MINERALOGICAL AND COMPOSITIONAL ANALYSIS OF TURQUOISE ARTIFACTS LINKED TO PREHISTORIC MINES IN NEW MEXICO, USA

by

CYNTHIA HOTUJEC

(Under the Direction of Samuel E. Swanson)

ABSTRACT

Petrography, Electron microprobe analysis, and X-ray diffraction analysis of thirty turquoise samples from four mine locations compared to ten artifact samples demonstrates that major element chemistry of the turquoise mineral group members is a potential indicator of geologic source. Mineralogical heterogeneity of turquoise has historically complicated attempts at determining the geologic source location of cultural artifacts. Mineralogy combined with chemical analysis provides major element ranges for comparison. Overlapping ranges of the cations Cu, Al, and Fe involved in the solid solution series of the minerals turquoise, chalcosiderite, and planerite show promise for providing chemical signatures of turquoise sources. Preliminary results show that samples from an Ancestral Puebloan archaeological site near Thoreau, New Mexico have more compositional similarity to a prehistoric mine at Hachita than geographically closer mines in the Cerrillos mining district.

INDEX WORDS: turquoise, chalcosiderite, planerite, petrography, electron microprobe, X-ray diffraction, prehistoric mining, Ancestral Puebloan, Hachita, Cerrillos, New Mexico

MINERALOGICAL AND COMPOSITIONAL ANALYSIS OF TURQUOISE ARTIFACTS LINKED TO PREHISTORIC MINES IN NEW MEXICO, USA

by

CYNTHIA HOTUJEC

BA Anthropology, Georgia State University, 2003

A Thesis Submitted to the Graduate Faculty of The University of Georgia in Partial Fulfillment

of the Requirements for the Degree

MASTER OF SCIENCE

ATHENS, GEORGIA

2011

MINERALOGICAL AND COMPOSITIONAL ANALYSIS OF TURQUOISE ARTIFACTS

LINKED TO PREHISTORIC MINES IN NEW MEXICO, USA

by

CYNTHIA HOTUJEC

Major Professor: Samuel E. Swanson

Committee: Douglas Crowe
Ervan G. Garrison

Electronic Version Approved:

Maureen Grasso
Dean of the Graduate School
The University of Georgia
May 2011

TABLE OF CONTENTS

LIST OF TABLES

Page

LIST OF FIGURES

Page

<u>**Chapter1 Introduction**</u>

Prehistoric Mining of Cultural Turquoise in the American Southwest

People have valued turquoise since prehistoric times. Native Americans in the southwestern United States, Mesoamerica, and South America, as well as prehistoric cultures in Mesopotamia, Australia, Egypt, China, Tibet, and India have all used the stone in various ways. Each culture ascribed turquoise a unique symbolic and economic significance. One of the prehistoric cultural traditions that had an affinity for turquoise was the Anasazi or Ancestral Puebloans of the American Southwest. Archaeologists have recovered blue green minerals from a variety of contexts indicating they used them for personal ornamentation, pigments, tesserae in mosaic overlay, and as ritual and grave goods (Mathien, 2001; Snow, 1891; Snow, 1973; Windes, 1992). Researchers are aware of many prehistoric turquoise mines in the southwestern United States, yet few have been investigated thoroughly from both archaeological and geological perspectives. Habitation and ritual sites where turquoise was consumed in the southwestern United States have been preferentially studied by archaeologists compared to the often neglected, rarely recorded and consequently less understood procurement sites where the commodity was extracted (Welch and Triadan, 1991).

Archaeologists are not solely responsible for the lack of available information on prehistoric mines and mining practices because historical and modern mining efforts have contributed substantially to the destruction of many prehistoric turquoise mines. Researcher bias that favors the study of habitation and ceremonial sites in addition to the irreversible effects of modern mining activity interfere with the ability to better understand this interesting facet of prehistory that persists in current times. The potential relationships between prehistoric turquoise mining activity and the subsequent trade and exchange of this commodity has been the subject of conjecture more than rigorous scientific testing. Reproducible and convincing geochemical evidence of prehistoric turquoise trade and exchange patterns has not been discovered, but a connection between Mesoamerica and the prehistoric American Southwest has been suggested by several researchers (Lekson, 1999; Mathien, 2001; Weigand, 1999; Weigand and Harbottle, 1993; Weigand et al., 1977). The ability to identify the procurement location of raw material used for turquoise artifacts would be very useful in studies of ancestral Puebloan political economy and could potentially contribute to existing models of social structure.

Archaeological literature uses the term cultural turquoise to refer to blue-green rocks recovered in association with cultural material at archaeological sites (Weigand and Harbottle, 1993). It is visually determined to be distinct from many other blue-green minerals based on observable physical properties. Cultural turquoise is not necessarily mineralogical or chemical turquoise, which refers specifically to the mineral group of hydrous copper phosphates. It may actually be one of several blue-green minerals similar in appearance to, but chemically different than, the turquoise group of minerals.

Field archaeologists continue to visually categorize cultural turquoise as such due to lack of access to expensive analytical techniques that require specialized training to identify mineralogical turquoise. The legal and ethical implications of using even minimally destructive techniques to burial items and irreplaceable artifacts is an important consideration in addition to accessibility and cost of analysis. Therefore, archaeological reports of cultural turquoise are typically the result of workers with highly variable rock and mineral visual identification skills. A widely accessible, inexpensive, nondestructive, reproducible and easily comparable method for turquoise sourcing must be developed. Until then, archaeologists will be restricted to the unreliable method of visual identification for turquoise.

Mineralogy

Turquoise is one of the minerals in the turquoise group of minerals. The general formula for the "turquoise group" is: $A_{0\text{-}1}B_6(PO_4)_{4-x}(PO_3OH)_x(OH)_8 \cdot 4H_2O$, where x = 0-2. The A site can be vacant in varying degrees or occupied by Cu, Zn, or Fe^{2+} (Table 1.1), and the B site can contain Al or Fe^{3+}. As the A site occupancy decreases, the charge balance is maintained by protonation and the development of (PO_3OH) groups which occurs in planerite (Foord and Taggart, 1998). Included within the turquoise group are the end members:

turquoise	$CuAl_6(PO_4)_4(OH)_8{\cdot}4(H_2O)$
planerite	$\square Al_6(PO_4)_2(PO_3OH)_2(OH)_8{\cdot}\ 4(H_2O)$
chalcosiderite	$CuFe^{3+}{}_6(PO_4)_4(OH)_8{\cdot}4(H_2O)$
faustite	$(Zn, Cu)Al_6(PO_4)_4(OH)_8{\cdot}4(H_2O)$
aheylite	$Fe^{2+}Al_6(PO_4)_4(OH)_8{\cdot}4(H_2O)$

Table 1.1 Theoretical turquoise endmember composition determined by stoichiometry.

Wt. %	turquoise	planerite	chalcosiderite	faustite	aheylite
CuO	9.78		8.06		
Cu2O				1.74	
ZnO				7.9	4.04
FeO					4.46
Fe2O3			48.6		
Al2O3	37.6	40.68		37.13	37.95
P2O5	34.9	37.76	28.77	34.46	35.22
H2O	17.72	21.56	14.61	18.59	18.44
TOTAL	100	100	100.04	99.82	100.11
Cations	**based on**	**28 O**			
Cu	1.0		1.0		
Cu2+				.2	
Zn				.79	.4
Fe2+					.5
Fe3+			6.0		
Al	6.0	6.0		5.92	5.97
P	4.0	4.0	4.0	3.94	3.98
H	16.0	18.0	16.0	16.76	16.41

The geologic setting where the mineral turquoise is found is the potassic alteration zone of porphyry copper deposits. Turquoise fills veins in volcanic rocks and phosphate-rich sediments. The turquoise mineral chalcosiderite is found in the oxidized zone of some hydrothermal deposits. Planerite forms in phosphate-rich aluminous deposits. Aheylite is a hydrothermal mineral in base metal tin deposits. Faustite occurs in argillized shales associated with copper mineralization.

Turquoise group minerals are hydrous aluminum phosphate minerals that are classified within the larger group of hydrous phosphates (Gaines et al., 1997). The existence of a sixth group member, coeruleolactite $(Ca, Cu)Al_6((PO_4)_4(OH)_8 \cdot 4(H_2O)$, is considered unlikely after analysis by Foord and Taggart (1998) whose samples of coeruleolactite were characterized as planerite. They suggest that coeruleolactite is not a valid species because the Ca^{2+} ion has a radius that is too large for the A site compared to the other cations (Foord and Taggart, 1998). Faustite is a Zn-bearing turquoise mineral. The extent of Zn substitution possible in the A site is unknown. The rarity of faustite has deterred documentation of this relationship, but a solid solution series may exist between faustite and turquoise (Foord and Taggart, 1998). All the turquoise group minerals including faustite are isostructural (Kolitsch and Giester, 2000).

The solid solution series known to exist in the turquoise mineral group are between turquoise and chalcosiderite and turquoise and planerite. The series between turquoise and chalcosiderite is between Al and Fe^{3+} in the B site (Fig. 1.1). Chalcosiderite is considered a rare mineral, although not as rare as faustite, aheylite and an unnamed ferrian, Fe^{2+} - Fe^{3+} member (Foord and Taggart, 1998). The series between turquoise and planerite is from Cu to vacancy in the A-site (Fig. 1.1). Planerite is the member with A site predominantly to completely vacant

(Foord and Taggart, 1998). Foord and Taggart propose that aheylite also has the potential for substitution with the components of planerite and faustite (Foord and Taggart, 1998).

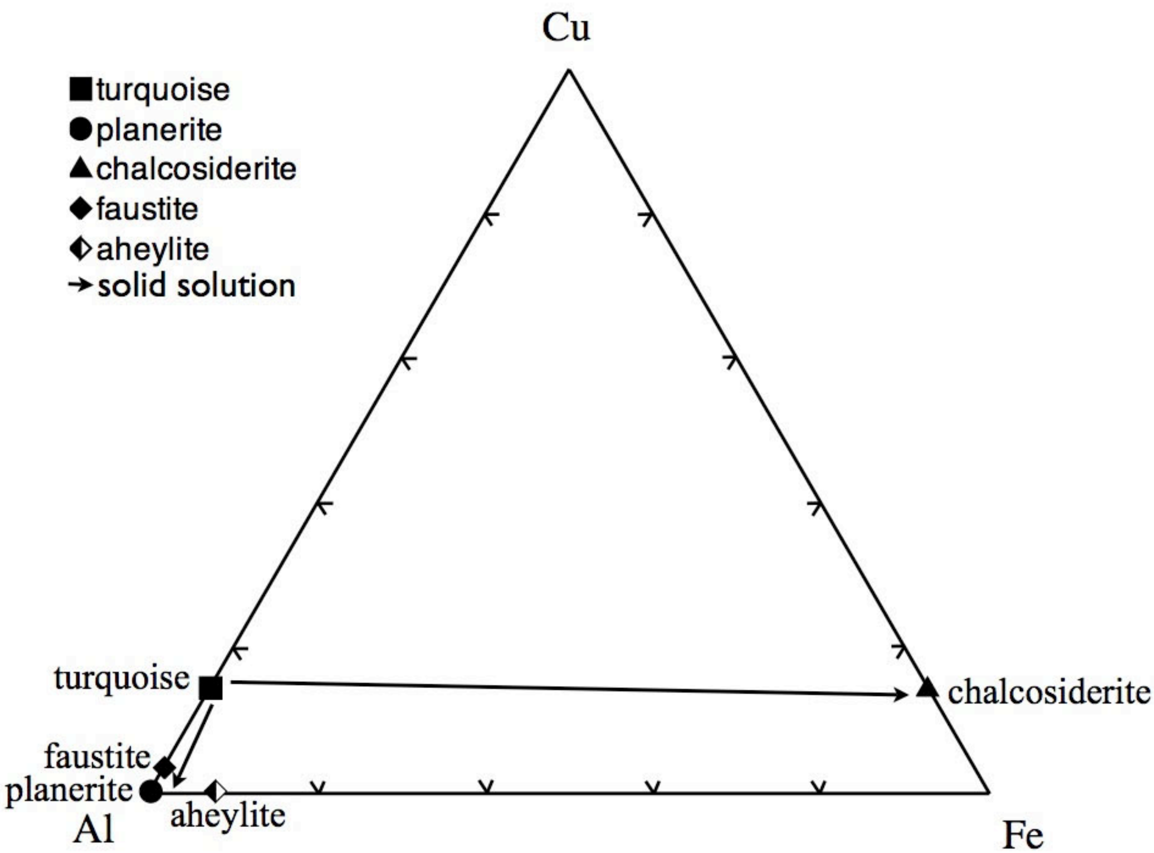

Figure 1.1 Ternary diagram of turquoise group endmembers and solid solution series.

Physical properties of the mineral turquoise include conchoidal fracture, hardness of 5-6 and perfect cleavage on {001} and good on {010}. It has a light green blue, light bluish white, to white streak. Turquoise crystals are vitreous, bright blue, rare, and usually smaller than 0.1 mm (Foord and Taggart, 1998). Most turquoise specimens are fine grained to cryptocrystalline and of variable density (Foord and Taggart, 1998). The luster of the common massive variety is earthy or dull to waxy. Color of the massive type ranges from blue to light blue, blue green, green to light green, and green gray. It forms concretions, encrustations, or veinlets (Nriagu and Moore, 1984). Turquoise occurs as globular crusts, flat and thin samples as a result of formation in cracks or veins, or nodular shapes due to isolated formation within a matrix.

The turquoise group mineral chalcosiderite has conchoidal fracture, hardness of 4.5, perfect cleavage on {001} good on {010}, and a pale green, green, or white streak. The luster is vitreous and the color is bright green to dark green. Chalcosiderite typically occurs as encrustations. The turquoise group mineral planerite has hardness of 5, no cleavage, and streak that is greenish white, blue white, or white. The luster is vitreous to dull and the color can be light green, olive green, bluish green, light blue, or white. Planerite can have a botryoidal habit and also occurs as encrustations. The turquoise group mineral aheylite has a hackly fracture, hardness of 5-6, perfect cleavage on {001} good on {010}, and a greenish white streak. The luster is dull to vitreous and the color range includes blue green, light blue and light green. Aheylite has a habit that can be botryoidal, felted or aggregate. The turquoise mineral faustite is brittle with a conchoidal fracture, has a hardness of 5.5, and poor or indistinct cleavage. The streak is white, greenish white, or light yellow green. The luster is earthy or dull to waxy and the color is bright green. Faustite has a habit that is massive, nodular, or in nugget form.

Previous Turquoise Source Studies

Sigleo (1970) attempted to use arc atomic emission spectroscopy (AES) to characterize turquoise. Traditional arc emission spectroscopy sample preparation involves grinding up a solid sample and destroying it during analysis. It is also a bulk technique that provides quantitative analysis of the major and trace elements present throughout the entire sample. The amount of variability within geologic sources analyzed in this study resulted in substantial overlap between the sources, preventing the ability to distinguish between them (Sigleo, 1970). Sigleo concluded that larger sample sizes from each source would reduce the intersource elemental variation and intrasource overlap (Mathien, 1981).

Sigleo (1975) also used instrumental neutron activation (INAA) to evaluate 24 possible geologic sources of 13 turquoise artifacts from the Snaketown Site, Arizona. Although this method is nondestructive, the solid sample must fit within the irradiation vial and it is also a bulk analytic technique that measures trace elements. This method succeeded in the identification of a diagnostic aspect of turquoise from only one area in Halloron Springs, California that had distinct levels of Co, Cr, Eu, Sb, Sc, and Ta among 30 elements analyzed for. The fortunately low levels of trace elements such as cobalt and chromium in this particular geologic source happened to coincide with similar levels in the artifacts based on similarity coefficients. Unfortunately the other sources had considerable overlap in the data and lacked their own unique chemical signature of trace elements. Additionally, the data formed two unexpectedly distinct groups of Sc levels within both the Halloron Springs samples and the archaeological samples. Sigleo (1975) stressed the importance of analyzing multiple samples from each source to identify this type of internal characteristic.

Neutron activation analysis (NAA) is minimally destructive and are therefore appealing to archaeologists working with irreplaceable artifacts (Mathien, 1981). However, because it is a bulk analytic technique, it can not provide *in situ* information about specific areas within a heterogeneous sample. Turquoise artifacts from Chacoan sites analyzed with NAA showed considerable homogeneity, but samples from geologic sources were not yet available for comparison and none of the artifact data were reported (Mathien, 1981).

X-ray fluorescence (XRF) has also been used to determine trace element variability in turquoise samples (Mathien and Olinger, 1992; Ronzio and Salmon, 1967; Salmon and Ronzio, 1962; Weigand et al., 1977). XRF is another destructive bulk analytic technique that traditionally requires the solid sample to be ground into a powder and pressed into a tablet. Newer portable XRF instruments have developed nondestructive methods, yet still provide bulk analytic results for major and trace elements. Results show large amounts of variation within one mine that causes overlap with other mines (Salmon and Ronzio, 1962). A large number of samples from various mines in the Cerrillos mining district in New Mexico also showed a great amount variation and was not diagnostic (Mathien and Olinger, 1992). These studies provide evidence that trace elements can not be used to successfully characterize turquoise sources, especially those in the Cerrillos mining district.

Others (Harbottle et al., 1994; Weigand, 1982; Weigand, 1999; Weigand and Harbottle, 1993; Weigand et al., 1977) have used the bulk analytic technique of neutron activation analysis (NAA) extensively in attempts to identify trade and exchange routes between ancient Mesoamerica and the prehistoric American Southwest. Some of the geologic sources of turquoise are alleged to have been homogenous and subsequently characterized, but no raw data were published to quantify the level of homogeneity purportedly observed. Patterns reported in multivariate numerical taxonomies and cluster analyses of the NAA results were not reproducible when tested by XRF, another bulk analytic technique (Mathien and Olinger, 1992). The inability to replicate patterns observed in bulk analysis of trace elements found in turquoise samples illustrates the important, yet often overlooked aspect of geochemistry that the suite of probable trace elements differs from mineral to mineral causing the range and levels of trace elements to vary widely in heterogeneous materials such as turquoise. This results in considerable overlap between sources and prevents diagnostic characterization using bulk analysis.

Electron microprobe analysis (EMPA) was used by Ruppert (1982) to explore the possible trade routes for turquoise throughout the Americas. EMPA does not provide bulk analysis, but is a microprobe technique with the capability of measuring the major element composition of a solid sample *in situ*. EMPA results successfully showed that turquoise samples from the southwest US and Mexico were chemically distinct from turquoise samples at archaeological sites in South America with no overlap in data (Ruppert, 1982). Welch and Triadan used X-ray diffraction analysis (XRD) to analyze a sample of turquoise from a prehistoric turquoise mine and compared it to a turquoise artifact from a nearby archaeological site, both in Arizona. XRD is not a bulk analytic technique, although sample preparation often involves grinding a solid sample into a powder. Although only one sample of each was analyzed, the mineralogy identified consisted of the mineral turquoise and metatorbernite, a copper uranium phosphate (Welch and Triadan, 1991). Based on mineralogy alone, it is suggested that the artifact came from the mine due to the presence of metatorbernite, an uncommon mineral associated with uranium deposits (Welch and Triadan, 1991). Additional analyses are clearly required, but the previous two studies show substantial promise for the continued use of both XRD and EMPA in obtaining the mineralogical and compositional data needed in turquoise sourcing studies.

Kim et al. (Kim et al., 2003) used proton-induced X-ray emission (PIXE) in conjunction with X-ray diffraction (XRD) to analyze cultural turquoise artifacts. XRD provided the identification of various blue green mineral phases present within the artifact sample set including the mineral turquoise that was subsequently characterized by PIXE. The ratio of Al to Cu was used to distinguish the mineral turquoise from the other phases and provided a foundation for future turquoise provenance studies. The relationship between color and chemical composition was also recorded and results showed that color varied with chemical composition (Kim et al., 2003).

Cu and H isotope ratios have recently undergone consideration as a possible method of turquoise characterization with the expectation that isotopic ranges will have distinctive variations among sources (Hull et al., 2008). The method uses a secondary ion mass spectrometer (SIMS), another microprobe technique that allows *in situ* analysis of solid samples. The isotope data are not collected through bulk analysis and sample preparation is minimally destructive. The method is apparently independent of "minor variations in the chemical composition of turquoise", but no supporting evidence has been provided to support this assertion (Hull et al., 2008). This method also assumes that copper isotope variation results from an abiotic process (Hull et al., 2008), disregarding the possibility of biotic fractionation and the challenges that would present to the success of this method. Nonetheless, the method shows promise because of its focus on major element isotopes and the ability to target specific areas within a turquoise sample.

Hull et. al. (2008) defined isotopic signatures for 12 turquoise sources after analyzing 17 samples: one sample from each of ten sources, two samples from the Castillian mine, and five samples from the Sleeping Beauty mine. Seventeen turquoise artifacts were also analyzed for comparison and had similar Cu to H ratios to several of the sources (Hull et al., 2008). Preliminary conclusions assert there is no isotopic variation at the deposit scale based on data from five samples from one mine (Hull et al., 2008). It is a tenuous assumption at best that five samples from one mine are enough to conclude that a particular source is homogeneous. A much larger sample set from each source is also necessary to determine if the Cu - H isotope ratio "signature" actually persists at the mine level for all occurrences. The 11 other source signatures are derived from the data of only one sample per mine (two samples from the Castillian mine). While this method has potential, much more robust sampling at the deposit scale is needed before considering Cu-H ratios truly reliable geochemical fingerprints for turquoise artifacts.

Justification for the Study

Archaeologists need a widely available, economical, nondestructive, and reproducible method of characterizing cultural turquoise. Experimentation with various methods thus far has revealed the need for extensive sampling from each geologic source to identify the range of variability possible. Studies have also shown that combining mineralogical and compositional analyses in conjunction are more useful (Kim et al., 2003) than geochemical techniques alone. Two different clay minerals, pyrophyllite $Al_4(Si_8O_{20})(OH)_4$ and gibbsite $Al(OH)_3$, have been observed in turquoise samples, but it is not yet clear how this mineral intergrowth might affect the results of sourcing studies (Hull et al., 2008). Additionally, artifact samples have been found to contain mineralogical mixtures of not only several phases of the turquoise group of minerals, but also several other blue-green phases such as chrysocolla, malachite, azurite, and even blue-green quartz, as well as phases of different color such as calcite (Kim et al., 2003). Mineralogical analysis can identify various phase combinations that might explain distinctive patterns observed in compositional data. The connection between mineralogy and geochemistry may be complicated and more time intensive, but continued examination of these relationships is necessary for defining the extent of turquoise variability at the deposit scale and ultimately, our ability to provenance turquoise artifacts.

XRD and electron microprobe analysis (EMPA) have provided a better understanding of the turquoise mineral group and how solid solution series can be responsible for variation even when seemingly homogenous samples are chosen (Foord and Taggart, 1998; Foord et al., 1986).

The inherent mineralogical variation in turquoise prevents bulk analytic methods from successfully characterizing mines and associating them with artifacts. An approach that attempts to identify the mineralogy of each sample and then focus chemical analysis on the most homogenous turquoise areas will provide the best comparative information about the composition of turquoise. Once the turquoise minerals have been isolated, a compositional analysis can provide a unique set of information about the geologic source to consider in relation to the mineralogy present at that location. This study attempts to apply this approach to multiple samples from prehistoric turquoise mines for comparison with cultural turquoise samples.

The initial stage of this thesis research requires variation between geologic sources to outweigh the variation within one source in order to identify the origin of artifact material (Weigand et al., 1977). A suite of turquoise samples from two separate mine sources was examined prior to analysis of turquoise artifacts. Conservation of artifacts is of concern because the assemblage is limited and the methods are minimally destructive. Additionally, identification of the compositional variation of turquoise artifacts alone will not provide any significant insights into the behavior of prehistoric Native Americans related to production, consumption and trade. Information about the trade and exchange patterns can be learned from methods that provide the ability to determine the location of raw material procurement. The chemical fingerprint of possible geologic sources needs to be identified before artifacts can be assigned to them. This research also attempts to provide a better understanding of the turquoise group minerals through the description of chemical composition and mineral variability identified within and among independent geologic occurrences.

Hypothesis: Major element chemistry of the turquoise mineral group members are an indicator of geologic source.

In other words,

If mineralogy and major element chemistry of the turquoise mineral group are indicators of geologic source, then mineralogical and compositional analysis of turquoise sources will provide a distinctive range that can be matched to cultural turquoise artifacts.

Chapter 2 Archaeological Setting of Turquoise Artifacts

Prehistory of the American Southwest

Most archaeologists agree that evidence of human occupation in the Americas begins around 12,000 – 15,000 years ago. When *Homo sapiens sapiens* arrived on the North American continent, their mode of subsistence was hunting and gathering. The development of agriculture allowed some groups to shift from a nomadic to a more sedentary lifestyle. Groups with various subsistence strategies subsequently produced distinct material remains. Geographic regions often encompassed areas where groups with different lifestyles lived in close proximity for centuries. One of these regions was the American Southwest, which includes the entire states of New Mexico and Arizona, southern Utah and southern Colorado, and portions of the northern Chihuahua and Sonora deserts.

Three distinct traditions are defined for the archaeological record in the American Southwest: the Hohokam, Mogollon, and Anasazi. Archaeologists refer to the last two groups as the "Ancestral Puebloans" because they are the ancestors of the modern Pueblo people (Kantner, 2004). All of these cultures were roughly contemporaneous and therefore, most likely had contact with each other. It is also reasonable to consider that they had contact with surrounding nomadic groups such as the Apache and Utes in addition to their Mesoamerican neighbors to the south. All of these groups to various degrees throughout time, considered turquoise to have spiritual significance and treated it as a valuable commodity. The Ancestral Puebloan cultural tradition is visible in the archaeological record of the southwestern United States from around

700 A.D. until sustained Spanish contact after 1540 A.D. Descendants of the Ancestral Puebloans continue to live in 21 pueblos throughout the American Southwest today.

The largest archaeological deposit of prehistoric cultural turquoise in the American Southwest was found in Chaco Canyon, New Mexico (Pepper 1909, 1920), a major center of Ancient Puebloan activity occupied from roughly 900 A.D. - 1250 A.D. The canyon contains over 100 archaeological sites, some including large core and veneer stone masonry architectural structures consisting of rooms, plazas, and circular rooms called kivas believed to have been used for ritual purposes. Human remains were either interred in debris mounds called middens outside of the structures or occasionally buried inside of sealed rooms within the main structure. Distributed between the burials of two males in Room 33 in the northern part of Pueblo Bonito were over 40,000 pieces of turquoise (Snow, 1973). Although the Hohokam site of Snaketown, Arizona is the earliest archaeological site in the region with turquoise artifacts (Sigleo, 1975), Pueblo Bonito has the largest recorded concentration of turquoise at one site. The majority of ruins in Chaco Canyon have not been excavated, so the total amount of turquoise actually present is unknown. There is no known geologic source for turquoise in Chaco Canyon, so the provenance of these artifacts is a topic of much speculation. The Cerrillos Mining District located about 105 miles east of Chaco Canyon has long been suspected as the source because it is the closest (see Fig 2.1) known prehistoric turquoise mine (Mathien, 2001).

The Ancient Puebloan culture was responsible for the extensive architecture and associated artifacts found at Chaco Canyon. During the period 1050-1100 A.D. there was an increase in activity in Chaco Canyon evident in the construction of more imposing architectural structures and predictive astronomical features. Intensification and expansion of social activity is also represented by larger cultural deposits with more varied exotic luxury goods. Luxury

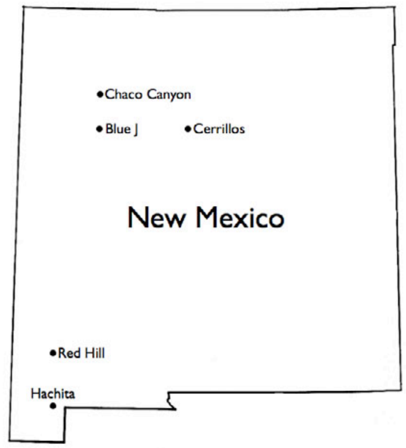

Figure 2.1 Map of places mentioned in text.

items include macaw feathers, copper bells, large cylinder jars with cacao residue, painted wooden staffs, cylinder jars covered with turquoise inlay, and many ornaments and objects made with lignite, marine shell, and turquoise. Chacoan cultural characteristics appear in the material culture of many smaller outlying communities at this time, indicating a large sphere of influence extended throughout the northern region of New Mexico into southern Colorado (Kantner, 2004). Chaco Canyon's influence eventually spread to Arizona and Utah. Some of these communities, also called outliers or great house communities, had their own smaller version of a Chacoan great house, a larger architectural structure than a normal residence that was probably used for ceremonial purposes.

Chacoan archaeologists deliberate at length over what similarities in material culture between Chaco Canyon sites and outlier sites could possibly suggest about social relationships. Several main models dominate the research based on various forms of evidence within and outside of the canyon. Some claim that Chaco Canyon developed an imperialistic state that relied on military prowess to subdue the outlying communities. The missionary model suggests that the canyon was a religious center that sent out individuals to acquire converts who then built similar architecture. A related model views the canyon as a religious pilgrimage site where individuals traveled long distances bringing gifts into the canyon and then returned home to emulate what they experienced on a smaller scale. Yet another model proposes a regional redistributive system where agricultural surpluses were stored in the canyon and allotted to communities in need during times of drought. These models all share the similar theme that participation in the system increased access to beneficial knowledge, protection, and/or material goods otherwise unavailable, resulting in the increased geographic range of Chacoan material culture.

One of these outlying communities occupied during the Pueblo II phase, named the Blue J community, was excavated as part of a field project conducted by the Georgia State University Anthropology Department and funded by the National Science Foundation. Although it does not have a confirmed great house, several neighboring communities featured Chacoan great houses, suggesting that Chaco Canyon was well known in the region surrounding the Blue J site.

Blue J Project

The Blue J project was conducted through archaeological field schools and laboratory methods courses in the Anthropology Department at Georgia State University. Five field seasons were spent surveying and excavating the Blue J community in McKinley County, New Mexico (Zone 12 769111E 3925251N). Among the artifacts recovered were a variety of ornament types, or objects believed to have been used for bodily adornment, recovered in various stages of production. These ranged from unmodified raw material to apparently finished ornaments: discoid beads, rectangular bead blanks, pendants, rings, etc. Subsequent ornament analysis results were compared to those of contemporaneous proximal sites. The ornament assemblage at Blue J was much larger and more varied than expected for a community without a great house

(Hotujec and Kantner, 2007). 24 of the Blue J ornaments were classified as turquoise based on observable mineral physical properties.

The Georgia State University archaeological field school located about 80 sites scattered within a 2.5 sq km area along the base of a mesa. Most of the sites were sandstone and limestone masonry structures consisting of adjacent square or rectangular rooms used for habitation and storage. Radiocarbon dating and ceramic chronology place the occupation of this community from 900 – 1200 A.D. (Kantner, unpublished data), overlapping with the height of Chaco Canyon. Initially, it was believed that Blue J was a great house community with one main structure exhibiting several of the architectural and stylistic traits often interpreted as an emulation of Chacoan culture. No great house was found after excavation of several habitations and a kiva, as well as extensive field survey in the surrounding area. Despite the lack of a great house and apparently no direct participation in the Chacoan social system, Blue J still had access to a wide variety of resources, including luxury materials used for ornaments (Hotujec and Kantner, 2007). Archaeologists consider enhanced access to resources as one of the main reasons why communities outside Chaco Canyon attempted to include themselves in what was happening there. The Blue J community presents a unique research opportunity because it is considered an anomaly among most contemporaneous outlying communities.

The Blue J ornament subassemblage includes 24 turquoise artifacts recovered from middens, room fill and the base of wall trenches. The archaeological term ornament includes any rock or mineral used for pigment, mosaics, personal adornment or ritual offerings. Most of the Blue J turquoise is small unmodified lumps, but bead and pendant fragments and incomplete abraded blanks also occur in the subassemblage. Although the amount of turquoise found at Blue J seems insignificant compared to the amount of turquoise found at Chaco Canyon, the entire ornament assemblage is comparable in size and considerably more varied than contemporaneous proximal Puebloan sites of similar size that have great houses (Hotujec and Kantner, 2007). Artifact samples analyzed for this research were selected from the group of unmodified turquoise within the Blue J ornament assemblage.

Chapter 3 Geologic Setting of Prehistoric Turquoise Mines

Occurrence

Turquoise may form in one of three geologic settings. The most common occurrence is in weathered igneous rocks rich in silica and aluminum that contain both copper and apatite (Pogue, 1915). Hydrothermally altered igneous rocks related to copper mineralization, in particular Cu porphyry deposits, often have turquoise in their distal regions. Turquoise also forms in sedimentary or metamorphic rocks near contact with igneous rocks. The least common occurrence is in non-igneous rocks such as sandstone or shale that have no apparent genetic relation to an igneous body (Pogue, 1915).

In the United States, turquoise has been recovered in the largest quantities in the states of New Mexico, Arizona, Nevada, California with lesser amounts also mined in Colorado, Texas, and Virginia. Sterrett (1911) reported that the occurrence of turquoise in the United States is "generally in or near such igneous or volcanic rocks as granite, quartz or monzonite porphyry, and rhyolite or trachyte" that also show evidence of sericitization, kaolinization or both. He was one of the earliest to record the frequency of turquoise in the vicinity of large copper ore deposits and noted that prospectors often profited from observing this association. Figure 3.1 shows the location of the porphyry copper belts worldwide.

Copper Porphyry Deposits

Plutons associated with copper porphyry deposits tend to be composed of granodiorites and quartz monzonites. Several different intrusive events, each with dissimilar compositions, can occur within the same system and obscure previous compositions and textures. Copper porphyry systems may extend from deep seated plutonic to shallow volcanic depths, ranging from one to

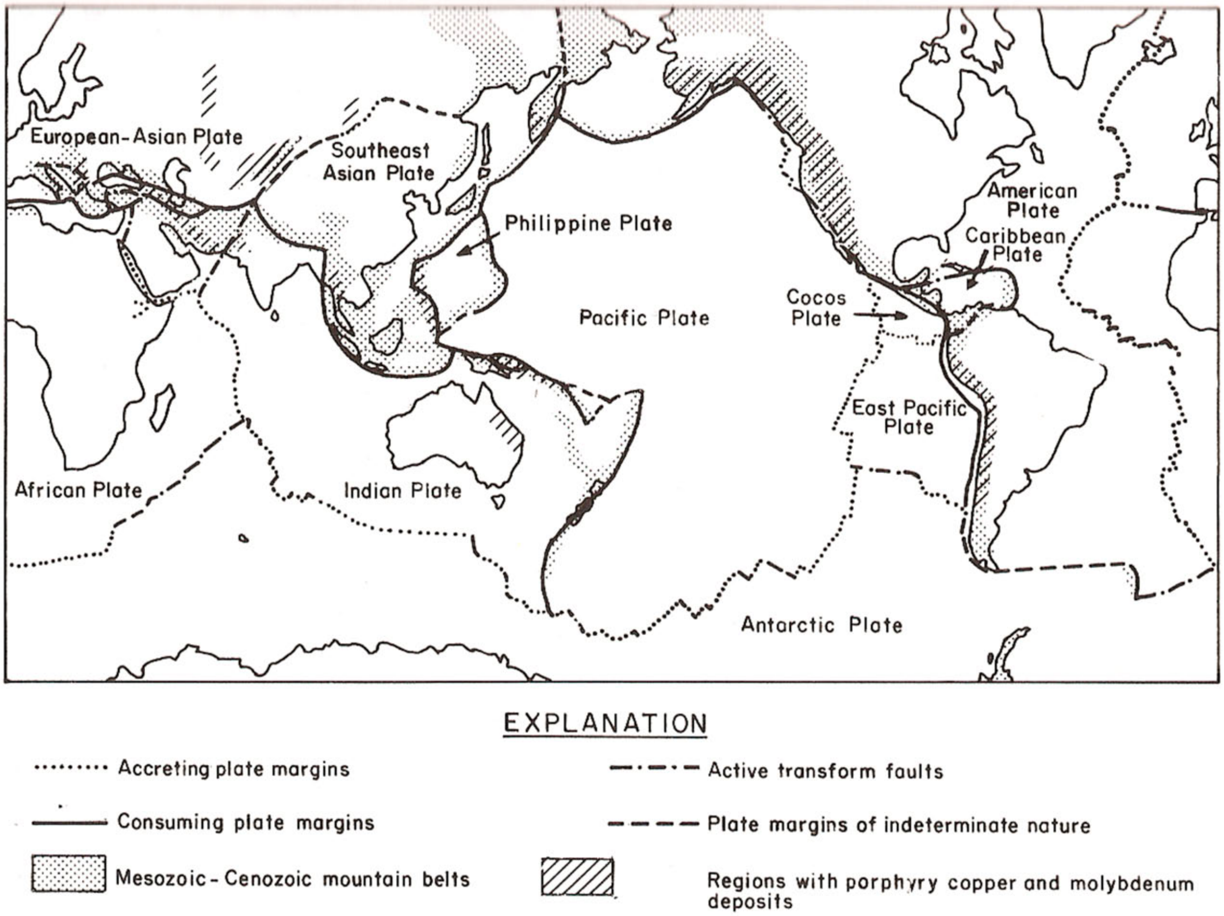

Figure 3.1 Porphyry copper belts of the world (Sawkins, 1990).

eight kilometers (Sawkins, 1990). Constraints on the formation of magmas associated with porphyry copper-forming igneous rocks include a water content in the magma of two to three weight percent and initial temperatures of $> 800°$ C, high amounts of metal, sulfur, and chlorine, and a high oxidation state (Guilbert and Park, 1986; Sawkins, 1990).

Hydrothermal fluids circulating within and adjacent to porphyry intrusions react chemically with the surrounding rocks as they travel further from the hot pluton. These fluids precipitate metallic ores that may be copper-rich in large, low-grade porphyry deposits. Turquoise deposits occur during the late stages of hydrothermal activity when fluids move upwards along fractures and encounter decreased pressure and cooling (Craig et al., 2001).

Figure 3.2 illustrates where hydrothermal veins generally form in a copper porphyry system. Turquoise mineralization frequently occurs in association with these veins.

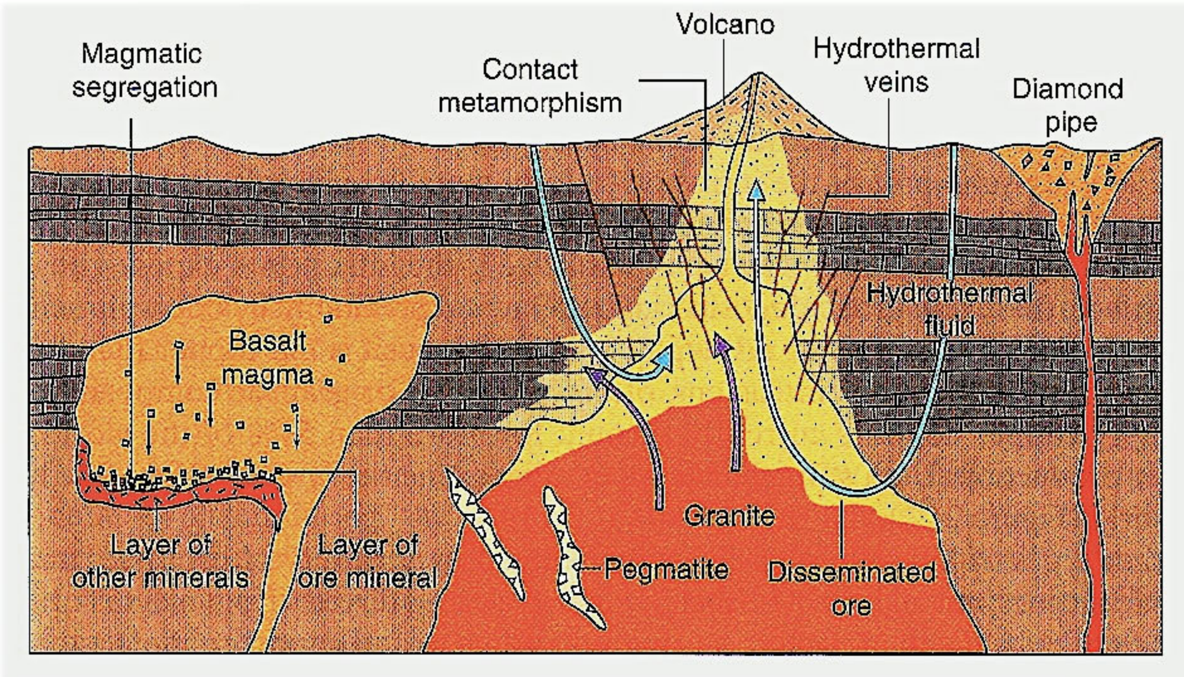

Figure 3.2 Location of hydrothermal veins (Hamblin and Christiansen, 2004).

Hydrothermal Fluids

The term hydrothermal fluid refers simply to heated water. Ore-bearing fluids are divided into six categories: magma and magmatic fluids, hydrothermal fluids that have separated from a magma, meteoric waters, seawater, connate waters, and metamorphic fluids (Guilbert and Park, 1986). All categories are possible sources of hydrothermal fluids and follow similar physical and chemical constraints as they move through country rock (Guilbert and Park, 1986). Hydrothermal fluid is sometimes used synonymously with the term *hypogene* which is generally defined as "a mineral deposit formed by ascending solutions; also, said of the solutions and of that environment." (Jackson et al., 2005).

Hypogene can be considered the opposite of supergene in the didactic sense, but this does not preclude the possibility that they may interact with each other in a particular geologic setting. Hydrothermal/hypogene and supergene fluids while separate in origin, are not necessarily spatially exclusive (Fig. 3.3). Supergene fluids related to post-mineralization weathering serve to remobilize hypogene assemblages. Turquoise minerals may form from these supergene fluids, as well as from the earlier, hypogene fluids.

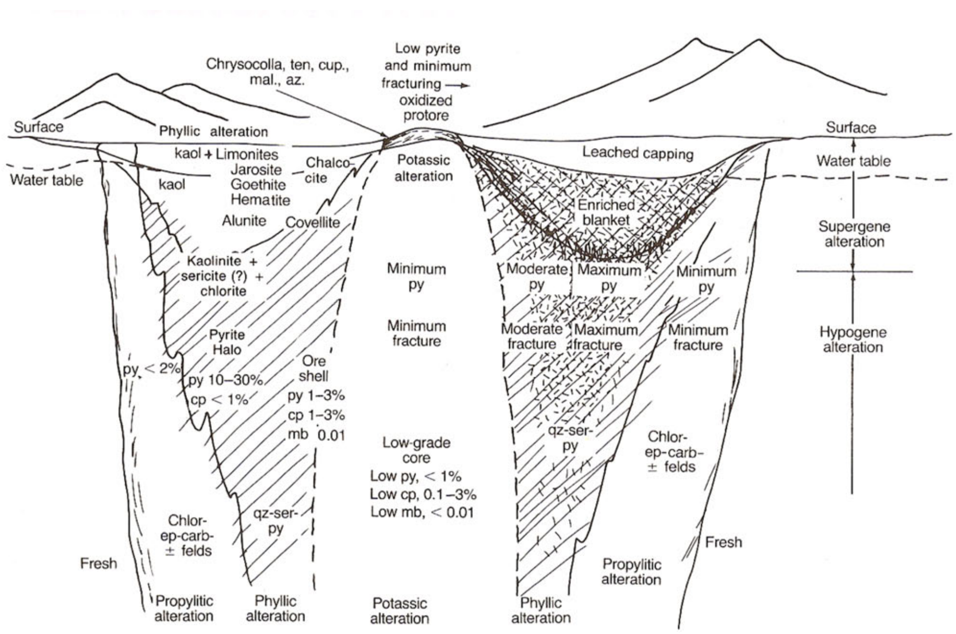

Figure 3.3 Idealized results of the interaction of hypogene and supergene alteration at a porphyry copper deposit (Guilbert and Park, 1986).

Alteration Zones

One of the distinguishing characteristics of copper porphyry systems are zones of ore minerals and alteration phases in the enclosing country rock. Turquoise tends to occur in a reasonably predictable fashion in certain alteration zones containing copper. Wall-rock alteration is a change in mineralogic composition prompted by contact with hydrothermal fluids (Guilbert and Park, 1986). A calc-alkaline pluton thermally and chemically alters the surrounding country rock when hydrothermal fluids circulate around the cooling pluton. The result is a set of concentric alteration zones characterized by distinctive mineral assemblages (Fig. 3.4). Factors such as size of the pluton, initial temperature of the magma, fluid content of the magma, and composition of the magma and/or country rock all affect the formation of minerals in the alteration zones. Minerals at equilibrium in higher-temperatures such as sillimanite form closest to the intrusion and those stable in lower-temperature environments, like epidote, form in the outer zones (Wicander and Monroe, 1995).

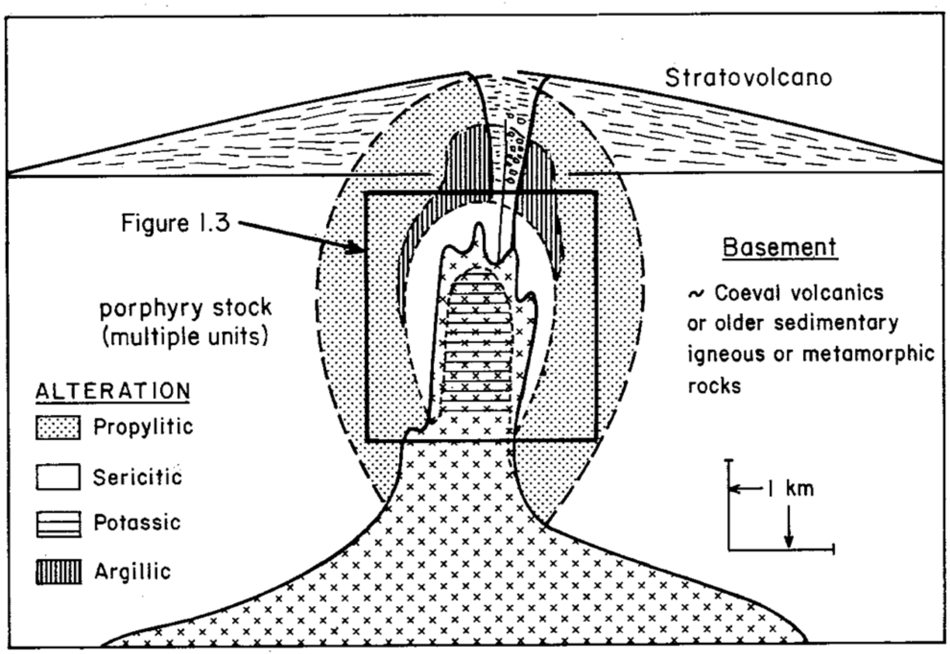

Figure 3.4 Generalized model of porphyry copper formation (Sawkins, 1990)

Alteration zones form a general pattern in copper porphyry systems (Fig. 3.5). From the intrusion outward, the progression is: potassic, phyllic, then mixed phyllic-argillic or argillic-propylitic (Sawkins, 1990). The innermost alteration is called the potassic alteration zone and is associated with the minerals quartz, biotite, and K-feldspar and/or anhydrite that replace the original texture or occur in veinlets. Other minerals potentially found in the potassic zone are chlorite, epidote, magnetite, actinolite and albite. The phyllic zone contains quartz, sericite, and pyrite mostly in veinlets. This zone has the maximum amount of sulfides and is surrounded by the next alteration zone, the propylitic zone. Propylitic alteration is characterized by chlorite, epidote, and carbonates. Isolated areas of argillic alteration containing quartz, kaolinite, and chlorite may also be located in the propylitic zone. These outer zone minerals are typically found in discrete veins in copper porphyry systems (Sawkins, 1990).

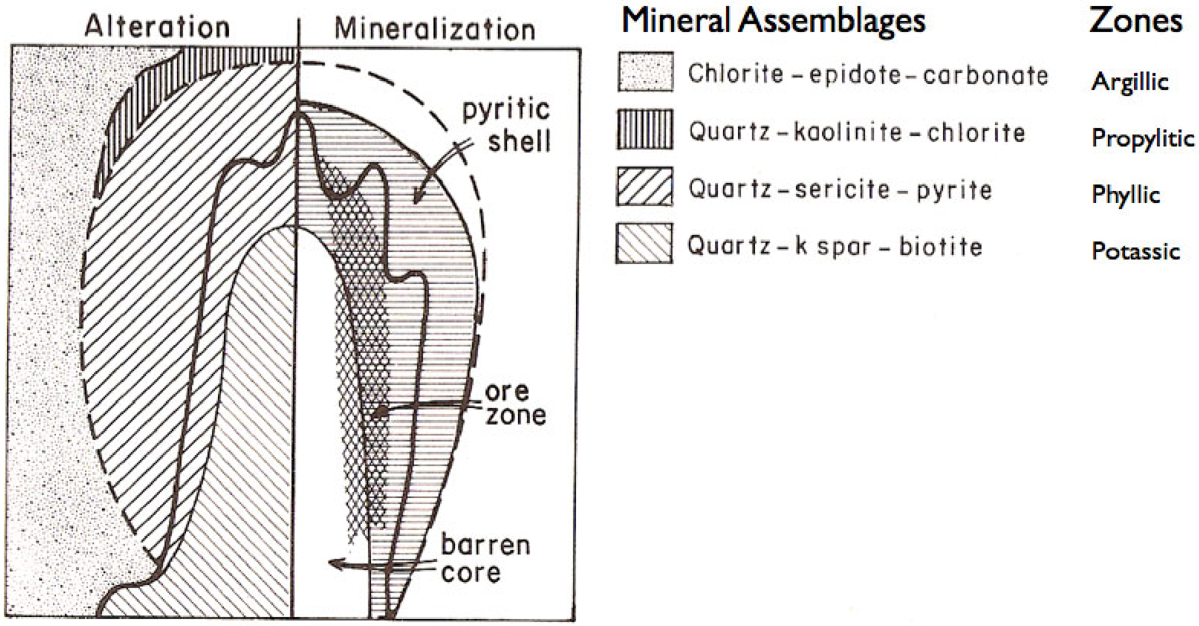

Figure 3.5 Alteration and mineralization zones of copper porphyries (Sawkins, 1990).

Alteration occurs in two stages, the orthomagmatic, or principal stage of silicate crystallization in a magma, and the meteoric stage. The first stage is caused by reactions with magmatic fluids and produces potassic and propylitic alteration assemblages. The second, meteoric, stage is related to the addition of meteoric waters and results in phyllic and argillic zones that overprint the propylitic zone. Evidence for this comes from both fluid inclusion and stable isotope studies that indicate where the orthomagmatic stage occurred due to the presence of fluids with high salinity at high temperature whereas the meteoric stage involves fluids of lower temperature and salinity (Sawkins, 1990). The end result is a combination of alteration facies overprinted on each other due to mixing of the hydrothermal fluids of both magmatic and nonmagmatic origin. Turquoise deposits are usually found in veins and veinlets in these argillic (potentially within the propylitic) and phyllic alteration zones.

Weathering

The alteration zones of the copper porphyry system described in the previous section can be exposed by erosion at the surface or become closer to it. When this occurs, the minerals undergo changes mainly caused by chemical weathering. These changes occur at temperatures of less than 100°C at low or surface pressure in the phreatic zone. This complicated process is often referred to as supergene weathering and involves a combination of possible chemical events such as oxidation/reduction reactions, chelation, hydration and hydrolysis, carbonation, and cation exchange. Supergene weathering is initiated by the introduction of slightly acidic groundwater and oxidizing agents which release highly mobile elements such as copper and transport them away depending on the specific hydrodynamics of the region. This weathering may result in the deposition of new, or secondary, minerals formed from the constituents of primary mineralization and is called secondary enrichment. The mobile nature of copper results in copper enrichment and also deposits of secondary copper minerals (Bland and Rolls, 1998).

It is assumed that the copper found in turquoise molecules is derived from the chemical weathering of porphyry copper minerals. While deposits of copper oxides such as chrysocolla, cuprite, malachite and others may be hypogene (Fig. 3.5) (Guilbert and Park, 1986), supergene turquoise minerals are not as predictable or regular in their occurrence. Turquoise minerals in copper porphyry systems are not restricted to occurrence in the exposed proto-ore and are also found in alteration mineralization zones that have been oxidized and leached.

Numerous phosphates form as secondary minerals from primary phosphates including the turquoise minerals chalcosiderite and faustite, for example (Nriagu and Moore, 1984). Turquoise deposits were initially thought to originate from copper-bearing solutions rising along fractures in granite porphyry that combined with phosphatic solutions moving along a second set of fractures which has been observed at turquoise deposits in the Burro Mountains (Gillerman, 1964). In this scenario, phosphate was derived from apatite and alumina from feldspar, both of which were present in the granite. The second formation process proposes that turquoise occurs when copper minerals oxidize in situ. Sulphate solutions from pyrite oxidation cause decomposition of apatite and provide phosphate. This fluid interaction results in the secondary formation of turquoise minerals (Gillerman, 1964). Both types of occurrence involve the interaction of fluids containing copper, aluminum and phosphate but the second interpretation proposing a supergene origin of turquoise is more widely recognized. Additional elements may contribute to the formation of different turquoise minerals. Iron is needed for the formation of aheylite (Fe^{2+}), $Fe3^{+}$ for chalcosiderite and the unnamed iron (Fe^{2+} - Fe^{3+}) analogue, but iron may also be taken up by turquoise. If zinc is present in the environment, the turquoise mineral faustite may form.

Thermogravimetric analysis (TGA) measures the amount of weight that is lost as the temperature of a sample is progressively raised. The data are presented in a weight loss curve that can provide information about change in mass due to decomposition, oxidation, or dehydration. The results are directly related to the characteristic molecular structure of a mineral and are therefore unique. The type of water present in minerals can also be determined by TGA. All turquoise minerals contain hydroxide that is structural and four water molecules that are not. These have been associated with two weight loss events at 280° and 170°C respectively in planerite. Crystallized samples from the type locality for turquoise have only one weight loss event at 420°C and is presumed to loose both water and hydroxide at that temperature (Foord and Taggart, 1998).

Information about phosphate weathering provides a guideline for understanding the weathering process in the turquoise group of minerals. Phosphates are divided into four groups depending on their alteration characteristics:

1) phosphate minerals relatively resistant to alteration processes
2) phosphate minerals which become unstable and are destroyed by alteration
3) phosphate minerals which are replaced by one or more new phosphates having different composition and structures
4) phosphate minerals showing deficiencies in cations and anionic groups but with preservation of their structures (Van Wambeke, 1971).

Turquoise minerals fall into the fourth category.

Alteration processes in phosphates are caused by low temperature solutions in addition to surficial weathering. Partial substitution of anionic groups involves the replacement of (PO_4) by (H_4O_4) and sometimes (CO_3), but (OH) when fluorine is present. Selective cations may be leached with or without simultaneous oxidation of iron (Van Wambeke, 1971). Charge balance for A-site vacancy is maintained by protonation of up to two (PO_3OH) groups, so H_20 for OH (Foord and Taggart, 1998) is the most likely anion substitution during alteration. The variable occupancy in the A-site of the turquoise group minerals is apparently unrelated to alteration processes (Foord and Taggart, 1998). Therefore, the solid solution series between vacancy and Cu in the A-site for planerite and turquoise should occur independently of alteration. The B-site cations, Fe^{3+} and Al^{3+} are very insoluble and Fe^{3+} is already oxidized, so it is also improbable that solid solution between turquoise and chalcosiderite is controlled by alteration processes.

Microbes are potentially involved in the alteration and erosion of turquoise minerals (Murr and Berry, 1976). Certain bacteria responsible for bioleaching selectively attach to low-grade sulfide ores and other minerals such as turquoise (Murr and Berry, 1976). A microbe similar to *Thiobacillus ferroxidans* attached to the surface of the turquoise-like phase in a sample from the Kingman mine, Arizona and avoided the matrix of ferric iron with oxygen. The iron in the turquoise mineral phase must have been ferrous and therefore, provided the energy source for biosynthesis through oxidation (Murr and Berry, 1976). Elemental X-ray mapping, energy dispersive analyzer and secondary electron images also reveal distinct halos around attached microbes described as "a shallow pit or eroded area" that gave "the impression of a secretion, reaction, or surface erosion" (Murr and Berry, 1976). Attempts to identify element content of a halo were unsuccessful and it was assumed to be organic matter, possibly an enzyme catalyst for the organism's reactions with the mineral (Murr and Berry, 1976).

Burkholderia ferrariae and *Burholderia carbensis* bacteria are phosphate solubilizing bacteria strains that interact with iron ore gangue phosphatic phases. They grow and form halos around tricalcium phosphate, grow but do not produce solubilization halos around berlinite ($AlPO_4$), and neither grow nor form halos around silicate rock containing turquoise (Delvasto et al., 2008). Copper in turquoise may have gone into solution during the high temperatures of sterilization and had a bactericidal effect which inhibited growth (Delvasto et al., 2008) or they might not interact with turquoise minerals at all. The interaction between turquoise minerals and bacterial strains suggested thus far involves indigenous chemoautotrophic microorganisms in the oxidation zone selecting ferrous iron from a very iron-rich turquoise mineral and creating a more compositionally pure turquoise-like mineral as a result. This particular process requires aheylite to be a common mineral, but the rarity of aheylite makes these propositions problematic. Bacterial involvement during turquoise weathering may eventually be found to occur via a different process, but the possibility of bacterial involvement in turquoise formation merits equal consideration.

Grant County Turquoise Mines

The Red Hill turquoise mine and the Azure turquoise mine are located in Grant County in southwest New Mexico (Fig. 3.6). Grant County is one of the most intensely mineralized areas of New Mexico. Many turquoise deposits have been mined there since prehistory.

Geology of Mines Analyzed

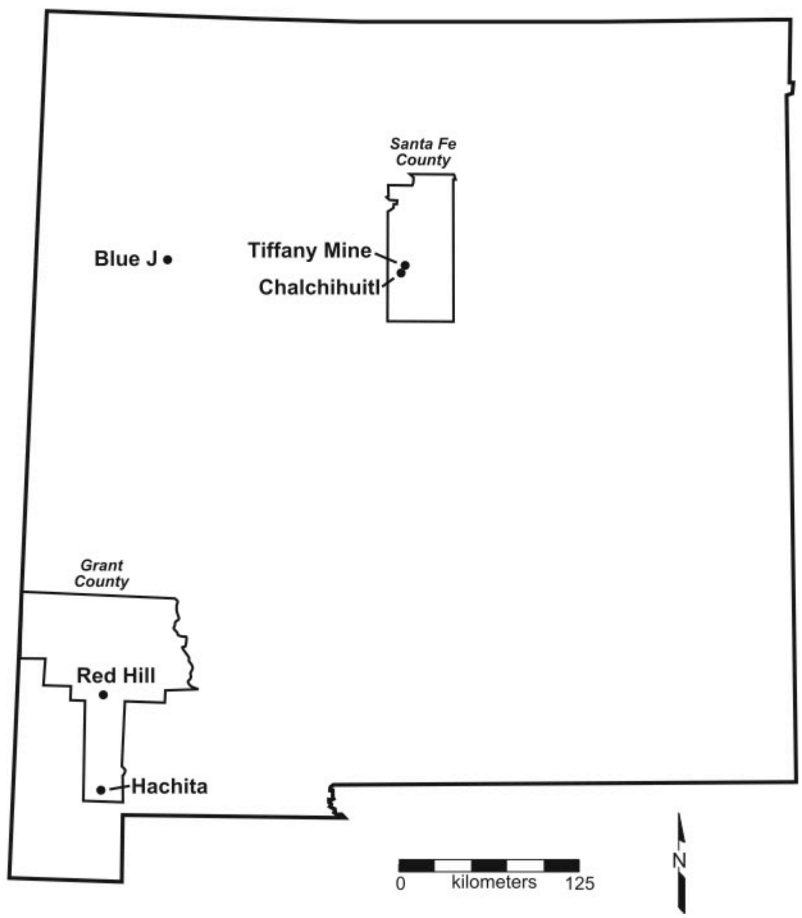

Figure 3.6 Locations sampled in New Mexico.

Red Hill Turquoise Mine

The Red Hill turquoise mine (not to be confused with the mining district and mine of the same name located in the Animas Mountains, NM) is located in the southern part of the Burro Mountains (742886E 3533713N). Referred to as the "Big Burro Mountains" in the southwest and the "Little Burro Mountains" in the northeast, they are a topographically high area that runs northwest from the town of White Signal (Fig. 3.7). The central area of the Big Burro Mountains contains porphyry style copper mineralization associated with the Tertiary age Tyrone stock.

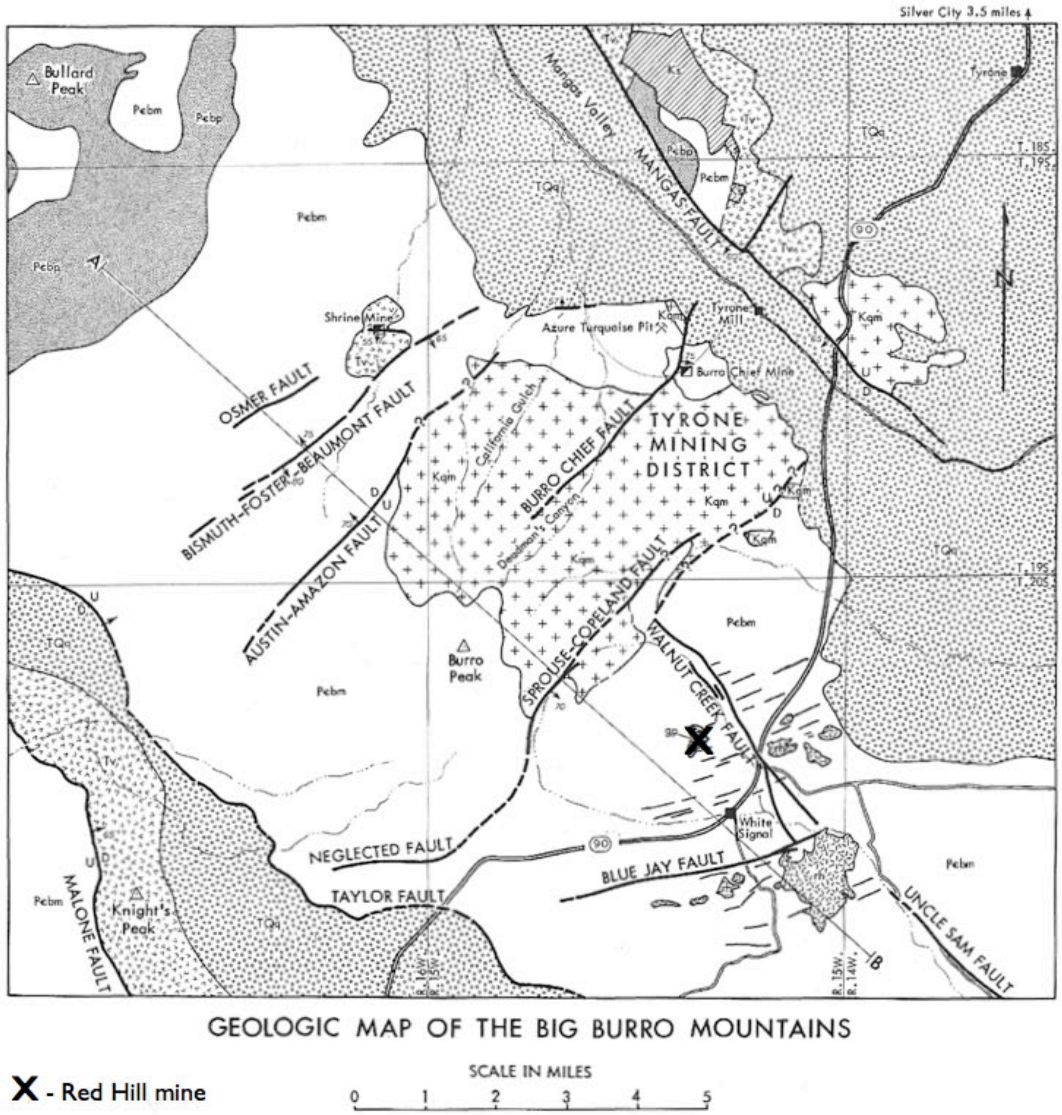

Figure 3.7 Location of the Red Hill turquoise mine, Burro Mtns., NM (Gillerman, 1970).

The Red Hill turquoise mine located about two miles southeast of the Tyrone mining district in the White Signal mining district. The country rock is described (Gillerman, 1964) as a reddish brown coarse-grained granite with large amounts of quartz, possibly the Precambrian

Burro Mountain granite (Fig. 3.7). The turquoise mines consist of three pits, one adit, one large open cut south of the adit and one small adit near the face of the cut.

Azure Turquoise Mine

The Azure turquoise mine is in the Little Hatchet Mountains in Grant County, New Mexico (740198E 3612763N). The Azure mine (not to be confused with a mine of the same name located in the Burro Mountains) is located between 5,000 and 5,400 feet in elevation in the Eureka Mining District (Fig. 3.8). It is west of the ghost town of Old Hachita where mines produced one and a half million dollars worth of lead and silver with lesser amounts of zinc and copper (Zeller, 1970). Throughout the Little Hatchet Mountains, the most mineralized areas are associated with stocks, dikes, and sills that have intruded sedimentary rocks.

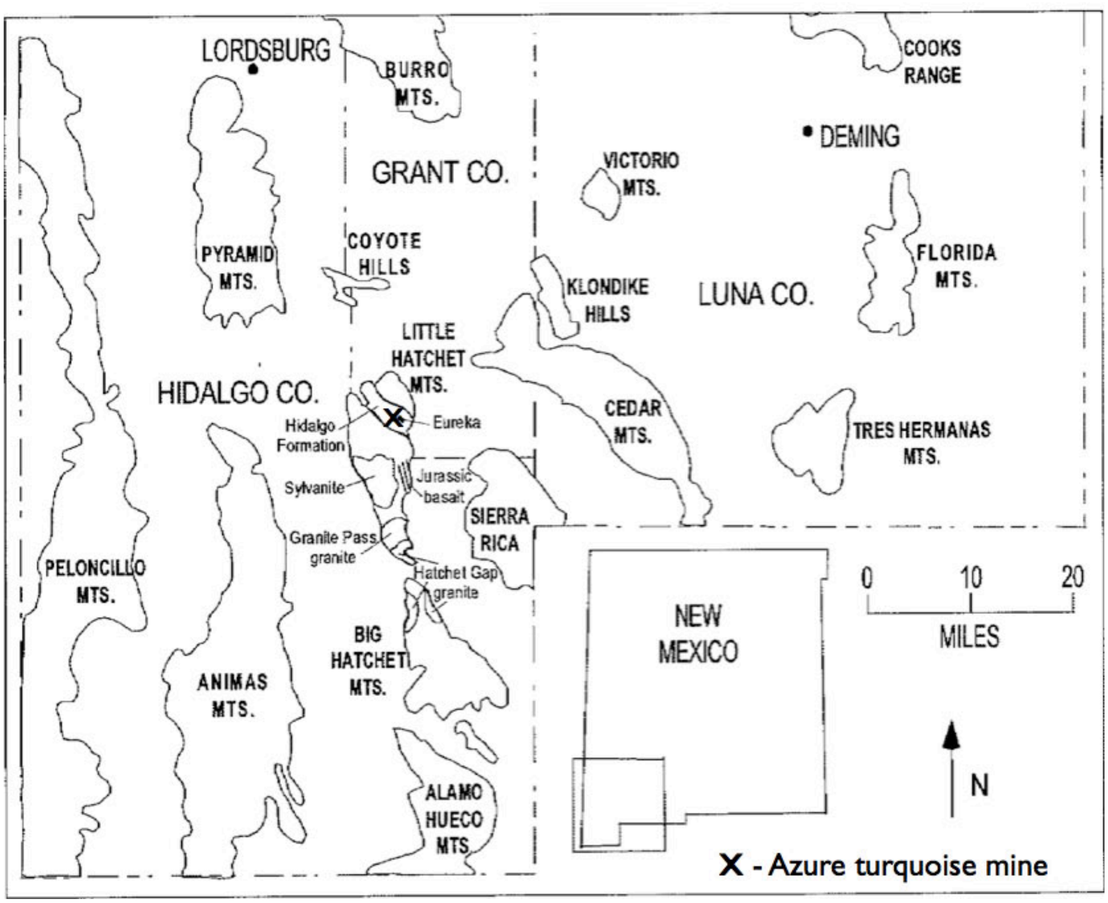

Figure 3.8 Location of Azure turquoise mine, Little Hatchet Mtns., NM (Channell, 2000).

The Azure mine is in the Hidalgo Formation that consists of a Late Cretaceous to early Tertiary series of laterally discontinuous and interbedded andesitic autobreccias, heterolithologic breccias, monolithologic breccias, lava flows, dikes and possibly ash flows along with reworked sedimentary and volcanic detritus (Young, 2000). The Hidalgo Formation is intruded by Eureka quartz monzonite and diorite stocks. Propylitic alteration of the Hidalgo formation occurred as hydrothermal alteration and weathering during and after deposition, during Laramide and Basin-and-Range tectonism, and intrusion of the Eureka stock (Young, 2000).

The turquoise occurrence at Hachita was initially reported "in seams in porphyry" (Sterrett, 1909). Turquoise was later identified near the contact of "a very fine-grained trachyte and a porphyry, probably monzonite", where it was mostly in the heavily iron oxide-stained trachyte (Sterrett, 1911). The turquoise deposit has also been described to occur along the edges of the monzonite stock in the altered rocks (Zeller, 1970). More recently, the Hachita turquoise deposits have been described as veinlets and fill fractures in altered trachyte, andesite and ash-flow tuff (McLemore, 2000). The samples collected for this research project came from the Azure No.2 mine described by Sterrett (1911). In 1909 the mine was observed to be a 40 ft. shaft "sunk in decomposed trachyte with andesite nearby on the east" (Sterrett, 1911). The deposit consisted of veinlets within the altered and fractured andesitic breccia, trachyte and possibly latite.

Santa Fe County Turquoise Mines

The Chalchihuitl and Tiffany turquoise mines are located about 25 miles southwest of the city of Santa Fe in Santa Fe County, New Mexico (Fig 3.6). They are in the Cerrillos Hills, a group of six low peaks that form the most northern portion of the San Pedro-Ortiz porphyry belt. Lead, silver, gold, zinc in north central New Mexico copper ores have been mined from the

Cerrillos Hills in addition to turquoise. (Smith, 1995). The turquoise mines are within the Cerrillos Mining district which covers an area of about 30 square miles.

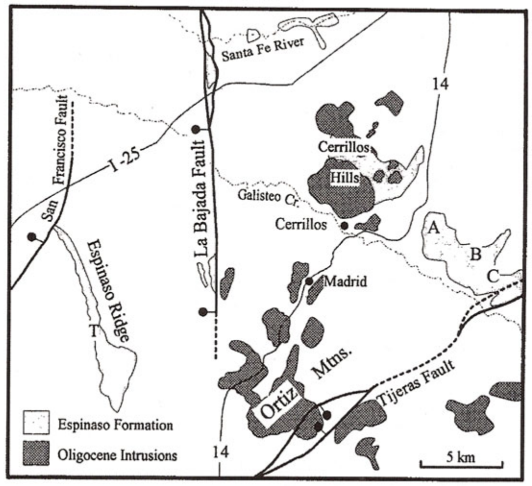

Figure 3.9 Intrusives and extrusives of the Cerrillos Hills (Erskine and Smith, 1993)

The Cerrillos Hills are a multiple intrusive complex of Oligocene laccoliths, dikes, sills and stocks that intrude upper Mesozoic and Eocene sedimentary strata (Giles, 1995). The igneous rocks are mostly monzonite ranging from syenite to diorite that intruded the volcaniclastic rocks of the Espinaso Formation (Fig. 3.9) which are extrusive equivalents of the plutonic rocks (Giles, 1995). There are two main intrusive centers, the Bonanza lobe in the north where Turquoise Hill is located and the San Marcos in the south that includes Chalchihuitl and the Cerrillos porphyry copper deposit (Fig. 3.10).

The intrusive laccolithic rocks are plagioclase-k-feldspar-hornblende-quartz porphyry, or quartz andesite, and date from 33.2 to 36.2 Ma while augite- and hornblende-monzonite stocks date from 27.9 to 31.4 Ma (Maynard, 2005). The Espinaso Formation consists of volcanic clasts, lava flows, and pyroclastic units ranging from basalt and basaltic andesite to trachyte with the majority being latites (Erskine and Smith, 1993). The lithologies of the volcanic rock are separated between calc-alkaline with hornblende or hornblende+clinopyroxene and alkaline

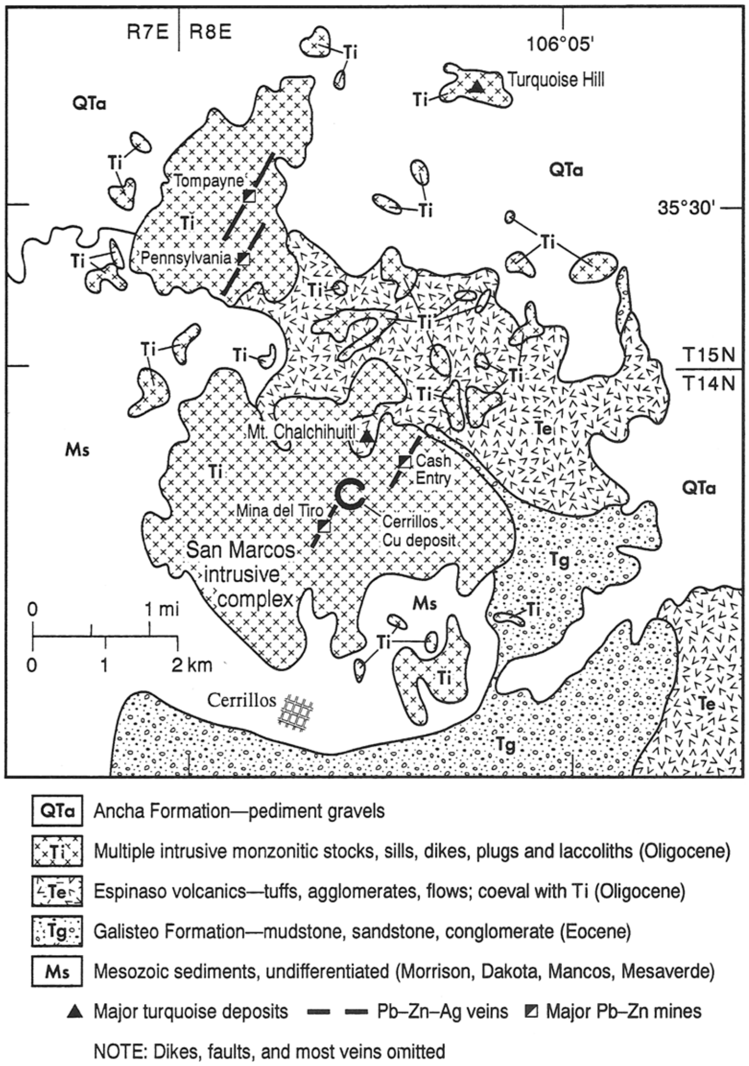

Figure 3.10 Major turquoise deposits of the Cerrillos Mining District (Giles, 1995).

containing clinopyroxene±biotite. The Cerrillos Hills only have the calc-alkaline version of the Espinaso volcanics (Erskine and Smith, 1993). The laccoliths are cut by the younger stocks and plugs as well as radiating dikes of a variety of quartz-poor compositions thought to have a center or vent in the northeastern area of the Cerrillos Hills (Maynard, 2005). The volcanic edifices that produced the Espinaso Formation have been eroded away and what remains are portions of mostly water-lain aprons (Maynard, 2005).

Tiffany Mine

The Tiffany Mine is located on Turquoise Hill (402172E 3928045N), one of a group of three small hills northeast of the central peaks of the Cerrillos Hills (Fig. 3.10). Turquoise Hill has four summits up to 6,462 ft. This isolated multiple intrusion laccolithic complex area is about 3500 x 2000 feet and consists of several quartz-poor augite monzonites that intruded Mancos Shale and Espinaso volcanics (Giles, 1995). The host rocks were domally upturned and metamorphosed near contacts (Giles, 1995). Copper-bearing hydrothermal solutions from the central monzonite stock or plug altered and mineralized surrounding igneous and sedimentary rocks creating a pyritic halo of mineralization concentrated along NE and NW-trending fracture zones especially at intersections (Giles, 1995).

Evidence of prehistoric mining at Tiffany is present in the marks made by stone tools that extend for about 25 feet down from the surface into the shaft which was further mined by the American Turquoise Company from around 1890 to 1905. Estimates quote the value of turquoise sold from this mine to be around $2 million but the value of finished stones sold on the New York retail market was probably much more (Smith, 1995). The Tiffany and The Old Castilian mines are the two largest turquoise mines on Turquoise Hill but several other smaller claims on and around the hill produced turquoise also. The turquoise occurs in nodules and veinlets in fractures. The fractured host rock of the turquoise deposits has undergone intense argillic alteration and the original equigranular monzonite is hardly recognizable.

Chalchithuitl Mine

The intrusive center including the Chalchihuitl turquoise mine (399062E 3925769N) and the copper porphyry is located about three miles south of Turquoise Hill (Fig. 3.10). The porphyry system contains .3% Cu and has the distinctive potassic-phyllic-argillic-propylitic alteration zones and high copper/potassic and high pyrite/propylitic zones expected for this type of system (Giles, 1995). Unique to this system are high chalcopyrite/pyrite ratios, high magnetite, significant gold, and no zones of lead and zinc (Giles, 1995). There is no chalcosite blanket and the goethitic oxide cap is 100-400 ft. thick while at Turquoise Hill the depth of the oxidized zone is unknown. Lead-zinc-silver vein deposits that postdate the porphyry occurred in shear zones and faults that follow the NNE fracture pattern throughout the district.

The turquoise of the Cerrillos District occurs in patches of "strongly argillized and weakly tourmalinized monzonite and Espinaso volcanics" and indicates a high initial hydrothermal pyrite content of up to 10% (Giles, 1995). The host rock at Chalchihuitl has been identified as hornblende quartz latite (Stearns, 1953). Maynard mapped the host rock of the turquoise deposit as part of the Espinaso volcanics, described as "light gray to lavender gray, clast-supported agglomerate (lahars?), volcaniclastic sandstone, and minor white volcanic tuff. Latite clasts are subrounded to subangular and range up to two meters (7 ft)" (Maynard et al., 2002). Turquoise occurs as veinlets and nodules and has a large range of color variability.

The Chalchihuitl mine is located on a low hill called Mount Chalchihuitl to the east of the Cerrillos Hills central peaks. The mine consists of one large main pit roughly 200 feet in diameter with two excavated adits still visible in the side walls, one about 135 ft deep and the other ~35 ft deep. The center of the pit contains a large waste dump with tailings up to 30 feet thick where the hill used to be in the center (Sterrett, 1911). There are also pits on the summit of the hill and along the southeast side. There is little to no turquoise currently visible in the wall rock but small amounts can still be observed in the tailings.

Chapter 4 Methodology

The research plan entailed selection of ten samples of prehistoric turquoise artifacts with no evidence of human modification. Artifacts were recovered during surface collection and excavation at a variety of subsurface depths within the Blue J community. They were interpreted to be raw material for ornament production or ritual use due to associated cultural material and because no turquoise deposits have been reported in the area. Ten artifacts were available for analysis, seven were from different habitation sites within the community and three came from the same habitation site 12. All artifact samples were prepared into grain mounts for electron microprobe analysis.

Mine samples were obtained from four locations in New Mexico. They all have reported evidence of prehistoric collection and propinquity to the archaeological site. One mine location is in the Little Hatchet Mountains, where over a hundred samples were collected in the field. A second set of samples donated by the Turquoise Museum in Albuquerque was from a mine in the Burro Mountains. Additional samples were collected from two separate mine locations in the Cerrillos Hills. The mine samples were analyzed using a combination of petrography, X-ray diffraction, and electron microprobe analysis according to the methods described below.

Sample numbering

The samples were numbered and recorded in an inventory prior to selection for analysis. The numbering system for the artifacts included the preface "BJ" plus the site number the artifact came from within the community. Therefore, because site 12 had three separate samples, they are numbered BJ12(1), BJ12(2) and BJ12(3). The samples from Hachita are prefaced by "TM" for their location plus their sequentially assigned inventory number. Red Hill samples are similarly numbered using the prefix: "RH", Chalchihuitl "CH" and Tiffany "TF".

Sample Collection

Turquoise artifact samples were selected from the ornament assemblage of a Puebloan II period archaeological site in McKinley County, Thoreau, New Mexico. The majority of these samples were collected personally or by members of the team under the author's supervision during fieldwork on the Blue J community project from 2000-2005. Archaeological morphological analysis of the ornament assemblage from the Blue J collection included blue green artifacts that were identified as azurite, malachite, or turquoise based on mineral physical properties observed in hand samples (Hotujec and Kantner, 2007). Azurite and malachite were identified based on the visible crystal habit of radiating fibers aggregated into botryoidal masses (Hurlbut and Sharp, 1998). When crystal habit was not apparent due to weathered surfaces, hydrochloric acid confirmed the presence of carbonates. Chrysocolla artifacts were identified based on a hardness of 2-4 and the characteristic of sticking to the tongue when touched. Artifacts were classified as turquoise according to hardness of 5-6 and a very fine-grained or cryptocrystalline habit (Hurlbut and Sharp, 1998).

Out of a total of 24 cultural turquoise artifacts found at Blue J, a sample set of ten artifacts classified as turquoise manufacture debris was chosen from separate habitation sites distributed geographically throughout the community area of 2.4 sq km. The dates of each sample provenience are based on mean ceramic dating, with calibrated C^{14} dates in parentheses. The depth of artifact deposition ranges between surface and 180 cm below surface. In addition to the notation of artifact dimensions and examination for evidence of human modification conducted during ornament analysis, the ten samples chosen were recorded in photomicrographs

Table 4.1 Sites and dates of turquoise artifacts (John Kantner, pers. comm., 2009).

Site number/Sample #	Occupation date
1	AD 934 to 1127 (AD 888 to 998; AD 1016 to 1179; AD 995 to 1159)
11	AD 991 to 1117 (AD 1115 to 1281)
12 (3 samples)	AD 988 to 1118 (AD 771 to 994)
21	AD 895 to 1116
43	AD 798 to 1057
46	AD 840 to 1095
47	AD 859 to 1112
49	AD 958 to 1119 (AD 607 to 670)

using a Canon S50 Powershot and both the Leica DM EP Polarizing microscope and Leica Zoom 2000 prior to analysis.

Two geologic turquoise occurrences in Grant County, New Mexico were chosen based on reasonable proximity to the archaeological site, the Red Hill mine and an outcrop in the Hachita Mining District (Fig. 4.1). Both locations were reported to have cultural evidence of prehistoric mining noted in the original geologic reports of the areas.

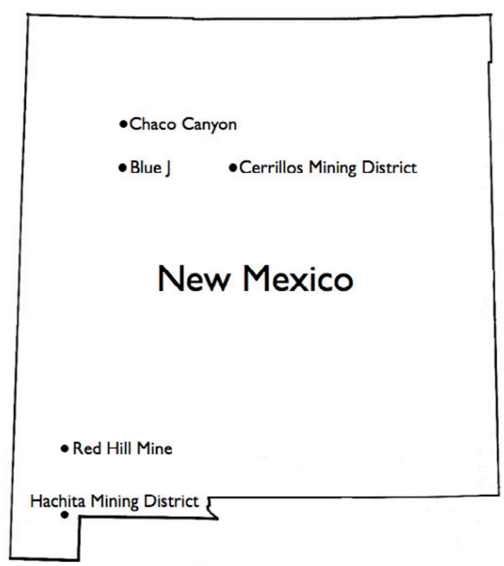

Figure 4.1 Locations of archaeological sites and prehistoric turquoise mines.

Sample collection was conducted at the Azure Mine in the Hachita Mining District, New Mexico. Over 100 samples of blue green material were randomly removed from the surface, tailings and directly from exposed veins. 12 samples were selected for thin section based on visual variability, size, and hardness appropriate for ornament production. Color variation was represented by choosing at least one of each color present from the material seen at the mine. Sample size was considered appropriate if it could provide the material for a small turquoise artifact. Pieces had to be large enough to reasonably produce a biconically drilled discoid bead or serve as a ceremonial offering. Variability of hardness was sought in order to analyze both softer, weathered-looking material and fresh material from veins. Ultimately, the limit of hardness was determined by sample preparation and if the material remained solid during the procedures described in the following section. All selection criteria were used to obtain sample sets representative of geologic occurrences in addition to the assumption that these properties may have also influenced prehistoric cultural material procurement.

The second source location was the Red Hill Mine, New Mexico. 21 pieces of Red Hill turquoise were obtained from the mine owner via the Turquoise Museum in Albuquerque, New Mexico. Six samples were selected out of the set of 21 available for thin section based on the same criteria as the Hachita source. Each Red Hill mine sample's visual variability in texture, color, and size was recorded in the sample inventory.

Cerrillos district samples were collected from the Chalchihuitl mine. Permission to collect samples from mine tailings was obtained via the property manager. The samples were collected from the main pit based on the same variability criteria as the other mines. The Tiffany Mine was visited on a separate occasion accompanied by the property owner. This mine is also no longer active, but permission to collect from the tailings was granted. Several pieces were sampled from the debris down slope from the main shaft. Samples from both Cerrillos mines were recorded in the inventory as well.

Sample Color

Samples chosen for analysis were examined for color variation. A standardized color reproduction system (Pantone Matching System, Formula Guide Solid Uncoated, Carlstadt, NJ, USA) was used to quantify the specific color(s) in each individual sample. This system was chosen in lieu of the Munsell Geological Rock Color Chart whose amount of blue and green hues were limited in comparison. The Pantone Matching System has 1,341 color options which include over 200 blue and green options. The uncoated chips were used to visually determine the best match for each dry turquoise hand sample in direct sunlight.

Sample Preparation

Mine samples selected were washed with deionized water and cut with a diamond saw to expose an appropriate surface for thin section. Samples were eliminated if material softness interfered with the saw's ability to cut an intact cross section of the sample. Twelve samples of Hachita turquoise and six samples of Red Hill turquoise chosen for analysis were sent to Vancouver Petrographics, Inc. for preparation of electron microprobe-quality polished thin sections. These thin sections were also used for petrographic analysis.

The artifact samples were washed with deionized water and lightly broken into smaller, 1-3 mm size pieces with a ceramic mortar and pestle. Appropriate portions were designated for grain mounts used in electron microprobe analysis. Grain mounts were prepared of samples less than .25 in. diameter by setting with epoxy in metal tubes. Epoxy was prepared with a 5:1 ratio that resulted in a mixture of 2.5 g of Buehler Epoxycure resin to .5 g of Epoxycure hardener which was stirred with a glass rod in an aluminum weighing dish for 2 minutes. The samples were covered with the epoxy mixture and left to dry for 24 hours. When dry, the exposed surface was cut and polished manually beginning with 280 microcut paper discs. Next, grain mounts were incrementally polished by decreasing from 5.0 to 1.0 to .3 micron aluminum oxide polishing powder on a Buehler Minimet 1000 grinder polisher. All samples, both grain mounts and thin sections, were carbon coated prior to EMPA analysis with the JEOL JEE-4x vacuum evaporator.

Five bulk powder mounts of Hachita samples were prepared for XRD analysis. The vein material was separated from the country rock for sample 109 and each was analyzed separately resulting in a sample set of six. TM109 was first crushed lightly with a ceramic mortar and pestle until matrix grains could be separated manually under 10x - 40x magnification. The other samples appeared to be homogenous turquoise with no visible matrix and were not separated in this manner. Once the sample material was chosen, it was gently crushed with the mortar and pestle and placed in a solution of sample powder and ethyl alcohol on a glass slide. The slurry was manually spread out with a glass extension from a pipette until it appeared to be evenly distributed across the slide surface and left to air dry. This minimized preferred orientation and provided the random orientation and infinite thickness required for Bragg's equation.

Petrography

Thin sections were examined with the Leica DM EP Polarizing microscope. Transmitted light was used to identify visually homogenous, fine-grained, areas believed to be turquoise. Optical microscopy of thin section samples provided information not available from the small samples prepared in grain mounts. Variations in color, texture, grain size, and inclusions were observed and recorded. Turquoise was distinguished from azurite or malachite by crystal habit and differentiated from heavily altered areas. Areas identified as unaltered turquoise were targeted for electron microprobe analysis.

X-ray Diffraction

XRD analysis was conducted at the University of Georgia Savannah River Ecology Laboratory. The scanning range was set from 2 to 60 degrees 2θ with a step scan rate of .04 degrees per minute. Cu radiation of wavelength 1.5418 was used. Data were processed with the Crystal Impact Match! Phase Identification from Powder Diffraction software. Background was not removed and the peaks were smoothed. Alpha 2 was subtracted and no 2-theta corrections were applied. Measured peaks were matched to the reference pattern database available in the Crystallography Open Database (COD) including The American Mineralogist Crystal Structure Database (AMCSD).

Electron Microprobe Analysis

Chemical analysis with the electron microprobe in the Geology Department of the University of Georgia determined the turquoise mineral composition. The JEOL JXA-8600 Superprobe was used to identify the ideal probe conditions for this particularly volatile material. 15 Kv, 10 Na current, and 0 - 5 μm beam width were the conditions determined to minimize sample damage. A routine was designed for the turquoise group minerals and initially analyzed the elements: Cu, Fe, Al, P, Zn, Ti, Mg, Mn, Ca, and Si. RH9 was designated the substandard and analyzed on a regular basis to monitor the reproducibility of these analytic methods. Over time there was little variation observed in sample RH9 (Table 4.2).

Energy dispersive spectra (EDS) were used for qualitative analysis of veins and country rock as well as zoned areas to determine general mineralogy and verify the presence of copper aluminum phosphates. Once turquoise group minerals were located, the most compositionally homogenous areas observed were targeted for wavelength dispersive spectra (WDS) quantitative analysis of the major elements. Target areas were probed at several points in several separate

separate areas per sample to capture variability at the sample level. All areas analyzed quantitatively were recorded with backscattered electron imaging (BSE) in composition mode.

Table 4.2 Turquoise substandard analyses results, means, and standard deviations.

Substandard Sample RH9

Weight Percent Oxides

	Date Analyzed																		
2009	**2/18**	**"**	**3/18**	**3/17**	**"**	**"**	**"**	**"**	**"**	**3/24**	**"**	**"**	**4/21**	**5/11**	**5/19**	**5/22**	**"**	**"**	**AVG**	**STDDEV**
CuO	5.97	6.32	7.79	6.74	7.67	7.58	7.83	7.1	7.32	5.74	6.3	7.04	6.41	7.89	6.35	7.23	7.79	8.46	**7.09**	**0.77**
MnO	0	0	0	0	0	0	0	0.05	0	0	0	0	0	0.05	0	0	0	0	**0.01**	**0.02**
ZnO	0	0	0	0	0	0	0	0	0	0	0	0	0	0	0	0	0	0	**0.00**	**0.00**
TiO2	0.51	0.57	0.47	0.55	0.49	0.44	0.39	0.54	0.42	0.5	0.59	0.43	0.4	0.55	0.42	0.51	0.56	0.56	**0.49**	**0.06**
MgO	0	0	0	0	0	0	0	0	0	0	0	0	0	0	0	0	0	0	**0.00**	**0.00**
CaO	0	0	0	0	0	0	0	0	0	0	0	0	0	0	0	0	0	0	**0.00**	**0.00**
K2O	0.13	0.09	0.1	0.12	0.12	0.11	0.13	0.11	0.11	0.11	0.12	0.07	0.07	0.16	0.11	0.17	0.12	0.15	**0.12**	**0.03**
Fe2O3	10.4	9.05	11.9	9.29	9.83	9.24	11.4	11.8	11.9	9.58	10.1	9.54	8.71	10.9	14.8	9.74	8.44	9.97	**10.36**	**1.53**
Al2O3	28	29.9	27.8	29.3	31.2	29.7	31.4	28.6	30.5	28.6	32.3	29.1	28.1	32.3	27.3	29.6	30.9	29.3	**29.65**	**1.52**
SiO2	0	0	0	0	0	0	0	0.12	0	0	0.12	0.11	0	0	0	0.09	0	0	**0.02**	**0.05**
P2O5	33.4	32	32	30.1	30.1	29.1	30.6	31.5	30.9	31.3	30.2	30.7	30.9	31.8	30.8	28.8	29.7	31.3	**30.84**	**1.12**
TOTAL	78.4	78.1	80	76.1	79.4	76.2	81.6	80.8	81.1	75.8	79.8	76.9	74.6	83.6	79.6	76.2	77.5	79.8	**78.64**	**2.40**

An area was defined as a location in the sample that had similar texture and a relatively uniform composition (± <.2 cations for elements involved: Cu, Fe, and Al). All areas analyzed within a sample were compared for overlapping cation ranges. If areas met the criteria (Table 4.3), they were included in the homogeneous turquoise material cation averages calculated for that sample. All analyses included in the sample averages were also in the cation averages for the entire location. This process was repeated for all analyses of mine locations and artifact samples.

Table 4.3 Criteria for inclusion of individual analyses in averages of turquoise material.

	Criteria for an area:
1.	Overlap in range.
2.	Range within .2 (if no overlap) for major elements in solid solution series (Cu, Fe, Al):
3.	Major elements must fall within range of turquoise mineral group:
	a) Cu between 0-9.78 wt.% (0-1.0 cations)
	b) Fe between 0-48.6 wt.% (0-6.0 cations)
	c) Al between 0-40.68wt.% (0-6.0 cations)
	d) P levels between 28.77-37.76 wt% (2.94-4.0 cations)
4.	Non-turquoise mineral components in common.
5.	Micro-texture is similar.
6.	Differences are not due to analysis on a different day with different probe conditions.

Data Processing

Once the output was collected, each analysis was individually examined for measurements below the minimum detection limits of that particular analysis (Fig. 4.4). When present, these measurements were removed from further calculations. Weight percent oxide analyses were stoichiometrically converted into atomic proportions of elements based on 28 oxygen atoms in the molecular formula for ideal turquoise. Iron was calculated as ferric. H_2O was calculated by difference of the total weight percent oxide from 100 for each analysis. Atomic proportions were used in statistical analyses and variability plots.

Table 4.4 Representative sample of typical minimum detection limits.

Oxide	**MDL**
P_2O_5	.09
SiO_2	.07
TiO_2	.09
Al_2O_3	.04
Fe_2O_3	.20
MgO	.04
CuO	.27
ZnO	.31
Ca	.04

Analyses focused on spatial areas within each sample for purposes of comparison between samples. Homogeneous turquoise was targeted, but areas of mineral intergrowth, weathered material, inclusions, etc. were analyzed when encountered. The data from analyses of areas that were not homogenous turquoise were considered separately in statistical calculations and variability plots. This provided a compositional analysis of the purest, most homogeneous turquoise areas available separate from additional mineralogical information obtained from each sample. Afterwards, the data from all areas analyzed were considered in conjunction to identify patterns useful for characterization.

Descriptive statistics for each major element measured were calculated and compared for all of the samples. A Pearson's correlation coefficient matrix for Cu, Fe+3, and Al was used to quantify the strength and direction of cation relationships among all the analyses. The matched pairs t-test was applied to the various cation levels between each sample and between each mine overall to determine significant differences.

Chapter 5 Results

Hachita

Hand Sample Description

The color of Hachita turquoise in hand sample is equivalent to Pantone 304U, 310U, 311U, 312U, 317U, and 3248U. There is no consistent association between color and texture, color and hardness, or color and color of host rock. Soft, presumably weathered portions of material range from light blue to dark blue (Fig. 5.1).

Figure 5.1 Weathered Hachita turquoise.

A fine-grained, white or tan, surface deposit <.5 mm coversparts of the weathered host rock and small portions of blue-green material. The tan surface deposit does not always occur in association with blue-green minerals and does not have any physical properties in common with turquoise minerals. The turquoise veins range in thickness from 0.5 mm - 5 mm, with the majority between 4 - 5 mm (Fig. 5.2). The veins are variable in thickness with some sections widening to 9 -10 mm. Nodular samples are up to 15 mm in diameter and may actually be thicker sections of vein.

Figure 5.2 Turquoise veins at Hachita.

Petrographic Description

The Hachita turquoise has a dense to fine-grained texture when viewed with a petrographic microscope. Individual crystals are typically too small to see, but sample TM127 has a larger grain size and spherulitic texture visible in thin section (Fig. 5.3). TM114 is also slightly spherulitic and has grain size intermediate between TM127 and the rest of the fine-grained Hachita samples. Samples TM68 and TM102 do not have pronounced spherules and instead consist of rounded areas of turquoise separated by microveinlets of a fine-grained light brown mineral, possibly iron-stained sericite. The term sericite refers to fine-grained sheet silicates, such as white mica, chlorite and clay minerals. The web-like microstructure is composed of small turquoise grains confined within rounded or elliptical sections. Variation within these webbed sections of turquoise occurs in sample TM102 (Fig. 5.4) where a mixture of densities and mineralogy is visible. Some sections contain mostly a light colored mineral, possibly quartz and/or sericite, and little to no turquoise.

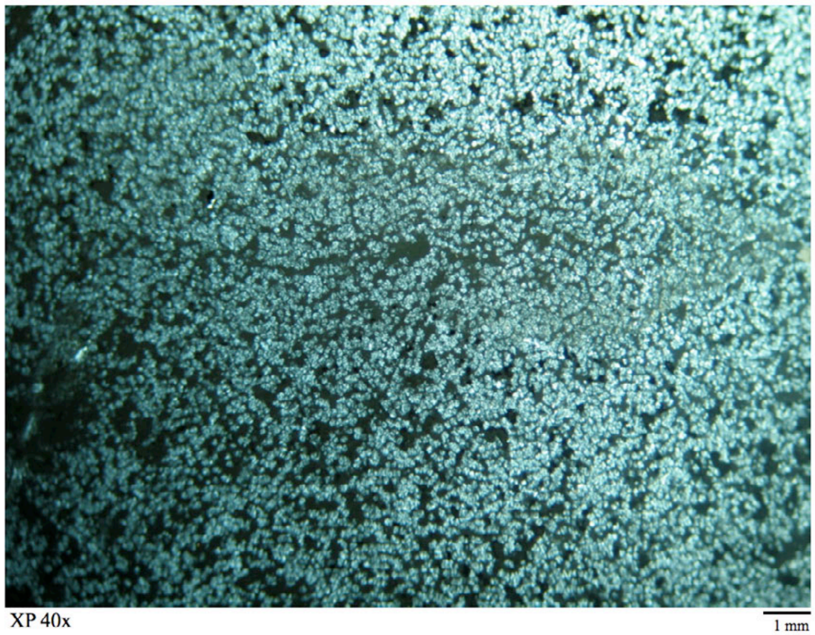

Figure 5.3 Spherulitic turquoise in sample TM127. XP (crossed polars)

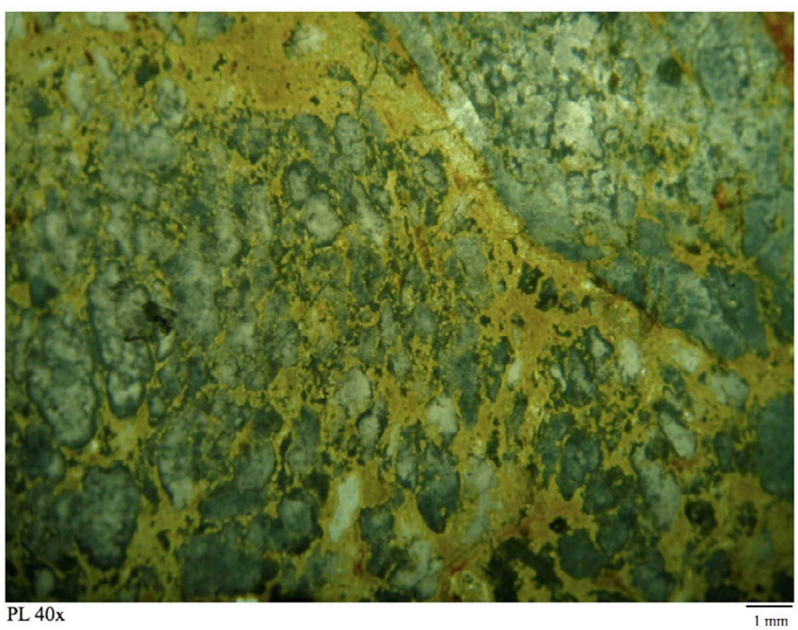

Figure 5.4 Sample TM102 vein-like network structure. PL (plane light)

Turquoise association with sericite in the form of fine-grained sheet silicates appears to be related to alteration of the local host rock. Zones of sericite are more pronounced along the edges of turquoise veins and in micro-fissures within the turquoise (Fig. 5.5). A fibrous texture is occasionally seen and appears to be the result of a fine-grained intergrowth with turquoise and phyllosilicates or sheet-silicates. Some Hachita samples also have silica or carbonate deposits along the outer margins of the turquoise veins separating turquoise from contact with the host rock (Fig. 5.6).

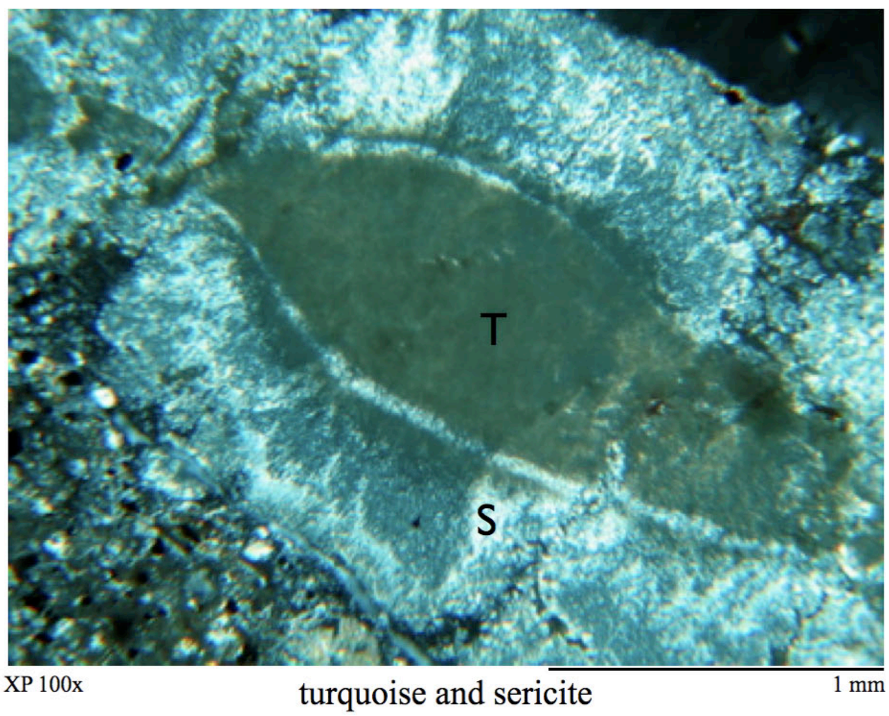

Figure 5.5 Hachita sample TM115. T=turquoise, S=sericite.

The Hachita turquoise commonly has inclusions of quartz, but opaque grains are also abundant. Samples TM118 has dark red inclusions that could be hematite or limonite-stained grains or sulphides. These inclusions are confined to the host in other samples where they are present, but in sample TM118 they are directly adjacent to the turquoise and partially enclosed within it (Fig. 5.6). Almost all samples from Hachita also have reddish brown and/or brown iron oxides within the turquoise material.

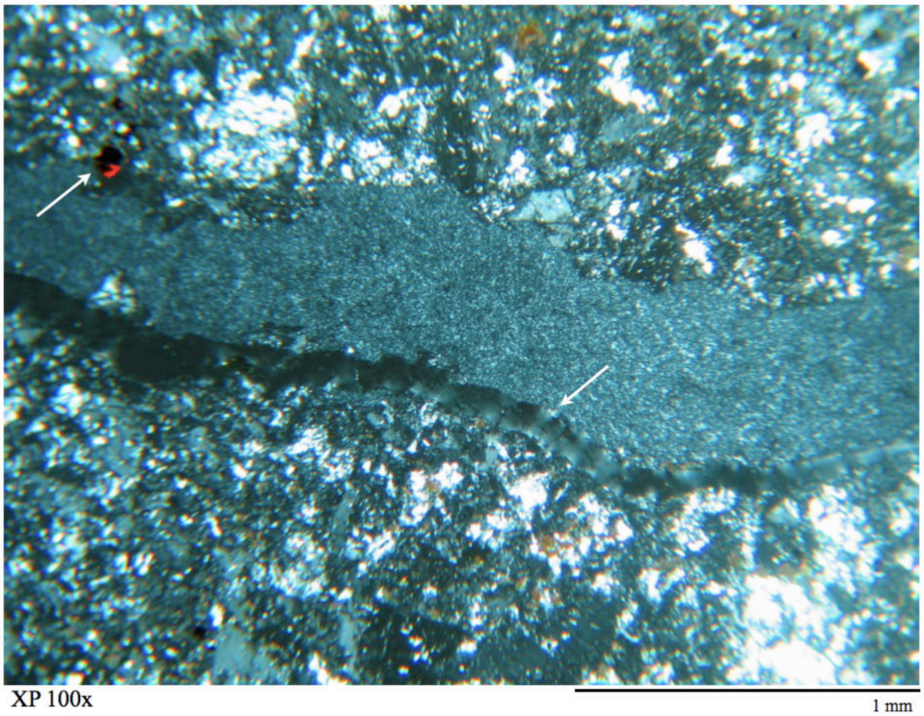

Figure 5.6 TM118 silica border (lower arrow) along turquoise vein and red inclusion (upper arrow).

The host rock of the Hachita turquoise samples appears to be a porphyritic dacite or rhyolite (Fig. 5.7). The groundmass is composed of clay and carbonate minerals. Samples TM127 and TM109 have brown iron oxides in the host rock (Fig. 5.8).Phenocrysts are predominantly fractured and consist of altered feldspars with quartz, altered biotite/chlorite (5.9a), opaque grains and white mica. Dark brown phenocrysts with 90° cleavage appear to be augite. Remnants of alkali feldspar phenocrysts occasionally exhibit simple twinning (Fig. 5.9b).

Microprobe analysis

Microprobe analysis of the Hachita samples identified the areas of copper aluminum phosphate in each sample. Three to four separate areas of copper aluminum phosphate were

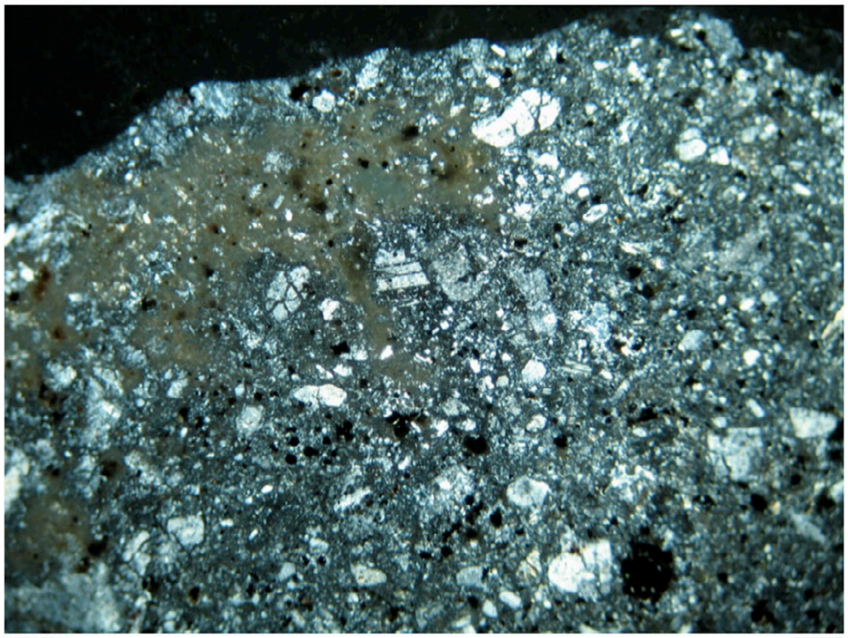

XP 40x 1 mm

Figure 5.7 Sample TM115 fractured and altered phenocrysts of the host rock. 40x XP

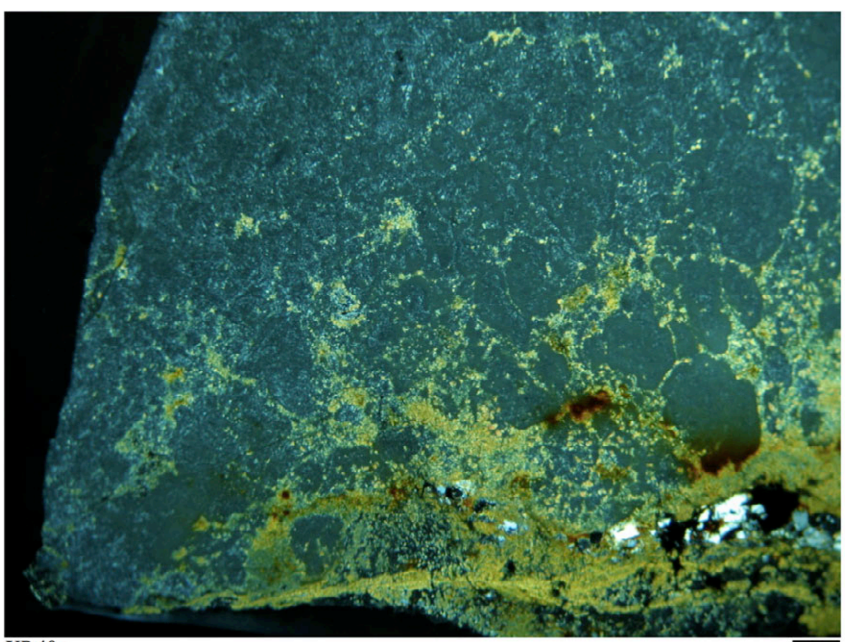

XP 40x 1 mm

Figure 5.8 Sample TM102 iron stains near host rock.

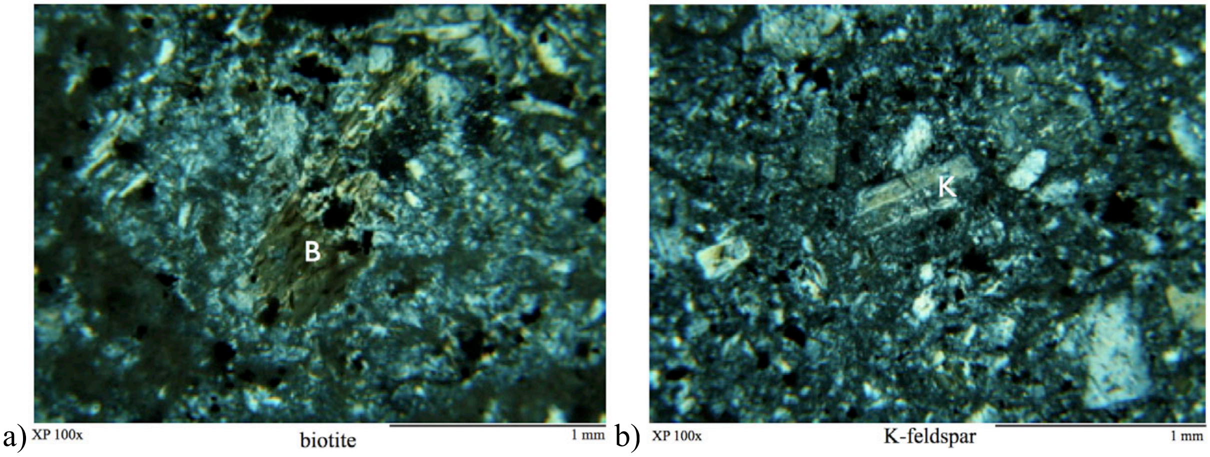

Figure 5.9 Phenocrysts in Hachita host rock a) biotite b) K-feldspar.

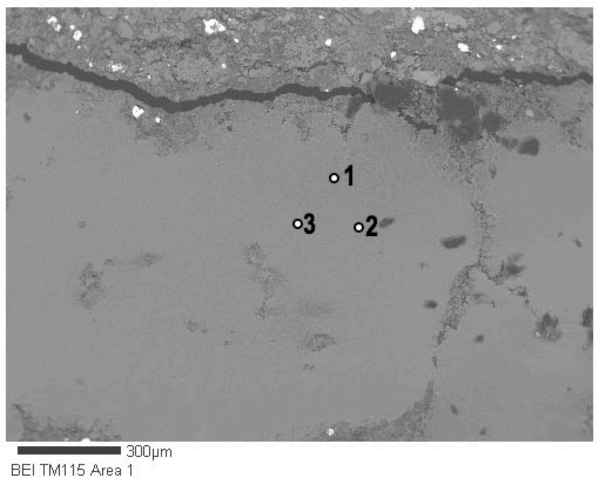

Figure 5.10 Analysis points targeted areas void of host rock, inclusions and alteration.

analyzed three times each totaling at least 9-12 separate analyses per sample. The result was a total of 120 individual analyses for this particular geologic occurrence (Table 5.1). The Hachita samples were heterogeneous. Isolated grains of host rock, zones of sericite, and inclusions such as quartz or opaque grains were avoided (Fig. 5.10). The remaining copper aluminum phosphate material analyzed formed two compositional groups differing in both iron and aluminum content. There is a high-Fe group with low Al and a low-Fe group with higher Al indicative of substitution. The majority of turquoise material analyzed had Fe_2O_3 between 1-3 wt.%. The high-

Fe areas were in one sample with Fe_2O_3 of 14-17 wt.% throughout and another sample with inclusions of concentrated Fe_2O_3 at 15-25% wt.% in the turquoise. Higher amounts of Fe_2O_3 in sample TM114 are identified only in composition while inclusions are evident in the texture of sample TM127.The high-iron inclusions are lighter in color and brighter in backscattered electron images due to higher density than the surrounding material.

The two high-iron area analyses of samples TM114 and TM127 Area 2 plot along the chalcosiderite-turquoise series where Fe^{+3} substitutes for Al (Fig. 5.11). The remaining Hachita analyses form a tight cluster close to the turquoise endmember and extend slightly downward towards aheylite-turquoise. This sample set demonstrates a transition from chalcosiderite to turquoise that involves alteration. The high-iron analyses are not included in the average of homogeneous turquoise minerals for this location and are considered separately.

Sample TM127 was a vein-shaped hand sample with no visible weathering and was harder than many Hachita samples. Sample TM127 had three analyses with no copper or phosphorous and high silica and aluminum values. These analyses (3-1, 3-2, and 3-3, Fig. 5.13) were determined to be clay minerals that surrounded spherules of copper aluminum phosphate. The bright centers of the spherules contained high levels of Fe (TM127 Area 2, Table 5.1). The remaining majority of the spherule material was darker grey in backscattered electron images (1-1, 1-2, 1-3, 1-4, & 1-5, Fig. 5.13). It had lower Fe and higher Al than the bright center (Table 5.2) and plots close to the turquoise endmember (Figure 5.11). The spherules contain silica although not nearly as much as the clay matrix between them. The high iron areas have lower Si, Ca, and K than the surrounding spherule material and may represent an earlier, unaltered chalcosiderite phase of turquoise.

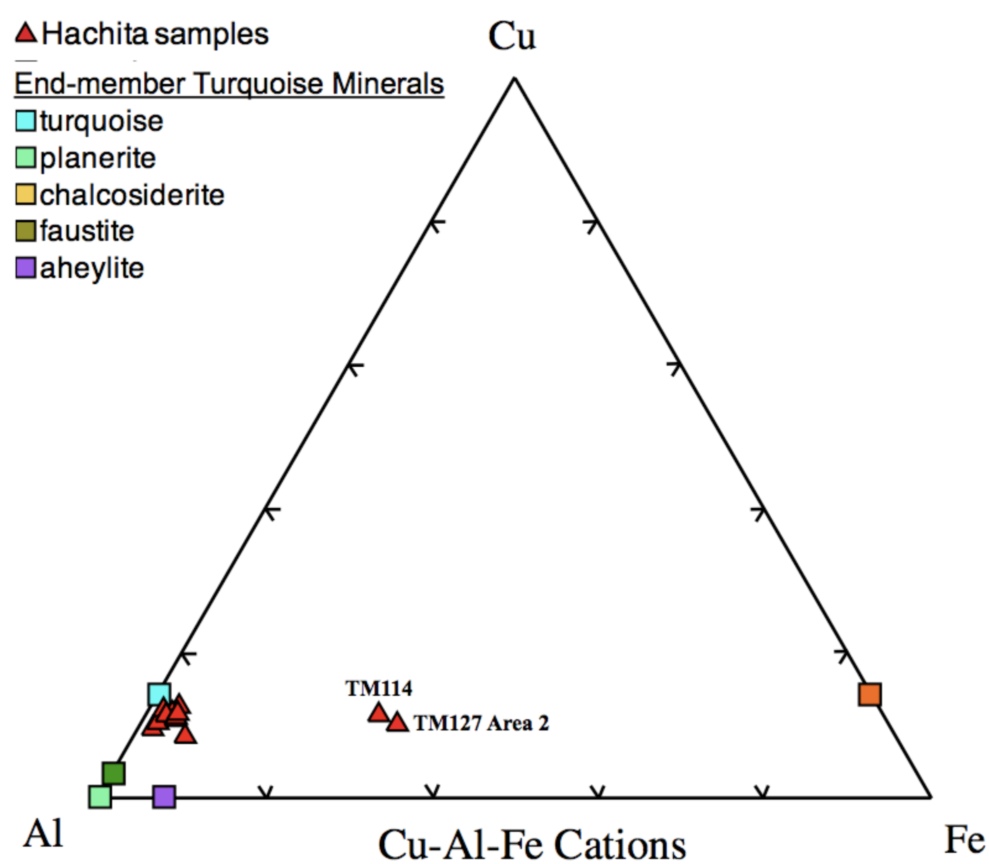

Figure 5.11 Hachita sample averages plotted with turquoise minerals.

Sample TM114 in hand sample was botryoidal and the color faded towards the sample edges. In both thin section and backscattered electron images TM114 has a spherulitic pattern albeit less defined than that in TM127 (Fig. 5.12a &b). In BEI aggregates are surrounded by darker and less dense material (Fig. 5.12a). In thin section, the rounded aggregates are separated by light colored, fine grained minerals, possibly a sericite intergrowth. TM127 and TM114 possibly suggest an association between elevated iron content and spherulitic micro-texture based on the Hachita sample set alone.

The two Hachita samples with spherules draw attention to the possibility that type or degree of weathering may potentially be indicated by the presence of a spherulitic texture. For example, lack of high iron concentrations at spherule centers and only remnant spherulitic texture in sample TM114 may suggest that alteration occurred throughout the sample due to dissemination of Fe^{+3}. This more extensive alteration might be the result of more intense weathering conditions or longer periods of exposure to an oxidative environment.

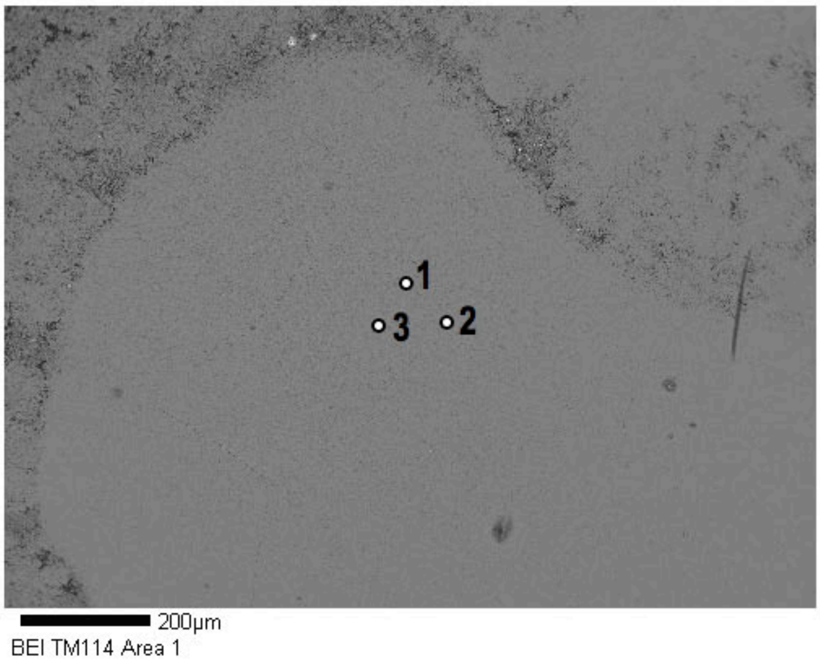

a)

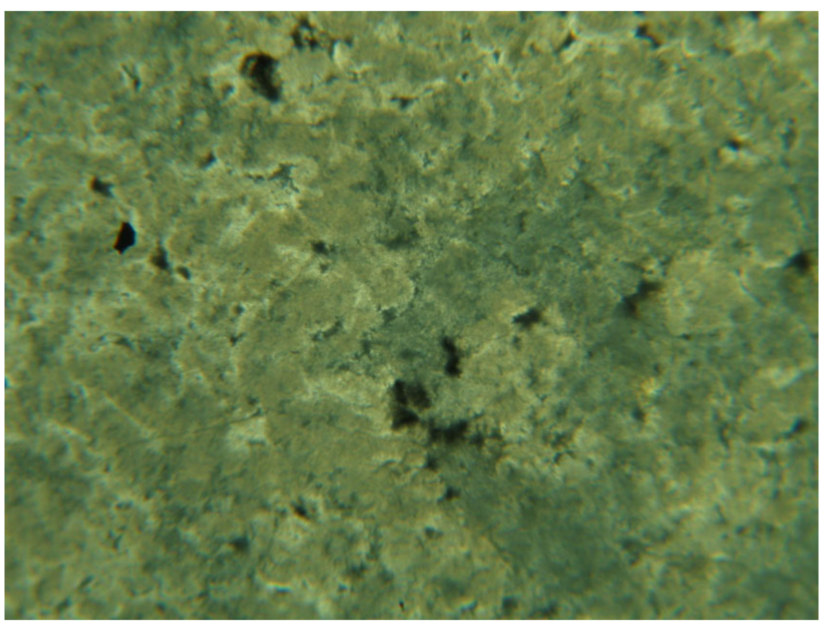

b)

Figure 5.12 TM114 spherules in a) back scattered electron image b) thin section 100x PL.

Table 5.1 Major cation range, average, and standard deviation for each Hachita sample.

TM57

n=12	MIN	MAX	AVG	STD
Cu	0.47	0.60	0.53	0.04
Fe	0.06	0.09	0.08	0.01
Al	4.34	5.59	4.85	0.40

TM102

n=9	MIN	MAX	AVG	STD
Cu	0.53	0.87	0.73	0.10
Fe	0.16	0.19	0.17	0.01
Al	4.89	5.66	5.24	0.31

TM66

n=13	MIN	MAX	AVG	STD
Cu	0.66	1.01	0.77	0.10
Fe	0.09	0.19	0.14	0.03
Al	5.43	6.25	5.76	0.25

TM109

n=12	MIN	MAX	AVG	STD
Cu	0.59	0.82	0.75	0.06
Fe	0.10	0.18	0.14	0.02
Al	4.91	6.12	5.56	0.46

TM68

n=11	MIN	MAX	AVG	STD
Cu	0.51	0.79	0.70	0.08
Fe	0.07	0.14	0.11	0.02
Al	5.33	6.41	5.81	0.38

TM115

n=9	MIN	MAX	AVG	STD
Cu	0.61	0.80	0.68	0.05
Fe	0.18	0.25	0.21	0.02
Al	4.60	5.79	5.12	0.41

TM70

n=9	MIN	MAX	AVG	STD
Cu	0.62	0.90	0.74	0.09
Fe	0.01	0.25	0.18	0.07
Al	4.50	5.20	4.85	0.27

TM118

n=10	MIN	MAX	AVG	STD
Cu	0.68	0.92	0.76	0.07
Fe	0.18	0.24	0.22	0.02
Al	4.81	6.24	5.43	0.48

TM91

n=9	MIN	MAX	AVG	STD
Cu	0.72	0.95	0.83	0.08
Fe	0.07	0.14	0.10	0.03
Al	5.09	6.21	5.79	0.32

TM127

n=5	MIN	MAX	AVG	STD
Cu	0.51	0.62	0.54	0.04
Fe	0.33	0.40	0.37	0.03
Al	5.03	5.65	5.33	0.28

TM95

n=12	MIN	MAX	AVG	STD
Cu	0.64	0.80	0.70	0.05
Fe	0.17	0.29	0.23	0.03
Al	5.06	5.85	5.44	0.30

Hachita homogeneous material

n=120	MIN	MAX	AVG	STD
Cu	0.47	1.01	0.71	0.11
Fe	0.01	0.40	0.17	0.07
Al	4.34	6.41	5.40	0.48

Analyses Excluded from Homogeneous Average

TM114

n=9	MIN	MAX	AVG	STD
Cu	0.64	0.78	0.70	0.05
Fe	1.56	1.82	1.67	0.09
Al	3.23	4.04	3.64	0.28

TM127 Area 2

n=4	MIN	MAX	AVG	STD
Cu	0.58	0.70	0.66	0.05
Fe	1.56	2.73	1.96	0.53
Al	2.92	4.31	3.77	0.60

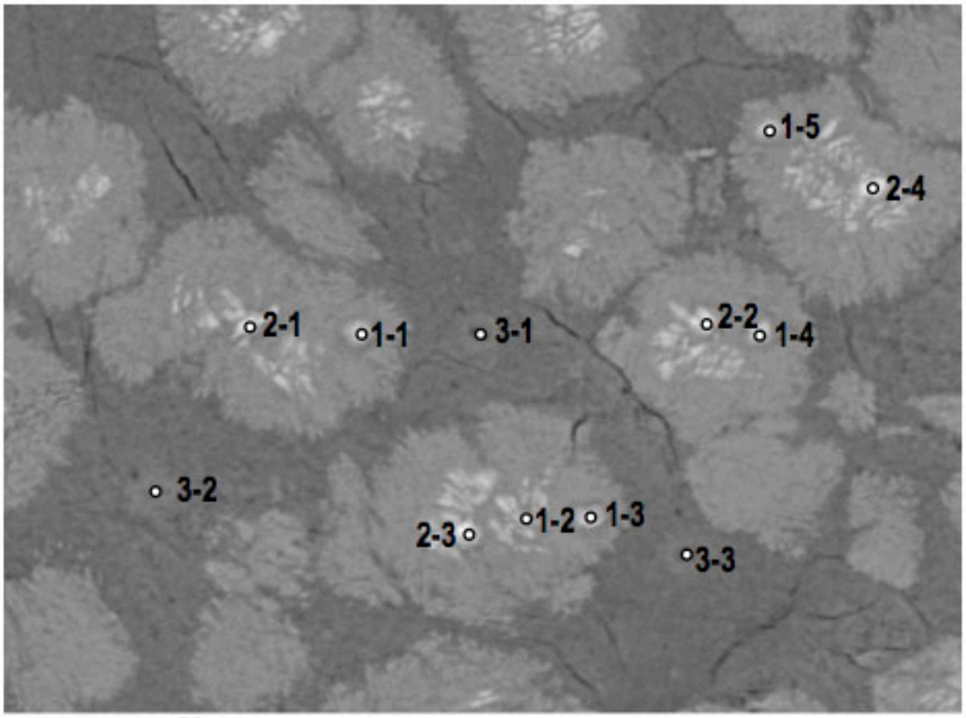

Figure 5.13 TM127 spherules with iron-rich centers surrounded by aluminum silicates.

Table 5.2 Individual analyses for sample TM127

	TM127 1-1	TM127 1-2	TM127 1-3	TM127 1-4	TM127 1-5	TM127 2-1	TM127 2-2	TM127 2-3	TM127 2-4	TM127 3-1	TM127 3-2	TM127 3-3
CuO	5.54	5.16	5.43	6.15	5.19	5.66	6.35	6.61	6.5	0	0	0
MnO	0	0	0	0	0	0	0	0	0	0	0	0
ZnO	0.05	0	0	0	0	0	0	0	0	0	0	0
TiO2	0	0	0	0	0.13	0	0	0.13	0.13	0	0	0
MgO	0	0	0	0	0	0	0	0	0	0.11	0	0
CaO	0.25	0.2	0.23	0.2	0.18	0.12	0.11	0.17	0.09	0.11	0.16	0.14
K2O	0.08	0.08	0.13	0	0	0	0	0	0	0	0	0.09
Fe2O3	3.79	3.95	3.44	3.93	3.64	15.19	16.41	17.36	25.41	1.4	1.32	0.92
Al2O3	33.03	35.68	33.16	35.12	35.29	24.74	26.31	23.7	17.33	33.03	34.52	34.45
SiO2	7.57	15.66	5.84	6.29	10.14	5.23	2.67	3	2.18	40.69	43.59	40.86
P2O5	26.01	21.07	27.82	28.38	23.84	27.63	28.35	27.75	28.14	0	0.17	0.25
Total	76.32	81.8	76.05	80.07	78.4	78.58	80.2	78.73	79.78	75.34	79.76	76.71
H2O (by diff.)	23.68	18.2	23.95	19.93	21.6	21.42	19.8	21.27	20.22	24.66	20.24	23.29
TOTAL (w/H2O)	100	100	100	100	100	100	100	100	100	100	100	100
Based on 28O												
Cu	0.54	0.52	0.53	0.62	0.51	0.58	0.67	0.69	0.7	0	0	0
Fe	0.37	0.4	0.33	0.39	0.36	1.56	1.72	1.81	2.73	0.13	0.13	0.09
Al	5.04	5.65	5.03	5.5	5.45	3.97	4.31	3.86	2.92	4.87	5.23	5.12
Mn	0	0	0	0	0	0	0	0	0	0	0	0
Zn	0	0	0	0	0	0	0	0	0	0	0	0
Ti	0	0	0	0	0.01	0	0	0.01	0.01	0	0	0
Mg	0	0	0	0	0	0	0	0	0	0.02	0	0
Ca	0.03	0.03	0.03	0.03	0.02	0.02	0.02	0.03	0.01	0.01	0.02	0.02
K	0.01	0.01	0.02	0	0	0	0	0	0	0	0	0.01
Si	0.98	2.1	0.75	0.84	1.33	0.71	0.37	0.41	0.31	5.09	5.6	5.15
P	2.85	2.4	3.03	3.2	2.65	3.18	3.34	3.25	3.4	0	0.02	0.03
TOTAL	9.82	11.11	9.72	10.58	10.33	10.02	10.43	10.06	10.08	10.12	11	10.42

X-ray Diffraction Analysis

Six samples from the Hachita mining district were analyzed with X-ray diffraction from random powder mounts. The experimental patterns exhibited numerous small peaks (Fig. 5.14) due to small grain size of turquoise observed in thin section and the presence of clay minerals. The background was not removed in order to retain information related to these smaller peaks. Random powder mounts prevented crystal orientation and differences in experimental and reference pattern intensity were observed. The turquoise reference pattern is a good match for all of the experimental patterns. Several patterns imply a possible mixture of the turquoise group minerals turquoise, faustite, or chalcosiderite in combination with the other minerals identified.

Hachita sample TM95 has a large number of peaks that match turquoise minerals. The reference patterns of turquoise, faustite, and chalcosiderite have 500 peaks each and matched the experimental pattern for 255, 253, and 275 peaks respectively. Similar numbers of matched peaks for these minerals were seen in all the other samples where they were present also. These three patterns are very similar in 2θ and d-spacing which may be the cause for the broad peaks observed in experimental patterns. This widening potentially due to a combination of turquoise minerals is expressed by shoulders visible on both sides of the turquoise peaks. In addition to turquoise minerals, several clay minerals also match closely to sample TM95's pattern: illite, vermiculite, and chlorite. Muscovite 2M1 and quartz were also present.

Fine-grained, light brown, hard host rock in sample TM109 was removed from blue green veins under low magnification and the two portions were analyzed separately, called TM109A and TM109B. The X-ray patterns for TM109A and the separated turquoise portion (TM109B) differed greatly. Sample TM109A provides useful information about the mineralogy of Hachita's turquoise host rock. The reference patterns most closely matched to the experimental pattern were quartz, microcline, vermiculite, bementite, biotite, kaolinite, muscovite 2M1, metaswitzerite, and albite in order of decreasing similarity. The patterns for kaolinite and bementite are somewhat similar and could have a little overlap. Since bementite is associated with zinc deposits and metamorphic rocks, misidentification is likely and kaolinite should be considered the better match. The closeness of the pattern to the experimental peaks was very high however, so it was not removed from the list. Zinc was indeed historically mined from the Hachita complex. Bementite also appears to be present in sample TM127.

Sample TM109B, the blue green vein material, was matched to turquoise minerals turquoise, faustite, and chalcosiderite. Clay minerals present include illite and vermiculite while biotite and chlorite patterns matched closely as well. It seems likely that there are mixed layer clays in this sample.

Sample TM114 matched three turquoise minerals: faustite, turquoise, and chalcosiderite in decreasing order starting with the best match. Quartz, vermiculite and muscovite 2M1 were also found in this sample. The presence of another hydrated phosphate, benyacarite, was surprising but considered because benyacarite has a similar chemical formula and different crystal structure (orthorhombic-dipyramidal) from turquoise, allowing detection in X-ray diffraction and not chemical analyses. Although often found in association with other phosphates, benyacarite occurs in phosphate-bearing pegmatites, not copper porphyry systems, so it's presence in sample TM114 is deemed unlikely.

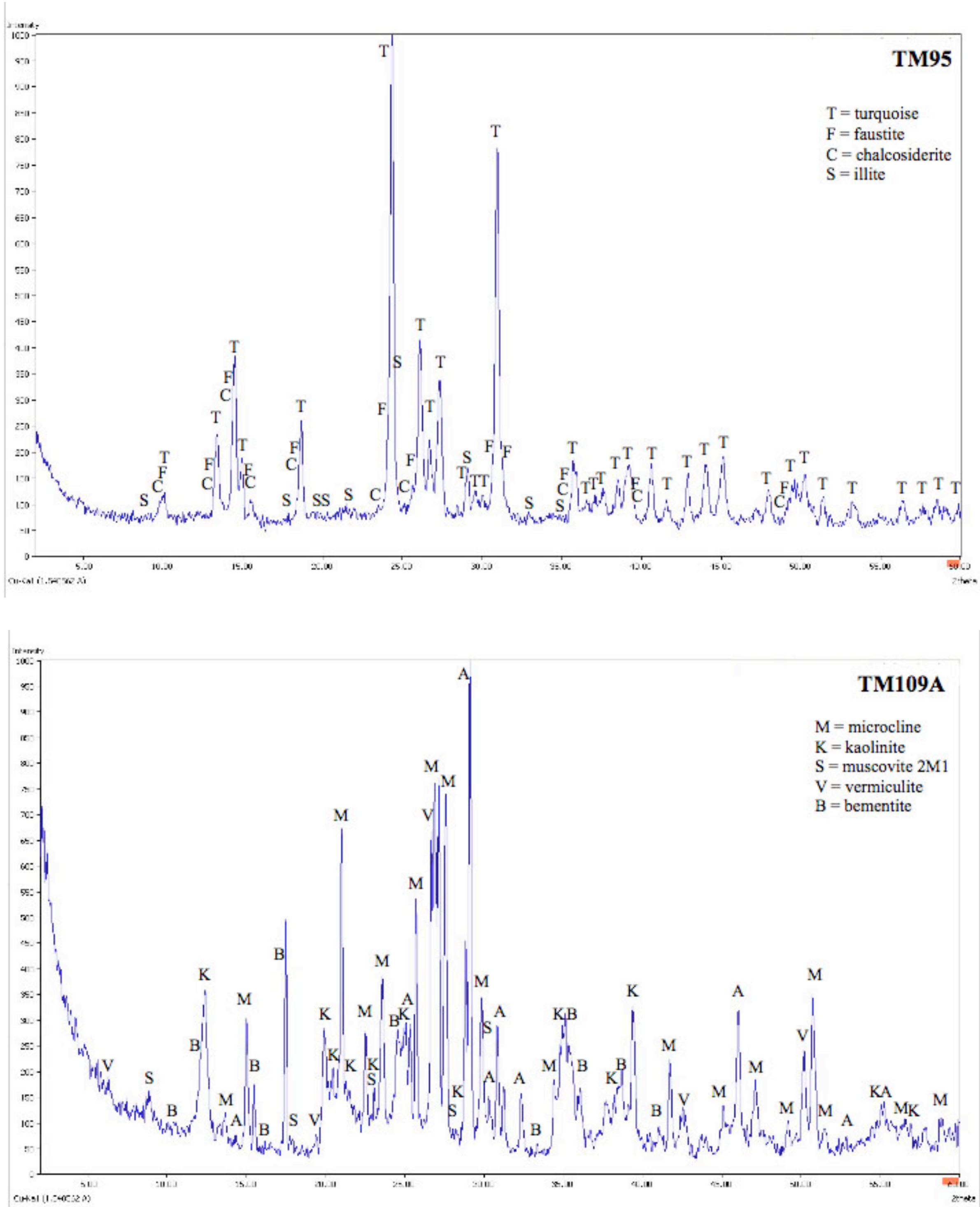

Figure 5.14 Experimental X-ray diffraction patterns of samples a) TM95 b) TM109A.

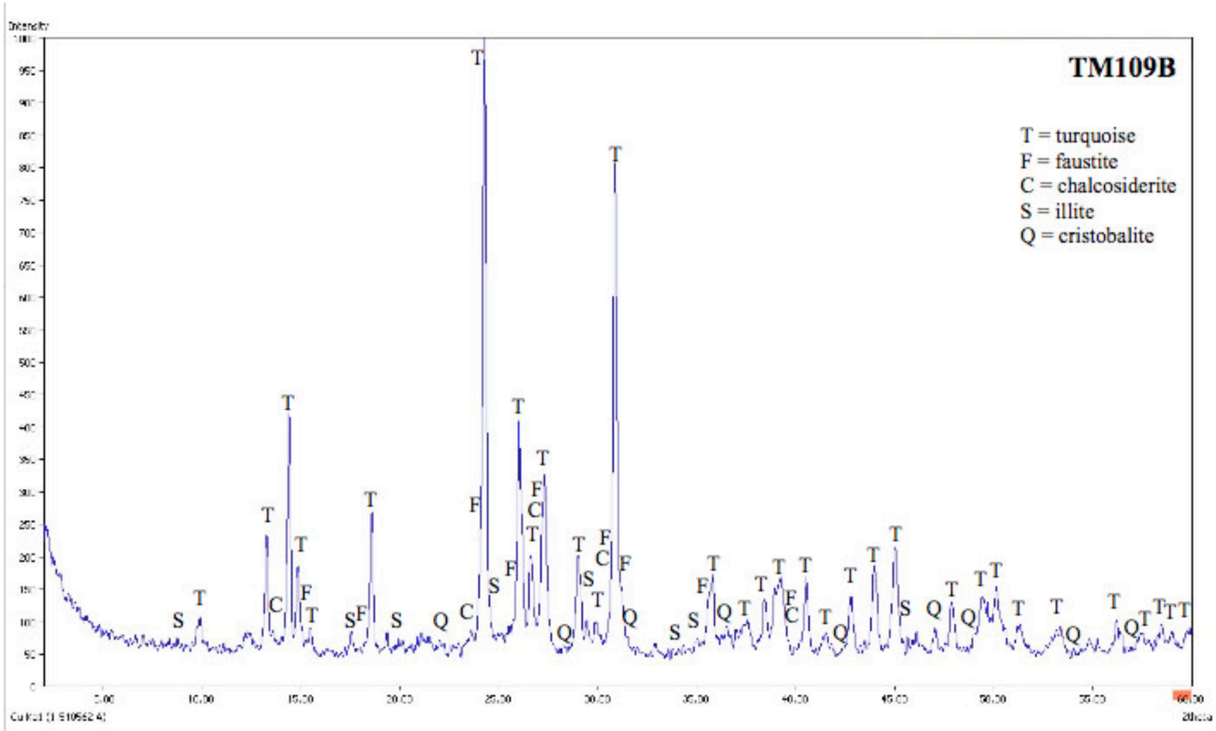

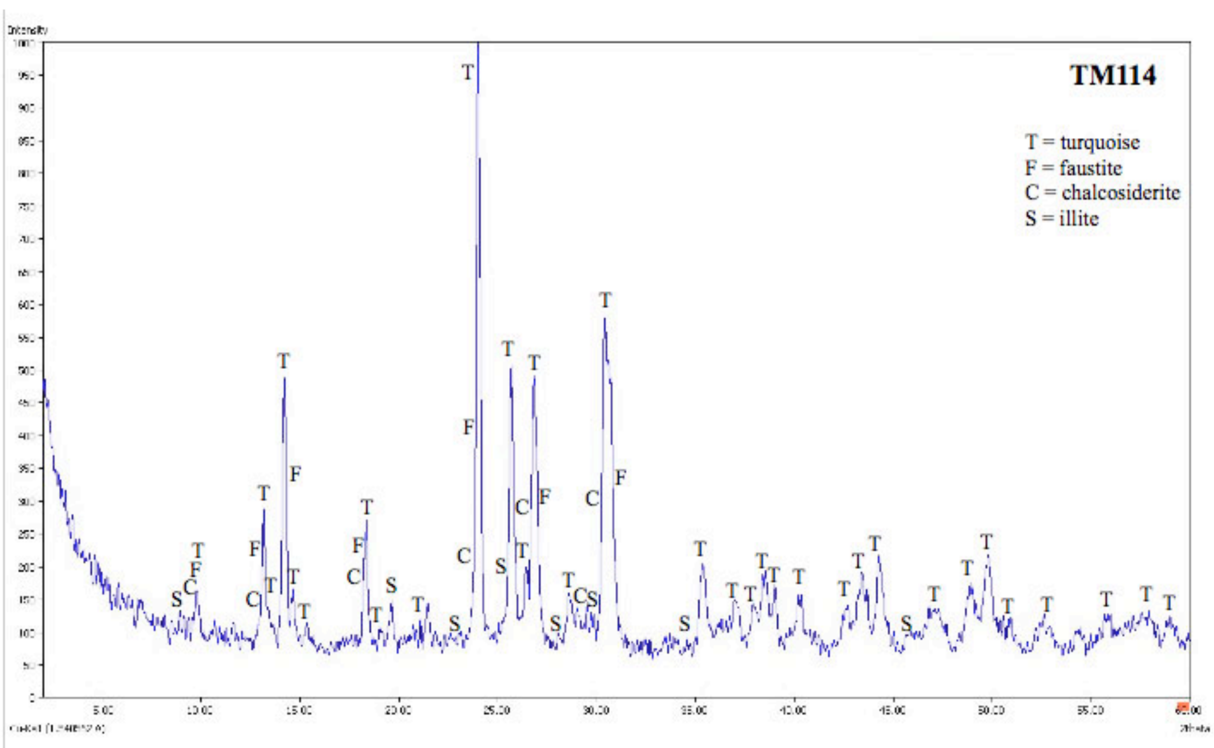

Figure 5.14 Experimental X-ray diffraction patterns of samples c) TM109B d) TM114.

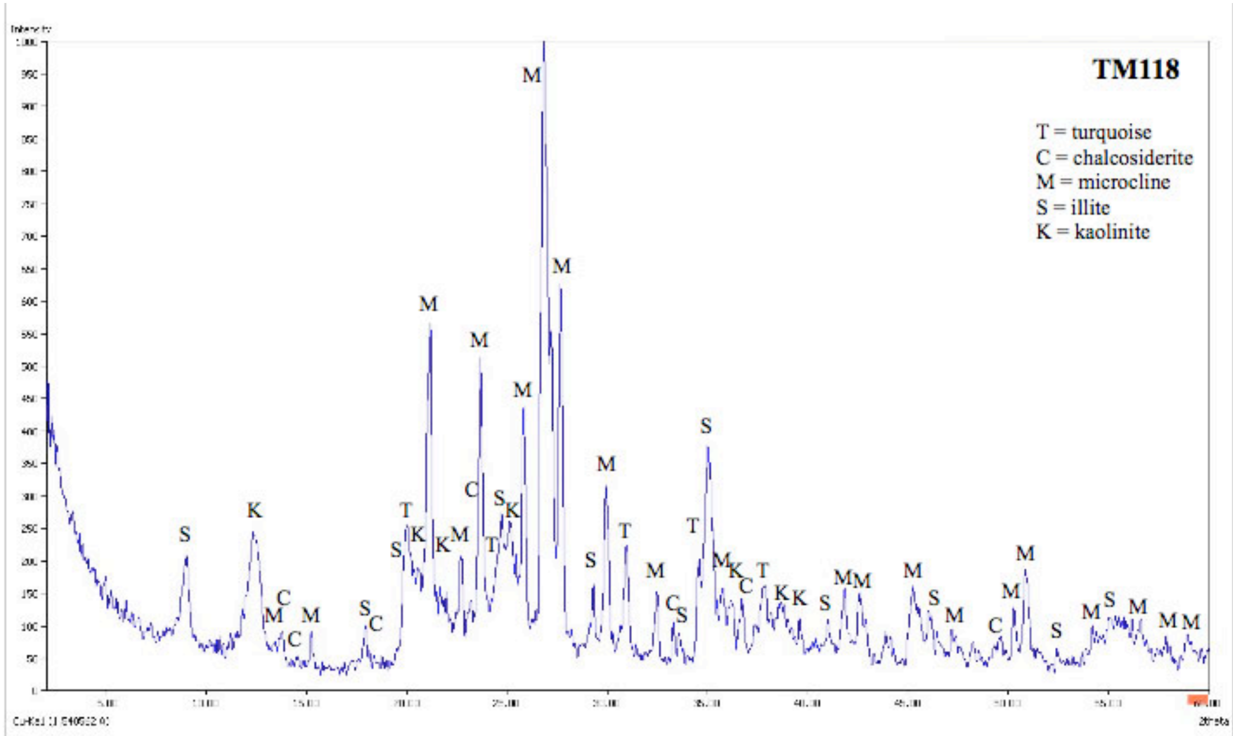

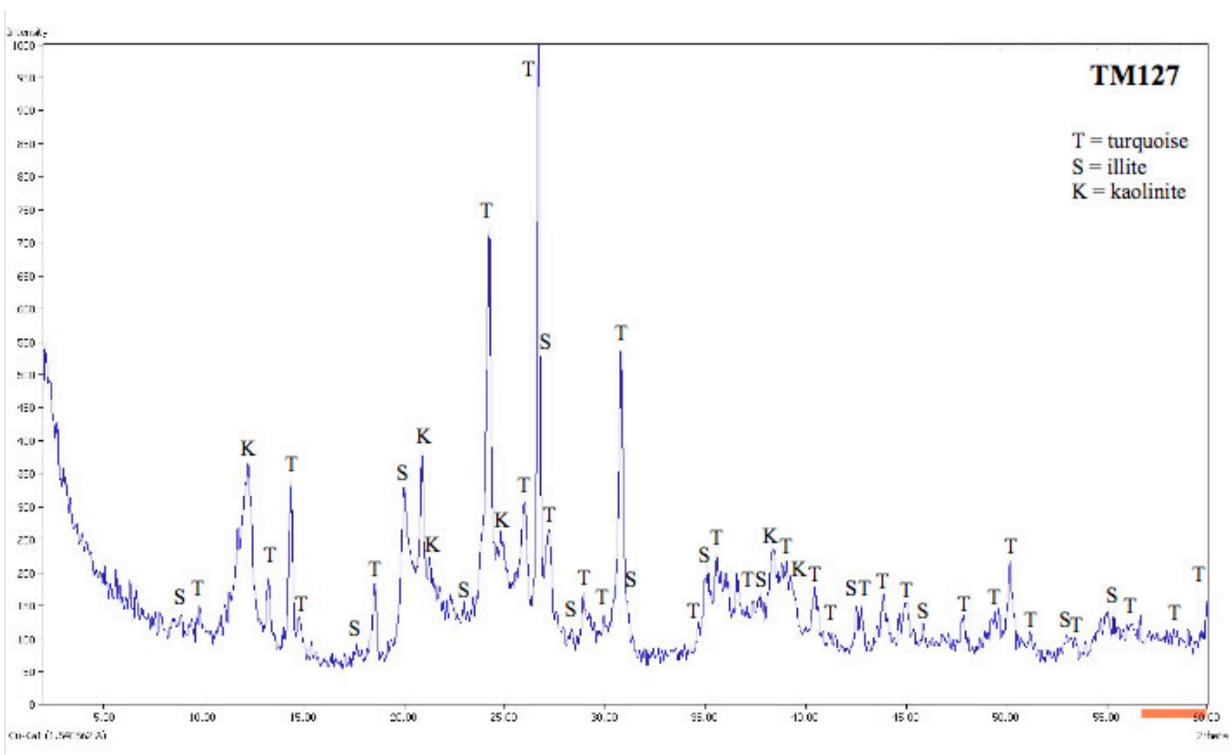

Figure 5.14 Experimental X-ray diffraction patterns of samples e)TM118 f) TM127.

Sample TM118 was a blue green vein separated from its soft grey host rock and only the turquoise portion was analyzed. Sample preparation, analytic, and data processing conditions remained constant for all samples. The turquoise minerals turquoise and chalcosiderite both matched this experimental pattern, not faustite. Illite and vermiculite were also present in sample TM118. Additional minerals found in this vein sample were microcline and kaolinite. These minerals are also present in the sample containing only host rock (TM109A).

Sample TM127 was a hard vein with light brown matrix attached. This experimental pattern matched the turquoise group mineral turquoise only. Clay minerals illite, vermiculite, and kaolinite were also present. Bementite and ramdohrite also provided close fits to many of the peaks in this sample not addressed by the other reference patterns mentioned. Ramdohrite, although unlikely, is considered as a possible phase in this sample and TM109A because large amounts of lead and silver were mined historically at the Hachita mining district and it might be present in the Hachita host rock.

Red Hill

Hand Sample Description

A set of samples from the Red Hill mine was provided by the Turquoise Museum in Albuquerque, New Mexico (Fig.5.15). The Red Hill sample colors are equivalent to Pantone 338U, 563U, 564U, 3252U, 3258U, 7472U. All pieces were recorded in the inventory and six samples were chosen for their representative variability. The six samples selected were cut, thin sectioned and analyzed with optical microscopy and electron microprobe analysis.

The Red Hill material in hand sample was very hard and mostly vein material. There were two samples with nodular shapes, one was possibly part of an undulating vein. There was no observed association between color and texture or hardness suggestive of weathering. Fractures in turquoise were coated with a brown-tan material. These host rock grains were too small to identify, but could possibly be from an igneous porphyry.

Figure 5.15 Samples from Red Hill Mine, White Signal Mining District, New Mexico (photo Cynthia Hotujec).

<u>Petrography Description</u>

Red Hill samples were dense or very fine-grained (<0.33 mm grain size). All of the samples had spherules or rounded aggregates of fine grains. A vein-like network filled with either a dark blue high-relief mineral, sericite, or iron oxides surrounds pockets of dense turquoise material. This texture forms a web-like pattern (Fig. 5.16).

The Red Hill turquoise mineral was intergrown with variable amounts of a very fine grained, light colored, mineral that appears to be sericite. Sample RH10 had a zone of increased sericite along the edge of the sample as well as microveinlets of the mineral that penetrate the sample (Fig. 5.17a & b). Rounded aggregates of turquoise had zones of denser turquoise minerals near the center and sericite intergrowths on the edges and between turquoise aggregates.

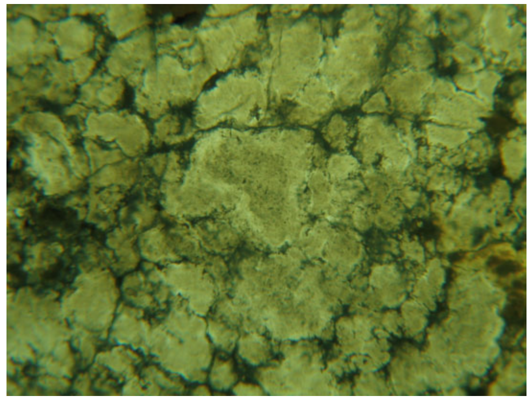

Figure 5.16 Rounded aggregates in Red Hill Sample RH13. 100x PL.

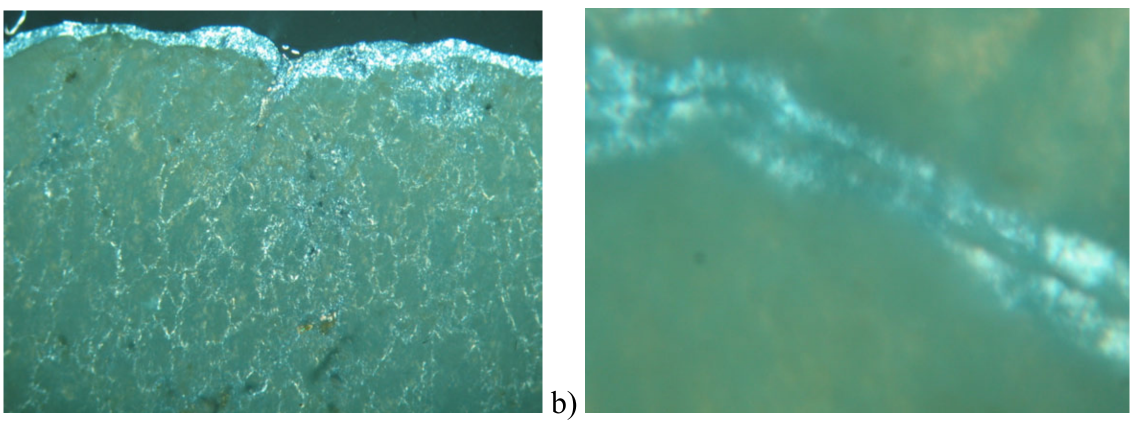

a) b)

Figure 5.17 Sample RH10 a) sericite zone (white color) 100x XP b) micro fissures 630xXP

Occasionally the turquoise minerals are completely intergrown with sericite throughout the sample and no discrete sericite zones are visible (Fig. 5.18a & b).

There were no signs of silicification or quartz inclusions as seen in the Hachita samples. All of the Red Hill turquoise samples contained iron oxides. The association of iron oxide and opaque grains may suggest replacement or oxidation of a preexisting mineral such as pyrite. This process may have mobilized elements necessary for the formation of secondary opaque grains and perhaps the turquoise minerals as well. (Fig. 5.19). Additional analyses focused on opaque mineral inclusions and their compositions are necessary to verify this tentative interpretation.

a) 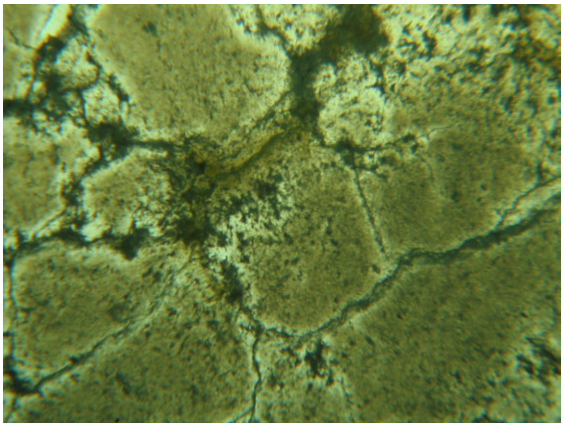 b) 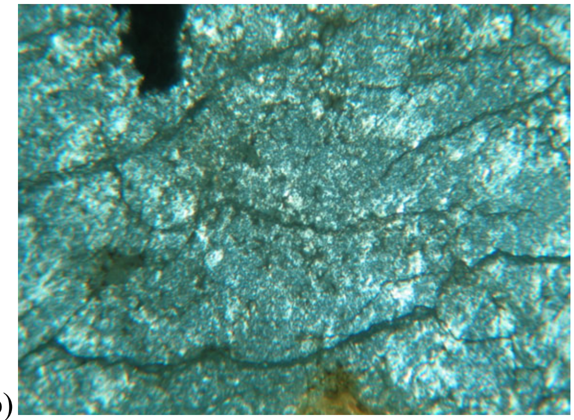

Figure 5.18 Two types of sericite intergrowth a) in zones on edges of dense pockets in RH9, 100x PL and b) throughout turquoise mineral grains of RH17, 100x XP.

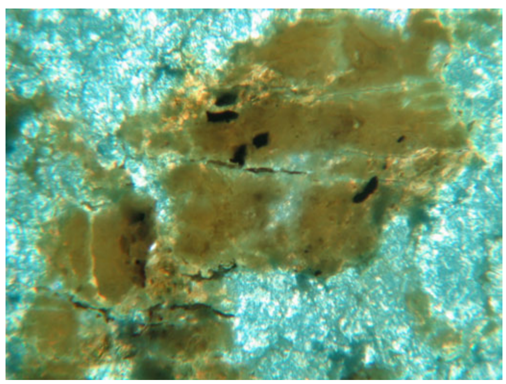

Figure 5.19 Iron oxide in sample RH13 with opaque inclusions. 100x XP

The six Red Hill samples had very little host rock attached to the turquoise samples. Small areas identified as host rock appeared to be an altered igneous porphyry. The minerals identified in the host rock were altered biotite/chlorite and anhedral opaque grains with lesser amounts of feldspar and some quartz. Microprobe analysis with EDS later identified rutile and possibly jarosite. Chloritized biotite grains appears to show evidence of dissolution and replacement as they consist of anhedral fragments with greenish zones on the peripheries of brownish centers (Fig. 5.20).

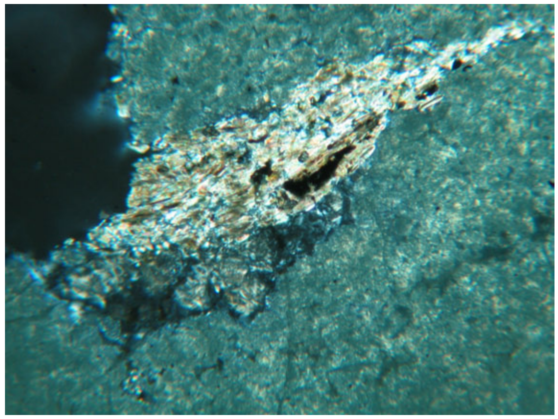

Figure 5.20 Alteration of biotite and chlorite of host rock in sample RH19. 100x XP

A spherulitic yellow mineral at the boundary between turquoise and host rock cuts into the blue green minerals of sample RH9 and follows microfissures indicating that it is more recent (Fig. 5.21a &b). The yellow mineral appears to be an iron oxide, perhaps radiating aggregates

a) 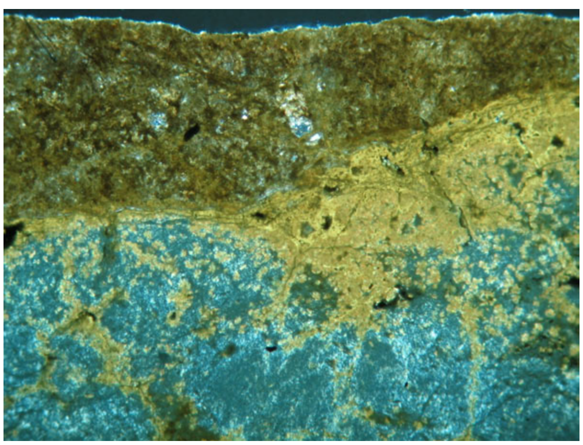 b) 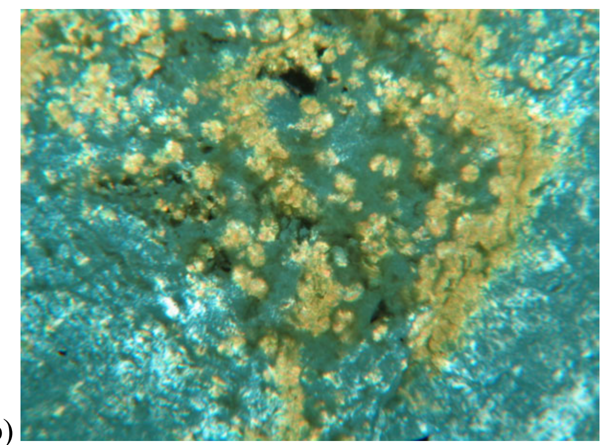

Figure 5.21 Sample RH9 a) host rock, iron oxide and blue green minerals, 40x XP and b) iron oxide and turquoise mineral association, 100x XP.

of goethite with small crystals due to aluminum substitution, jarosite, or a mixture of both. Yellow spherules extending into the blue green material in some areas are intergrown with a denser blue green mineral lacking sericite intergrowths present throughout the rest of sample RH9 (Fig. 5.21b). Preliminary data suggest this is a fine grained intergrowth of high-Fe turquoise and jarosite. The dark blue turquoise mineral is very similar to that in the vein-like network often separating rounded turquoise aggregates in other samples. More analyses focused on the relationship between host rock and turquoise group minerals are warranted to determine if and what role this yellow mineral may play in turquoise alteration and weathering.

Microprobe Analysis

Six samples from the Red Hill Mine were analyzed and two compositional groups formed within the data. The areas analyzed are separated into two distinct groups (Fig. 5.22). The Red Hill samples had the lowest Al content (average is 4.84) of all the mines and artifacts and the Fe is also the highest (Table 5.3). The blue green mineral in the vein network separating rounded turquoise aggregates plots closer to chalcosiderite than the material within the aggregates (Fig. 5.22). Sixteen analyses from areas in samples RH13, RH16, and RH17 were not included in the averages of homogeneous turquoise. These samples had veinlets which were comparatively lower in Cu, Al, and P and higher in Fe when analyzed (Fig. 5.23).

High Fe analyses were not completely eliminated from the examination of turquoise composition variability, but evaluated separately in order to identify possible associations with microtextures observed in thin section or BEI. For example, microtextures associated with high Fe analyses are somewhat similar in both Red Hill and Hachita samples. Red Hill Sample RH13 has the most pronounced spherulitic texture of the Red Hill samples. Sample RH17 has globular areas separated by micro-veins filled with different minerals and the spherulites are not as small, numerous and circular as those in RH13. Sample RH16 also had a vein-like network separating rounded aggregates of turquoise. These three sample areas had the highest Fe (Fig. 5.22). This is a similar pattern to that observed for Hachita where spherulitic aggregates of turquoise were associated with high Fe in samples TM114 and TM127 (Fig. 5.11). Hachita's spherulitic samples

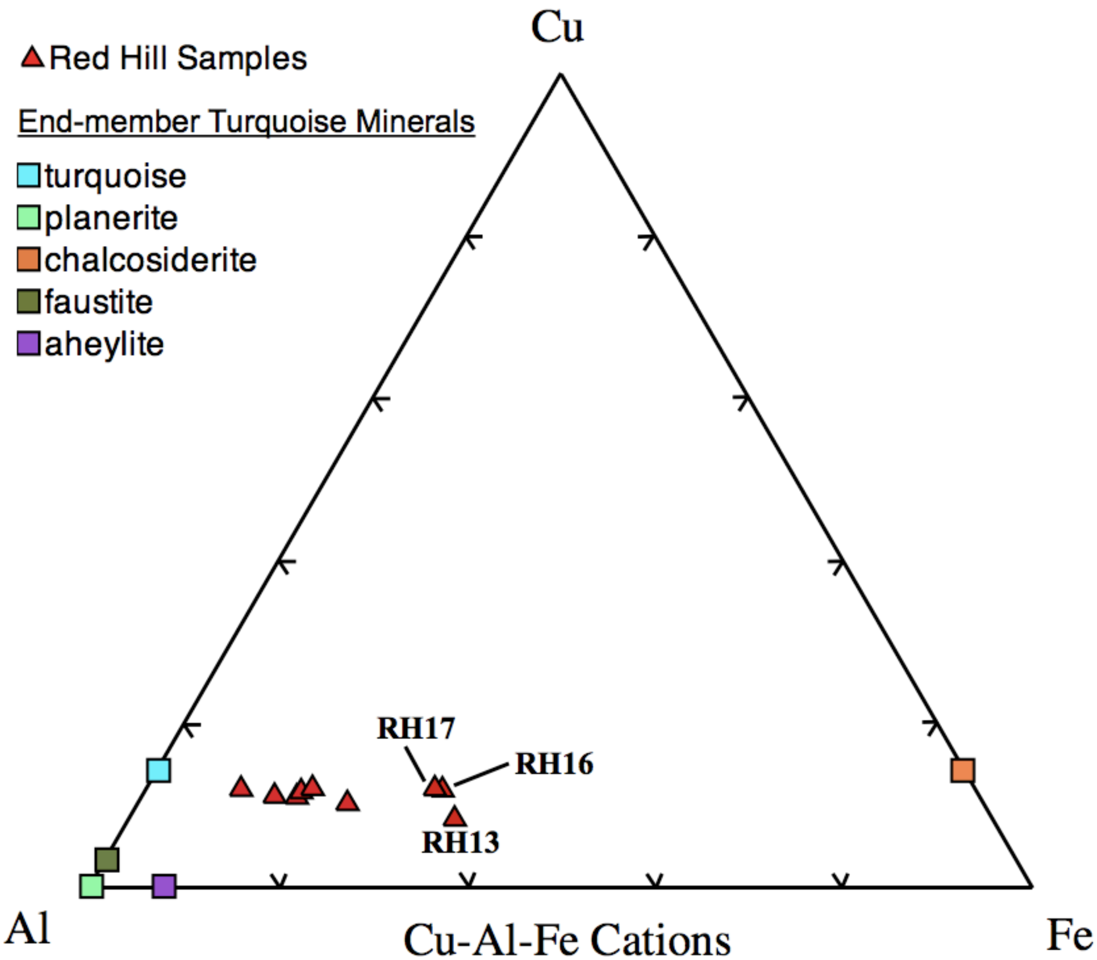

Figure 5.22 Red Hill sample averages plotted with turquoise minerals.

TM127 and TM114 actually plot within the range of the Red Hill high Fe veins and are closer to them compositionally than the rest of the Hachita samples (Fig. 5.23). Although both groups of samples exhibit these high Fe textures, the overall composition of Red Hill samples is more chalcosideritic as a group than Hachita (Fig. 5.23). Separation of mine data into homogeneous and high Fe microtexture subsets both prevents overlap between these two mines and provides information about turquoise mineral alteration that might otherwise be lost.

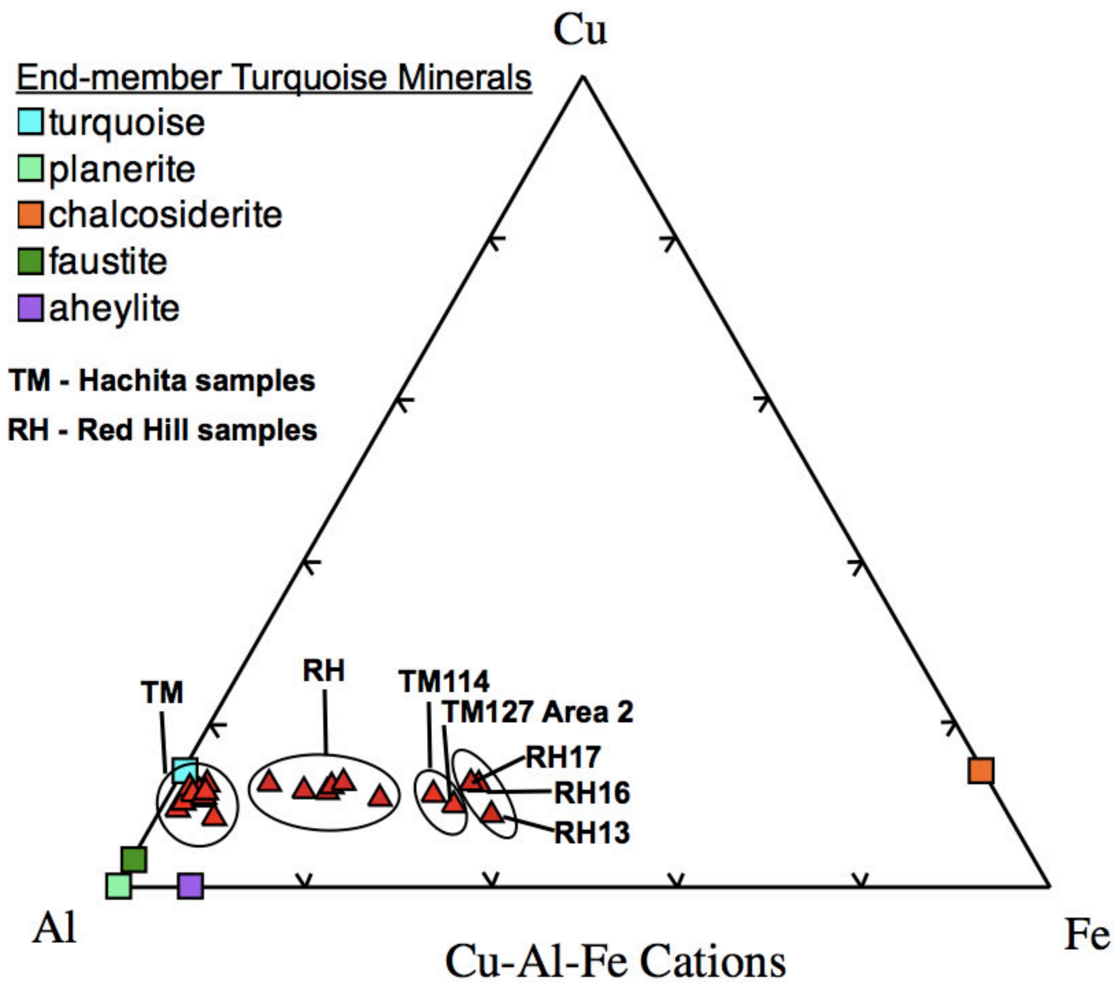

Figure 5.23 Red Hill and Hachita homogeneous averages plotted with high-Fe analyses.

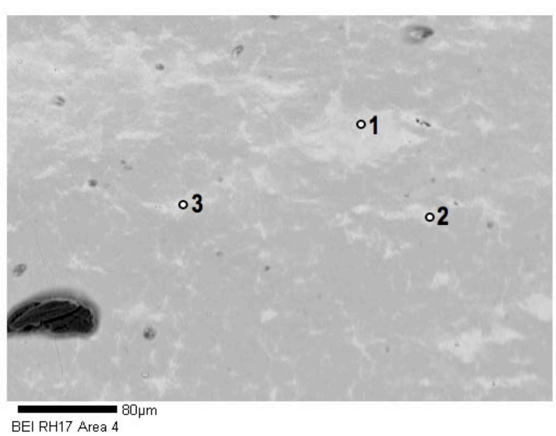

Figure 5.24 Sample RH17 veinlets (lighter gray) with lower Cu, Al, and P, and higher Fe than surrounding material.

Table 5.3 Major Cation Range, Average, and Standard Deviation for Red Hill Samples.

RH9

n=18	MIN	MAX	AVG	STD
Cu	0.57	0.88	0.73	0.09
Fe	0.85	1.53	1.06	0.17
Al	4.31	5.37	4.73	0.30

RH16

n=7	MIN	MAX	AVG	STD
Cu	0.69	0.86	0.81	0.06
Fe	0.85	1.36	1.12	0.19
Al	4.59	5.36	4.90	0.26

RH10

n=13	MIN	MAX	AVG	STD
Cu	0.67	0.85	0.76	0.06
Fe	0.78	1.12	0.93	0.09
Al	4.68	5.39	5.03	0.23

RH17

n=7	MIN	MAX	AVG	STD
Cu	0.71	0.90	0.84	0.06
Fe	0.46	0.96	0.68	0.18
Al	5.14	5.64	5.39	0.20

RH13

n=12	MIN	MAX	AVG	STD
Cu	0.59	0.74	0.67	0.04
Fe	1.14	1.74	1.42	0.19
Al	4.04	4.70	4.35	0.22

RH19

n=12	MIN	MAX	AVG	STD
Cu	0.75	0.92	0.86	0.06
Fe	1.05	1.41	1.22	0.12
Al	4.49	5.26	4.93	0.26

Red Hill homogeneous material

n=68	MIN	MAX	AVG	STD
Cu	0.57	0.92	0.77	0.09
Fe	0.46	1.74	1.09	0.26
Al	4.04	5.64	4.84	0.38

Analyses Excluded from Homogeneous Average

RH13 Area 4

n=3	MIN	MAX	AVG	STD
Cu	0.49	0.55	0.51	0.03
Fe	1.79	2.34	2.07	0.28
Al	3.07	3.66	3.43	0.32

RH17 Area 2 & 4

n=6	MIN	MAX	AVG	STD
Cu	0.68	0.87	0.81	0.08
Fe	1.31	2.40	2.02	0.44
Al	3.21	4.61	3.80	0.55

RH16 Area 1, 1-4 & 2, 1-3

n=7	MIN	MAX	AVG	STD
Cu	0.71	0.85	0.79	0.05
Fe	1.61	2.28	2.05	0.29
Al	3.07	4.22	3.70	0.45

Chalchihuitl

Hand Sample Description

Seven samples were selected from the field collection made from tailings on Mount Chalchihuitl. The color ranged from pale blue to deep blue and pale green to deep green and some samples had both blue and green (Fig. 5.25). The colors were equivalent to Pantone 304U, 317U, 577U, 576U, 579U, 3115U, 3242U, 7465U, and 7466U.

This small sample set exhibited a wide range of visual variability. Blue green minerals were both vein-shaped and nodular. Some of the pieces were softer and had a slightly powdery texture in hand sample, others were brittle and hard. Host rock attached to the turquoise samples was an altered igneous porphyry consisting of a tan fine-grained groundmass and rounded phenocrysts of quartz and feldspar. Iron stains streak the samples and one sample had a soft, white, clay-like coating on one small area. Seven samples were set into grain mounts for electron microprobe analysis.

Figure 5.25 Sample CH23 exhibits color variability at the sample scale.

Microprobe Analysis

The seven Chalchihuitl mine samples had copper aluminum phosphate analyzed n=51 times (Table 5.4). Six of the analyses from sample CH23 were not included in the average of homogeneous material because they had high iron. Samples CH26 and CH35 were eliminated from the homogeneous average completely because there were no turquoise minerals present. CH26 had phosphate between 21-26 wt.% which is lower than the lowest amount found in a turquoise mineral (chalcosiderite has P 28.77 wt.%). CH35 had very low Cu and high Ti of 1.3-2.8 wt.%. Chalchihuitl had the highest levels of Si among all the locations analyzed averaging 1.06 wt% SiO2. The silica is apparently quartz intergrown with turquoise. Three analyses also not included in the sample averages from CH35, CH26, and CH27 were within quartz inclusions that had high silica values of up to 99.29 wt%.

Table 5.4 Major Cation Range, Average, and Standard Deviation for Chalchihuitl samples.

CH22

n=12	MIN	MAX	AVG	STD
Cu	0.64	0.83	0.71	0.06
Fe	0.06	0.10	0.08	0.01
Al	4.99	6.22	5.65	0.39

CH28

n=12	MIN	MAX	AVG	STD
Cu	0.67	0.74	0.70	0.02
Fe	0.08	0.13	0.11	0.02
Al	5.08	5.59	5.36	0.14

CH23

n=3	MIN	MAX	AVG	STD
Cu	0.68	0.72	0.70	0.02
Fe	0.19	0.21	0.20	0.01
Al	5.30	5.96	5.53	0.38

CH34

n=9	MIN	MAX	AVG	STD
Cu	0.38	0.50	0.44	0.04
Fe	0.20	0.37	0.27	0.05
Al	5.10	5.49	5.25	0.11

CH27

n=9	MIN	MAX	AVG	STD
Cu	0.51	0.69	0.62	0.06
Fe	0.04	0.09	0.07	0.02
Al	4.51	5.59	5.09	0.39

Chalchihuitl homogeneous material

n=45	MIN	MAX	AVG	STD
Cu	0.38	0.83	0.64	0.11
Fe	0.04	0.37	0.13	0.08
Al	4.51	6.22	5.20	0.50

Analyses Excluded from Homogeneous Average

CH23 Area 1 & 2				
n=6	MIN	MAX	AVG	STD
Cu	0.50	0.61	0.55	0.05
Fe	0.52	0.77	0.64	0.08
Al	4.34	4.69	4.49	0.16

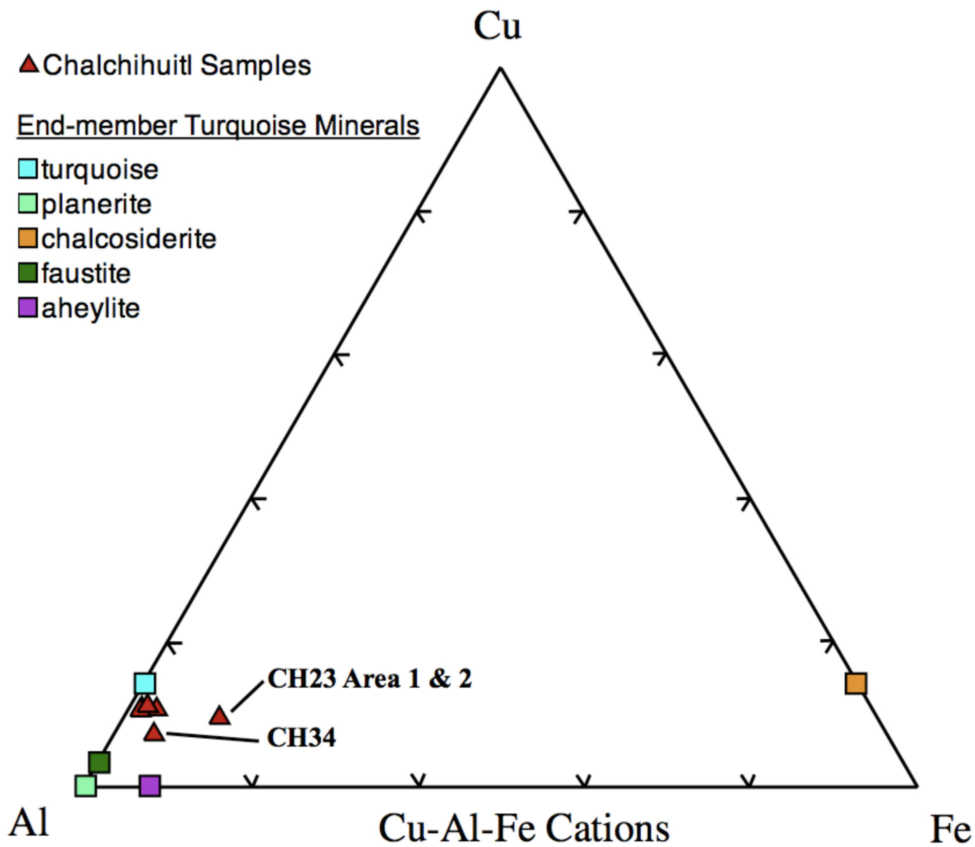

Figure 5.26 Chalchihuitl sample averages plotted with turquoise minerals.

The five samples that contained copper aluminum phosphate plot very close to the turquoise endmember (Fig. 5.26). Chalchihuitl sample CH34 had lower Cu than the other samples from this mine and plots between turquoise and endmember aheylite. Although bright, lighter colored/higher density presumably high-iron inclusions were observed in the Chalchihuitl samples, they were not routinely analyzed because data collection focused on homogeneous turquoise mineral composition. Two Chalchihuitl sample areas from CH23 however, have high Fe and plot closer to chalcosiderite than other analyses. The result is two subsets of data from high Fe and low Fe analyses similar to the Hachita and Red Hill sample sets.

Back scattered electron images identified textural differences. Texture ranged from smooth and dense to spherulitic (Fig. 5.27 a & b). The three samples close to the turquoise

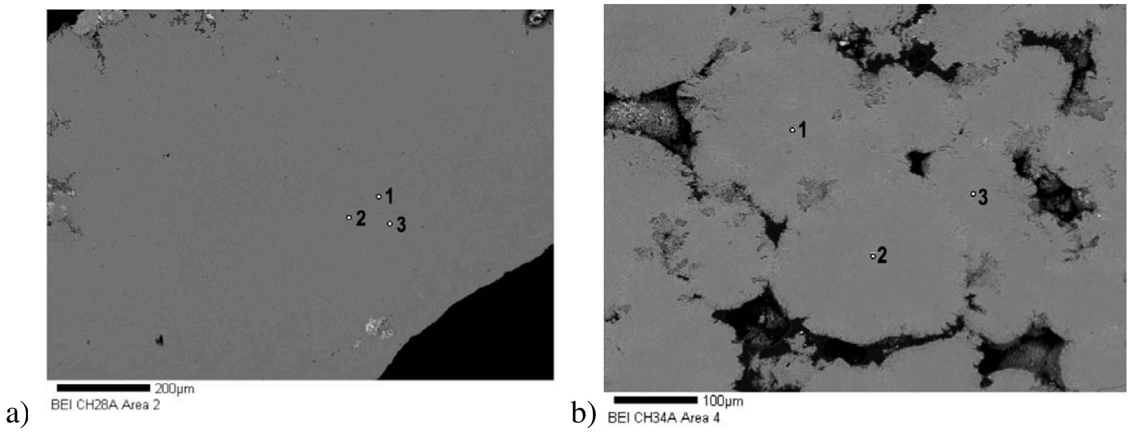

Figure 5.27 Chalchihuitl sample textures a) smooth & dense b) spherulitic.

endmember (CH22, CH27, & CH28) had different textures despite similar compositions. Some textures are not associated with high Fe composition. CH28 was very dense and homogenous (Fig. 5.27a). CH34 had well-defined spherulites (Fig. 5.27b) with faint zones of higher and lower density in some areas (Figure 5.29a). Sample CH22 had both bright, high Fe and dark, less dense inclusions (Fig. 5.28a). CH27 had rounded aggregates, possibly remnant spherules (Fig. 5.28b). CH23 Area 3 that plotted closest to chalcosiderite, had a porous, possibly remnant spherulitic texture (Fig. 5.29b). The Chalchihuitl textures should exhibit the most weathering characteristics because they were collected from the tailings pile and not directly from veins in the host rock. The textural variability observed therefore may be due to factors other than weathering.

The Chalchihuitl samples demonstrated a relation between color in hand sample and composition. The sample closest to chalcosiderite (Fig. 5.26) with the most iron on average, CH23 is pale blue (317U, 577U) and had slightly less Cu than the others besides CH34 (Table 5.4) The three samples closest to turquoise are blue (304U, 317U, 3115U, 577U) and have the

a) 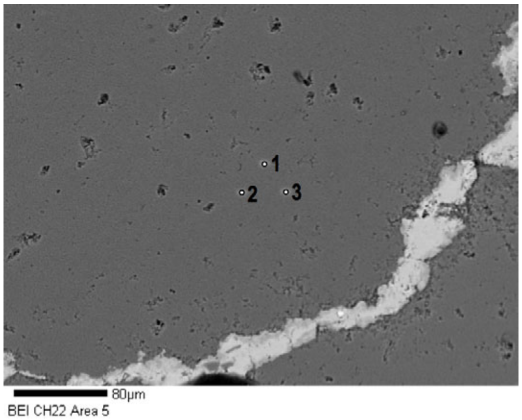

b) 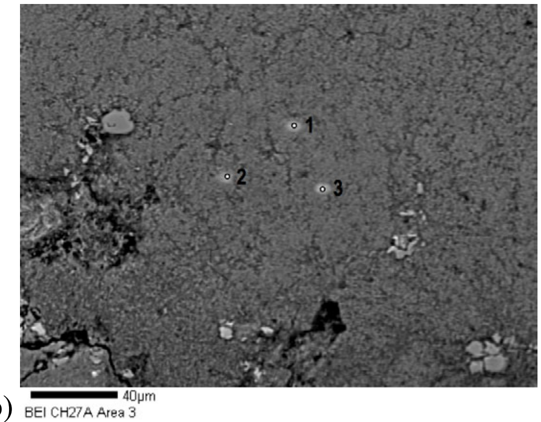

Figure 5.28 Textural variation in Chalchihuitl samples a) CH22 and b) CH27.

a) 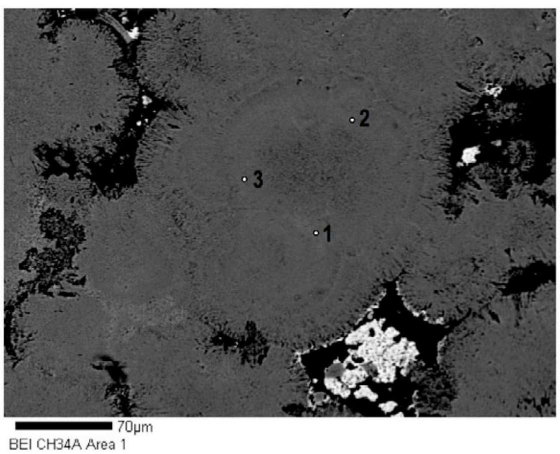

b) 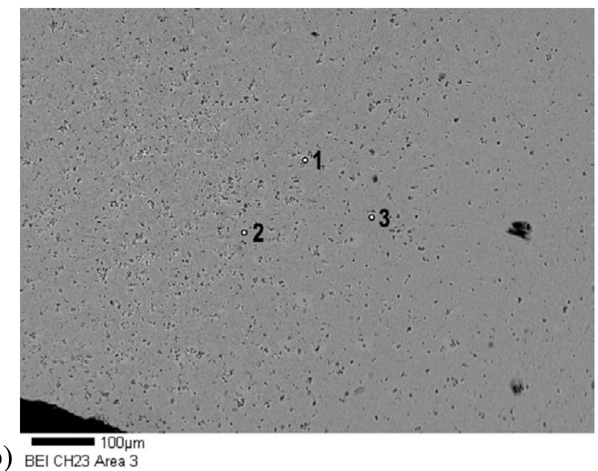

Figure 5.29 a) Spherulitic texture of sample CH34 and b) dense inclusions of sample CH23.

highest Cu averages (Table 5.4). CH34 is between turquoise and aheylite with the least amount of Cu and the next highest amount of Fe after CH23 (Table 5.4) and is a shade of pale blue-green (3242U). The two samples determined to not be turquoise minerals were both green. Sample CH35 (Fig. 5.29) is green (7465U, 7466U) and CH26 is pale green (579U, 576U). It is possible that the greater color variability in hand samples of Chalchihuitl turquoise is a result of greater mineralogical variability.

Figure 5.30 CH35 had high Ti and low Cu and was not a turquoise mineral.

Tiffany

Hand Sample Description

Fifteen samples were collected from the tailings of the Tiffany Mine in the Cerrillos Mining District according to the same variability criteria as the other locations. The color of the samples is equivalent to Pantone 317U, 319U, 3105U, 3115U, 3125U. One sample had a small pale greenish area within predominantly light blue material and this sample was selected as one of the five samples for electron microprobe analysis.

The blue-green minerals were mostly nodular but were also present in the form of veins. The majority of the samples were dense and hard. The host rock was an igneous porphyry with a light brown fine-grained groundmass with many very small black grains. Phenocrysts of quartz and altered feldspars were observed in the groundmass. Bands of iron oxide stains were visible throughout the samples.

Microprobe Analysis

The Tiffany mine samples had homogeneous turquoise analyzed n=60 times. All of the individual analyses of Tiffany samples were included in the homogenous turquoise mineral averages because none had values outside of the compositional range for turquoise minerals

(Table 5.5). The Tiffany mine samples were the most homogenous of all the sample sets analyzed. Backscattered electron images display very dense turquoise material. Inclusions were mostly bright and dense but variable (Fig. 5.31a & b). The mine sample analyses form a very tight compositional cluster near the ideal turquoise end-member (Fig. 5.32).

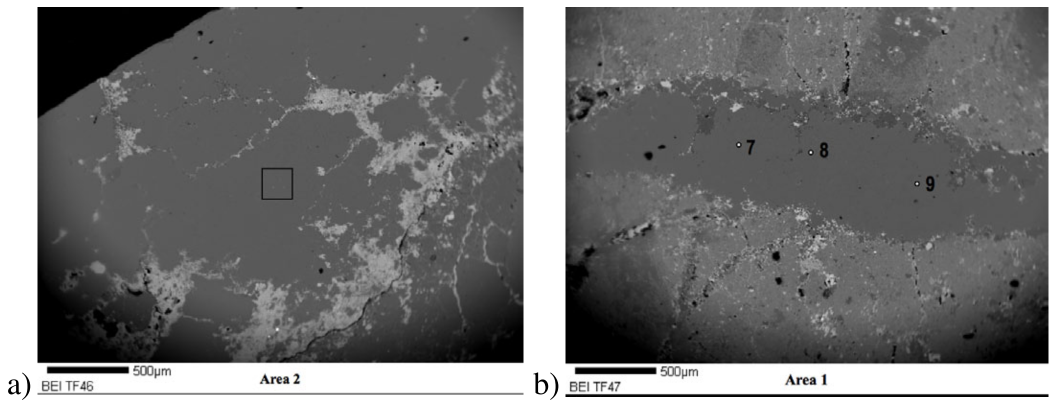

Figure 5.31 Inclusions in Tiffany samples a)TF46 and b) TF47.

Table 5.5 Major cation range, average, and standard deviation for Tiffany samples.

TF39

n=12	MIN	MAX	AVG	STD
Cu	0.70	0.81	0.75	0.03
Fe	0.09	0.14	0.12	0.02
Al	5.31	6.15	5.70	0.32

TF47

n=12	MIN	MAX	AVG	STD
Cu	0.76	0.86	0.80	0.03
Fe	0.04	0.10	0.07	0.02
Al	5.49	6.19	5.79	0.28

TF44

n=12	MIN	MAX	AVG	STD
Cu	0.73	0.82	0.77	0.03
Fe	0.07	0.12	0.09	0.01
Al	5.49	6.03	5.74	0.19

TF49

n=12	MIN	MAX	AVG	STD
Cu	0.80	0.89	0.84	0.03
Fe	0.09	0.18	0.13	0.03
Al	5.57	6.08	5.80	0.20

TF46

n=12	MIN	MAX	AVG	STD
Cu	0.71	0.79	0.75	0.02
Fe	0.15	0.22	0.19	0.02
Al	5.43	5.90	5.66	0.16

Tiffany samples average

n=60	MIN	MAX	AVG	STD
Cu	0.70	0.89	0.78	0.05
Fe	0.04	0.22	0.12	0.05
Al	5.31	6.19	5.74	0.24

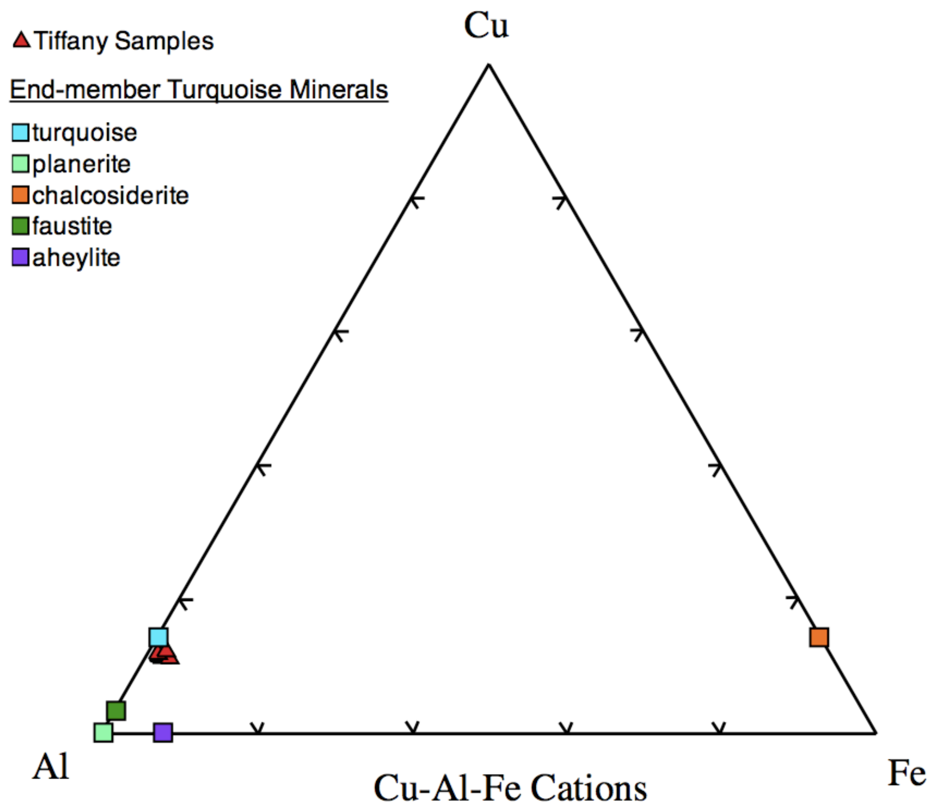

Figure 5.32 Tiffany sample averages plotted with turquoise minerals.

The texture of the Tiffany samples clearly contrasts textures seen at Chalchihuitl, although both sites are in the Cerrillos mining district. Lower density material surrounding turquoise grain aggregates was seen in sample TF46 (Figure 5.33a). The remaining samples from Tiffany had a very dense and fine grained texture (Fig. 5.33b). The Tiffany samples, like those from Chalchihuitl, were also collected from mine tailings and expected to exhibit more evidence of alteration than either Hachita or Red Hill samples. However, no signs of alteration were observed at Tiffany. This provides additional support of the assertion that weathering of turquoise does not result from exposure at surface conditions. Sample TF47 had color variability and was not compositionally distinct. This evidence suggests that color variability is not due to weathering at surface conditions.

a) 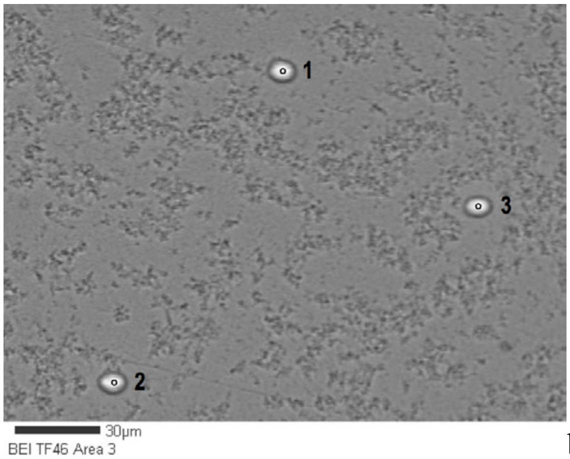

b) 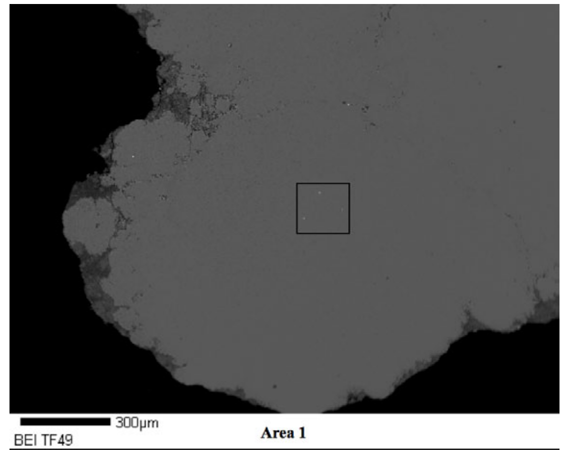

Figure 5.33 Textures of Tiffany samples a)TF46 and b) TF49.

Blue J Artifacts

Hand Sample Description

Ten artifacts were excavated and recovered during surface collection from the Blue J Community archaeological site. The color of the artifact sample set was equivalent to Pantone 317U, 318U, 319U, 325U, 326U, 344U, 348U, and 3105U. Four samples were nodular, four were vein-shaped and the original form of two artifacts could not be determined. The nodules had very little to no host rock. The vein-shaped samples have small amounts of adhering host rock. When visible, host rock appeared to be a light brown fine-grained rock that was variably reddish from iron stains (Fig. 5.34a & b). The ten artifact samples were prepared in epoxy grain mounts for electron microprobe analysis.

Microprobe Analysis

The turquoise minerals in the Blue J Community artifact samples were analyzed 103 times. The artifact sample set was not homogenous as a group (Fig. 5.35). The copper cation values averaged 0.76 ± 0.07. Greater variation was found in the cations of Fe (avg. 0.27 ± 0.16) and Al (avg. 5.50 ± 0.25) than in copper. Ten high Fe analyses were from veinlets or between spherules depending on the specific micro-texture of the sample. These were not included

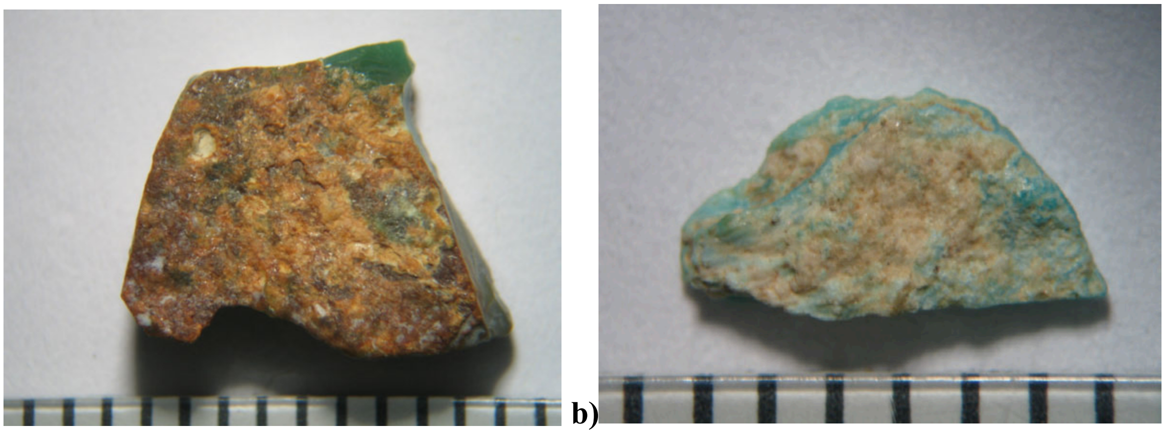

a) b)

Figure 5.34 Host rock on Blue J artifacts a) sample BJ21 and b) BJ12(2). 1 division = 1 mm

in averages of homogeneous material (Table 5.6), but plotted with the turquoise minerals. The data form two groups similar to the mine samples sets. Eight analyses from four samples fell outside of the compositional range for turquoise minerals and were excluded from the plot.

Analyses of homogeneous material range from very close to endmember turquoise to points just below chalcosiderite-turquoise. The artifact sample set had the highest measured values for cation Zn (avg. 0.18 ± 0.16) which supports the possibility of turquoise solid solution with faustite and aheylite (Foord and Taggart,1998). One of the high Fe areas (BJ12(3) Area 2) from three artifact samples extend further towards chalcosiderite than any of the mine samples (Fig. 5.35).

The Blue J artifact samples contain inclusions high in Cu (Fig. 5.36a,b,c, & d). Inclusions in BJ11 Area 5, BJ46 Area 4-1, and BJ49 Area 4 have Cu values outside of the compositional range for turquoise minerals (Table 1.1). The inclusions are high in Cu and low in P relative to the turquoise minerals. Many samples contained bright, high density inclusions that were observed and noted but not analyzed in favor of turquoise minerals. It is possible that these inclusions may have also been high in Cu. High Cu inclusions may have been overlooked in an attempt to determine homogenous turquoise compositions and may potentially supplement information gained about turquoise mineral alteration from high Fe inclusions.

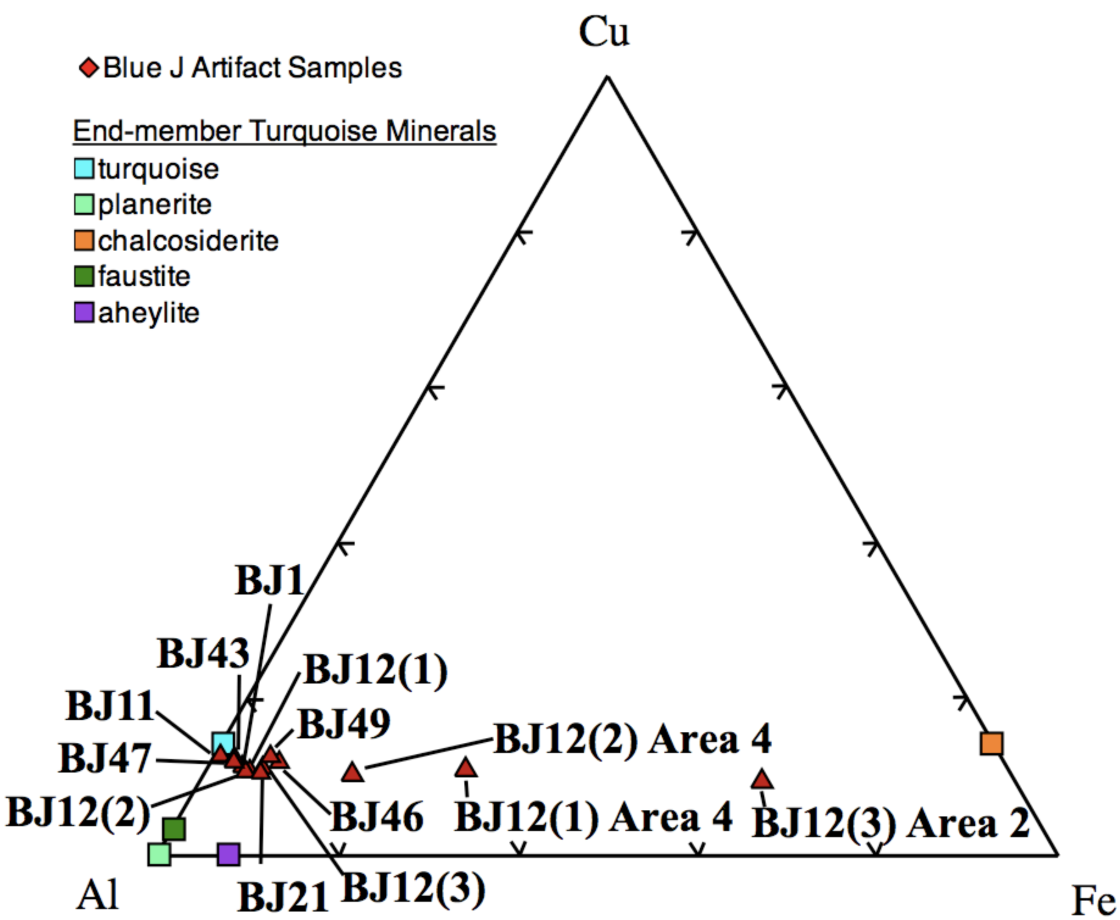

Figure 5.35 Artifact sample averages plotted with turquoise minerals.

Data Analysis

Cu, Fe, and Al content from all sample locations was tested statistically using the independent sample t-test (assuming unequal variances) at a confidence level of 95%. All individual homogeneous analyses, not sample averages, from each mine were tested as a group against every other set including the artifact set. The null hypothesis is that there is no significant

Table 5.6 Major cation range, average, and standard deviation for Blue J samples.

BJ1

n=9	MIN	MAX	AVG	STD
Cu	0.67	0.83	0.75	0.05
Fe	0.19	0.30	0.23	0.03
Al	5.39	5.91	5.65	0.21

BJ11

n=14	MIN	MAX	AVG	STD
Cu	0.74	0.91	0.82	0.05
Fe	0.00	0.03	0.02	0.01
Al	5.53	5.69	5.60	0.05

BJ12(1)

n=9	MIN	MAX	AVG	STD
Cu	0.62	0.77	0.71	0.05
Fe	0.20	0.49	0.30	0.11
Al	5.35	5.77	5.58	0.16

BJ12(2)

n=12	MIN	MAX	AVG	STD
Cu	0.48	0.79	0.72	0.08
Fe	0.24	0.33	0.28	0.03
Al	5.48	6.13	5.75	0.19

BJ12(3)

n=12	MIN	MAX	AVG	STD
Cu	0.66	0.77	0.73	0.03
Fe	0.22	0.94	0.38	0.21
Al	4.83	5.85	5.44	0.28

BJ21

n=9	MIN	MAX	AVG	STD
Cu	0.61	0.71	0.66	0.03
Fe	0.21	0.59	0.37	0.12
Al	5.00	5.49	5.25	0.18

BJ43

n=9	MIN	MAX	AVG	STD
Cu	0.75	0.84	0.8	0.03
Fe	0.11	0.16	0.13	0.02
Al	5.34	5.84	5.51	0.18

BJ46

n=9	MIN	MAX	AVG	STD
Cu	0.68	0.84	0.75	0.05
Fe	0.33	0.62	0.46	0.10
Al	4.85	5.32	5.10	0.17

BJ47

n=9	MIN	MAX	AVG	STD
Cu	0.68	0.80	0.76	0.04
Fe	0.10	0.20	0.14	0.03
Al	5.35	5.57	5.47	0.08

BJ49

n=11	MIN	MAX	AVG	STD
Cu	0.71	0.89	0.83	0.06
Fe	0.36	0.44	0.39	0.03
Al	4.70	5.80	5.35	0.34

Blue J Artifact homogeneous material

n=103	MIN	MAX	AVG	STD
Cu	0.48	0.91	0.76	0.07
Fe	0.00	0.94	0.27	0.16
Al	4.83	6.13	5.50	0.25

Analyses Excluded from Homogeneous Average

BJ12(1) Area 4

n=4	MIN	MAX	AVG	STD
Cu	0.68	0.81	0.73	0.06
Fe	1.21	3.08	1.88	0.83
Al	2.78	4.53	3.96	0.79

BJ12(3) Area 2

n=3	MIN	MAX	AVG	STD
Cu	0.55	0.70	0.61	0.08
Fe	3.45	4.50	3.97	0.53
Al	1.59	1.93	1.78	0.17

BJ12(2) Area 4

n=3	MIN	MAX	AVG	STD
Cu	0.61	0.71	0.67	0.05
Fe	0.84	1.28	1.04	0.22
Al	4.31	5.12	4.68	0.41

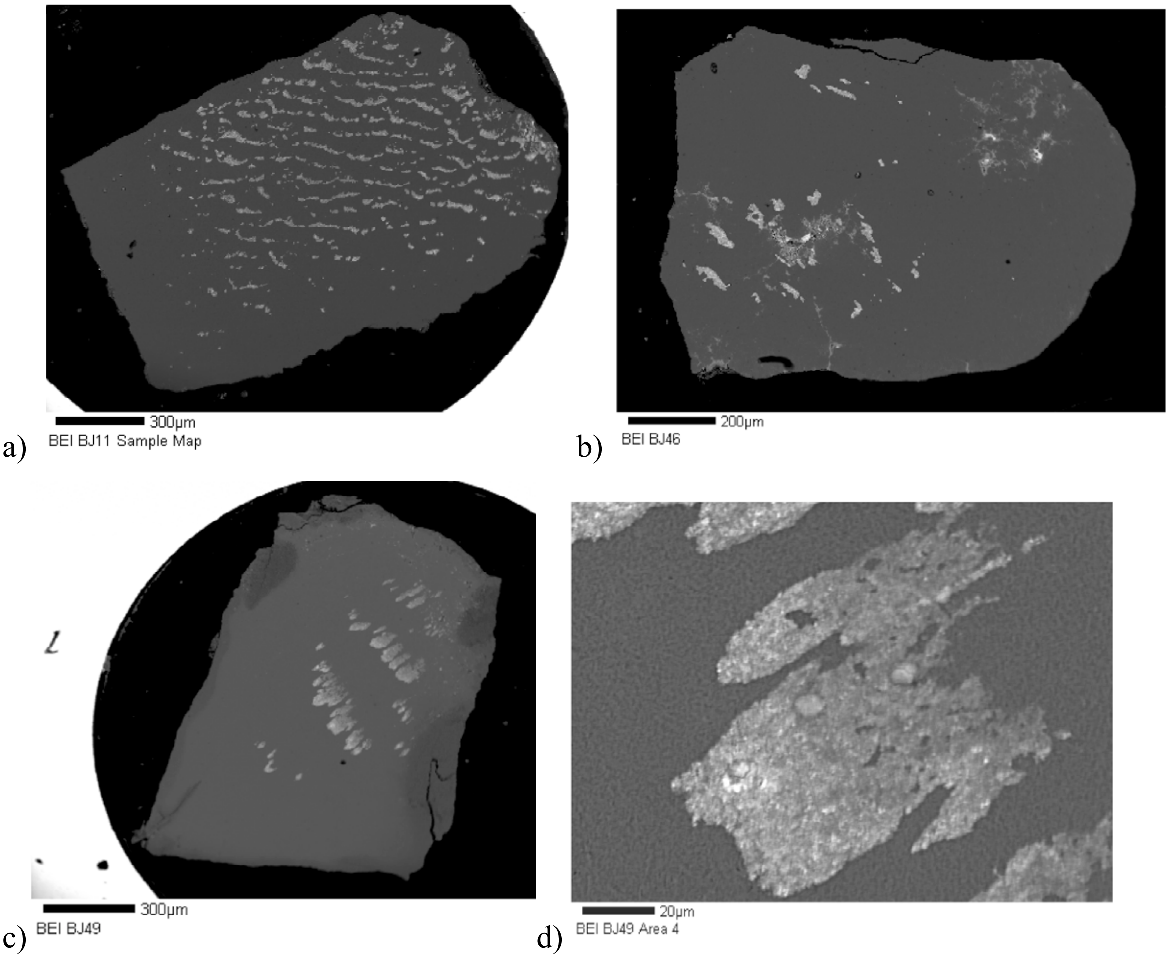

Figure 5.36 High Cu inclusions in Blue J samples a) BJ11 b) BJ46 c) BJ49 d) BJ49 Area 4.

difference between these three cations for each group of samples. Most tests resulted in rejection of the null hypothesis with only five that could not reject it (Table 5.7). The copper levels of the Red Hill and Tiffany Mines were not significantly different. Also, the artifact samples were not significantly different from the Red Hill mine samples in copper. The iron values of the Chalchihuitl and Tiffany mine analyses were not significantly different from each other. Comparison tests for the aluminum values resulted in the inability to reject the null hypothesis between the Hachita and Chalchihuitl mines and between Hachita and the artifacts. Overall, the majority of these analyses have significant differences between Cu, Fe, and Al values except for the five comparisons just mentioned. Cu and Al have two rejections each and Fe has only one.

Two of the five p-values not rejected involve similarities with the artifact set, which due to variability, suggest they are not all from the same source. That leaves only one combination from each element with significant similarities between the four mines. These three elements, Cu, Fe, and Al show the most promise for providing a characteristic range of major elements. Based on the significant differences in means of Cu, Fe, and Al bivariate plots will compare each pair of elements for similarity between homogeneous mine and individual artifact data in addition to all the homogeneous data observed in a ternary plot.

Table 5.7. Pair-wise comparisons of p-values for individual homogeneous turquoise mineral analysis of Cu, Fe, and Al cations.
H=Hachita, R=Red Hill, C=Chalchihuitl, T=Tiffany, A=Artifacts

Cu p-values

	Hachita	Red Hill	Chalchihuitl	Tiffany
A	0.0003	0.4139	0.0000	0.0048
T	0.0000	0.2244	0.0000	
C	0.0003	0.0000		
R	0.0002			

Fe p-values

	Hachita	Red Hill	Chalchihuitl	Tiffany
A	0.0000	0.0000	0.0000	0.0000
T	0.0000	0.0000	0.4199	
C	0.0111	0.0000		
R	0.0000			

Al p-values

	Hachita	Red Hill	Chalchihuitl	Tiffany
A	0.0612	0.0000	0.0385	0.0000
T	0.0000	0.0000	0.0000	
C	0.7324	0.0000		
R	0.0000			

In Figure 5.37 each individual analysis of turquoise mineral is plotted. Some separation can been seen which is statistically significant according to Table 5.7, but there is too much overlap to visually assess the results. Instead it is more useful to plot only the averages of the individual analyses by sample (Fig. 5.38). Here it is possible to discern on the most basic level, that the Red Hill mine is separate from the three other mines. It is not possible to observe the difference between the three remaining mines with this plot. The artifact data overlap with all of the mine locations because they plot in the center of mine data.

When the cation Fe data are plotted with the Cu and Al in a ternary plot, the effects of the solid solution series on the data can be seen. The points are clearly spread out along the solid solution series between turquoise and chalcosiderite as iron replaces aluminum. There is also a

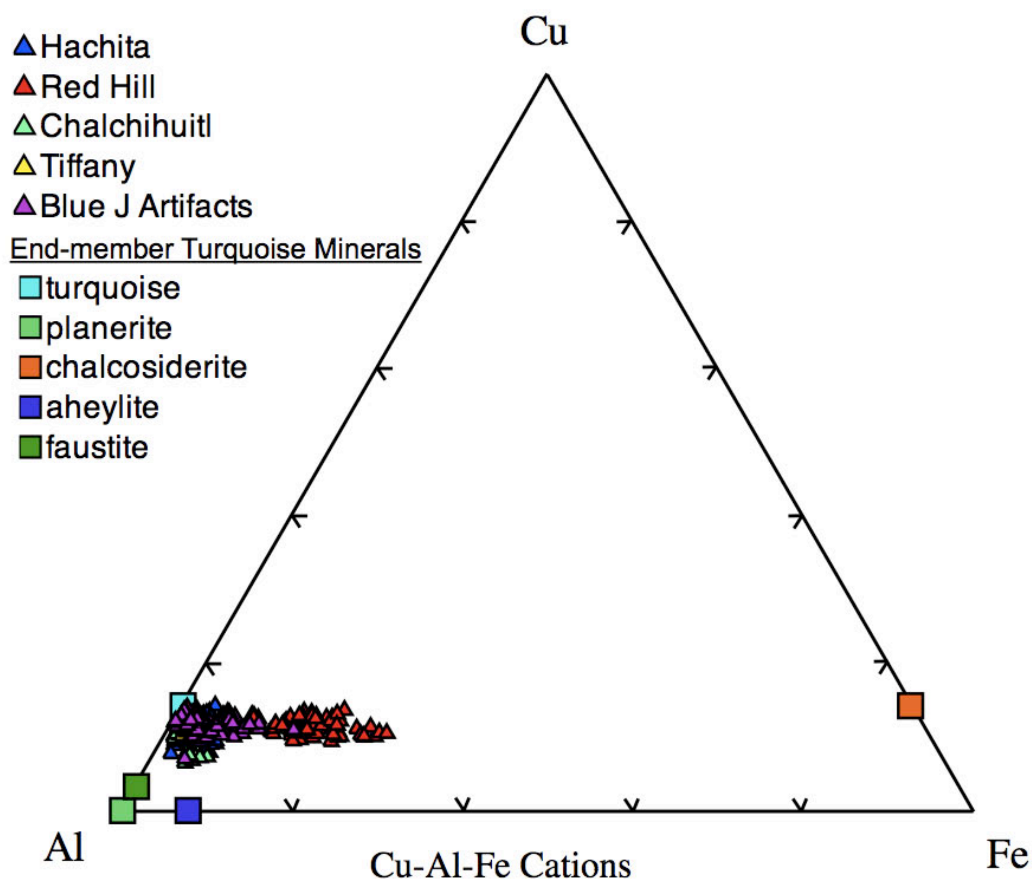

Figure 5.37 Individual analyses with turquoise group ideal endmembers.

gradation of copper between turquoise-chalcosiderite and aheylite-planerite. While Figures 5.37 and 5.38 are useful in visualizing the data, they are not very helpful when trying to determine the source of artifacts. To eliminate the overlap, one of the three variables is removed to illustrate the statistically significant variation in a more visually simplified format (Fig. 5.39).

The first of three bivariate scatterplots compares Fe^{+3} to Al cation averages of each sample (Fig. 5.39). This plot shows an inverse relationship between the two elements due to substitution. The range of ferric iron between ideal endmember turquoise and chalcosiderite is from 0 to 6 cations and Al from 6 to 0 respectively. The Fe-Al plot confirms that the overall data set is more like endmember turquoise than the other turquoise minerals. The Hachita mine

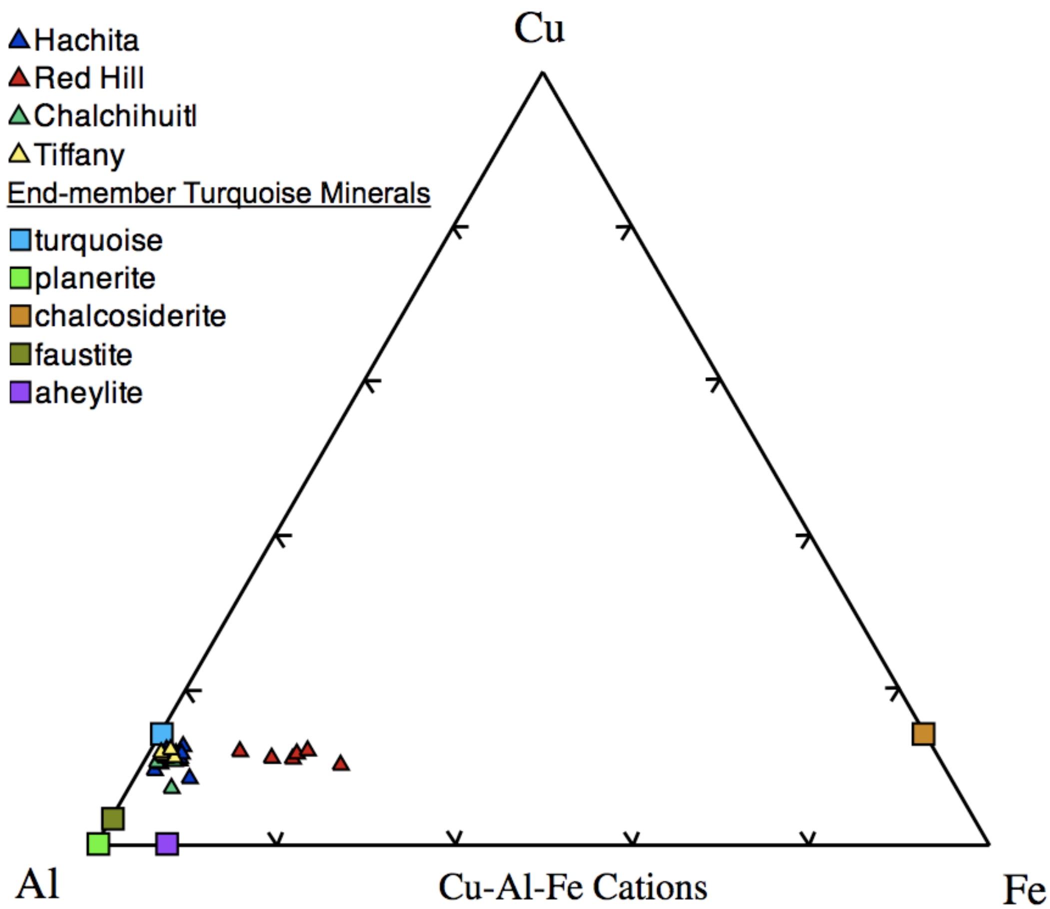

Figure 5.38 Analysis averages by sample with turquoise group ideal endmembers.

overlaps both Chalchihuitl and Tiffany while Chalchihuitl and Tiffany form two clusters of data points who share an Al range between 5.6 - 5.7 cations. Red Hill clearly stands apart as turquoise-chalcosiderite due to higher iron. The majority of artifacts appear to fall along the upper Fe limit of the Hachita data. All six of these artifacts (BJ21, BJ12(3), BJ12(1), BJ49, BJ12 (2), and BJ1) could potentially fit within the Hachita data set although BJ1 is very close to Tiffany also. BJ46 doesn't have similarity for Fe with any other mine data set but has Al ~5.2 cations, within the Hachita or possibly Chalchihuitl ranges. Two artifact points, BJ47 and BJ43, fall directly within the Chalchihuitl cluster which is also in the Hachita range. Sample BJ11 has lower Fe^{+3} and falls just beyond the Chalchihuitl and Hachita overlap.

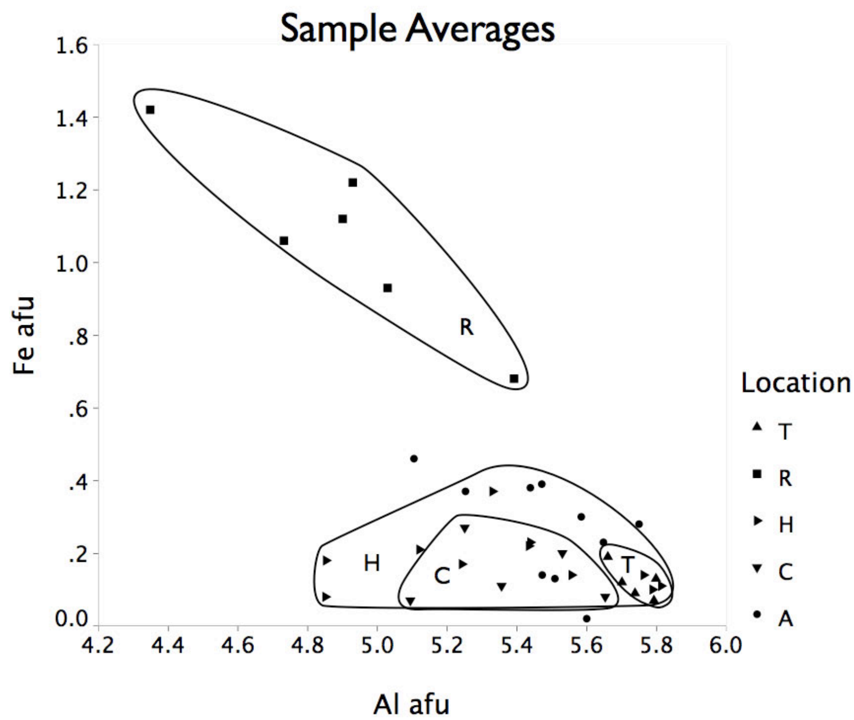

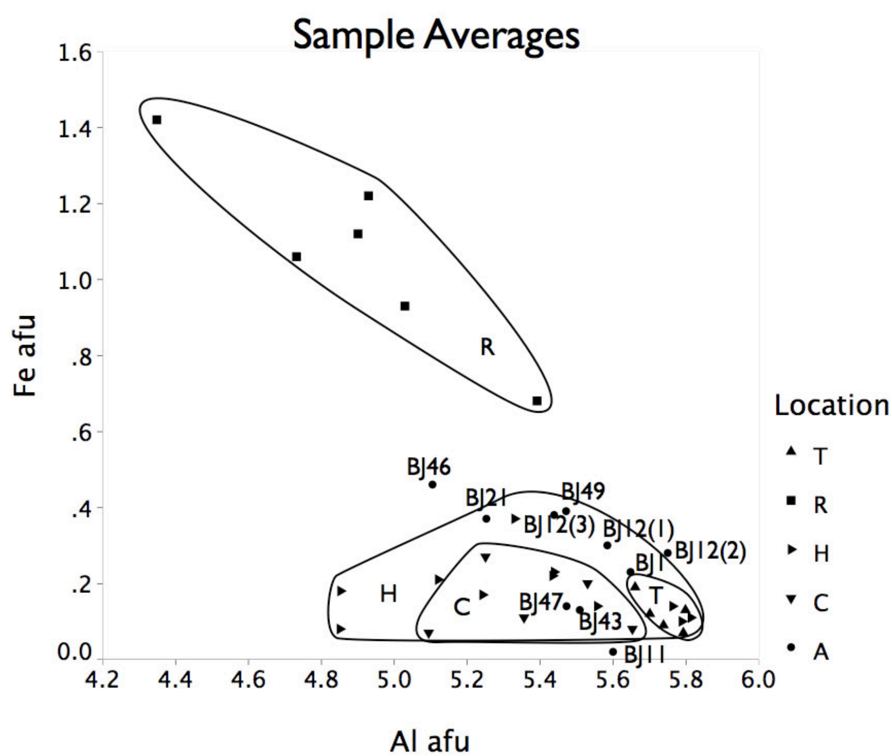

Figure 5.39 Al and Fe^{+3} sample averages for mines and artifacts T=Tiffany, R=Red Hill, H=Hachita, C=Chalchihuitl, A=Artifacts
afu = atoms per formula unit

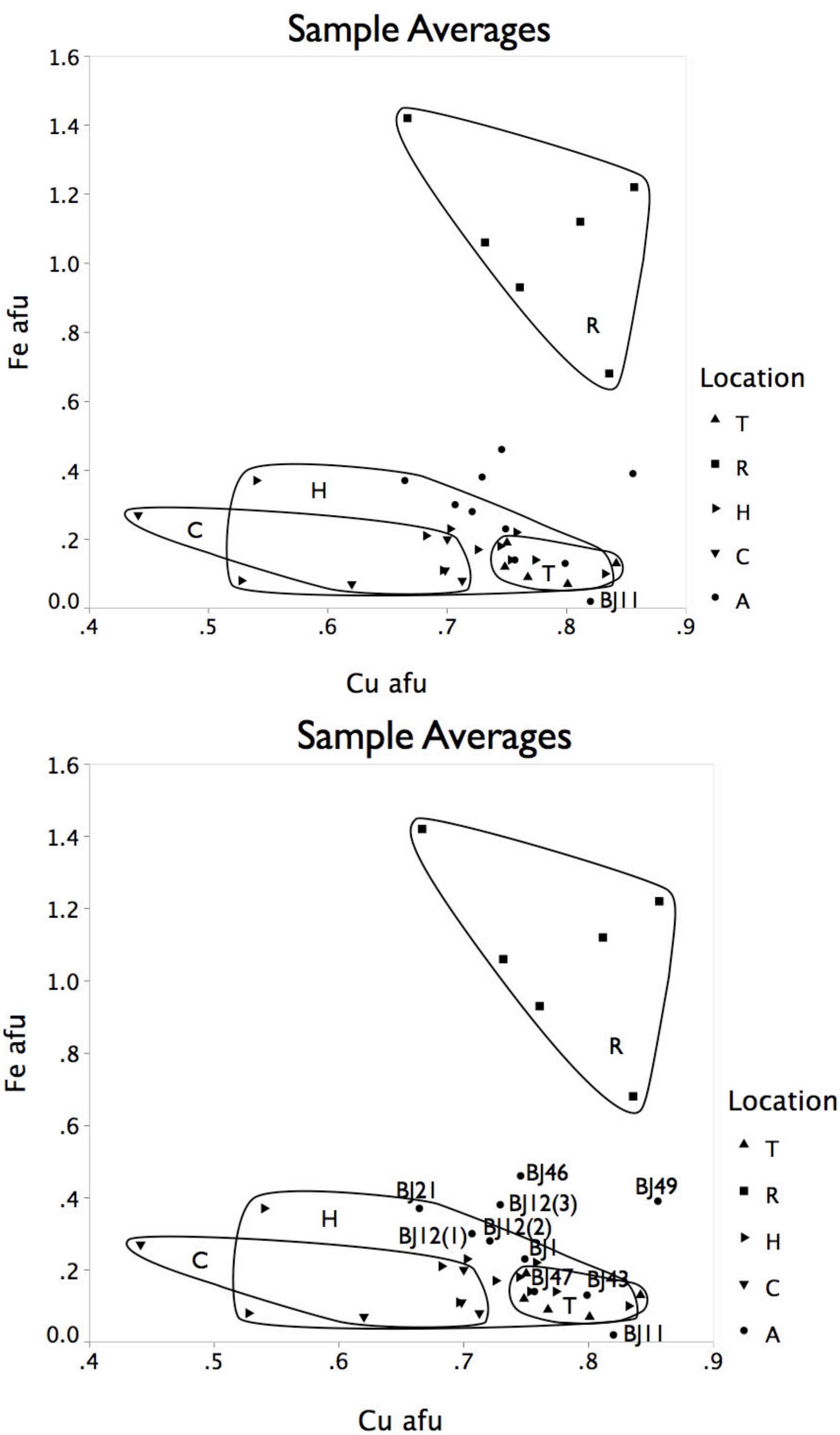

Figure 5.40 Cu and Fe^{+3} sample averages for mines and artifacts T=Tiffany, R=Red Hill, H=Hachita, C=Chalchihuitl, A=Artifacts afu = atoms per formula unit

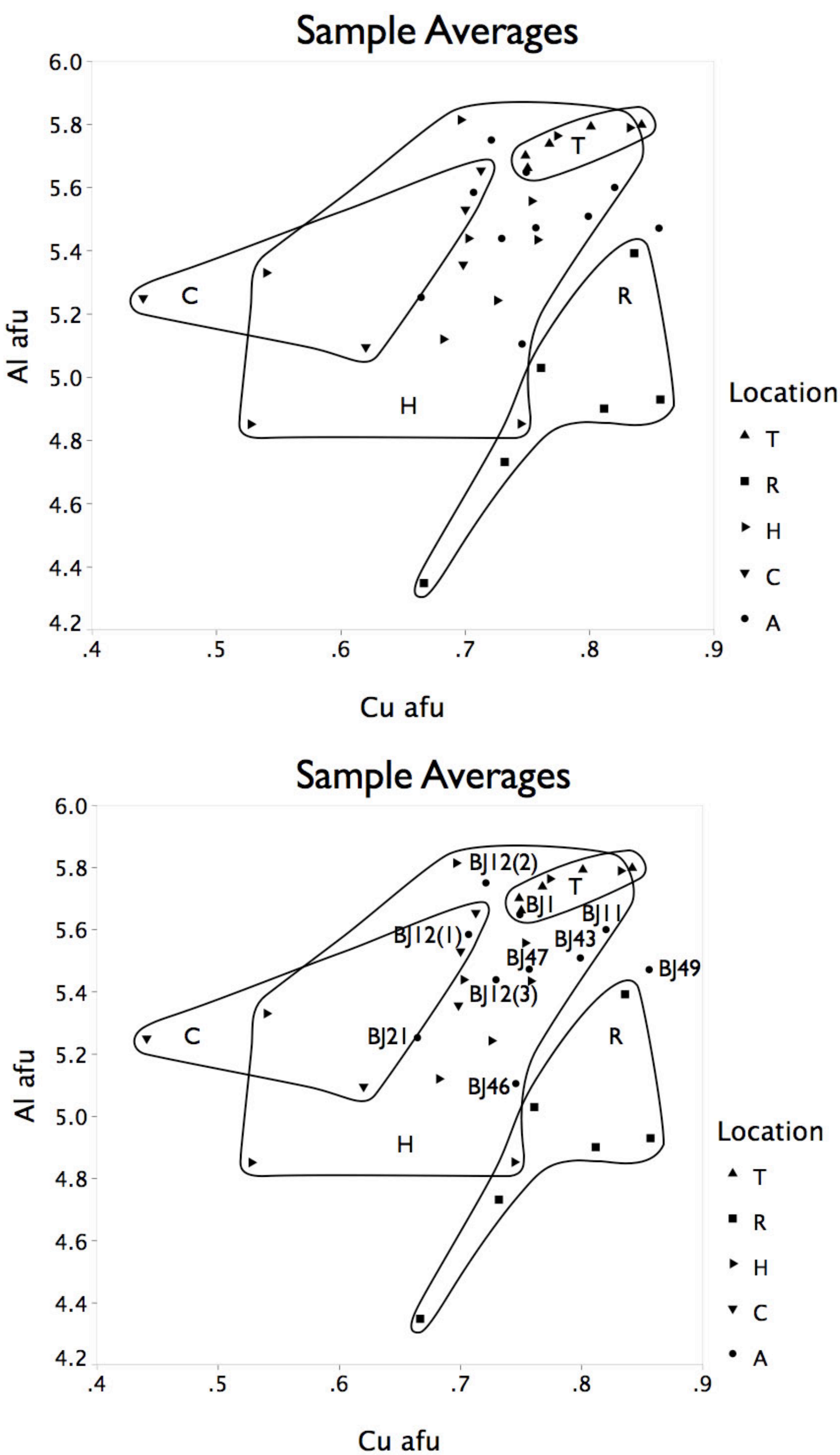

Figure 5.41 Cu and Al sample averages for mines and artifacts.
T=Tiffany, R=Red Hill, H=Hachita, C=Chalchihuitl, A=Artifacts
afu = atoms per formula unit

The plot of Cu to Fe^{+3} cation averages (Fig. 5.40) differs slightly from Figure 5.38 and shows a little more separation between mines. The Red Hill mine remains a distinct cluster while the other three mines spread out along the Cu axis. Hachita is superimposed on portions of Chalchihuitl and Tiffany but in this plot, both Chalchihuitl and Tiffany are distinct from each other. A group of artifact samples are along the border of the Hachita data. BJ1,BJ21, BJ12(2) and BJ12(1) and possibly BJ12(3) all fall reasonably within the Hachita data set. BJ46 and BJ49 have higher Fe and plot beyond Hachita but not yet into the Red Hill range. Artifact samples BJ47 and BJ43, are directly within the Tiffany and Hachita data range, not Chalchihuitl and Hachita as in the Al-Fe plot. Sample BJ11 also plots just outside the lower Tiffany and Hachita border instead of Chalchihuitl as in Figure 5.39.

The comparison of Cu to Al cation averages (Fig. 5.41) expands the mine data differently than Al to Fe^{+3} or Cu to Fe^{+3} and provides a different aspect of mine to artifact relations. Artifacts with copper above ~ 0.72 afu did not come from the Chalchihuitl mine. Artifacts with aluminum values below ~ 5.6 afu did not come from the Tiffany mine. When an artifact fits both of those criteria, the Cerrillos district in general could be eliminated as a potential source. The Hachita mine data set overlies Chalchihuitl, Tiffany and a small area of Red Hill also. Chalchihuitl, Tiffany, and Red Hill remain distinctly different from each other. Six artifacts fall within the Hachita range only: BJ11, BJ12(2), BJ12(3), BJ43, BJ46, BJ47. Artifact samples BJ21 and BJ12 (1) are within the range of either Chalchihuitl or Hachita. BJ1 plots almost directly on top of a Tiffany sample, but it is also within the Hachita area. BJ49 is the only sample that does not fit within a mine area, but it is close to the Red Hill range.

Table 5.8 Mine comparisons by artifact.
T=Tiffany, R=Red Hill, H=Hachita, C=Chalchihuitl

Artifact Sample	Al-Fe	Cu-Fe	Cu-Al
BJ1	H or T	H or T	T or H
BJ11	---	---	H
BJ12(1)	H	H	C or H
BJ12(2)	H	H	H
BJ12(3)	H	H	H
BJ21	H	H	C or H
BJ43	C or H	T or H	H
BJ46	---	---	H
BJ47	C or H	T or H	H
BJ49	H	---	---

When all three of the comparisons are considered together, the degree of similarity between artifact and source is more apparent (Table 5.8). If an artifact has similarity for all three comparisons, the relationship is more suggestive of source. This occurs between Hachita and samples BJ12(2), BJ12(3) and BJ21. Sample BJ1 consistently shows similarity between both Hachita and Tiffany, which strengthens the possibility that it is from Tiffany because it has such a restricted compositional range. Samples BJ 43 and BJ47 are similar to Hachita in all three cases and only Chalchihuitl or Tiffany in two. Three samples, BJ11, BJ46, and BJ49 are similar to Hachita in only one comparison which suggests a weaker relationship as a potential source. Overall, the majority of artifacts are more similar to Hachita while only a few could have also originated from Cerrillos. These results are contrary to what one might expect when considering that the Hachita source is much further away from Blue J than the Cerrillos source.

The compositional range of Hachita is much larger than that of Red Hill, Chalchihuitl and Tiffany which remain distinct in the bivariate plots. This difference is probably due to sampling variability. The Hachita sample set included both collection from tailings and directly from veins in the host rock. A variety of material was intentionally sought to identify the full extent of compositional variability possible. Tiffany and Chalchihuitl have been mined out and no longer have vein material present in host rock. The only turquoise minerals available were from the tailings of mine workings that ended in the late 19th century. Therefore, these samples have been exposed to surface conditions for at least a century. The Red Hill mine sample set was provided by a turquoise collector who obtained them from the mine owners. These samples represent the highest grade, most desirable material from the occurrence and therefore, have not experienced weathering conditions like the other sample sets. Lastly, the turquoise artifacts have come from both surface collection and excavation and have experienced a range of weathering conditions for over a thousand years. Yet, the artifact samples still form a relatively restricted group on plots. The potential effect, or lack thereof, that both surface and subsurface weathering conditions may have on compositional range must be taken into consideration when analyzing prehistoric mines and artifacts.

The solid solution series between turquoise and chalcosiderite has been observed in the results and responsible for the largest amount of variability. The increased mobility of iron in near surface oxidizing conditions related to ore deposits could be a potential cause for increased turquoise mineral alteration to chalcosiderite. The longer a sample is exposed to this environment, the more chalcosiderite-like the composition might become. This possible process contradicts the results of this study, however. The Red Hill samples are not weathered and contain the highest iron levels. Alternately, the artifact samples have arguably been exposed to surface weathering conditions the longest of all the samples, yet do not have the highest Fe levels. The high Fe inclusions observed in the samples with spherulitic texture suggest that alteration is caused by the loss of Fe^{+3} and results in a composition more like endmember turquoise. Oxidation from ferrous to ferric iron could possibly weaken bonds and release it from the crystal structure creating a more stable composition. The direction of alteration then, seems more likely to move from chalcosiderite to turquoise and not the reverse. This would explain why the majority of samples, besides Red Hill, are close to endmember turquoise in composition.

The prevalence of iron oxides observed in all samples shows that factors such as temperature, pH, eH, and pressure must also contribute to turquoise alteration in addition to availability of Fe^{+3}. The pervasive intergrowth of sericite and presence of quartz in samples suggests that the turquoise formed under conditions found in phyllic alteration zones of copper porphyry systems. This would make the turquoise minerals unstable at surface and near surface conditions and could explain why they are often found soft, crumbled, and apparently weathered. Pyrite present in the phyllic alteration mineral assemblage may have provided the Fe of high Fe inclusions, vein-like networks, and numerous iron oxides observed in the turquoise minerals. The separation of high Fe analyses from the calculation of homogeneous turquoise material is useful for identifying mine compositions most similar to turquoise artifacts.

Continued analyses of material from the same mines along with the addition of others will hopefully further clarify the relationship between Fe content, alteration, and weathering in turquoise. These results call attention to the need for large sample sets in order to definitively characterize mines for provenance studies.

Chapter 6 Conclusions

The turquoise mineral analyzed in this study was mineralogically and compositionally heterogeneous. Small-scale sample heterogeneity is visible on all scales. The heterogeneity involves variation within the turquoise group of minerals in addition to close association in the form of intergrowths with other minerals in (e.g. quartz, sericite). Sericite formation as a result of hydrothermal alteration of feldspar occurs during higher temperatures than those where turquoise deposits are currently located. Jarosite also forms in a range of temperatures that may exceed those at surface and near surface conditions. The fine grained intergrowth of turquoise minerals with these minerals raises questions that require continued examination and may have direct bearing on our current understanding of the environment of turquoise mineral formation. Further examination of high Cu inclusions as well as high Fe and others may also prove to be useful in understanding the processes involved in turquoise mineral formation and alteration.

It may be possible that turquoise minerals crystallize under more than one discrete set of geochemical conditions. A variety or range of formation conditions may be responsible for the variety of turquoise occurrences and mineral heterogeneity observed. This heterogeneous aspect of the turquoise mineral group can be advantageous, rather than a hindrance, for studies that address and accommodate turquoise mineral variability. Workers must not only recognize, but address the heterogeneous character of turquoise by using the appropriate techniques. Microscale analysis of turquoise is necessary to achieve the goal of artifact source identification. The use of bulk analysis for turquoise material is not supported by this study because it can not identify and target areas of copper aluminum phosphates for analyses. Micro-techniques (petrography, microprobe, SIMS, etc.) that can resolve and quantify variability on the micrometer scale should be used in lieu of bulk techniques that can not adequately address mineralogical and/or compositional variability.

The results of this study underscore the need for careful sampling methods and detailed study of the geological setting of turquoise deposits. It has also initiated the process of quantification of turquoise deposit variability within and between mining districts. Multiple samples of both fresh and weathered material from a variety of formation environments as well as multiple analyses of each sample are equally important when considering the relevance of results one artifact at a time.

Significant differences between copper, iron, and aluminum levels at various mines have been identified. Close association between turquoise minerals and sericite and quartz on a micro-scale has been observed and recorded. Evidence contrary to common assumptions that turquoise minerals fade in color when exposed to weathering environments has also been found. Continued study of the relationship between physical properties such as color, texture, hardness, and the chemical and mineralogical character of samples will provide archaeologists with improved field identification techniques for working with turquoise artifacts.

Based on preliminary results, it is reasonable to conclude that most of the turquoise artifacts from the Blue J community did not come from the Red Hill mine, Tiffany mine, or Chalchihuitl mine. Caution must be taken when considering the potential source of these artifacts as the Hachita mine. Although there is overlap in compositional ranges, these results are based on only limited samples from four mines and more samples from Hachita and more mine deposits should be included in the dataset before definitive assertions of similarity are made. This provenance study entails the process of elimination where the lack of compositional range overlap between an artifact and source is a conclusive result that provides useful information for archaeologists. The ability to effectively rule out a suite of potential sources of turquoise artifacts presents interesting and exciting possibilities for further archaeological research especially when combined with information about the origins of other artifact classes.

The next step in this study will be to define the range of major elements in greater detail by additional sampling, analysis, and comparison of outcrops within the Hachita and Cerrillos mining districts and subsequent addition of new mining districts and artifacts. There will also be continued evaluation of non-destructive XRD techniques for use with artifacts. The mineralogical heterogeneity identified in this study provides an additional indicator of source based on minerals unique to the geology of each mine.

The full range of compositional variety has yet to be thoroughly identified at the deposit and sample scale. The use of additional approaches involving isotopic analysis will be considered once this has been achieved. Major element isotope analysis that accommodates variability in turquoise minerals could be used to refine the characterization process as would trace elements indicative of specific geologic sources. These techniques in addition to XRD could provide decisive methods for distinguishing source in areas of compositional overlap.

This approach will continue to attempt to elucidate the understudied processes of turquoise mineral genesis, alteration, and weathering through detailed study of the host rocks and environments of formation. The goal is to continue to identify and understand the potential factors responsible for the heterogeneity observed in turquoise deposits and artifacts using appropriate techniques. Once the full extent of geochemical variability possible in the turquoise mineral group has been quantified, it can be successfully applied to determine the geologic origin of cultural turquoise artifacts.

References

Beard, R.D., 2001, Turquoise at Turquoise Mountain, Old Hachita, New Mexico, 22nd Annual New Mexico Mineral Symposium: Socorro, New Mexico, New Mexico Institute of Mining and Technology.

Bland, W., and Rolls, D., 1998, Weathering : an introduction to the scientific principles: London; New York, Arnold, x, 271 p. p.

Craig, M.S., Vaughn, D.J., and Skinner, B.J., 2001, Resources of the Earth: New York, Prentice Hall.

Channell, R., 2000, Magmatic history of the Little Hatchet Mountains, Hidalgo and Grant Counties, southwestern New Mexico, *in* McMillan, N.J., Lawton, T.F., Heizler, M.T., Esser, R.P., and McLemore, V.T., eds., Guidebook - New Mexico Geological Society, Volume 51: United States, New Mexico Geological Society : Socorro, NM, United States, p. 141-148.

Craig, M.S., Vaughn, D.J., and Skinner, B.J., 2001, Resources of the Earth: New York, Prentice Hall.

Delvasto, P., Valverde, A., Ballester, A., Munoz, J.A., Gonzalez, F., Blazquez, M.L., Igual, J.M., and GarcÌa-Balboa, C., 2008, Diversity and activity of phosphate bioleaching bacteria from a high-phosphorus iron ore: Hydrometallurgy, v. 92, p. 124-129.

Erskine, D.W., and Smith, G.A., 1993, Compositional characterization of volcanic products from a primarily sedimentary record; the Oligocene Espinaso Formation, north-central New Mexico; with Suppl. Data 9325: Geological Society of America Bulletin, v. 105, p. 1214-1222.

Foord, E.E., and Taggart, J.E., 1998, A reexamination of the turquoise group: the mineral aheylite, planerite (redefined), turquoise and coeruleolactite: Mineralogical Magazine, v. 62, p. 93-111.

Foord, E.E., Taggart, J.E., and Prewitt, C.T., 1986, Reassessment of the turquoise group; redefinition of planerite, ([1])Al (sub 6) (PO (sub 4)) (sub 2) (PO (sub 3) OH) (sub 2) (OH) (sub 8) .4H (sub 2) O and aheylite, FeAl (sub 6) (PO (sub 4)) (sub 4) (OH) (sub 8) .4H (sub 2) O, a new member of the group, Papers and Proceedings of the General Meeting - International Mineralogical Association, p. 102.

Gaines, R.V., Skinner, H.C.W., Foord, E.E., Mason, B., and Rosenzweig, A., 1997, Dana's New Mineralogy: The System of Mineralogy of James Dwight Dana and Edward Salisbury Dana: New York, John Wiley and Sons.

Giles, D.L., 1995, Cerrillos mining district, Guidebook - New Mexico Geological Society, Volume 46: United States, New Mexico Geological Society : Socorro, NM, United States, p. 61-62.

Gillerman, E., 1964, Mineral deposits of western Grant County, New Mexico: United States, New Mexico Bureau of Mines and Mineral Resources : Socorro, NM, United States.

—1970, Mineral deposits and structural pattern of the Big Burro Mountains, New Mexico: United States, New Mexico Geological Society : Socorro, NM, United States, 115-121 p.Guilbert, J.M., and Park, C.F., 1986, The Geology of Ore Deposits: New York, W. H. Freeman.

Hamblin, W.K., and Christiansen, E.H., 2004, Earth's Dynamic Systems: Upper Saddle River, Prentice-Hall, Inc., 759 p.

Harbottle, G., Weigand, P.C., and Foster, M.S., 1994, Archaeological turquoise from Pueblo Grande and comparison with the turquoise database, Material Culture, Phoenix : Soil Systems Publications in Archaeology, p. 369-389.

Hedlund, D.C., 1985, Geology, mines, and prospects of the Tyrone Stock and vicinity, Grant County, New Mexico: United States, U. S. Geological Survey : Reston, VA, United States.

Hotujec, C., and Kantner, J., 2007, Ornaments from Chaco-Era Outlying Communities: The Case of the Blue J Community, 72nd Society for American Archaeology Annual Meeting: Austin, Texas.

Hull, S., Fayek, M., Mathien, F.J., Shelley, P., and Durand, K.R., 2008, A new approach to determining the geological provenance of turquoise artifacts using hydrogen and copper stable isotopes: Journal of Archaeological Science, v. 35, p. 1355-1369.

Hurlbut, J., Cornelius S., and Sharp, E.W., 1998, Dana's Minerals and How to Study Them: New York, John Wiley and Sons.

Jackson, J.A., Mehl, J.P., Neuendorf, K.K.E., and American Geological Institute., 2005, Glossary of geology: Alexandria, Va., American Geological Institute, xii, 779 p. p.

Johnson, D.W., 1903, The geology of the Cerrilos Hills, New Mexico: Annals of the New York Academy of Sciences, p. 173-246. 85

Kantner, J., 2004, Ancient Puebloan Southwest: Cambridge, UK ; New York, Cambridge University Press, xii, 324 p. p.

Kim, J., Simon, A.W., Ripoche, V., Mayer, J.W., and Wilkens, B., 2003, Proton-induced x-ray emission analysis of turquoise artefacts from Salado Platform Mound sites in the Tonto Basin of central Arizona: Measurement Science & Technology, v. 14, p. 1579-1589.

Kolitsch, U., and Giester, G., 2000, The crystal structure of faustite and its copper analogue turquoise: Mineralogical Magazine, v. 64, p. 905-913.

Lekson, S.H., 1999, The Chaco meridian : centers of political power in the ancient Southwest: Walnut Creek, Calif., AltaMira Press, 235 p. p.

Mathien, F.J., 1981, Neutron Activation of Turquoise Artifacts From Chaco Canyon, New Mexico: Current Anthropology, v. 22, p. 293-294.

—, 2001, The organization of turquoise production and consumption by the prehistoric Chacoans: American Antiquity, v. 66, p. 103-118.

Mathien, F.J., and Olinger, B., 1992, An experiment with X-ray fluorescence to determine trace element variability in turquoise composition, *in* Duran, M.S., and Kirkpatrick, D.T., eds., Archaeology, Art, and Anthropology: Papers in Honor of J. J. Brody, Volume 18: Albuquerque, The Archaeological Society of New Mexico, p. 123–134.

Maynard, S.R., 2005, Laccoliths of the Ortiz porphyry belt, Santa Fe County, New Mexico: New Mexico Geology, v. 27, p. 3-21.

Maynard, S.R., Lisenbee, A.L., and Rogers, J., 2002, Preliminary Geologic Map of the Picture Rock 7.5-Minute Quadrangle Santa Fe County, Central New Mexico, Volume Open-File Report DM-49, New Mexico Bureau of Mines and Mineral Resources.

McLemore, V.T., 2000, The Eureka mining district, Grant County, New Mexico, Guidebook - New Mexico Geological Society, Volume 51: United States, New Mexico Geological Society : Socorro, NM, United States, p. 21-22.

Murr, L.E., and Berry, V.K., 1976, Direct observations of selective attachment of bacteria on low-grade sulfide ores and other mineral surfaces: Hydrometallurgy, v. 2, p. 11-24.

Nriagu, J.O., and Moore, P.B., 1984, Phosphate minerals: Berlin ; New York, Springer-Verlag, p. vi, 442 p.

O'Neill, A.J., and Thiede, D.S., 1982, Silver City Quadrangle, New Mexico and Arizona: National Uranium Resource Evaluation: Grand Junction, US Department of Energy.

Paige, S., 1912, The origin of turquoise in the Burro Mountains, New Mexico: Economic Geology, v. 7, p. 382-392.

Plog, S., 1997, Ancient peoples of the American Southwest: New York, N.Y., Thames and Hudson, 224 p. p.

Pogue, J.E., 1915, Turquois: Glorieta, New Mexico, The Rio Grande Press.

Ronzio, A.R., and Salmon, M.L., 1967, Relation between source and composition of turquoise: The Journal of the Colorado-Wyoming Academy of Science, v. 5, p. 30-31.

Ruppert, H., 1982, Zur Verbreitung und Herkunft von Turkis und Sodalith in prekolumbischen Kulturen der Kordilleren. [On the diffusion and origin of turquoise and sodalite in Precolumbian cultures of the Cordilleras.]: Baessler-Archiv, p. 69-124.

—, 1983, Geochemische Untersuchungen an Turkis und Sodalith aus Lagerstatten und prekolumbianischen Kulturen der Kordilleren. [Geochemical investigation of turquoise and sodalite from mineral deposits and Precolumbian cultures of the Cordilleras.]: Berliner Beitrege zur Archeometrie, p. 101-209.

—, 1984, Fremdelemente in Tuerkisen als Indikator fuer Herkunft und Handelsaustausch des Minerals in praekolumbischen andinen Kulturen (Foreign elements in turquoise as an indicator of the origin and trade of minerals in pre-Colombian Andean culture): Fortschritte der Mineralogie, Beiheft, v. 62, p. 199-200.

Salmon, M., and Ronzio, A.R., 1962, The X-ray fluorescence analysis of turquoise: The Journal of the Colorado-Wyoming Academy of Science, v. 5, p. 19.

Sawkins, F.J., 1990, Metal deposits in relation to plate tectonics: Berlin ; New York, Springer-Verlag, xix, 461 p. p.

Sigleo, A.C., 1975, Turquoise mine and artifact correlation for Snaketown site, Arizona: Science, v. 189, p. 459-560.

Sigleo, A.M.C., 1970, [Master's thesis]: Albuquerque, University of New Mexico.

Smith, G.A., 1995, Supplemental road log 3, Cerrillos to I-25 via Waldo, Guidebook - New Mexico Geological Society, Volume 46: United States, New Mexico Geological Society : Socorro, NM, United States, p. 77-79.

Snow, C.H., 1891, Turquois in southwestern New Mexico: American Journal of Science, v. 41, p. 511-512.

Snow, D.H., 1973, Prehistoric Southwestern turquoise industry: Palacio, v. 79, p. 33-51.
86

Stearns, C.E., 1953, Early Tertiary vulcanism in the Galisteo- Tonque area, north-central New Mexico: American Journal of Science, v. 251, p. 415-452.

Sterrett, D.B., 1908, Precious Stones: Mineral Resources of the United States, v. Part 2- Nonmetallic Products, p. 795-832.

—, 1909, Precious Stones: Mineral Resources of the United States, v. Part 2 - Nonmetallic Products, p. 805-853.

—, 1911, Gems and Precious Stones: Mineral Resources of the United States, v. Part 2 - Nonmetals, p. 739-795.

Van Wambeke, L., 1971, The problem of cation deficiencies in some phosphates due to alteration processes: American Mineralogist, v. 56, p. 1366-1384.

Weigand, P.C., 1982, Sherds associated with turquoise mines in the southwestern U.S.A: Pottery southwest, v. 9, p. 4-6.

—, 1999, Observations on ancient mining within the northwestern regions of the Mesoamerican civilization, with emphasis on turquoise, In Quest of Mineral Wealth: Aboriginal and Colonial Mining and Metallurgy in Spanish America, Baton Rouge : Geoscience Publications, Louisiana State University.

Weigand, P.C., and Harbottle, G., 1993, Role of turquoises in the ancient Mesoamerican trade structure, American Southwest and Mesoamerica: Systems of Prehistoric Exchange, New York : Plenum, p. 159-177.

Weigand, P.C., Harbottle, G., and Sayre, E.V., 1977, Turquoise sources and source analysis: Mesoamerica and the southwestern U.S.A, Exchange systems in prehistory, New York : Academic Press, c1977, p. 15-34.

Welch, J.R., and Triadan, D., 1991, Canyon Creek turquoise mine, Arizona: Kiva, v. 56, p. 145-164.

Wicander, R., and Monroe, J.S., 1995, Essentials of geology: Minneapolis/St. Paul, West Pub. Co., xxvi, 428 p. p.

Windes, T.C., 1992, Blue Notes: The Chacoan Turquoise Industry in the San Juan Basin, *in* Doyle, D.E., ed., Anasazi Regional Organization and the Chaco System, Volume 5: Albuquerque, Maxwell Museum of Anthropology, p. 159-168.

Young, J.R., 2000, Volcanology, geochemistry and structural geology of the Upper Cretaceous Hidalgo Formation, southwestern New Mexico, *in* McMillan, N.J., Lawton, T.F., and Esser, R.P., eds., Guidebook - New Mexico Geological Society, Volume 51: United States, New Mexico Geological Society : Socorro, NM, United States, p. 149-156.

Zalinski, E.R., 1907, Turquoise in the Burro Mountains, New Mexico: Economic Geology, v. 2, p. 464-492.

Zeller, R.A., Jr., 1970, Geology of the Little Hatchet mountains, Hidalgo and Grant counties, New Mexico: United States, New Mexico Bureau of Mines and Mineral Resources : Socorro, NM, United States.

Appendix A: Artifact Photographs

Artifact Sample BJ1
1 division = 1 mm

Provenience: Blue J Archaeological Project, NM, Site 1 8S2W Level 17 6/03

Artifact Sample BJ11
1 division = 1 mm

Provenience: Blue J Archaeological Project, New Mexico
Site #11, Wall 29 West, 6/17/05

Artifact Sample BJ12(1)
1 division = 1 mm

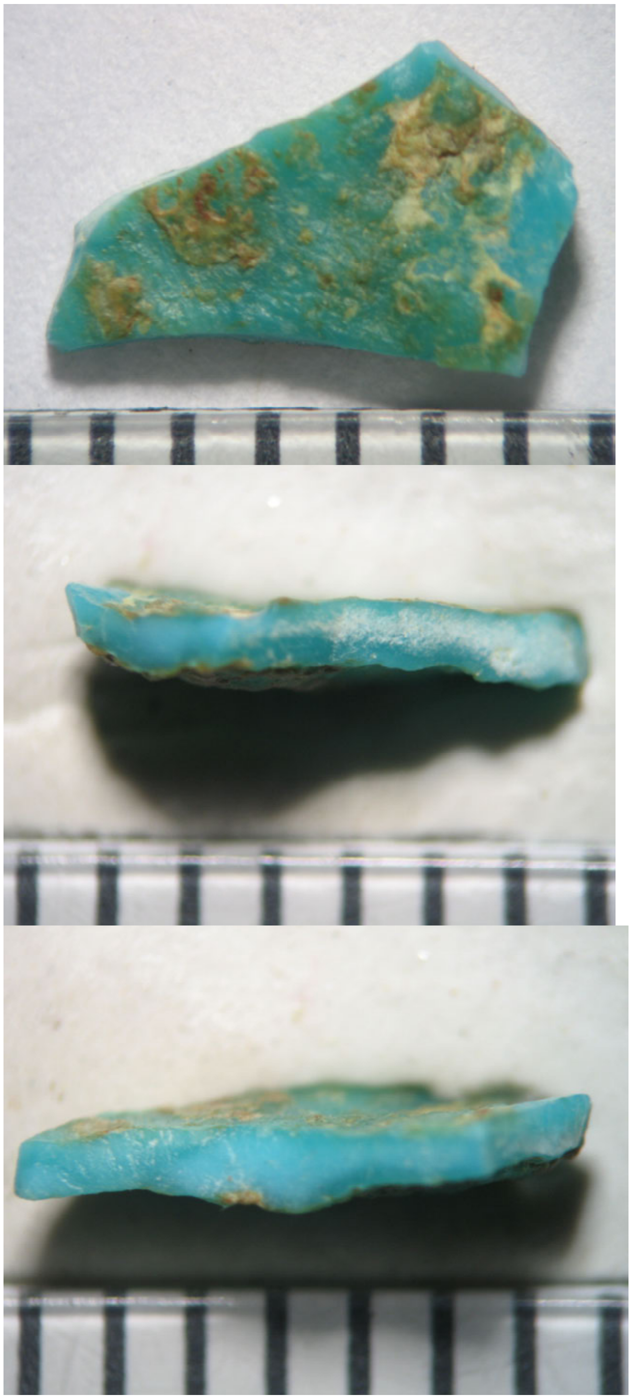

Provenience: Blue J Archaeological Project
Site 12 Surface Collection 6/14/06

Artifact Sample BJ12(2)
1 division = 1 mm

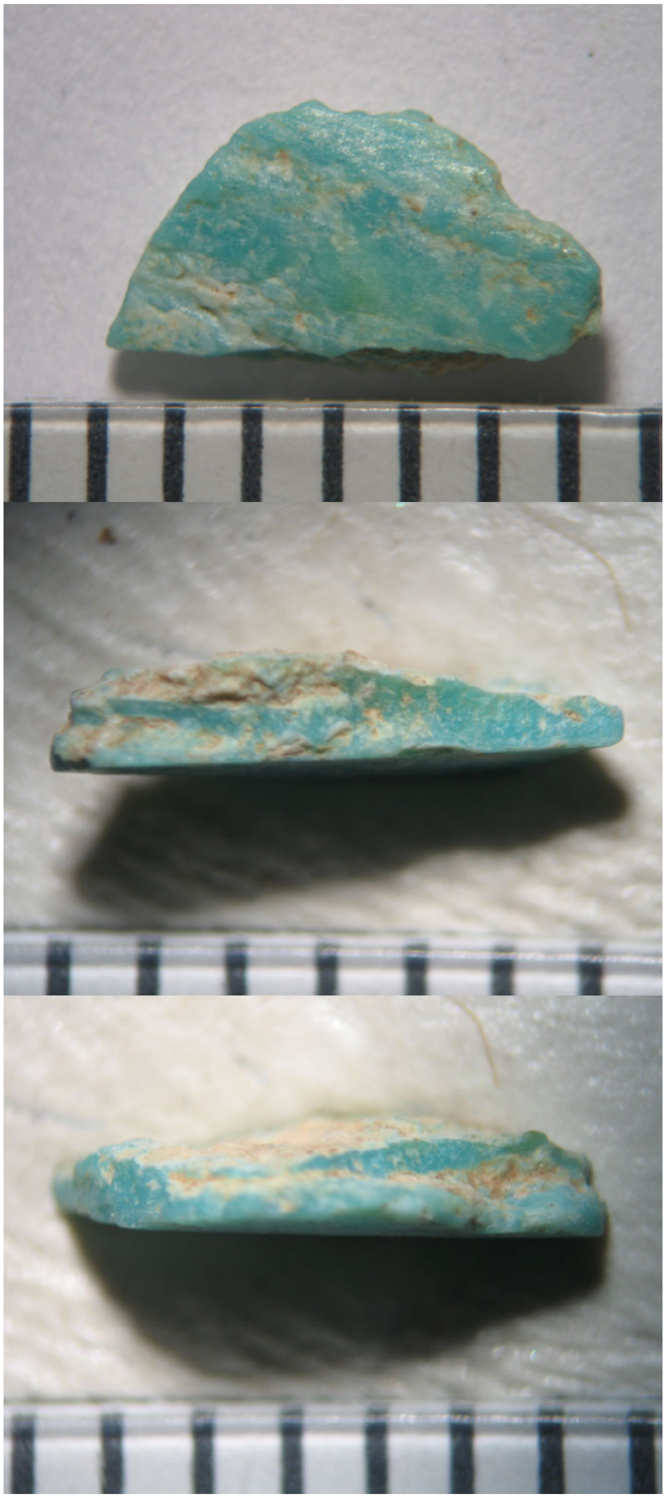

Provenience: Blue J Archaeological Project
Site 12 Surface Collection 6/14/06

Artifact Sample BJ12(3)
1 division = 1 mm

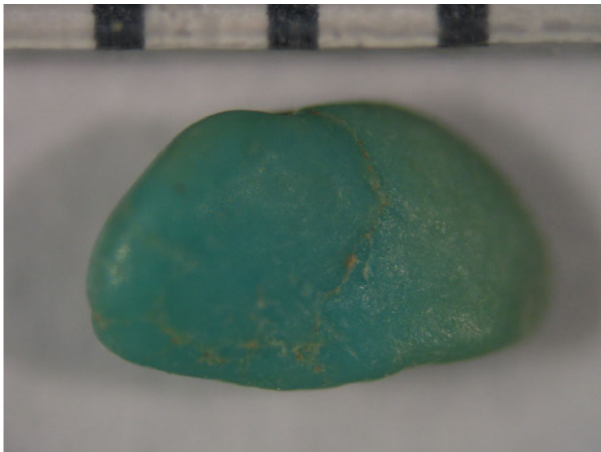


Provenience: Blue J Archaeological Project
Site 12 Surface Collection 6/14/06

Artifact Sample BJ21
1 division = 1 mm

Provenience: BJ Archaeological Project, NM
Site # 21, Unit 2S 3E, Level 1
(surface - 50 cmbmd), 5/31/06

Artifact Sample BJ43
1 division = 1 mm

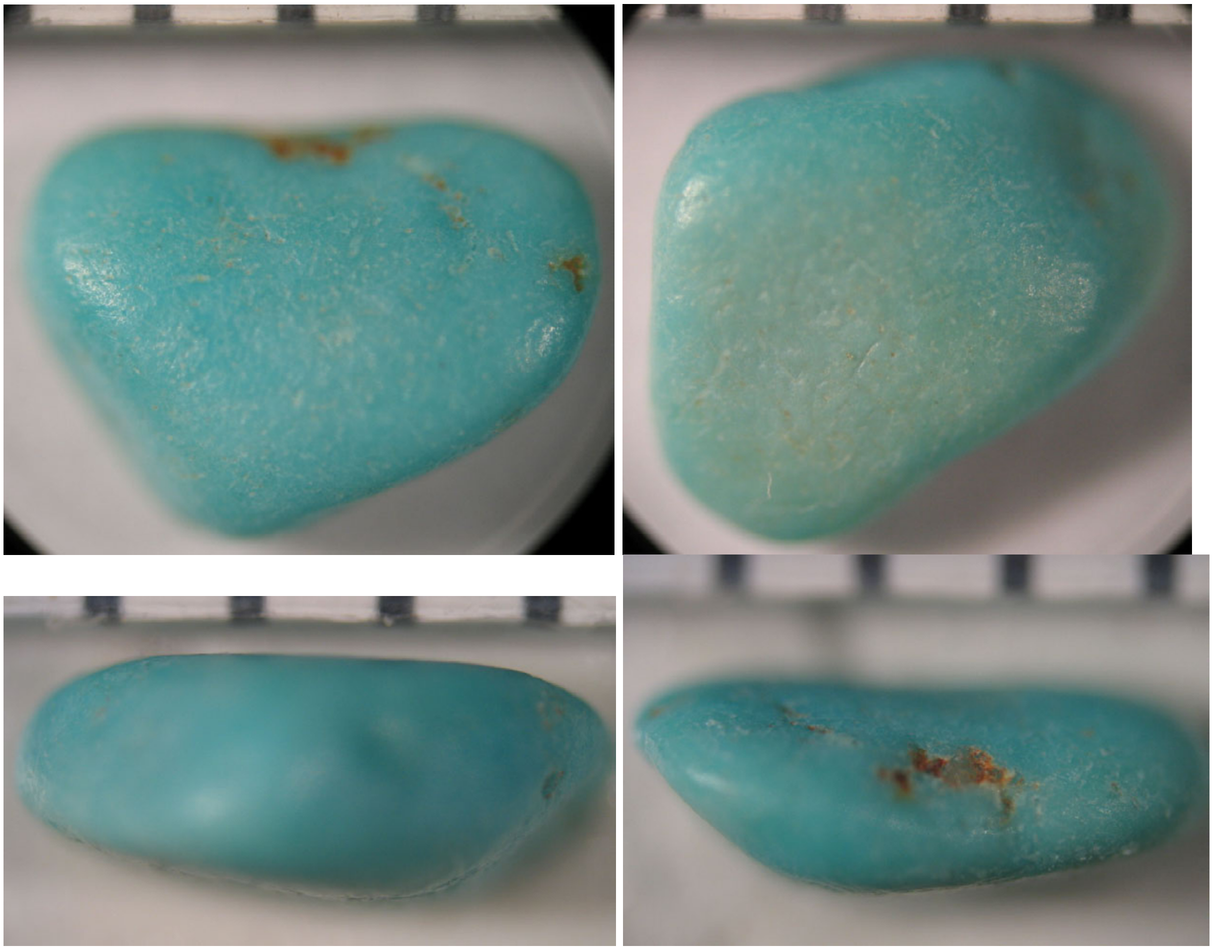

Provenience: Blue J Archaeological Project
Site #43 Surface Collection

Artifact Sample BJ46
1 division = 1 mm

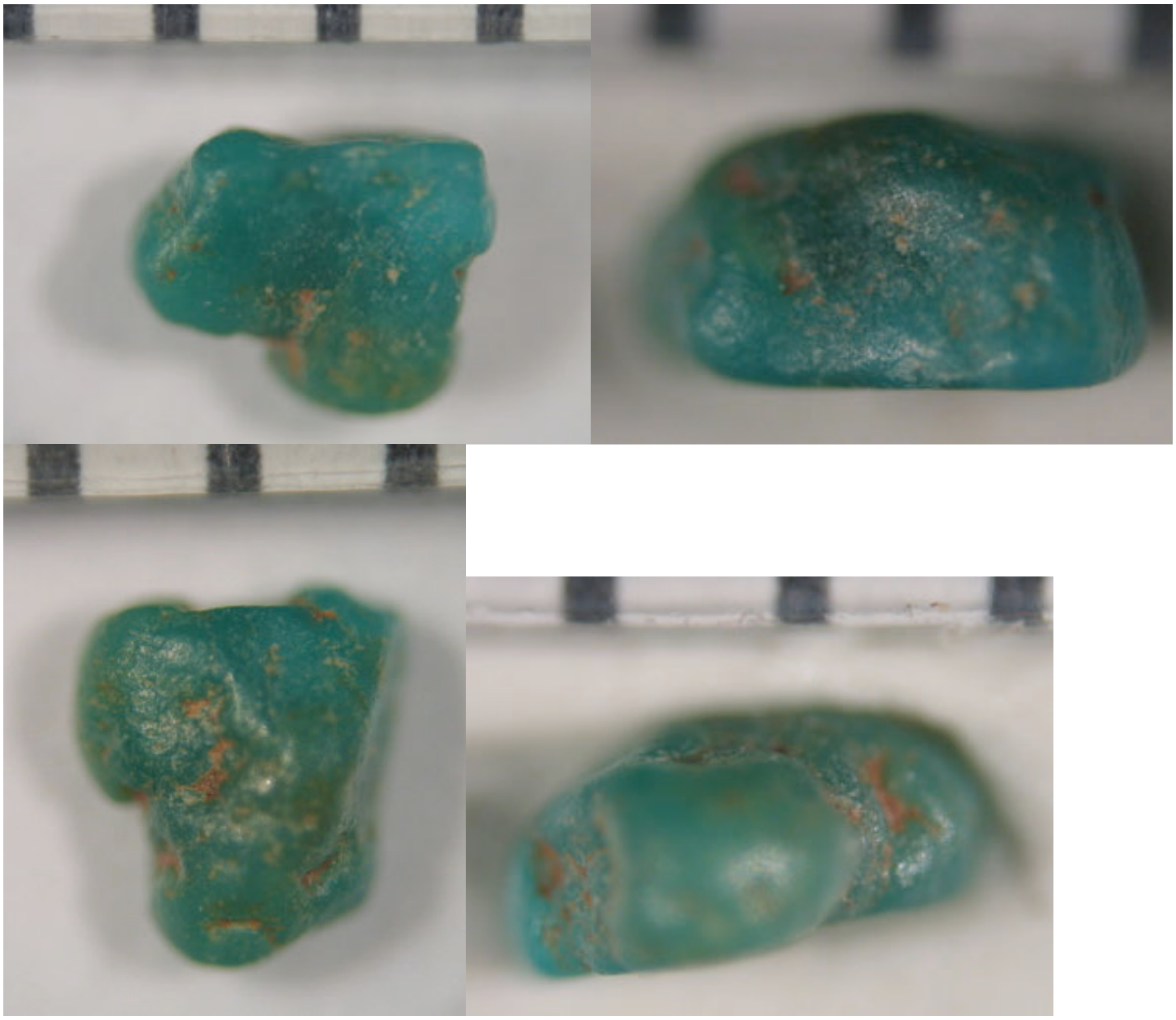

Provenience:
Blue J Archaeological Project, NM
Site #46, Surface Collection

Artifact Sample BJ47
1 division = 1 mm

Provenience: Blue J Archaeological Project, NM
Site #47 Surface Collection

Artifact Sample BJ49
1 division = 1 mm

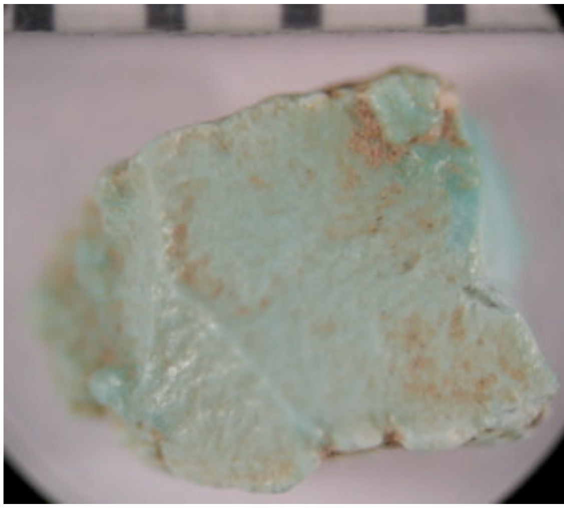

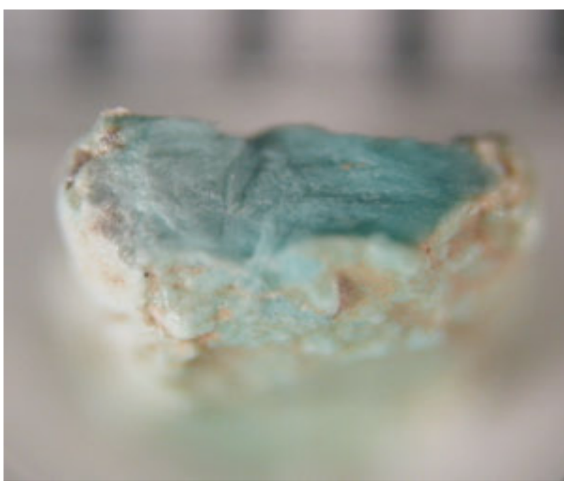

Provenience: BJ Archaeological Project
Site #49, Wall 1 Exterior, 6/10/04

<u>Appendix B: Mine Sample Photographs</u>

Azure Mine, Hachita Mining District, New Mexico

Turquoise Mountain

Azure Mine, Turquoise Mountain. Backpack at bottom left for scale.

Mine wall view facing southwest.

Mine wall view facing northeast.

Turquoise veins in fractures.

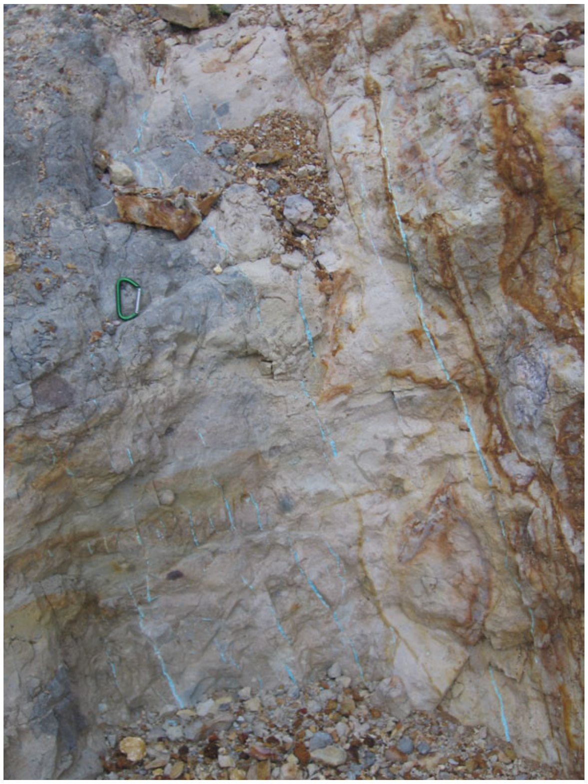


Turquoise occurs in contact zone between gray and tan altered, oxidized rocks.

Samples were collected directly from veins.

Samples were also collected from tailings.

Samples of weathered material were collected.


Samples were rinsed in water and air-dried.


Variability in texture, relative hardness and host rock was recorded.

Sample TM57

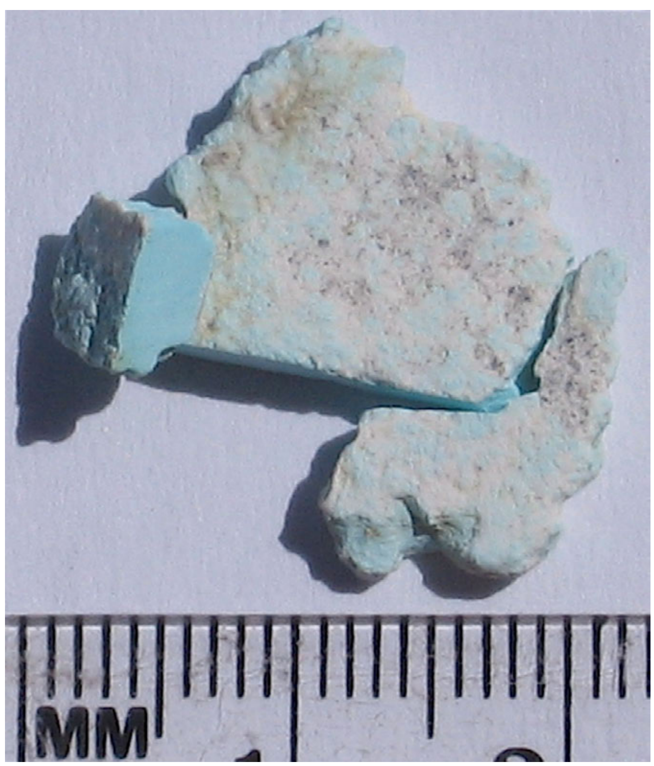

Sample TM66

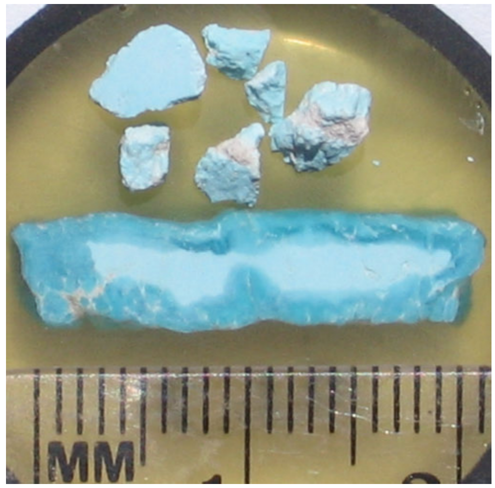

Sample TM68

Sample TM70

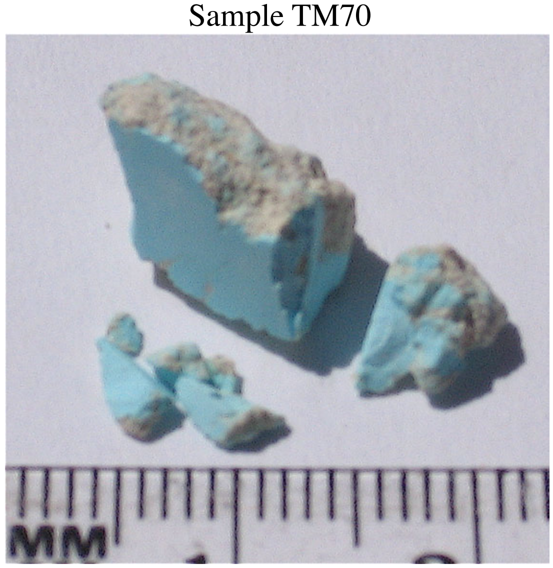

Sample TM91

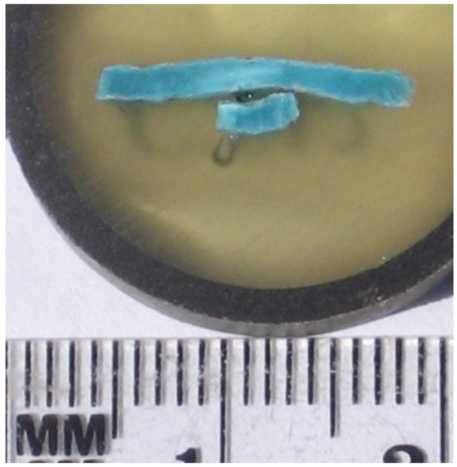

Sample TM95

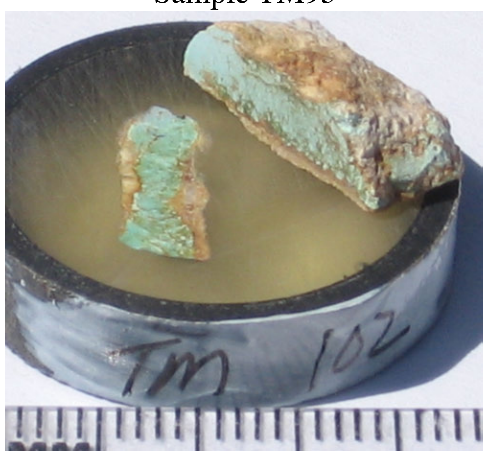

Sample TM102

Sample TM109

Sample TM114

Sample TM115

Sample TM118

Sample TM127

Red Hill Mine, White Signal Mining District, New Mexico

A set of samples were donated by the Turquoise Museum in Albuquerque, NM

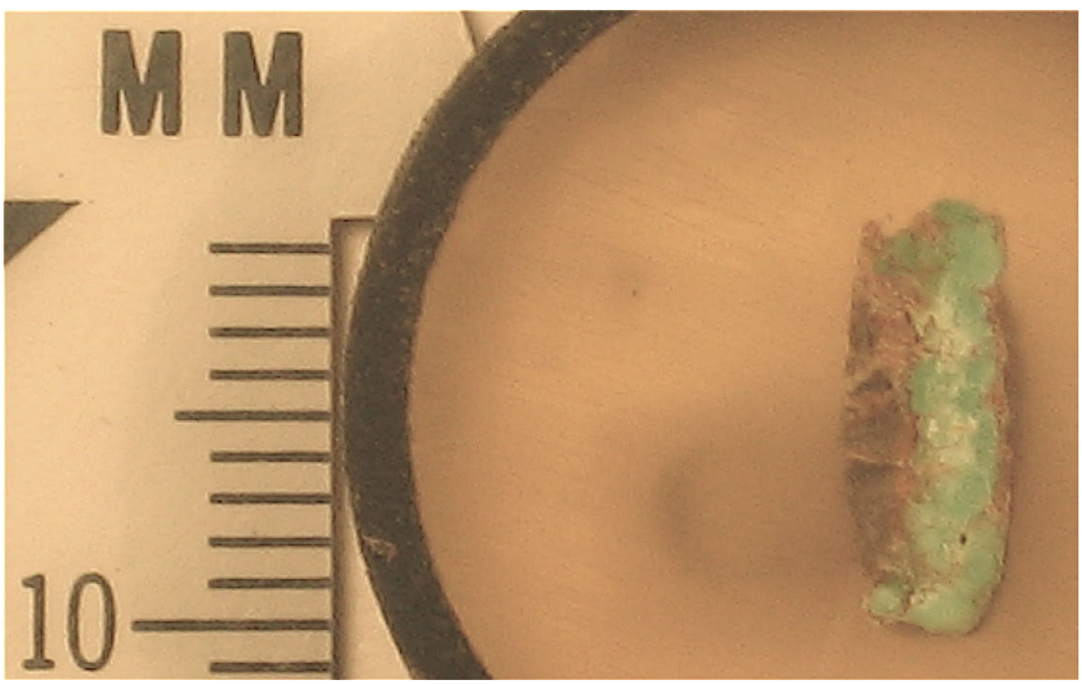

Sample RH9

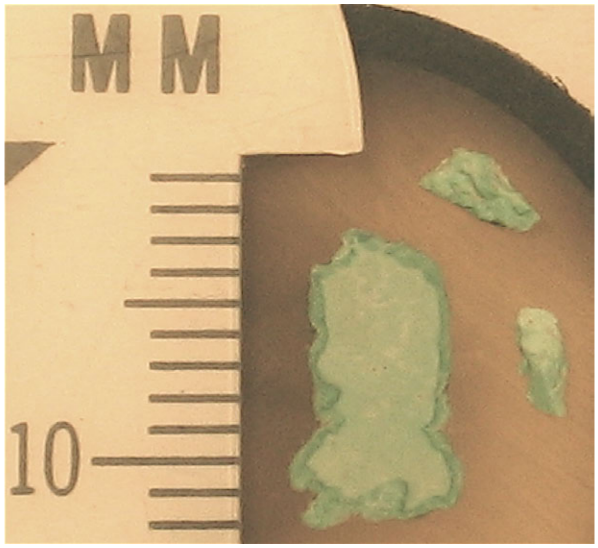

Sample RH10

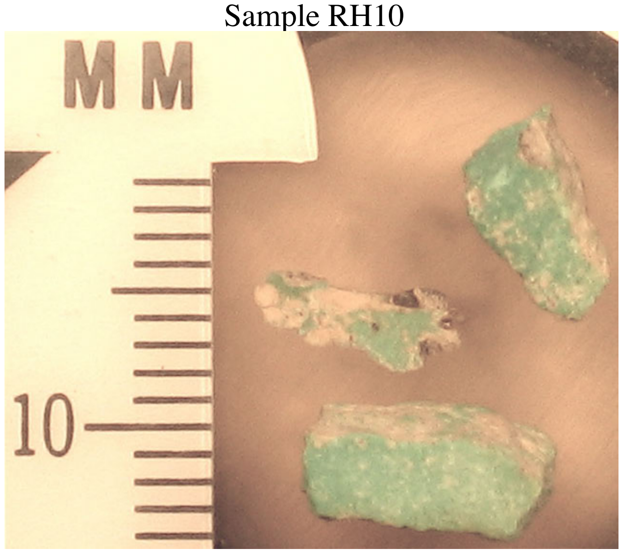

Sample RH13

Sample RH16

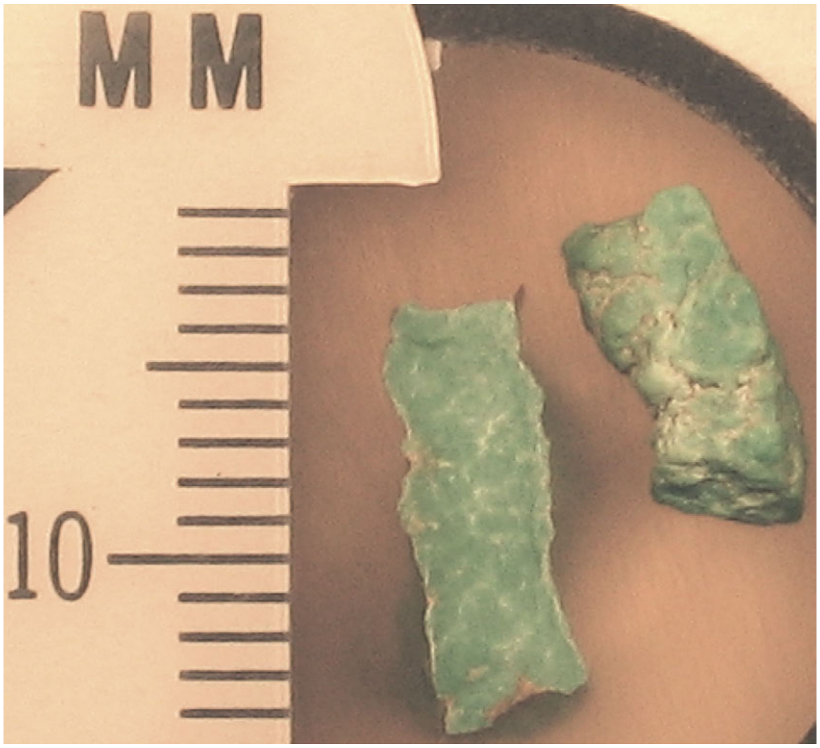

Sample RH17

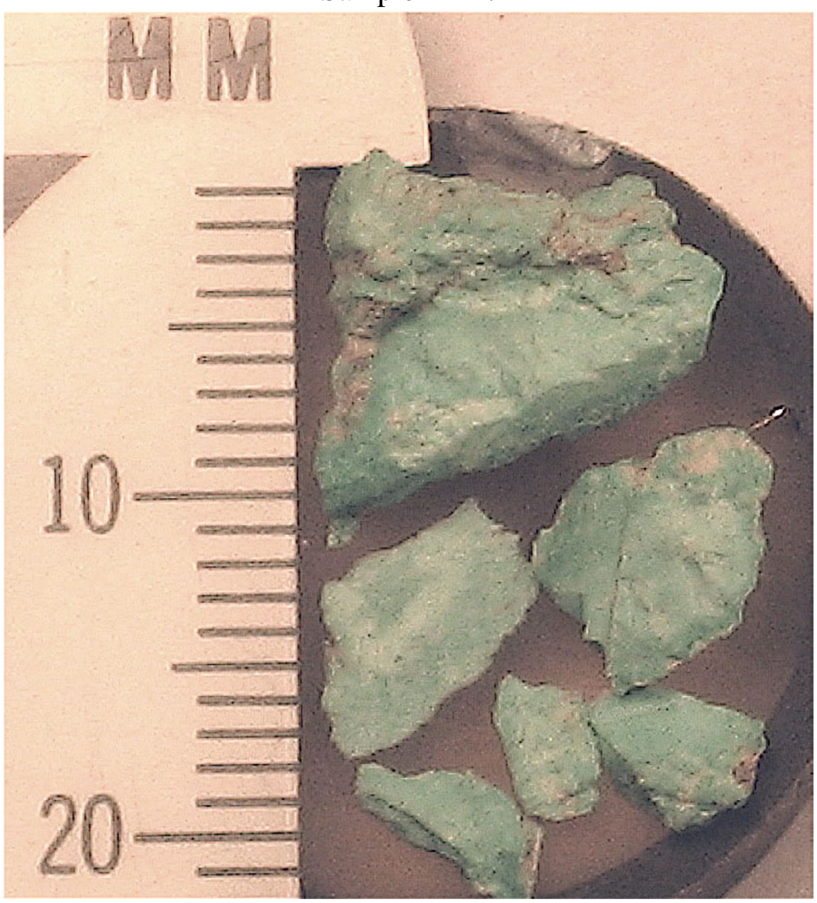

Sample RH19

Chalchihuitl Mine, Cerrillos Mining District, New Mexico

Mount Chalchihuitl is in the Cerrillos Hills, today part of an historic park.


This is one of several prehistoric turquoise mines on Mount Chalchihuitl.

The entrance to some turquoise mines are not overtly apparent aiding in preservation.

Evidence of fire is preserved in charcoal deposits and soot-stained roofs.

Fragments of stone mining implements can be seen scattered among the tailings.

Prehistoric mining tools found at Cerrillos are on display at the local mining museum.


The main pit has two depressions in the walls with vein scars, one seen in the center of the photo.

The other is at the base of the wall on the opposite side of the pit, nearer the top of the mountain.

Evidence of fire can be seen on the rooftop of the entrance.

Mining activity has ceased and only a very small amount of turquoise is left in the vein.

Samples were collected from the tailings in the main pit.

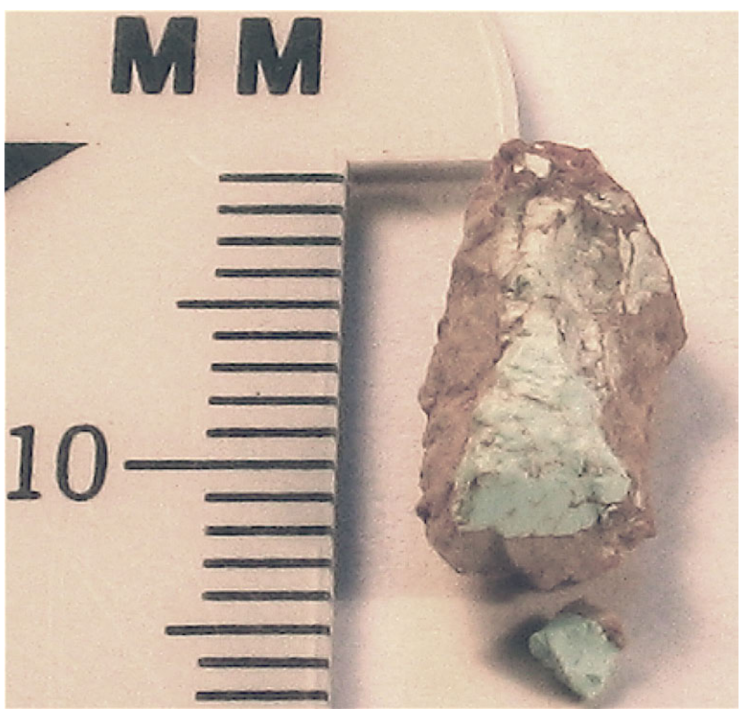

Sample CH22

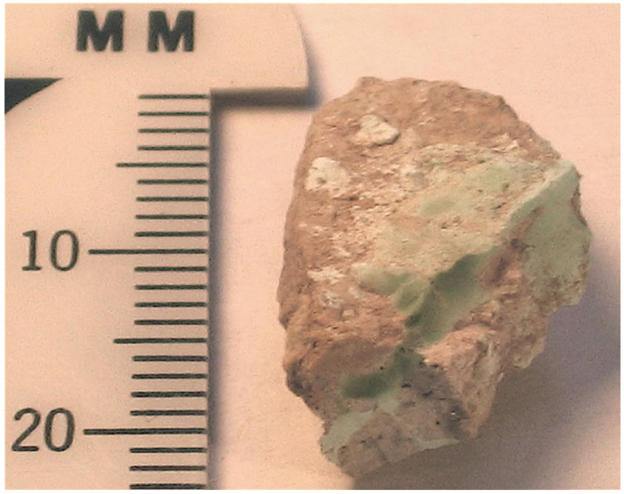

Sample CH23

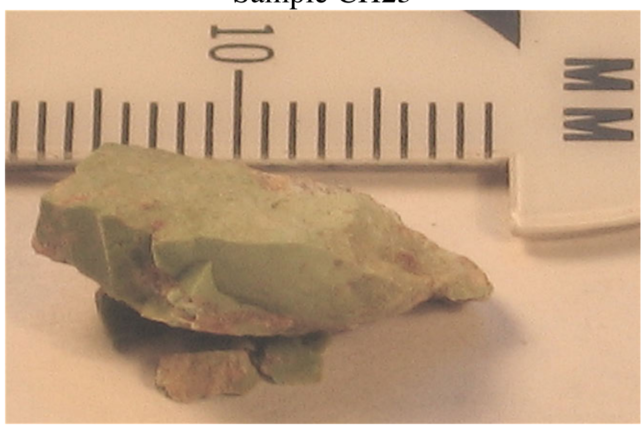

Sample CH26

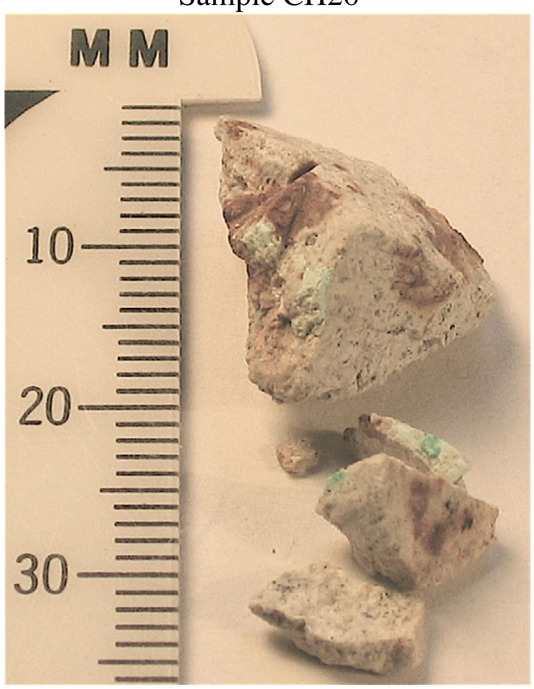

Sample CH27

Sample CH28

Sample CH34

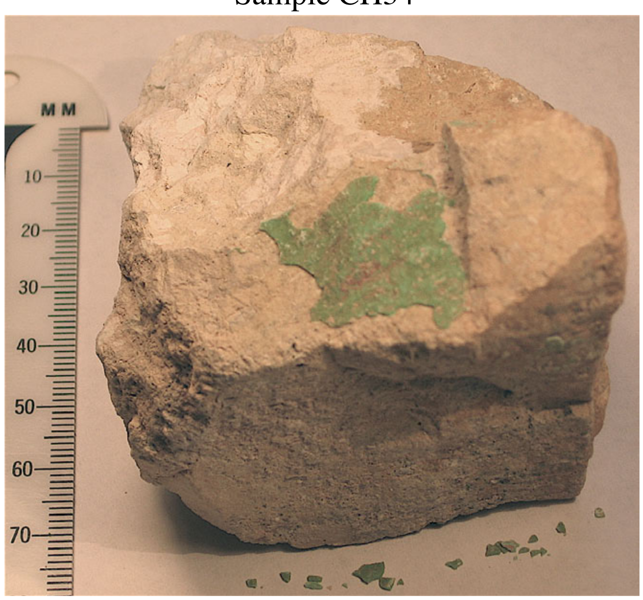

Sample CH35

The Tiffany Mine, Cerrillos Mining District, New Mexico

Currently called the Millennium Mine and located on private property.

.

The main mine shaft.


Prehistoric tool scars visible near the top of the shaft.

Prehistoric stone mining tools.

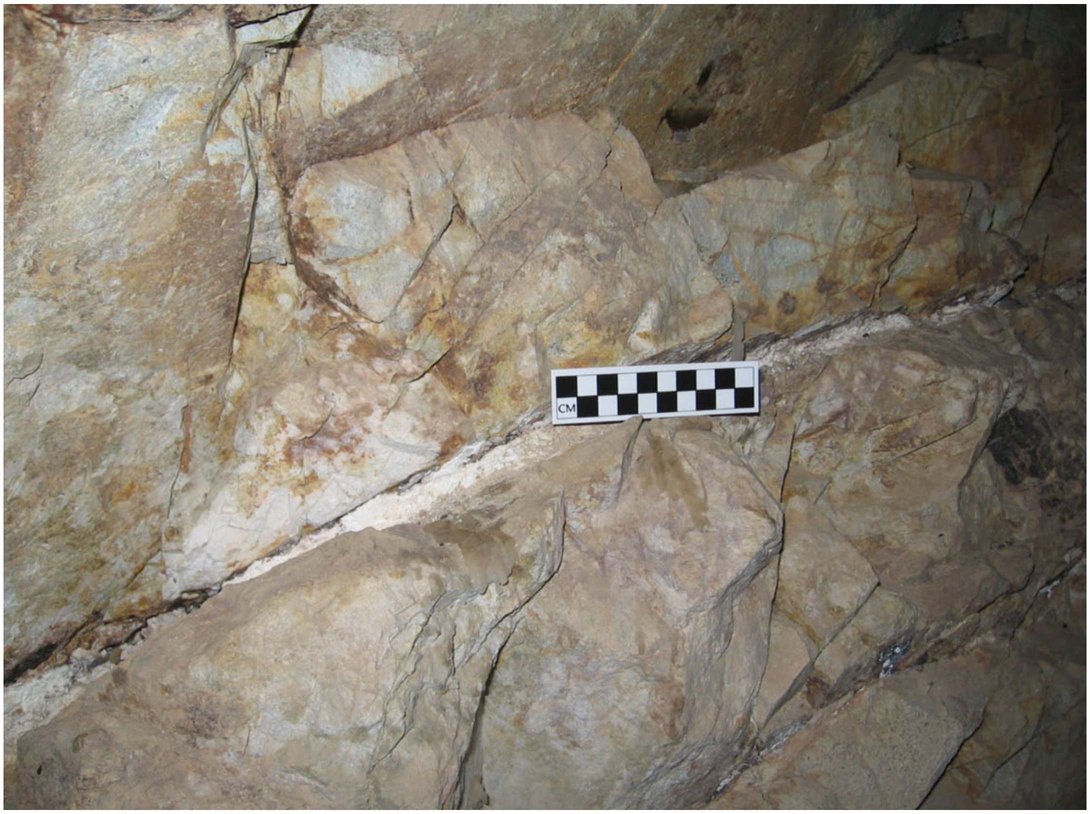

Scar where turquoise vein was removed by modern mining.

Turquoise veinlet in situ.

Mining has ceased at this location but other claims on the property are currently active.

Samples were collected from the tailings surrounding the shaft entrance.

Sample TF39

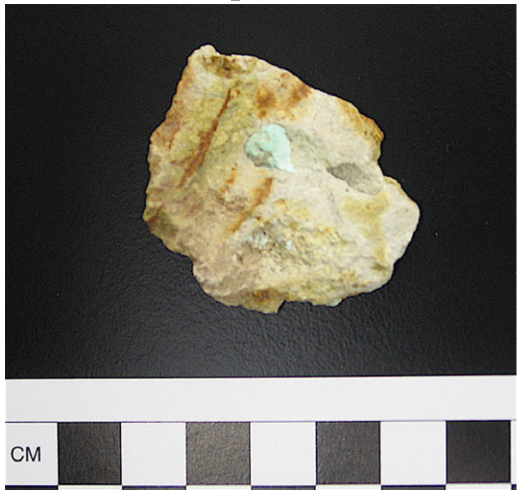

Sample TF44

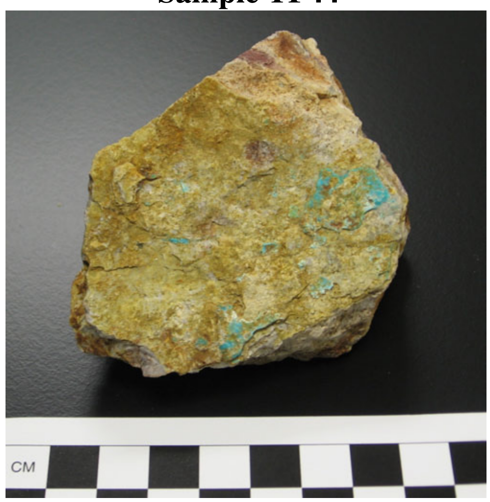

Sample TF46

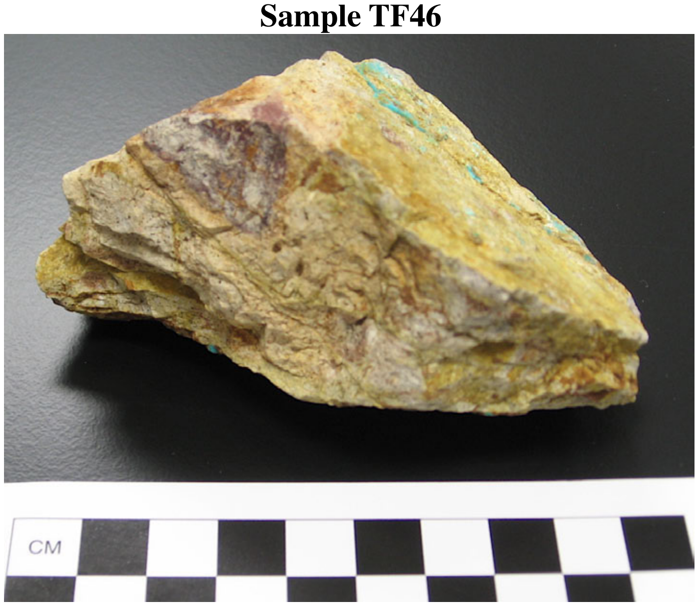

Sample 47

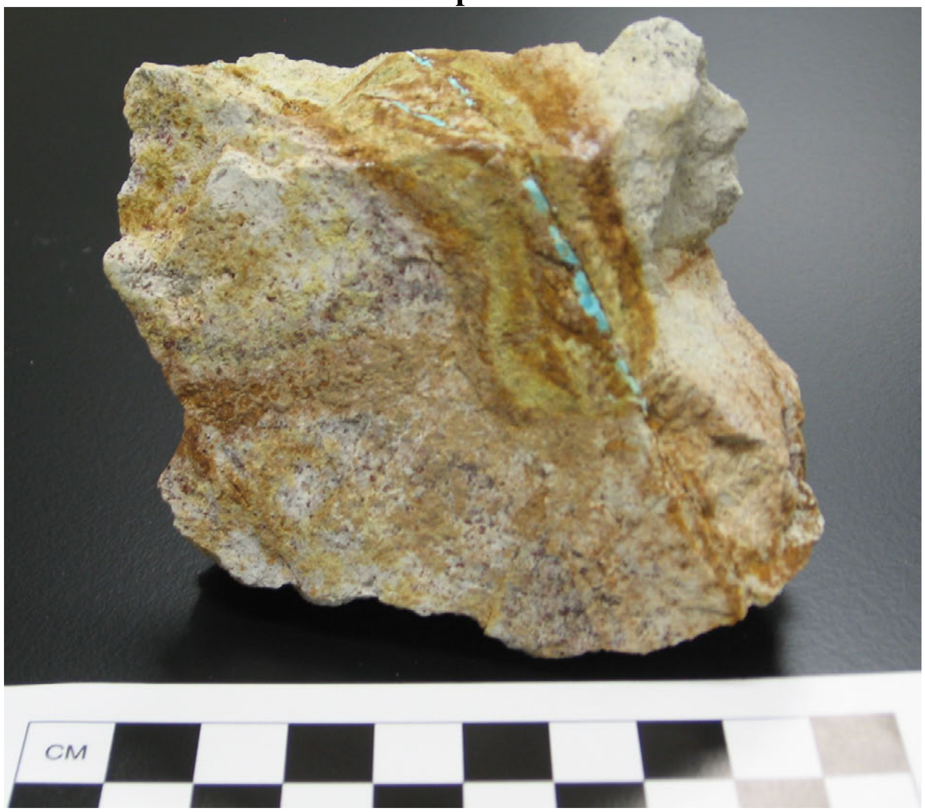

Sample 49

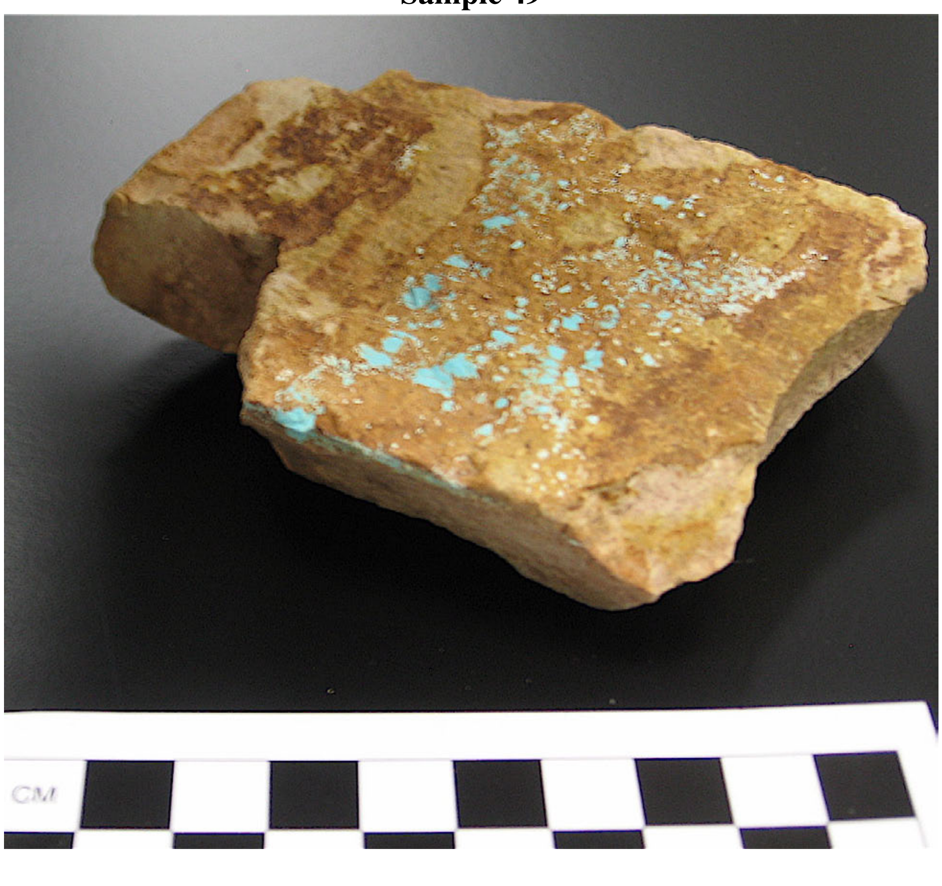

Appendix C: Color Reference

Location	Sample #	Pantone Reference #	Blue	Green	B/G mixture
Red Hill	RH9	3252U			
	RH10	564U			
	RH13	7472U			
	RH16	338U			
	RH17	563U			
	RH19	3258U			
Hachita	TM57	304U			
	TM66	310U & 311U			
	TM68	310U			
	TM70	317U			
	TM91	310U			
	TM95	311U & 312U			
	TM102	317U			
	TM109	317U			
	TM114	3248U			
	TM115	310U			
	TM118	310U			
	TM127	310U			
Chalchihuitl	CH22	304U			
	CH23	317U & 577U			
	CH26	579U - 576U			
	CH27	317U			
	CH28	3115U & 577U			
	CH34	3242U			
	CH35	7465U & 7466U			
Tiffany	TF39	317U			
	TF44	3115U			
	TF46	3125U			
	TF47	319U - 317U			
	TF49	3105U			
Artifacts	BJ1	325U			
	BJ11	3105U			
	BJ12(1)	325U			
	BJ12(2)	325U			
	BJ12(3)	325U			
	BJ21	348U - 344U			
	BJ43	318U			
	BJ46	326U			
	BJ47	319U			
	BJ49	317U			

Appendix D: Inventory of Turquoise Samples Collected

#	Location	length mm	width mm	thick-ness mm	Country Rock	Blue Green Mineral
1	Red Hill	8.9	5.8	2.9	very fine grained light brown	seam/vein-shaped piece
2	Red Hill	8.6	6.7	2.3	very fine grained light brown	seam/vein-shaped piece
3	Red Hill	11.1	8.2	3.4	very fine grained light brown	seam/vein-shaped piece
4	Red Hill	13.1	11.7	2.4	very fine grained light brown	seam/vein-shaped piece
5	Red Hill	13.2	9.5	3.5	very fine grained light brown	seam/vein-shaped piece
6	Red Hill	11.7	7.2	2.2	very fine grained light brown	seam/vein-shaped piece
7	Red Hill	15.9	9.3	3.9	very fine grained light brown	seam/vein-shaped piece
8	Red Hill	9.9	8	2.3	very fine grained light brown	seam/vein-shaped piece
9	Red Hill	13.7	11.6	4.6	very fine grained light brown	seam/vein-shaped piece
10	Red Hill	11.4	9.3	6.1	very fine grained light brown	somewhat nodular, but possibly thick, undulating vein formation
11	Red Hill	19	12	6.3	very fine grained light brown	seam/vein-shaped piece
12	Red Hill	17.8	11	6.7	very fine grained light brown	seam/vein-shaped piece
13	Red Hill	18	10.15	4.3	very fine grained light brown	seam/vein-shaped piece
14	Red Hill	15.8	7.3	7.2	very fine grained light brown	twisted, curved seam/vein-shaped piece
15	Red Hill	15.4	10.3	5.7	very fine grained light brown	seam/vein-shaped piece
16	Red Hill	16.2	12.5	4.7	very fine grained light brown	seam/vein-shaped piece
17	Red Hill	15.4	12.4	5.3	very fine grained light brown	seam/vein-shaped piece
18	Red Hill	17	12.8	3.6	very fine grained light brown	seam/vein-shaped piece
19	Red Hill	17.1	13.6	7.6	very fine grained light brown	nodular
20	Red Hill	19.6	19.2	3.9	very fine grained light brown	seam/vein-shaped piece
21	Red Hill	11.7	10	2.1	very fine grained light brown	2 pieces crossmend, polish marks, broke on lapidary wheel ?
22	Mt Chalchihuitl	14.5	5.6	4.8	light colored, altered	on surface, 1.5 mm thick, 7.3 mm long
23	Mt Chalchihuitl	24.3	12.4	7.8	light colored, altered	on surface and in vein, 1.5 mm thick
24	Mt Chalchihuitl	17.6	12.8	5.9	light colored, altered	on surface, .6 mm thick, 7 mm long
25	Mt Chalchihuitl	21.6	12	9.3	light colored, altered	nodule exposed on surface 2x3mm
26	Mt Chalchihuitl	18.6	13.3	4.4	very fine grained light brown	seam/vein-shaped piece
27	Mt Chalchihuitl	21.7	13.8	10.1	light colored, altered	on surface, .5 mm thick, 13.2 long
28	Mt Chalchihuitl	26.9	19.3	11.3	light colored, altered	on surface, 1 mm thick, 10 mm long
29	Mt Chalchihuitl	29.8	19.3	12.8	light colored, altered	on surface, 1 mm thick, discontinuous
30	Mt Chalchihuitl	40	21.8	8.2	light colored, altered	on surface, 1 mm thick, discontinuous
31	Mt Chalchihuitl	27.8	21.6	4.3	grey, light colored, altered	intergrown with host rock, no distinct seam or surface deposit
32	Mt Chalchihuitl	72.3	35.6	26.6	light colored, altered	on surface, .5 mm thick, discontinuous
33	Mt Chalchihuitl	74	34	22.5	light colored, altered	on surface, .5 mm thick, and in part of a crack

34	Mt Chalchihuitl	120	60	30	light colored, altered	one vein, 1.5 mm thick
35	Mt Chalchihuitl	90	60	57.5	light colored, altered	2 on surface and 1 lens, .5 mm thick
36	Tiffany	21.2	20	13.2	light colored w/iron bands, altered	discontinuous somewhat rounded inclusions, a few are completely white -altered?
37	Tiffany	21.6	16.6	12.9	light colored w/iron bands, altered	discontinuous somewhat rounded inclusions most on surface <.5 mm
38	Tiffany	35	31.1	22.1	light colored w/iron bands, altered	on surface, .5 mm, some inclusions and possible < .5 mm small vein
39	Tiffany	41.4	34.7	17.2	light colored w/iron bands, altered	nodular, the largest at 8.4x6.3x4.5
40	Tiffany	47	37.7	14.1	light colored w/iron bands, altered	nodules within the iron bands
41	Tiffany	6.5	27.7	24.6	light colored w/iron bands, altered	on surface, <.5 thickx20x12.3 mm, some nodular inclusions also
42	Tiffany	47	45	21.4	fine grained light & blk, w/iron bands, altered	nodular inclusions
43	Tiffany	51.3	49.1	25.7	light colored w/iron bands, altered	on surface, 1.5 mm thick 41x19
44	Tiffany	92	44	22	fine grained light & blk, w/iron bands, altered	discontinuous, nodules of variable thickness on surface
45	Tiffany	120	49	40	fine grained light & blk, w/iron bands, altered	on surface .75 mm thick 24.5x16.2 & some nodules
46	Tiffany	95.5	64	47.4	fine grained light & blk, w/iron bands, altered	on surface 1 mm thick & some nodules
47	Tiffany	103	87.7	53.2	fine grained light & blk, w/iron bands, altered	in veins .5 - 1.8 mm thick
48	Tiffany	105	96	50.4	fine grained light & blk, w/iron bands, altered	on surface .5 - 1.5 mm thick and in a small vein <.5mm
49	Tiffany	115	105	27.7	light colored w/iron bands, altered	nodules exposed on surface around 4x4 mm thickness uncertain
50	Tiffany	145	80	60	fine grained light & blk, w/phenocrysts, iron bands, altered	zoned nodules on surface and vein
51	Hachita District	15.7	8.9	5.8	very fine grained light brown	seam/vein shaped piece, color fades in cross section to powdery white on exterior
52	Hachita District	17.2	10.4	3.8	very fine grained light brown	seam/vein shaped piece, color fades in cross section to powdery white on exterior
53	Hachita District	16.2	12.8	7	very fine grained light brown	seam/vein shaped piece, soft
54	Hachita District	15.8	13	4.6	very fine grained light brown	seam/vein shaped piece, soft
55	Hachita District	17.7	12.6	1.2	very fine grained light brown	seam/vein shaped piece, soft
56	Hachita District	17.2	10.4	1.1	very fine grained, light brown with black grains (lichen?)	seam/vein shaped piece, less soft
57	Hachita District	15.1	9.9	5.6	very fine grained light brown	seam/vein shaped piece, soft
58	Hachita District	15.3	14.1	4.6	very fine grained light brown	seam/vein shaped piece, soft
59	Hachita District	15.8	12.4	6.4	very fine grained light brown	seam/vein shaped piece, soft

60	Hachita District	17.3	10.4	3.5	very fine grained, light brown with black grains (lichen?)	seam/vein shaped piece, less soft
61	Hachita District	18.2	11.6	5.8	very fine grained, light brown with black grains (lichen?)	seam/vein shaped piece, less soft
62	Hachita District	20.3	13.3	8.4	very fine grained light brown with yellow areas and black grains (lichen?)	seam/vein shaped piece, less soft
63	Hachita District	15.1	10.9	3.8	very fine grained light brown with black grains (lichen?)	seam/vein shaped piece, less soft
64	Hachita District	22.5	7.9	1.7	very fine grained light brown with black grains (lichen?)	seam/vein shaped piece, less soft
65	Hachita District	8.5	5.7	3.5	very fine grained light brown with black grains (lichen?)	seam/vein shaped piece, less soft
66	Hachita District	21.9	18.3	3.5	very fine grained light brown with black grains (lichen?)	seam/vein shaped piece, less soft
67	Hachita District	21.5	15.8	10.1	very fine grained light brown with black grains (lichen?)	seam/vein shaped layer on surface 1.7 mm thick
68	Hachita District	23.2	13.9	7.5	very fine grained light brown with black grains (lichen?)	seam/vein shaped piece, less soft & powdery
69	Hachita District	18.12	16	5.6	very fine grained light brown	seam/vein shaped piece, soft
70	Hachita District	25.4	12.1	4.7	very fine grained light brown with black grains (galena?)	seam/vein shaped piece, less soft
71	Hachita District	19.9	10.4	4.5	very fine grained light brown with a few black grains (lichen?)	seam/vein shaped piece, soft
72	Hachita District	16	13.6	1.8	very fine grained light brown with black grains (lichen?)	seam/vein shaped piece, less soft
73	Hachita District	42.7	31.6	11.7	very fine grained light brown with black grains (lichen?)	nodules exposed on surface and small vein .9mm thick
74	Hachita District	12.1	8.8	6	very fine grained, light brown	somewhat nodular, possibly thick, undulating vein formation, soft/powdery
75	Hachita District	10.6	6.9	4.7	very fine grained light brown with black grains (lichen?)	seam/vein shaped piece, less soft
76	Hachita District	12	9.7	5	very fine grained, light brown	seam/vein shaped piece, color fades in cross section to powdery white on exterior
77	Hachita District	29.3	18.8	5.4	very fine grained, light brown with black grains	seam/vein shaped piece, 1.5 mm thick, less soft
78	Hachita District	17.9	10.3	6.7	very fine grained light brown with black grains	seam/vein shaped piece, less soft
79	Hachita District	19.1	9.9	4.9	very fine grained light brown with few black grains	seam/vein shaped piece, soft
80	Hachita District	23.4	14.6	5.6	very fine grained light brown with few black grains	seam/vein shaped piece, soft
81	Hachita District	30.2	17.8	2	very fine grained light brown with many black grains	seam/vein shaped piece, less soft
82	Hachita District	11.4	8.6	2.5	very fine grained light brown with few black grains	seam/vein shaped piece, soft
83	Hachita District	12.8	10.2	4.2	very fine grained light brown with few black grains	nodule somewhat seam/vein-shaped piece, soft

84	Hachita District	16	12.7	7.4	very fine grained light brown with black grains	seam/vein shaped piece, less soft
85	Hachita District	18.2	11.2	5.4	very fine grained light brown with black grains	seam/vein shaped piece, color fades in cross section to white on exterior
86	Hachita District	14.4	8.6	4.5	very fine grained light brown with few black grains	seam/vein shaped piece, soft
87	Hachita District	13.6	9.5	2.4	very fine grained light brown with many black grains	seam/vein shaped piece, less soft
88	Hachita District	20	9.3	6.4	very fine grained light brown with black grains	seam/vein shaped piece, soft
89	Hachita District	17	13.8	2.5	very fine grained light brown with black grains	seam/vein shaped piece, comparatively hard
90	Hachita District	19.1	12.2	6.8	very fine grained gray & light brown with many black grains	seam/vein shaped piece, comparatively hard
91	Hachita District	15.9	12.2	8.4	very fine grained light brown rock with reflective black grains	nodule with country rock interspersed
92	Hachita District	10.8	7.1	5.3	very fine grained light brown	seam/vein shaped soft piece, color fades in cross section to white on exterior
93	Hachita District	15.3	9	3.9	fine grained light brown w/iron bands & quartz, altered	seam/vein shaped piece, soft
94	Hachita District	9.2	8.25	4	very fine grained light brown rock with few black & qtz grains, altered	nodular (poss. vein) soft piece, color fades in cross section to white on exterior
95	Hachita District	19.9	12.5	1.7	very fine grained light brown with many black grains	seam/vein shaped piece, comparatively hard
96	Hachita District	20	14.2	3.7	very fine grained light brown with qtz and black grains	seam/vein shaped piece, comparatively hard
97	Hachita District	11.6	9.6	5.7	very fine grained light brown with black grains	seam/vein shaped piece, soft & powdery
98	Hachita District	12.7	11.6	5.6	very fine grained light brown with few qtz and few black grains	seam/vein shaped piece, soft
99	Hachita District	13.2	9.9	3.5	very fine grained light brown rock with qtz and few black grains	seam/vein shaped piece, soft, powdery, crumbling
100	Hachita District	11	8.6	4.2	very fine grained light brown with few qtz and black grains	seam/vein shaped soft piece, color fades in cross section to white on exterior
101	Hachita District	14.3	11.3	2.4	very fine grained light brown with qtz and black grains	seam/vein shaped piece, soft
102	Hachita District	18.4	16.6	6.3	fine grained light brown w/iron bands & black grains, altered	seam/vein shaped piece, less soft
103	Hachita District	18.3	13.8	6.2	very fine grained light brown with black grains	seam/vein shaped piece, less soft
104	Hachita District	17	11.1	7.4	very fine grained light brown with many black grains, iron stained	seam/vein shaped piece, less soft
105	Hachita District	18.5	14.3	6	very fine grained light brown with many black grains, iron stained	seam/vein shaped piece, less soft

106	Hachita District	21.3	15.7	9.8	very fine grained light brown with few black grains	nodular, 9.5x8.5 mm, poss. edge of seam/vein-shaped piece, soft
107	Hachita District	26.7	24	16	very fine grained light brown with black grains	seam/vein shaped piece, 1.5 mm thick, less soft
108	Hachita District	26.5	23	14	very fine grained light brown with few black grains	seam/vein shaped piece, soft, powdery, crumbling
109	Hachita District	31.4	20	14	very fine grained light brown with black grains	seam/vein shaped piece, 3.5 mm thick, less soft
110	Hachita District	31.3	25	17.4	very fine grained light brown with many black grains	seam/vein shaped piece, .6 mm thick, less soft
111	Hachita District	33.8	24.5	13	very fine grained light brown with few black grains	seam/vein shaped piece, soft, powdery, crumbling
112	Hachita District	32.7	14.8	2.8	very fine grained light brown with black grains	seam/vein shaped piece, hard and brittle
113	Hachita District	17	12.3	7.9	very fine grained light brown with black grains	seam/vein shaped piece, less soft
114	Hachita District	19.8	17.5	11.3	very fine grained light brown with dark grains	nodular, somewhat granular, darker blue in one section fading to light blue on edges
115	Hachita District	28.6	24.6	9	very fine grained light brown with many black grains	seam/vein shaped piece, 1mm thick, less soft
116	Hachita District	25.7	14.6	9.7	very fine grained light brown with dark grains	seam/vein shaped piece, 2mm thick, less soft
117	Hachita District	21.8	18.7	11.2	very fine grained light brown with few black grains	seam/vein .5 mm thick seen in cross section
118	Hachita District	30	26	16	very fine grained light brown with many black grains	nodules exposed on surface, also small vein visible
119	Hachita District	43.4	30	19.2	very fine grained light brown with dark grains	nodular, soft, chalky, crumbling
120	Hachita District	21.9	15.5	8.9	very fine grained light brown with shiny black grains	seam/vein shaped piece, less soft
121	Hachita District	45.24	34.3	20	fine grained light brown w/iron bands & black grains, altered	seam/vein shaped 8x6x.5 mm, soft
122	Hachita District	57	34.5	17.5	very fine grained light brown with many black grains	several nodules or pockets thickest 1.5 mm, less soft
123	Hachita District	54.5	43	26.4	light brown and light red fine grained with black bands	seam/vein shape 2.5 wide within black band, white around edges, otherwise deeper blue
124	Hachita District	95	75	55	very fine grained light brown with iron stains & few black grains	nodules and seam/veins up to 4mm thick, soft
125	Hachita District	95	55	50	very fine grained gray and light brown with iron stains and many black grains	seam/vein shaped piece, less soft
126	Hachita District	95	55	45	very fine grained light brown with iron bands and black grains	seam/vein .5mm thick exposed on one surface
127	Hachita District	16	15	6	fine grained light brown w/iron bands & black grains, altered	seam/vein shaped piece, less soft

Appendix E: Petrography

Sample RH9

Turquoise:

- Color - brown to light brown and bluish brown in fissures
- Texture - dense to fine-grained
- Alteration - intergrowth with sericite, zone of higher sericite along fissures separating turquoise aggregates
- Turquoise fissures have a higher relief, different color, possibly a different mineral or less altered turquoise

Host:

- Porphyritic with numerous altered biotite phenocrysts
- Quartz, altered feldspars and opaque phenocrysts
- Iron oxide spherules adjacent to and intergrown with turquoise, blue high relief mineral, and opaque inclusions

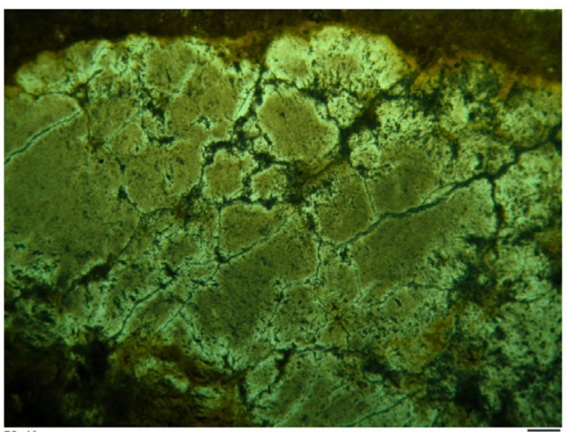

PL 40x turquoise spherules and fissures 1 mm

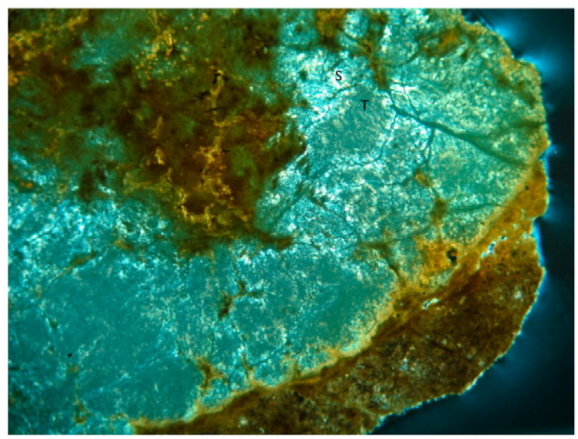

XP 40x turquoise intergrown with sericite 1 mm

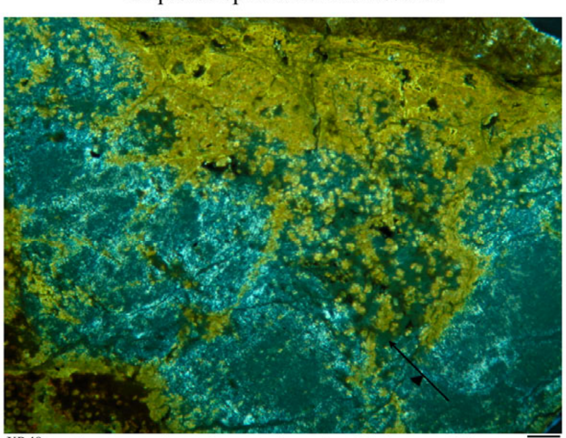

XP 40x fissure mineral associated with iron oxides 1 mm

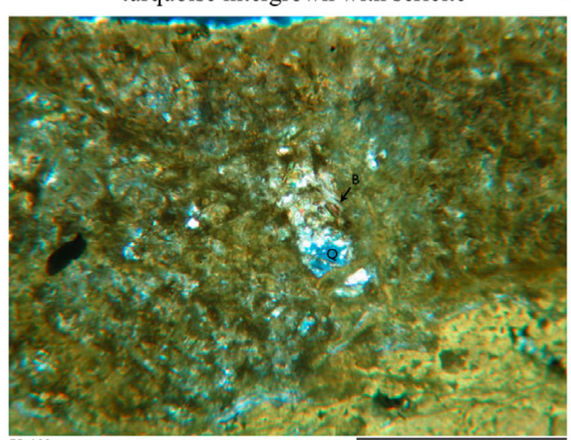

PL 100x quartz and biotite in host 1 mm

Sample RH10

Turquoise:

- Color - bluish brown to dark brown, darker than most samples
- Texture - dense, fine-grained, spherulitic
- Quartz grain inclusions
- Alteration of turquoise next to a vein of silica originating from a quartz grain - turquoise is fibrous at a perpendicular angle to the vein
- Turquoise zoned areas have higher amounts of intergrown sericite
- Area between spherules has higher relief, different mineral
- Biotite, partially altered to chlorite
- Opaque grains
- Possible epidote or jarosite in altered turquoise
- Altered feldspars

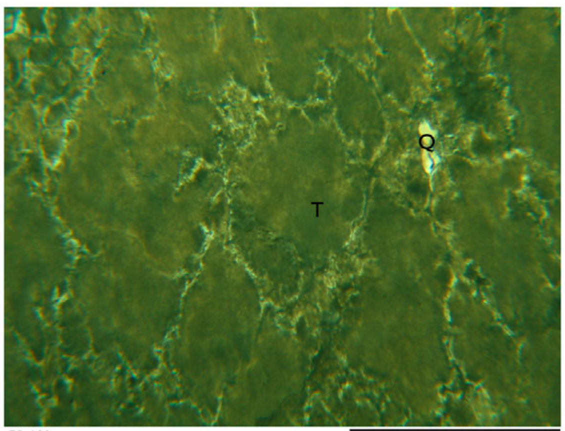

PL 100x turquoise spherules and quartz grain 1 mm

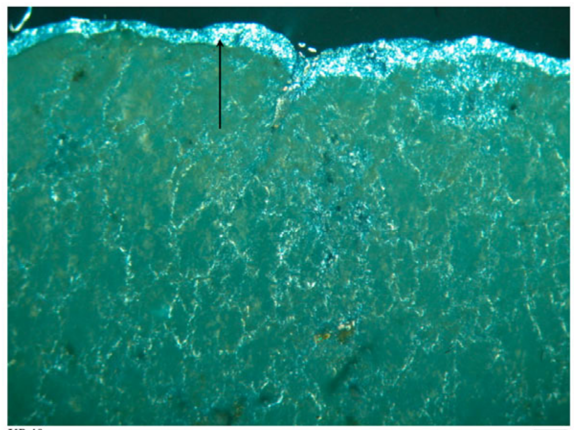
XP 40x turquoise alteration zone 1 mm

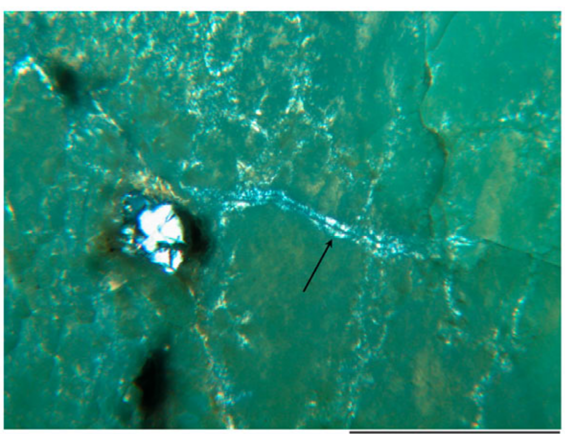
XP 100x silicate veinlet 1 mm

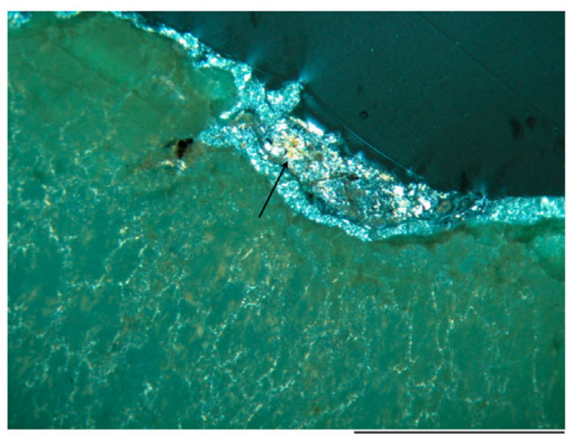
XP 100x altered biotite in altered turquoise 1 mm

Sample RH13

Turquoise:

- Color - brown to bluish brown
- Texture - spherulitic, dense to fine-grained
- Alteration - sericite intergrowth, increased sericite content at spherule edges
- Mineral separating the spherules has a higher relief and darker color.
- Iron oxides associated with opaque mineral grains and possible chlorite

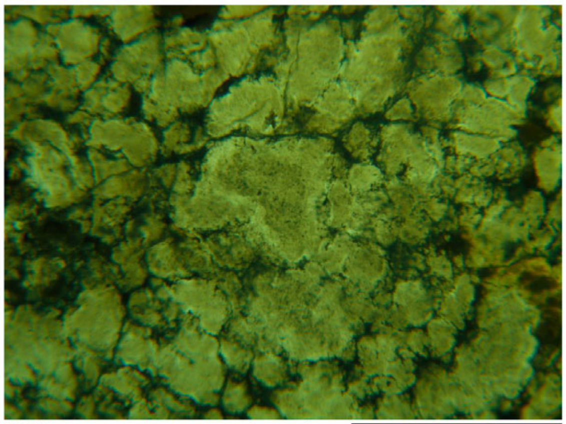

PL 100x turquoise spherules 1 mm

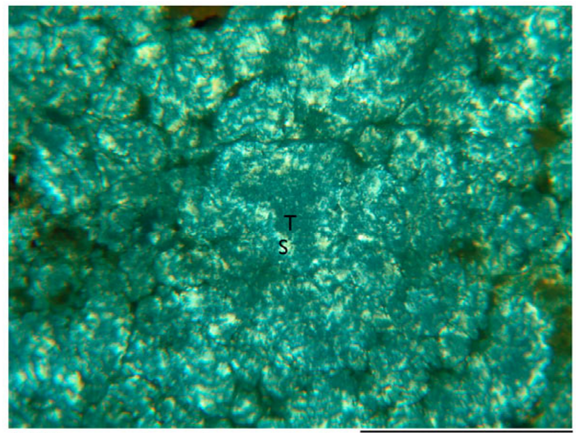

XP 100x turquoise-sericite intergrowth 1 mm

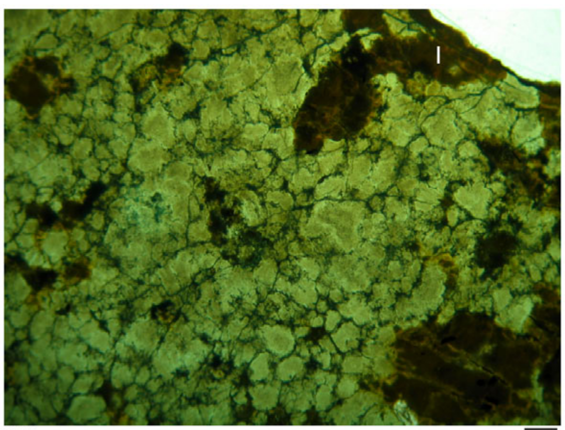

PL 40x Iron oxides 1 mm

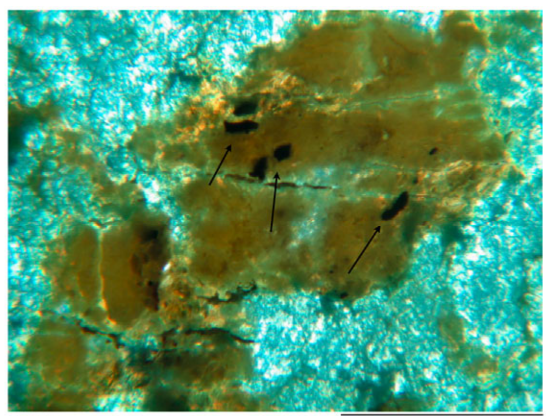

XP 100x opaque grains in iron oxide 1 mm

Sample RH16

Turquoise:

- Color - light brown to brown
- Texture - dense to fine-grained
- Alteration - intergrowth with sericite, possibly also kaolinite
- Sericite content of intergrowth seems to increase around some fissures forming zones
- A darker, higher relief mineral in some fissures
- Chlorite has medium to high birefringence, brown color masks birefringence
- Opaque inclusions

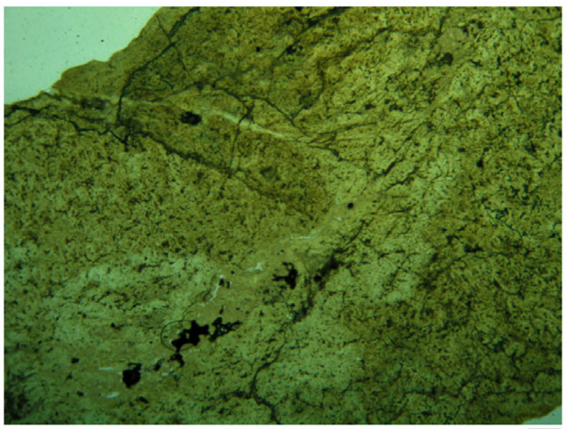

PL 40x fine-grained turquoise 1 mm

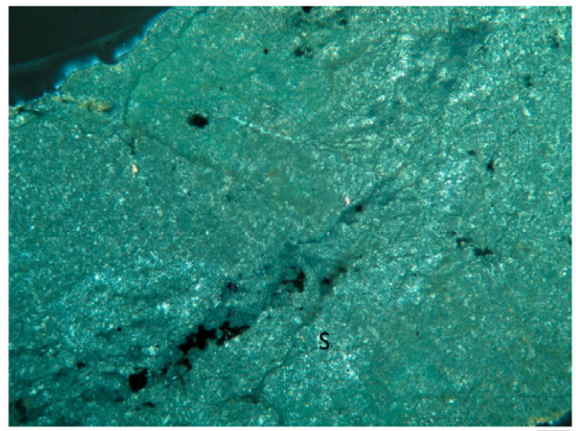

XP 40x sericite intergrowth along fissures 1 mm

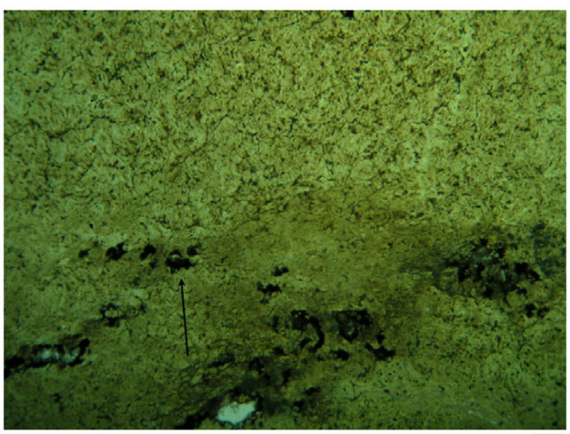

PL 40x opaque inclusions 1 mm

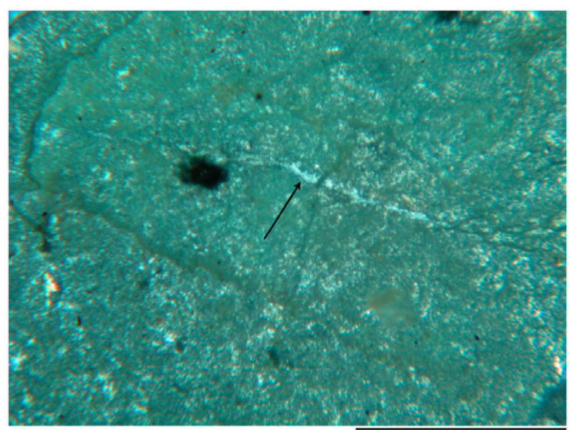

XP 100x sericite veinlet 1 mm

Sample RH17
Turquoise:

- Color - light brown
- Texture - dense to fine-grained
- Alteration - disseminated sericite, intergrowth with turquoise
- Iron oxide stained edges
- Opaque inclusions
- Fissures have a bluish brown color and high relief, different mineral or unaltered turquoise

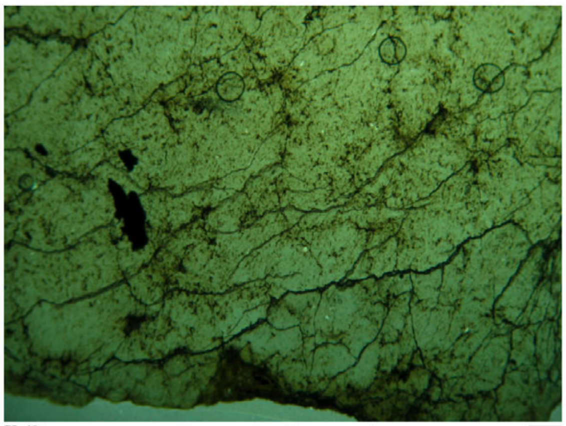
PL 40x fine-grained turquoise 1 mm

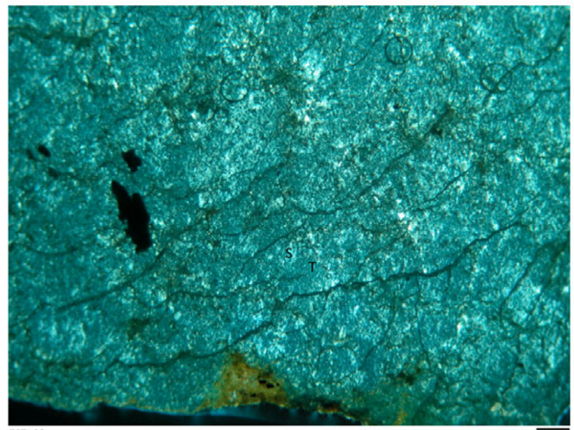

XP 40x sericite and turquoise intergrowth 1 mm

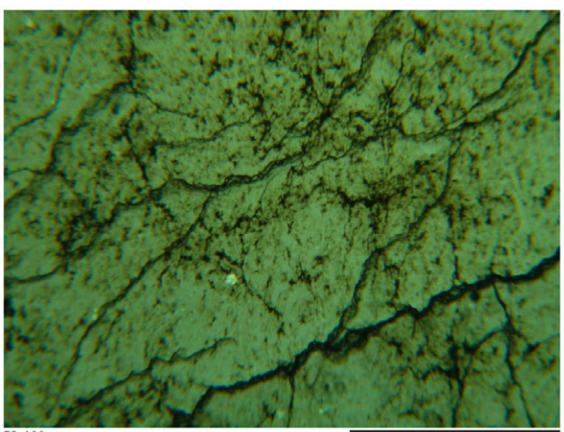
PL 100x high relief mineral in fissures 1 mm

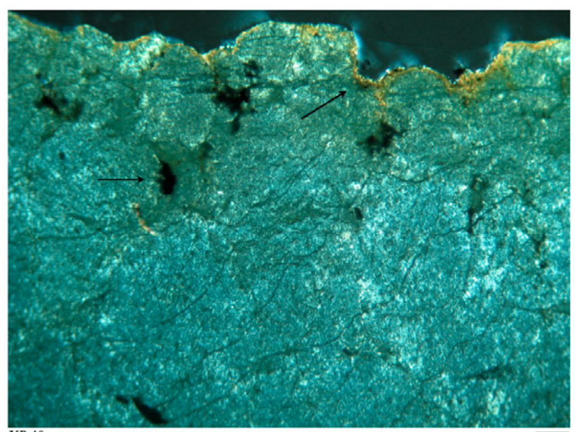
XP 40x opaque inclusions and iron-stained edges 1 mm

Sample RH19

Turquoise:

- Color - bluish brown
- Texture - dense to fine-grained, somewhat spherulitic
- Alteration - intergrowth with sericite increases along fissures, micro-veins and at sample edge
- Darker, high relief mineral seems to define spherules, sometimes sericite instead, sometimes both

Host/Inclusions:

- Altered biotite, chlorite, and coarse-grained sericite in veins cutting turquoise
- Altered feldspar grains near biotite, possibly replaced by sericite
- Opaque grains throughout both turquoise and host rock

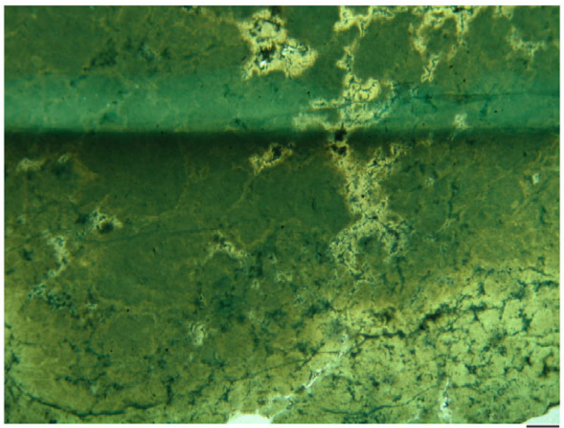

PL 40x fine-grained turquoise 1 mm

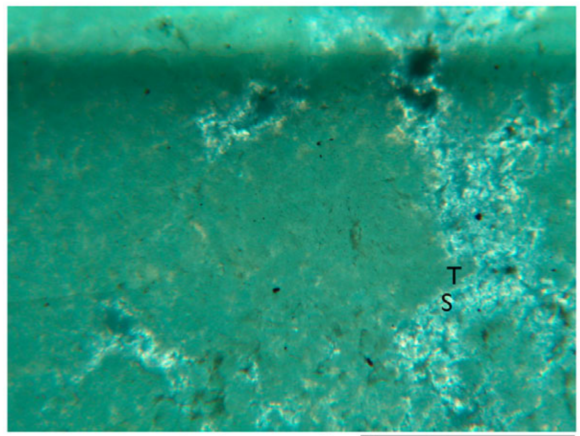

XP 100x turquoise intergrowth with sericite 1 mm

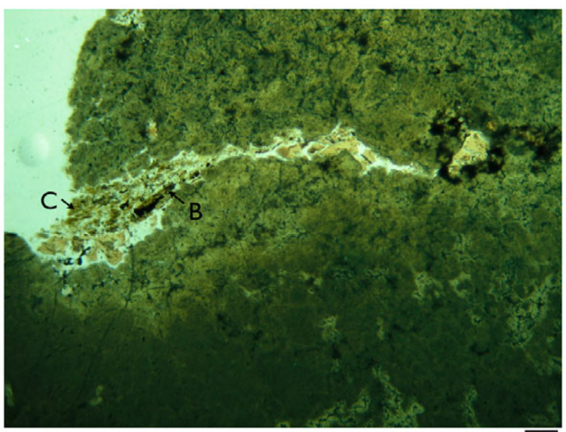

PL 40x biotite and chlorite in vein 1 mm

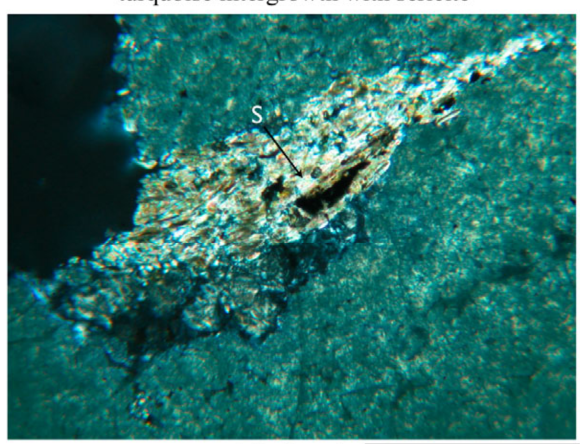

XP 100x sericite in vein 1 mm

Sample TM57

Turquoise:

- Color - brown to light brown in altered areas
- Texture - dense, fine-grained and fibrous where intergrown with sericite
- Alteration - zoning along edge of sample
- A few coarse-grained mica inclusions in addition to disseminated sericite

Host:

- Porphyritic
- Opaque inclusions
- Colorless, high relief phenocrysts with grayish/yellow-white interference colors
- Fine-grained altered feldspar
- Altered biotite

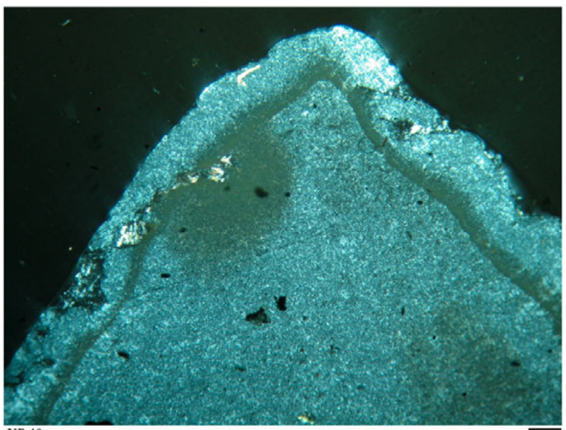

XP 40x fine-grained turquoise 1 mm

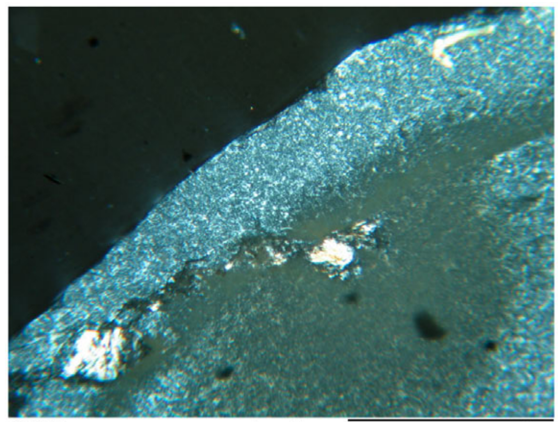

XP 100x turquoise alteration 1 mm

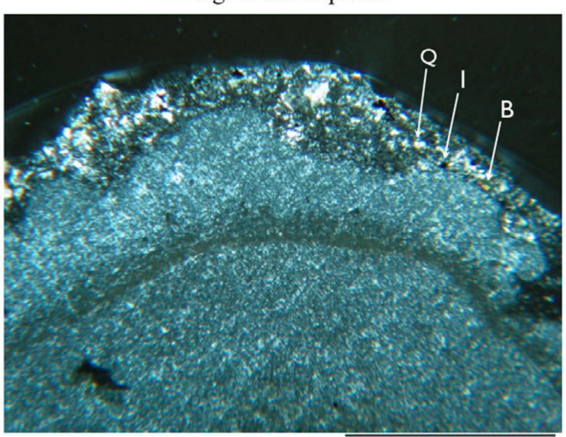

XP 100x quartz, opaque inclusions, biotite in host 1 mm

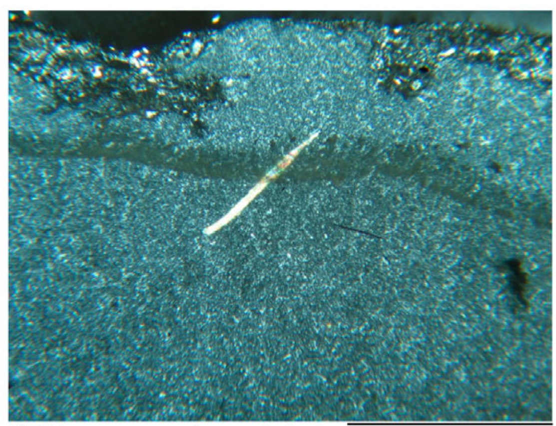

XP 100x mica grain inclusion 1 mm

Sample TM66

Turquoise:

- Color - bluish dark brown to light brown
- Texture - fine-grained, dense, slight spherulitic appearance due to micro-veinlets
- Alteration - zone along edge near micro-veinlets is altered turquoise intergrown with fine-grained sericite. Sericite content much greater at contact with host rock.

Host:

- Porphyritic
- Feldspar laths
- Possible kaolinite, clay minerals
- Iron oxides
- Opaque inclusions

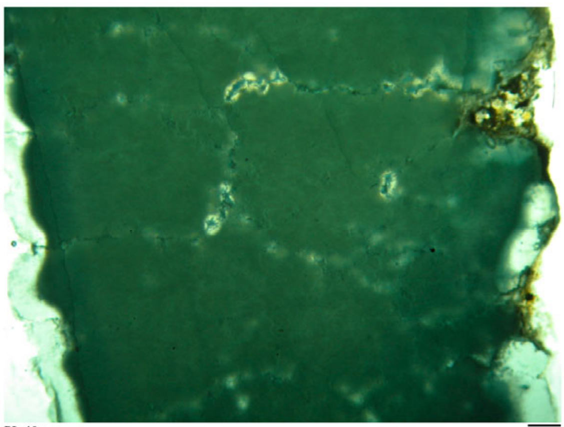

PL 40x fine-grained dense turquoise texture 1 mm

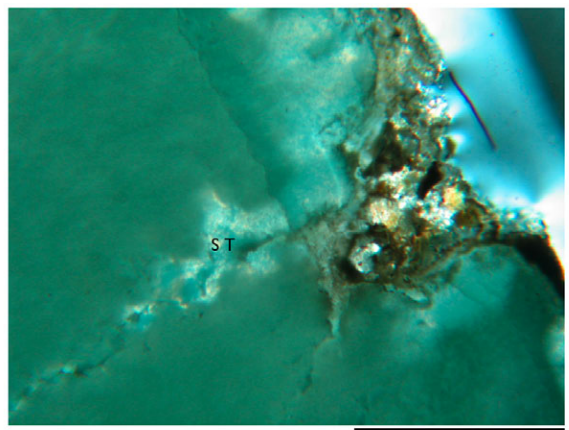

XP 100x altered turquoise intergrown with sericite 1 mm

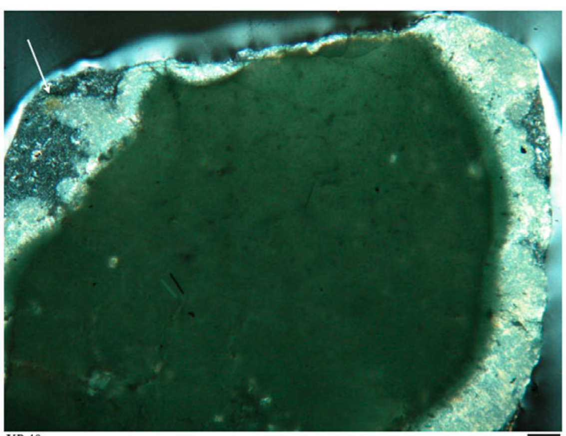

XP 40x host rock with iron stain 1 mm

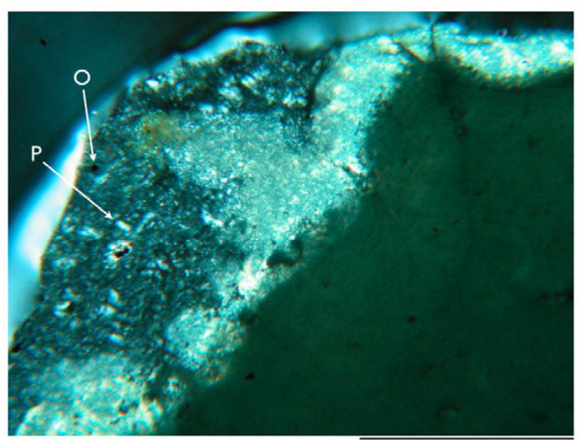

XP 100x opaque inclusions and plagioclase in host 1 mm

Sample TM68

Turquoise:

- Color - dark bluish brown in unaltered areas to light brown in altered
- Texture - dense, fine-grained, fibrous in some altered areas
- Alteration - zones visible where turquoise becomes sericitized and interference colors range from anomalous grey to 3rd order yellow-pink-blue, zoning more prevalent along fissures or micro-veinlets, but also present where no fissures are visible.

Host rock:

- Opaque inclusions - some are linear
- Dark brown, euhedral grains, ~.35 mm, possibly garnet

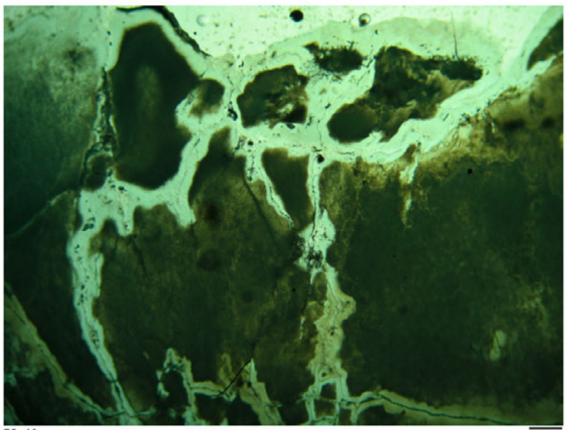

PL 40x fine-grained bluish brown turquoise 1 mm

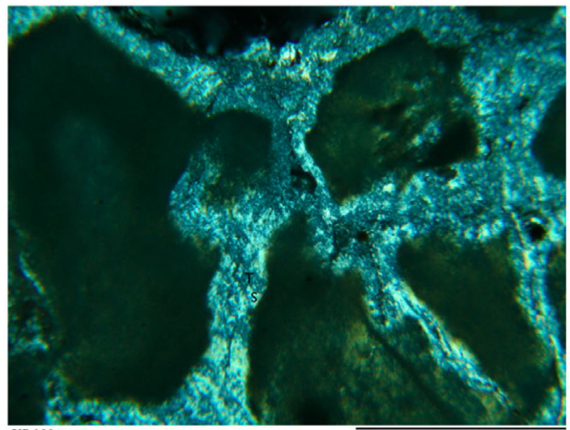

XP 100x turquoise-sericite intergrowth 1 mm

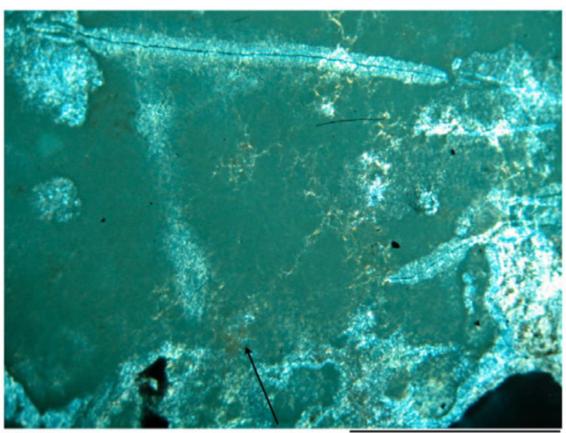

XP 100x iron oxides in altered turquoise 1 mm

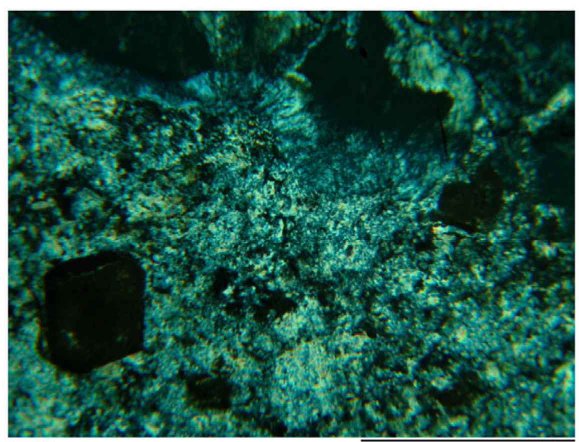

XP 100x host rock next to altered fibrous turquoise 1 mm

Sample TM70

Turquoise:

- Color – dark to light brown
- Texture – dense to fine-grained
- Birefringence – anomalous
- Alteration – turquoise intergrowth with fine-grained white mica/ sericite. Zone along outer edge has higher sericite content.
- Sericite intergrowth along micro-veinlet has brown inclusions and follows fissure cutting unaltered, or less altered, turquoise.
- Iron oxides

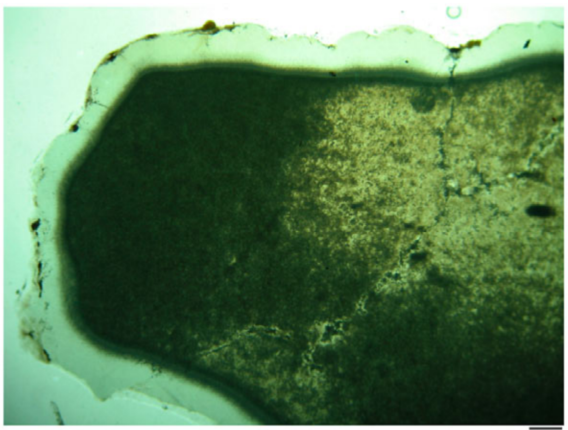

PL 40x dark and light brown turquoise 1 mm

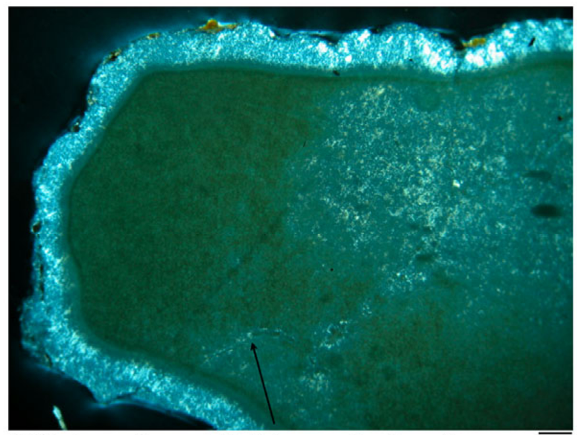

XP 40x turquoise-sericite intergrowth along fissure 1 mm

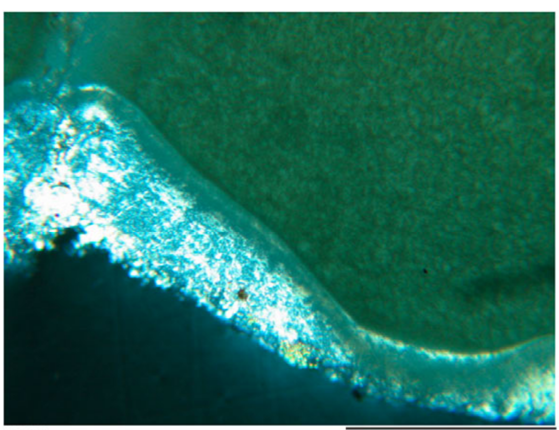

XP 100x turquoise-sericite alteration zone 1 mm

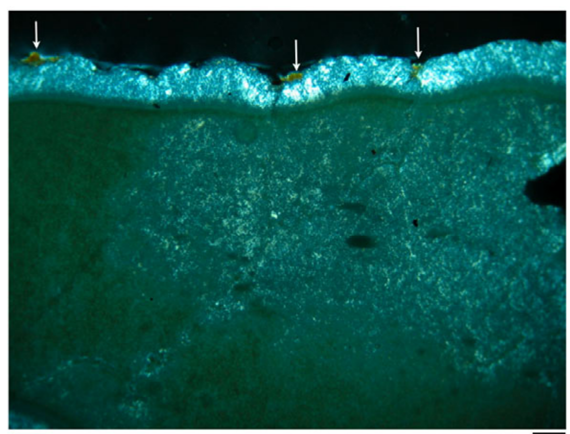

XP 40x iron oxides 1 mm

Sample TM91

Turquoise:

- Color - dark brown, bluish brown to light brown
- Texture - fine-grained and dense in center
- Alteration - zones have variable amounts of sericite, edges have the most sericite intergrowth, quartz grains in outermost zone

Host:

- Porphyritic
- Altered feldspar, chlorite and opaque phenocrysts
- Altered anhedral red brown grains, possibly garnet or hematite
- Iron oxides

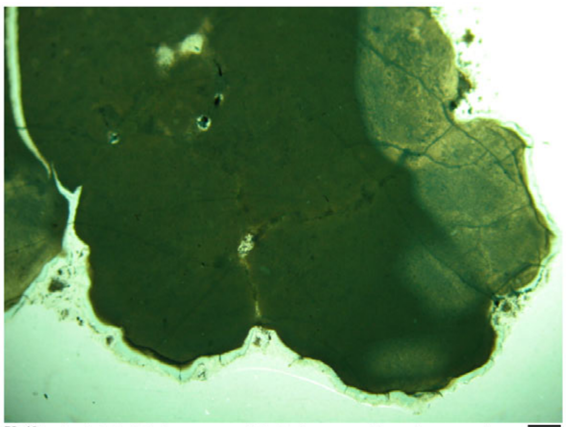

PL 40x dark bluish brown and light brown altered turquoise 1 mm

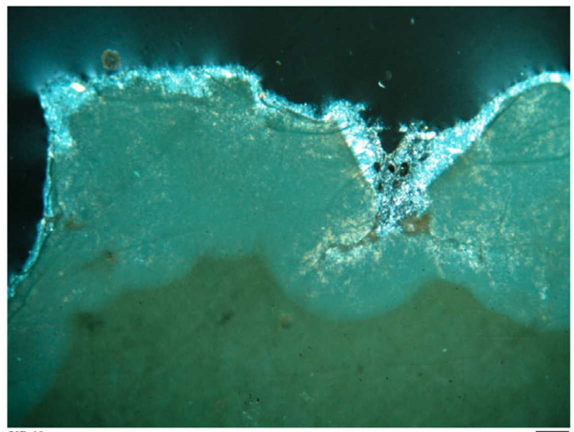

XP 40x turquoise alteration zones 1 mm

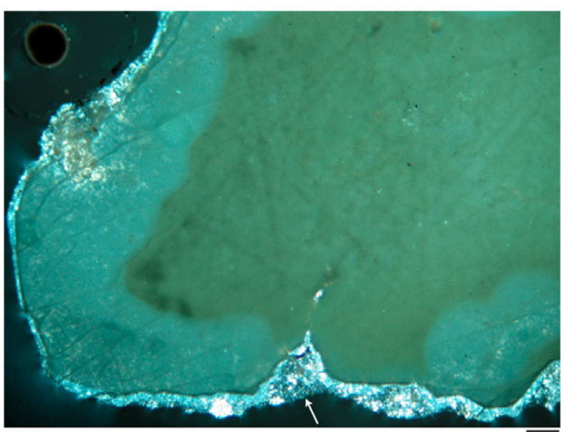

XP 40x remnant of volcanic host 1 mm

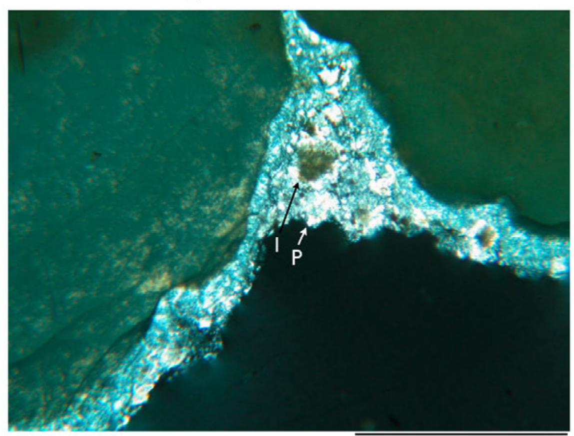

XP 100x altered plagioclase and iron stains in host 1 mm

Sample TM95

Turquoise:

- Color - light brown to bluish light brown in one area, lighter in color than most samples
- Texture - dense, fine-grained, intergrown with sericite
- Turquoise inclusion within turquoise, possibly crossed veins
- Alteration - zoned, altered turquoise has higher sericite phase content than less altered zones

Host rock:

- Porphyritic
- Altered feldspar - some twinning visible, could be sanidine or plagioclase
- Epidote - .02 - .04 mm light green grains, 2nd order interference
- Iron-stained
- Opaque inclusions

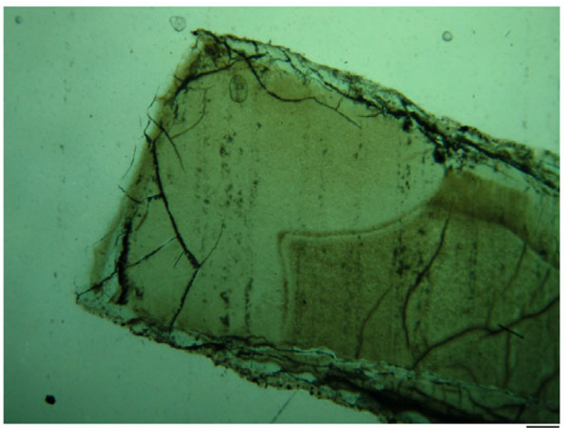

PL 40x fine-grained texture in light brown turquoise 1 mm

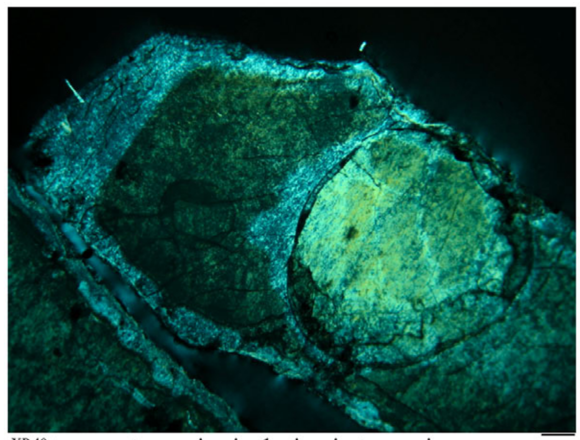

XP 40x turquoise inclusion in turquoise 1 mm

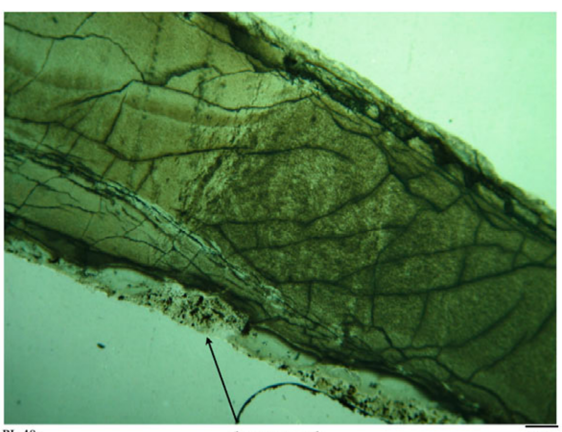

PL 40x host rock 1 mm

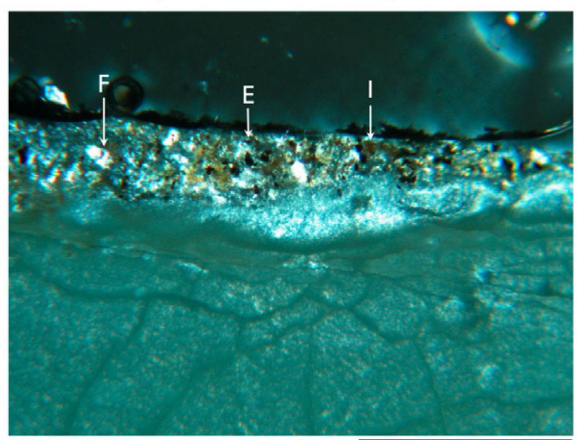

XP 100x feldspar, epidote, and iron oxide in host 1 mm

<u>Sample TM102</u>

Turquoise:

- Color - bluish brown to light brown
- Texture - dense, fine-grained, spherules in a webbed veinlet network
- Alteration - where altered, turquoise is intergrown with sericite. Pockets or spherules of unaltered turquoise are separated from altered, sericitized pockets by an iron oxide and/or chlorite web or veinlet zone. Some spherules have a dense rim with an altered center.

Host rock:

- Quartz
- Feldspar
- Jarosite or possibly apatite
- Altered biotite and chlorite
- Opaque grains

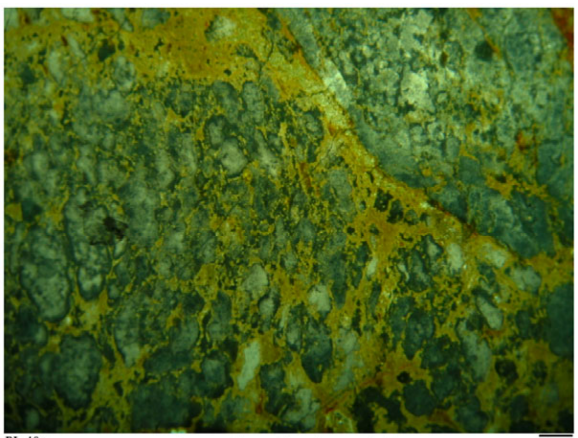

PL 40x turquoise spherules in veinlet zone 1 mm

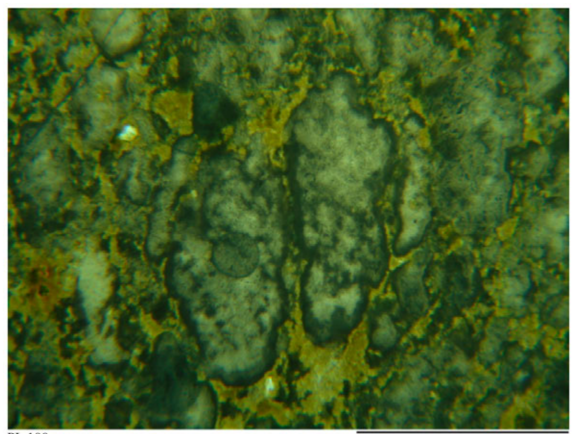

PL 100x altered turquoise in centers of spherules 1 mm

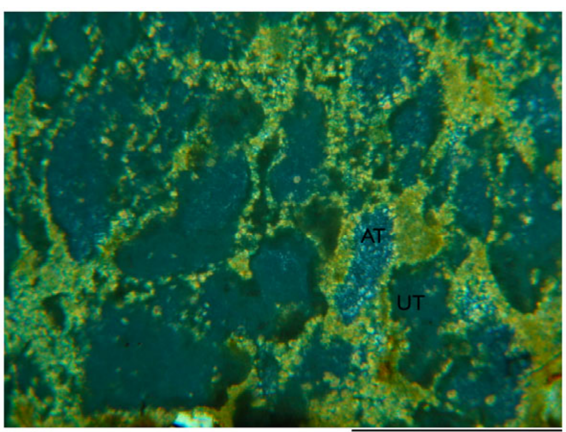

XP 100x spherules of altered or unaltered turquoise 1 mm

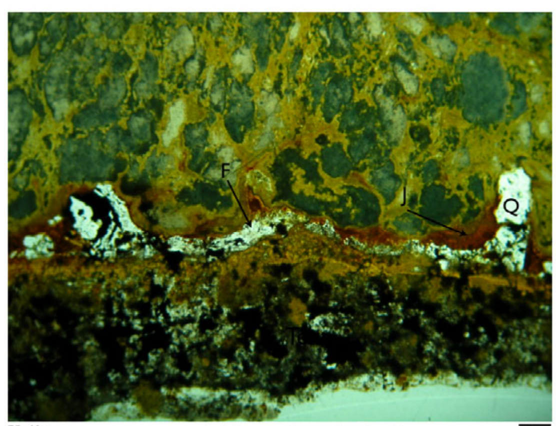

PL 40x quartz, feldspar, jarosite in host 1 mm

<u>Sample TM109</u>

Turquoise:

- Color - brown to light brown
- Texture - dense to fine-grained
- Alteration - turquoise intergrown with sericite in altered areas

Host rock:

- Fine-grained mixture of plagioclase, feldspars, epidote, chlorite and altered biotite and quartz
- Dense unaltered area of turquoise intergrown with host
- Vein of altered plagioclase and/or quartz next to chlorite spherules

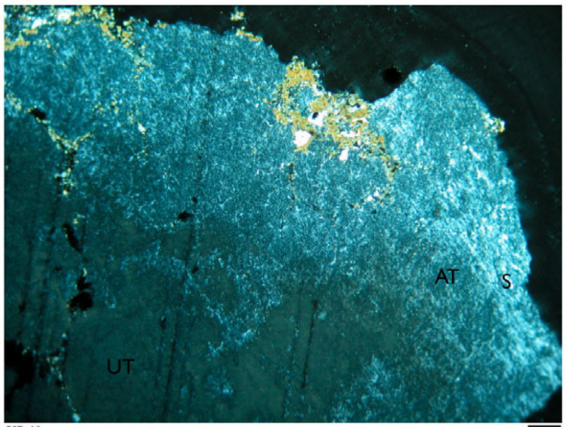

XP 40x unaltered turquoise and intergrown with sericite 1 mm

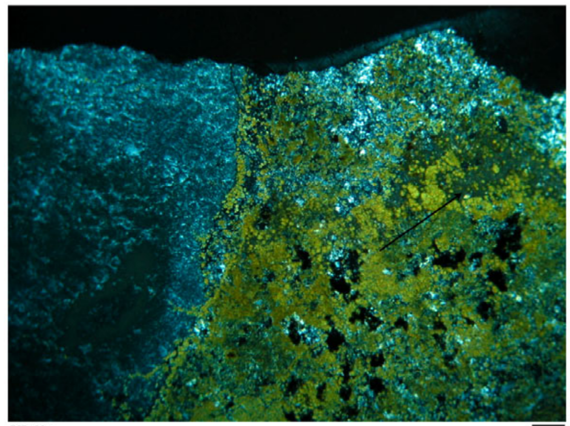
XP 40x dense turquoise within host 1 mm

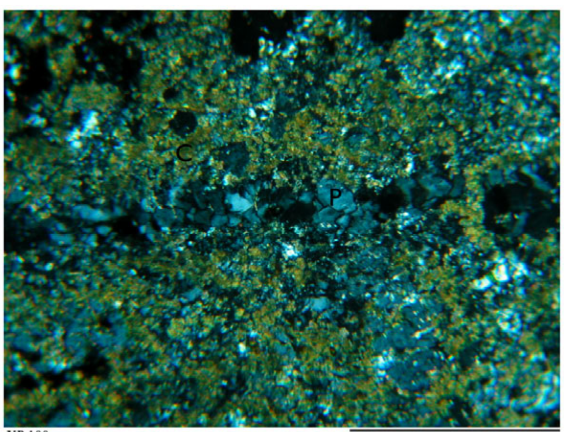

XP 100x plagioclase vein and chlorite in host 1 mm

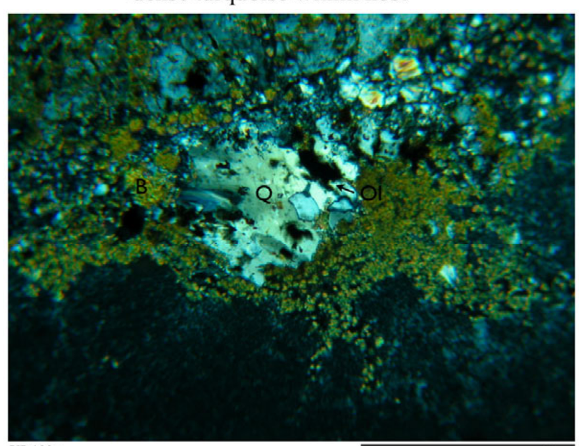

XP 100x quartz, altered biotite and opaque inclusions 1 mm

Sample TM114

Turquoise:

- Color - brown to light brown
- Texture - dense, fine-grained intergrowth with sericite
- Quartz inclusions
- Oxide-stained

Host:

- Porphyritic
- Quartz phenocrysts
- Yellowish light brown mineral, .5 mm grain, along sample edges and filling veins, possibly altered jarosite grains

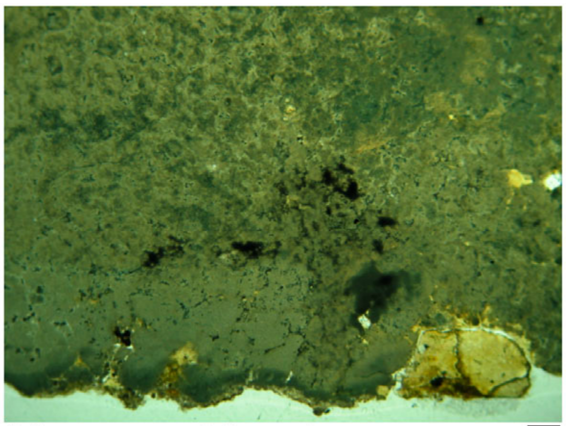

PL 40x mottled turquoise texture 1 mm

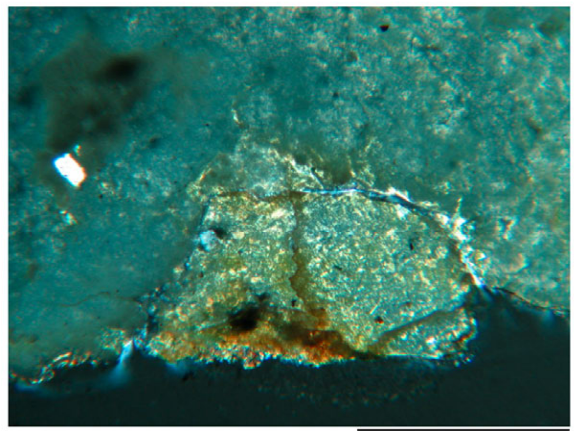

XP 100x turquoise intergrown with sericite 1 mm

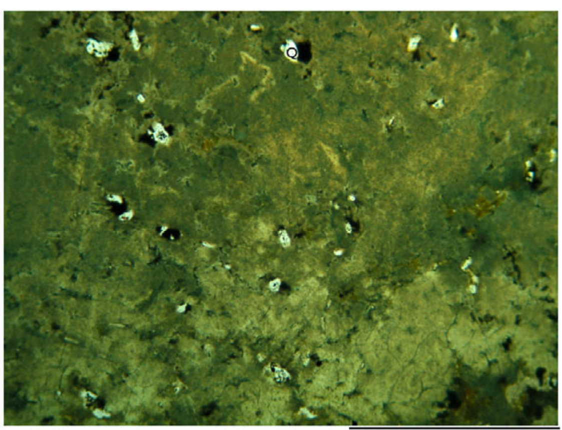

PL 100x quartz inclusions 1 mm

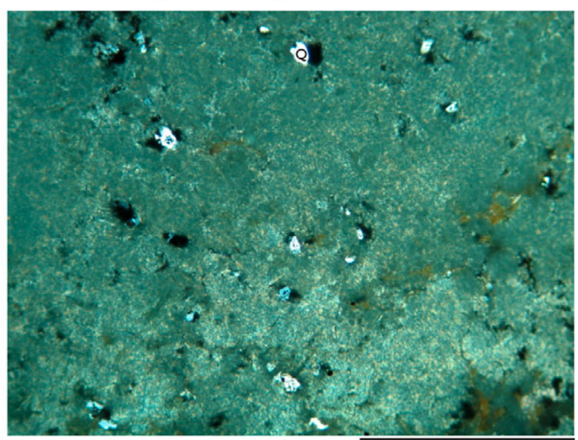

XP 100x quartz inclusions 1 mm

Sample TM115

Turquoise:

- Color - greenish brown
- Texture - dense to fine-grained
- Alteration – zoned around periphery of unaltered center.
- Light brown altered turquoise is intergrown with sericite

Host:

- Volcanic, fine-grained groundmass w/phenocrysts up to 1 mm
- Biotite altered to chlorite
- Altered plagioclase laths, twinning visible in some grains
- Altered alkaline feldspar
- Carbonate
- Sericite

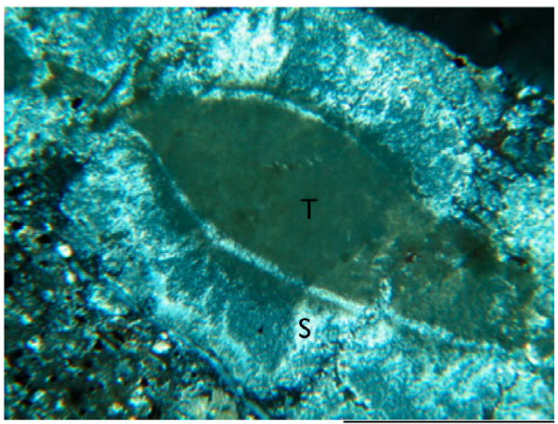

XP 100x turquoise and sericite 1 mm

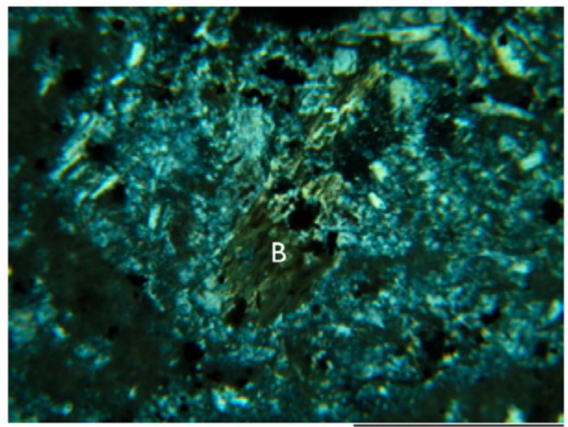

XP 100x biotite 1 mm

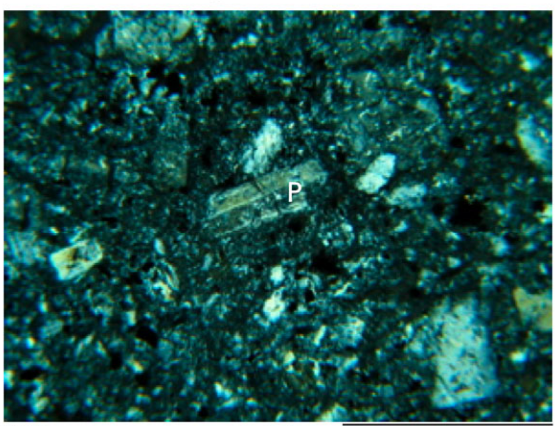

XP 100x plagioclase 1 mm

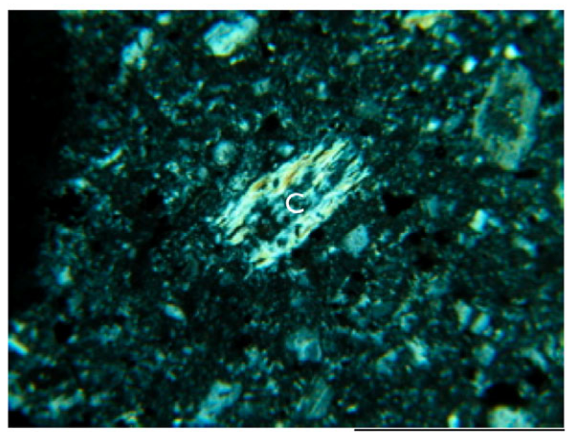

XP 100x chlorite 1 mm

Sample TM118

Turquoise:

- Color - light brown to dark brown
- Texture - dense to fine-grained
- Alteration - turquoise intergrowth with sericite, sericite has perpendicular orientation to vein wall in some areas
- Silicate cuts through chlorite grains, also a thin zone or crust of silicate separates turquoise vein from host rock

Host:

- Fine-grained groundmass with chlorite, altered feldspar, and opaque phenocrysts
- Red brown mineral inclusions in host and directly next to turquoise, garnet or possibly hematite
- Silicate veinlet
- Iron oxides

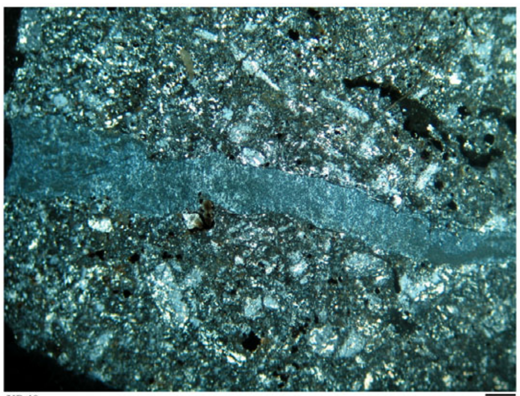

XP 40x fine-grained turquoise vein 1 mm

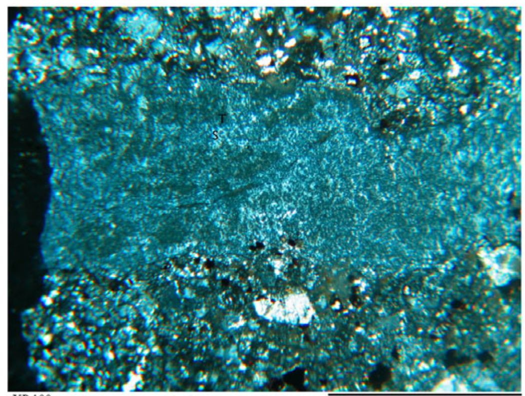

XP 100x turquoise-sericite intergrowth 1 mm

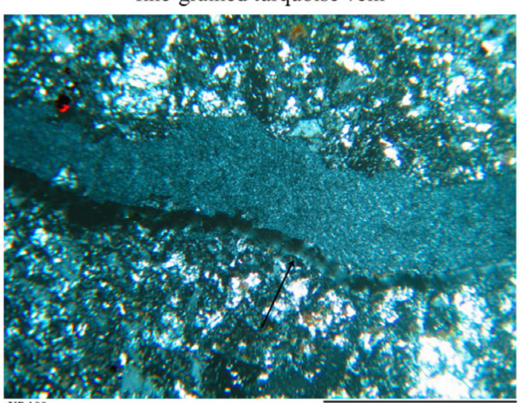

XP 100x silicate border between turquoise & host 1 mm

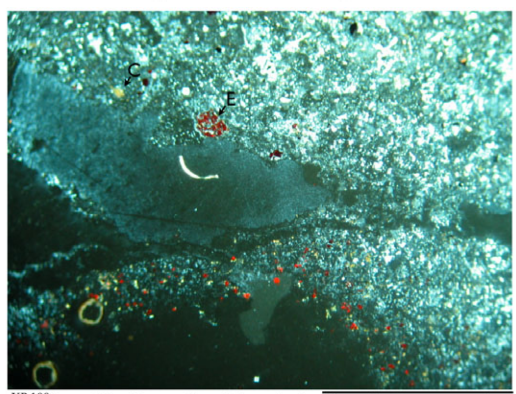

XP 100x chlorite and epidote inclusions in host 1 mm

Sample TM127

Turquoise:

- Color - light brown to dark brown
- Texture - dense, fine-grained spherules .02 - .04 mm diameter, porous
- Alteration - centers of spherules have higher relief and 1st order white and yellow interference colors and rims have lower relief and yellowish brown color in plane light.
- Turquoise in one area is intergrown with dark brown mineral with light brown interference color, either oxide-stained sericite or chlorite

Host:

- Denser turquoise is separated from less dense turquoise by altered biotite/chlorite/iron oxide vein.
- Chlorite or sericite stained with iron oxides
- Altered feldspar, possibly epidote, and a red brown mineral

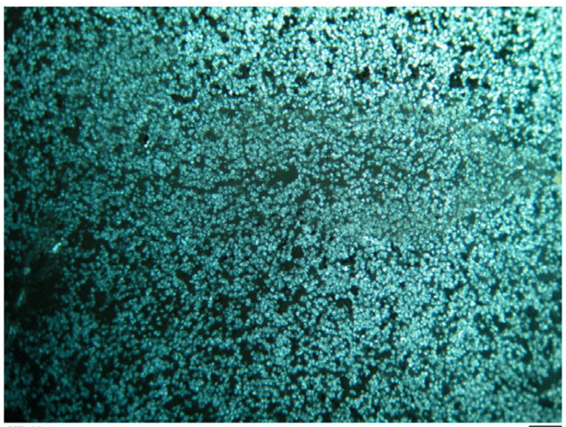

XP 40x turquoise spherules 1 mm

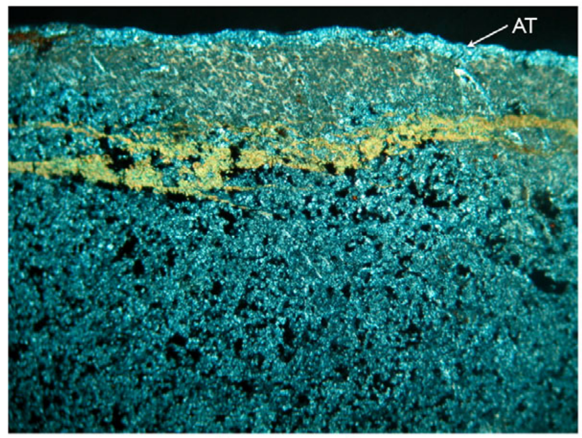

altered turquoise

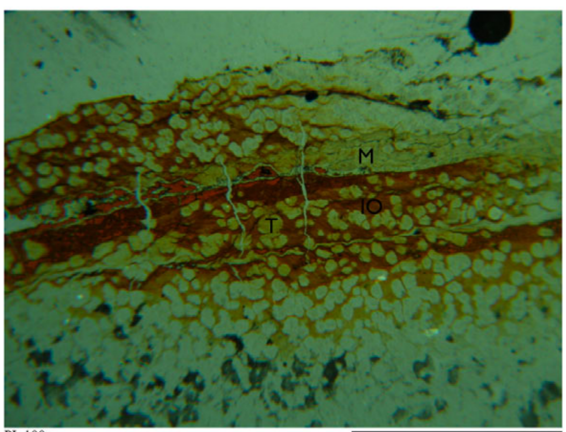

PL 100x turquoise intergrown with iron oxides and mica 1 mm

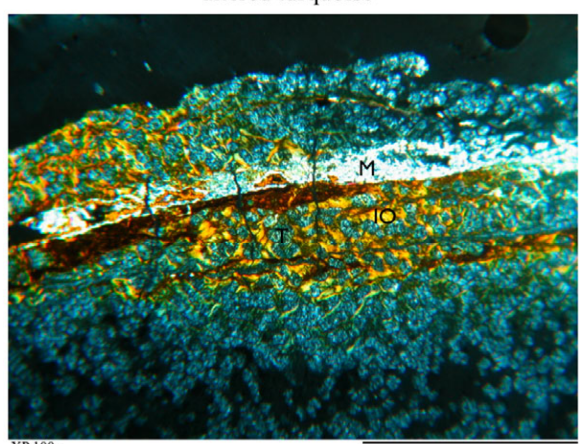

XP 100x turquoise intergrown with iron oxides and mica 1 mm

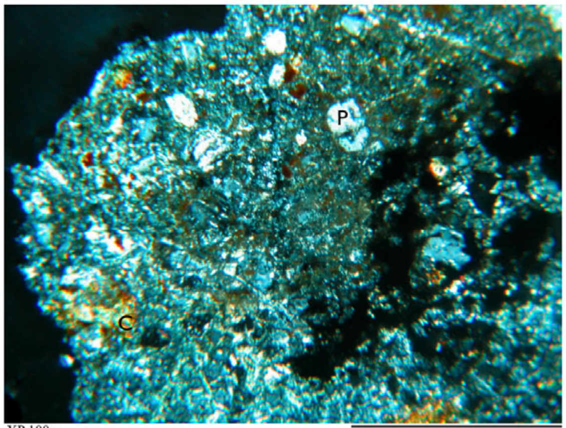

XP 100x plagioclase and chlorite in host 1 mm

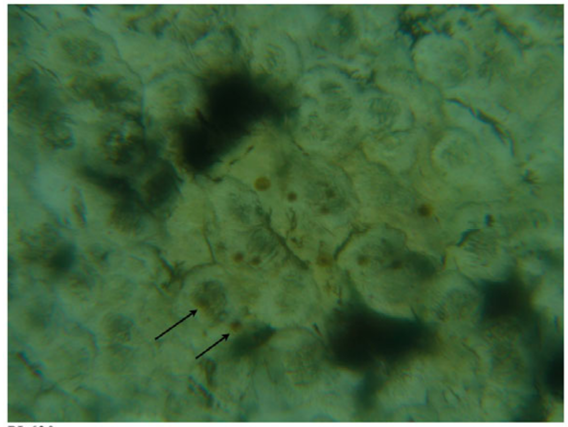

PL630x electron microprobe scars on turquoise spherules

Appendix F: Electron Microprobe Aanalyses of Turquoise Samples

Hachita Sample TM57

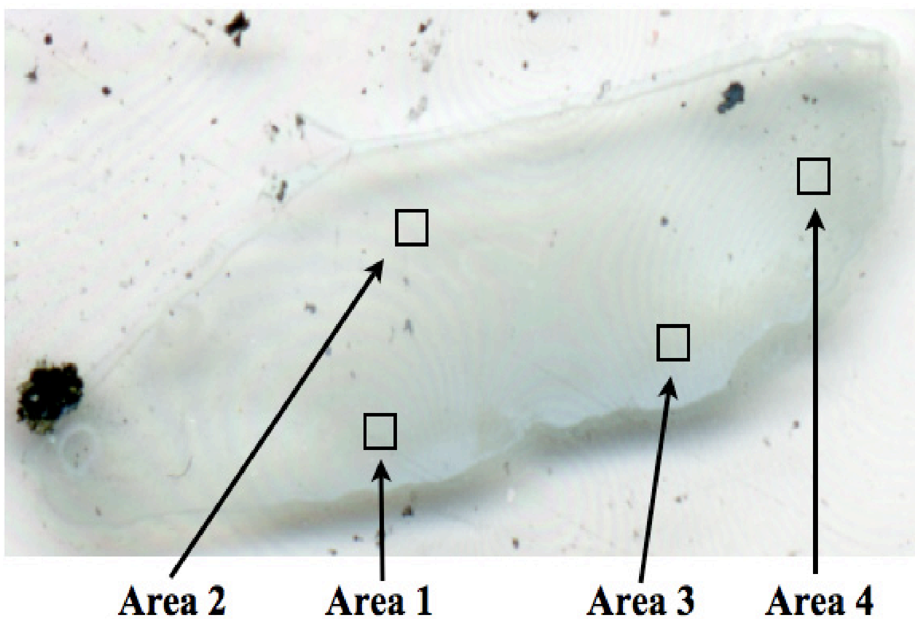

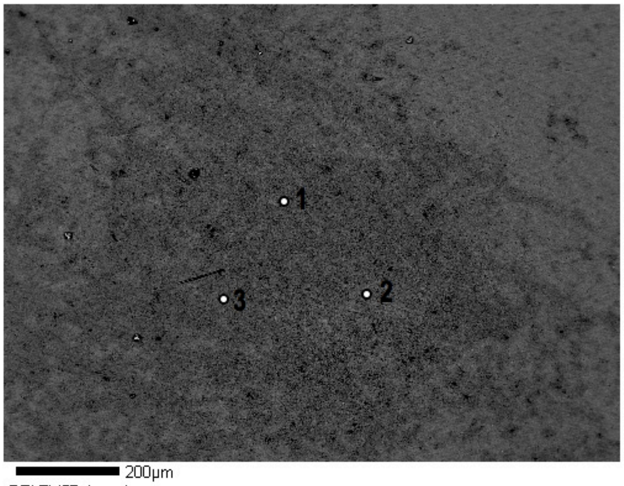

BEI TM57 Area 1

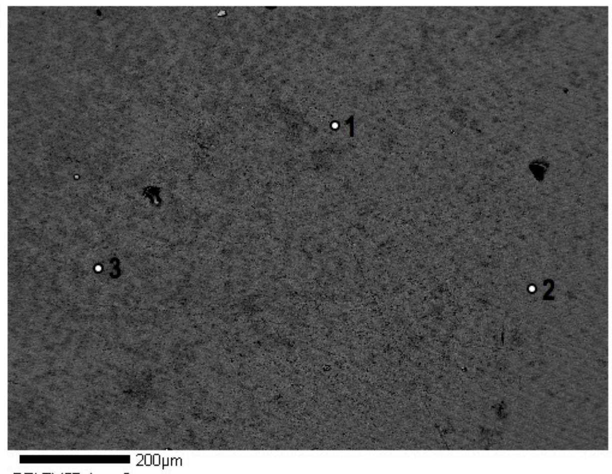

BEI TM57 Area 2

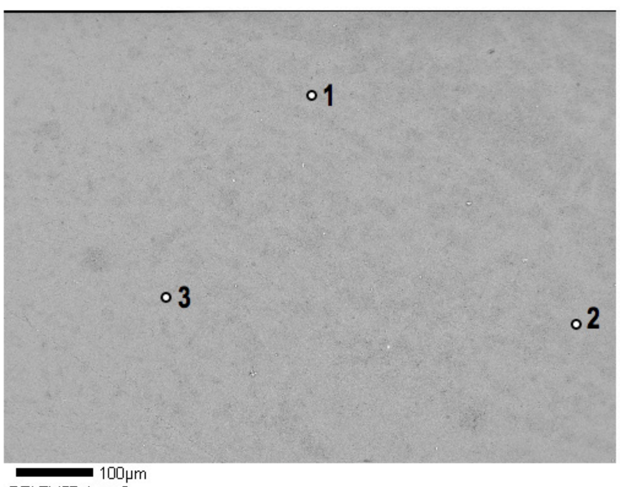

BEI TM57 Area 3

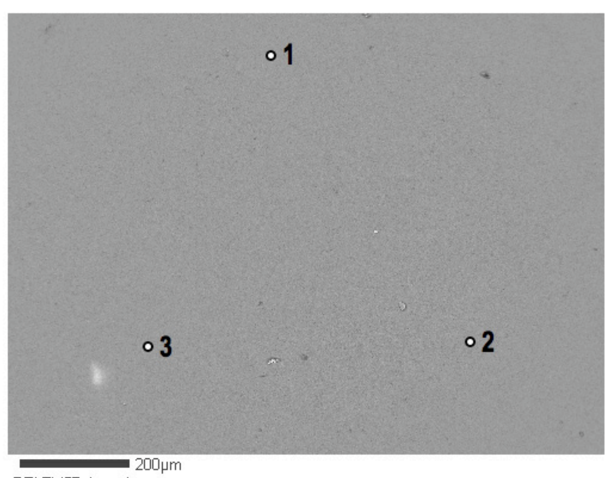

BEI TM57 Area 4

	TM57 1-1	TM57 1-2	TM57 1-3	TM57 2-1	TM57 2-2	TM57 2-3	TM57 3-1	TM57 3-2	TM57 3-3	TM57 4-1	TM57 4-2	TM57 4-3
CuO	5.52	6.16	5.45	5.47	5.75	5.65	5.79	5.91	6.26	5.27	5.91	5.27
MnO	0	0	0	0	0	0	0	0	0	0	0	0
ZnO	0	0	0	0	0	0	0	0	0	0	0	0
TiO2	0	0	0	0	0	0	0	0	0	0	0	0
MgO	0	0	0	0	0	0	0	0	0	0	0	0
CaO	0	0	0	0	0	0	0	0	0	0	0	0.09
K2O	0	0	0	0.1	0.08	0.07	0	0	0.06	0	0	0.08
Fe2O3	0.78	0.88	1.12	0.96	0.91	1.01	0.96	0.83	0.96	0.73	0.91	1.07
Al2O3	33.87	31.89	33.9	32.16	37.38	31.81	34.96	32.67	36.72	30.88	34.56	31.63
SiO2	0	0	0	0	0	0	0	0	0	0	0	0
P2O5	29.5	27.97	28.81	29.11	30.66	29.15	29.96	30.55	30.13	28.86	29.12	29.17
Total	69.67	66.9	69.28	67.8	74.78	67.69	71.67	69.96	74.13	65.74	70.5	67.3
H2O (by diff.)	30.33	33.1	30.72	32.2	25.22	32.31	28.33	30.04	25.87	34.26	29.5	32.7
TOTAL (w/H2O)	100	100	100	100	100	100	100	100	100	100	100	100
Based on 28O												
Cu	0.51	0.56	0.5	0.5	0.55	0.52	0.54	0.55	0.6	0.47	0.55	0.48
Fe	0.07	0.08	0.1	0.09	0.09	0.09	0.09	0.08	0.09	0.07	0.08	0.1
Al	4.89	4.54	4.89	4.59	5.59	4.54	5.12	4.73	5.49	4.34	5.03	4.5
Mn	0	0	0	0	0	0	0	0	0	0	0	0
Zn	0	0	0	0	0	0	0	0	0	0	0	0
Ti	0	0	0	0	0	0	0	0	0	0	0	0
Mg	0	0	0	0	0	0	0	0	0	0	0	0
Ca	0	0	0	0	0	0	0	0	0	0	0	0.01
K	0	0	0	0.02	0.01	0.01	0	0	0.01	0	0	0.01
Si	0	0	0	0	0	0	0	0	0	0	0	0
P	3.06	2.86	2.98	2.98	3.29	2.99	3.15	3.17	3.23	2.91	3.04	2.98
TOTAL	8.53	8.04	8.47	8.18	9.53	8.15	8.9	8.53	9.42	7.79	8.7	8.08

Hachita Sample TM66

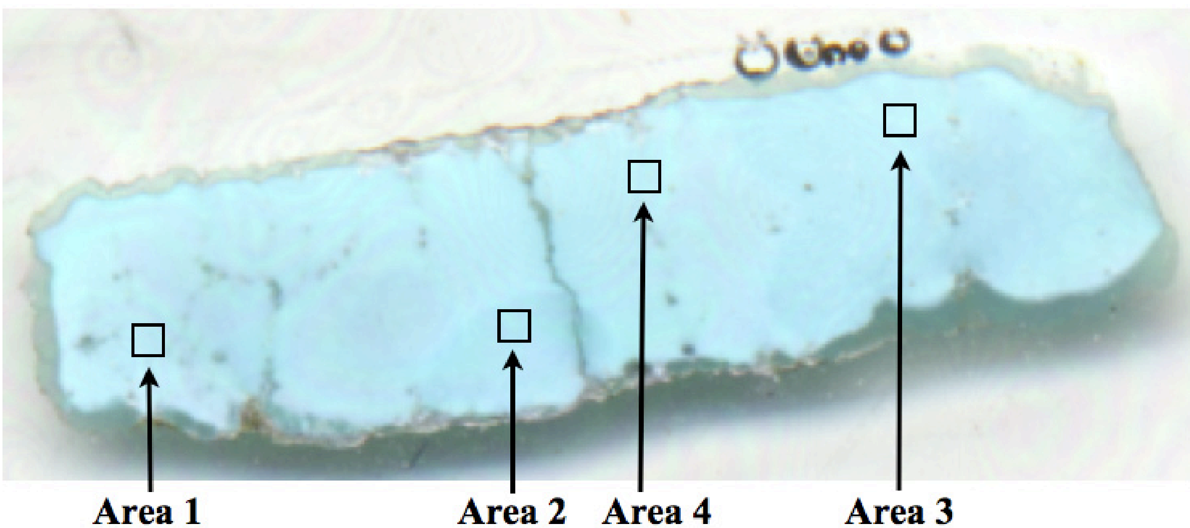

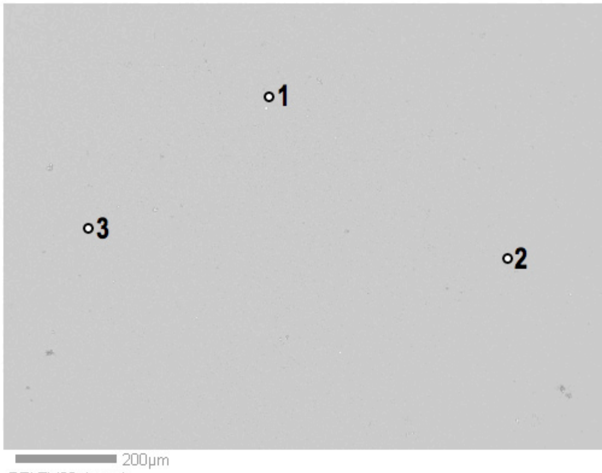

BEI TM66 Area 1

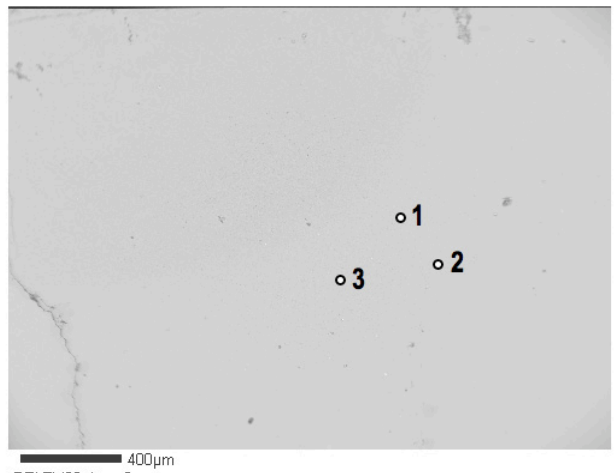

BEI TM66 Area 2

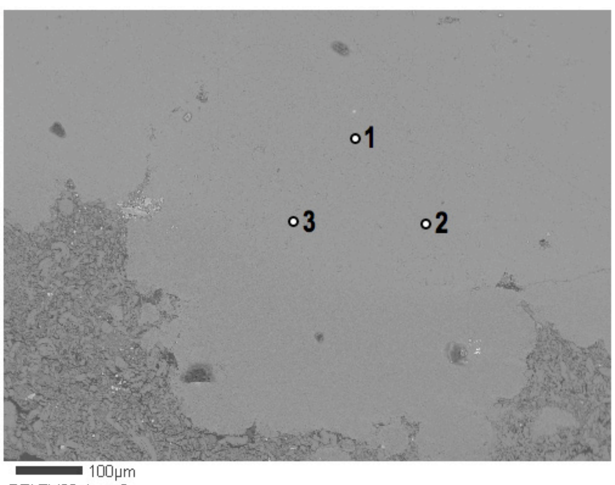

BEI TM66 Area 3

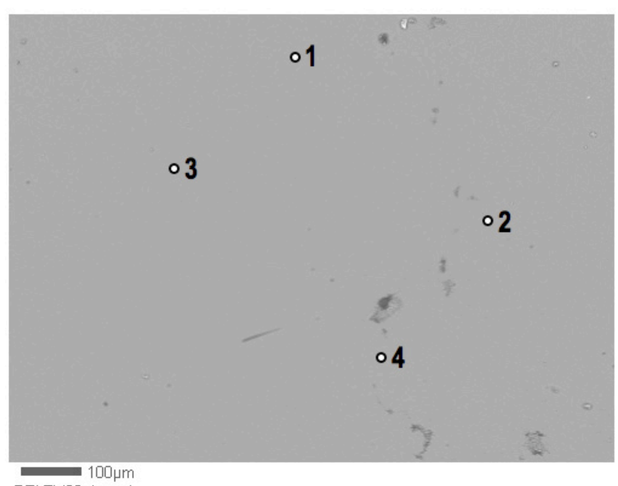

BEI TM66 Area 4

	TM66 1-1	TM66 1-2	TM66 1-3	TM66 2-1	TM66 2-2	TM66 2-3	TM66 3-1	TM66 3-2	TM66 3-3	TM66 4-1	TM66 4-2	TM66 4-3	TM66 4-4
CuO	7.03	7.95	7.14	7.87	7.07	7.69	6.82	7.35	7.32	9.64	8.35	8.88	7.94
MnO	0	0	0	0	0	0	0	0	0	0	0	0	0
ZnO	0	0	0	0	0	0	0	0	0	0	0	0	0
TiO2	0	0	0	0	0	0	0	0	0	0	0	0	0
MgO	0	0.09	0	0	0	0	0	0	0	0	0	0	0
CaO	0.13	0	0.14	0.13	0.11	0.11	0.18	0.21	0.16	0.18	0.15	0.14	0.15
K2O	0	0	0	0	0.06	0.09	0	0	0.07	0	0.05	0.06	0
Fe2O3	1.01	1.52	1.72	1.57	1.46	1.45	1.24	1.43	1.43	1.29	1.55	0.84	1.9
Al2O3	38.26	36.65	36.68	37.38	38.44	36.18	36.07	38.55	35.86	38.38	36.35	38.09	35.97
SiO2	0	0.1	0.13	0	0.1	0.1	0.09	0	0.14	0.11	0	0	0.11
P2O5	33	31.58	30.93	31.45	31.85	31.64	30.46	31.3	30.41	34.88	32.4	33.08	31.87
Total	79.43	77.9	76.74	78.4	79.09	77.26	74.87	78.84	75.39	84.47	78.85	81.1	77.94
H2O (by diff.)	20.57	22.1	23.26	21.6	20.91	22.74	25.13	21.16	24.61	15.53	21.15	18.9	22.06
TOTAL (w/H2O)	100	100	100	100	100	100	100	100	100	100	100	100	100
Based on 28O													
Cu	0.7	0.79	0.7	0.78	0.7	0.76	0.66	0.73	0.71	1.01	0.83	0.9	0.79
Fe	0.1	0.15	0.17	0.16	0.14	0.14	0.12	0.14	0.14	0.13	0.15	0.09	0.19
Al	5.93	5.67	5.61	5.8	5.97	5.56	5.43	5.99	5.44	6.25	5.67	6.03	5.57
Mn	0	0	0	0	0	0	0	0	0	0	0	0	0
Zn	0	0	0	0	0	0	0	0	0	0	0	0	0
Ti	0	0	0	0	0	0	0	0	0	0	0	0	0
Mg	0	0.02	0	0	0	0	0	0	0	0	0	0	0
Ca	0.02	0	0.02	0.02	0.02	0.01	0.03	0.03	0.02	0.03	0.02	0.02	0.02
K	0	0	0	0	0.01	0.02	0	0	0.01	0	0.01	0.01	0
Si	0	0.01	0.02	0	0.01	0.01	0.01	0	0.02	0.01	0	0	0.01
P	3.68	3.51	3.4	3.51	3.55	3.49	3.3	3.49	3.31	4.08	3.63	3.76	3.54
TOTAL	10.43	10.15	9.92	10.27	10.4	9.99	9.55	10.38	9.65	11.51	10.31	10.81	10.12

Hachita Sample TM68

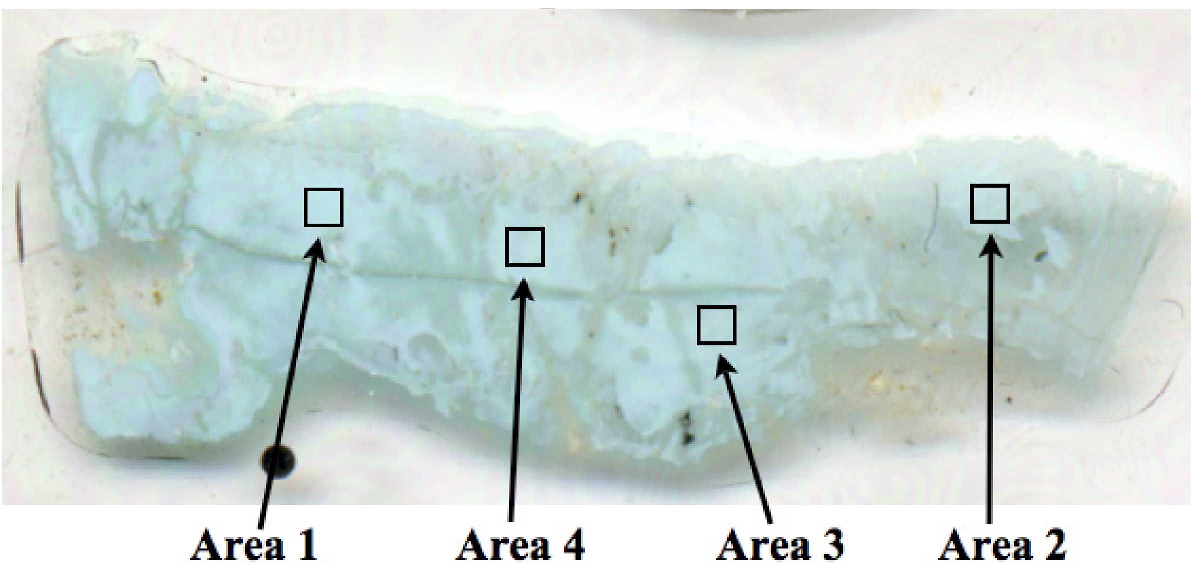

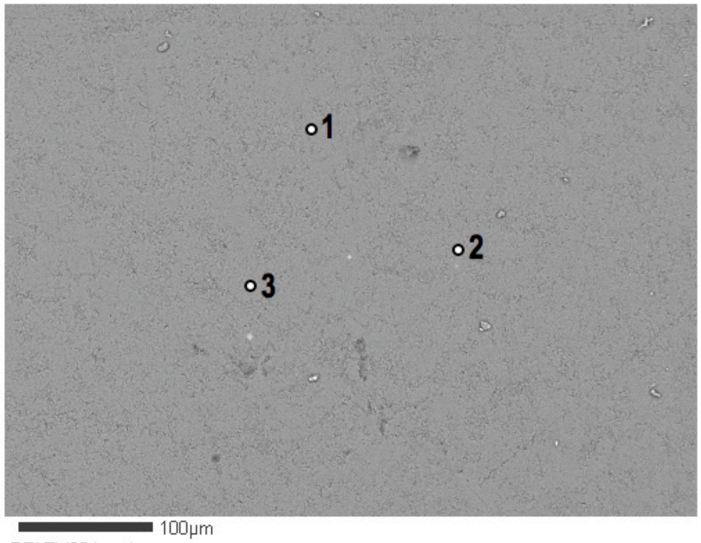

BEI TM68Area1

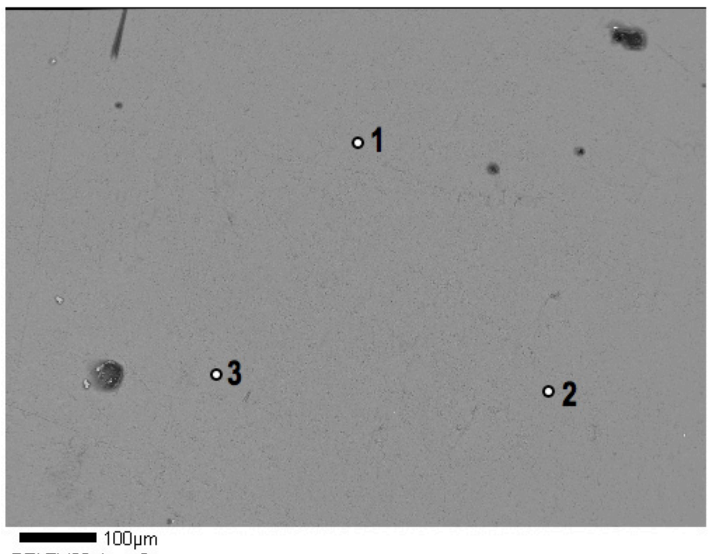

BEI TM68 Area 2

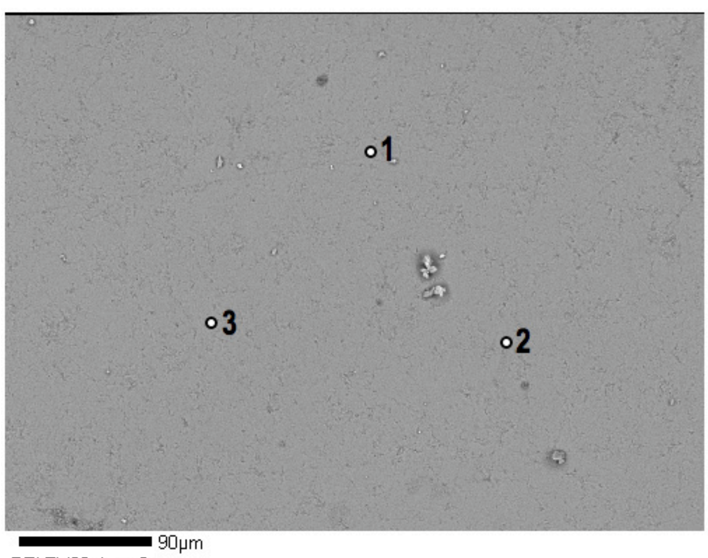

BEI TM68 Area 3

	TM68 1-1	TM68 1-2	TM68 1-3	TM68 2-1	TM68 2-2	TM68 2-3	TM68 3-1	TM68 3-2	TM68 3-3	TM68 4-1	TM68 4-2
CuO	7.05	7.95	7.53	6.92	6.51	7.1	7.61	6.76	6.98	7.65	7.17
MnO	0	0	0	0	0	0	0	0	0	0	0
ZnO	0	0	0	0	0.43	0	0	0	0	0	0
TiO2	0	0	0	0	0	0	0	0	0	0	0
MgO	0	0	0	0	0	0	0	0	0	0	0
CaO	0	0	0	0	0.09	0	0	0	0	0	0
K2O	0.06	0	0	0	0	0.06	0.05	0.07	0.06	0.06	0.08
Fe2O3	1.1	0.81	1.28	0.84	1.19	1.14	0.77	0.87	1.49	1.23	1.07
Al2O3	38.67	36.91	36.24	38.27	35.36	38.79	34.99	38.01	35.34	40.25	40.33
SiO2	0	0	0	0	0	0	0	0	0	0	0
P2O5	32.25	34.08	33.62	31.35	33.05	33.27	33.67	34.61	31.26	33.28	31.94
Total	79.25	79.84	78.81	77.47	76.76	80.49	77.18	80.42	75.3	82.61	80.72
H2O (by diff.)	20.75	20.16	21.19	22.53	23.24	19.51	22.82	19.58	24.7	17.39	19.28
TOTAL (w/H2O)	100	100	100	100	100	100	100	100	100	100	100
Based on 28O											
Cu	0.51	0.79	0.75	0.68	0.63	0.71	0.74	0.67	0.68	0.78	0.72
Fe	0.11	0.08	0.13	0.08	0.12	0.11	0.07	0.09	0.14	0.13	0.11
Al	6	5.75	5.61	5.86	5.38	6.07	5.34	5.91	5.34	6.42	6.33
Mn	0	0	0	0	0	0	0	0	0	0	0
Zn	0	0	0	0	0.04	0	0	0	0	0	0
Ti	0	0	0	0	0	0	0	0	0	0	0
Mg	0	0	0	0	0	0	0	0	0	0	0
Ca	0	0	0	0	0.01	0	0	0	0	0	0
K	0.01	0	0	0	0	0.01	0.01	0.01	0.01	0.01	0.01
Si	0	0	0	0	0	0	0	0	0	0	0
P	3.6	3.82	3.74	3.45	3.61	3.74	3.69	3.87	3.39	3.81	3.6
TOTAL	10.23	10.44	10.23	10.07	9.79	10.64	9.85	10.55	9.56	11.15	10.77

Hachita Sample TM70

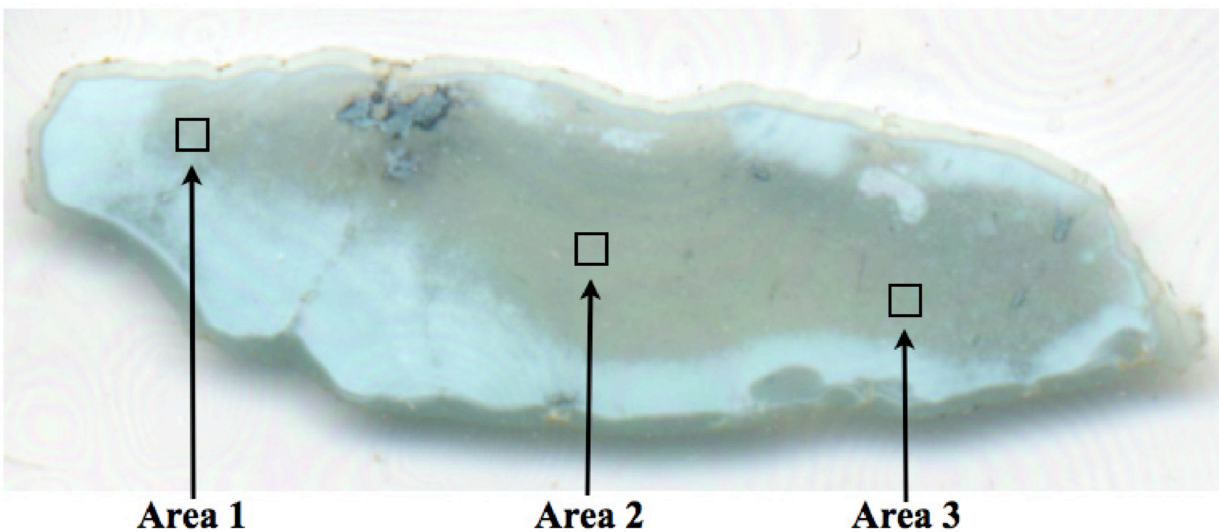

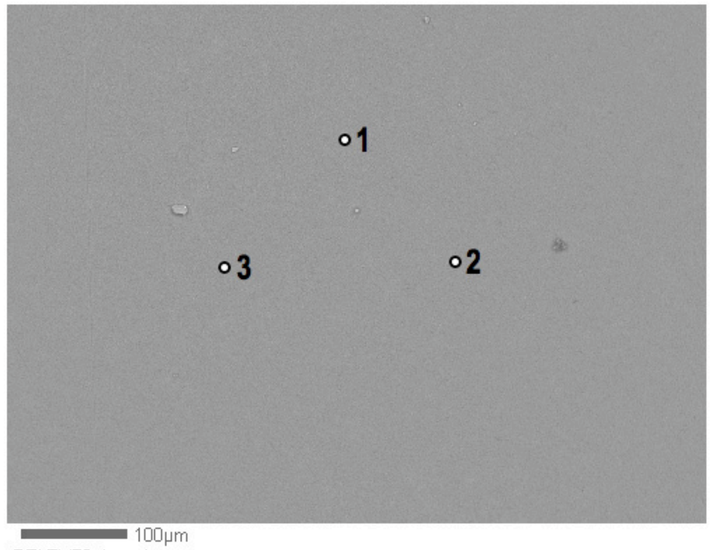

BEI TM70 Area 1

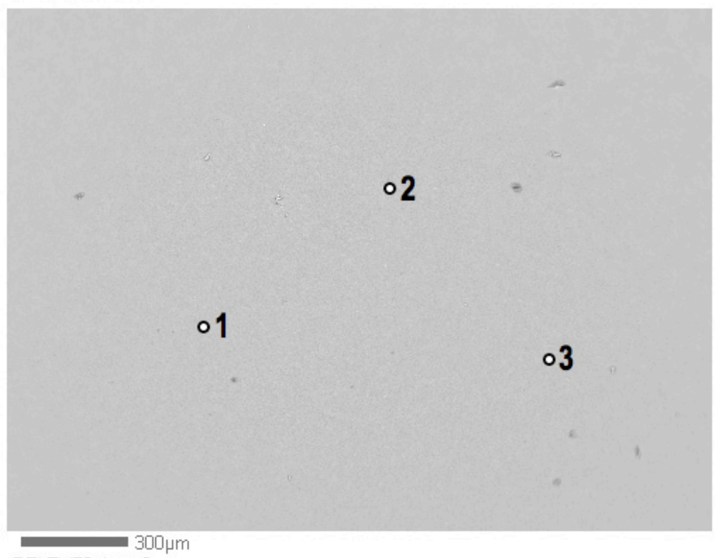

BEI TM70 Area 2

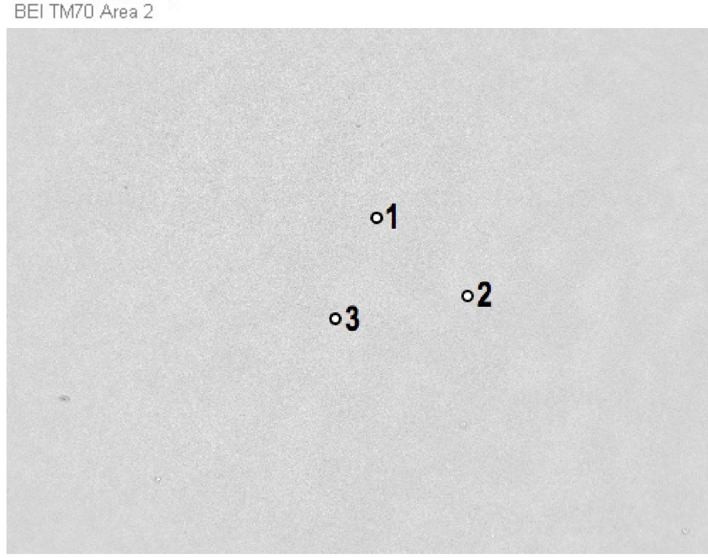

BEI TM70 Area 3

	TM70 1-1	TM70 1-2	TM70 1-3	TM70 2-1	TM70 2-2	TM70 2-3	TM70 3-1	TM70 3-2	TM70 3-3
CuO	6.65	7.48	7.87	7.13	7.13	7.63	8.93	8.21	9.18
MnO	0	0	0	0	0	0	0	0	0
ZnO	0	0	0	0	0	0	0	0	0
TiO2	0	0	0	0	0	0	0	0	0
MgO	0	0	0	0	0.09	0	0	0.11	0
CaO	0.14	0.2	0.12	0.2	0.15	0.11	0.23	0.15	0.21
K2O	0.06	0	0	0.06	0	0	0	0.07	0.12
Fe2O3	2.2	2.57	2.04	2.43	1.83	2.04	2.08	2.08	2.36
Al2O3	32.01	33.39	31.52	33.84	31.07	33.61	34.06	30.34	33.93
SiO2	0	0	0.1	0	0	0.12	0.11	0.14	0.11
P2O5	27.67	28.87	29.37	28.1	29.01	27.53	27.3	30.1	28.92
Total	68.73	72.51	71.02	71.76	69.29	71.04	72.71	71.2	74.84
H2O (by diff.)	31.27	27.49	28.98	28.24	30.71	28.96	27.29	28.8	25.16
TOTAL (w/H2O)	100	100	100	100	100	100	100	100	100
Based on 28O									
Cu	0.62	0.72	0.75	0.68	0.67	0.72	0.86	0.78	0.9
Fe	0.2	0.25	0.19	0.01	0.17	0.19	0.2	0.2	0.23
Al	4.65	4.99	4.66	5.03	4.52	4.98	5.14	4.5	5.2
Mn	0	0	0	0	0	0	0	0	0
Zn	0	0	0	0	0	0	0	0	0
Ti	0	0	0	0	0	0	0	0	0
Mg	0	0	0	0	0.02	0	0	0.02	0
Ca	0.02	0.03	0.02	0.03	0.02	0.01	0.03	0.02	0.03
K	0.01	0	0	0.01	0	0	0	0.01	0.02
Si	0	0	0.01	0	0	0.01	0.01	0.02	0.01
P	2.89	3.1	3.12	3	3.03	2.93	2.96	3.2	3.18
TOTAL	8.39	9.09	8.75	8.76	8.43	8.84	9.2	8.75	9.57

Hachita Sample TM91

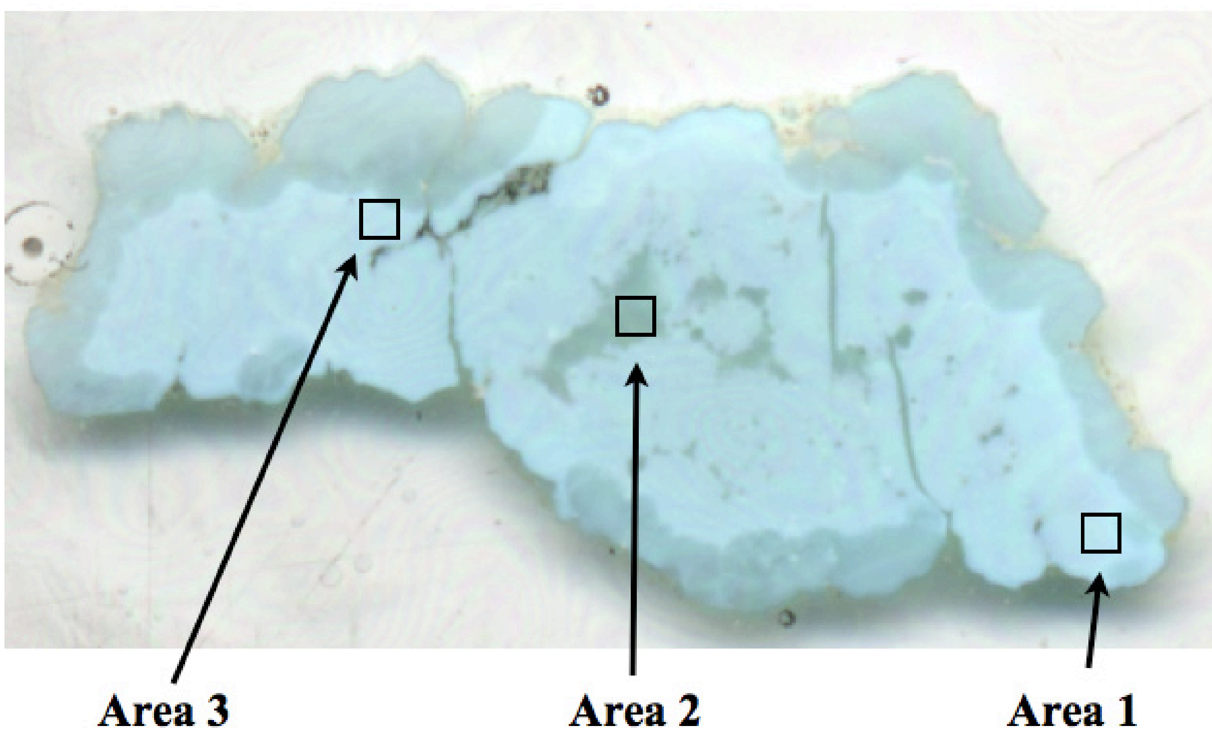

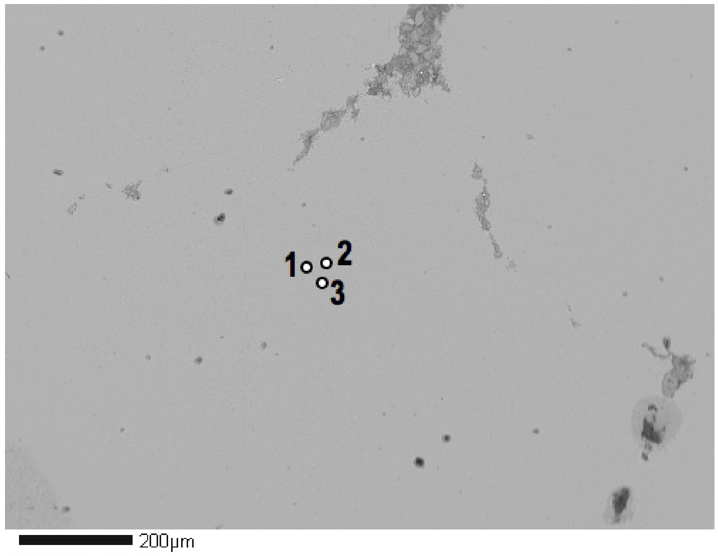

BEI TM91 Area 1

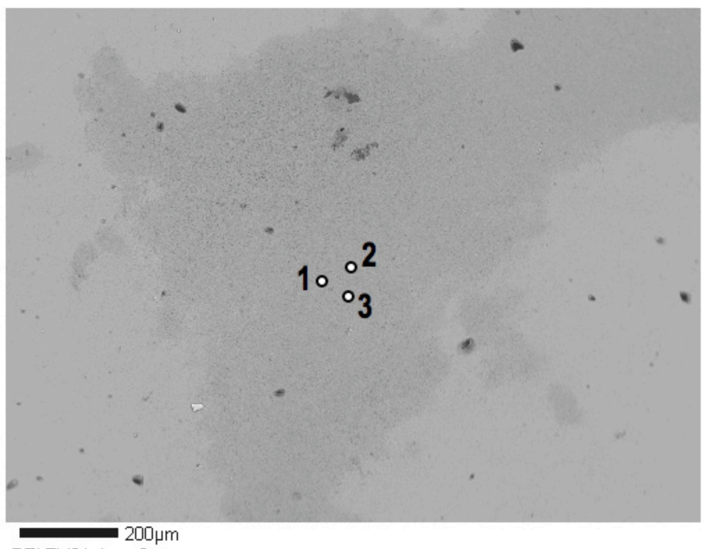

BEI TM91 Area 2

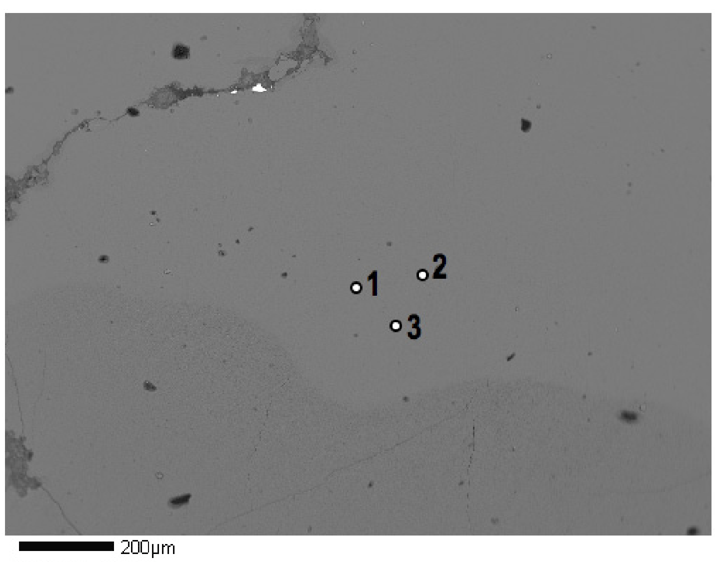

BEI TM91 Area 3

	TM91 1-1	TM91 1-2	TM91 1-3	TM91 2-1	TM91 2-2	TM91 2-3	TM91 3-1	TM91 3-2	TM91 3-3
CuO	7.59	9.2	8.69	7.66	7.54	8.15	8.89	8.64	8.5
MnO	0	0	0	0	0	0	0	0.17	0
ZnO	0	0	0	0	0	0	0	0	0
TiO2	0	0	0	0	0	0	0	0	0
MgO	0	0	0	0	0	0	0	0	0
CaO	0	0.09	0	0	0	0	0.08	0.08	0
K2O	0.08	0.05	0.09	0.07	0.07	0.07	0	0.06	0
Fe2O3	1.41	1.08	0.73	0.96	0.75	0.96	1.15	0.68	1.29
Al2O3	37.23	38.62	36.81	37.32	34.26	37.11	37.26	38.5	37.01
SiO2	0	0.1	0.15	0.12	0.17	0.15	0.12	0.13	0.09
P2O5	34.3	33.87	32.67	31.81	29.7	30.15	31.14	34.52	33.13
Total	80.61	83.02	79.13	77.94	72.49	76.59	78.64	82.78	80.02
H2O (by diff.)	19.39	16.98	20.87	22.06	27.51	23.41	21.36	17.22	19.98
TOTAL (w/H2O)	100	100	100	100	100	100	100	100	100
Based on 28O									
Cu	0.76	0.95	0.87	0.76	0.72	0.8	0.89	0.89	0.85
Fe	0.14	0.11	0.07	0.09	0.07	0.09	0.11	0.07	0.13
Al	5.84	6.21	5.74	5.75	5.09	5.69	5.82	6.15	5.81
Mn	0	0	0	0	0	0	0	0.02	0
Zn	0	0	0	0	0	0	0	0	0
Ti	0	0	0	0	0	0	0	0	0
Mg	0	0	0	0	0	0	0	0	0
Ca	0	0.01	0	0	0	0	0.01	0.01	0
K	0.01	0.01	0.01	0.01	0.01	0.01	0	0.01	0
Si	0	0.01	0.02	0.02	0.02	0.02	0.02	0.02	0.01
P	3.86	3.91	3.66	3.52	3.17	3.32	3.49	3.96	3.73
TOTAL	10.61	11.21	10.37	10.15	9.08	9.93	10.34	11.13	10.53

Hachita Sample TM95

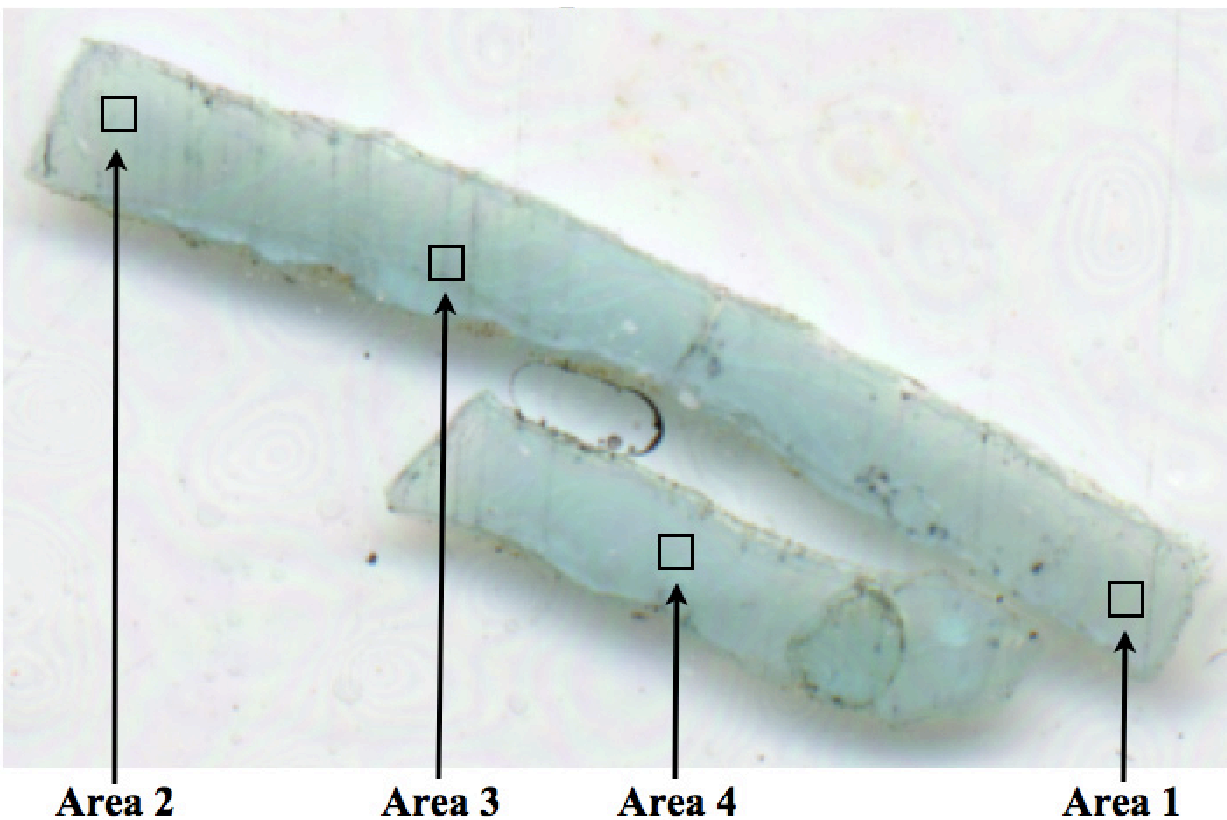

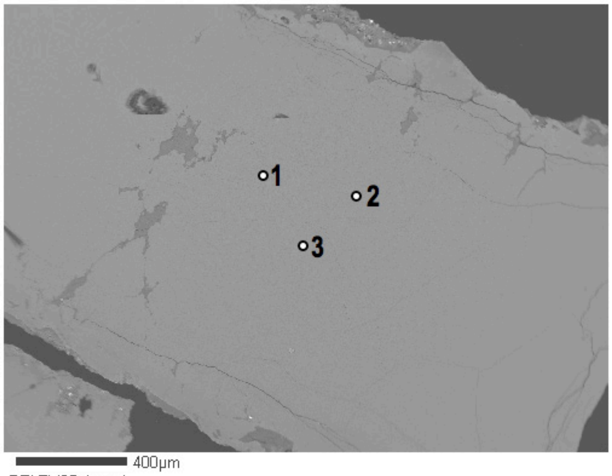

BEI TM95 Area 1

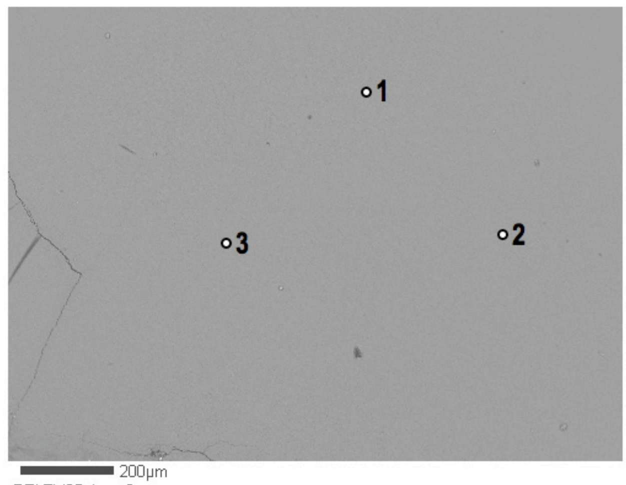

BEI TM95 Area 2

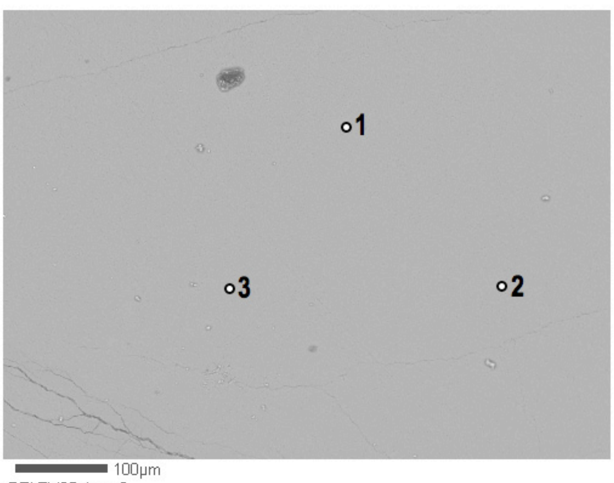

BEI TM95 Area 3

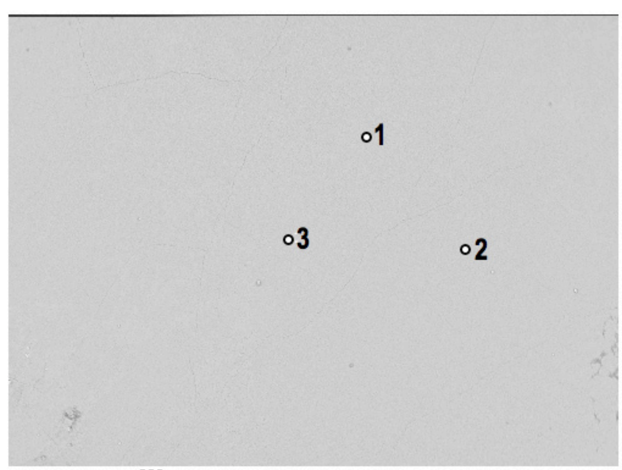

BEI TM95 Area 4

	TM95 1-1	TM95 1-2	TM95 1-3	TM95 2-1	TM95 2-2	TM95 2-3	TM95 3-1	TM95 3-2	TM95 3-3	TM95 4-1	TM95 4-2	TM95 4-3
CuO	8.09	7.17	8.08	6.71	6.58	7.12	6.65	6.71	6.92	6.98	7.26	7.44
MnO	0	0	0	0	0	0	0	0	0	0	0	0
ZnO	0	0	0	0	0	0	0	0	0	0	0	0
TiO2	0	0	0	0	0	0	0	0	0	0	0	0
MgO	0	0	0	0	0	0	0	0	0	0.11	0	0.16
CaO	0.17	0.11	0.2	0	0.17	0.11	0	0.09	0.08	0.18	0	0.17
K2O	0.06	0	0.08	0.11	0.08	0.07	0.09	0.08	0.11	0	0.06	0.07
Fe2O3	2.23	2.37	2.4	2.25	2.2	2.56	1.79	1.8	2.44	2.66	2.46	2.95
Al2O3	33.94	36.93	34.32	37.39	33.61	37.31	34.26	36.72	35.01	37.59	34.39	33.81
SiO2	0.44	0.52	0.58	0.51	0.57	0.53	0.31	0.32	0.35	0.66	0.58	0.88
P2O5	31.94	31.43	30.5	31.21	31.73	32.04	31.68	32.14	31.57	30.64	30.79	29.84
Total	76.88	78.53	76.16	78.18	74.94	79.75	74.78	77.85	76.48	78.82	75.54	75.31
H2O (by diff.)	23.12	21.47	23.84	21.82	25.06	20.25	25.22	22.15	23.52	21.18	24.46	24.69
TOTAL (w/H2O)	100	100	100	100	100	100	100	100	100	100	100	100
Based on 28O												
Cu	0.8	0.71	0.79	0.66	0.64	0.71	0.64	0.66	0.68	0.7	0.71	0.73
Fe	0.22	0.23	0.24	0.22	0.21	0.26	0.17	0.18	0.24	0.26	0.24	0.29
Al	5.22	5.73	5.27	5.77	5.06	5.84	5.15	5.64	5.35	5.85	5.23	5.15
Mn	0	0	0	0	0	0	0	0	0	0	0	0
Zn	0	0	0	0	0	0	0	0	0	0	0	0
Ti	0	0	0	0	0	0	0	0	0	0	0	0
Mg	0	0	0	0	0	0	0	0	0	0.02	0	0.03
Ca	0.02	0.01	0.03	0	0.02	0.02	0	0.01	0.01	0.03	0	0.02
K	0.01	0	0.01	0.02	0.01	0.01	0.01	0.01	0.02	0	0.01	0.01
Si	0.06	0.07	0.08	0.07	0.07	0.07	0.04	0.04	0.05	0.09	0.07	0.11
P	3.53	3.5	3.36	3.46	3.43	3.6	3.42	3.55	3.46	3.43	3.36	3.27
TOTAL	9.86	10.25	9.78	10.2	9.44	10.51	9.43	10.09	9.81	10.38	9.62	9.61

Hachita Sample TM102

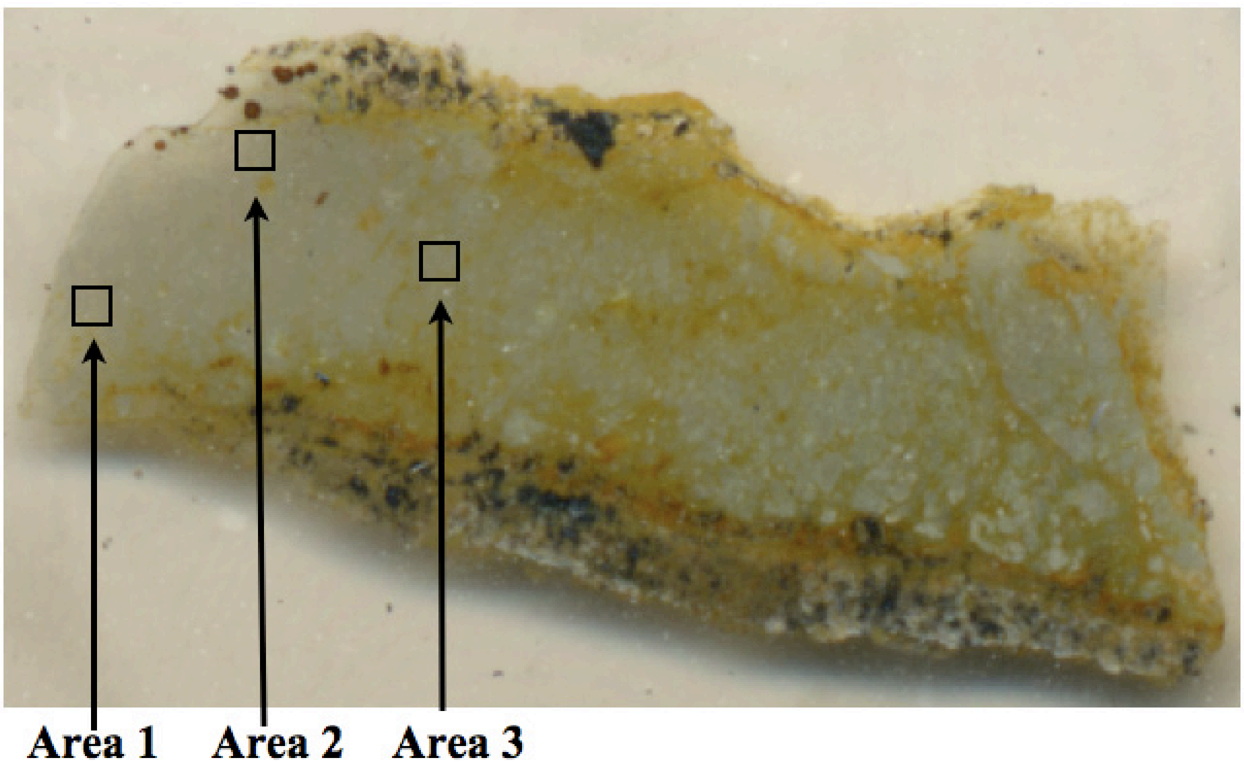

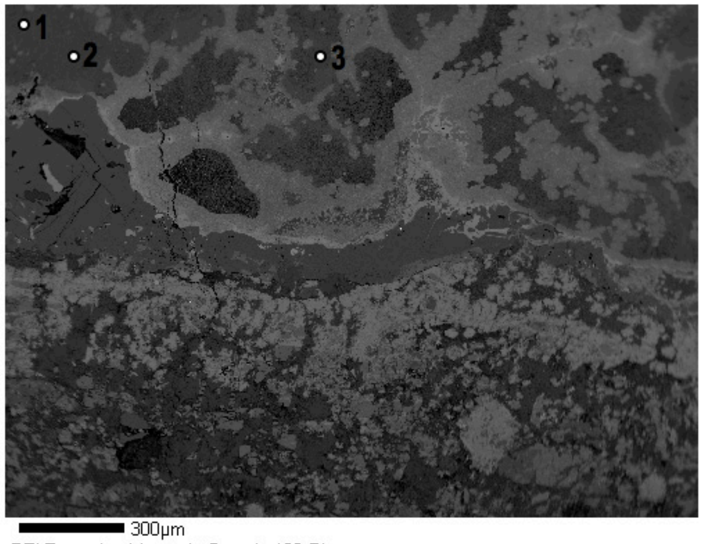

BEI Turquoise Mountain Sample 102 Rim

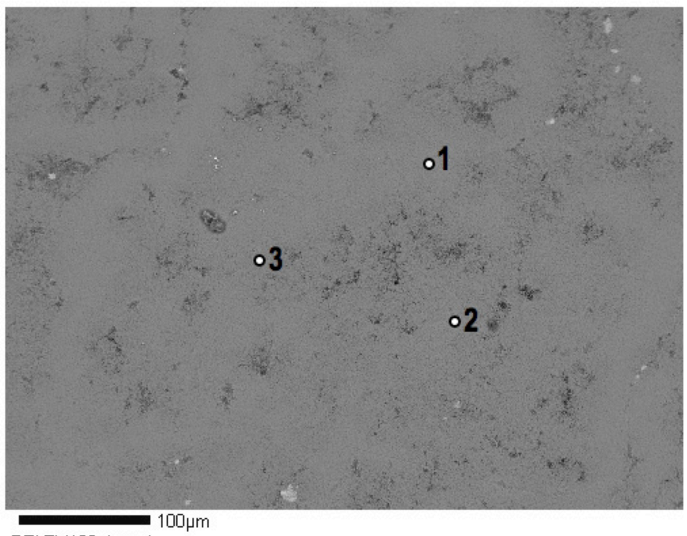

BEI TM102 Area 1

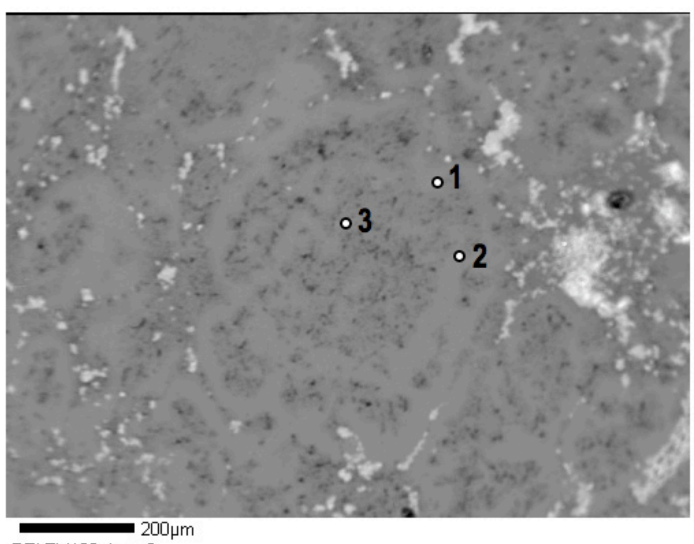

BEI TM102 Area 2

	TM102 1-1	TM102 1-2	TM102 1-3	TM102 2-1	TM102 2-2	TM102 2-3	TM102 3-1	TM102 3-2	TM102 3-3
CuO	7.72	8.1	7.53	8.51	7.51	7.55	5.47	6.97	6.03
MnO	0	0	0	0	0	0	0	0	0
ZnO	0	0	0.05	0	0	0	0	0	0
TiO2	0	0	0	0	0	0	0	0	0
MgO	0	0	0	0	0	0	0	0	0
CaO	0.7	0.62	0.71	0.73	0.73	0.74	0.57	0.59	0.56
K2O	0.19	0.23	0.23	0.24	0.17	0.27	0.18	0.24	0.24
Fe2O3	1.68	1.87	1.68	1.85	1.78	1.54	1.78	1.75	1.63
Al2O3	32.56	35.69	32.07	35.01	32	35.04	33.6	33.2	34.35
SiO2	6.7	5.57	6.29	6.46	5.95	6.58	4.25	6.28	6.5
P2O5	27.93	28.81	27.2	29.42	28.12	29.81	29.21	30.6	31.36
Total	77.48	80.89	75.76	82.22	76.26	81.52	75.05	79.62	80.68
H2O (by diff.)	22.52	19.11	24.24	17.78	23.74	18.48	24.95	20.38	19.32
TOTAL (w/H2O)	100	100	100	100	100	100	100	100	100
Based on 28O									
Cu	0.76	0.82	0.74	0.87	0.74	0.77	0.53	0.7	0.6
Fe	0.17	0.19	0.16	0.19	0.17	0.16	0.17	0.17	0.16
Al	5.02	5.66	4.89	5.61	4.89	5.55	5.04	5.17	5.35
Mn	0	0	0	0	0	0	0	0	0
Zn	0	0	0	0	0	0	0	0	0
Ti	0	0	0	0	0	0	0	0	0
Mg	0	0	0	0	0	0	0	0	0
Ca	0.1	0.09	0.1	0.11	0.1	0.11	0.08	0.08	0.08
K	0.03	0.04	0.04	0.04	0.03	0.05	0.03	0.04	0.04
Si	0.88	0.75	0.81	0.88	0.77	0.88	0.54	0.83	0.86
P	3.1	3.28	2.98	3.39	3.09	3.39	3.15	3.42	3.51
TOTAL	10.06	10.83	9.72	11.09	9.79	10.91	9.54	10.41	10.6

Hachita Sample TM109

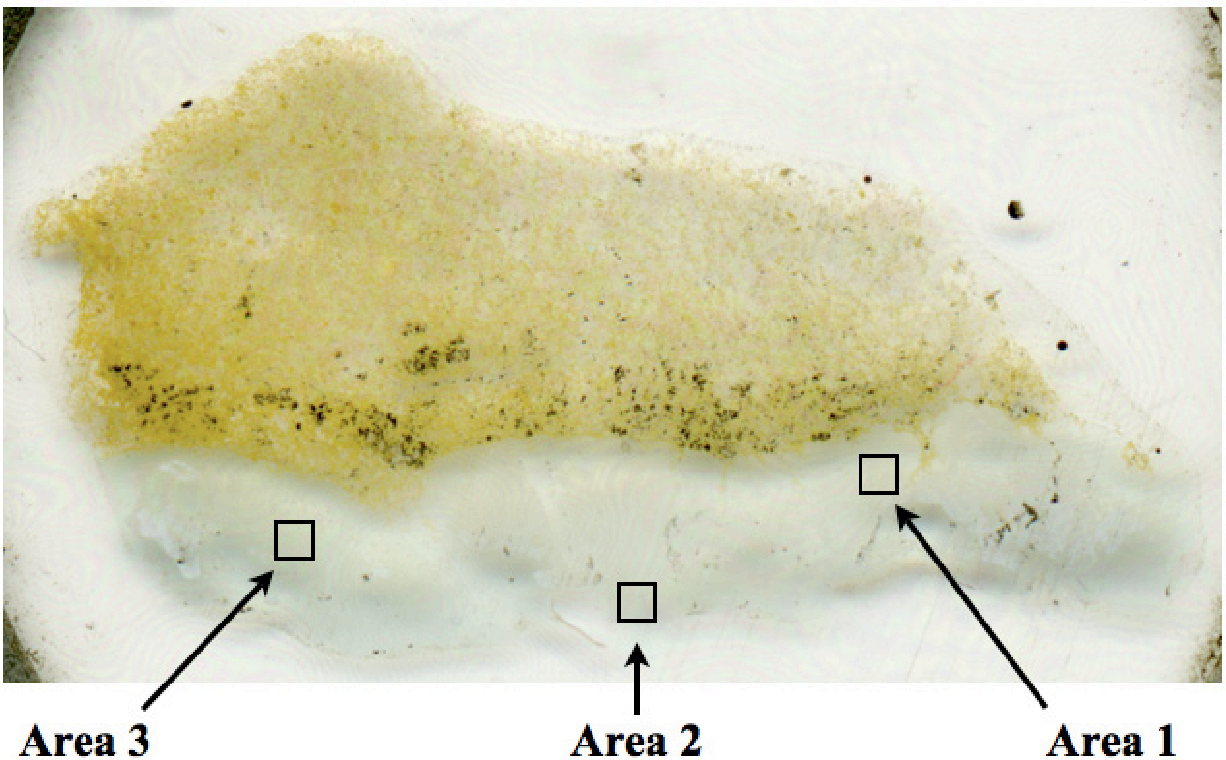

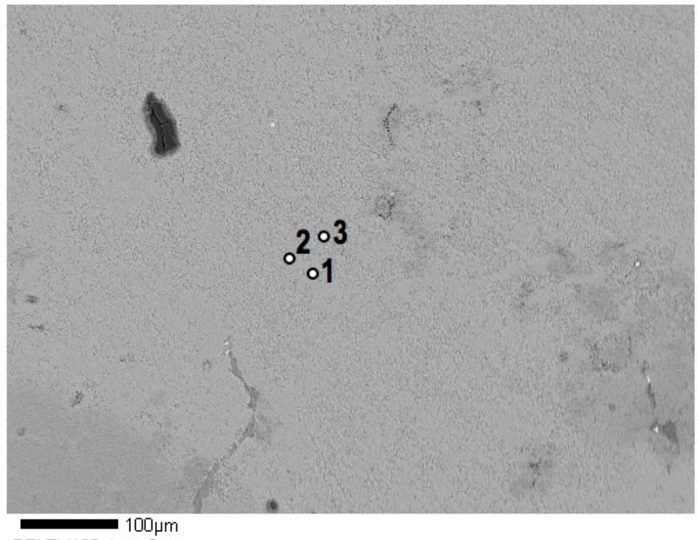

BEI TM109 Area 3

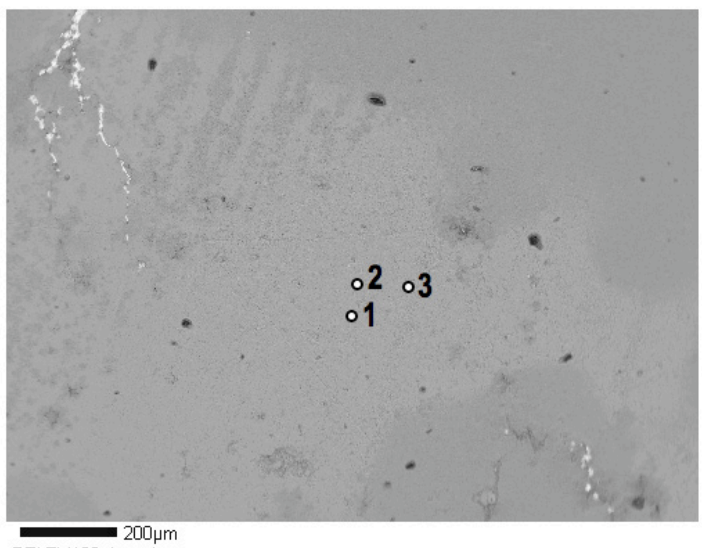

BEI TM109 Area 1

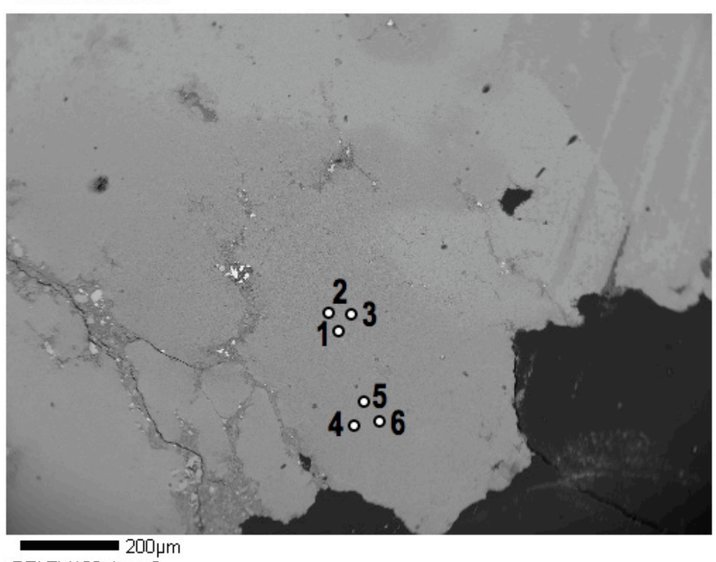

BEI TM109 Area 2

	TM109 1-1	TM109 1-2	TM109 1-3	TM109 2-1	TM109 2-2	TM109 2-3	TM109 2-4	TM109 2-5	TM109 2-6	TM109 3-1	TM109 3-2	TM109 3-3
CuO	7.99	7.59	7.96	8.04	7.54	7.64	7.75	7.86	6.21	8.04	7.38	8.09
MnO	0	0	0	0	0	0	0	0	0	0	0	0
ZnO	0.04	0	0	0.14	0	0	0	0	0	0	0	0
TiO2	0	0	0	0	0	0	0	0	0	0	0	0
MgO	0	0	0	0	0	0	0	0	0	0	0	0
CaO	0.11	0	0.07	0	0	0.11	0.09	0	0	0.14	0.11	0.12
K2O	0	0	0.06	0	0	0	0	0	0.11	0	0	0
Fe2O3	1.74	0.32	1.17	1.47	1.43	1.45	1.74	1.29	1.09	1.36	1.55	1.36
Al2O3	38.7	36.15	38.43	35.02	33.28	33.15	37.17	33.35	36.14	36.86	38.5	38.36
SiO2	0.13	0.13	0	0	0	0.15	0.09	0.11	0.15	0.18	0.16	0.11
P2O5	32.19	30.98	32.79	29.45	30.09	29.27	30.27	29.45	29.15	33	32.39	32.72
Total	80.9	76.16	80.48	74.13	72.34	71.77	77.11	72.06	72.84	79.58	80.09	80.76
H2O (by diff.)	19.1	23.84	19.52	25.87	27.66	28.23	22.89	27.94	27.16	20.42	19.91	19.24
TOTAL (w/ H2O)	100	100	100	100	100	100	100	100	100	100	100	100
Based on 28O												
Cu	0.81	0.74	0.8	0.78	0.72	0.73	0.76	0.75	0.59	0.8	0.74	0.82
Fe	0.18	0.13	0.12	0.14	0.14	0.14	0.17	0.12	0.1	0.14	0.16	0.14
Al	6.12	5.51	6.04	5.29	4.94	4.91	5.72	4.95	5.36	5.76	6.03	6.05
Mn	0	0	0	0	0	0	0	0	0	0	0	0
Zn	0	0	0	0.01	0	0	0	0	0	0	0	0
Ti	0	0	0	0	0	0	0	0	0	0	0	0
Mg	0	0	0	0	0	0	0	0	0	0	0	0
Ca	0.02	0	0.01	0	0	0.01	0.01	0	0	0.02	0.02	0.02
K	0	0	0.01	0	0	0	0	0	0.02	0	0	0
Si	0.02	0.02	0	0	0	0.02	0.01	0.01	0.02	0.02	0.02	0.02
P	3.66	3.39	3.7	3.2	3.21	3.12	3.35	3.14	3.11	3.7	3.64	3.71
TOTAL	10.81	9.79	10.68	9.42	9.01	8.93	10.02	8.97	9.2	10.44	10.61	10.76

Hachita Sample TM114

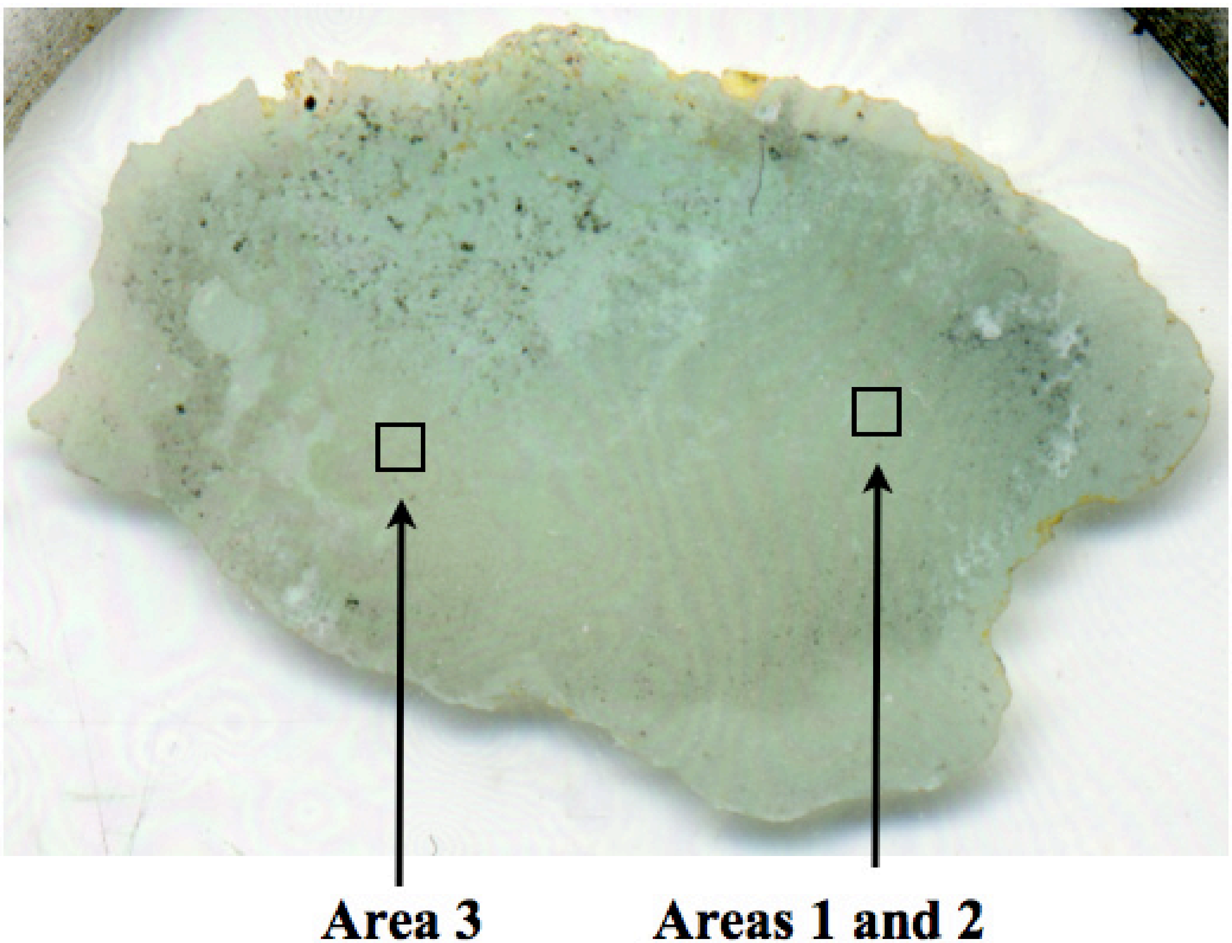

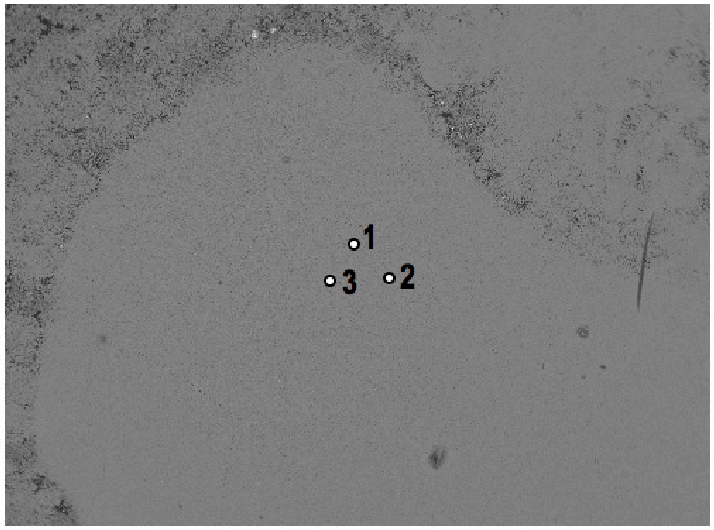

200µm
BEI TM114 Area 1

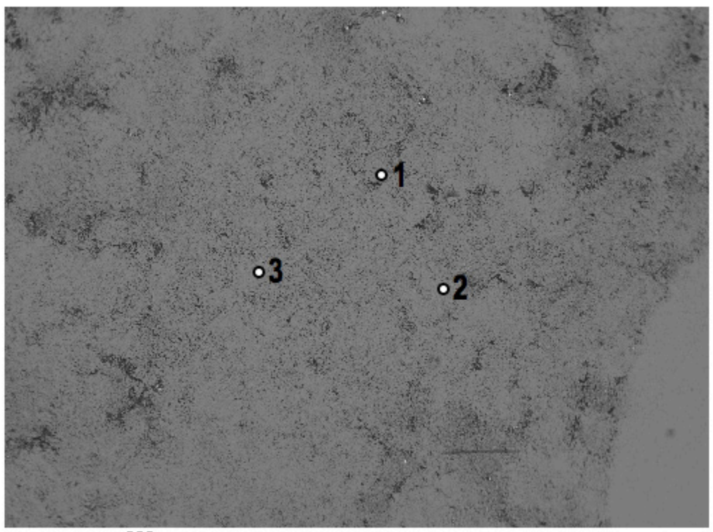

200µm
BEI TM114 Area 2

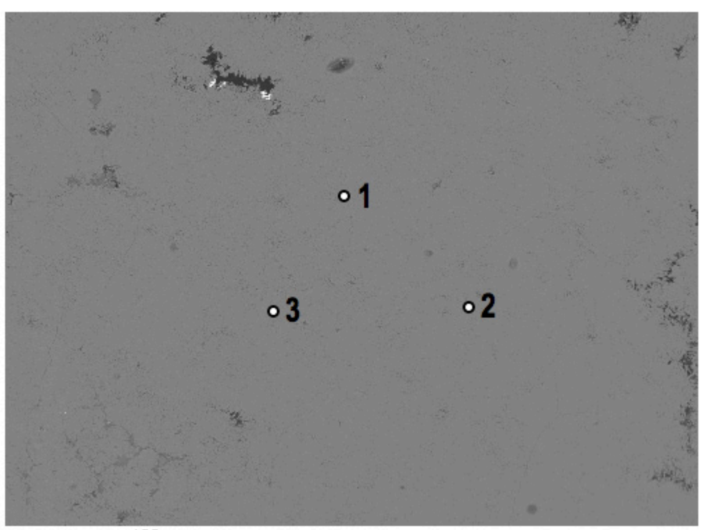

100µm
BEI TM114 Area 3

	TM114 1-1	TM114 1-2	TM114 1-3	TM114 2-1	TM114 2-2	TM114 2-3	TM114 3-1	TM114 3-2	TM114 3-3
CuO	6.27	6.48	6.06	6.54	6.5	6.81	7.31	7.19	7.4
MnO	0	0	0	0	0	0	0	0	0
ZnO	0	0	0	0	0	0	0	0	0
TιO2	0.11	0.12	0.12	0.19	0.13	0.18	0.16	0	0
MgO	0.3	0.33	0.31	0.05	0.2	0.22	0	0	0
CaO	0.29	0.4	0.53	0.2	0.33	0.29	0.27	0.3	0.27
K2O	0.15	0.21	0.21	0.11	0.13	0.09	0.1	0.08	0.09
Fe2O3	15.58	15.97	16.9	15.82	17.58	15.73	15.68	16.37	15.96
Al2O3	21.82	22.08	22.27	20.87	21.85	20.91	24.11	24.44	23.57
SiO2	7.31	7.47	6.46	2.03	5.52	4.23	2.33	4.64	3.78
P2O5	26.6	25.58	25.52	26.04	25.39	27.15	29.1	27.78	28.98
Total	78.45	78.64	78.37	71.94	77.62	75.59	79.04	80.81	80.06
H2O (by diff.)	21.55	21.36	21.63	28.06	22.38	24.41	20.96	19.19	19.94
TOTAL (w/H2O)	100	100	100	100	100	100	100	100	100
Based on 28O									
Cu	0.65	0.67	0.64	0.65	0.67	0.69	0.76	0.76	0.78
Fe	1.6	1.65	1.79	1.56	1.82	1.59	1.63	1.73	1.67
Al	3.52	3.58	3.7	3.23	3.54	3.31	3.93	4.04	3.87
Mn	0	0	0	0	0	0	0	0	0
Zn	0	0	0	0	0	0	0	0	0
Ti	0.01	0.01	0.01	0.02	0.01	0.02	0.02	0	0
Mg	0.06	0.07	0.07	0.03	0.04	0.04	0	0	0
Ca	0.04	0.06	0.08	0.03	0.05	0.04	0.04	0.05	0.04
K	0.03	0.04	0.04	0.02	0.02	0.01	0.02	0.01	0.02
Si	1	1.03	0.91	0.27	0.76	0.57	0.32	0.65	0.53
P	3.08	2.98	3.04	2.89	2.95	3.09	3.4	3.3	3.42
TOTAL	9.99	10.09	10.28	8.7	9.86	9.36	10.12	10.54	10.33

Hachita Sample TM115

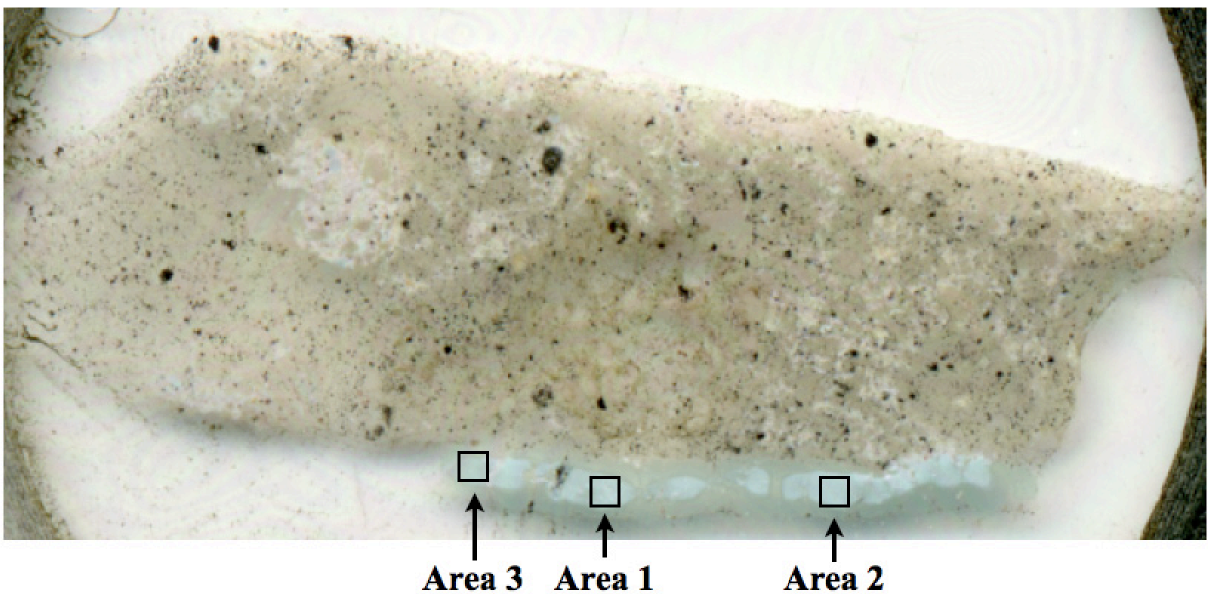

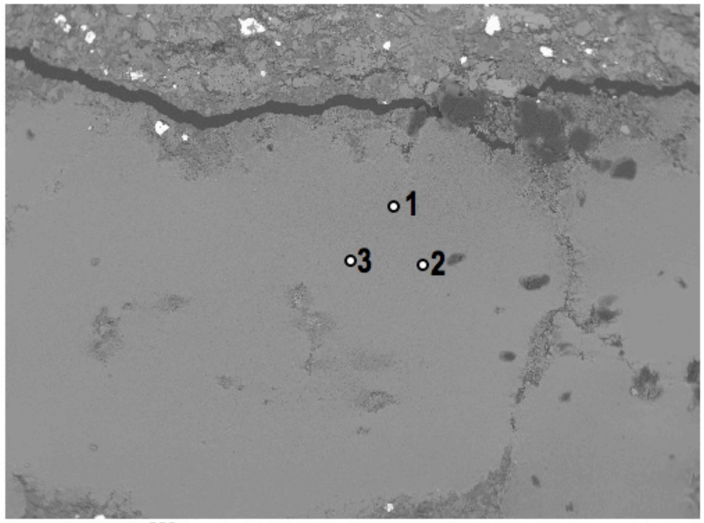

300µm
BEI TM115 Area 1

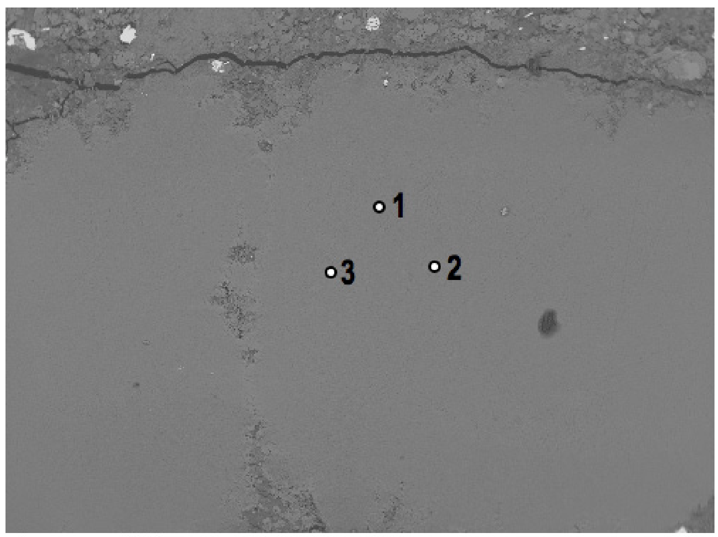

200µm
BEI TM115 Area 2

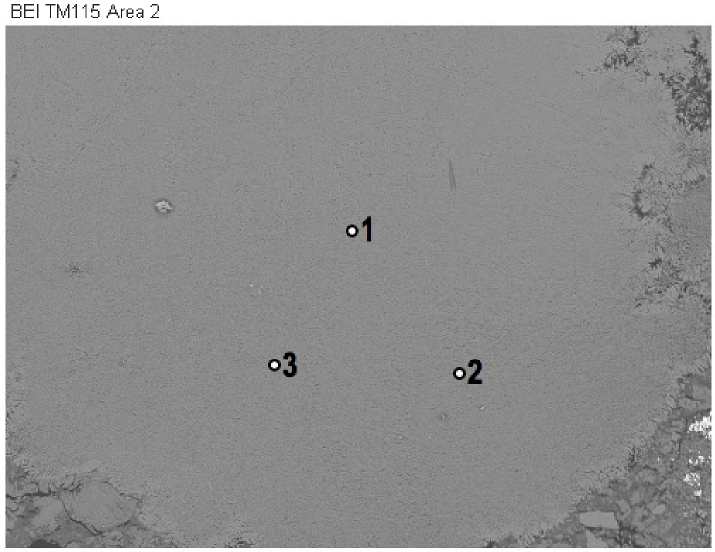

100µm
BEI TM115 Area 3

	TM115 1-1	TM115 1-2	TM115 1-3	TM115 2-1	TM115 2-2	TM115 2-3	TM115 3-1	TM115 3-2	TM115 3-3
CuO	6.54	6.56	7.09	7.06	7.19	7.02	7.29	8.3	6.94
MnO	0	0	0	0	0	0	0	0	0
ZnO	0	0	0	0	0	0	0	0	0
TiO2	0	0	0	0	0	0.13	0	0	0
MgO	0	0	0	0	0	0	0	0	0
CaO	0	0	0	0	0	0	0	0	0
K2O	0	0	0	0	0	0	0	0	0.1
Fe2O3	2.7	2.2	2.08	2.36	2	1.86	2.31	1.95	2.15
Al2O3	31.4	35.4	33.38	37.21	33.59	37.71	33.43	33.73	31.76
SiO2	0	0	0	0.11	0	0	0.1	0	0
P2O5	29.75	28.8	30.92	29.18	29.95	30.4	29.86	29.55	29.67
Total	70.39	72.96	73.47	75.93	72.73	77.12	72.99	73.53	70.62
H2O (by diff.)	29.61	27.04	26.53	24.07	27.27	22.88	27.01	26.47	29.38
TOTAL (w/H2O)	100	100	100	100	100	100	100	100	100
Based on 28O									
Cu	0.61	0.63	0.68	0.69	0.69	0.69	0.7	0.8	0.65
Fe	0.25	0.21	0.2	0.23	0.19	0.18	0.22	0.19	0.2
Al	4.6	5.28	4.99	5.68	5	5.79	5	5.08	4.66
Mn	0	0	0	0	0	0	0	0	0
Zn	0	0	0	0	0	0	0	0	0
Ti	0	0	0	0	0	0.01	0	0	0
Mg	0	0	0	0	0	0	0	0	0
Ca	0	0	0	0	0	0	0	0	0
K	0	0	0	0	0	0	0	0	0.02
Si	0	0	0	0.01	0	0	0.01	0	0
P	3.13	3.09	3.32	3.2	3.21	3.35	3.21	3.2	3.13
TOTAL	8.59	9.21	9.19	9.81	9.09	10.02	9.14	9.27	8.66

Hachita Sample TM118

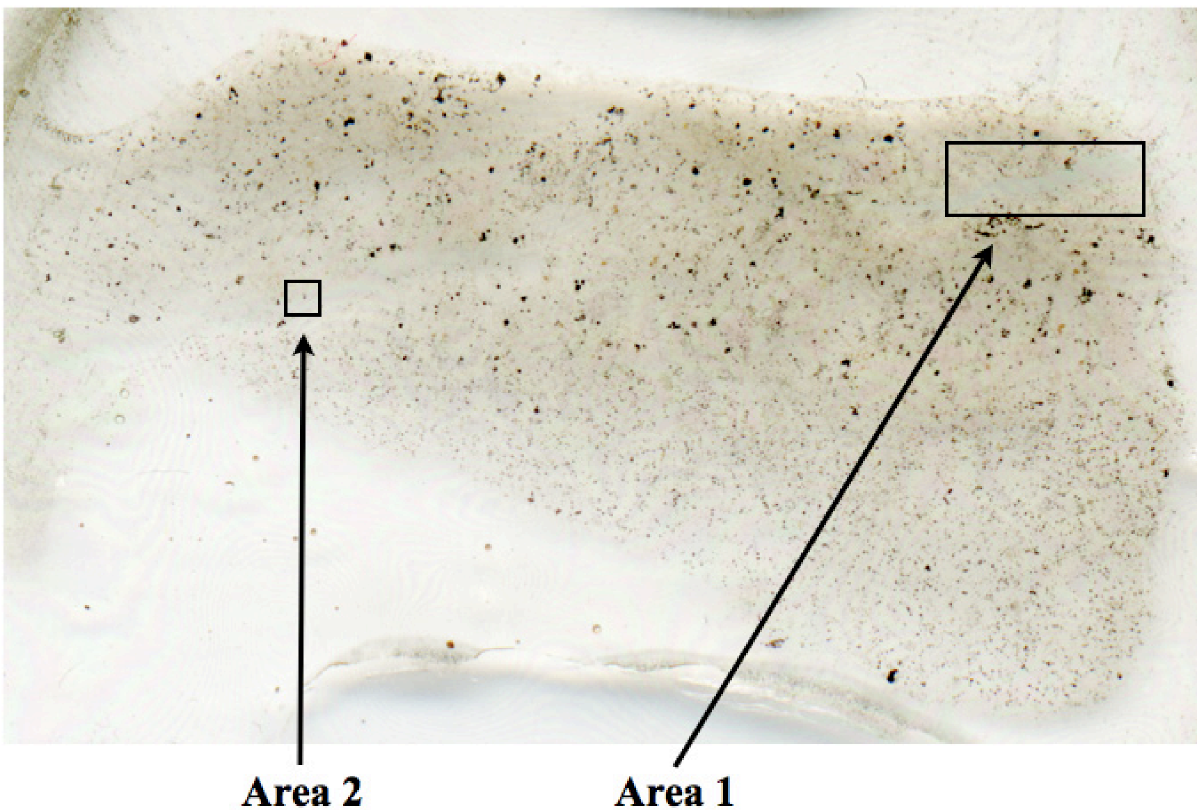

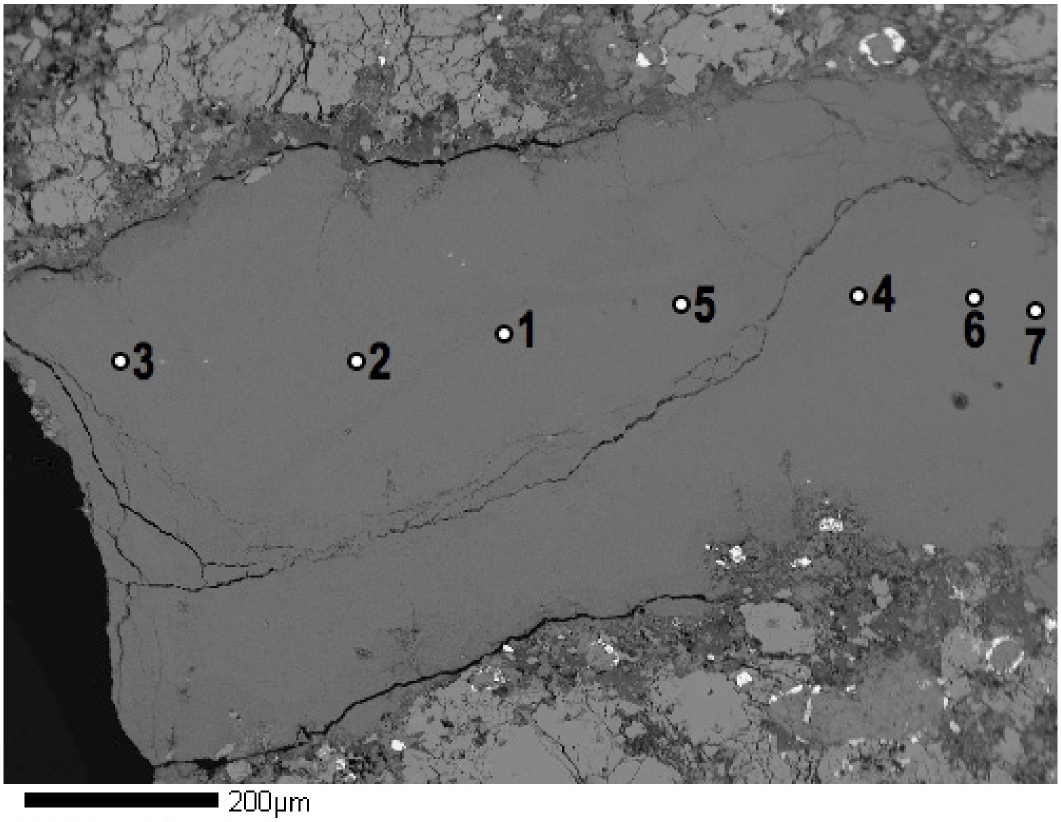

BEI TM118 Area 1

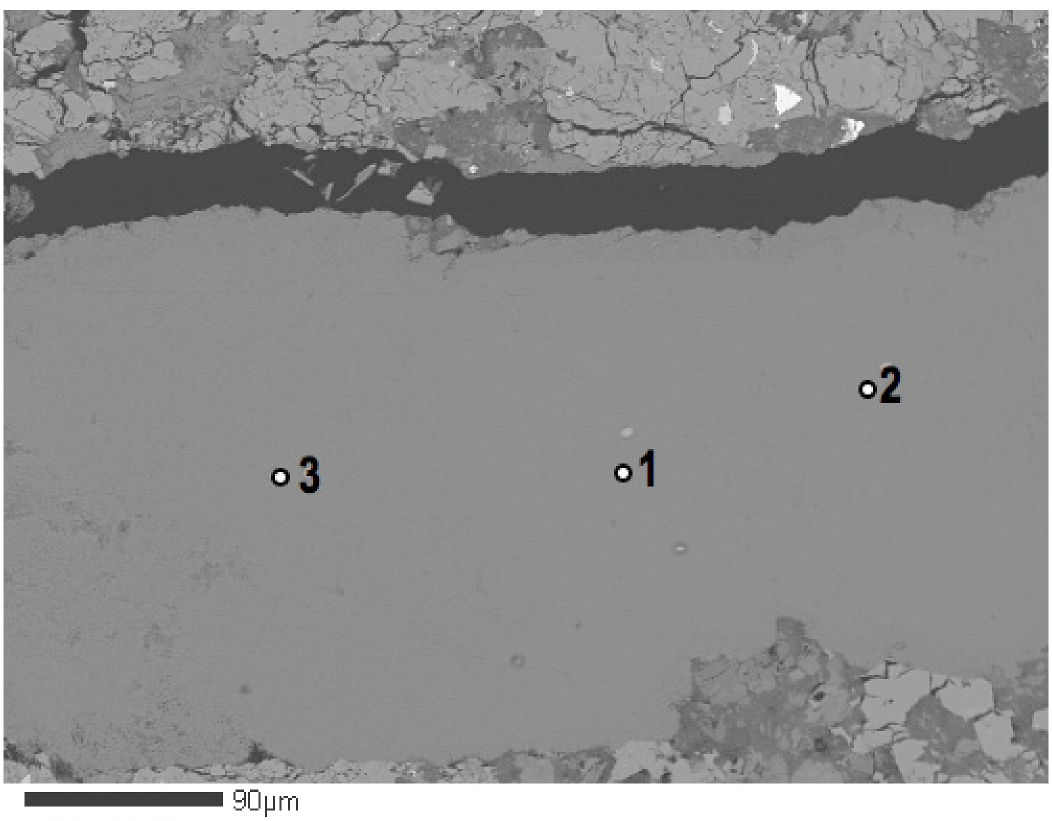

BEI TM118 Area 3

	TM118 1-1	TM118 1-2	TM118 1-3	TM118 1-4	TM118 1-5	TM118 1-6	TM118 1-7	TM118 2-1	TM118 2-2	TM118 2-3
CuO	7.48	8.9	7.15	7.25	7.94	7.77	7.11	8.23	7.49	7.59
MnO	0	0	0	0	0	0	0	0	0	0
ZnO	0	0	0	0	0	0	0	0	0	0
TiO2	0	0	0	0	0	0	0	0	0	0
MgO	0	0	0	0	0	0.17	0	0	0	0
CaO	0	0.1	0	0	0	0	0	0	0	0
K2O	0.06	0	0.08	0	0.06	0.07	0	0	0	0.07
Fe2O3	2.35	2.25	2.16	1.89	2.42	2.36	2.44	2.28	2.17	2.19
Al2O3	38.23	38.67	32.44	34.23	36.1	32.8	35.53	37.04	34.71	33.4
SiO2	0	0.17	0	0.24	0.22	0.13	0.12	0.16	0.17	0.09
P2O5	33.24	32.98	30.16	31.18	31.96	29.85	30.86	30.63	30.64	31.99
Total	81.37	83.07	71.99	74.8	78.7	73.14	76.07	78.34	75.18	75.33
H2O (by diff.)	18.63	16.93	28.01	25.2	21.3	26.86	23.93	21.66	24.82	24.67
TOTAL (w/H2O)	100	100	100	100	100	100	100	100	100	100
Based on 28O										
Cu	0.76	0.92	0.68	0.7	0.79	0.75	0.69	0.82	0.73	0.74
Fe	0.24	0.23	0.2	0.18	0.24	0.23	0.24	0.23	0.21	0.21
Al	6.05	6.24	4.81	5.16	5.63	4.92	5.42	5.77	5.27	5.07
Mn	0	0	0	0	0	0	0	0	0	0
Zn	0	0	0	0	0	0	0	0	0	0
Ti	0	0	0	0	0	0	0	0	0	0
Mg	0	0	0	0	0	0.03	0	0	0	0
Ca	0	0.01	0	0	0	0	0	0	0	0
K	0.01	0	0.01	0	0.01	0.01	0	0	0	0.01
Si	0	0.02	0	0.03	0.03	0.02	0.02	0.02	0.02	0.01
P	3.78	3.82	3.21	3.38	3.58	3.22	3.38	3.43	3.34	3.49
TOTAL	10.84	11.24	8.91	9.45	10.28	9.18	9.75	10.27	9.57	9.53

Hachita Sample TM127

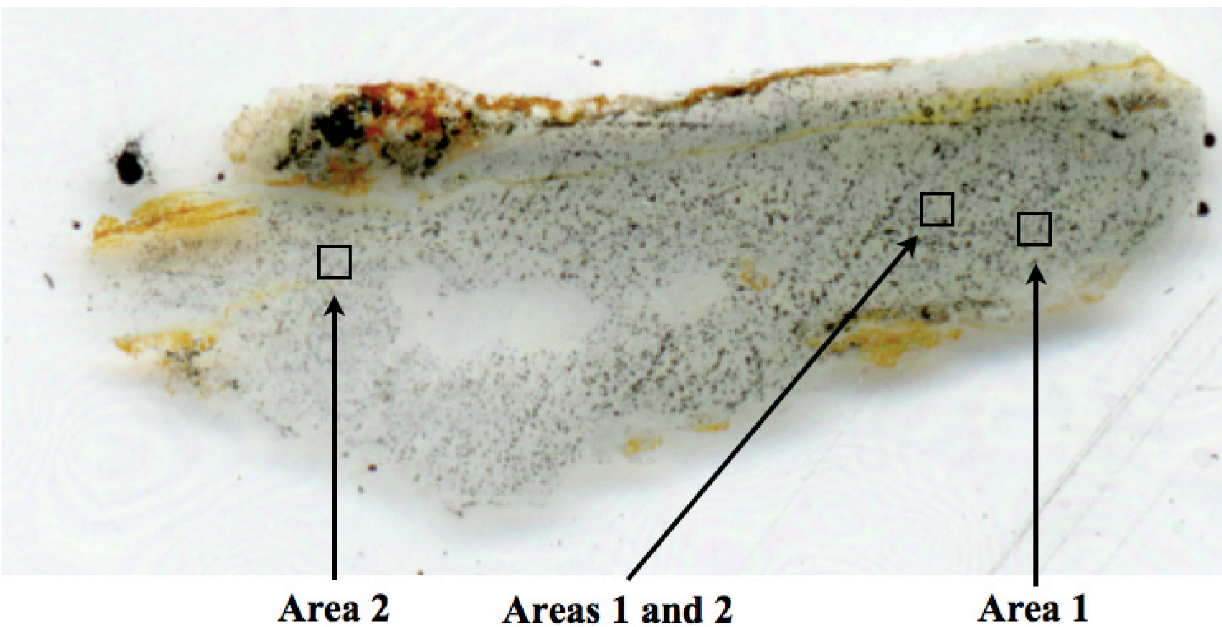

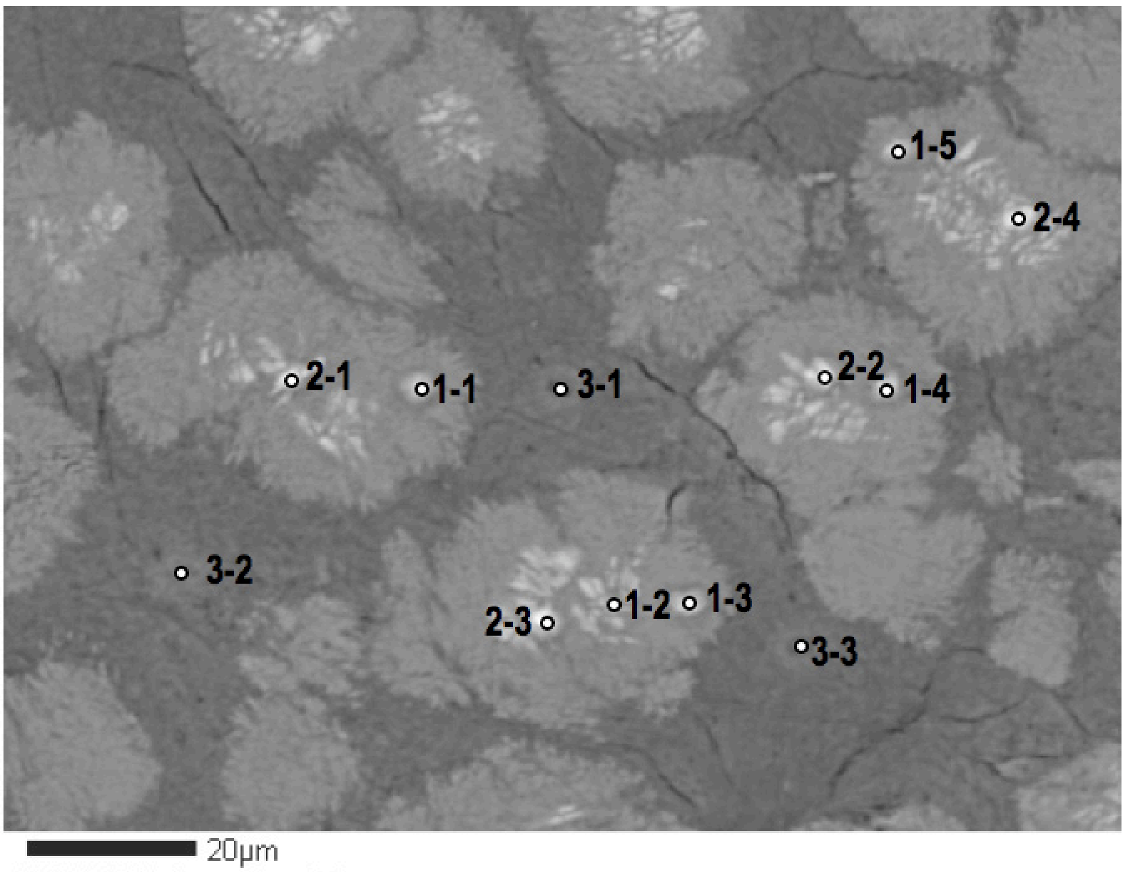

BEI TM127 Areas 1 and 2

	TM127 1-1	TM127 1-2	TM127 1-3	TM127 1-4	TM127 1-5	TM127 2-1	TM127 2-2	TM127 2-3	TM127 2-4	TM127 3-1	TM127 3-2	TM127 3-3
CuO	5.54	5.16	5.43	6.15	5.19	5.66	6.35	6.61	6.5	0	0	0
MnO	0	0	0	0	0	0	0	0	0	0	0	0
ZnO	0.05	0	0	0	0	0	0	0	0	0	0	0
TiO2	0	0	0	0	0.13	0	0	0.13	0.13	0	0	0
MgO	0	0	0	0	0	0	0	0	0	0.11	0	0
CaO	0.25	0.2	0.23	0.2	0.18	0.12	0.11	0.17	0.09	0.11	0.16	0.14
K2O	0.08	0.08	0.13	0	0	0	0	0	0	0	0	0.09
Fe2O3	3.79	3.95	3.44	3.93	3.64	15.19	16.41	17.36	25.41	1.4	1.32	0.92
Al2O3	33.03	35.68	33.16	35.12	35.29	24.74	26.31	23.7	17.33	33.03	34.52	34.45
SiO2	7.57	15.66	5.84	6.29	10.14	5.23	2.67	3	2.18	40.69	43.59	40.86
P2O5	26.01	21.07	27.82	28.38	23.84	27.63	28.35	27.75	28.14	0	0.17	0.25
Total	76.32	81.8	76.05	80.07	78.4	78.58	80.2	78.73	79.78	75.34	79.76	76.71
H2O (by diff.)	23.68	18.2	23.95	19.93	21.6	21.42	19.8	21.27	20.22	24.66	20.24	23.29
TOTAL (w/H2O)	100	100	100	100	100	100	100	100	100	100	100	100
Based on 28O												
Cu	0.54	0.52	0.53	0.62	0.51	0.58	0.67	0.69	0.7	0	0	0
Fe	0.37	0.4	0.33	0.39	0.36	1.56	1.72	1.81	2.73	0.13	0.13	0.09
Al	5.04	5.65	5.03	5.5	5.45	3.97	4.31	3.86	2.92	4.87	5.23	5.12
Mn	0	0	0	0	0	0	0	0	0	0	0	0
Zn	0	0	0	0	0	0	0	0	0	0	0	0
Ti	0	0	0	0	0.01	0	0	0.01	0.01	0	0	0
Mg	0	0	0	0	0	0	0	0	0	0.02	0	0
Ca	0.03	0.03	0.03	0.03	0.02	0.02	0.02	0.03	0.01	0.01	0.02	0.02
K	0.01	0.01	0.02	0	0	0	0	0	0	0	0	0.01
Si	0.98	2.1	0.75	0.84	1.33	0.71	0.37	0.41	0.31	5.09	5.6	5.15
P	2.85	2.4	3.03	3.2	2.65	3.18	3.34	3.25	3.4	0	0.02	0.03
TOTAL	9.82	11.11	9.72	10.58	10.33	10.02	10.43	10.06	10.08	10.12	11	10.42

Red Hill Sample RH9

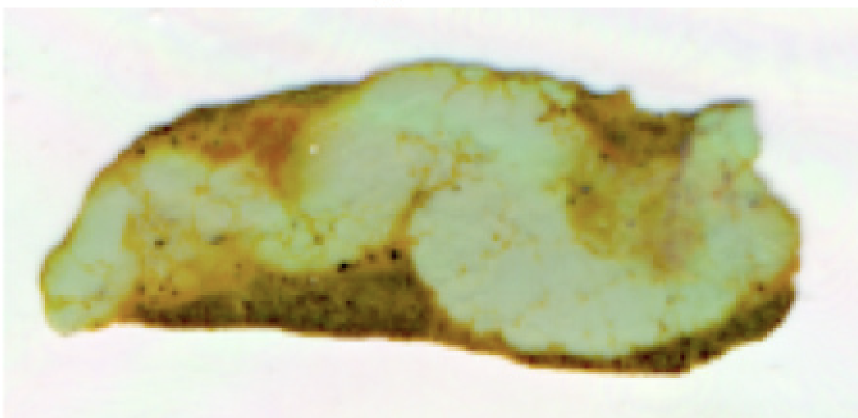

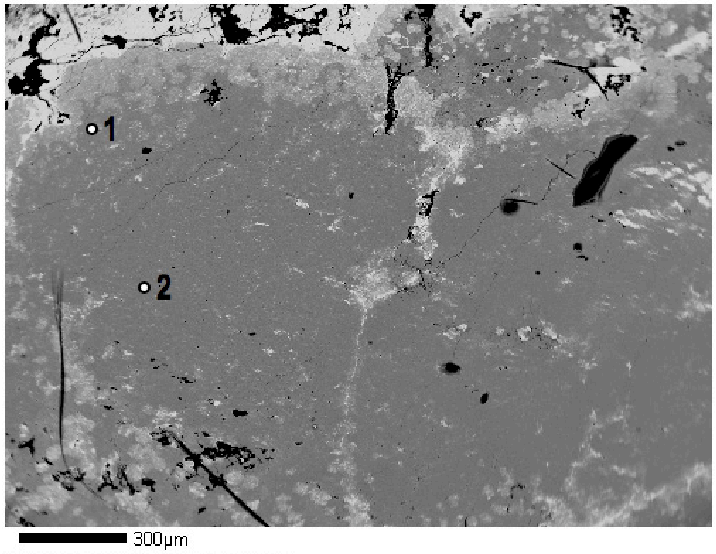

BEI Red Hill Mine Sample 9 Area 1

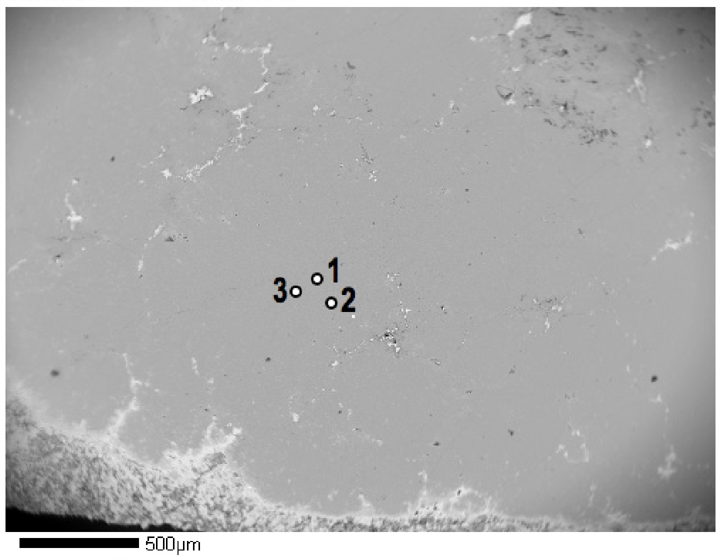

BEI RH9 Area 1

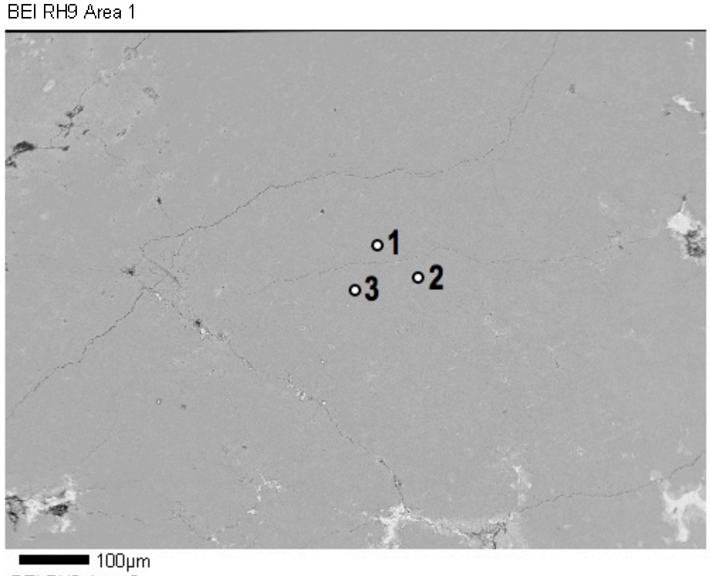

BEI RH9 Area 2

RH9	2/18-1	2/18-2	3/3	3/17-1	3/17-2	3/17-3	3/17-4	3/17-5	3/17-6	3/24-1	3/24-2	3/24-3	4/21	5/11	5/19	5/22-1	5/22-2	5/22-3
CuO	5.97	6.32	7.79	6.74	7.67	7.58	7.83	7.1	7.32	5.74	6.3	7.04	6.41	7.89	6.35	7.23	7.79	8.46
MnO	0	0	0	0	0	0	0	0.05	0	0	0	0	0	0.05	0	0	0	0
ZnO	0	0	0	0	0	0	0	0	0	0	0	0	0	0	0	0	0	0
TiO2	0.51	0.57	0.47	0.55	0.49	0.44	0.39	0.54	0.42	0.5	0.59	0.43	0.4	0.55	0.42	0.51	0.56	0.56
MgO	0	0	0	0	0	0	0	0	0	0	0	0	0	0	0	0	0	0
CaO	0	0	0	0	0	0	0	0	0	0	0	0	0	0	0	0	0	0
K2O	0.13	0.09	0.1	0.12	0.12	0.11	0.13	0.11	0.11	0.11	0.12	0.07	0.07	0.16	0.11	0.17	0.12	0.15
Fe2O3	10.41	9.05	11.89	9.29	9.83	9.24	11.37	11.77	11.92	9.58	10.13	9.54	8.71	10.86	14.75	9.74	8.44	9.97
Al2O3	28.01	29.86	27.76	29.33	31.2	29.71	31.36	28.55	30.48	28.55	32.34	29.05	28.12	32.27	27.25	29.59	30.91	29.33
SiO2	0	0	0	0	0	0	0	0.12	0	0	0.12	0.11	0	0	0	0.09	0	0
P2O5	33.39	32.04	32.03	30.1	30.05	29.1	30.56	31.49	30.86	31.3	30.2	30.68	30.93	31.79	30.76	28.82	29.68	31.34
Total	78.42	78.11	80.04	76.12	79.36	76.18	81.64	80.79	81.11	75.77	79.8	76.92	74.64	83.57	79.64	76.16	77.49	79.82
H2O*	21.58	21.89	19.96	23.88	20.64	23.82	18.36	19.21	18.89	24.23	20.2	23.08	25.36	16.43	20.36	23.84	22.51	20.18
TOTAL	100	100	100	100	100	100	100	100	100	100	100	100	100	100	100	100	100	100
28 O																		
Cu	0.64	0.6	0.81	0.67	0.79	0.76	0.82	0.85	0.77	0.57	0.65	0.71	0.63	0.84	0.66	0.73	0.79	0.88
Fe	0.91	1.05	1.23	0.92	1.01	0.93	1.19	1.23	1.24	0.94	1.04	0.96	0.85	1.15	1.53	0.98	0.85	1.03
Al	4.7	4.42	4.5	4.57	5.01	4.66	5.15	4.67	4.98	4.41	5.18	4.56	4.31	5.37	4.42	4.64	4.88	4.74
Mn	0	0	0	0	0	0	0	0.01	0	0	0	0	0	0.01	0	0	0	0
Zn	0	0	0	0	0	0	0	0	0	0	0	0	0	0	0	0	0	0
Ti	0.06	0.05	0.05	0.05	0.05	0.04	0.04	0.06	0.04	0.05	0.06	0.04	0.04	0.06	0.04	0.05	0.06	0.06
Mg	0	0	0	0	0	0	0	0	0	0	0	0	0	0	0	0	0	0
Ca	0	0	0	0	0	0	0	0	0	0	0	0	0	0	0	0	0	0
K	0	0.02	0.02	0.02	0.02	0.02	0.02	0.02	0.02	0.02	0.02	0.01	0.01	0.03	0.02	0.03	0.02	0.03
Si	0	0	0	0	0	0	0	0.02	0	0	0.02	0.01	0	0	0	0.01	0	0
P	4.7	3.78	3.73	3.37	3.47	3.28	3.61	3.7	3.62	3.47	3.48	3.46	3.41	3.8	3.58	3.25	3.37	3.64
TOTAL	11.01	9.92	10.34	9.6	10.35	9.69	10.83	10.56	10.67	9.46	10.45	9.75	9.25	11.26	10.25	9.69	9.97	10.38

Red Hill Sample RH10

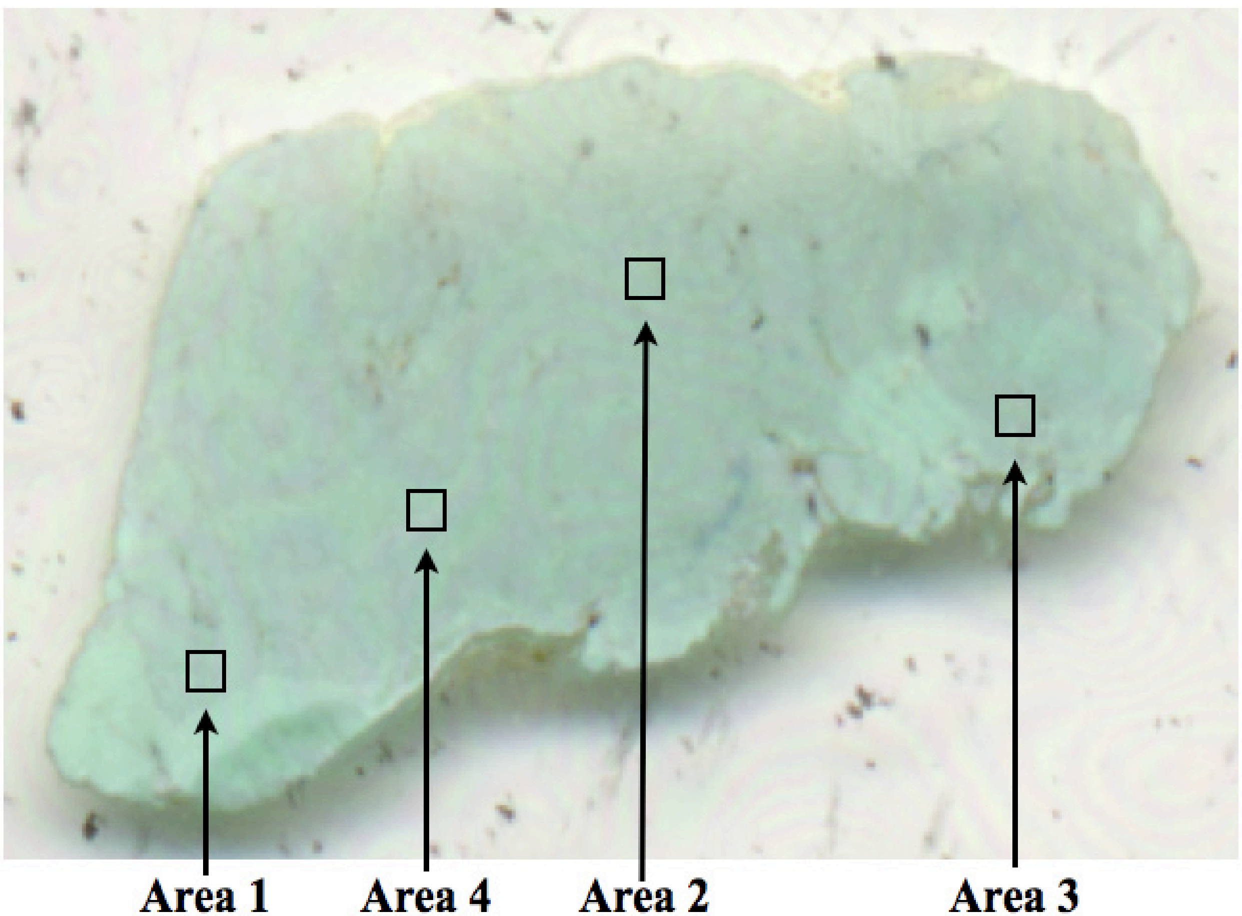

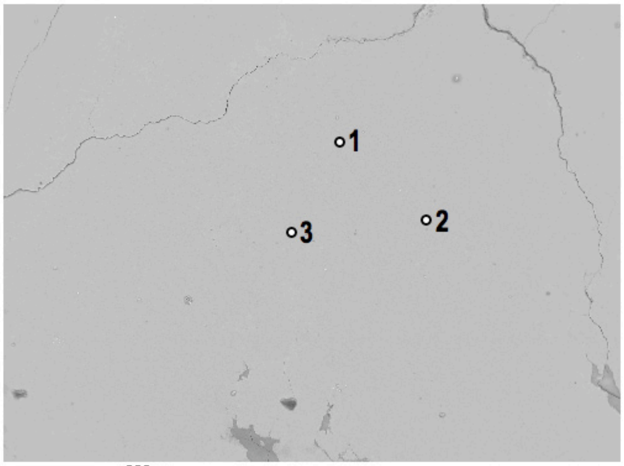

200µm
BEI RH10 Area 1

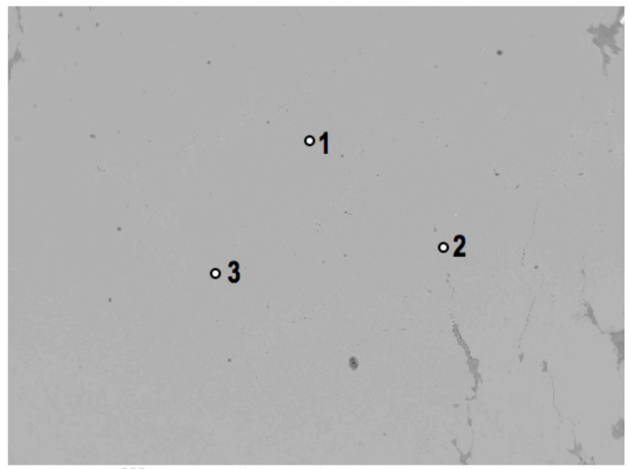

300µm
BEI RH10 Area 2

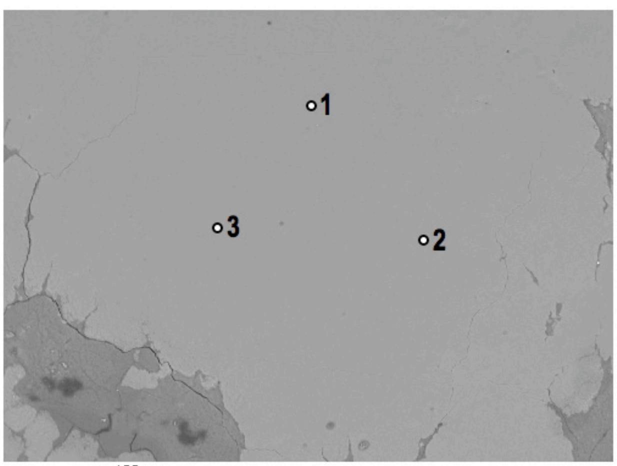

100µm
BEI RH10 Area 3

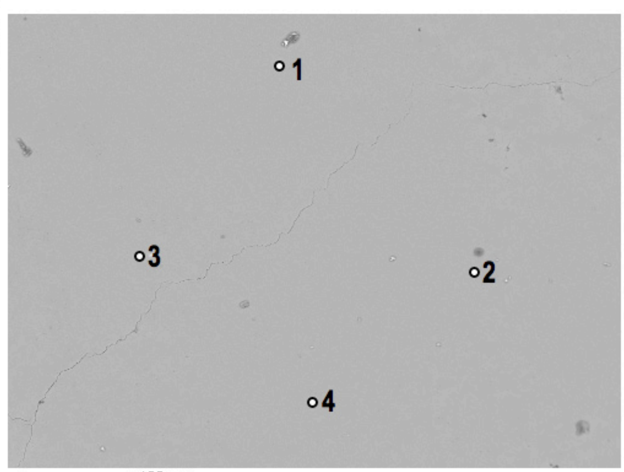

100µm
BEI RH10 Area 4

	RH10 1-1	RH10 1-2	RH10 1-3	RH10 2-1	RH10 2-2	RH10 2-3	RH10 3-1	RH10 3-2	RH10 3-3	RH10 4-1	RH10 4-2	RH10 4-3	RH10 4-4
CuO	7.29	7.52	7.05	6.95	7.13	7.52	7.07	6.64	6.72	8.12	8.18	8.25	7.98
MnO	0	0	0	0	0	0	0	0	0	0	0	0	0
ZnO	0	0	0	0	0	0	0	0	0	0	0	0	0
TiO2	0.51	0.63	0.53	0.5	0.5	0.51	0.5	0.64	0.5	0.57	0.51	0.47	0.46
MgO	0	0	0	0	0	0	0	0	0	0	0	0	0
CaO	0	0	0	0	0	0	0	0	0	0	0.07	0.07	0
K2O	0.14	0.17	0.13	0.2	0.18	0.22	0.17	0.18	0.18	0.21	0.13	0.16	0.23
Fe2O3	10.14	9.31	10.83	9.08	7.92	7.76	8.37	9.34	9.83	9.44	9.31	8.68	8.79
Al2O3	31.52	30.68	31.18	30.76	32.95	31.46	33.62	29.91	30.42	32.52	29.5	30.98	32.63
SiO2	0	0	0	0.12	0	0	0	0	0	0	0	0	0.09
P2O5	30.67	29.23	31.43	32.18	31.37	30.87	30.37	31.16	31.23	30.39	29.59	30.66	30.57
Total	80.27	77.54	81.15	79.79	80.04	78.34	80.1	77.87	78.88	81.25	77.3	79.27	80.75
H2O (by diff.)	19.73	22.46	18.85	20.21	19.96	21.66	19.9	22.13	21.12	18.75	22.7	20.73	19.25
TOTAL (w/H2O)	100	100	100	100	100	100	100	100	100	100	100	100	100
Based on 28O													
Cu	0.75	0.76	0.73	0.71	0.73	0.76	0.73	0.67	0.69	0.85	0.83	0.85	0.83
Fe	1.05	0.94	1.12	0.93	0.81	0.78	0.86	0.94	1	0.98	0.94	0.89	0.91
Al	5.09	4.86	5.07	4.91	5.27	4.98	5.39	4.72	4.84	5.31	4.68	4.97	5.29
Mn	0	0	0	0	0	0	0	0	0	0	0	0	0
Zn	0	0	0	0	0	0	0	0	0	0	0	0	0
Ti	0.05	0.06	0.05	0.05	0.05	0.05	0.05	0.06	0.05	0.06	0.05	0.05	0.05
Mg	0	0	0	0	0	0	0	0	0	0	0	0	0
Ca	0	0	0	0	0	0	0	0	0	0	0.01	0.01	0
K	0.02	0.03	0.02	0.03	0.03	0.04	0.03	0.03	0.03	0.04	0.02	0.03	0.04
Si	0	0	0	0.02	0	0	0	0	0	0	0	0	0.01
P	3.56	3.33	3.67	3.69	3.6	3.51	3.5	3.53	3.57	3.56	3.37	3.53	3.56
TOTAL	10.52	9.98	10.66	10.34	10.49	10.12	10.56	9.95	10.18	10.8	9.9	10.33	10.69

Red Hill Sample RH13

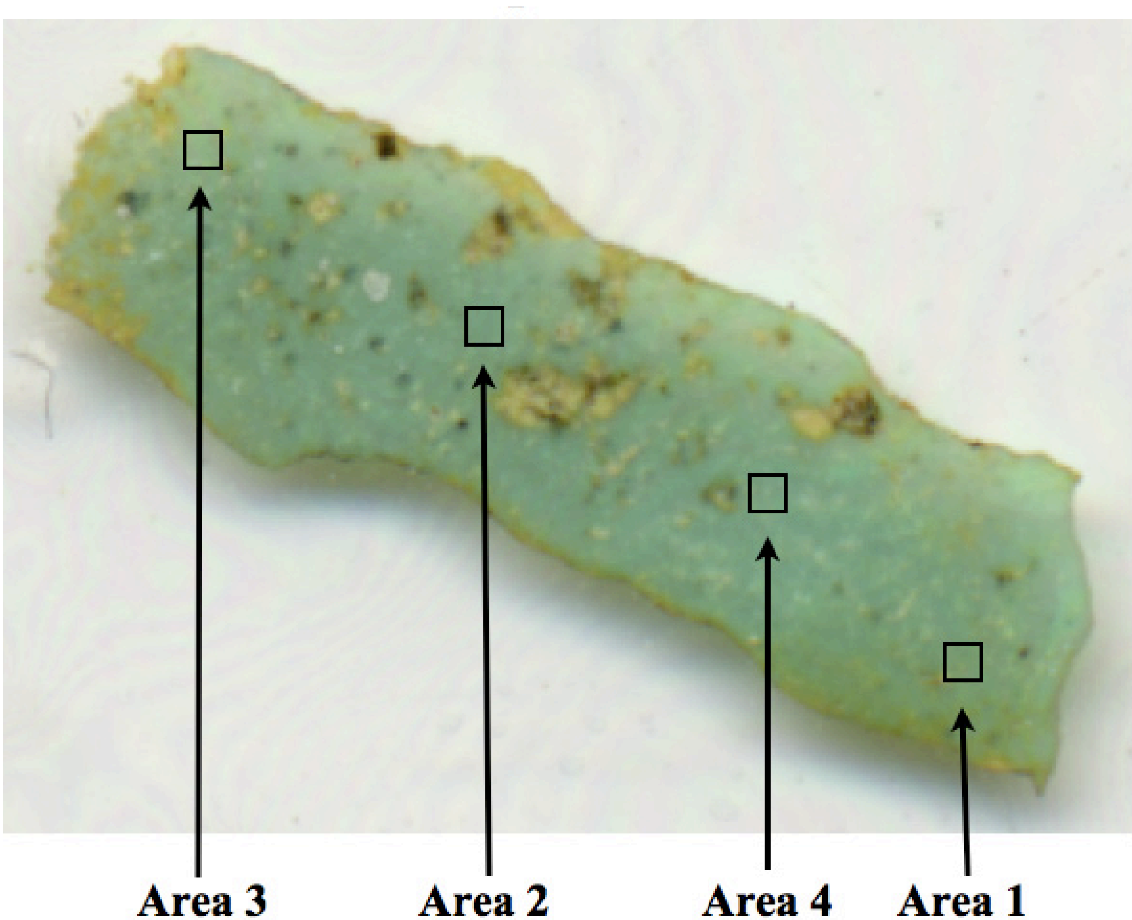

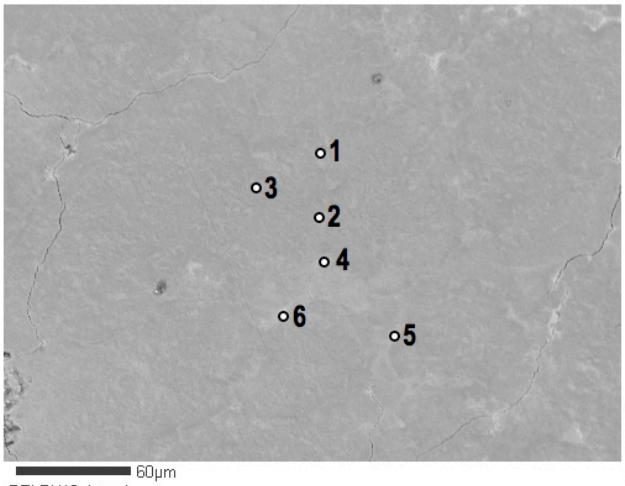

BEI RH13 Area 1

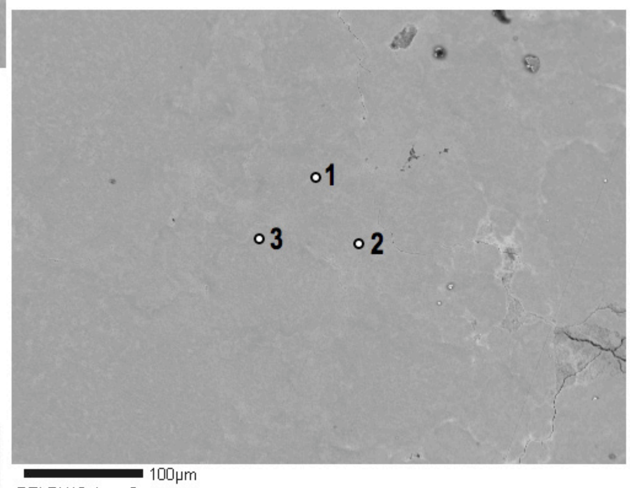

BEI RH13 Area 2

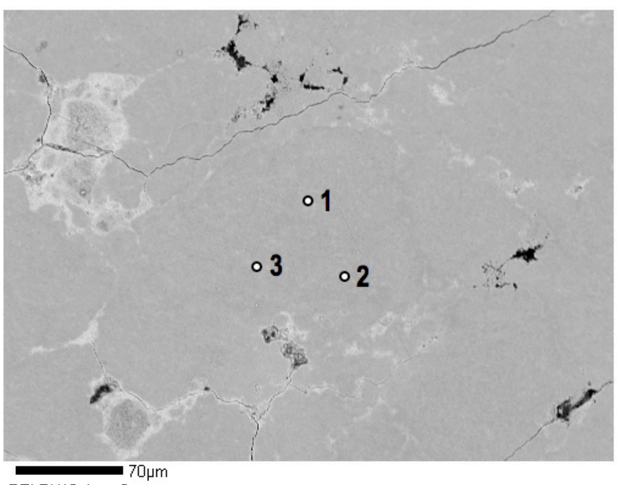

BEI RH13 Area 3

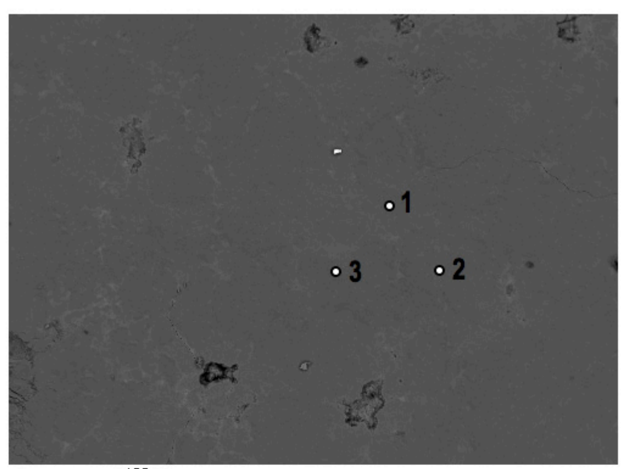

BEI RH13 Area 4

	RH13 1-1	RH13 1-2	RH13 1-3	RH13 1-4	RH13 1-5	RH13 1-6	RH13 2-1	RH13 2-2	RH13 2-3	RH13 3-1	RH13 3-2	RH13 3-3	RH13 4-1	RH13 4-2	RH13 4-3
CuO	6.25	6.47	5.83	5.39	4.72	4.88	7.11	6.69	6.45	6.45	6.71	6.02	6.65	6.22	6.61
MnO	0	0	0	0	0	0	0	0	0	0	0	0	0	0	0
ZnO	0	0	0	0	0	0	0	0	0	0	0	0	0	0	0
TiO2	1.06	1.3	1.18	1.18	1.18	0.78	0.97	1.23	1.12	1.1	1.1	1.17	1.26	1.18	1.22
MgO	0	0	0	0	0	0	0	0	0	0	0	0	0	0	0
CaO	0	0	0	0.25	0.14	0.35	0	0	0	0	0	0	0	0	0
K2O	0.24	0.17	0.22	1.45	1.54	2.19	0.13	0.09	0.13	0.23	0.26	0.13	0.17	0.14	0.22
Fe2O3	15.36	12.12	12.26	17.69	20.21	22.87	14.76	13.35	13.08	15.13	16.53	12.34	11.13	13.83	15.25
Al2O3	26.15	27	28.31	22.45	22.66	19.14	26.31	26.08	29.11	25.22	26.2	26.86	29.37	26.07	27.96
SiO2	0	0	0	0.27	0	0	0	0	0	0	0	0	0	0	0
P2O5	29.97	29.83	28.94	24.82	25.07	21.85	29.39	30.62	29.33	28.89	29.53	29.48	29.94	30.98	30.12
Total	79.03	76.89	76.74	73.5	75.52	72.06	78.66	78.06	79.23	77.03	80.34	75.99	78.53	78.42	81.38
H2O (by diff.)	20.97	23.11	23.26	26.5	24.48	27.94	21.34	21.94	20.77	22.97	19.66	24.01	21.47	21.58	18.62
TOTAL (w/H2O)	100	100	100	100	100	100	100	100	100	100	100	100	100	100	100
Based on 28O															
Cu	0.65	0.66	0.59	0.55	0.49	0.5	0.74	0.69	0.67	0.66	0.71	0.61	0.68	0.64	0.7
Fe	1.59	1.22	1.24	1.79	2.09	2.34	1.53	1.36	1.35	1.55	1.74	1.24	1.14	1.42	1.61
Al	4.24	4.27	4.47	3.56	3.66	3.07	4.27	4.17	4.7	4.04	4.32	4.21	4.69	4.18	4.62
Mn	0	0	0	0	0	0	0	0	0	0	0	0	0	0	0
Zn	0	0	0	0	0	0	0	0	0	0	0	0	0	0	0
Ti	0.11	0.13	0.12	0.12	0.12	0.08	0.1	0.13	0.12	0.11	0.12	0.12	0.13	0.12	0.13
Mg	0	0	0	0	0	0	0	0	0	0	0	0	0	0	0
Ca	0	0	0	0.01	0.02	0.05	0	0	0	0	0	0	0	0	0
K	0.04	0.03	0.04	0.25	0.27	0.38	0.02	0.02	0.02	0.04	0.05	0.02	0.03	0.02	0.04
Si	0	0	0	0.04	0	0	0	0	0	0	0	0	0	0	0
P	3.49	3.39	3.28	2.83	2.91	2.52	3.42	3.52	3.4	3.32	3.5	3.32	3.44	3.57	3.58
TOTAL	10.12	9.7	9.74	9.15	9.56	8.94	10.08	9.89	10.26	9.72	10.44	9.52	10.11	9.95	10.68

Red Hill Sample RH16

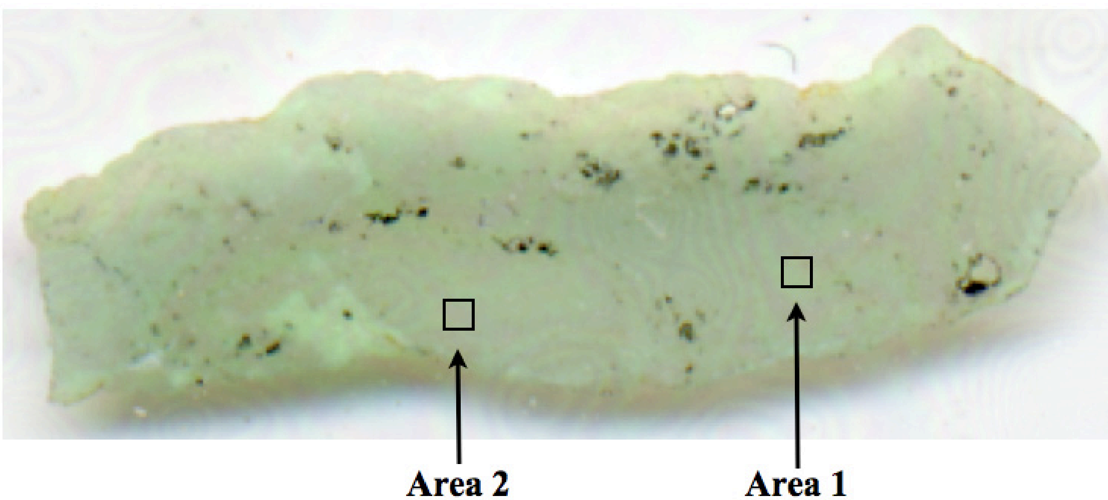

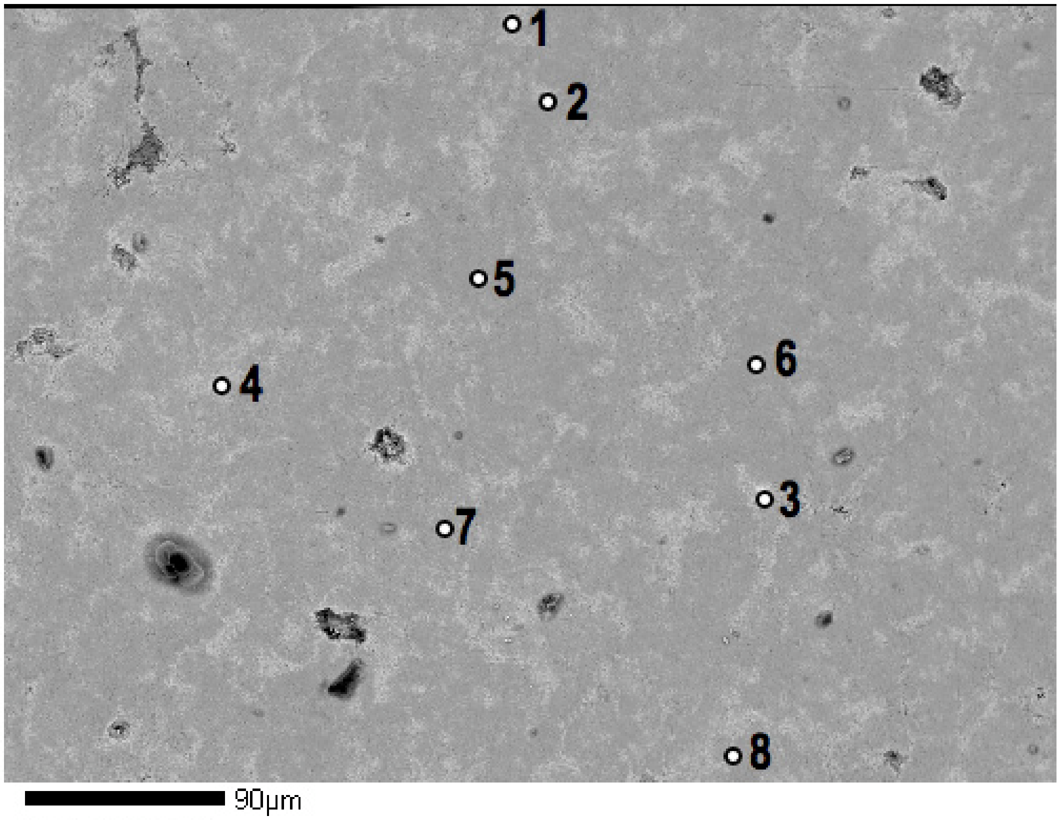

BEI RH16 Area 1

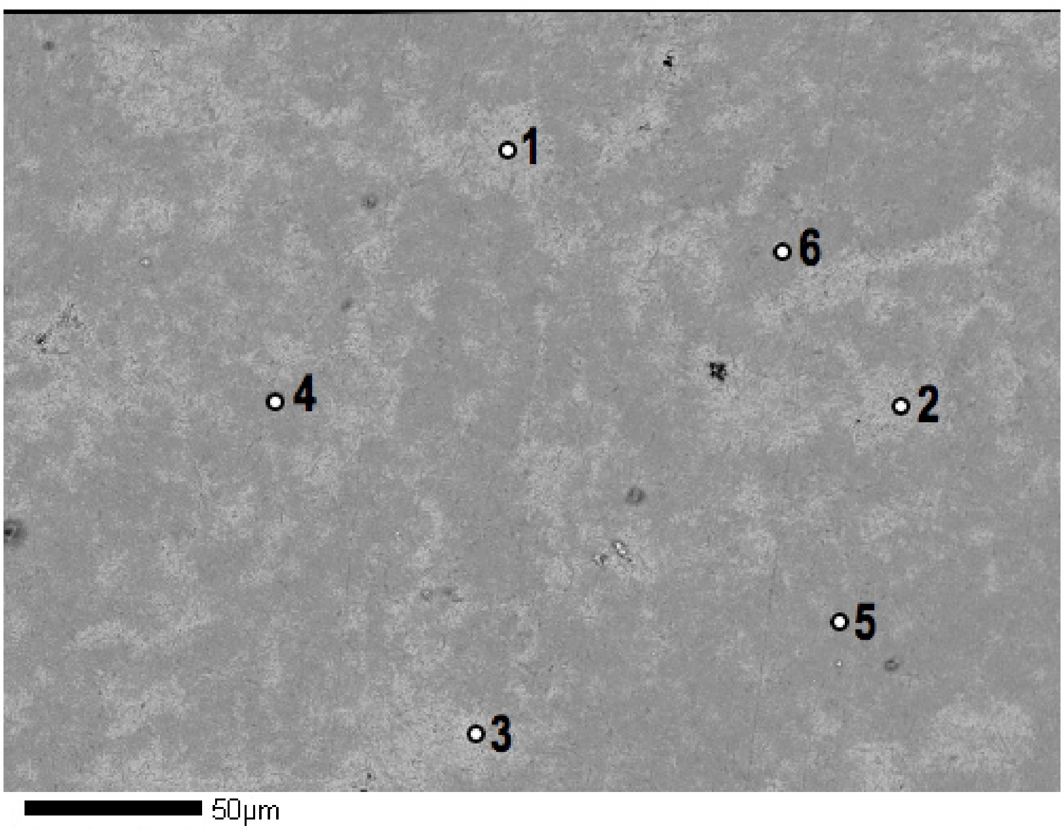

BEI RH16 Area 2

	RH16 1-1	RH16 1-2	RH16 1-3	RH16 1-4	RH16 1-5	RH16 1-6	RH16 1-7	RH16 1-8	RH16 2-1	RH16 2-2	RH16 2-3	RH16 2-4	RH16 2-5	RH16 2-6
CuO	7.45	7.81	7.92	7.44	8.06	7.7	8.08	8.11	7.96	6.75	7.21	7.43	8.23	6.65
MnO	0	0	0	0	0	0	0	0	0	0	0	0	0	0
ZnO	0	0	0	0	0	0	0	0	0	0	0	0	0	0
TiO2	0.92	0.65	0.55	0.51	1.2	1.25	1.03	1.18	0.57	0.55	0.2	1.38	1.46	1
MgO	0	0	0	0	0	0	0	0	0	0	0	0	0	0
CaO	0	0	0	0	0	0	0	0	0	0	0	0	0	0
K2O	0.09	0.1	0.13	0.14	0.1	0.08	0.11	0.14	0.1	0.11	0.1	0.12	0.07	0.21
Fe2O3	15.83	15.37	20.88	20.66	10.23	12.84	10.22	11.98	19.99	21.09	21.95	8.19	9.21	12.53
Al2O3	24.78	25.72	20.02	23.95	29.53	30.59	28.6	29.96	22.52	20.71	18.85	32.89	29.98	28.85
SiO2	0	0	0	0	0	0	0	0	0	0	0	0	0	0
P2O5	29.75	30	27.1	30.27	31.01	29.18	30.72	30.2	28.83	29.32	27.44	32.45	31.92	31.16
Total	78.82	79.66	76.6	82.97	80.13	81.63	78.76	81.57	79.97	78.53	75.75	82.46	80.88	80.39
H2O (by diff.)	21.18	20.34	23.4	17.03	19.87	18.37	21.24	18.43	20.03	21.47	24.25	17.54	19.12	19.61
TOTAL (w/H2O)	100	100	100	100	100	100	100	100	100	100	100	100	100	100
Based on 28O														
Cu	0.78	0.82	0.83	0.82	0.84	0.82	0.83	0.86	0.85	0.71	0.75	0.78	0.86	0.69
Fe	1.65	1.61	2.19	2.25	1.06	1.36	1.05	1.26	2.14	2.22	2.28	0.85	0.95	1.3
Al	4.04	4.22	3.28	4.09	4.78	5.06	4.59	4.95	3.77	3.41	3.07	5.36	4.87	4.69
Mn	0	0	0	0	0	0	0	0	0	0	0	0	0	0
Zn	0	0	0	0	0	0	0	0	0	0	0	0	0	0
Ti	0.1	0.07	0.06	0.06	0.12	0.13	0.11	0.12	0.06	0.06	0.02	0.14	0.15	0.1
Mg	0	0	0	0	0	0	0	0	0	0	0	0	0	0
Ca	0	0	0	0	0	0	0	0	0	0	0	0	0	0
K	0.02	0.02	0.02	0.03	0.02	0.01	0.02	0.02	0.02	0.02	0.02	0.02	0.01	0.04
Si	0	0	0	0	0	0	0	0	0	0	0	0	0	0
P	3.48	3.54	3.19	3.72	3.61	3.47	3.54	3.58	3.47	3.47	3.21	3.8	3.72	3.63
TOTAL	10.07	10.28	9.57	10.97	10.43	10.85	10.14	10.79	10.31	9.89	9.35	10.95	10.56	10.45

Red Hill Sample RH17

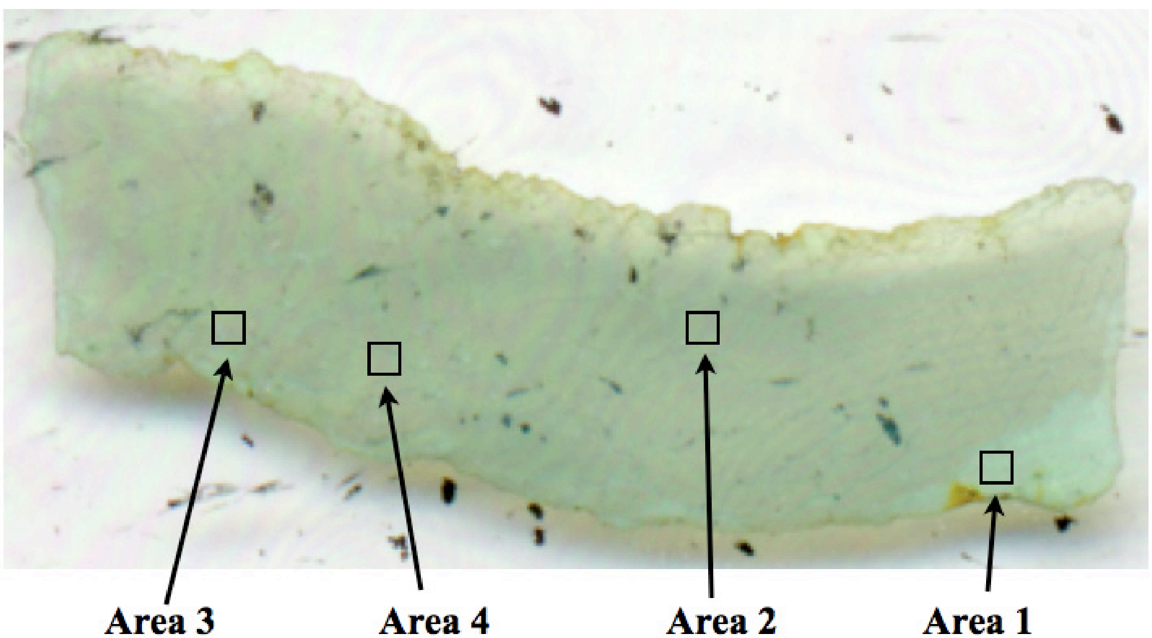

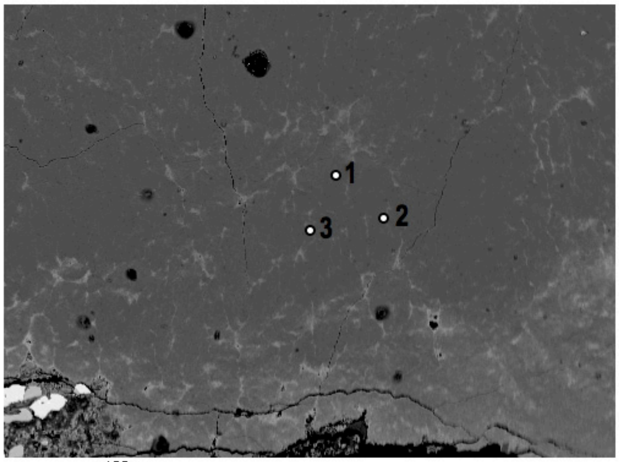

100µm
BEI RH17 Area 1

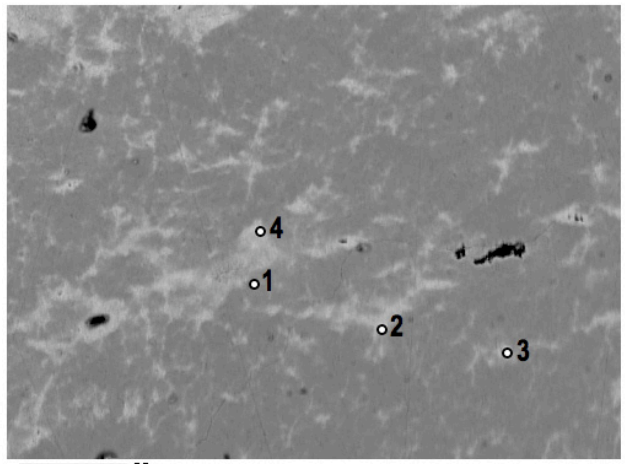

60µm
BEI RH17 Area 2

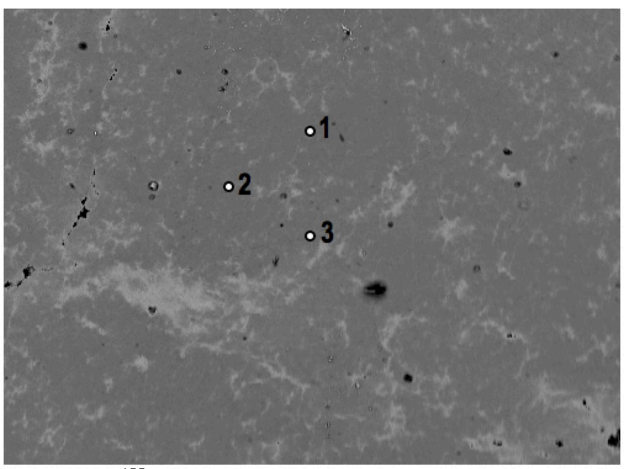

100µm
BEI RH17 Area 3

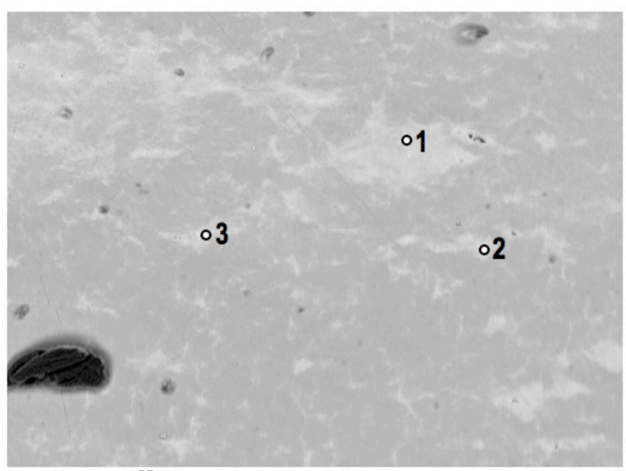

80µm
BEI RH17 Area 4

	RH17 1-1	RH17 1-2	RH17 1-3	RH17 1-4	RH17 2-1	RH17 2-2	RH17 2-3	RH17 3-1	RH17 3-2	RH17 3-3	RH17 4-1	RH17 4-2	RH17 4-3
CuO	8.29	8.54	8.42	7.98	7.1	6.49	7.8	7.02	7.98	8.01	8.06	7.91	7.67
MnO	0	0	0	0	0	0	0	0	0	0	0	0	0
ZnO	0	0	0	0	0	0	0	0	0	0	0	0	0
TiO2	0.98	0.98	1.06	0.69	0.36	0.49	0.43	0.57	0.71	0.5	0.26	0.18	0.14
MgO	0	0	0	0	0	0	0	0	0	0	0	0	0
CaO	0	0	0	0	0	0	0	0	0	0	0	0	0
K2O	0.1	0.13	0.09	0.08	0.07	0.06	0.12	0.08	0.13	0.11	0.12	0.07	0
Fe2O3	5.71	6.6	5.67	8.19	19.05	12.66	18	4.58	5.72	9.04	19.51	22.1	22.01
Al2O3	32.25	34.39	32.74	33.14	22.18	28.32	24.04	34.31	32.04	33.76	22.2	20.37	19.29
SiO2	0	0	0	0	0	0	0	0	0	0	0	0	0
P2O5	34.28	32.13	33.68	33.85	31.24	33.31	32.74	33.51	35.16	33.88	31.82	31.01	29.7
Total	81.61	82.77	81.66	83.92	80	81.33	83.12	80.07	81.73	85.31	81.97	81.64	78.82
H2O (by diff.)	18.39	17.23	18.34	16.08	20	18.67	16.88	19.93	18.27	14.69	18.03	18.36	21.18
TOTAL (w/H2O)	100	100	100	100	100	100	100	100	100	100	100	100	100
Based on 28O													
Cu	0.85	0.9	0.87	0.84	0.75	0.68	0.85	0.71	0.82	0.86	0.87	0.86	0.82
Fe	0.59	0.69	0.58	0.86	2.01	1.31	1.94	0.46	0.59	0.96	2.1	2.4	2.34
Al	5.19	5.62	5.28	5.46	3.67	4.61	4.07	5.41	5.14	5.64	3.75	3.46	3.21
Mn	0	0	0	0	0	0	0	0	0	0	0	0	0
Zn	0	0	0	0	0	0	0	0	0	0	0	0	0
Ti	0.1	0.1	0.11	0.07	0.04	0.05	0.05	0.06	0.07	0.05	0.03	0.02	0.02
Mg	0	0	0	0	0	0	0	0	0	0	0	0	0
Ca	0	0	0	0	0	0	0	0	0	0	0	0	0
K	0.02	0.02	0.02	0.01	0.01	0.01	0.02	0.01	0.02	0.02	0.02	0.01	0
Si	0	0	0	0	0	0	0	0	0	0	0	0	0
P	3.96	3.77	3.9	4.01	3.71	3.89	3.98	3.79	4.05	4.07	3.86	3.79	3.55
TOTAL	10.71	11.1	10.76	11.25	10.19	10.55	10.91	10.44	10.69	11.6	10.63	10.54	9.94

Red Hill Sample RH19

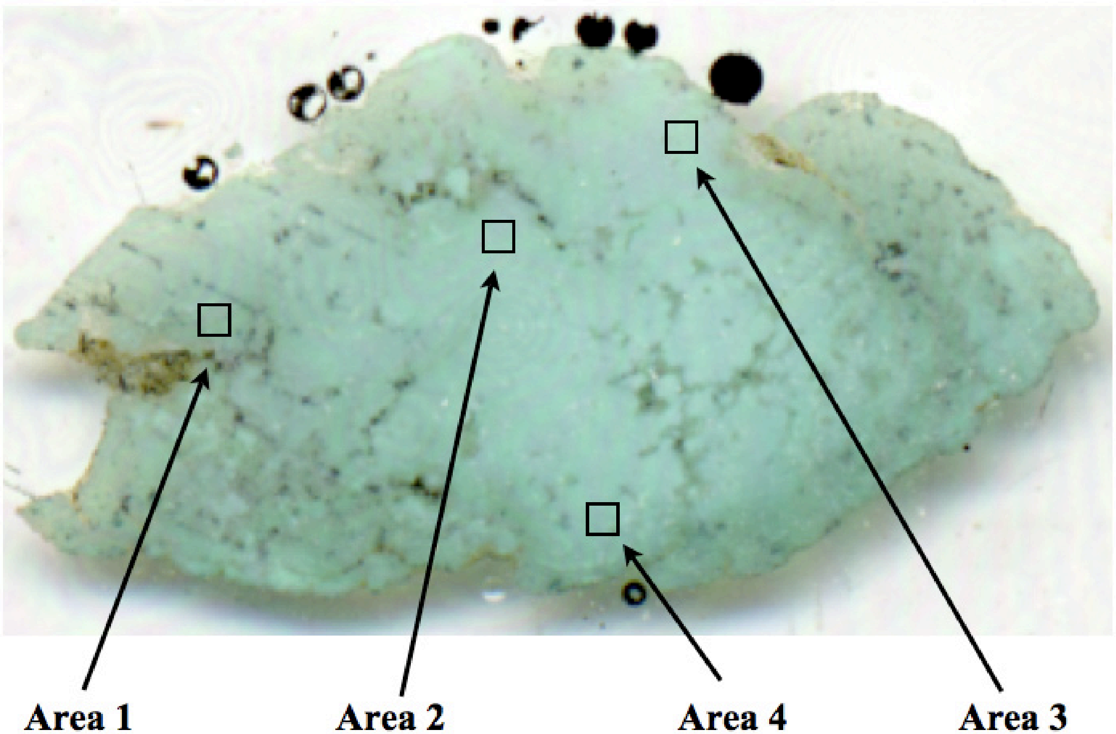

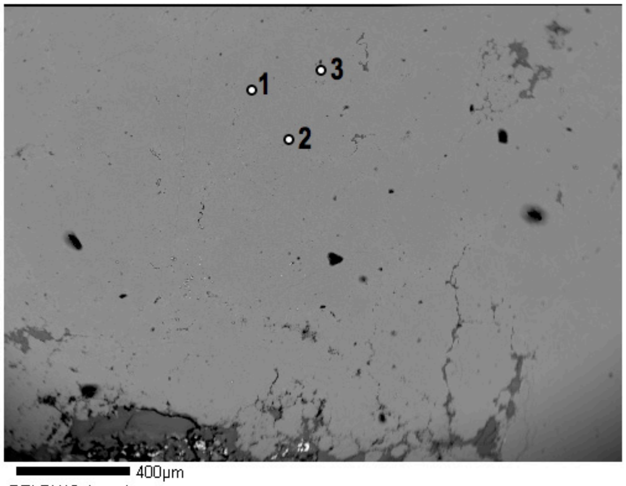

BEI RH19 Area 1

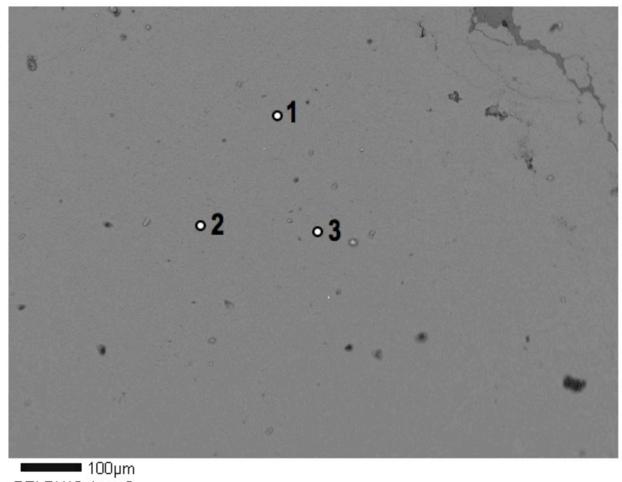

BEI RH19 Area 2

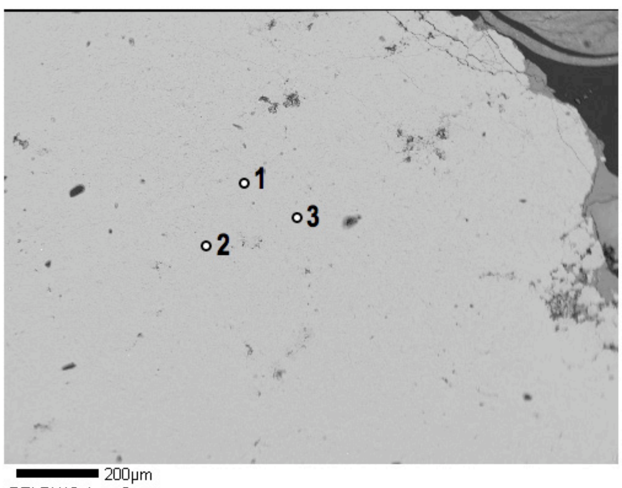

BEI RH19 Area 3

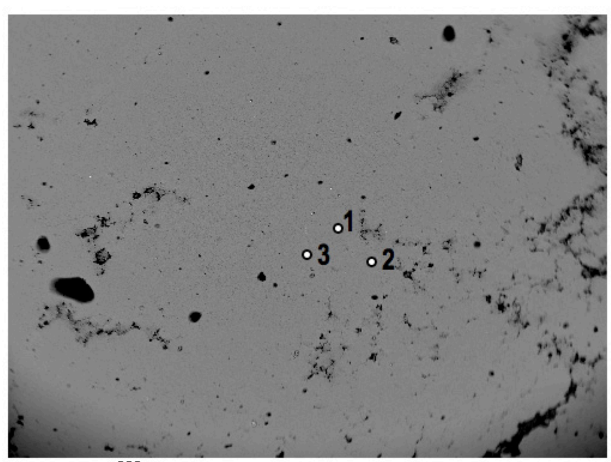

BEI RH19 Area 4

	RH19 1-1	RH19 1-2	RH19 1-3	RH19 2-1	RH19 2-2	RH19 2-3	RH19 3-1	RH19 3-2	RH19 3-3	RH19 4-1	RH19 4-2	RH19 4-3
CuO	7.18	8.14	7.33	8.17	7.9	8.45	8.7	8.35	7.71	8.49	8.56	7.89
MnO	0	0	0	0	0	0	0	0	0	0	0	0
ZnO	0	0	0	0	0	0	0	0	0	0	0	0
TiO2	0.73	0.69	0.71	0.43	0.68	0.49	0.86	0.81	0.78	0.54	0.59	0.94
MgO	0	0	0	0	0	0	0	0	0	0	0	0
CaO	0	0.07	0	0	0	0	0.06	0	0	0	0	0
K2O	0.12	0.11	0.11	0.2	0.15	0.15	0.18	0.11	0.14	0.25	0.17	0.11
Fe2O3	10.48	11.41	10.67	10.16	12.07	10.33	12.29	12.63	12.32	11.16	12.16	13.16
Al2O3	30.93	28.88	30.96	29.51	31.25	30.03	27.45	30.66	27.89	31	28.69	30.08
SiO2	0	0	0	0	0	0.1	0	0	0	0	0	0
P2O5	31.92	31.88	31.39	31.5	31.89	33.04	30.51	34.48	32.13	33.99	33.1	31.72
Total	81.35	81.19	81.17	79.98	83.94	82.59	80.06	87.03	80.97	85.42	83.27	83.9
H2O (by diff.)	18.65	18.81	18.83	20.02	16.06	17.41	19.94	12.97	19.03	14.58	16.73	16.1
TOTAL (w/H2O)	100	100	100	100	100	100	100	100	100	100	100	100
Based on 28O												
Cu	0.75	0.85	0.76	0.85	0.85	0.89	0.91	0.92	0.81	0.92	0.92	0.85
Fe	1.09	1.19	1.11	1.05	1.29	1.09	1.28	1.38	1.29	1.2	1.3	1.41
Al	5.03	4.73	5.04	4.77	5.23	4.95	4.49	5.26	4.56	5.24	4.79	5.06
Mn	0	0	0	0	0	0	0	0	0	0	0	0
Zn	0	0	0	0	0	0	0	0	0	0	0	0
Ti	0.08	0.07	0.07	0.04	0.07	0.05	0.09	0.09	0.08	0.06	0.06	0.1
Mg	0	0	0	0	0	0	0	0	0	0	0	0
Ca	0	0.01	0	0	0	0	0.01	0	0	0	0	0
K	0.02	0.02	0.02	0.04	0.03	0.03	0.03	0.02	0.02	0.04	0.03	0.02
Si	0	0	0	0	0	0.01	0	0	0	0	0	0
P	3.73	3.75	3.67	3.66	3.84	3.91	3.59	4.25	3.77	4.12	3.97	3.83
TOTAL	10.7	10.62	10.67	10.41	11.31	10.93	10.4	11.92	10.53	11.58	11.07	11.27

Chalchihuitl Sample CH22

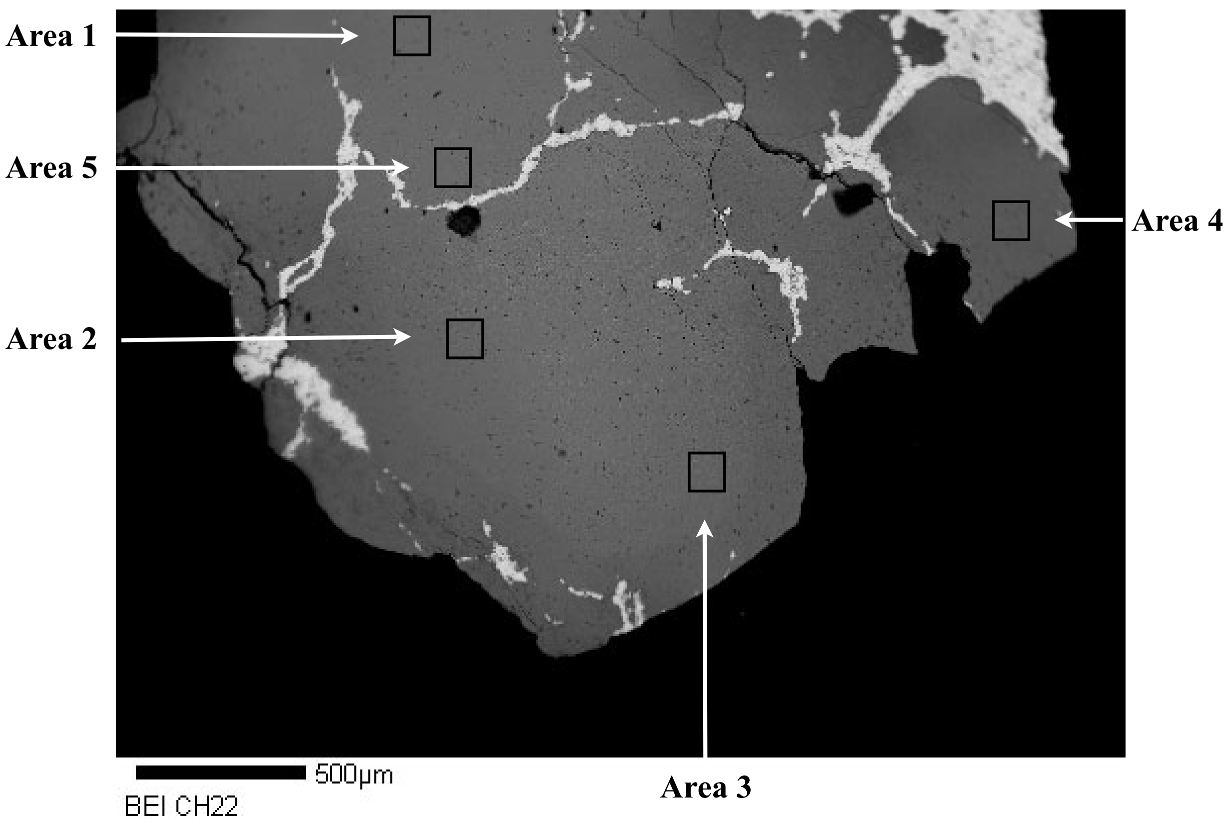

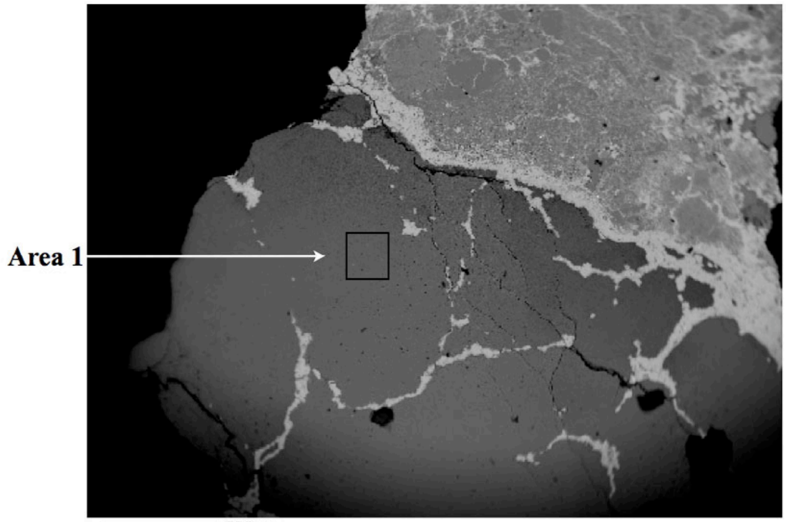

500µm

BEI CH22

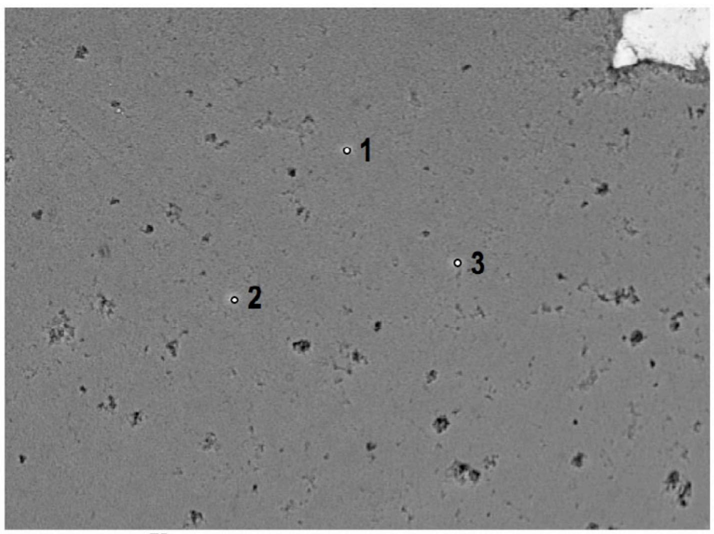

70µm

BEI CH22 Area 1

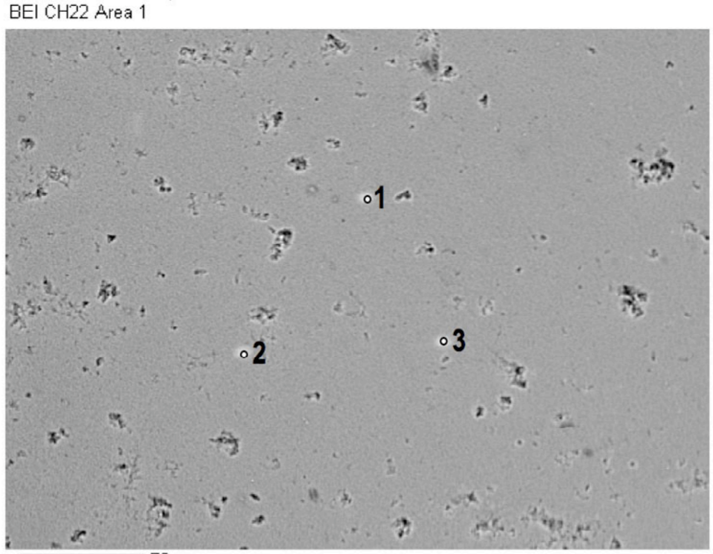

70µm

BEI CH22 Area 2

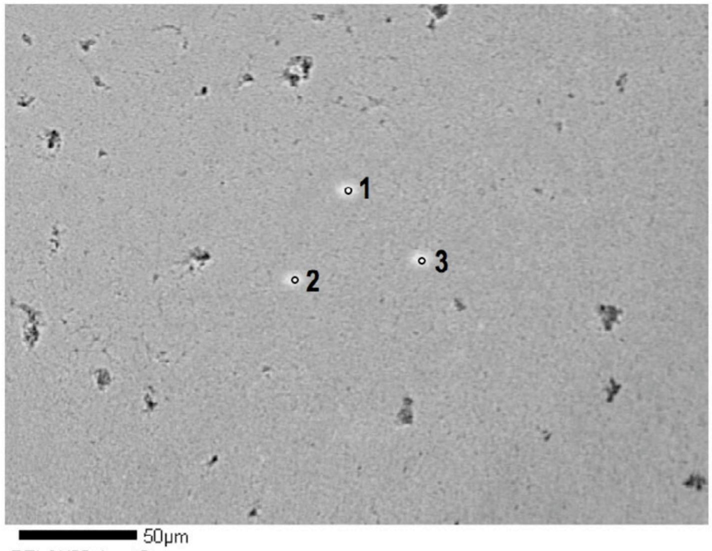

BEI CH22 Area 3

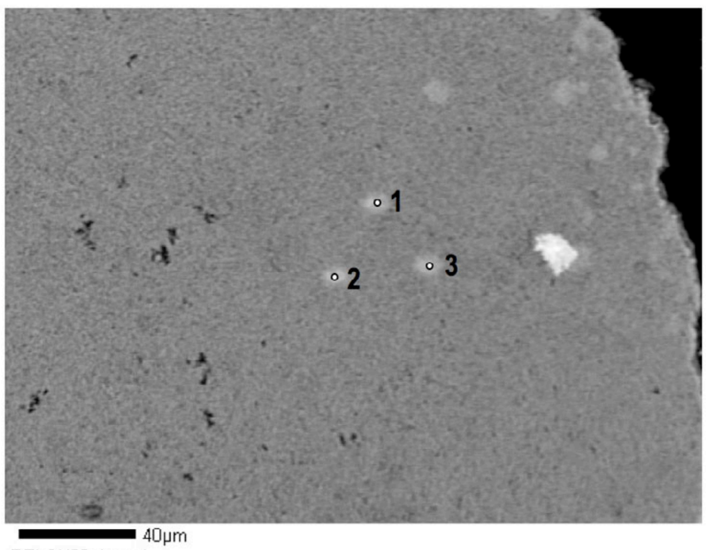

BEI CH22 Area 4

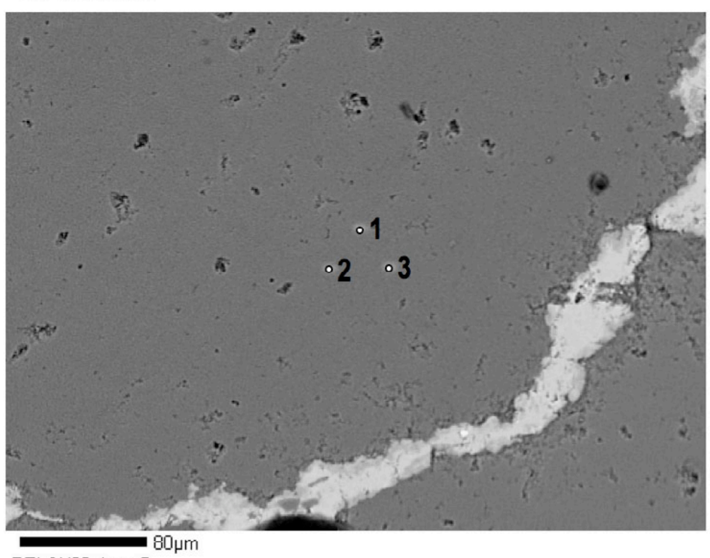

BEI CH22 Area 5

CH22	1-1	1-2	1-3	2-1	2-2	2-3	3-1	3-2	3-3	4-1	4-2	4-3	5-1	5-2	5-3
P2O5	30.57	29.53	29.17	31.82	30.96	33.14	29.83	29.26	29.82	26.39	25.82	25.45	30.39	30.85	30.19
SiO2	6.86	6.67	7.19	7.06	7.56	7.60	7.07	7.16	7.09	6.11	5.76	6.25	7.11	7.32	7.56
TiO2	0.00	0.09	0.00	0.00	0.13	0.00	0.00	0.00	0.00	0.00	0.00	0.00	0.00	0.00	0.00
Al2O3	36.21	33.76	35.76	34.05	38.44	36.14	37.50	32.80	36.76	29.25	33.93	28.86	37.46	33.34	37.73
Fe2O3	0.63	0.86	0.72	0.94	0.62	0.68	0.90	0.66	0.84	0.77	0.79	0.89	1.00	0.64	0.79
MgO	0.06	0.10	0.07	0.11	0.08	0.08	0.09	0.00	0.07	0.06	0.07	0.09	0.09	0.16	0.05
CuO	7.16	7.13	6.73	6.71	7.27	7.93	7.80	6.52	6.60	5.91	6.16	6.11	6.78	7.03	6.84
ZnO	0.32	0.33	0.40	0.00	0.00	0.00	0.00	0.36	0.39	0.32	0.00	0.00	0.00	0.00	0.00
CaO	0.29	0.31	0.33	0.45	0.48	0.44	0.32	0.35	0.33	0.38	0.38	0.42	0.34	0.54	0.31
Total	82.10	78.79	80.36	81.14	85.53	86.01	83.51	77.11	81.90	69.18	72.90	68.07	83.17	79.88	83.48
H2O (by diff.)	17.90	21.21	19.64	18.86	14.47	13.99	16.49	22.89	18.10	30.82	27.10	31.93	16.83	20.12	16.52
TOTAL	100	100	100	100	100	100	100	100	100	100	100	100	100	100	100
Based on 28O															
Cu	0.72	0.71	0.67	0.67	0.75	0.83	0.8	0.64	0.67	0.55	0.59	0.56	0.69	0.7	0.7
Fe	0.06	0.09	0.07	0.09	0.06	0.07	0.09	0.06	0.08	0.07	0.07	0.08	0.1	0.06	0.08
Al	5.72	5.22	5.58	5.32	6.22	5.87	6.01	4.99	5.79	4.22	5.03	4.14	5.95	5.17	6
Zn	0.03	0.03	0.04	0	0	0	0	0.03	0.04	0.03	0	0	0	0	0
Mg	0.01	0.02	0.01	0.02	0.02	0.02	0.02	0	0.01	0.01	0.01	0.02	0.02	0.03	0.01
Ti	0	0.01	0	0	0.01	0	0	0	0	0	0	0	0	0	0
Ca	0.04	0.04	0.05	0.06	0.07	0.06	0.05	0.05	0.05	0.05	0.05	0.06	0.05	0.08	0.04
Si	0.92	0.87	0.95	0.94	1.04	1.05	0.96	0.92	0.95	0.75	0.72	0.76	0.96	0.96	1.02
P	3.47	3.28	3.27	3.57	3.6	3.86	3.43	3.2	3.38	2.74	2.75	2.62	3.47	3.44	3.45
H	16.01	18.57	17.36	16.68	13.27	12.87	14.96	19.72	16.16	25.19	22.75	25.93	15.14	17.67	14.9
TOTAL	26.98	28.84	28	27.35	25.04	24.63	26.32	29.61	27.13	33.61	31.97	34.17	26.38	28.11	26.2

Chalchihuitl Sample CH23

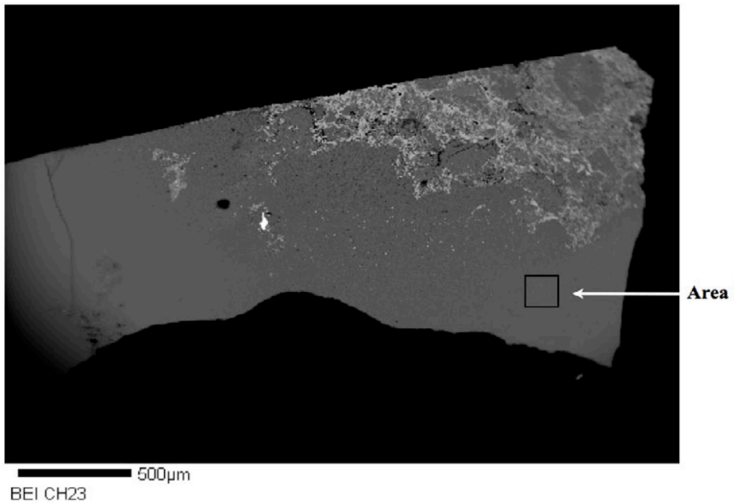

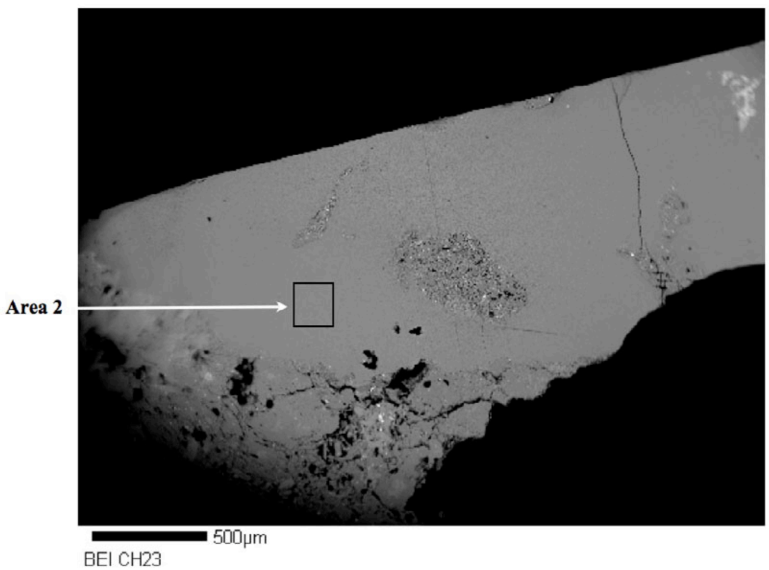

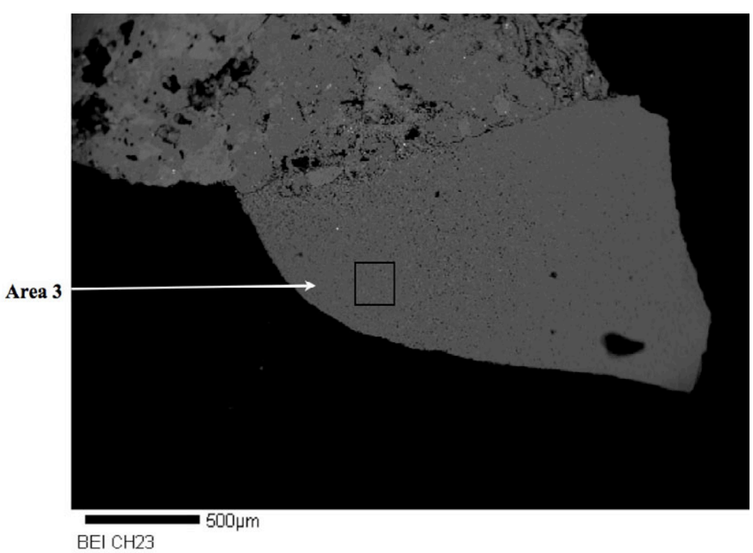

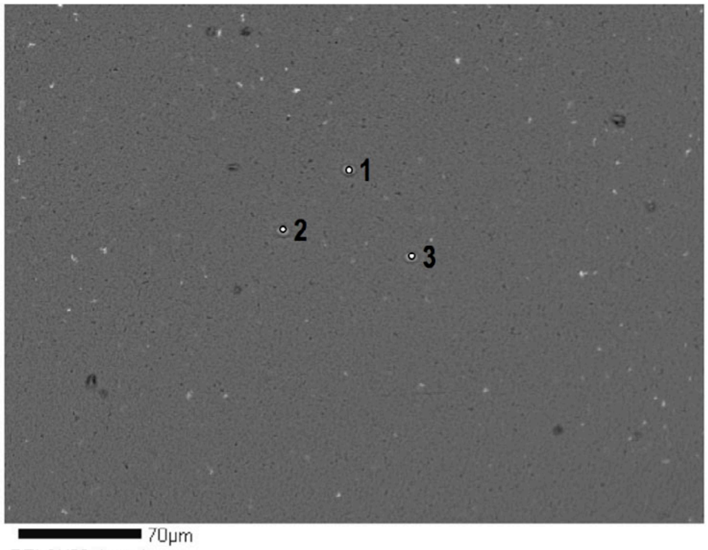

BEI CH23 Area 1

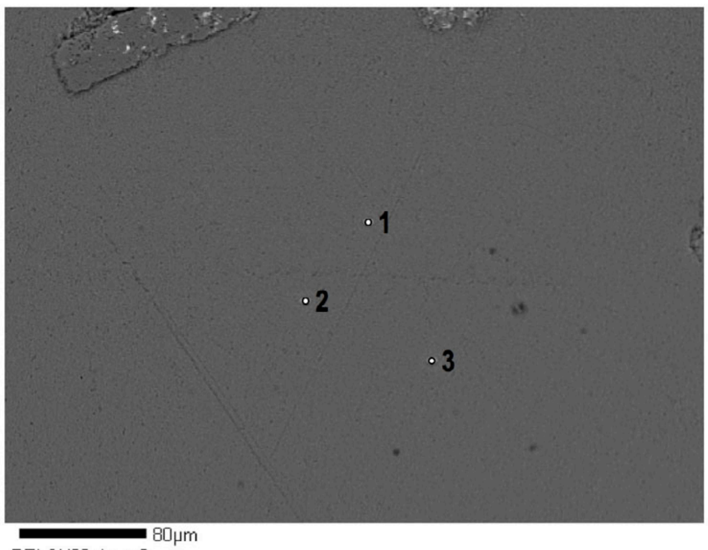

BEI CH23 Area 2

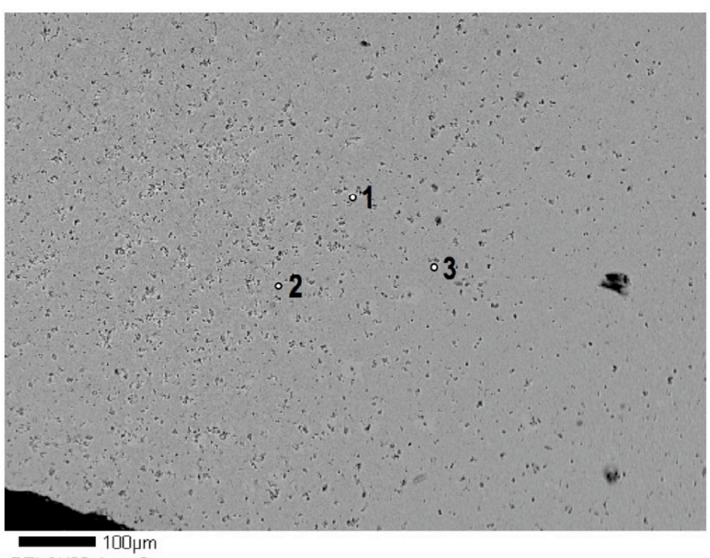

BEI CH23 Area 3

CH23	**CH23 1-1**	**CH23 1-2**	**CH23 1-3**	**CH23 2-1**	**CH23 2-2**	**CH23 2-3**	**CH23 3-1**	**CH23 3-2**	**CH23 3-3**
P2O5	24.01	23.89	25.49	23.34	22.98	22.91	29.86	30.16	30.68
SiO2	16.97	17.28	16.45	18.49	18.97	19.28	9.79	9.48	9.72
TiO2	0.00	0.00	0.00	0.00	0.00	0.00	0.00	0.00	0.00
Al2O3	27.81	29.32	27.45	28.23	27.00	27.84	33.25	36.47	33.21
Fe2O3	5.17	5.89	5.68	6.59	6.56	7.44	1.83	1.93	2.04
MgO	0.75	0.87	0.92	0.90	0.97	1.00	0.22	0.18	0.27
CuO	5.49	4.99	4.96	5.85	5.67	5.09	6.75	6.83	6.65
ZnO	0.34	0.00	0.00	0.39	0.00	0.00	0.51	0.47	0.45
CaO	0.85	0.73	0.73	0.79	0.78	0.84	0.70	0.71	0.77
Total	81.39	82.97	81.68	84.58	82.94	84.40	82.91	86.23	83.80
H2O*	18.61	17.03	18.32	15.42	17.06	15.60	17.09	13.77	16.20
TOTAL	100.00	100.00	100.00	100.00	100.00	100.00	100.00	100.00	100.00
28 O									
Cu	0.56	0.51	0.5	0.61	0.58	0.53	0.69	0.72	0.68
Fe	0.52	0.6	0.57	0.69	0.67	0.77	0.19	0.2	0.21
Al	4.41	4.69	4.34	4.61	4.34	4.53	5.3	5.96	5.32
Zn	0	0	0	0.04	0	0	0.05	0.05	0.05
Mg	0.03	0.18	0.18	0.19	0.2	0.21	0.04	0.04	0.05
Ti	0	0	0	0	0	0	0	0	0
Ca	0.12	0.11	0.1	0.12	0.11	0.12	0.1	0.11	0.11
Si	2.28	2.35	2.21	2.56	2.59	2.66	1.32	1.31	1.32
P	2.73	2.74	2.89	2.74	2.65	2.68	3.42	3.54	3.53
H	16.7	15.43	16.4	14.27	15.54	14.37	15.41	12.74	14.7
TOTAL	27.35	26.61	27.19	25.83	26.68	25.87	26.52	24.67	25.97

Chalchihuitl Sample CH26

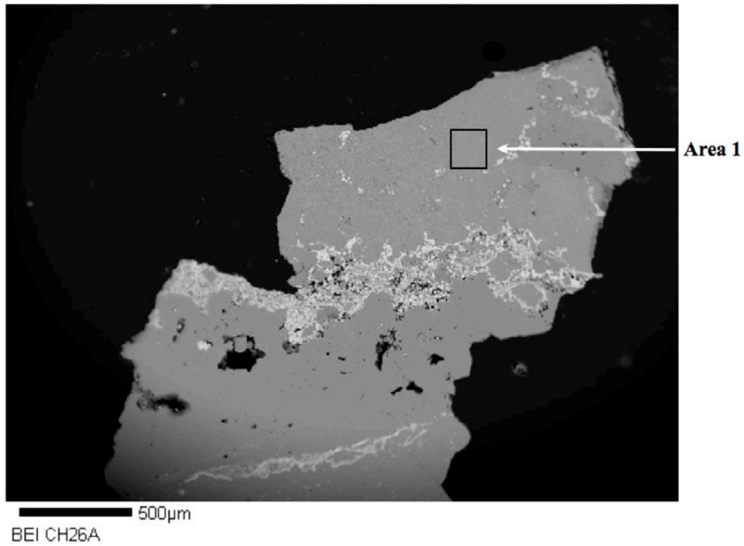

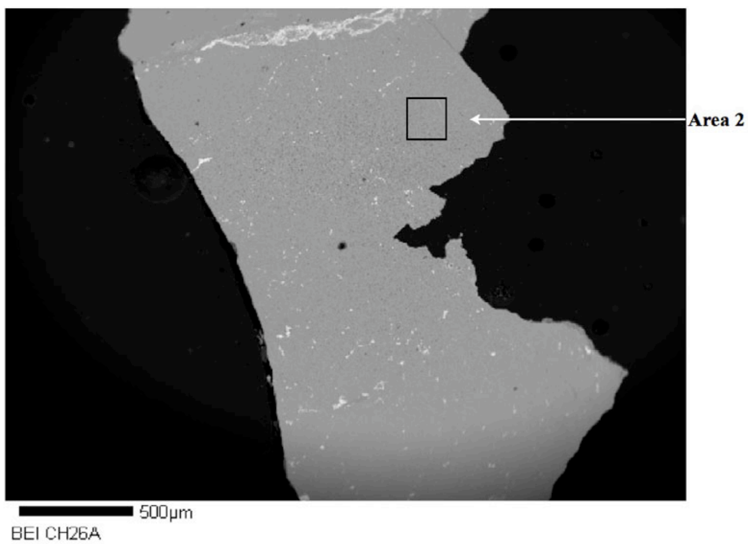

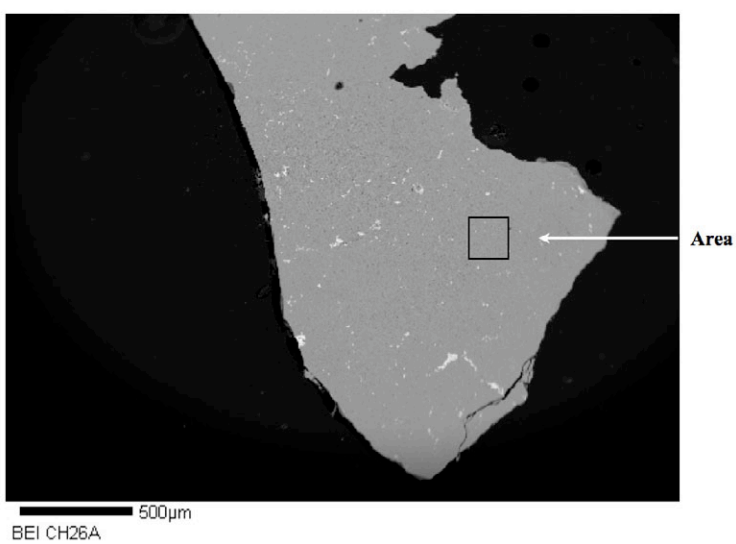

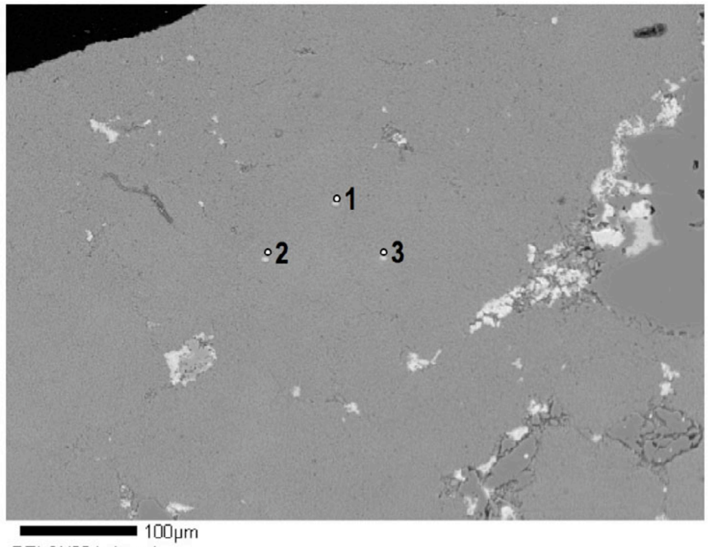

BEI CH26A Area !

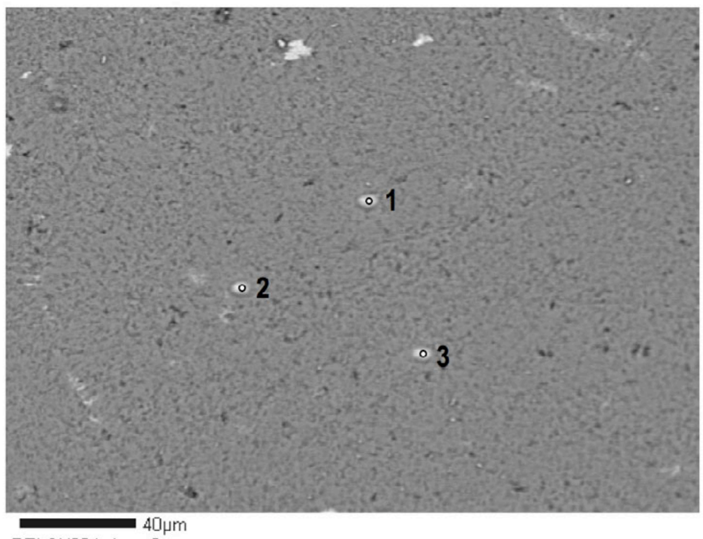

BEI CH26A Area 2

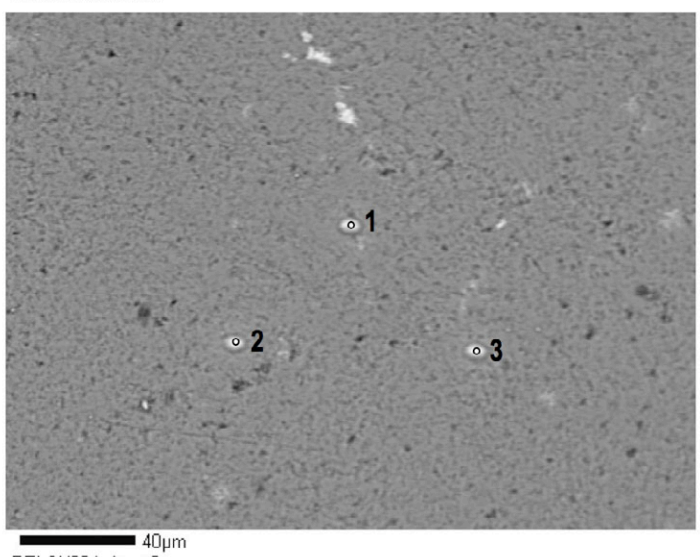

BEI CH26A Area 3

CH26	**CH26A 1-1**	**CH26A 1-2**	**CH26A 1-3**	**CH26A 2-1**	**CH26A 2-2**	**CH26A 2-3**	**CH26A 3-1**	**CH26A 3-2**	**CH26A 3-3**	**CH26B 1-1**	**CH26B 2-1**
P2O5	25.01	23.47	21.25	25.27	23.35	23.21	26.00	23.94	25.00	25.75	0.00
SiO2	15.42	17.12	19.61	16.35	17.72	18.24	16.01	15.85	16.09	14.71	99.29
TiO2	0.00	0.09	0.00	0.12	0.00	0.04	0.00	0.00	0.00	0.00	0.00
Al2O3	27.84	27.91	23.69	29.87	26.90	29.03	28.10	29.46	28.19	28.06	0.59
Fe2O3	6.77	8.17	9.33	5.07	5.57	5.37	5.33	4.54	5.08	7.29	0.00
MgO	0.63	0.69	0.84	0.53	0.58	0.58	0.49	0.44	0.48	0.63	0.00
CuO	5.65	5.12	4.49	5.39	4.99	4.99	4.90	5.36	5.26	5.21	0.00
ZnO	0.00	0.00	0.00	0.00	0.00	0.27	0.00	0.00	0.42	0.00	0.00
CaO	0.82	0.87	1.03	0.81	0.96	0.93	0.78	0.86	0.89	0.83	0.00
Total	82.14	83.45	80.24	83.41	80.06	82.66	81.61	80.45	81.41	82.48	99.88
H2O	17.86	16.55	19.76	16.59	19.94	17.34	18.39	19.55	18.59	17.52	0.12
TOTAL	100.00	100.00	100.00	100.00	100.00	100.00	100.00	100.00	100.00	100.00	100.00
28O											
Cu	0.58	0.53	0.46	0.55	0.5	0.51	0.49	0.54	0.53	0.53	0
Fe	0.69	0.85	0.94	0.52	0.56	0.55	0.54	0.45	0.51	0.75	0
Al	4.45	4.52	3.75	4.79	4.21	4.63	4.43	4.62	4.46	4.5	0.1
Zn	0	0	0	0	0	0.03	0	0	0.04	0	0
Mg	0.13	0.14	0.17	0.11	0.11	0.12	0.1	0.09	0.1	0.13	0
Ti	0	0.01	0	0.01	0	0	0	0	0	0	0
Ca	0.12	0.13	0.15	0.12	0.14	0.14	0.11	0.12	0.13	0.12	0
Si	2.09	2.35	2.64	2.22	2.35	2.47	2.14	2.11	2.16	2	13.9
P	2.87	2.73	2.42	2.91	2.62	2.66	2.94	2.7	2.84	2.96	0
H	16.18	15.19	17.73	15.05	17.67	15.68	16.42	17.36	16.65	15.9	0.11
TOTAL	27.11	26.45	28.26	26.28	28.16	26.79	27.17	27.99	27.42	26.89	14.11

Chalchihuitl Sample CH27

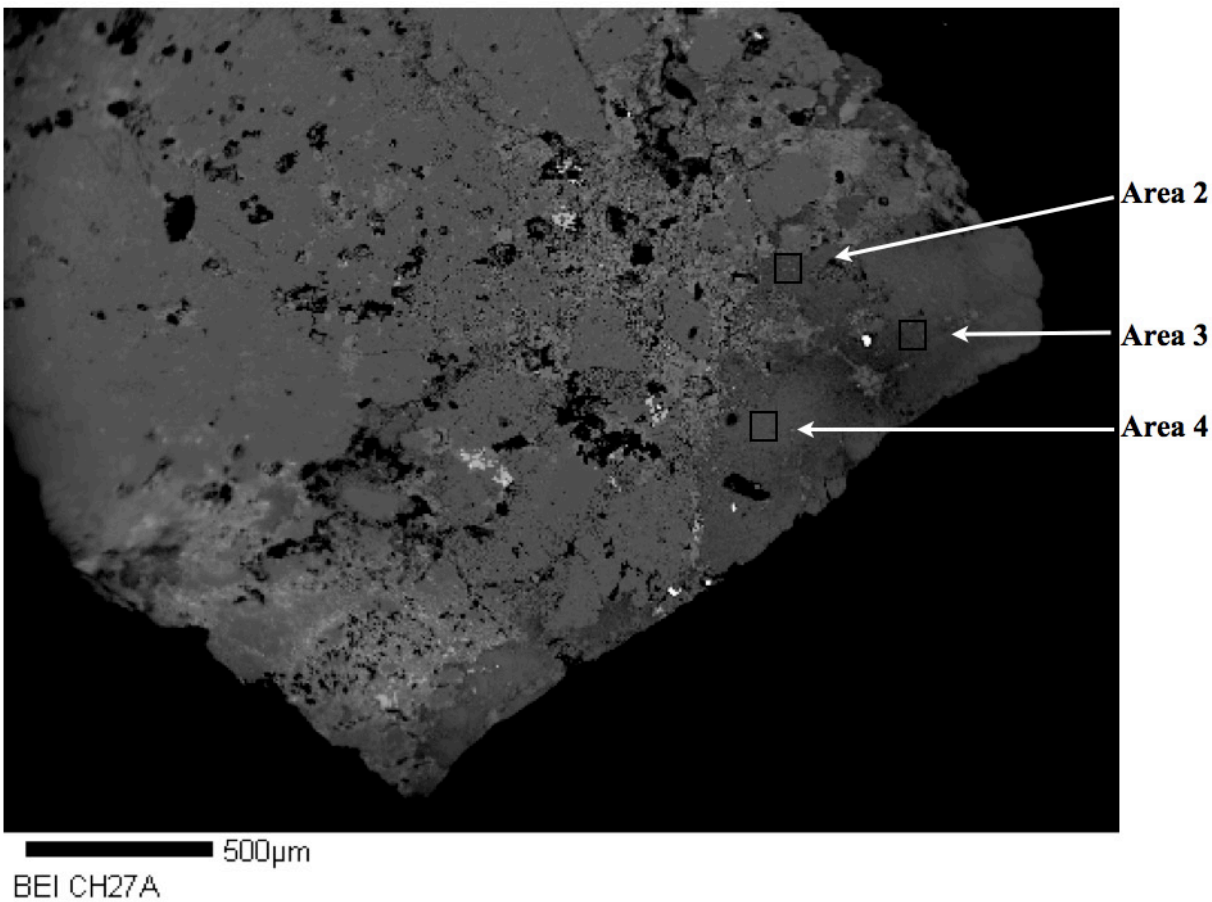

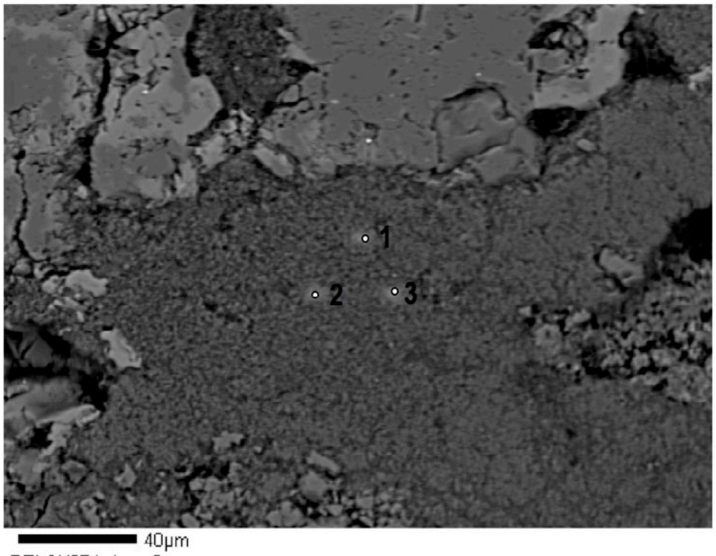

BEI CH27A Area 2

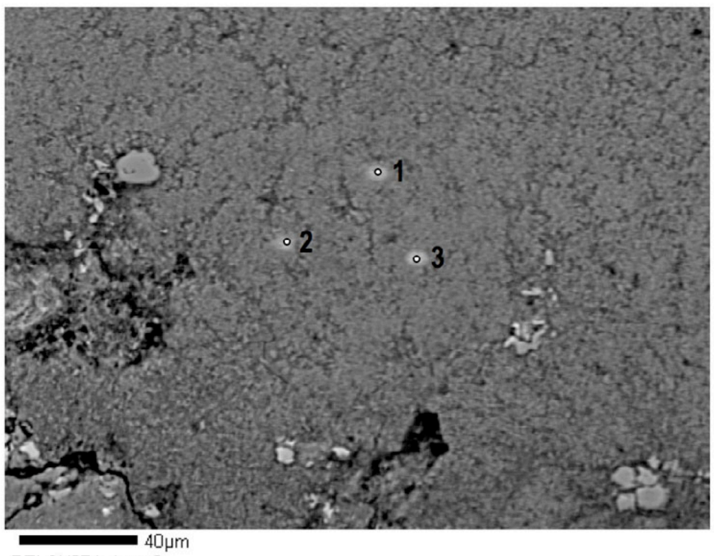

BEI CH27A Area 3

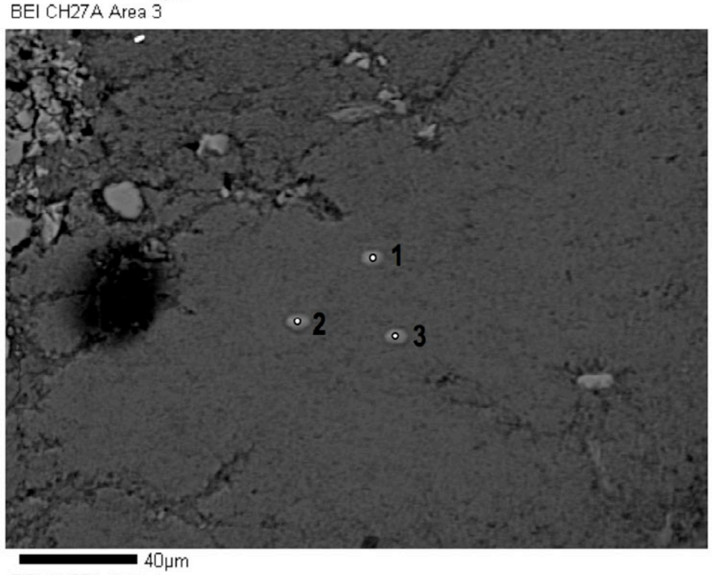

BEI CH27A Area 4

CH27	CH27A 1-1	CH27A 2-1	CH27A 2-2	CH27A 2-3	CH27A 3-1	CH27A 3-2	CH27A 3-3	CH27A 4-1	CH27A 4-2	CH27A 4-3
P2O5	0.00	29.43	30.56	30.59	30.99	29.33	31.11	31.77	31.06	31.63
SiO2	98.58	1.64	1.58	1.55	1.66	1.70	1.44	1.46	1.56	1.63
TiO2	0.00	0.26	0.12	0.24	0.19	0.19	0.17	0.21	0.20	0.23
Al2O3	0.74	31.29	35.89	32.71	36.16	31.87	32.79	36.58	33.75	35.94
Fe2O3	0.00	0.88	0.48	0.86	0.67	1.00	0.64	0.78	0.47	0.61
MgO	0.19	0.00	0.00	0.06	0.00	0.07	0.06	0.00	0.00	0.00
CuO	0.00	5.57	6.32	6.54	6.23	6.18	7.18	6.62	7.16	6.59
ZnO	0.00	0.00	0.11	0.00	0.00	0.00	0.00	0.00	0.00	0.00
CaO	0.04	0.27	0.24	0.26	0.21	0.28	0.25	0.22	0.29	0.23
Total	99.55	69.35	75.30	72.81	76.10	70.62	73.64	77.63	74.49	76.85
H2O*	0.45	30.65	24.70	27.19	23.90	29.38	26.36	22.37	25.51	23.15
TOTAL	100.00	100.00	100.00	100.00	100.00	100.00	100.00	100.00	100.00	100.00
28 O										
Cu	0	0.51	0.61	0.62	0.6	0.58	0.69	0.65	0.69	0.64
Fe	0	0.08	0.05	0.08	0.06	0.09	0.06	0.08	0.04	0.06
Al	0.12	4.51	5.39	4.84	5.46	4.65	4.89	5.59	5.06	5.46
Zn	0	0	0.01	0	0	0	0	0	0	0
Mg	0.04	0	0	0.01	0	0.01	0.01	0	0	0
Ti	0	0.02	0.01	0.02	0.02	0.02	0.02	0.02	0.02	0.02
Ca	0.01	0.04	0.03	0.04	0.03	0.04	0.03	0.03	0.04	0.03
Si	13.78	0.2	0.2	0.19	0.21	0.21	0.18	0.19	0.2	0.21
P	0	3.05	3.3	3.25	3.36	3.07	3.33	3.49	3.34	3.45
H*	0.42	25.01	21.03	22.78	20.44	24.26	22.25	19.37	21.65	19.92
TOTAL	14.37	33.42	30.63	31.83	30.18	32.93	31.46	29.42	31.04	29.79

Chalchihuitl Sample CH28

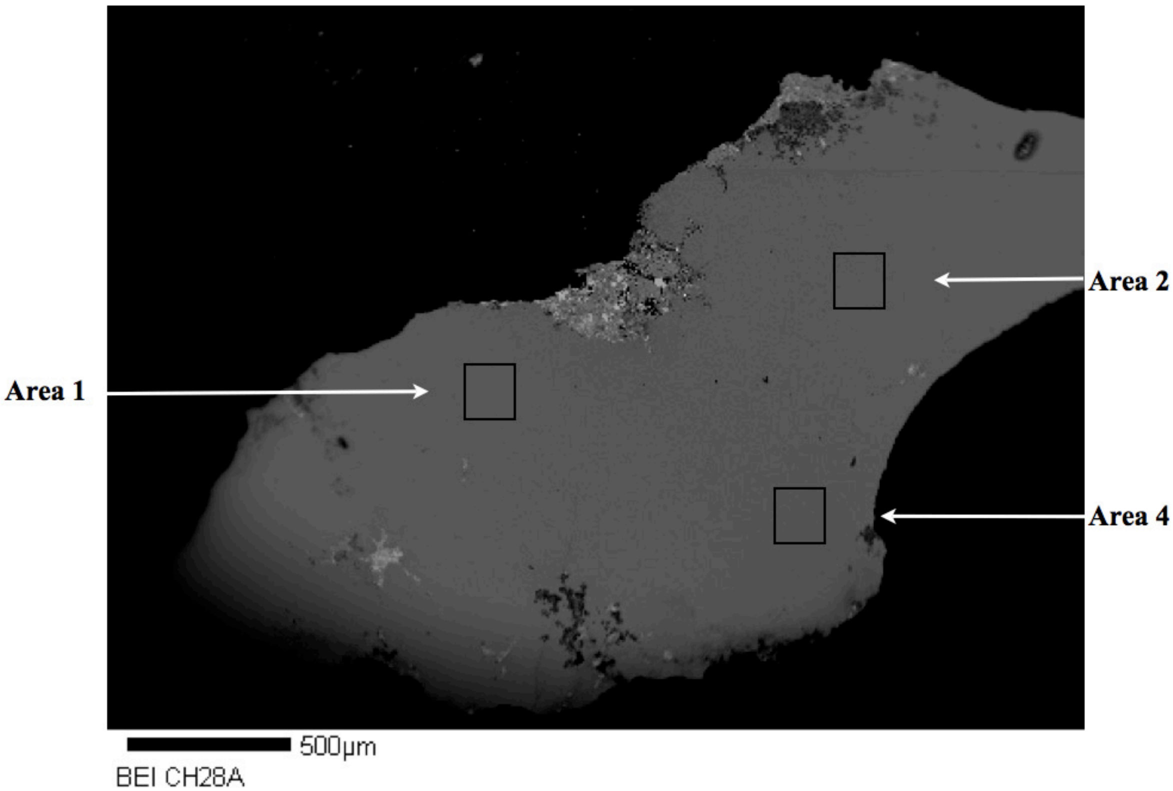

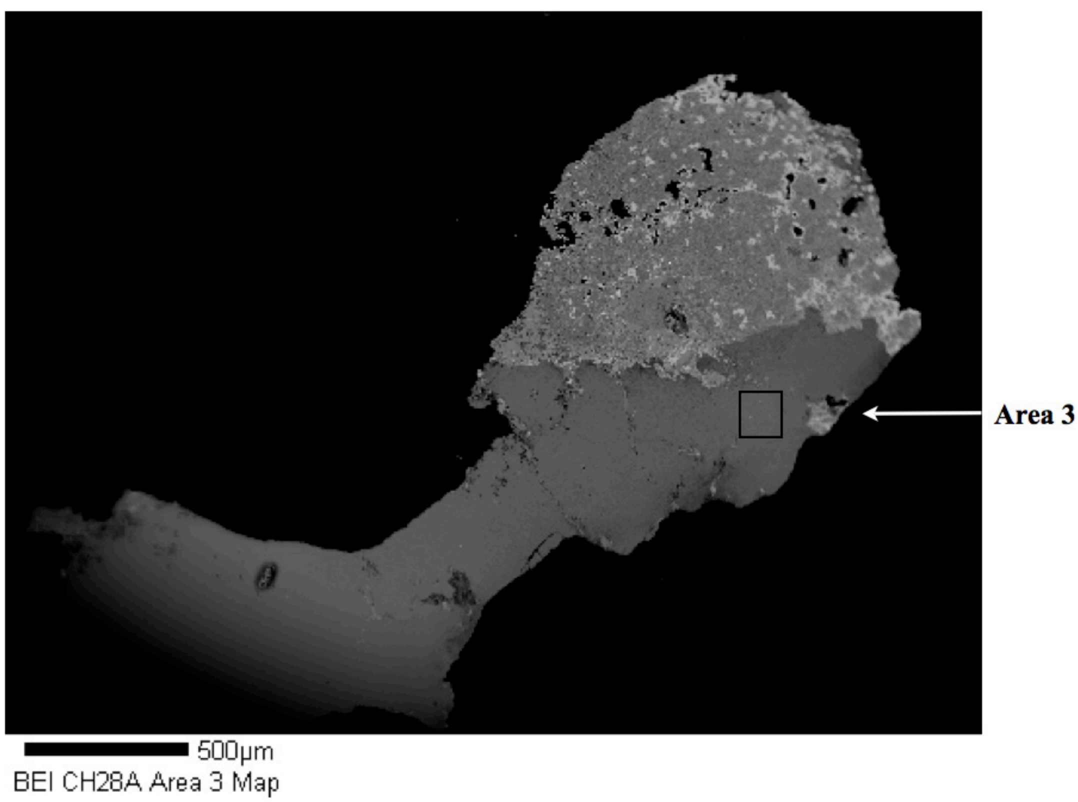

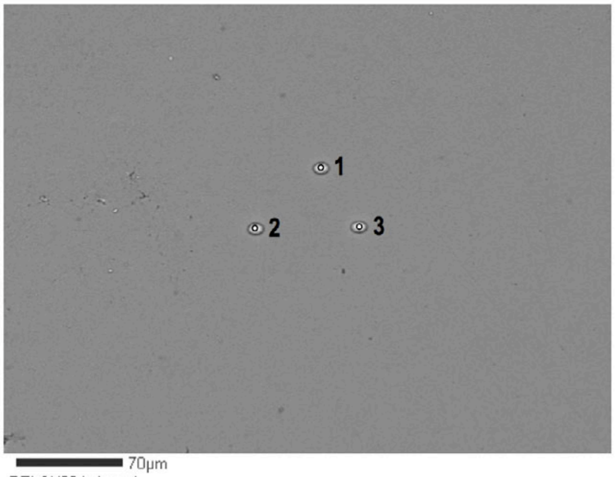

BEI CH28A Area 1

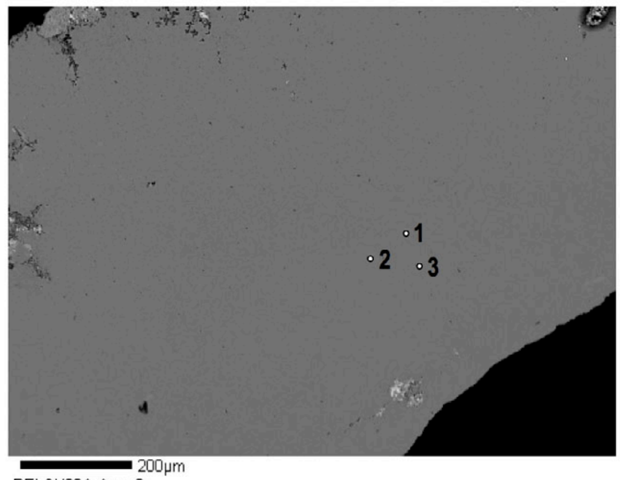

BEI CH28A Area 2

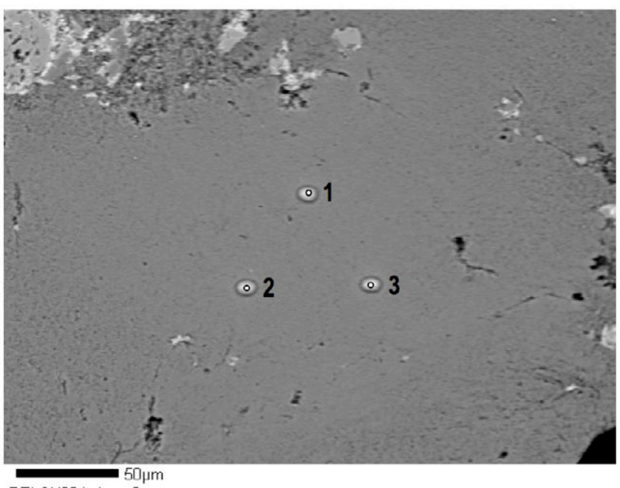

BEI CH28A Area 3

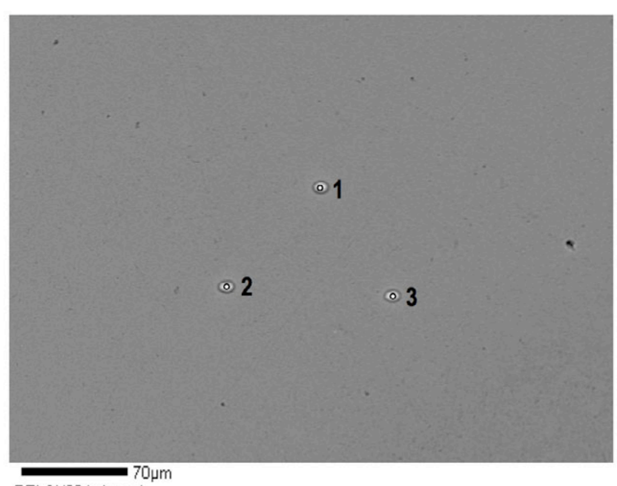

BEI CH28A Area 4

CH28A	**CH28A 1-1**	**CH28A 1-2**	**CH28A 1-3**	**CH28A 2-1**	**CH28A 2-2**	**CH28A 2-3**	**CH28A 3-1**	**CH28A 3-2**	**CH28A 3-3**	**CH28A 4-1**	**CH28A 4-2**	**CH28A 4-3**
P2O5	30.60	31.61	31.59	30.78	31.23	30.64	30.59	30.84	29.84	31.03	31.09	30.11
SiO2	5.85	4.51	5.16	6.88	6.00	6.58	6.50	7.38	8.23	7.42	6.98	7.06
TiO2	0.34	0.29	0.36	0.21	0.21	0.20	0.25	0.38	0.24	0.26	0.28	0.29
Al2O3	34.25	35.62	34.32	33.87	34.08	34.93	34.05	34.91	32.69	34.46	33.45	34.41
Fe2O3	0.93	0.81	1.04	1.04	1.03	1.12	1.09	1.21	1.33	1.27	1.14	1.22
MgO	0.16	0.12	0.13	0.15	0.15	0.16	0.10	0.08	0.12	0.15	0.09	0.11
CuO	7.09	7.32	7.33	6.72	6.90	7.26	6.94	6.63	6.89	6.69	6.90	6.88
ZnO	0.34	0.17	0.00	0.00	0.32	0.00	0.00	0.00	0.00	0.32	0.00	0.00
CaO	0.45	0.41	0.43	0.59	0.49	0.53	0.45	0.51	0.53	0.59	0.53	0.57
Total	80.01	80.86	80.36	80.23	80.41	81.42	79.98	81.93	79.87	82.18	80.45	80.64
H2O (by diff.)	19.99	19.14	19.64	19.77	19.59	18.58	20.02	18.07	20.13	17.82	19.55	19.36
TOTAL (w/H2O)	100.00	100.00	100.00	100.00	100.00	100.00	100.00	100.00	100.00	100.00	100.00	100.00
Based on 28O												
Cu	0.71	0.74	0.73	0.67	0.69	0.73	0.69	0.67	0.69	0.68	0.69	0.69
Fe	0.09	0.08	0.1	0.1	0.1	0.11	0.11	0.12	0.13	0.13	0.11	0.12
Al	5.34	5.59	5.36	5.27	5.32	5.5	5.29	5.49	5.08	5.44	5.21	5.38
Zn	0.03	0.02	0	0	0.03	0	0	0	0	0.03	0	0
Mg	0.03	0.02	0.03	0.03	0.03	0.03	0.02	0.02	0.02	0.03	0.02	0.02
Ti	0.03	0.03	0.04	0.02	0.02	0.02	0.03	0.04	0.02	0.03	0.03	0.03
Ca	0.06	0.06	0.06	0.08	0.07	0.08	0.06	0.07	0.08	0.09	0.07	0.08
Si	0.77	0.6	0.68	0.91	0.79	0.88	0.86	0.99	1.08	0.99	0.92	0.94
P	3.43	3.56	3.54	3.44	3.5	3.46	3.42	3.49	3.33	3.52	3.48	3.38
H	17.66	17.01	17.37	17.41	17.32	16.57	17.63	16.11	17.71	15.95	17.26	17.14
TOTAL	28.15	27.71	27.91	27.93	27.87	27.38	28.11	27	28.14	26.89	27.79	27.78

Chalchihuitl Sample CH34

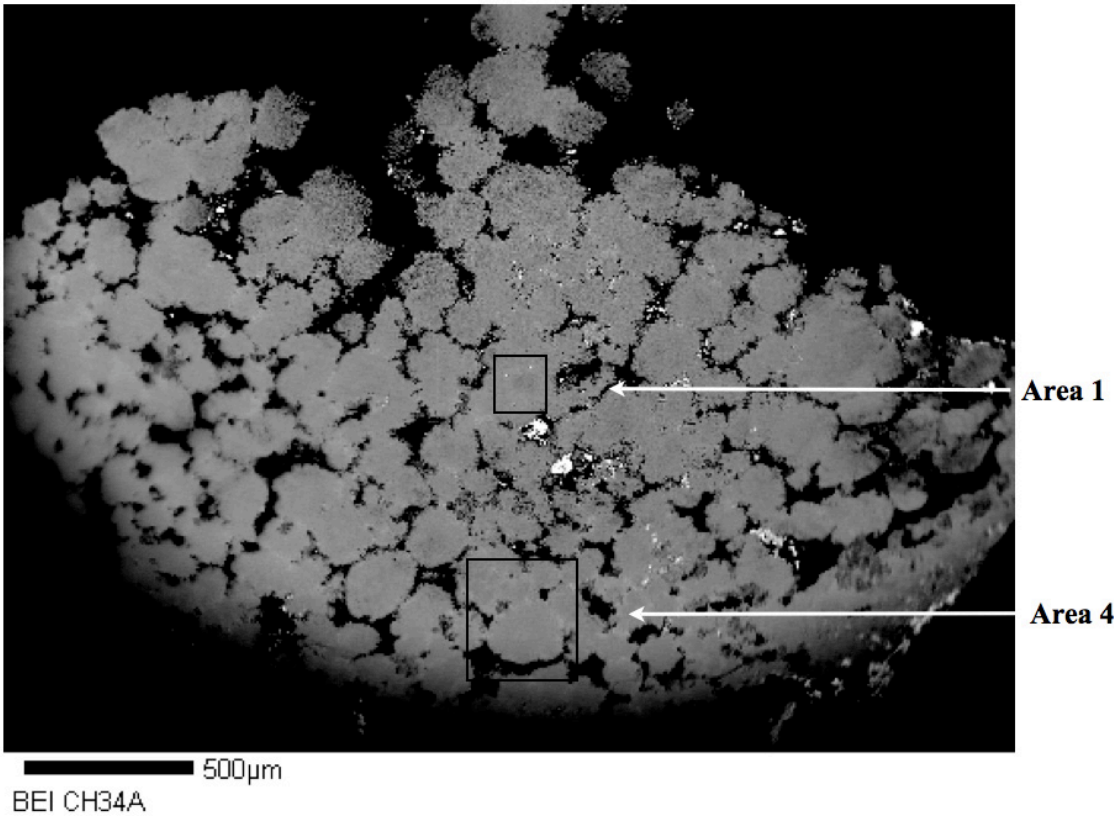

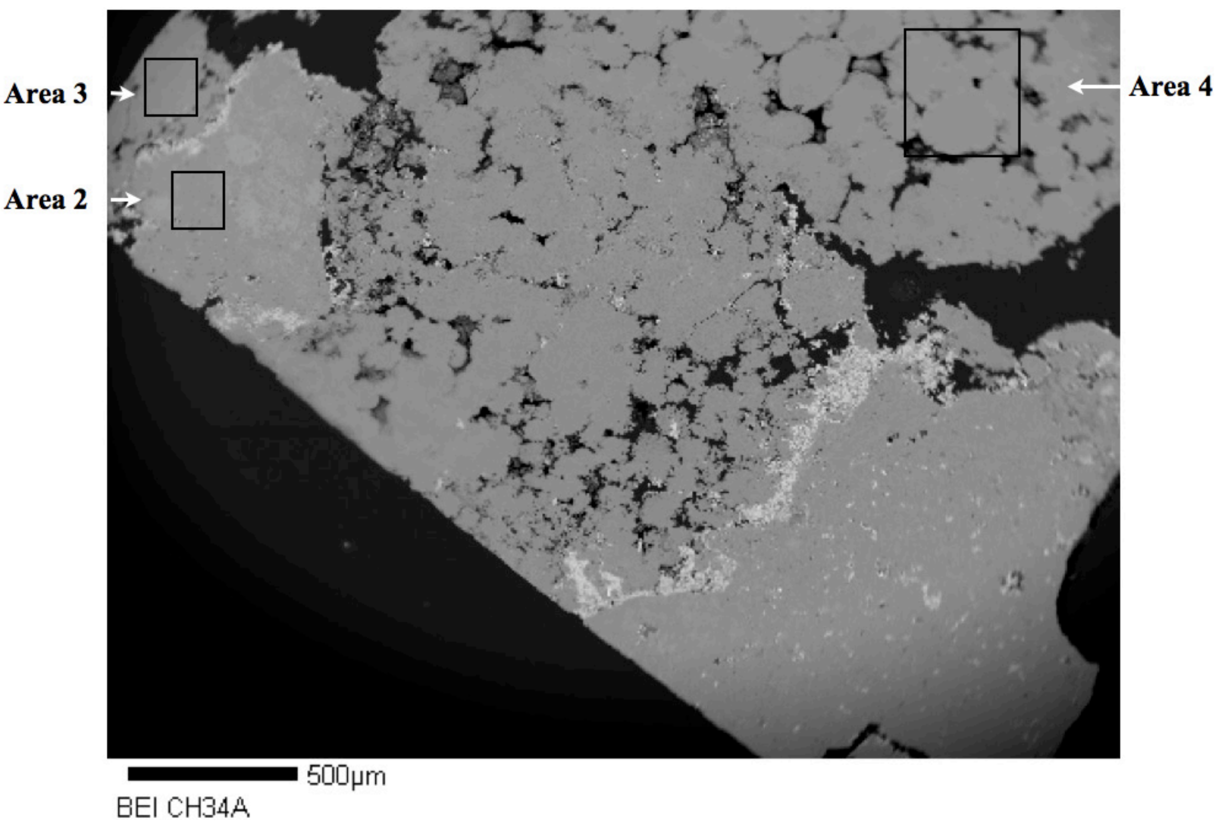

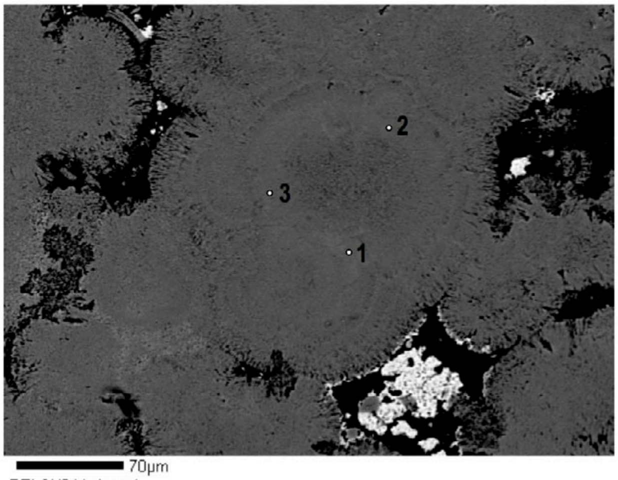

BEI CH34A Area 1

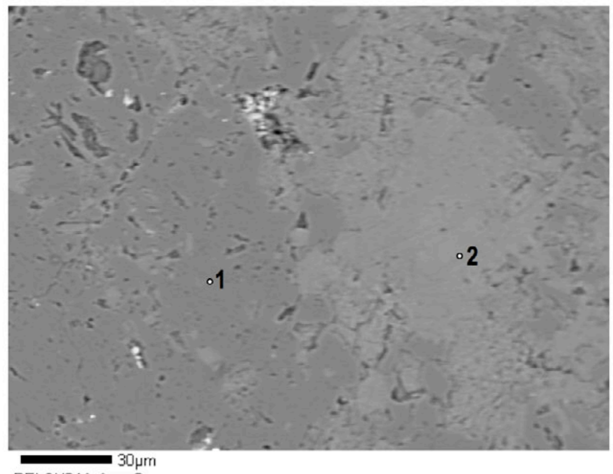

BEI CH34A Area 2

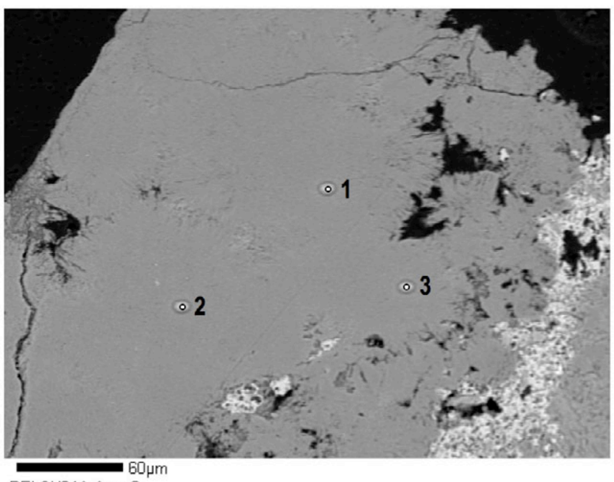

BEI CH34A Area 3

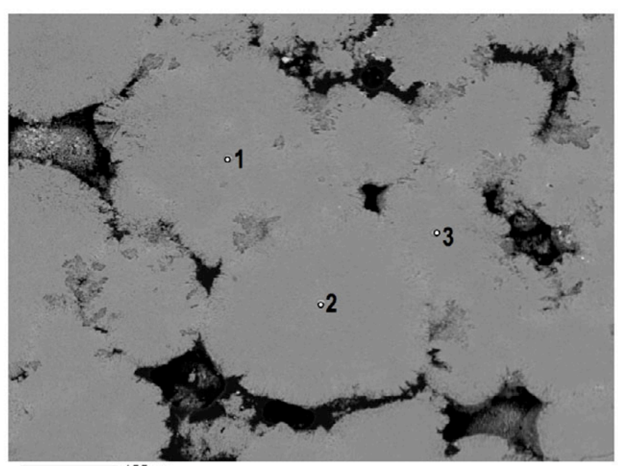

BEI CH34A Area 4

CH34A	CH34A 1-1	CH34A 1-2	CH34A 1-3	CH34A 2-1	CH34A 2-2	CH34A 3-1	CH34A 3-2	CH34A 3-3	CH34A 4-1	CH34A 4-2	CH34A 4-3
P2O5	32.03	32.77	32.24	0.09	0.00	32.39	30.25	32.38	30.74	33.41	30.09
SiO2	4.90	3.66	4.57	65.78	45.30	7.76	8.60	6.58	8.71	3.65	9.73
TiO2	0.18	0.16	0.28	0.00	0.44	0.21	0.14	0.23	0.16	0.15	0.23
Al2O3	33.70	33.84	35.32	19.73	32.84	32.82	34.17	33.75	33.23	33.95	34.05
Fe2O3	2.09	2.58	2.44	0.00	4.79	2.85	2.34	2.70	3.72	3.28	2.38
MgO	0.20	0.19	0.18	0.05	2.55	0.26	0.26	0.26	0.30	0.26	0.19
CuO	4.70	5.12	4.87	0.00	0.00	4.18	3.88	4.07	4.40	4.37	4.51
ZnO	0.00	0.00	0.00	0.00	0.00	0.00	0.00	0.00	0.00	0.00	0.00
CaO	0.78	0.76	0.76	0.37	0.00	0.88	0.92	0.81	0.82	0.90	0.88
Total	78.57	79.09	80.65	86.01	85.92	81.35	80.57	80.78	82.08	79.97	82.05
H2O*	21.43	20.91	19.35	13.99	14.08	18.65	19.43	19.22	17.92	20.03	17.95
TOTAL	100.00	100.00	100.00	100.00	100.00	100.00	100.00	100.00	100.00	100.00	100.00
28 O											
Cu	0.46	0.5	0.49	0	0	0.42	0.38	0.4	0.44	0.43	0.45
Fe	0.2	0.25	0.24	0	0.49	0.28	0.23	0.27	0.37	0.32	0.24
Al	5.15	5.21	5.49	3.05	5.27	5.1	5.28	5.22	5.22	5.25	5.33
Zn	0	0	0	0	0	0	0	0	0	0	0
Mg	0.04	0.04	0.03	0.01	0.52	0.05	0.05	0.05	0.06	0.05	0.04
Ti	0.02	0.02	0.03	0	0.04	0.02	0.01	0.02	0.02	0.01	0.02
Ca	0.11	0.11	0.11	0.05	0	0.12	0.13	0.11	0.12	0.13	0.13
Si	0.64	0.48	0.6	8.62	6.17	1.02	1.13	0.86	1.16	0.48	1.29
P	3.52	3.62	3.6	0.01	0	3.62	3.36	3.6	3.47	3.71	3.38
H*	18.54	18.23	17.03	12.23	12.81	16.42	17	16.85	15.94	17.54	15.91
TOTAL	28.68	28.46	27.62	23.97	25.3	27.05	27.57	27.38	26.8	27.92	26.79

Chalchihuitl Sample CH35

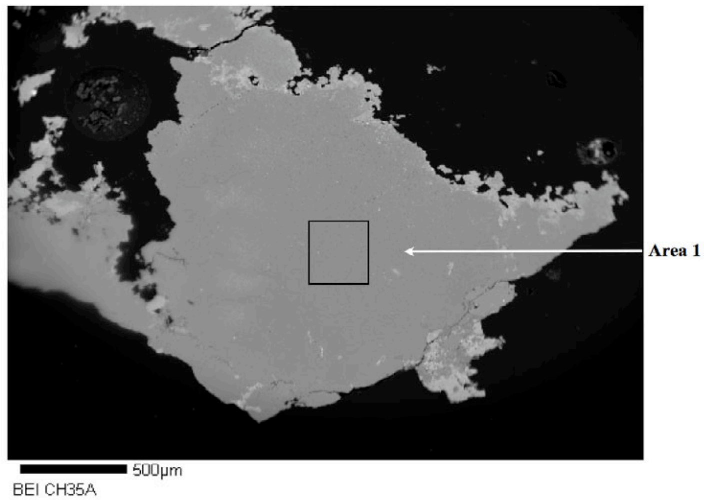

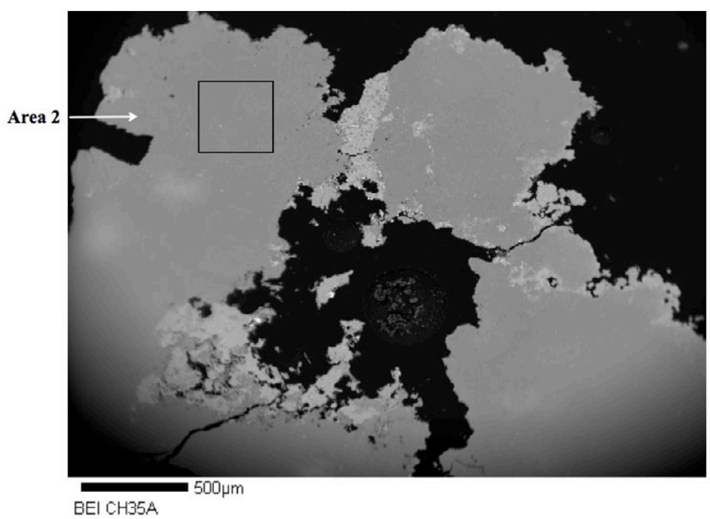

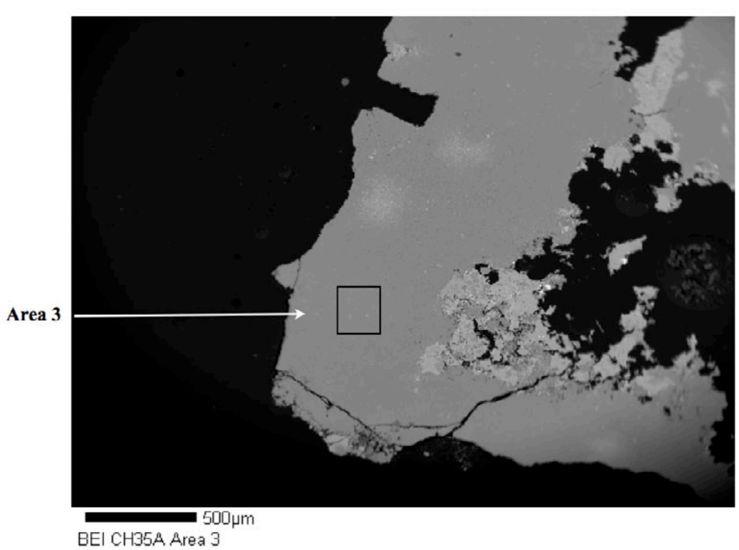

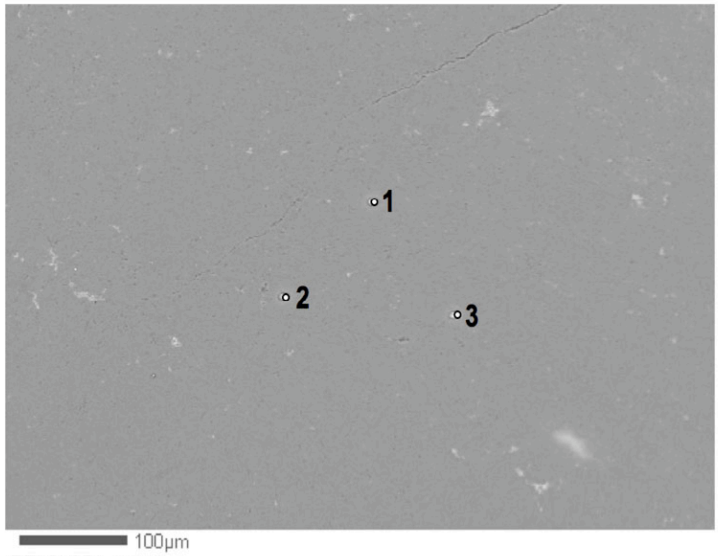

BEI CH35A Area 1

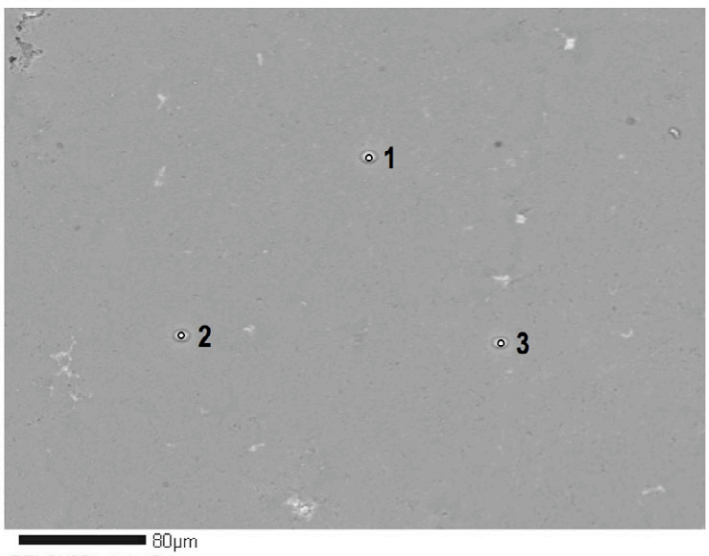

BEI CH35A Area 2

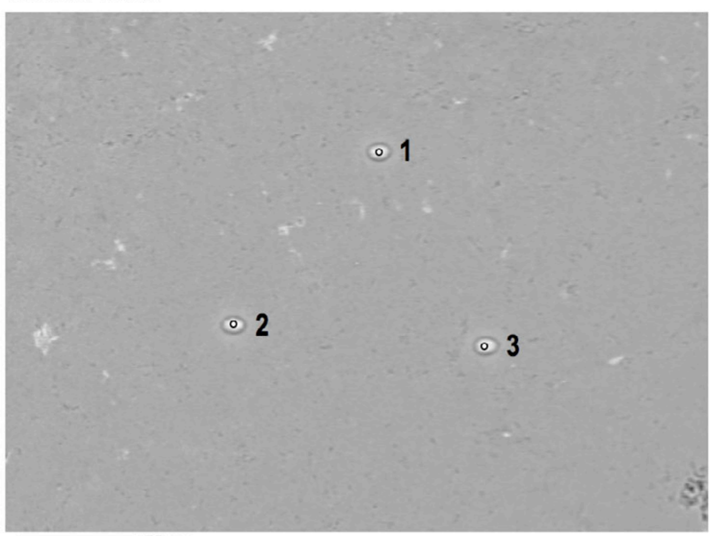

BEI CH35A Area 3

CH35	**CH35A 1-1**	**CH35A 1-2**	**CH35A 1-3**	**CH35A 2-1**	**CH35A 2-2**	**CH35A 2-3**	**CH35A 3-1**	**CH35A 3-2**	**CH35A 3-3**	**CH35A 4-1**
P2O5	37.87	36.28	35.55	36.00	35.16	35.77	35.76	35.25	36.04	34.99
SiO2	1.04	0.35	0.29	0.14	0.00	0.30	0.44	1.03	0.08	0.41
TiO2	2.29	2.65	2.47	1.32	2.47	2.45	2.53	1.83	2.84	1.89
Al2O3	39.12	37.63	36.10	37.48	35.67	37.98	35.67	37.08	36.38	35.35
Fe2O3	1.87	1.00	1.04	1.30	0.81	1.34	1.28	1.93	0.84	3.99
MgO	0.11	0.06	0.05	0.11	0.06	0.05	0.00	0.09	0.07	0.08
CuO	3.34	2.66	2.84	2.66	2.43	3.12	2.85	3.01	2.67	2.20
ZnO	0.00	0.00	0.00	0.00	0.00	0.00	0.00	0.00	0.00	0.00
CaO	0.45	0.30	0.37	0.64	0.59	0.42	0.37	0.39	0.53	1.09
Total	86.09	80.93	78.71	79.65	77.19	81.42	78.90	80.61	79.45	80.01
H2O*	13.91	19.07	21.29	20.35	22.81	18.58	21.10	19.39	20.55	19.99
TOTAL	100.00	100.00	100.00	100.00	100.00	100.00	100.00	100.00	100.00	100.00
28 O										
Cu	0.34	0.26	0.28	0.26	0.23	0.31	0.28	0.3	0.26	0.22
Fe	0.19	0.1	0.1	0.13	0.08	0.13	0.12	0.19	0.08	0.39
Al	6.25	5.77	5.46	5.7	5.33	5.87	5.4	5.7	5.53	5.44
Zn	0	0	0	0	0	0	0	0	0	0
Mg	0.02	0.01	0.01	0.02	0.01	0.01	0	0.02	0.01	0.02
Ti	0.23	0.26	0.24	0.13	0.24	0.24	0.24	0.24	0.28	0.19
Ca	0.07	0.04	0.05	0.09	0.08	0.06	0.05	0.18	0.07	0.15
Si	0.14	0.05	0.04	0.02	0	0.04	0.06	0.13	0.01	0.05
P	4.35	4	3.86	3.93	3.77	3.97	3.89	3.89	3.93	3.87
H*	12.59	16.57	18.23	17.53	19.31	16.27	18.11	16.89	17.68	17.43
TOTAL	24.18	27.06	28.27	27.81	29.05	26.9	28.15	27.54	27.85	27.76

Tiffany Sample TF39

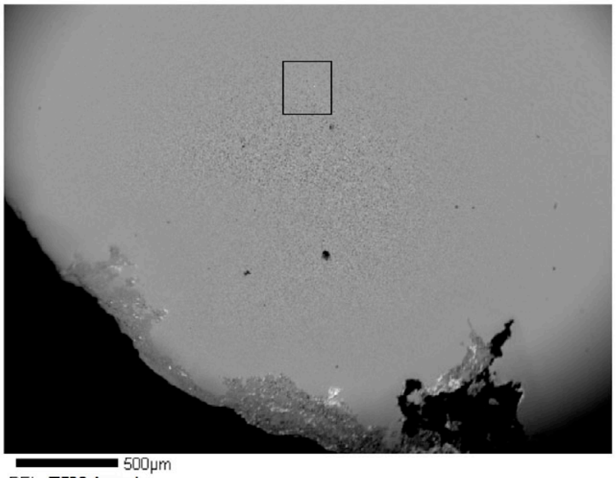

BEI TF39 Area 1

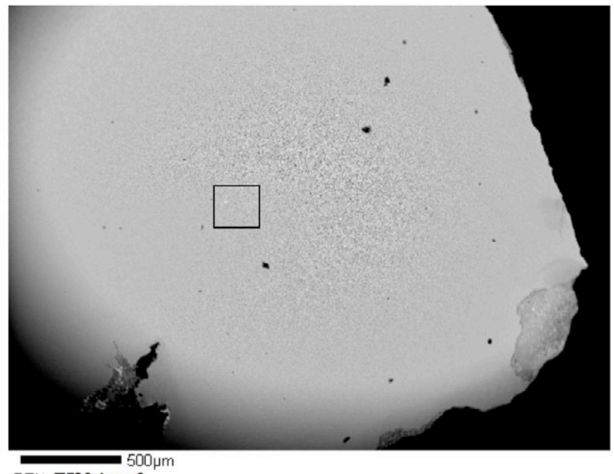

BEI TF39 Area 2

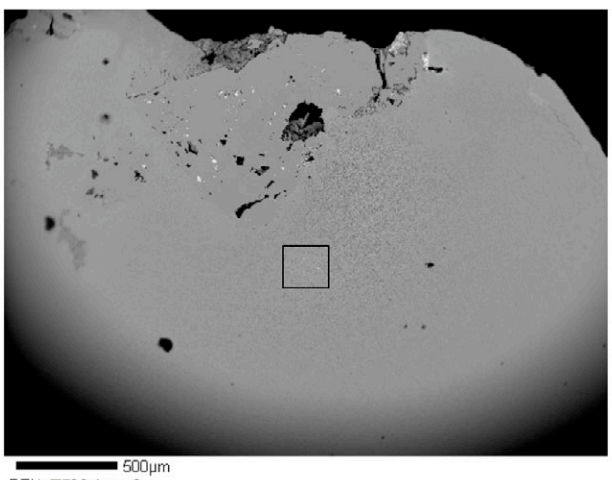

BEI TF39 Area 3

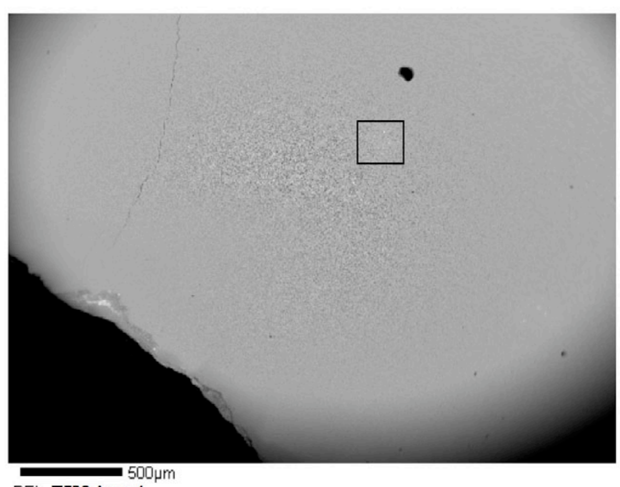

BEI TF39 Area 4

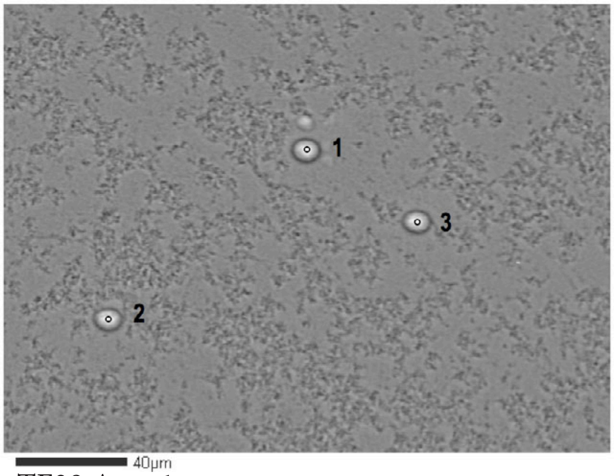

TF39 Area 1

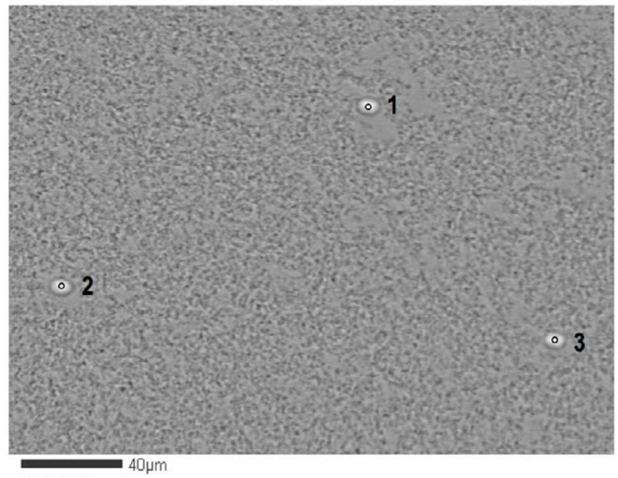

TF39 Area 2

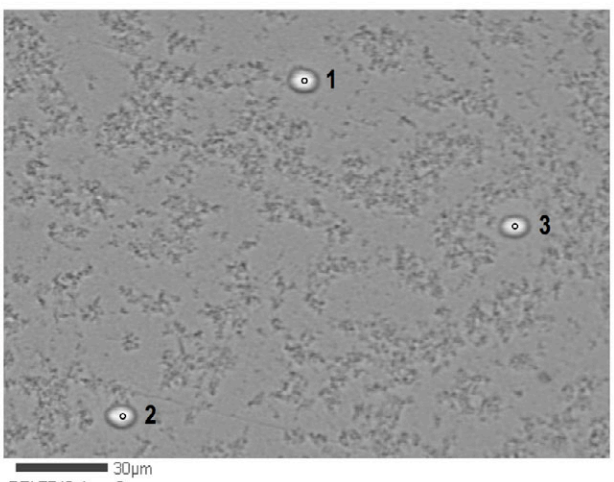

TF39 Area 3

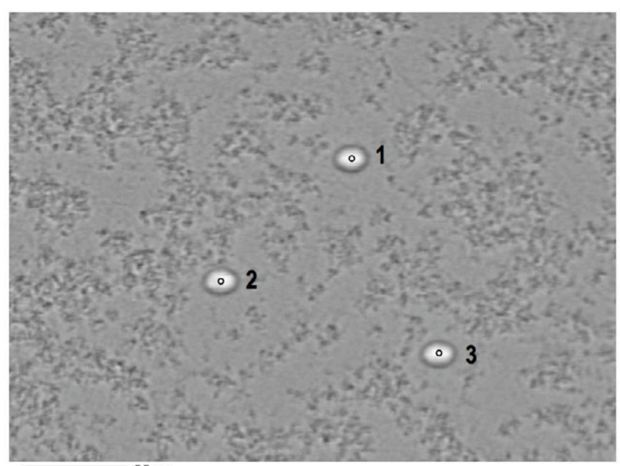

TF39 Area 4

TF39	TF39 1-1	TF39 1-2	TF39 1-3	TF39 2-1	TF39 2-2	TF39 2-3	TF39 3-1	TF39 3-2	TF39 3-3	TF39 4-1	TF39 4-2	TF39 4-3
P2O5	34.57	33.50	34.06	34.90	32.78	35.17	32.84	33.64	33.89	33.91	34.00	33.50
SiO2	0.30	0.29	0.32	0.38	0.33	0.33	0.46	0.36	0.42	0.39	0.33	0.38
TiO2	0.19	0.19	0.20	0.17	0.22	0.20	0.11	0.14	0.13	0.23	0.21	0.20
Al2O3	34.53	36.50	34.90	38.43	36.48	38.48	34.88	37.36	35.02	38.25	35.63	38.40
Fe2O3	1.16	1.06	0.87	1.31	0.92	1.15	1.46	1.05	1.29	1.12	1.18	1.29
MgO	0.00	0.00	0.00	0.00	0.00	0.05	0.00	0.00	0.00	0.00	0.00	0.00
CuO	7.44	7.67	7.27	7.92	7.65	6.91	7.36	7.36	7.63	7.94	7.53	7.29
ZnO	0.00	0.00	0.00	0.00	0.00	0.00	0.00	0.00	0.00	0.00	0.00	0.00
CaO	0.16	0.14	0.12	0.14	0.17	0.17	0.16	0.16	0.14	0.16	0.15	0.19
Total	78.36	79.35	77.74	83.26	78.55	82.46	77.26	80.08	78.52	82.01	79.02	81.24
H2O*	21.64	20.65	22.26	16.74	21.45	17.54	22.74	19.92	21.48	17.99	20.98	18.76
TOTAL	100.00	100.00	100.00	100.00	100.00	100.00	100.00	100.00	100.00	100.00	100.00	100.00
28 O												
Cu	0.73	0.76	0.71	0.81	0.76	0.7	0.72	0.74	0.75	0.81	0.75	0.74
Fe	0.11	0.11	0.09	0.13	0.09	0.12	0.14	0.1	0.13	0.11	0.12	0.13
Al	5.31	5.67	5.34	6.15	5.64	6.08	5.34	5.83	5.41	6.07	5.52	6.05
Zn	0	0	0	0	0	0	0	0	0	0	0	0
Mg	0	0	0	0	0	0.01	0	0	0	0	0	0
Ti	0.02	0.02	0.02	0.02	0.02	0.02	0.01	0.01	0.01	0.02	0.02	0.02
Ca	0.02	0.02	0.02	0.02	0.02	0.02	0.02	0.02	0.02	0.02	0.02	0.03
Si	0.04	0.04	0.04	0.05	0.04	0.04	0.06	0.05	0.05	0.05	0.04	0.05
P	3.82	3.74	3.74	4.01	3.64	3.99	3.61	3.77	3.76	3.86	3.78	3.79
H	18.86	18.18	19.29	15.17	18.78	15.7	19.72	17.6	18.79	16.17	18.4	16.73
TOTAL	28.91	28.54	29.25	26.36	28.99	26.68	29.62	28.12	28.92	27.11	28.65	27.54

Area 1

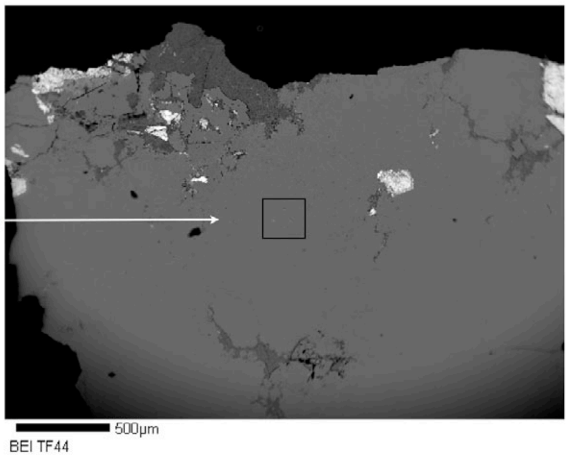

Tiffany Sample TF44

Area 2

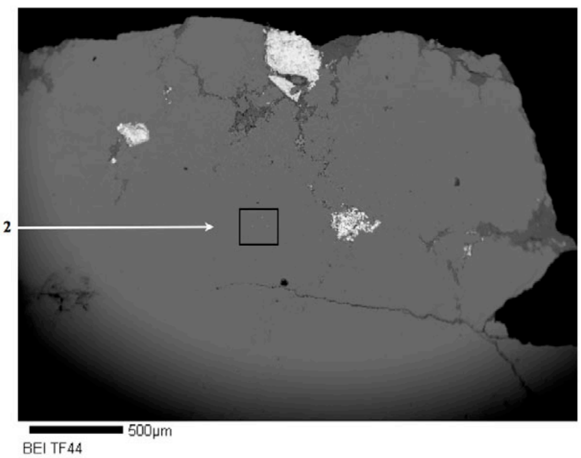

Area 3

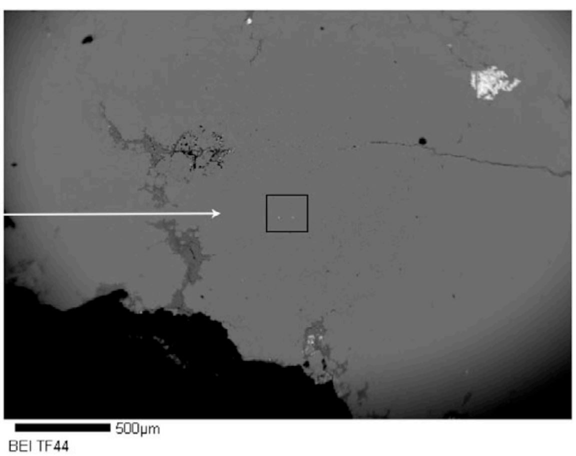

Area 4

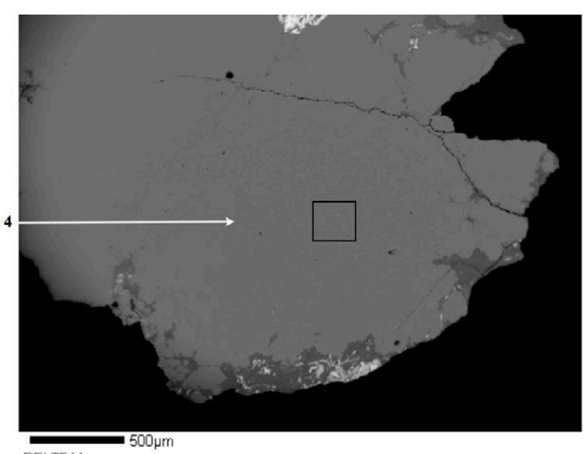

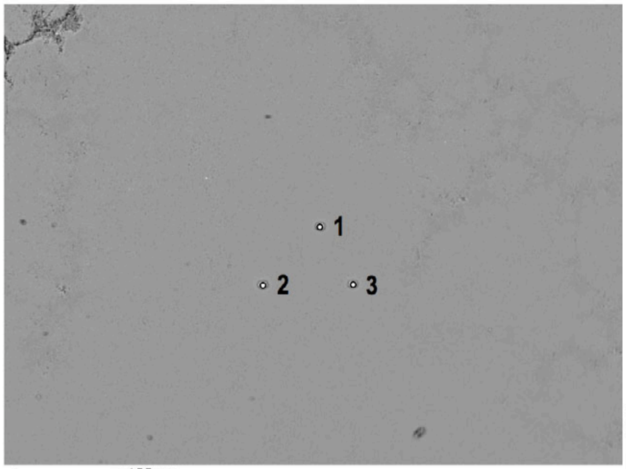

100μm

BEI TF44 Area 1

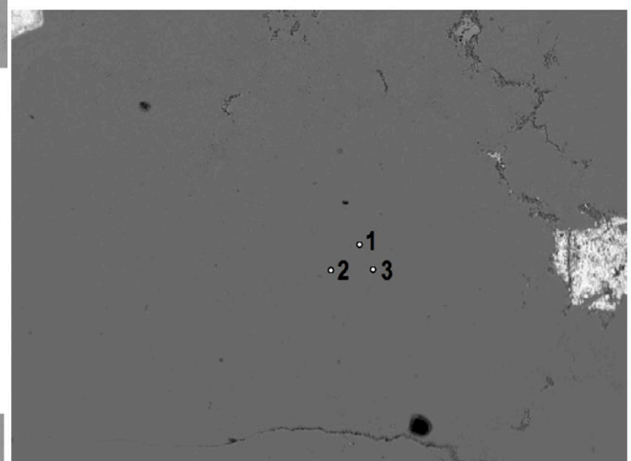

200μm

BEI TF44 Area 2

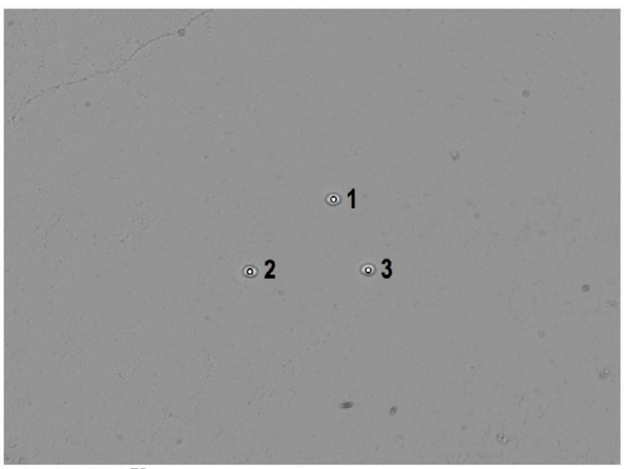

70μm

BEI TF44 Area 3

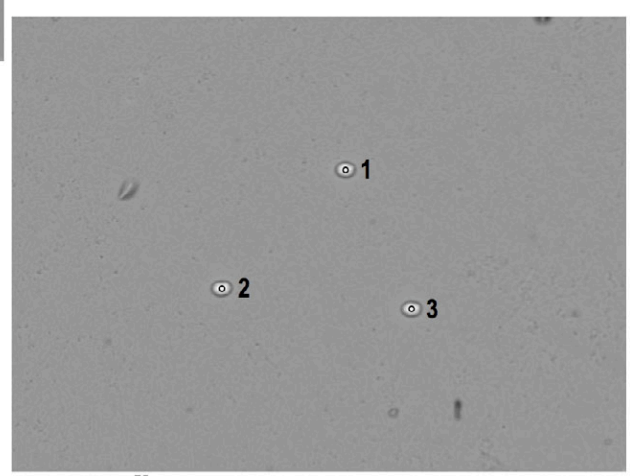

50μm

BEI TF44 Area 4

TF44	TF44 1-1	TF44 1-2	TF44 1-3	TF44 2-1	TF44 2-2	TF44 2-3	TF44 3-1	TF44 3-2	TF44 3-3	TF44 4-1	TF44 4-2	TF44 4-3
P2O5	34.61	33.70	33.04	32.81	33.57	33.48	34.57	32.28	33.84	34.95	33.09	32.56
SiO2	0.12	0.08	0.10	0.14	0.14	0.08	0.12	0.11	0.11	0.12	0.00	0.14
TiO2	0.31	0.32	0.33	0.33	0.30	0.26	0.24	0.37	0.22	0.29	0.28	0.35
Al2O3	35.81	37.95	35.98	37.67	36.12	37.68	35.56	37.42	36.27	37.95	35.92	38.03
Fe2O3	1.07	0.91	0.87	1.18	0.84	0.93	0.88	0.74	0.75	0.99	0.86	0.88
MgO	0.00	0.00	0.00	0.00	0.00	0.00	0.00	0.00	0.00	0.00	0.00	0.00
CuO	7.82	7.51	8.16	7.62	7.39	7.55	7.48	7.56	8.13	8.01	7.65	7.48
ZnO	0.00	0.00	0.00	0.00	0.00	0.00	0.00	0.00	0.00	0.00	0.00	0.00
CaO	0.12	0.13	0.17	0.16	0.18	0.10	0.13	0.16	0.16	0.16	0.16	0.16
Total	79.86	80.60	78.65	79.91	78.54	80.09	78.98	78.64	79.47	82.47	77.96	79.60
H2O*	20.14	19.40	21.35	20.09	21.46	19.91	21.02	21.36	20.53	17.53	22.04	20.40
TOTAL	100.00	100.00	100.00	100.00	100.00	100.00	100.00	100.00	100.00	100.00	100.00	100.00
28 O												
Cu	0.78	0.75	0.81	0.76	0.73	0.76	0.74	0.75	0.81	0.82	0.75	0.75
Fe	0.11	0.09	0.09	0.12	0.08	0.09	0.09	0.07	0.07	0.1	0.08	0.09
Al	5.58	5.95	5.58	5.89	5.57	5.88	5.49	5.79	5.65	6.03	5.53	5.92
Zn	0	0	0	0	0	0	0	0	0	0	0	0
Mg	0	0	0	0	0	0	0	0	0	0	0	0
Ti	0.03	0.03	0.03	0.03	0.03	0.03	0.02	0.04	0.02	0.03	0.03	0.03
Ca	0.02	0.02	0.02	0.02	0.03	0.01	0.02	0.02	0.02	0.02	0.02	0.02
Si	0.02	0.01	0.01	0.02	0.02	0.01	0.02	0.01	0.01	0.02	0	0.02
P	3.87	3.79	3.68	3.68	3.72	3.75	3.84	3.59	3.78	3.99	3.66	3.64
H	17.78	17.21	18.75	17.79	18.75	17.61	18.4	18.72	18.11	15.79	19.21	18
TOTAL	28.19	27.85	28.97	28.31	28.93	28.14	28.62	28.99	28.47	26.8	29.28	28.47

Tiffany Sample TF46

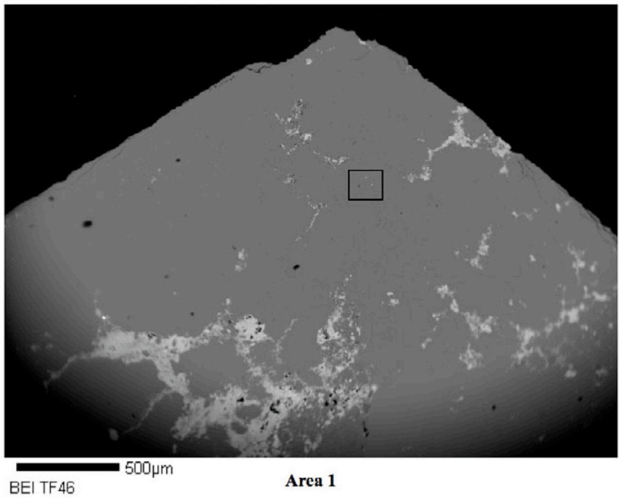

Area 1

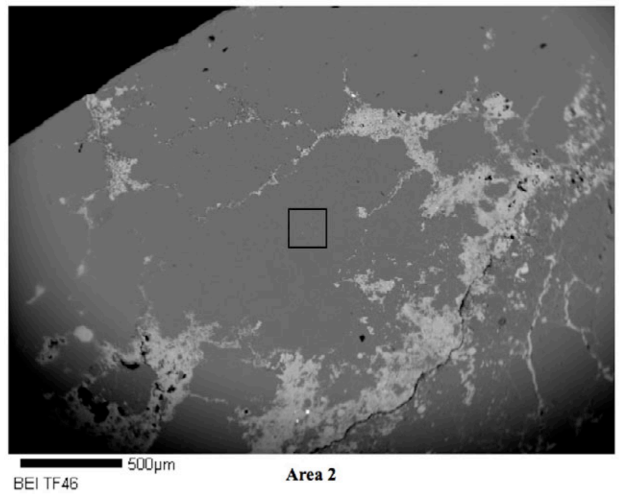

Area 2

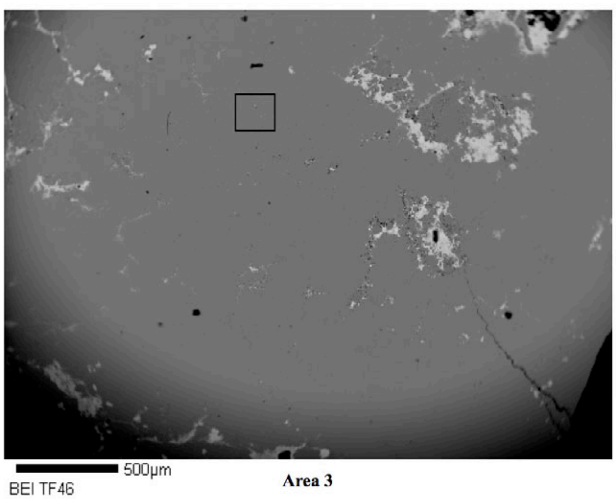

Area 3

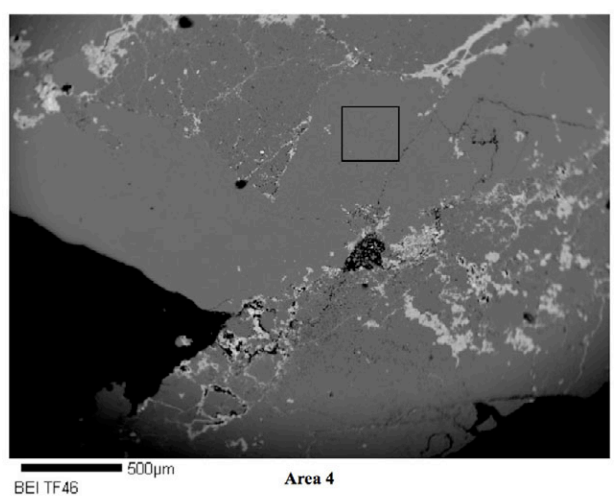

Area 4

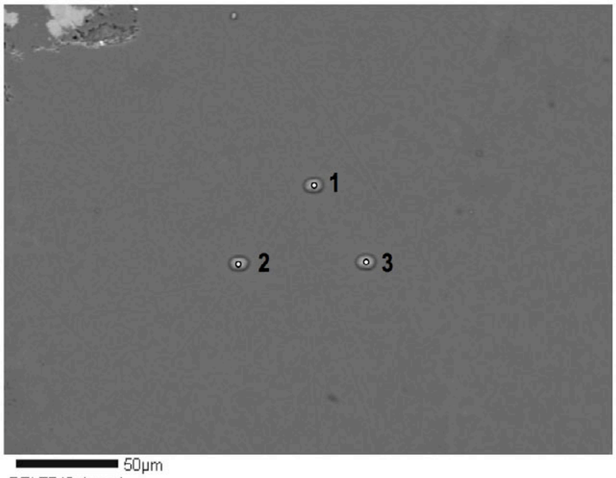

BEI TF46 Area 1

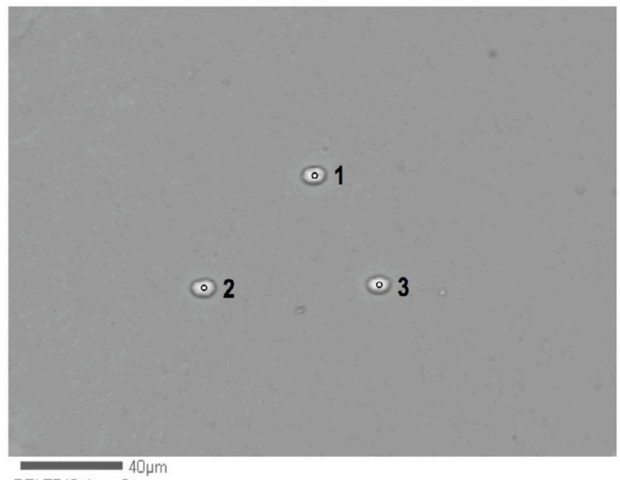

BEI TF46 Area 2

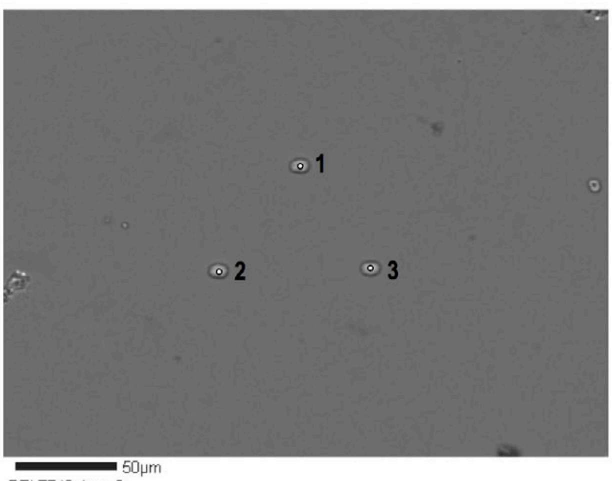

BEI TF46 Area 3

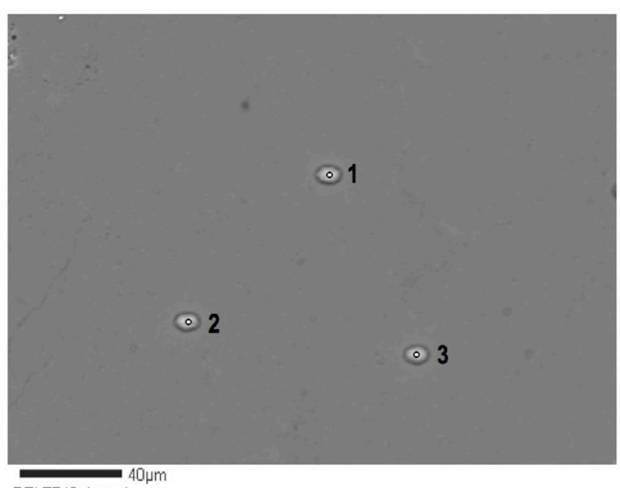

BEI TF46 Area 4

TF46	TF46 1-1	TF46 1-2	TF46 1-3	TF46 2-1	TF46 2-2	TF46 2-3	TF46 3-1	TF46 3-2	TF46 3-3	TF46 4-1	TF46 4-2	TF46 4-3
P2O5	33.02	34.16	33.43	33.41	34.11	34.65	35.03	33.26	33.69	33.13	33.11	33.26
SiO2	0.19	0.26	0.24	0.24	0.19	0.22	0.14	0.15	0.13	0.13	0.22	0.24
TiO2	0.00	0.00	0.00	0.00	0.00	0.00	0.00	0.00	0.00	0.00	0.00	0.00
Al2O3	35.22	36.58	35.21	36.64	35.45	36.90	35.62	37.41	35.68	37.31	35.87	36.46
Fe2O3	1.84	1.80	2.02	2.20	2.01	2.07	1.80	2.03	1.54	1.91	1.58	2.20
MgO	0.00	0.00	0.00	0.00	0.00	0.04	0.00	0.00	0.00	0.00	0.00	0.00
CuO	7.53	7.26	7.21	7.32	7.72	7.45	7.52	7.55	7.80	7.80	7.50	7.13
ZnO	0.00	0.51	0.35	0.40	0.46	0.00	0.34	0.00	0.51	0.46	0.00	0.00
CaO	0.15	0.17	0.14	0.13	0.13	0.12	0.12	0.14	0.17	0.16	0.18	0.17
Total	77.94	80.74	78.60	80.34	80.08	81.45	80.58	80.54	79.52	80.90	78.45	79.46
H2O*	22.06	19.26	21.40	19.66	19.92	18.55	19.42	19.46	20.48	19.10	21.55	20.54
TOTAL	100.00	100.00	100.00	100.00	100.00	100.00	100.00	100.00	100.00	100.00	100.00	100.00
28 O												
Cu	0.74	0.73	0.72	0.74	0.78	0.75	0.76	0.76	0.78	0.79	0.74	0.71
Fe	0.18	0.18	0.2	0.22	0.2	0.21	0.18	0.2	0.15	0.19	0.16	0.22
Al	5.43	5.75	5.45	5.76	5.56	5.82	5.59	5.88	5.57	5.9	5.54	5.68
Zn	0	0.05	0.03	0.04	0.05	0	0.03	0	0.05	0.05	0	0
Mg	0	0	0	0	0	0.01	0	0	0	0	0	0
Ti	0	0	0	0	0	0	0	0	0	0	0	0
Ca	0.02	0.02	0.02	0.02	0.02	0.02	0.02	0.02	0.02	0.02	0.03	0.02
Si	0.02	0.03	0.03	0.03	0.03	0.03	0.02	0.02	0.02	0.02	0.03	0.03
P	3.66	3.86	3.72	3.77	3.84	3.93	3.95	3.76	3.78	3.76	3.68	3.72
H*	19.26	17.16	18.78	17.5	17.7	16.58	17.26	17.33	18.13	17.11	18.87	18.12
TOTAL	29.31	27.78	28.95	28.08	28.18	27.35	27.81	27.97	28.5	27.84	29.05	28.5

Tiffany Sample TF47

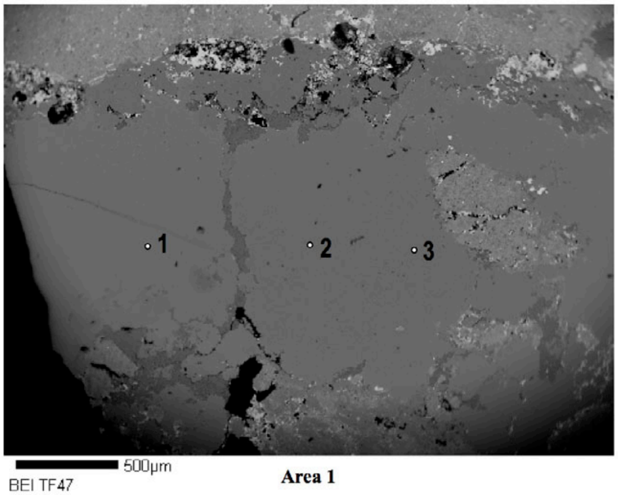

Area 1

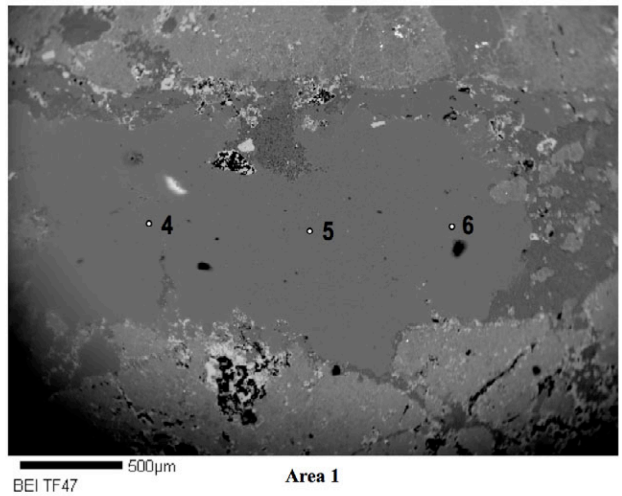

Area 1

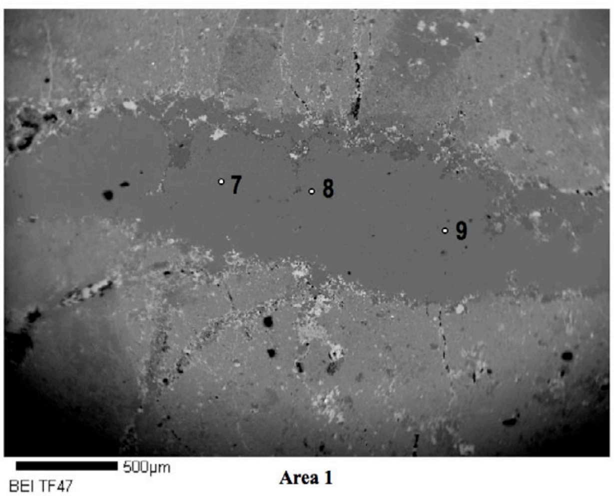

Area 1

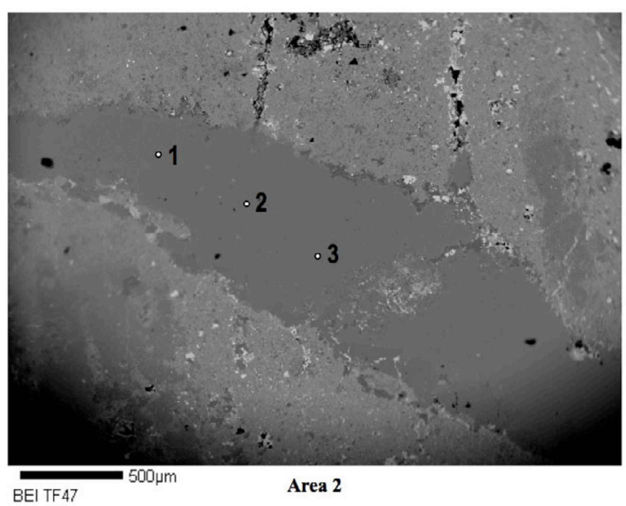

Area 2

TF47	**TF47 1-1**	**TF47 1-2**	**TF47 1-3**	**TF47 1-4**	**TF47 1-5**	**TF47 1-6**	**TF47 1-7**	**TF47 1-8**	**TF47 1-9**	**TF47 2-1**	**TF47 2-2**	**TF47 2-3**
P2O5	33.28	32.59	32.29	34.28	33.98	33.42	34.63	33.09	32.30	34.39	33.08	33.27
SiO2	0.77	0.67	0.63	0.51	0.42	0.28	0.24	0.32	0.26	0.33	0.44	0.48
TiO2	0.00	0.00	0.00	0.23	0.13	0.28	0.37	0.51	0.52	0.66	0.58	0.39
Al2O3	35.73	37.11	35.70	38.64	35.75	38.70	35.66	38.38	36.21	38.26	35.98	38.19
Fe2O3	0.66	0.55	0.64	0.81	0.87	0.67	0.45	0.52	0.56	0.93	1.04	0.80
MgO	0.00	0.00	0.00	0.07	0.00	0.00	0.00	0.00	0.00	0.00	0.00	0.00
CuO	8.24	8.07	8.13	8.42	7.65	7.74	7.78	8.36	8.23	7.86	7.69	7.86
ZnO	0.00	0.00	0.00	0.00	0.00	0.00	0.00	0.00	0.00	0.00	0.00	0.00
CaO	0.27	0.29	0.25	0.17	0.32	0.14	0.18	0.17	0.22	0.17	0.15	0.19
Total	78.95	79.27	77.64	83.12	79.12	81.24	79.31	81.36	78.30	82.61	78.96	81.17
H2O*	21.05	20.73	22.36	16.88	20.88	18.76	20.69	18.64	21.70	17.39	21.04	18.83
TOTAL	100.00	100.00	100.00	100.00	100.00	100.00	100.00	100.00	100.00	100.00	100.00	100.00
28 O												
Cu	0.82	0.8	0.8	0.86	0.76	0.78	0.77	0.85	0.82	0.8	0.76	0.79
Fe	0.06	0.05	0.06	0.08	0.09	0.07	0.04	0.05	0.06	0.09	0.1	0.08
Al	5.54	5.77	5.49	6.19	5.54	6.1	5.52	6.07	5.6	6.09	5.58	6.02
Zn	0	0	0	0	0	0	0	0	0	0	0	0
Mg	0	0	0	0.01	0	0	0	0	0	0	0	0
Ti	0	0	0	0.02	0.01	0.03	0.04	0.05	0.05	0.07	0.06	0.04
Ca	0.04	0.04	0.03	0.02	0.05	0.02	0.03	0.02	0.03	0.03	0.02	0.03
Si	0.1	0.09	0.08	0.07	0.05	0.04	0.03	0.04	0.03	0.04	0.06	0.06
P	3.71	3.64	3.57	3.94	3.78	3.78	3.85	3.76	3.59	3.93	3.69	3.77
H*	18.51	18.26	19.49	15.31	18.33	16.74	18.15	16.7	19.03	15.68	18.48	16.81
TOTAL	28.78	28.65	29.52	26.5	28.61	27.56	28.43	27.54	29.21	26.73	28.75	27.6

<u>Tiffany Sample TF49</u>

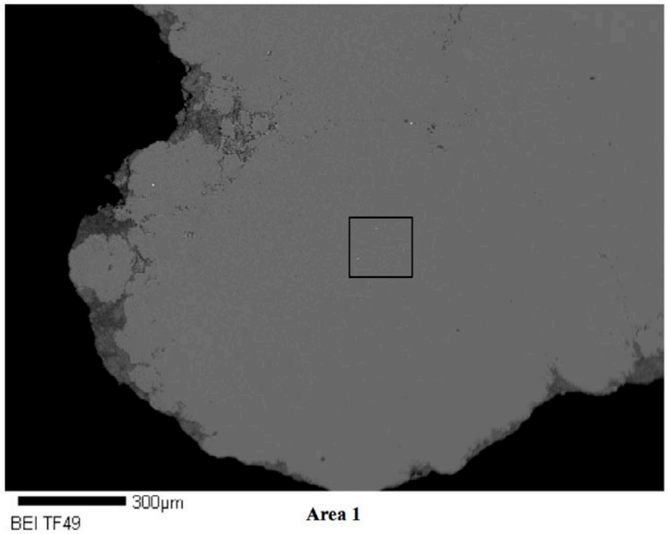

Area 1

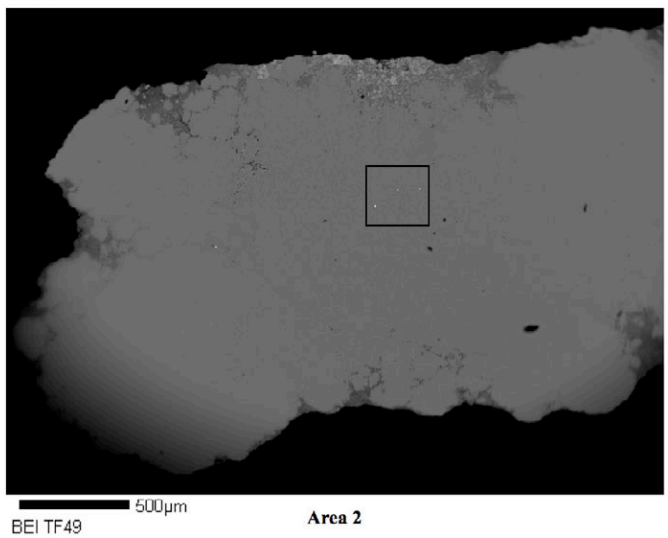

Area 2

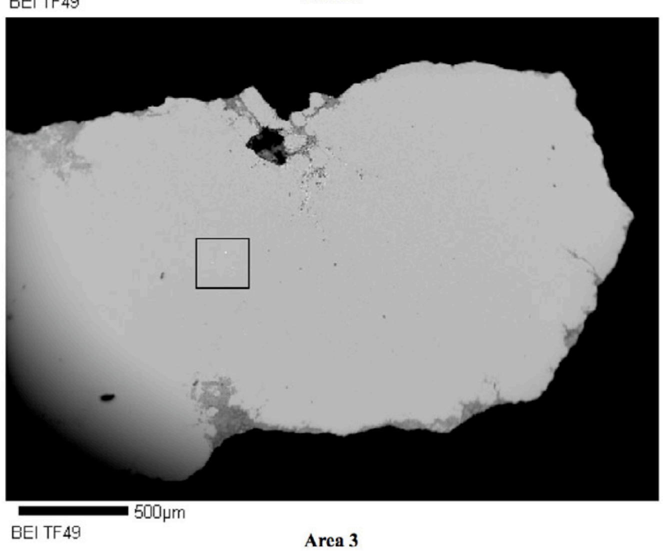

Area 3

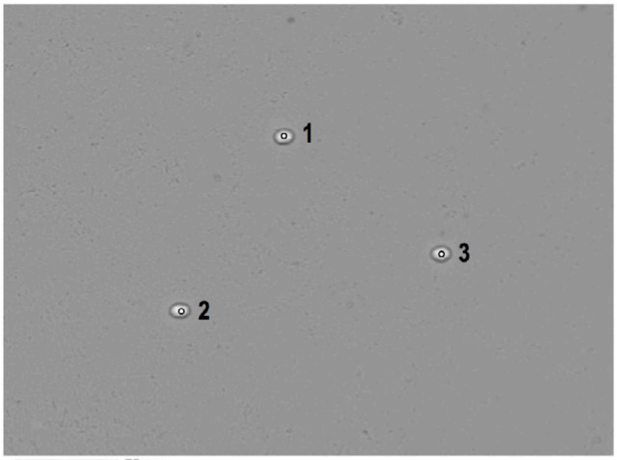

50µm
BEI TF49 Area 1

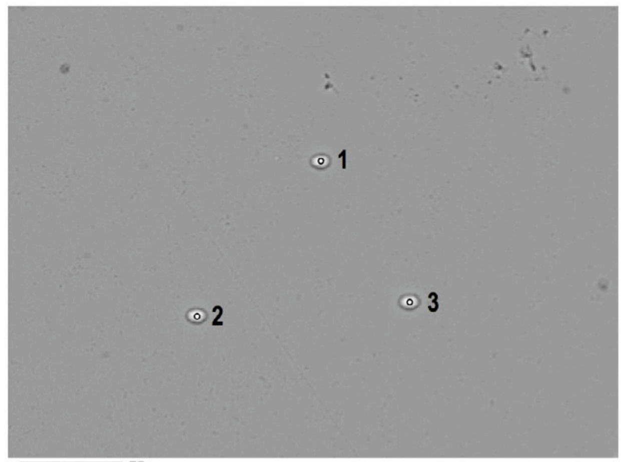

50µm
BEI TF49 Area 2

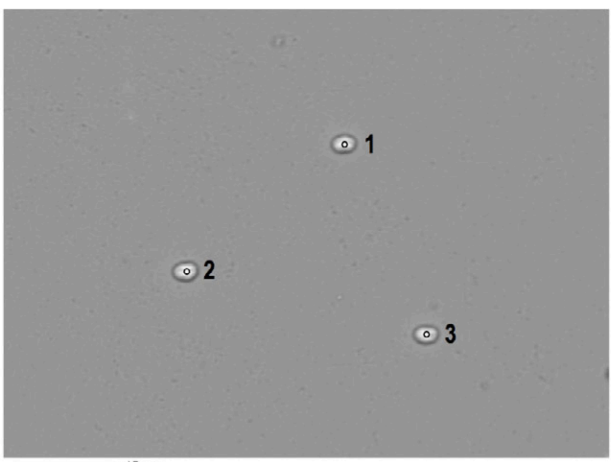

40µm
BEI TF49 Area 3

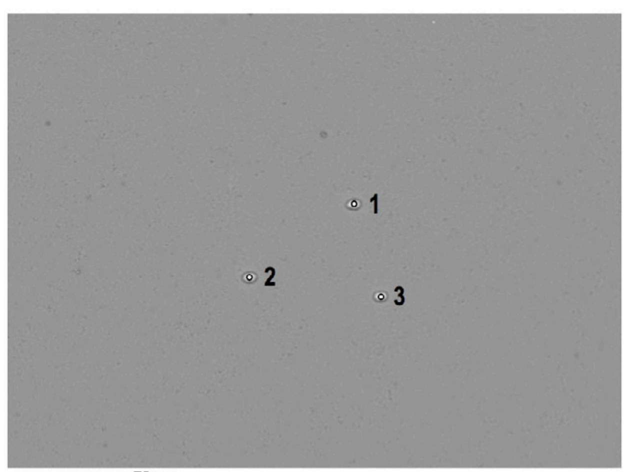

70µm
BEI TF49 Area 4

TF49	**TF49 1-1**	**TF49 1-2**	**TF49 1-3**	**TF49 2-1**	**TF49 2-2**	**TF49 2-3**	**TF49 3-1**	**TF49 3-2**	**TF49 3-3**	**TF49 4-1**	**TF49 4-2**	**TF49 4-3**
P2O5	34.22	34.25	34.02	33.46	33.24	33.11	33.25	33.82	33.41	32.94	33.99	33.14
SiO2	0.09	0.00	0.08	0.00	0.00	0.00	0.00	0.00	0.00	0.00	0.11	0.00
TiO2	0.00	0.00	0.00	0.00	0.00	0.00	0.00	0.00	0.00	0.00	0.00	0.00
Al2O3	35.88	37.37	36.41	38.40	36.04	38.00	36.08	38.11	35.93	37.89	35.74	37.20
Fe2O3	1.40	1.24	1.08	1.01	0.93	0.94	1.03	1.06	1.23	1.71	1.74	1.75
MgO	0.00	0.00	0.00	0.00	0.00	0.00	0.00	0.00	0.00	0.00	0.00	0.00
CuO	8.06	8.70	8.29	8.44	8.06	8.46	8.74	8.38	8.51	8.01	8.15	8.48
ZnO	0.00	0.00	0.00	0.00	0.00	0.00	0.00	0.00	0.00	0.00	0.00	0.00
CaO	0.12	0.13	0.10	0.12	0.13	0.13	0.14	0.11	0.14	0.10	0.11	0.15
Total	79.76	81.69	79.98	81.43	78.40	80.64	79.24	81.48	79.21	80.65	79.85	80.72
H2O*	20.24	18.31	20.02	18.57	21.60	19.36	20.76	18.52	20.79	19.35	20.15	19.28
TOTAL	100.00	100.00	100.00	100.00	100.00	100.00	100.00	100.00	100.00	100.00	100.00	100.00
28 O												
Cu	0.81	0.89	0.83	0.86	0.8	0.85	0.87	0.85	0.85	0.81	0.82	0.86
Fe	0.14	0.13	0.11	0.1	0.09	0.09	0.1	0.11	0.12	0.17	0.17	0.18
Al	5.6	5.94	5.7	6.08	5.57	5.99	5.63	6.03	5.6	5.97	5.59	5.88
Zn	0	0	0	0	0	0	0	0	0	0	0	0
Mg	0	0	0	0	0	0	0	0	0	0	0	0
Ti	0	0	0	0	0	0	0	0	0	0	0	0
Ca	0.02	0.02	0.01	0.02	0.02	0.02	0.02	0.02	0.02	0.01	0.02	0.02
Si	0.01	0	0.01	0	0	0	0	0	0	0	0.01	0
P	3.84	3.91	3.82	3.81	3.69	3.75	3.73	3.85	3.74	3.73	3.82	3.76
H	17.9	16.47	17.74	16.66	18.92	17.28	18.36	16.61	18.36	17.28	17.87	17.26
TOTAL	28.32	27.36	28.22	27.53	29.09	27.98	28.71	27.47	28.69	27.97	28.3	27.96

Blue J Sample BJ1

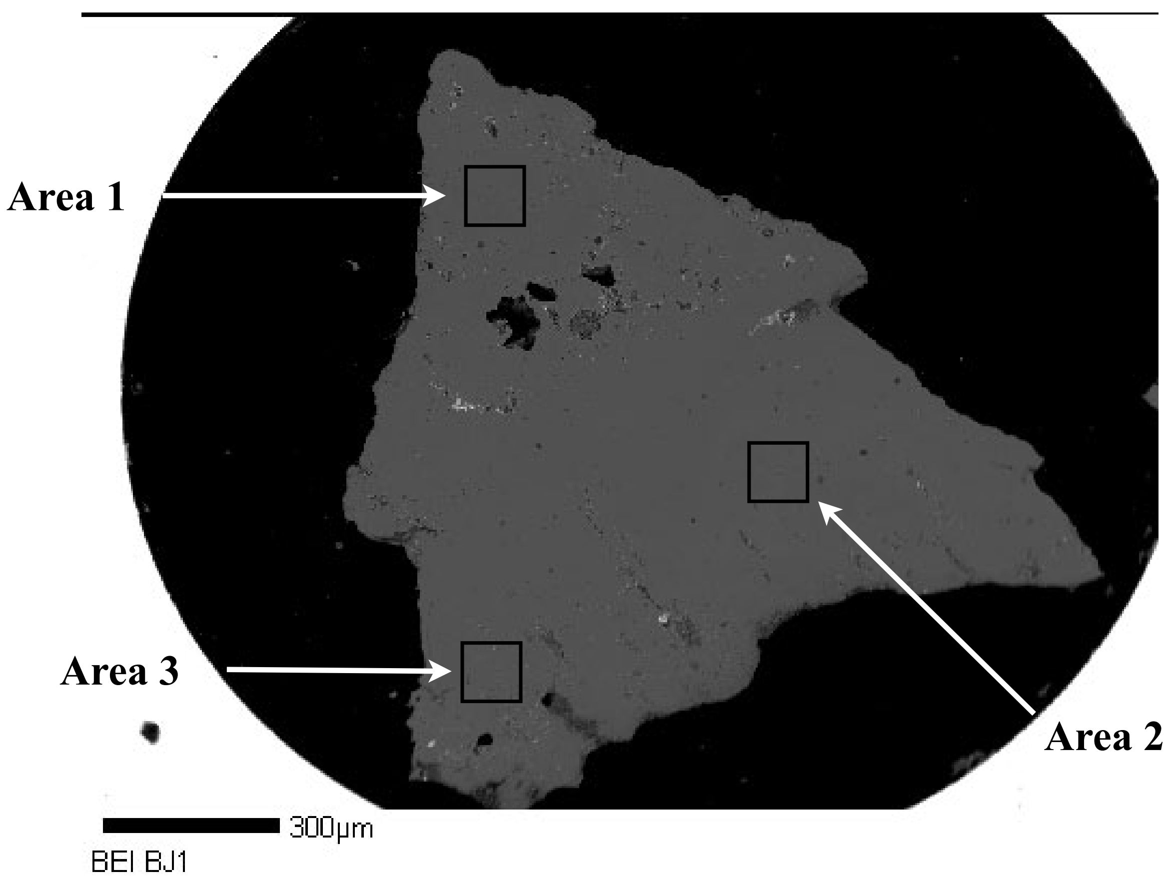

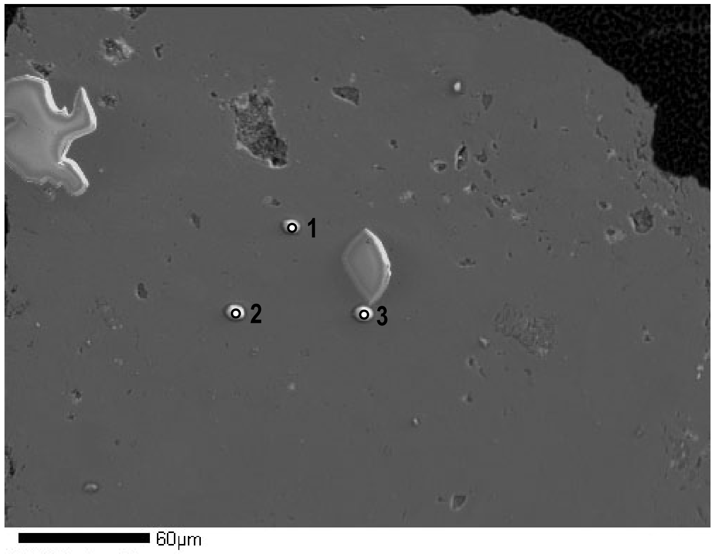

BEI BJ1 Area 1

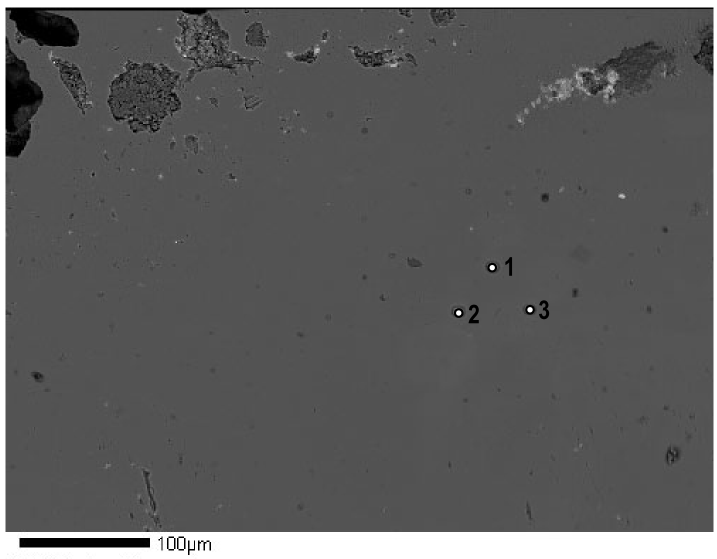

BEI BJ1 Area 2

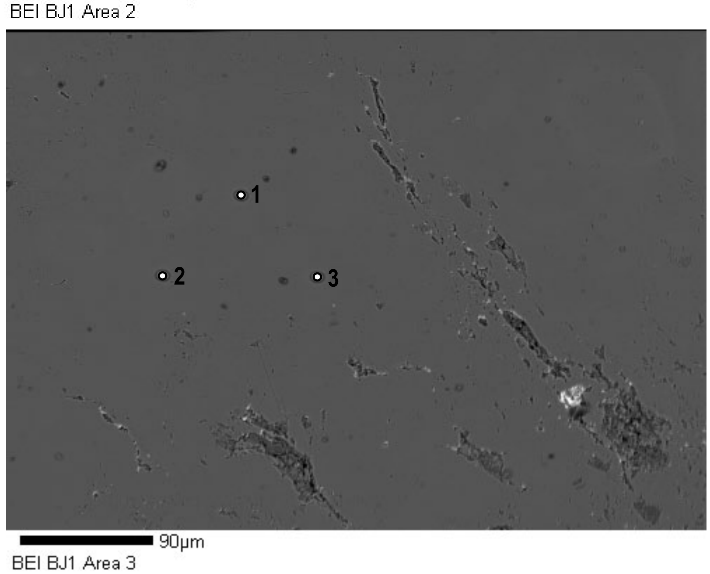

BEI BJ1 Area 3

	BJ1 1-1	BJ1 1-2	BJ1 1-3	BJ1 2-1	BJ1 2-2	BJ1 2-3	BJ1 3-1	BJ1 3-2	BJ1 3-3
CuO	7.54	7.7	6.65	7.63	7.62	7.54	7.01	7.17	8.09
ZnO	0	0	0	0	0	0	0	0	0
TiO2	0	0	0	0	0	0	0	0	0
MgO	0	0	0	0	0.038	0.052	0	0.050	0
Fe2O3	1.86	2.08	1.93	2.24	2.25	3.01	2.41	2.40	2.35
Al2O3	37.40	35.30	37.40	34.88	35.90	34.60	36.51	34.71	36.83
SiO2	0.10	0.14	0.11	0.10	0.24	0.53	0.00	0.14	0.42
P2O5	34.81	34.99	35.34	36.19	34.54	34.26	34.63	35.04	34.85
Total	81.71	80.22	81.43	81.04	80.59	79.99	80.56	79.52	82.54
H2O (by diff.)	18.29	19.78	18.57	18.96	19.41	20.01	19.45	20.48	17.46
TOTAL (w/H2O)	100.00	100.00	100.00	100.00	100.00	100.00	100.00	100.00	100.00
Based on 28O									
Cu	0.76	0.77	0.67	0.77	0.77	0.76	0.7	0.71	0.83
Fe	0.19	0.21	0.19	0.22	0.23	0.3	0.24	0.24	0.24
Al	5.91	5.52	5.87	5.48	5.64	5.42	5.72	5.39	5.88
Zn	0	0	0	0	0	0	0	0	0
Ti	0	0	0	0	0	0	0	0	0
Mg	0	0	0	0	0.01	0.01	0	0.01	0
Si	0.01	0.02	0.01	0.01	0.03	0.07	0	0.02	0.06
P	3.95	3.93	3.98	4.08	3.9	3.85	3.89	3.91	4
TOTAL	10.82	10.45	10.72	10.56	10.58	10.41	10.55	10.28	11.01

Blue J Sample BJ11

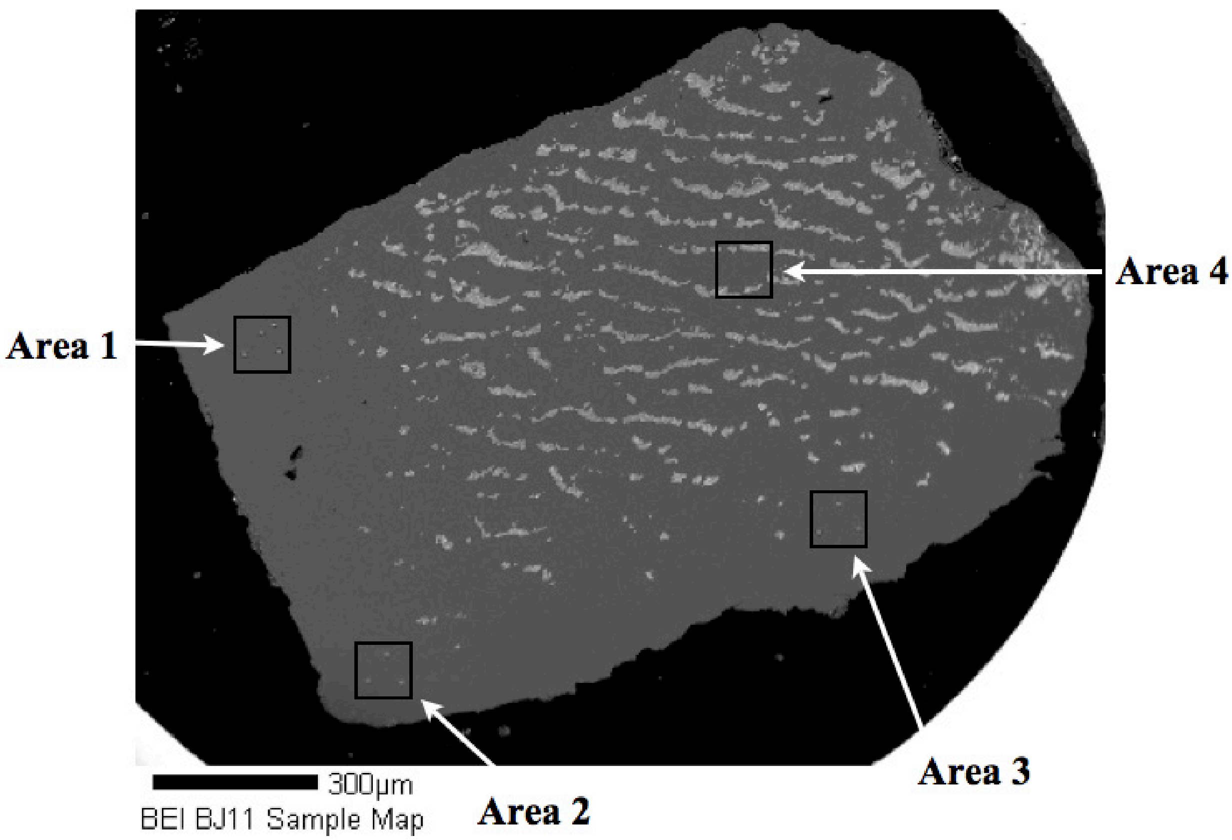

Blue J Sample BJ11

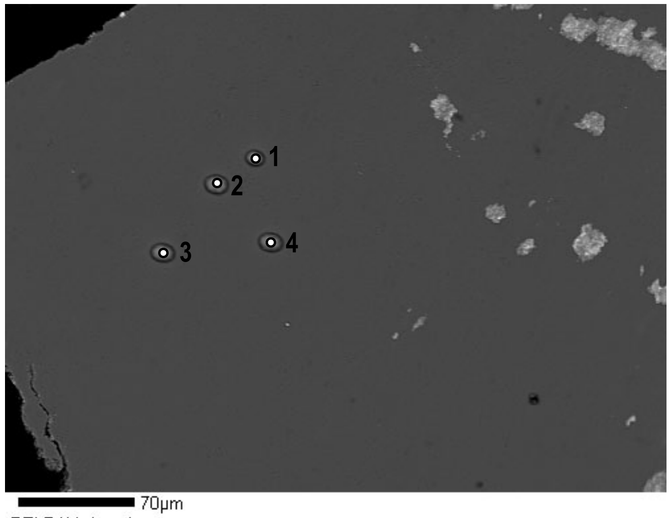

BEI BJ11 Area I

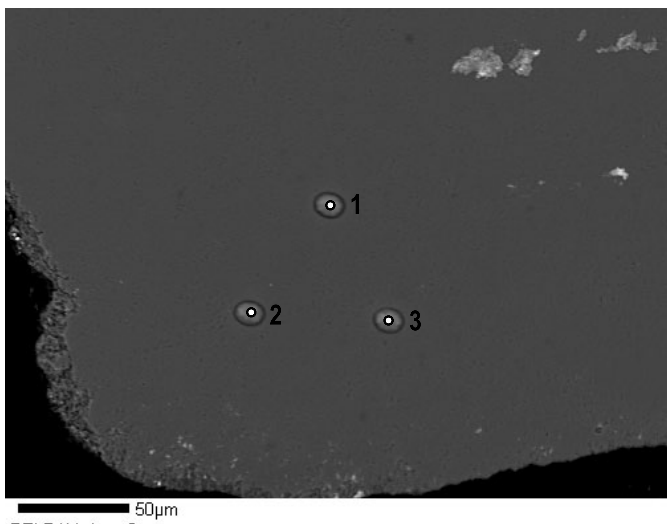

BEI BJ11 Area 2

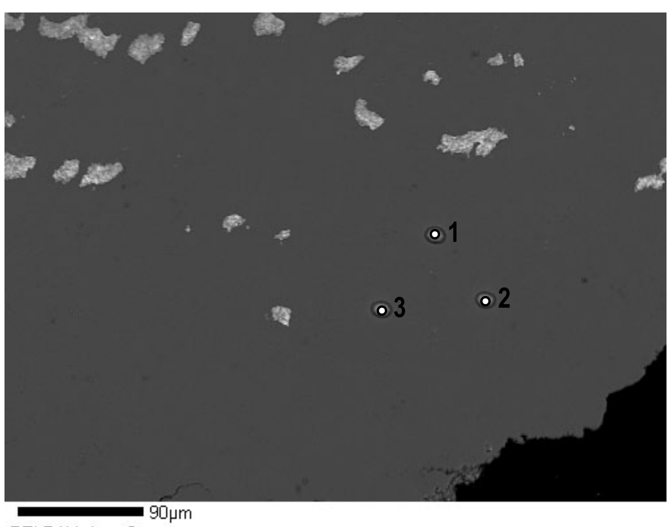

BEI BJ11 Area 3

	BJ11 1-1	BJ11 1-2	BJ11 1-3	BJ11 1-4	BJ11 2-1	BJ11 2-2	BJ11 2-3	BJ11 3-1	BJ11 3-2	BJ11 3-3	BJ11 4-1	BJ11 4-2	BJ11 4-3	BJ11 4-4
CuO	7.55	8.29	7.99	9.04	8.40	7.86	8.42	8.72	8.23	8.74	8.31	7.47	7.77	7.83
MnO	0	0	0	0	0	0	0	0	0	0	0	0		
ZnO	0	0	0	0	0.31	0.35	0.39	0	0	0	0.37	0.31	0	0
TiO2	0	0	0	0	0	0	0	0	0	0	0	0	0	0
MgO	0	0	0.04	0	0	0.06	0	0	0	0.04	0.04	0	0	0
CaO	0.41	0.42	0.36	0.41	0.38	0.37	0.40	0.34	0.36	0.44	0.27	0.43		0
K2O	0.05	0	0	0.05	0	0	0	0	0	0	0.43	0.06		
Fe2O3	0	0.20	0.31	0.26	0.24	0.23	0.28	0.31	0.20	0.24	0.25	0.31	0	0
Al2O3	36.26	36.02	35.84	35.53	36.09	36.24	36.01	35.55	35.99	35.59	35.97	36.80	36.63	36.46
SiO2	0	0	0	0	0	0	0	0	0	0.07	0	0	0	0
P2O5	32.68	34.33	34.20	35.25	33.76	34.76	34.01	34.67	33.55	33.83	34.93	33.31	35.07	34.39
Total	76.95	79.26	78.73	80.54	79.18	79.86	79.51	79.59	78.33	78.95	80.57	78.68	79.47	79.02
H2O (by diff.)	23.05	20.74	21.27	19.46	20.82	20.14	20.49	20.41	21.67	21.05	19.43	21.32	20.53	20.98
TOTAL (w/ H2O)	100	100	100	100	100	100	100	100	100	100	100	100	100	100
Based on 28O														
Cu	0.74	0.83	0.79	0.91	0.84	0.78	0.84	0.87	0.81	0.87	0.84	0.74	0.77	0.78
Fe	0	0.02	0.03	0.03	0.02	0.02	0.03	0.03	0.02	0.02	0.02	0.03	0	0
Al	5.53	5.59	5.54	5.58	5.62	5.65	5.62	5.54	5.56	5.53	5.66	5.69	5.66	5.63
Mn	0	0	0	0	0	0	0	0	0	0	0	0		
Zn	0	0	0	0	0.03	0.03	0.04	0	0	0	0.04	0.03	0	0
Ti	0	0	0	0	0	0	0	0	0	0	0	0	0	0
Mg	0	0	0.01	0	0	0.01	0	0	0	0.01	0.01	0	0	0
Ca	0.06	0.06	0.05	0.06	0.05	0.05	0.06	0.05	0.05	0.06	0.04	0.06		0.05
K	0.01	0	0	0.01	0	0	0	0	0	0	0.07	0.01		
Si	0	0	0	0	0	0	0	0	0	0.01	0	0	0	0
P	3.58	3.83	3.8	3.98	3.77	3.89	3.81	3.88	3.72	3.78	3.95	3.7	3.9	3.82
TOTAL	9.92	10.33	10.22	10.57	10.33	10.43	10.4	10.37	10.16	10.28	10.63	10.26	10.33	10.28

Sample BJ11

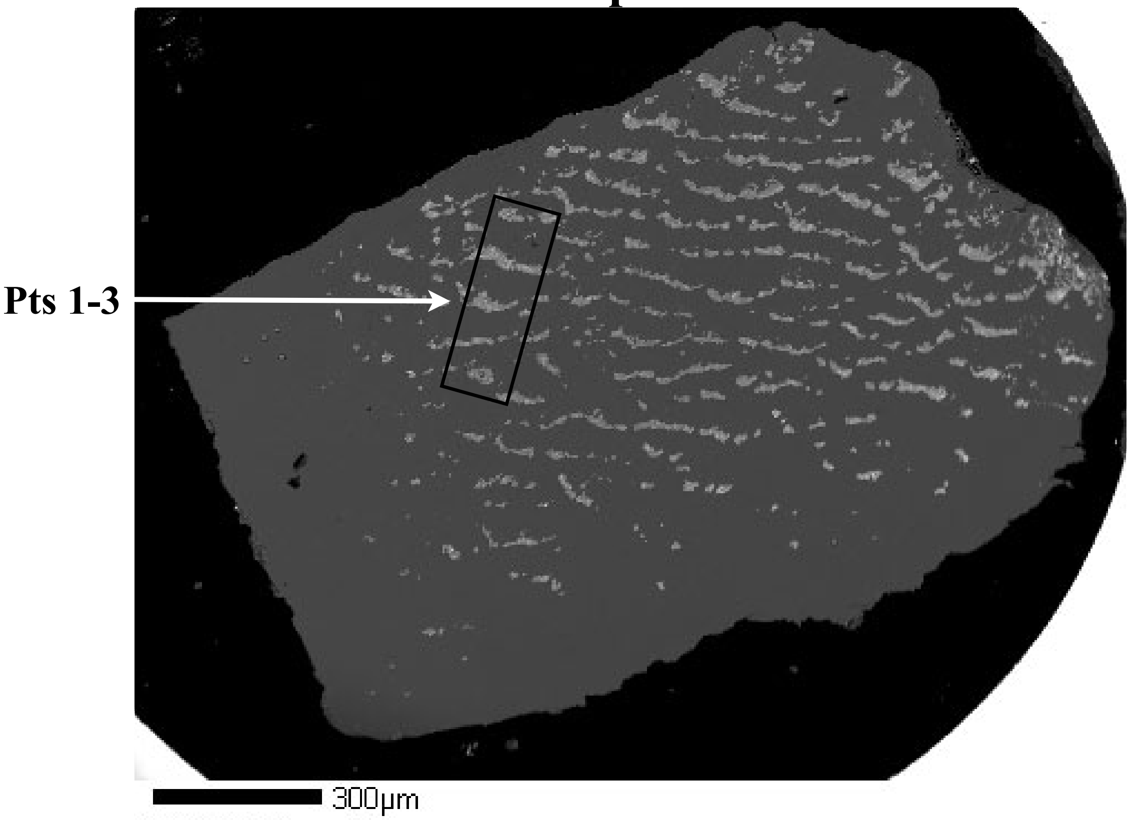

BEI BJ11 Sample Map

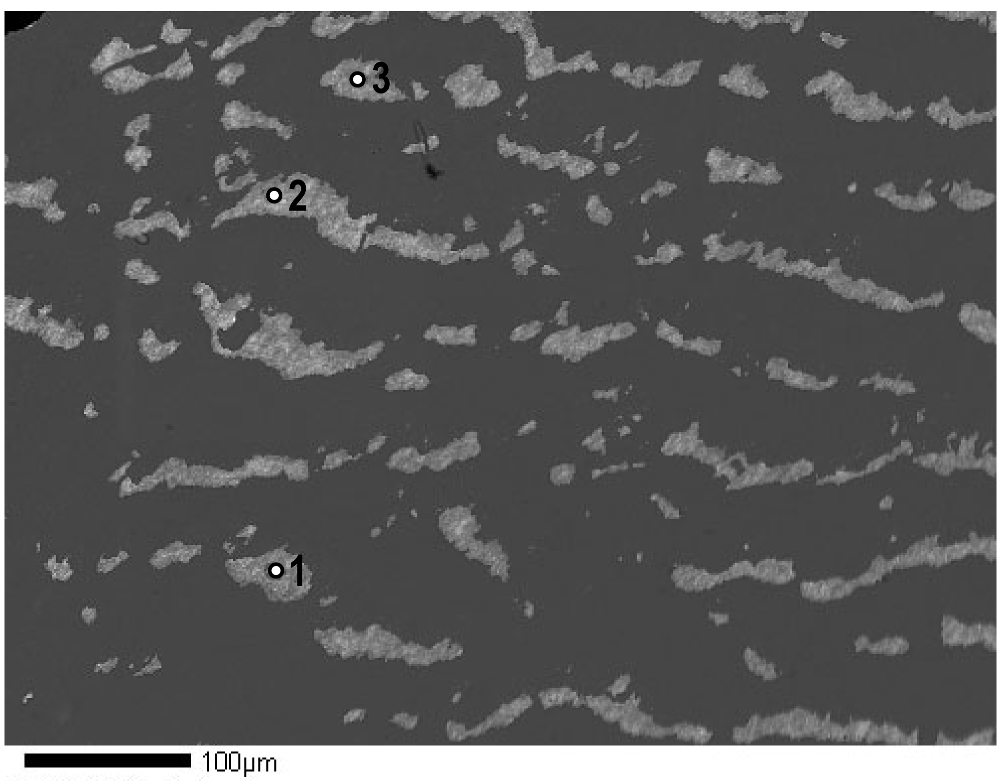

BEI BJ 11 Inclusions

	BJ11-1	BJ11-2	BJ11-3
CuO	17.62	18.38	17.16
MnO	0	0	0
ZnO	3.41	5.50	3.64
TiO2	0	0	0
MgO	0	0	0
CaO	0.33	0.39	0.37
K2O	1.98	0.07	0.06
Fe2O3	0.19	0	0.28
Al2O3	34.42	36.30	37.38
SiO2	0.22	0.27	0.21
P2O5	24.35	24.44	26.05
Total	82.52	85.35	85.15
H2O (by diff.)	17.48	14.65	14.85
TOTAL (w/H2O)	100.00	100.00	100.00
Based on 28O			
Cu	1.97	2.12	1.93
Fe	0.02	0	0.03
Al	6.01	6.52	6.58
Mn	0	0	0
Zn	0.37	0.62	0.4
Ti	0	0	0
Mg	0	0	0
Ca	0.05	0.06	0.06
K	0.37	0.01	0.01
Si	0.03	0.04	0.03
P	3.06	3.15	3.29
TOTAL	11.88	12.52	12.33

Blue J Sample BJ12(1)

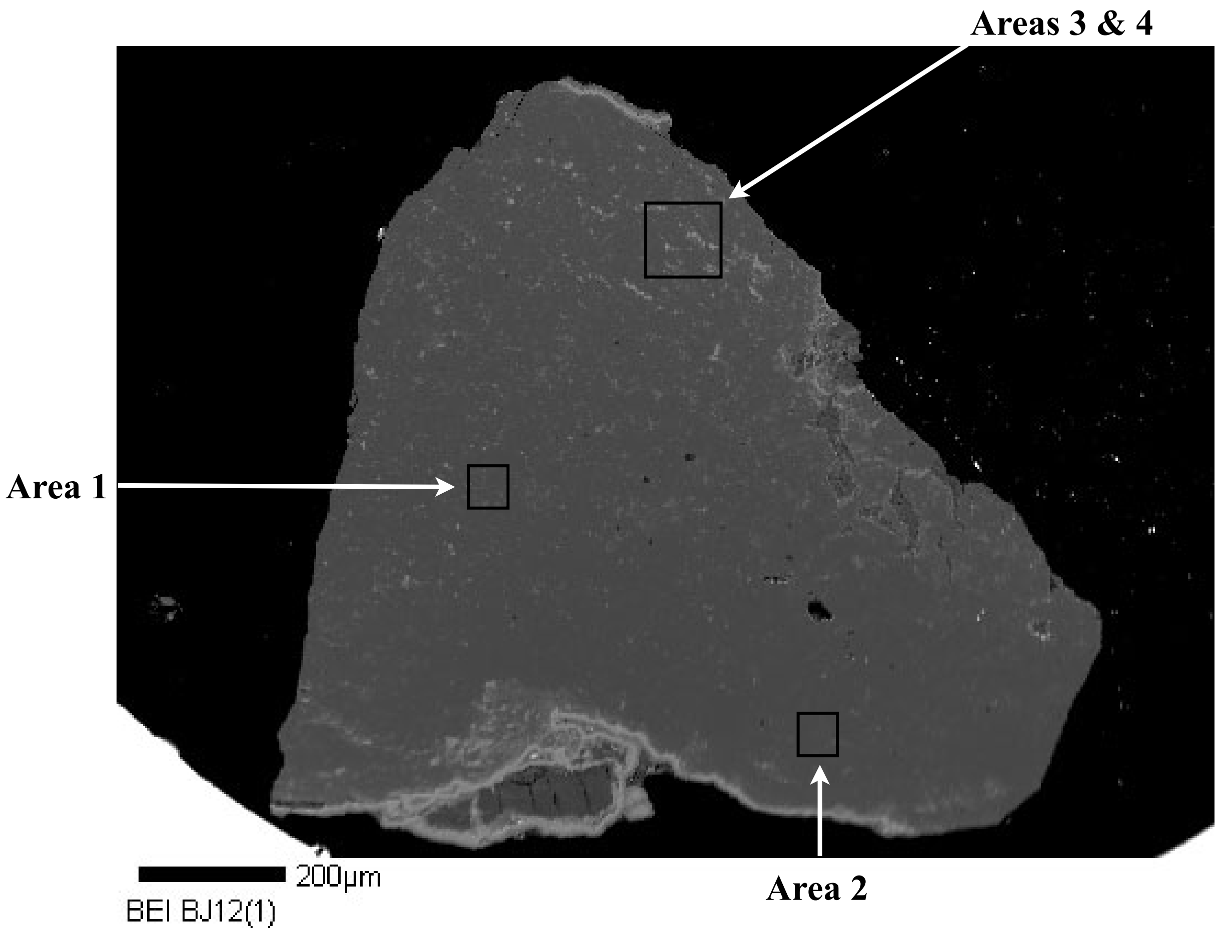

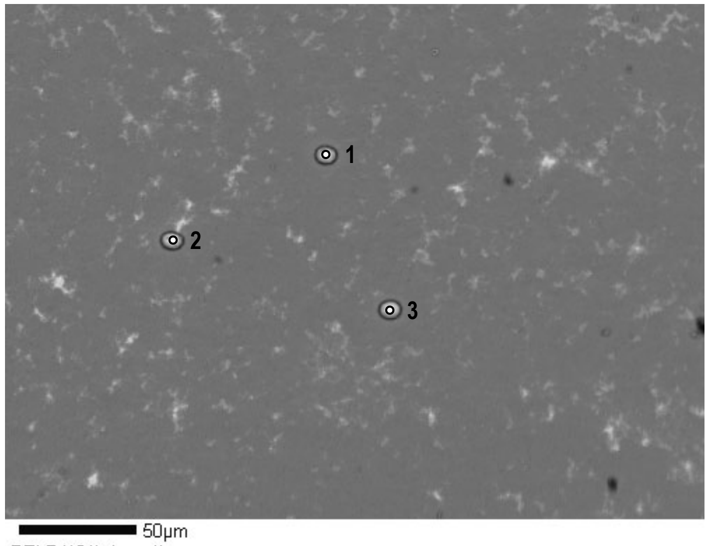

BEI BJ12(1 Area 1)

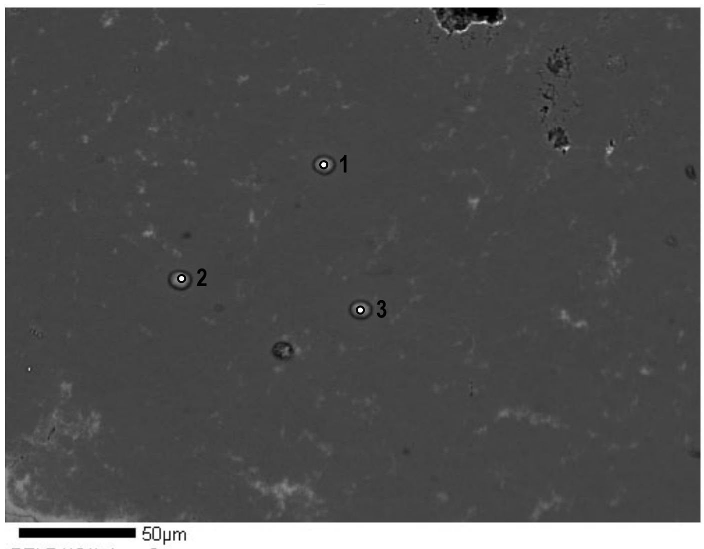

BEI BJ12(1 Area 2

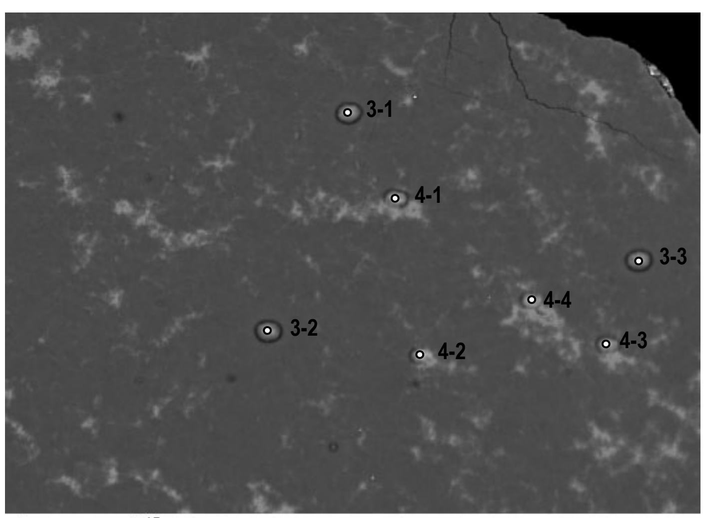

BEI BJ12(1 Area 3 _4

Sample BJ12(1)	1-1	1-2	1-3	2-1	2-2	2-3	3-1	3-2	3-3	4-1	4-2	4-3	4-4
CuO	6.17	6.74	7.04	7.3	6.68	7.22	6.78	7.61	7.47	6.46	7.25	6.86	6.82
ZnO	0	0	0	0	0	0	0	0	0	0.29	0	0	0
TiO2	0	0	0	0	0	0	0	0	0	0	0	0	0
MgO	0	0.08	0	0.06	0	0	0	0	0	0	0	0	0
CaO	0.23	0.21	0.23	0.24	0.24	0.21	0.22	0.24	0.27	0.26	0.15	0.29	0.22
Fe2O3	2.74	2.36	2.31	2.68	2.06	1.99	4.50	3.32	4.78	14.71	27.67	11.73	15.93
Al2O3	36.39	34.61	36.15	34.80	36.82	35.38	34.50	34.78	35.70	25.77	15.95	28.03	25.90
SiO2	0.49	0.50	0.46	0.21	0.26	0.27	0.22	0.19	0.24	0.17	0.00	0.13	0.12
P2O5	35.96	34.52	35.69	34.74	34.69	35.88	34.65	35.02	35.10	34.05	32.39	33.56	32.74
Total	81.99	79.03	81.87	80.03	80.76	80.94	80.88	81.16	83.55	81.71	83.41	80.60	81.73
H2O (by diff.)	18.01	20.97	18.13	19.97	19.24	19.06	19.12	18.84	16.45	18.29	16.59	19.40	18.27
TOTAL (w/H2O)	100.00	100.00	100.00	100.00	100.00	100.00	100.00	100.00	100.00	100.00	100.00	100.00	100.00
Based on 28O													
Cu	0.62	0.67	0.71	0.73	0.67	0.73	0.69	0.77	0.77	0.68	0.81	0.71	0.72
Fe	0.28	0.23	0.23	0.27	0.21	0.2	0.45	0.34	0.49	1.54	3.08	1.21	1.68
Al	5.73	5.35	5.71	5.44	5.76	5.55	5.45	5.5	5.77	4.23	2.78	4.53	4.28
Zn	0	0	0	0	0	0	0	0	0	0.03	0	0	0
Ti	0	0	0	0	0	0	0	0	0	0	0	0	0
Mg	0	0.02	0	0.01	0	0	0	0	0	0	0	0	0
Ca	0.03	0.03	0.03	0.03	0.03	0.03	0.03	0.03	0.04	0.04	0.02	0.04	0.03
Si	0.07	0.07	0.06	0.03	0.03	0.04	0.03	0.03	0.03	0.02	0	0.02	0.02
P	4.07	3.84	4.05	3.9	3.9	4.04	3.93	3.98	4.08	4.02	4.06	3.89	3.89
TOTAL	10.8	10.21	10.79	10.41	10.6	10.59	10.58	10.65	11.18	10.56	10.75	10.4	10.62

Blue J Sample BJ12(2)

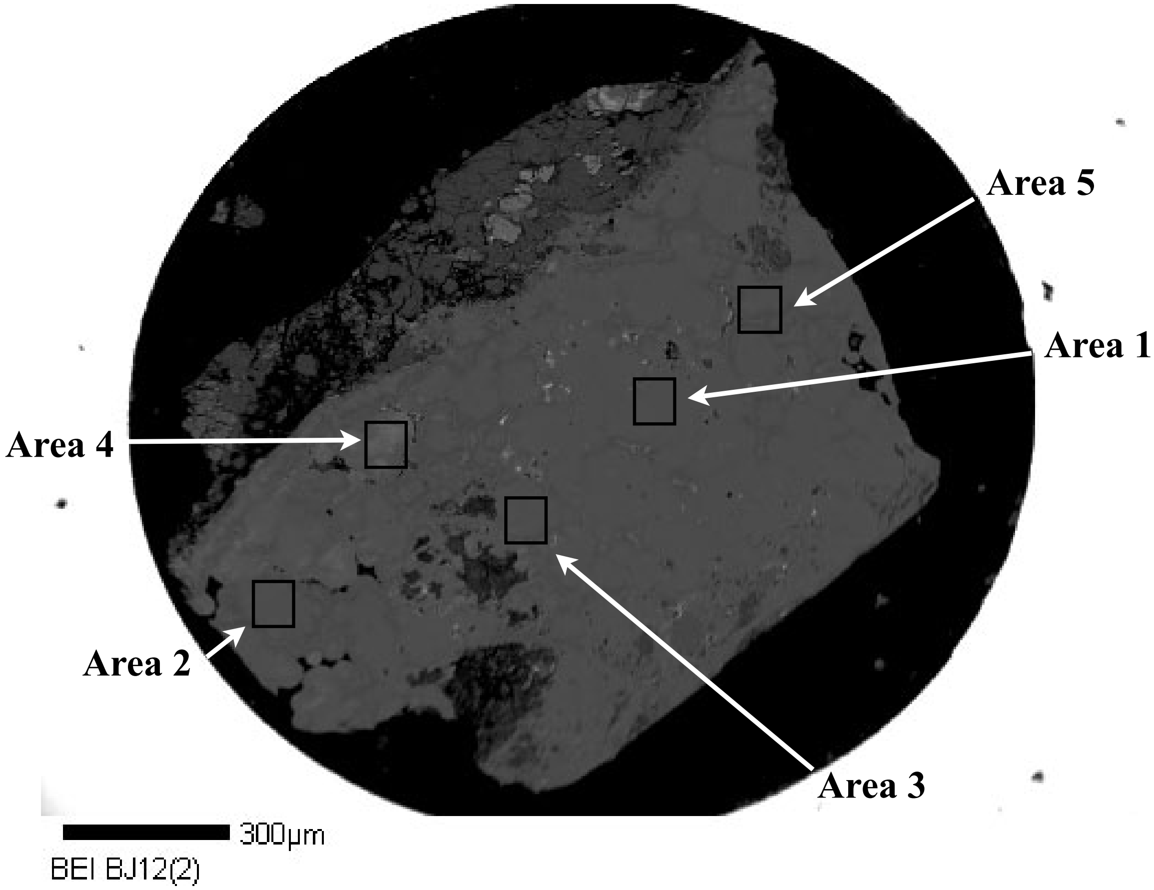

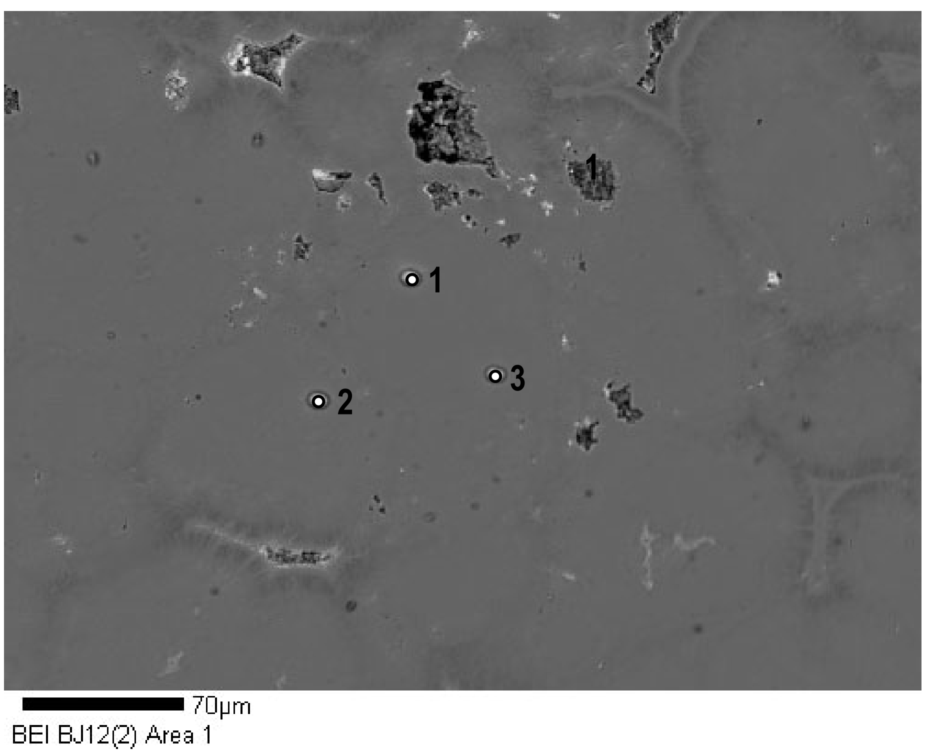

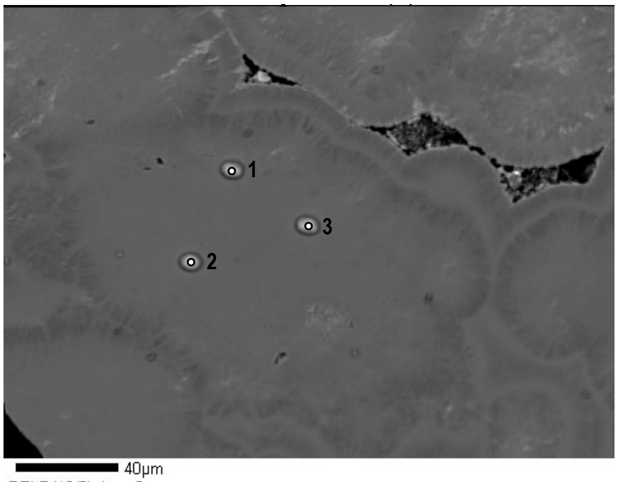

BEI BJ12(2) Area 2

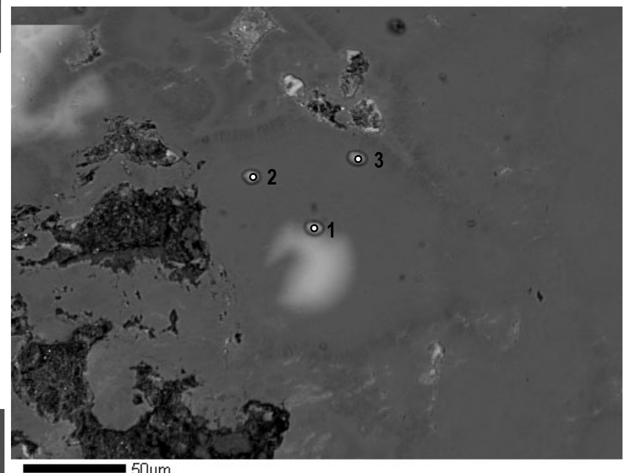

BEI BJ12(2) Area 3

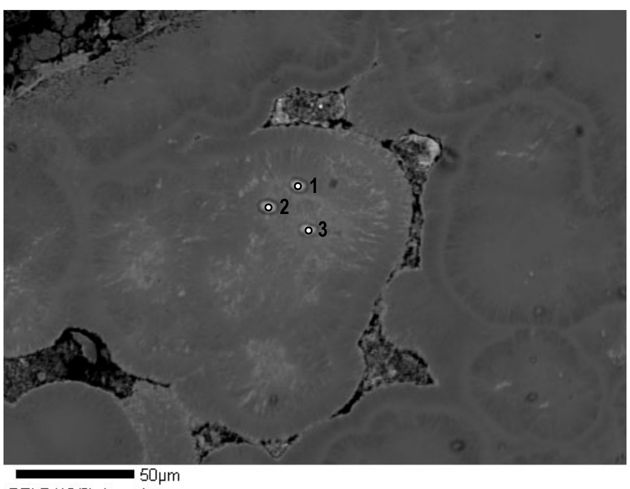

BEI BJ12(2) Area 4

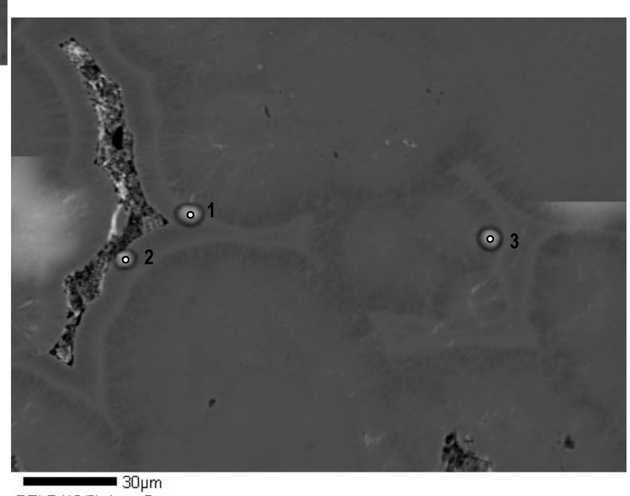

BEI BJ12(2) Area 5

Sample BJ12(2)	1-1	1-2	1-3	2-1	2-2	2-3	3-1	3-2	3-3	4-1	4-2	4-3	5-1	5-2	5-3
CuO	7.62	7.29	7.28	7.82	7.36	7.53	7	7.5	7.31	6.9	6.72	5.97	7.23	6.63	4.75
ZnO	0.31	0	0	0	0	0.36	0.55	0	0.31	0	0.34	0	0	0	0.40
TiO2	0	0	0	0	0	0	0	0	0	0	0	0	0	0	0
MgO	0	0	0.07	0.06	0.07	0	0	0	0	0	0	0	0	0	0
Fe2O3	2.79	2.75	2.68	2.71	2.53	2.45	2.89	3.23	2.44	9.87	8.16	12.51	3.21	2.97	2.44
Al2O3	36.16	35.26	36.91	34.88	36.67	34.98	36.25	35.28	36.99	28.91	31.91	26.98	36.58	37.20	38.87
SiO2	0.10	0	0	0	0.22	0	0	0	0.08	0	0.12	0	0.15	0.09	0
P2O5	35.46	35.37	34.05	35.94	35.92	34.80	35.83	35.10	34.55	34.76	34.19	34.11	35.31	35.71	36.74
Total	82.44	80.67	80.99	81.41	82.76	80.11	82.52	81.11	81.68	80.44	81.45	79.57	82.48	82.60	83.20
H2O (by diff.)	17.56	19.33	19.01	18.59	17.24	19.89	17.48	18.89	18.32	19.56	18.55	20.43	17.52	17.40	16.80
TOTAL (w/H2O)	100	100	100	100	100	100	100	100	100	100	100	100	100	100	100
Based on 28O															
Cu	0.78	0.73	0.74	0.79	0.75	0.76	0.71	0.76	0.74	0.71	0.69	0.61	0.74	0.67	0.48
Fe	0.28	0.28	0.27	0.27	0.26	0.24	0.29	0.33	0.25	1.01	0.84	1.28	0.33	0.3	0.25
Al	5.77	5.53	5.82	5.51	5.84	5.48	5.77	5.57	5.86	4.62	5.12	4.31	5.82	5.9	6.13
Zn	0.03	0	0	0	0	0.04	0.05	0	0.03	0	0.03	0	0	0	0.04
Ti	0	0	0	0	0	0	0	0	0	0	0	0	0	0	0
Mg	0	0	0.01	0.01	0.01	0	0	0	0	0	0	0	0	0	0
Si	0.01	0	0	0	0.03	0	0	0	0.01	0	0.02	0	0.02	0.01	0
P	4.06	3.99	3.85	4.08	4.11	3.92	4.1	3.98	3.93	3.99	3.94	3.91	4.04	4.07	4.16
TOTAL	10.93	10.53	10.69	10.66	11	10.44	10.92	10.64	10.82	10.33	10.64	10.11	10.95	10.95	11.06

Blue J Sample BJ12(3)

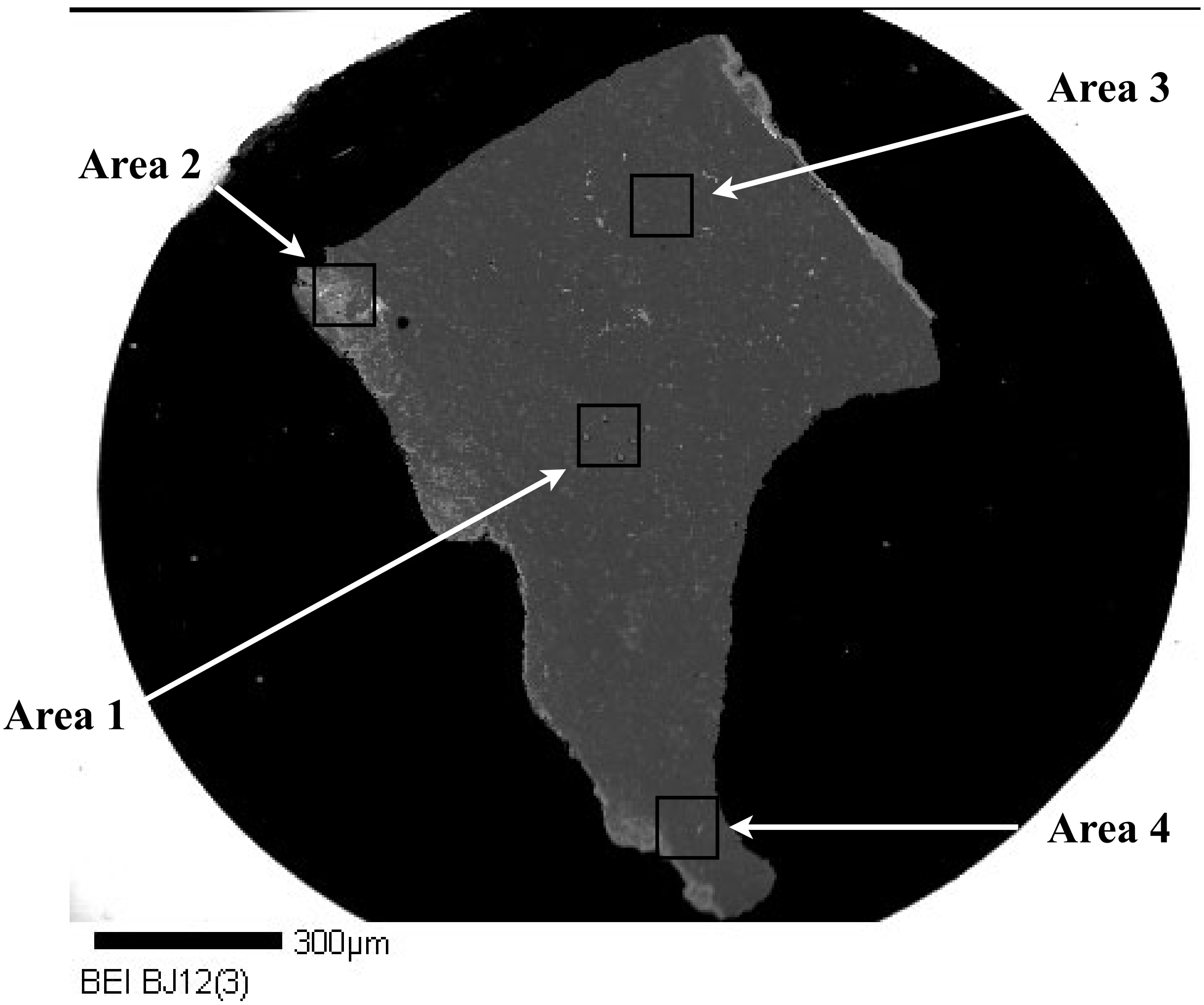

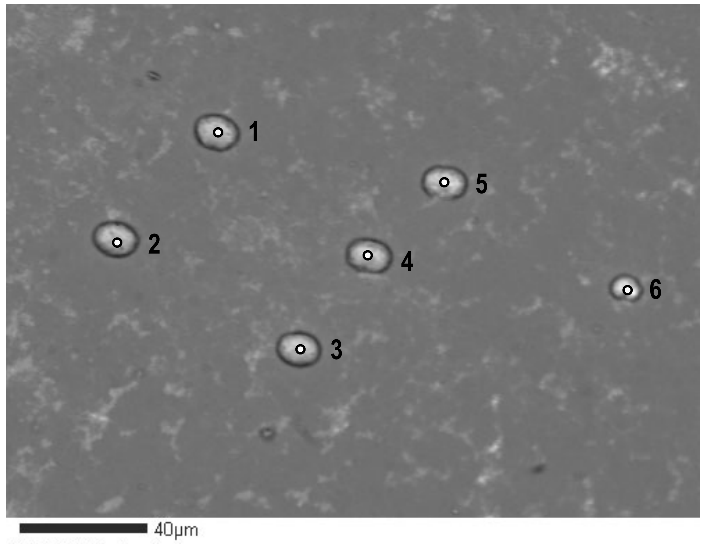

BEI BJ12(3) Area I

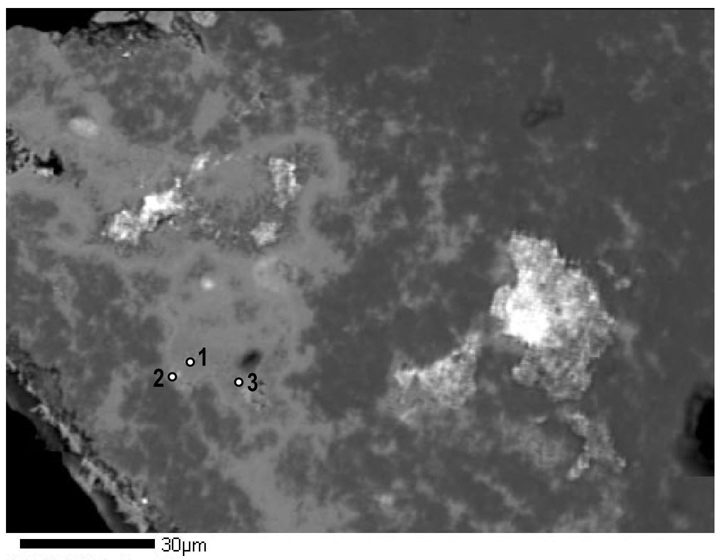

BEI BJ12(3) Area 2

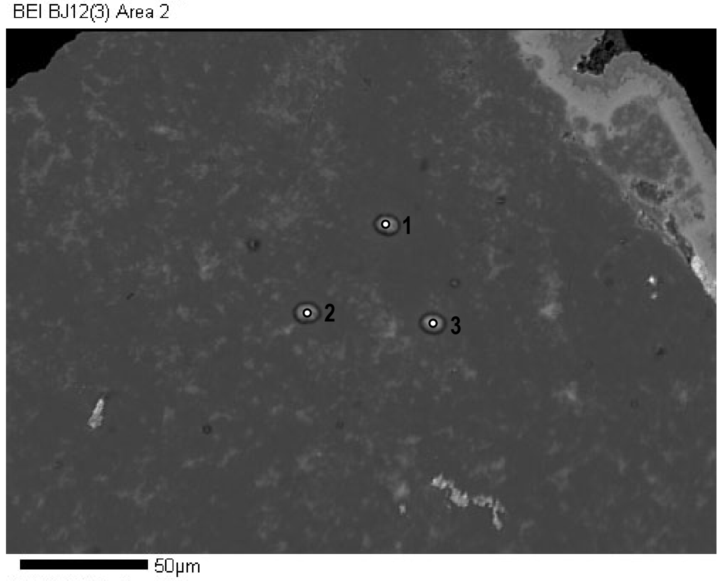

BEI BJ12(3) Area 3

Sample BJ12(3)	1-1	1-2	1-3	1-4	1-5	1-6	2-1	2-2	2-3	3-1	3-2	3-3	4-1	4-2	4-3
CuO	7.11	7.57	7.55	7.45	7.02	6.88	5.96	5.06	5.13	6.56	7.12	7.01	7.54	7.12	7.55
MnO	0	0	0	0	0	0	0	0	0	0	0	0	0	0	0
ZnO	0	0	0	0	0	0	0	0	0	0	0	0	0	0	0
TiO2	0	0	0	0	0	0	0	0	0	0	0	0	0	0	0.09
MgO	0	0	0.05	0	0	0.08	0	0	0	0	0	0	0	0	0
CaO	0.39	0.34	0.39	0.35	0.42	0.41	0.13	0.20	0.20	0.30	0.32	0.35	0.36	0.37	0.28
K2O	0.10	0.19	0.27	0.20	0.07	0.06	0	0	0	0.13	0.21	0.08	0.13	0.11	0.09
Fe2O3	2.39	2.15	2.55	3.22	6.48	9.16	38.61	31.73	35.22	3.15	2.93	3.63	3.94	2.87	2.56
Al2O3	34.58	34.88	35.12	34.52	31.67	30.10	8.74	11.32	10.38	36.20	34.56	35.78	33.70	36.79	35.22
SiO2	0.44	0.41	0.48	0.46	0.46	0.51	0.19	0.09	0.15	0.26	0.34	0.30	0.32	0.27	0.30
P2O5	34.83	35.37	35.35	35.30	34.42	33.60	31.07	31.36	31.33	34.23	34.52	34.30	34.23	34.57	34.73
Total	79.83	80.90	81.76	81.50	80.55	80.80	84.70	79.76	82.41	80.83	80.00	81.45	81.22	82.10	80.82
H2O (by diff.)	20.17	19.10	18.24	18.50	19.45	19.20	18.00	20.24	17.59	19.17	20.00	18.55	19.78	17.90	19.18
TOTAL (w/H2O)	100	100	100	100	100	100	100	100	100	100	100	100	100	100	100
Based on 28O															
Cu	0.71	0.76	0.77	0.76	0.71	0.71	0.70	0.55	0.58	0.66	0.71	0.71	0.76	0.73	0.76
Mn	0.24	0.22	0.26	0.33	0.66	0.94	4.50	3.45	3.96	0.32	0.29	0.37	0.40	0.29	0.26
Zn	5.39	5.49	5.57	5.47	5.03	4.83	1.59	1.93	1.83	5.69	5.41	5.67	5.31	5.85	5.55
Ti	0	0	0	0	0	0	0	0	0	0	0	0	0	0	0
Mg	0	0	0	0	0	0	0	0	0	0	0	0	0	0	0
Ca	0	0	0	0	0	0	0	0	0	0	0	0	0	0	0.01
K	0	0	0.01	0	0	0.02	0	0	0	0	0	0	0	0	0
Fe	0.06	0.05	0.06	0.05	0.06	0.06	0.02	0.03	0.03	0.04	0.05	0.05	0.05	0.05	0.04
Al	0.02	0.03	0.05	0.03	0.01	0.01	0	0	0	0.02	0.04	0.01	0.02	0.02	0.02
Si	0.06	0.05	0.07	0.06	0.06	0.07	0.03	0.01	0.02	0.03	0.05	0.04	0.04	0.04	0.04
P	3.90	4.00	4.03	4.02	3.93	3.87	4.07	3.83	3.96	3.87	3.88	3.91	3.88	3.95	3.93
TOTAL	10.38	10.60	10.82	10.72	10.46	10.51	10.91	9.80	10.38	10.63	10.43	10.76	10.46	10.93	10.61

Blue J Sample BJ21

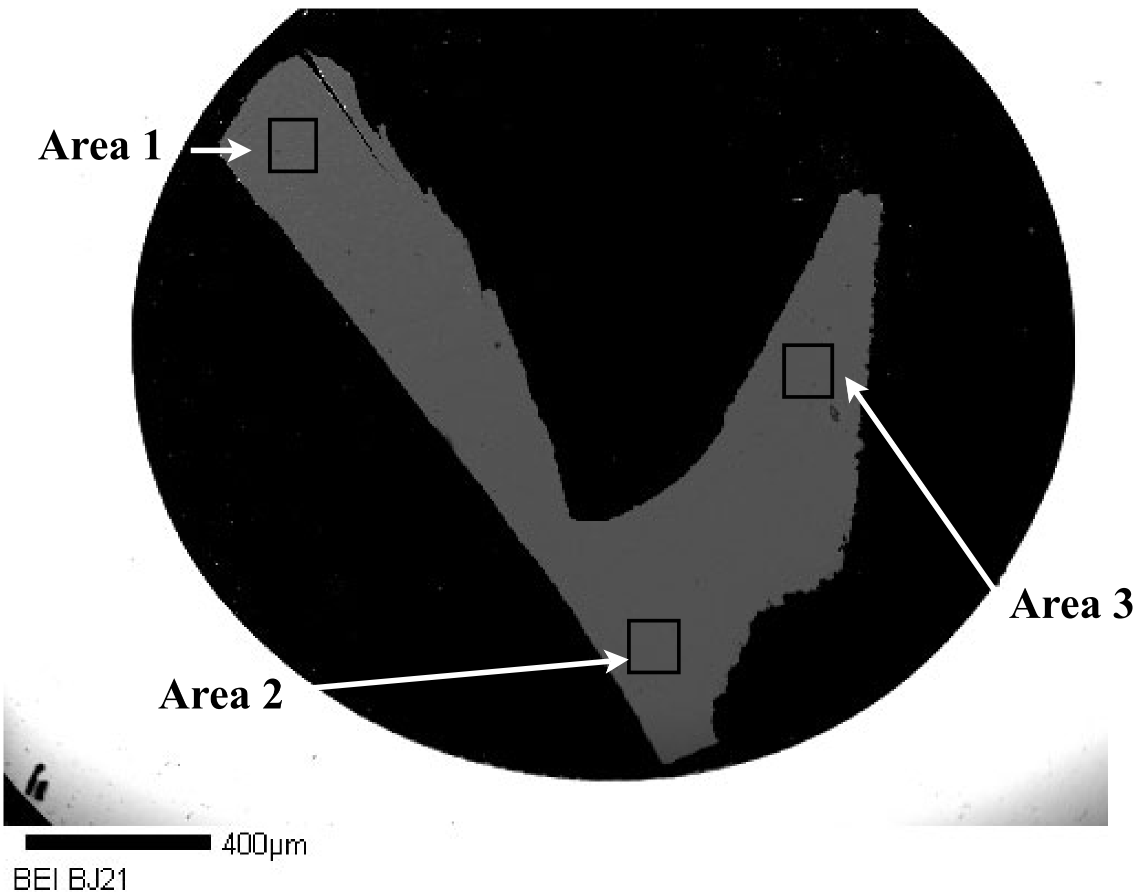

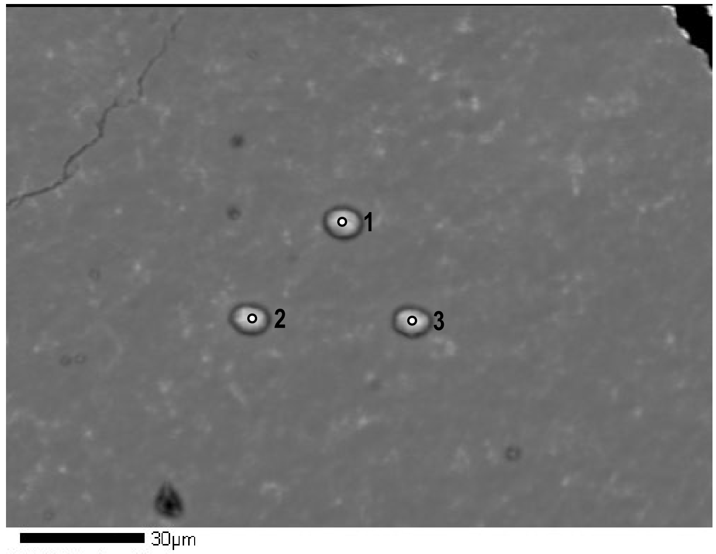

BEI BJ21 Area 1

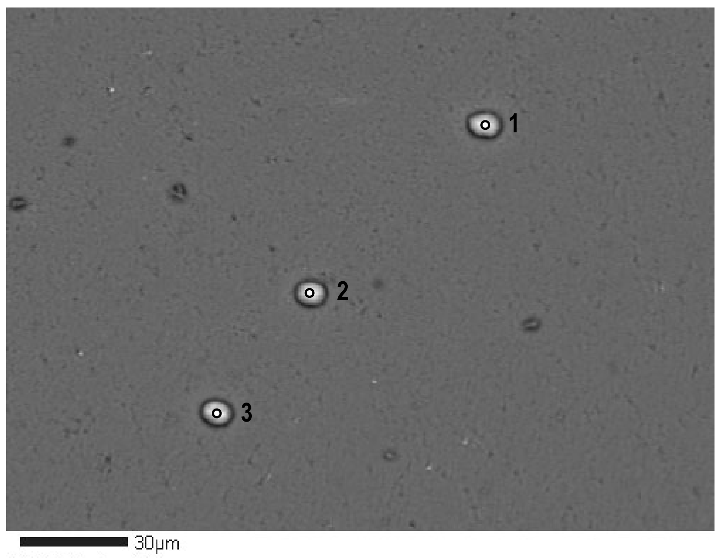

BEI BJ21 Area 2

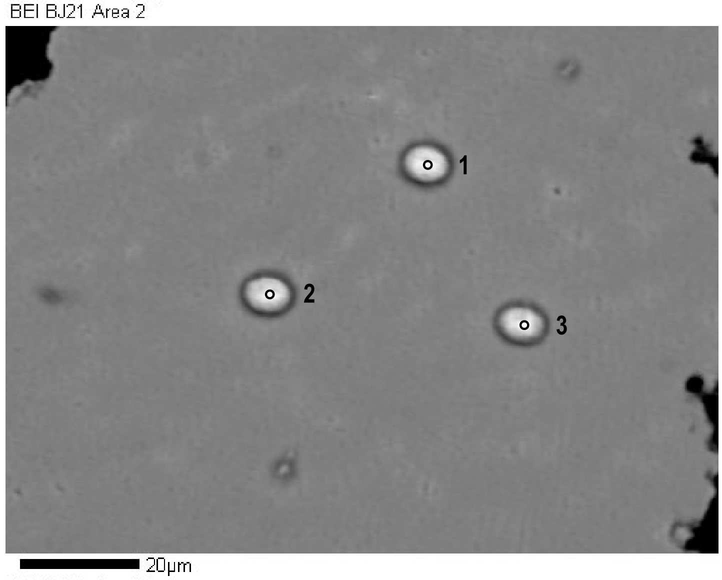

BEI BJ21 Area 3

	BJ21 1-1	BJ21 1-2	BJ21 1-3	BJ21 2-1	BJ21 2-2	BJ21 2-3	BJ21 3-1	BJ21 3-2	BJ21 3-3
CuO	6.47	6.85	6.11	6.77	6.88	6.94	6.4	6.39	6.71
ZnO	0	0.36	0.36	0	0	0.38	0	0	0.32
TiO2	0	0	0	0	0	0	0	0	0
MgO	0.05	0.12	0.08	0	0	0.10	0	0.11	0.11
Fe2O3	4.70	5.78	4.86	2.08	2.83	3.05	3.07	4.02	3.11
Al2O3	32.89	34.06	32.15	34.58	33.59	34.73	32.77	33.37	33.74
SiO2	1.33	1.64	1.57	2.34	2.75	3.76	2.06	3.44	2.73
P2O5	34.39	33.82	33.89	35.58	34.29	32.45	33.33	32.97	33.26
Total	79.83	82.63	79.02	81.35	80.34	81.42	77.63	80.30	79.98
H2O (by diff.)	20.17	17.37	20.98	18.65	19.66	18.58	22.37	19.70	20.02
TOTAL (w/H2O)	100.00	100.00	100.00	100.00	100.00	100.00	100.00	100.00	100.00
Based on 28O									
Cu	0.65	0.71	0.61	0.68	0.69	0.7	0.63	0.64	0.67
Zn	0.47	0.59	0.48	0.21	0.28	0.31	0.3	0.4	0.31
Ti	5.14	5.48	5	5.41	5.24	5.49	5.02	5.22	5.27
Mg	0	0.04	0.03	0	0	0.04	0	0	0.03
Fe	0	0	0	0	0	0	0	0	0
Al	0.01	0.03	0.02	0	0	0.02	0	0.02	0.02
Si	0.18	0.22	0.21	0.31	0.36	0.5	0.27	0.46	0.36
P	3.86	3.91	3.79	4	3.84	3.68	3.67	3.7	3.73
TOTAL	10.31	10.98	10.14	10.61	10.41	10.74	9.89	10.44	10.39

Blue J Sample BJ43

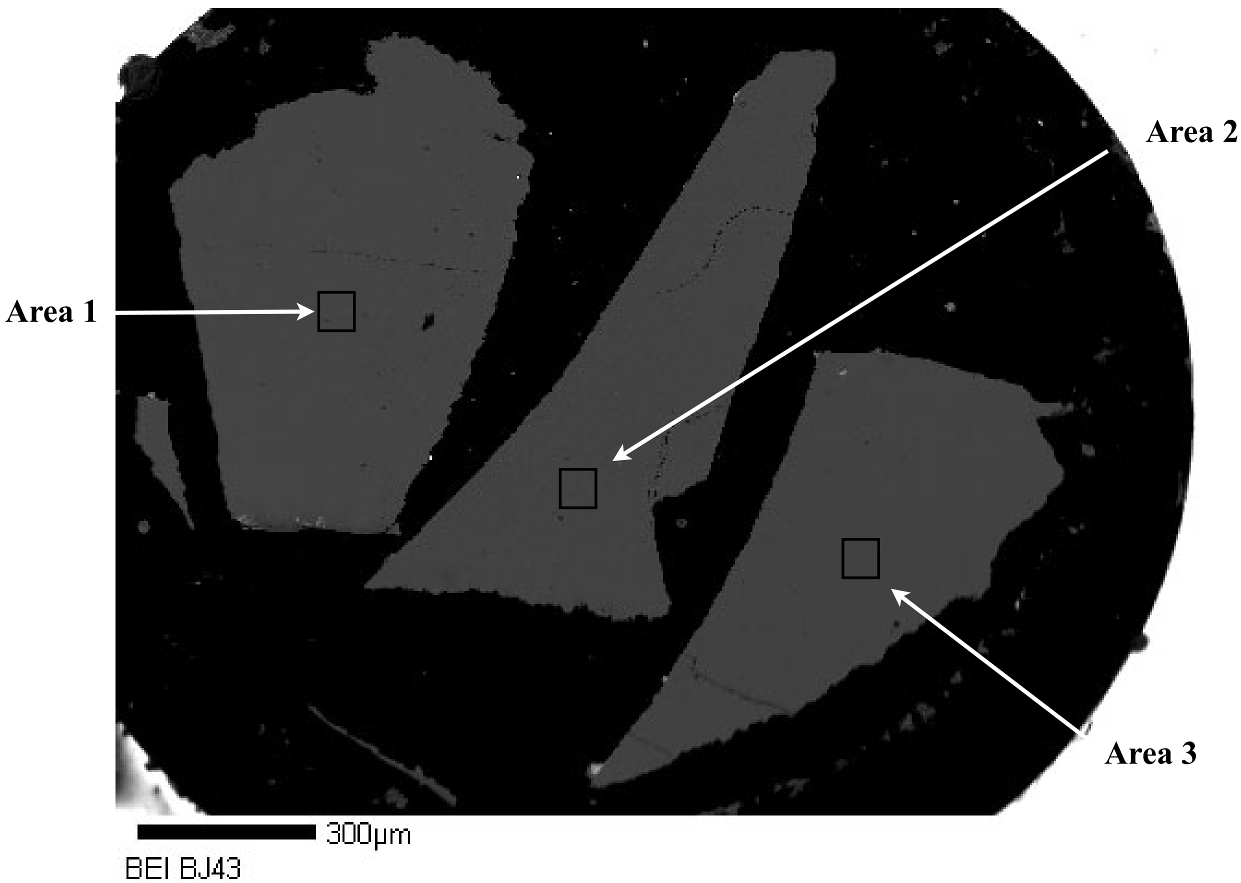

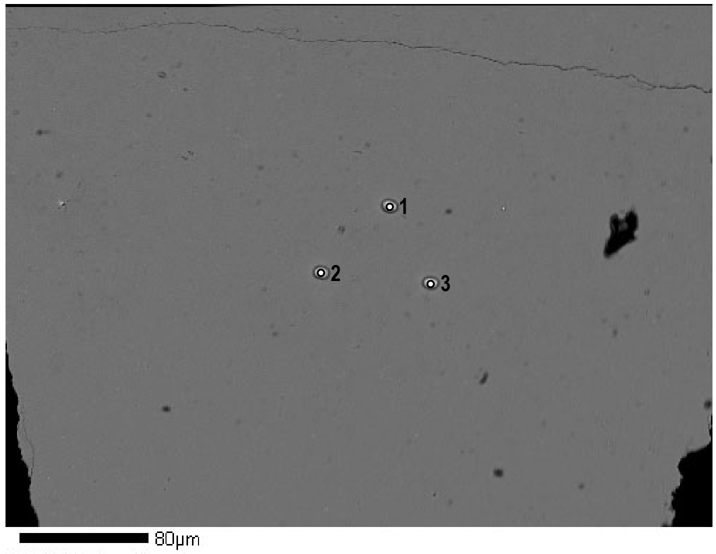

BEI BJ43 Area 1

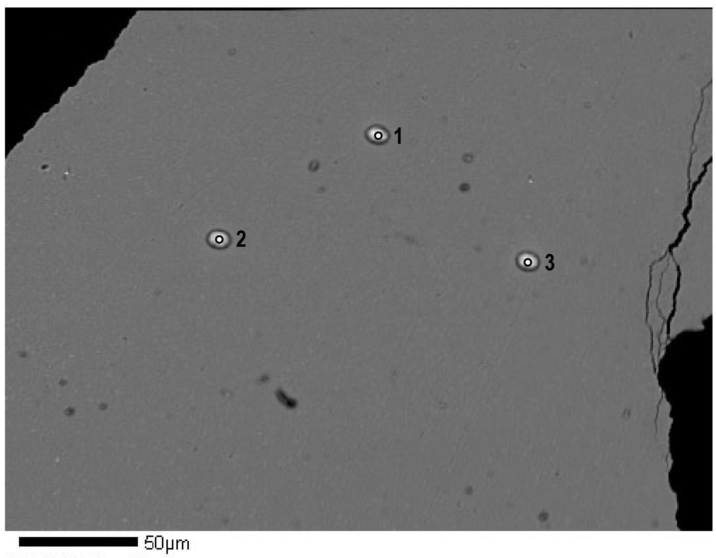

BEI BJ43 Area 2

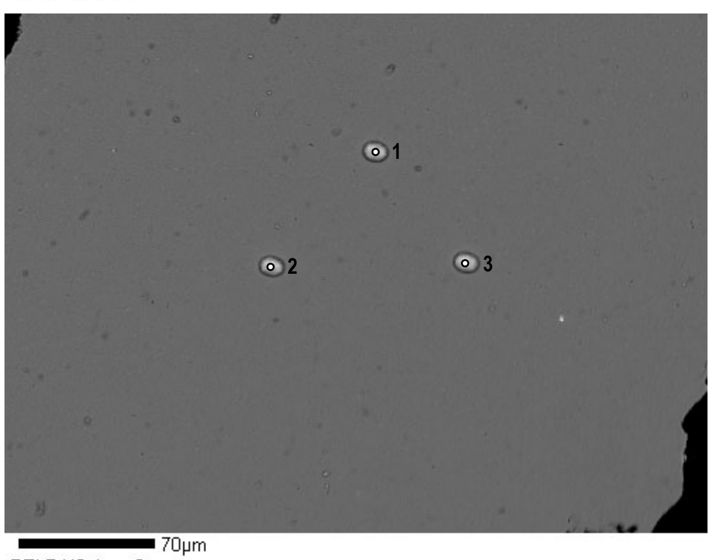

BEI BJ43 Area 3

	BJ43 1-1	BJ43 1-2	BJ43 1-3	BJ43 2-1	BJ43 2-2	BJ43 2-3	BJ43 3-1	BJ43 3-2	BJ43 3-3
CuO	7.47	8.38	7.99	8.33	7.57	7.86	7.78	8.26	8.28
MnO	0	0	0	0	0	0	0	0	0
ZnO	0	0	0	0	0	0	0.35	0	0
TiO2	0	0	0	0	0	0	0	0	0
MgO	0	0	0	0	0	0	0	0	0.05
CaO	0.32	0.30	0.30	0.38	0.31	0.37	0.37	0.29	0.31
K2O	0.13	0.13	0.17	0	0	0.05	0.06	0.10	0.07
Fe2O3	1.44	1.29	1.63	1.40	1.25	1.23	1.19	1.30	1.10
Al2O3	35.96	34.79	36.34	34.85	34.78	36.91	34.63	34.66	34.55
SiO2	0.93	0.87	0.92	0.98	1.05	0.94	0.96	0.95	1.05
P2O5	34.89	34.15	33.57	33.57	33.73	34.27	33.19	33.40	32.62
Total	81.15	79.91	80.92	79.52	78.70	81.63	78.52	78.96	78.05
H2O*	18.85	20.09	19.08	20.48	21.30	18.37	21.48	21.04	21.95
TOTAL	100.00	100.00	100.00	100.00	100.00	100.00	100.00	100.00	100.00
28 O									
Cu	0.75	0.84	0.81	0.83	0.75	0.8	0.77	0.82	0.82
Mn	0.15	0.13	0.16	0.14	0.12	0.12	0.12	0.13	0.11
Zn	5.65	5.45	5.73	5.44	5.37	5.84	5.37	5.39	5.34
Ti	0	0	0	0	0	0	0	0	0
Mg	0	0	0	0	0	0	0.03	0	0.01
Ca	0	0	0	0	0	0	0	0	0
K	0	0	0	0	0	0	0	0	0.01
Fe	0.05	0.04	0.04	0.05	0.04	0.05	0.05	0.04	0.04
Al	0.02	0.02	0.03	0	0	0.01	0.01	0.02	0.01
Si	0.12	0.12	0.12	0.13	0.14	0.13	0.13	0.13	0.14
P	3.94	3.84	3.81	3.77	3.74	3.89	3.69	3.73	3.62
Total	10.68	10.44	10.7	10.36	10.16	10.84	10.17	10.26	10.1

Blue J Sample BJ46

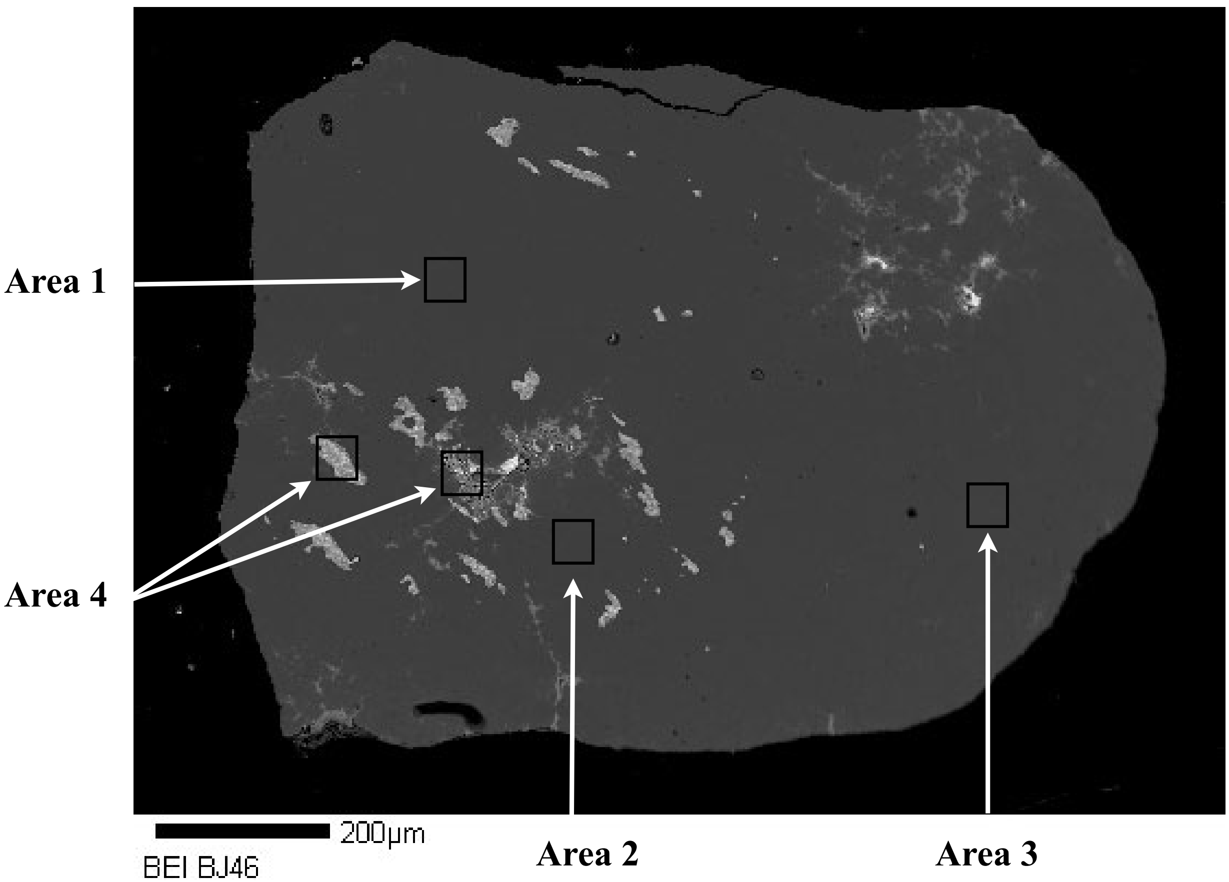

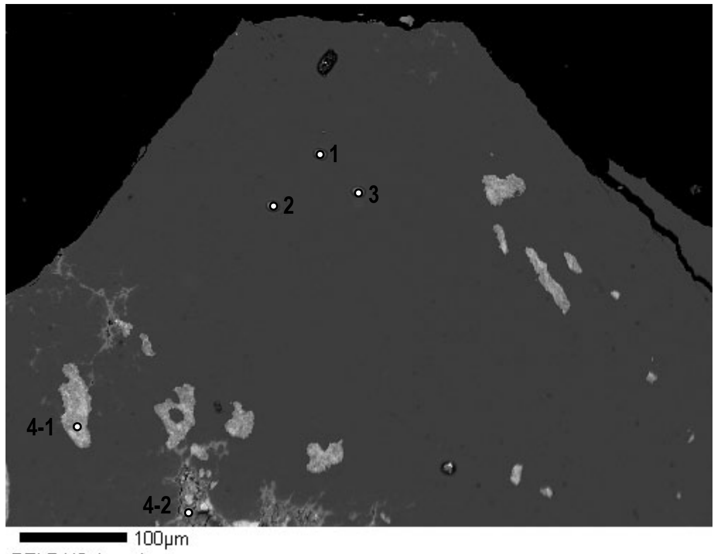

BEI BJ46 Area 1

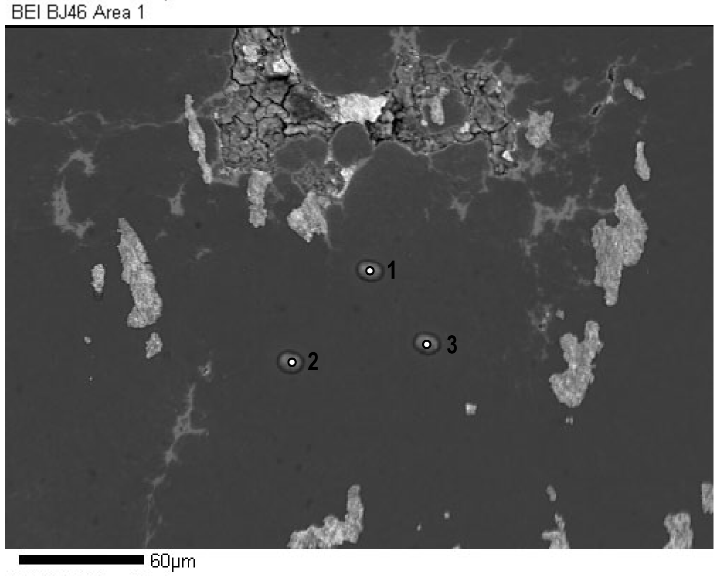

BEI BJ46 Area 2

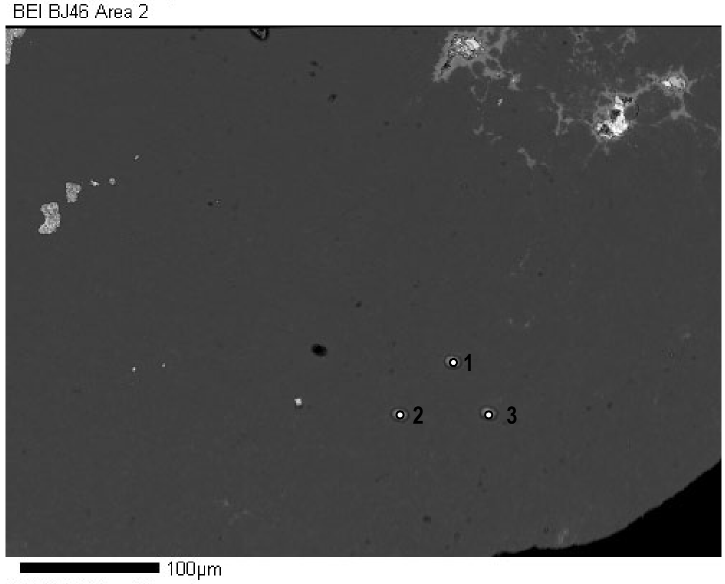

BEI BJ46 Area 3

	BJ46 1-1	BJ46 1-2	BJ46 1-3	BJ46 2-1	BJ46 2-2	BJ46 2-3	BJ46 3-1	BJ46 3-2	BJ46 3-3	BJ46 4-1	BJ46 4-2
CuO	7.24	8.01	8.29	7.09	7.63	7.17	6.89	7.26	7.28	18.06	1.94
MnO	0	0	0	0	0	0	0	0	0	0	0
ZnO	0	0	0.37	0	0	0	0	0	0	4.43	0.55
TiO2	0	0	0	0.14	0	0.12	0.11	0	0.13	0.12	0
MgO	0	0	0.05	0	0	0	0	0	0	0	0.45
CaO	0.31	0.34	0.27	0.35	0.34	0.36	0.37	0.31	0.37	0.32	13.63
K2O	0	0	0	0	0	0.05	0	0	0	0	0.48
Fe2O3	3.36	3.45	3.36	5.12	4.30	4.75	5.24	6.25	5.64	3.49	32.23
Al2O3	33.73	33.75	33.69	32.46	33.11	32.48	31.77	30.97	31.7	32.11	3.99
SiO2	0	0	0	0	0	0	0	0	0	0.23	3.83
P2O5	34.11	33.89	33.91	33.12	34.31	34.89	32.85	33.65	33.33	25.23	27.12
Total	78.75	79.44	79.94	78.27	79.69	79.83	77.23	78.44	78.44	83.99	84.23
H2O (by diff.)	21.25	20.56	20.06	21.73	20.32	20.17	22.77	21.56	21.56	16.01	15.77
TOTAL (w/H2O)	100.00	100.00	100.00	100.00	100.00	100.00	100.00	100.00	100.00	100.00	100.00
Based on 28O											
Cu	0.72	0.81	0.84	0.71	0.77	0.72	0.68	0.73	0.73	2.06	0.23
Mn	0.33	0.35	0.34	0.51	0.43	0.48	0.52	0.62	0.56	0.4	3.8
Zn	5.24	5.3	5.32	5.06	5.2	5.1	4.91	4.85	4.96	5.71	0.74
Ti	0	0	0	0	0	0	0	0	0	0	0
Mg	0	0	0.04	0	0	0	0	0	0	0.49	0.06
Ca	0	0	0	0.01	0	0.01	0.01	0	0.01	0.01	0
K	0	0	0.01	0	0	0	0	0	0	0	0.1
Fe	0.04	0.05	0.04	0.05	0.05	0.05	0.05	0.04	0.05	0.05	2.29
Al	0	0	0	0	0	0.01	0	0	0	0	0.1
Si	0	0	0	0	0	0	0	0	0	0.03	0.6
P	3.81	3.82	3.85	3.71	3.87	3.94	3.65	3.78	3.74	3.23	3.6
Total	10.14	10.33	10.44	10.05	10.32	10.31	9.82	10.02	10.05	11.98	11.52

Blue J Sample BJ47

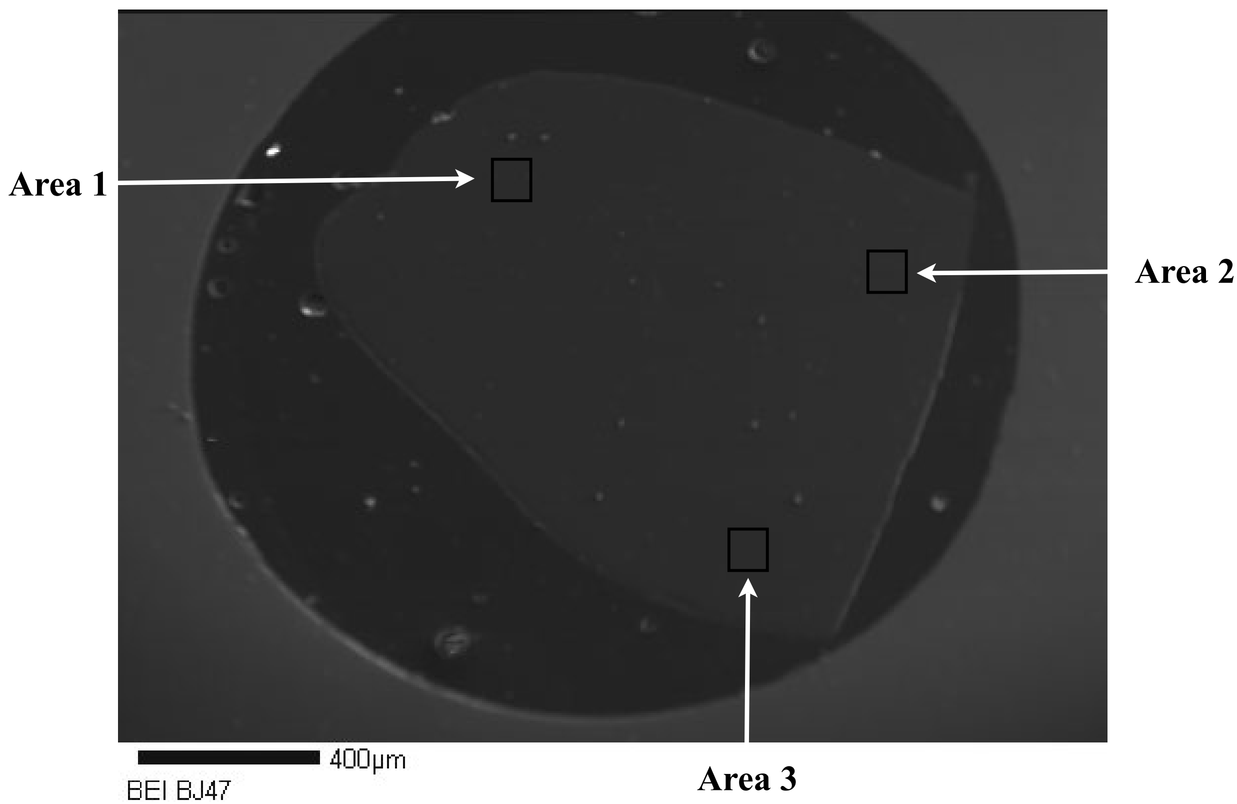

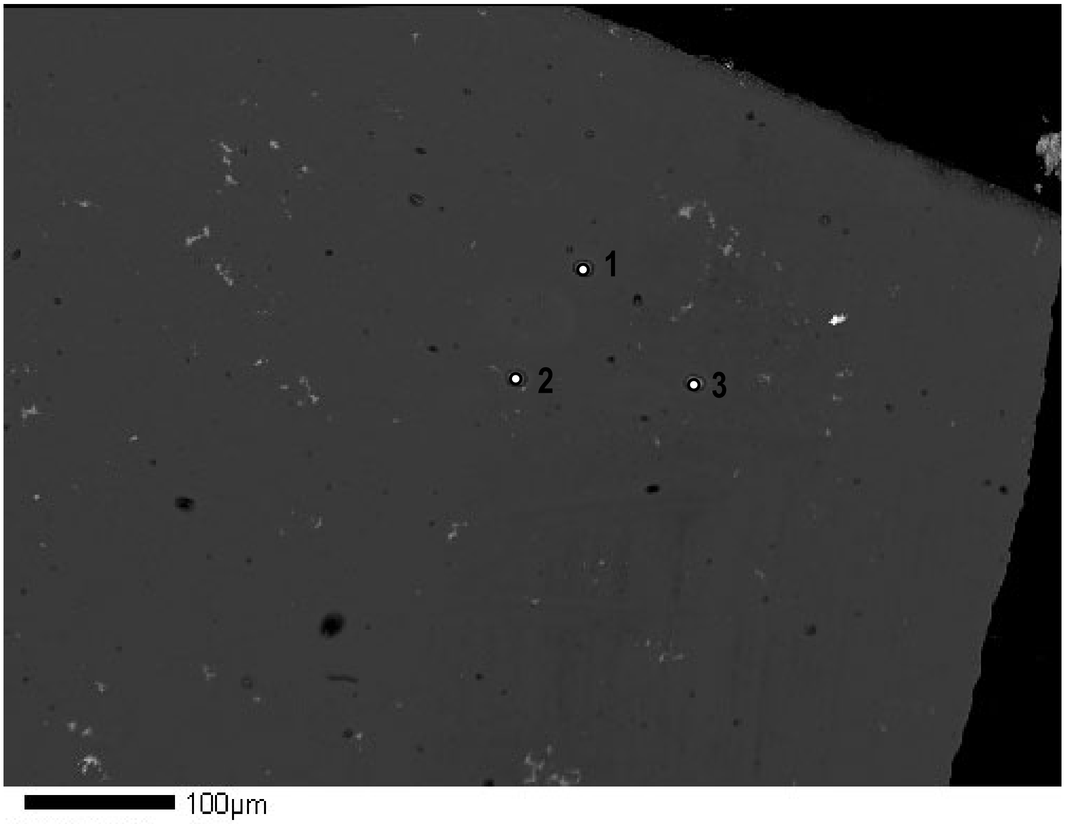

BEI BJ47 Area 2

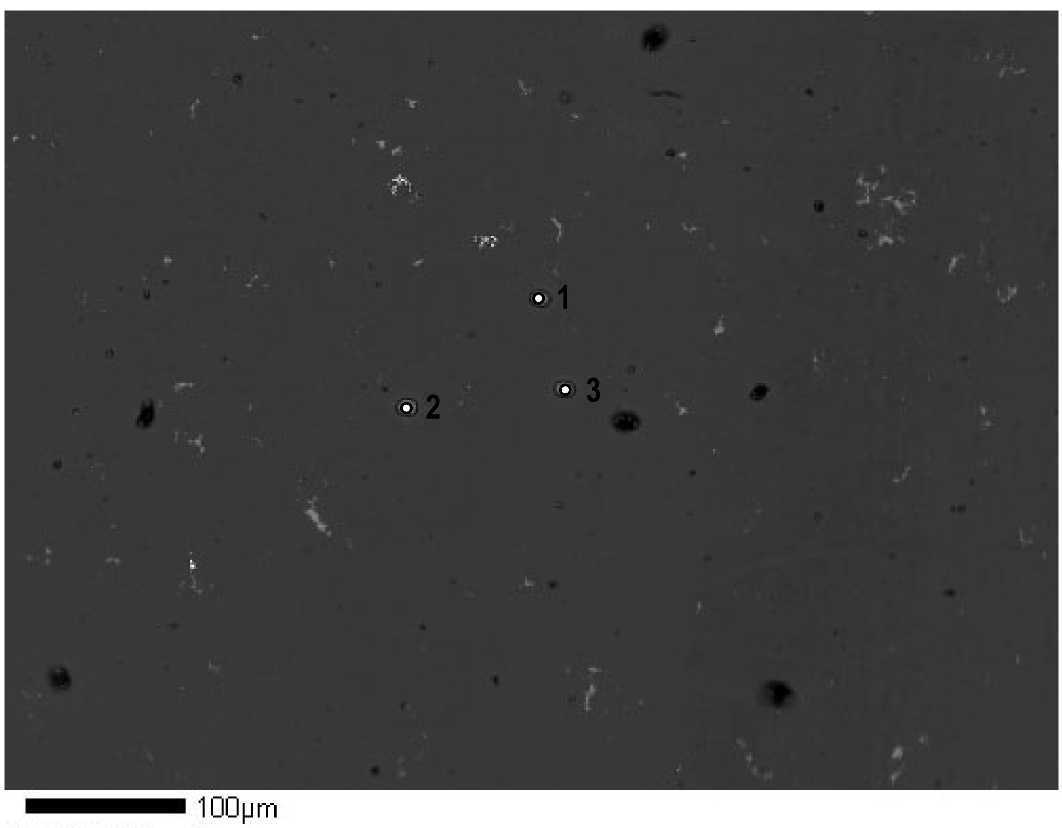

BEI BJ47 Area 3

	BJ47 1-1	BJ47 1-2	BJ47 1-3	BJ47 2-1	BJ47 2-2	BJ47 2-3	BJ47 3-1	BJ47 3-2	BJ47 3-3
CuO	7.38	7.9	7.34	7.89	6.83	7.95	7.71	7.34	7.85
MnO	0	0	0	0	0	0	0	0	0
ZnO	0	0	0	0	0	0	0.29	0	0
TiO2	0	0	0	0	0	0	0	0	0
MgO	0	0	0	0	0.08	0	0.05	0	0
CaO	0.46	0.40	0.43	0.54	0.62	0.46	0.41	0.40	0.43
K2O	0.35	0.29	0.08	0.22	0.09	0.10	0.08	0.06	0.07
Fe2O3	1.66	1.39	1.70	1.43	1.97	1.54	1.13	1.06	1.13
Al2O3	35.22	35.22	35.05	35.25	34.46	34.65	35.49	35.11	35.08
SiO2	0.43	0.53	0.48	0.47	0.59	0.44	0.39	0.39	0.37
P2O5	35.01	34.89	35.33	34.77	34.86	34.09	34.98	33.55	34.80
Total	80.51	80.62	80.41	80.58	79.50	79.23	80.53	77.90	79.72
H2O (by diff.)	19.49	19.38	19.59	19.42	20.50	20.77	19.47	22.10	20.28
TOTAL (w/H2O)	100	100	100	100	100	100	100	100	100
Based on 28O									
Cu	0.74	0.8	0.74	0.79	0.68	0.79	0.77	0.72	0.78
Mn	0.17	0.14	0.17	0.14	0.2	0.15	0.11	0.1	0.11
Zn	5.52	5.53	5.48	5.54	5.35	5.4	5.57	5.39	5.47
Ti	0	0	0	0	0	0	0	0	0
Mg	0	0	0	0	0	0	0.03	0	0
Ca	0	0	0	0	0	0	0	0	0
K	0	0	0	0	0.02	0	0.01	0	0
Fe	0.07	0.06	0.06	0.08	0.09	0.07	0.06	0.06	0.06
Al	0.06	0.05	0.01	0.04	0.02	0.02	0.01	0.01	0.01
Si	0.06	0.07	0.06	0.06	0.08	0.06	0.05	0.05	0.05
P	3.94	3.94	3.97	3.93	3.89	3.81	3.94	3.7	3.89
Total	10.56	10.59	10.49	10.58	10.33	10.3	10.55	10.03	10.37

Blue J Sample BJ49

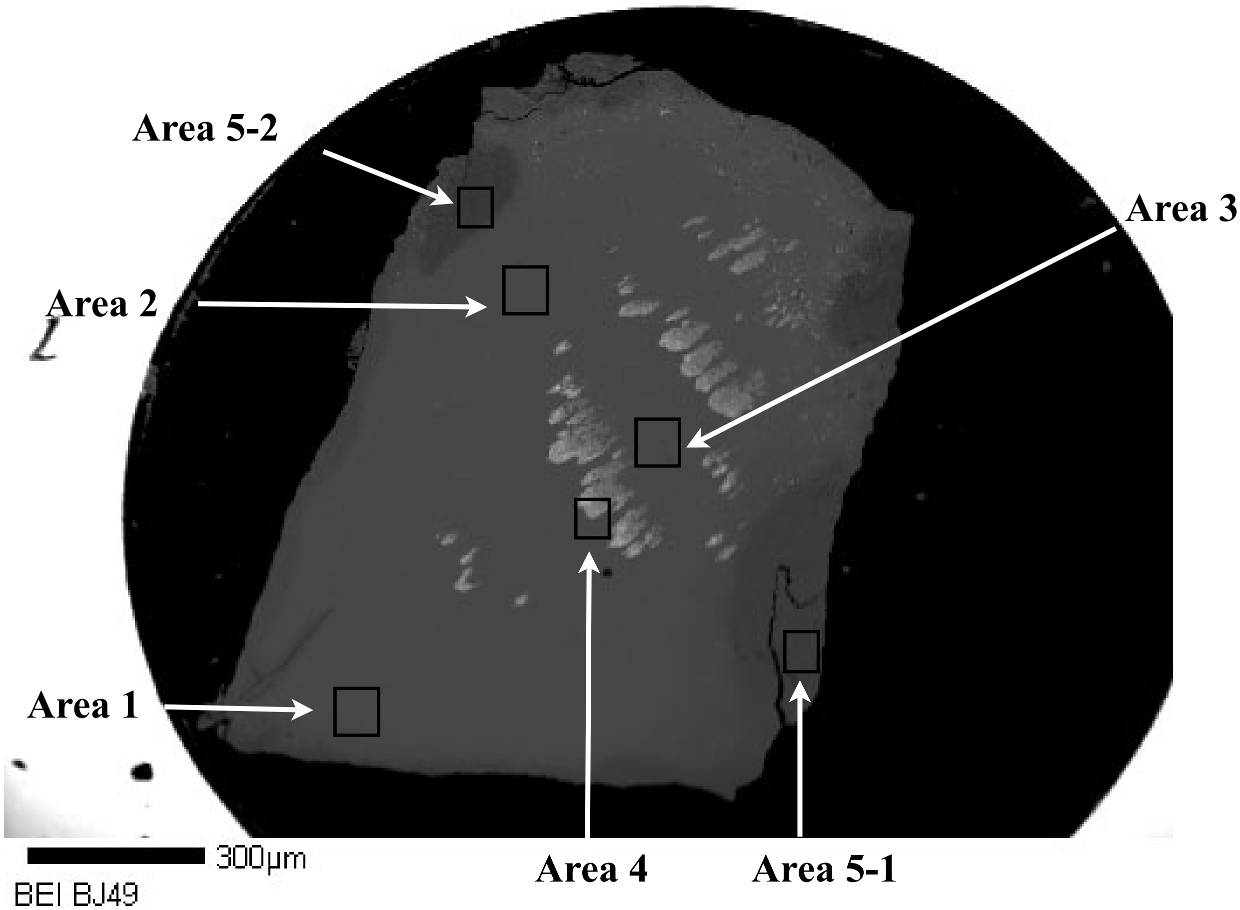

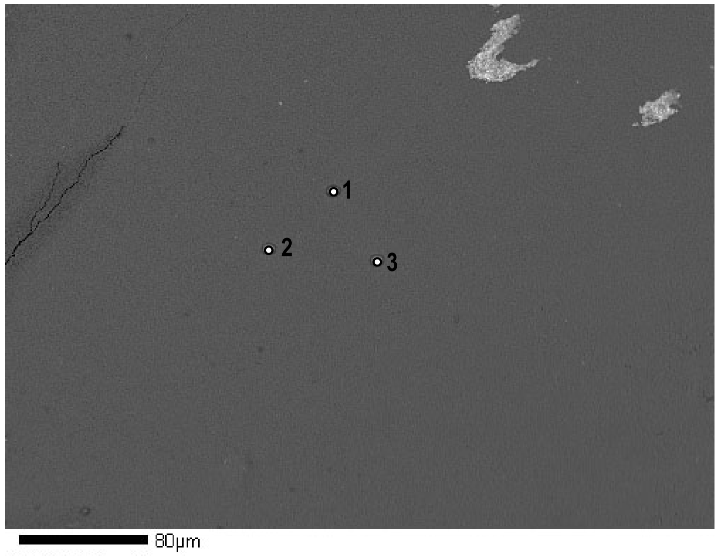

BEI BJ49 Area 1

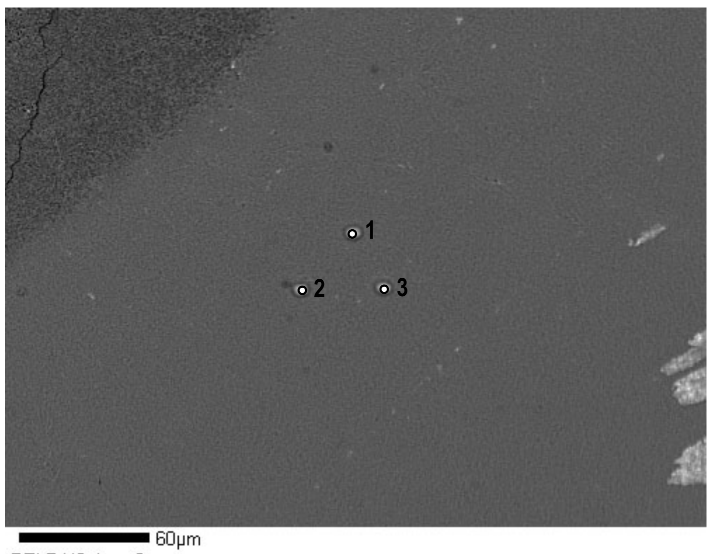

BEI BJ49 Area 2

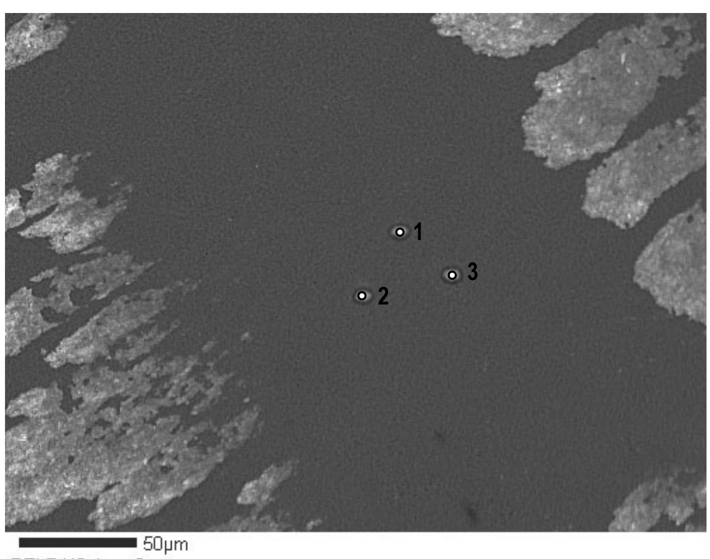

BEI BJ49 Area 3

	BJ49 1-1	BJ49 1-2	BJ49 1-3	BJ49 2-1	BJ49 2-2	BJ49 2-3	BJ49 3-1	BJ49 3-2	BJ49 3-3
CuO	8.61	8.43	7.87	8.55	8.25	8.17	8.33	8.56	8.37
Fe2O3	0	0	0	0.301	0	0	0	0	0
Al2O3	33.7	35.85	33.06	35.11	33.27	34.7	32.61	35.54	33.81
ZnO	0	0.05	0.04	0	0.07	0	0.04	0.05	0
TiO2	0.31	0.25	0.26	0.29	0.24	0.22	0.15	0.23	0.22
MgO	3.59	3.45	3.75	3.73	4.31	4.19	3.64	3.80	3.85
CaO	0.31	0.36	0.32	0.36	0.33	0.27	0.31	0.34	0.28
SiO2	0.51	0.58	0.51	0.34	0.34	0.46	0.55	0.44	0.45
P2O5	35.43	34.35	34.63	33.12	34.19	34.22	34.96	34.51	34.01
Total	82.45	83.33	80.44	81.80	81.00	82.23	80.59	83.47	80.99
H2O (by diff.)	17.55	16.67	19.56	18.20	19.00	17.77	19.41	16.53	19.01
TOTAL (w/H2O)	100.00	100.00	100.00	100.00	100.00	100.00	100.00	100.00	100.00
Based on 28O									
Cu	0.89	0.87	0.8	0.88	0.84	0.84	0.84	0.89	0.85
Fe	0.37	0.36	0.38	0.38	0.44	0.43	0.37	0.39	0.39
Al	5.41	5.8	5.22	5.64	5.3	5.57	5.16	5.76	5.38
Zn	0	0	0	0.03	0	0	0	0	0
Ti	0.03	0.04	0.03	0.04	0.03	0.03	0.03	0.04	0.03
Mg	0	0.01	0.01	0	0.01	0	0.01	0.01	0
Ca	0.04	0.04	0.04	0.04	0.03	0.03	0.02	0.03	0.03
Si	0.07	0.08	0.07	0.05	0.05	0.06	0.07	0.06	0.06
P	4.09	3.99	3.93	3.82	3.91	3.95	3.97	4.02	3.89
Total	10.9	11.19	10.48	10.88	10.61	10.91	10.47	11.2	10.63

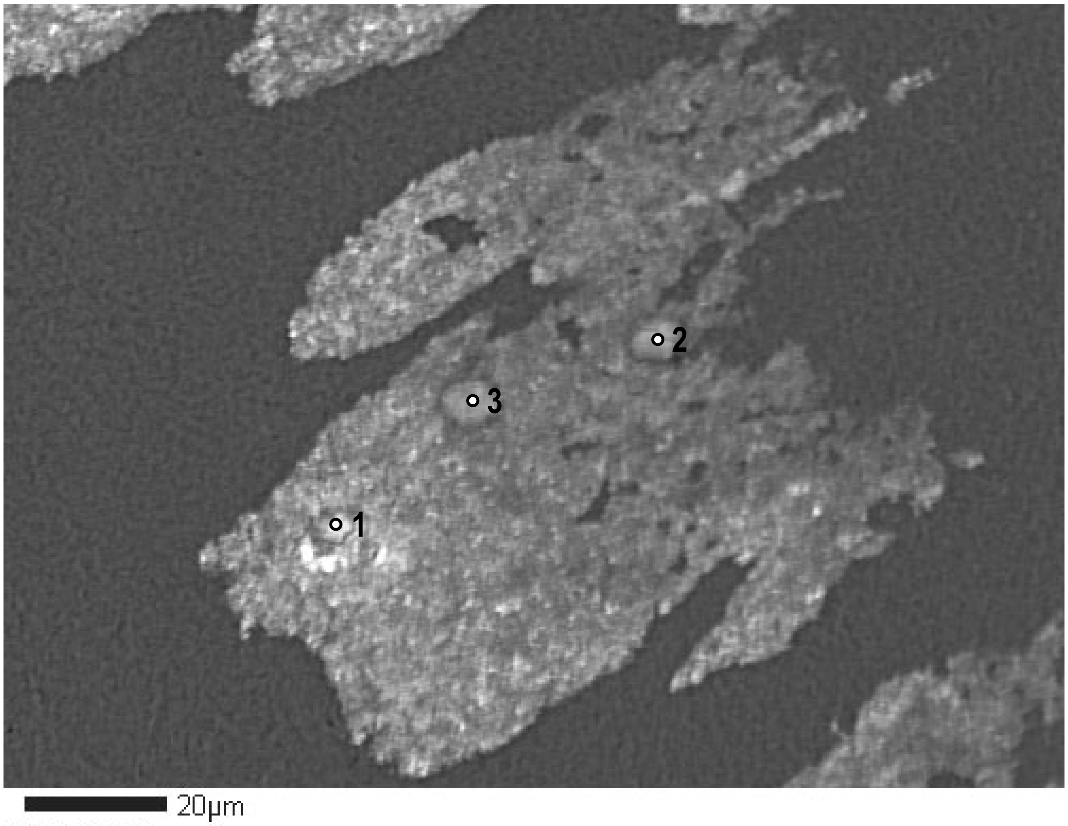

BEI BJ49 Area 4

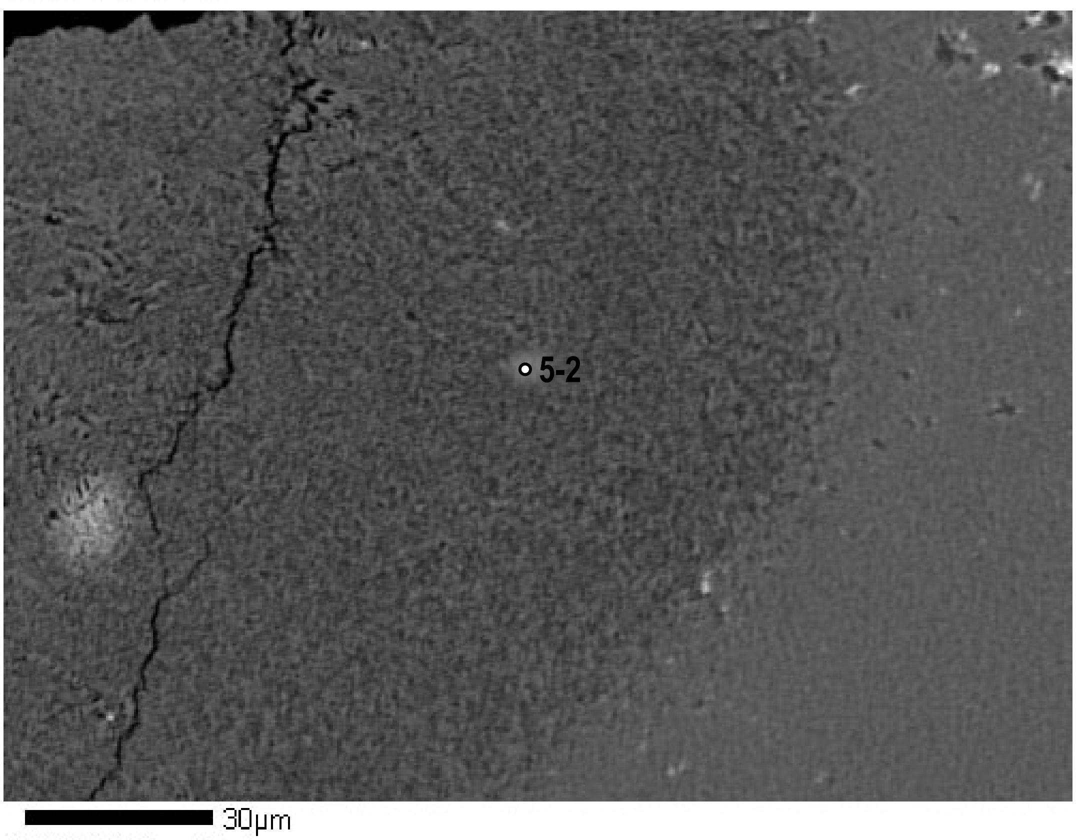

BEI BJ49 Area 5

	BJ49 4-1	BJ49 4-2	BJ49 4-3	BJ49 5-1	BJ49 5-2
CuO	20.74	11.8	13.6	7.34	7.4
Fe2O3	8.45	3.07	3.87	0	0
Al2O3	33.12	32.36	35.61	31.03	32.58
ZnO	0.05	0	0	0	0.04
TiO2	0.20	0.24	0.23	0.18	0.24
MgO	2.90	3.43	3.95	3.68	4.35
CaO	0.16	0.23	0.30	0.29	0.39
SiO2	0.48	0.43	0.55	0.29	0.46
P2O5	25.40	30.15	29.59	31.83	28.33
Total	91.50	81.71	87.69	74.64	73.78
H2O (by diff.)	8.50	18.29	12.31	25.36	26.22
TOTAL (w/H2O)	100	100	100	100	100
Based on 28O					
Cu	2.62	1.26	1.55	0.71	0.72
Fe	0.37	0.36	0.45	0.36	0.42
Al	6.53	5.38	6.32	4.7	4.95
Zn	1.04	0.32	0.43	0	0
Ti	0.02	0.02	0.03	0.03	0.04
Mg	0.01	0	0	0	0.01
Ca	0.04	0.04	0.04	0.02	0.03
Si	0.08	0.06	0.08	0.04	0.06
P	3.6	3.6	3.77	3.46	3.09
Total	14.31	11.04	12.67	9.32	9.32

Appendix G: Electron Microprobe Analyses of Homogeneous Turquoise Minerals

Range, Average and Standard Deviation of Homogenous Material by Location

Blue J Artifacts					**Hachita**					**Red Hill**					**Chalchihuitl**					**Tiffany**				
n=101	**MIN**	**MAX**	**AVG**	**STD**	n=111	**MIN**	**MAX**	**AVG**	**STD**	n=69	**MIN**	**MAX**	**AVG**	**STD**	n=45	**MIN**	**MAX**	**AVG**	**STD**	n=60	**MIN**	**MAX**	**AVG**	**STD**
CuO	4.75	9.04	7.51	0.68	**CuO**	5.16	9.64	7.26	0.97	**CuO**	5.74	8.70	7.37	0.79	**CuO**	2.43	7.93	5.78	1.64	**CuO**	6.91	8.74	7.81	0.42
ZnO	0.00	0.55	0.29	0.14	**ZnO**	0.00	0.43	0.14	0.17	**ZnO**	0.00	0.00	0.00	0.00	**ZnO**	0.00	0.51	0.34	0.11	**ZnO**	0.00	0.51	0.43	0.07
Fe2O3	0.00	9.16	2.54	1.63	**Fe2O3**	0.32	3.95	1.72	0.73	**Fe2O3**	4.58	16.53	10.58	2.43	**Fe2O3**	0.47	3.72	1.31	0.75	**Fe2O3**	0.11	2.20	1.00	0.61
TiO2	0.00	0.31	0.20	0.07	**TiO2**	0.00	0.13	0.14	0.07	**TiO2**	0.39	1.46	0.75	0.30	**TiO2**	0.00	2.84	0.68	0.90	**TiO2**	0.00	1.46	0.60	0.43
MgO	0.00	4.31	1.12	1.72	**MgO**	0.00	0.17	0.12	0.03	**MgO**	0.00	0.00	0.00	0.00	**MgO**	0.00	0.30	0.13	0.07	**MgO**	0.00	0.07	0.05	0.01
CaO	0.00	0.62	0.35	0.08	**CaO**	0.00	0.74	0.23	0.20	**CaO**	0.00	0.07	0.07	0.00	**CaO**	0.21	0.92	0.49	0.20	**CaO**	0.00	0.32	0.17	0.04
MnO	0.00	0.00	0.00	0.00	**MnO**	0.00	0.17	0.17	0.00	**MnO**	0.00	0.05	0.05	0.00	**SiO2**	0.00	9.79	5.09	3.09	**SiO2**	0.00	0.77	0.25	0.16
K2O	0.00	0.43	0.13	0.09	**K2O**	0.00	0.27	0.10	0.06	**K2O**	0.07	0.26	0.14	0.05	**Al2O3**	31.29	39.12	34.98	1.80	**Al2O3**	34.53	38.70	36.72	1.16
SiO2	0.00	3.76	0.68	0.76	**SiO2**	0.00	15.66	1.69	3.11	**SiO2**	0.00	0.12	0.11	0.01	**P2O5**	29.17	37.87	31.72	2.15	**P2O5**	32.28	35.17	33.62	0.71
Al2O3	30.10	38.87	34.98	1.52	**Al2O3**	30.34	40.33	35.34	2.31	**Al2O3**	25.22	34.39	29.95	2.16	**Total**	69.35	87.70	80.16	3.74	**Total**	77.26	83.26	79.92	1.43
P2O5	32.45	36.74	34.49	0.85	**P2O5**	21.07	34.88	30.60	2.14	**P2O5**	28.82	35.16	31.20	1.49	**H2O***	12.30	30.65	19.84	3.74	**H2O***	16.74	22.74	20.08	1.43
Total	76.95	83.55	80.45	1.42	**Total**	65.74	84.47	76.13	4.11	**Total**	74.64	87.03	80.03	2.49	**TOTAL**	100.00	100.00	100.00	0.00	**TOTAL**	100.00	100.00	100.00	0.00
H2O*	16.45	23.05	19.56	1.41	**H2O***	15.53	34.26	23.65	4.01	**H2O***	12.97	25.36	19.97	2.49										
TOTAL	100.00	100.00	####	0.00	**TOTAL**	100.00	100.00	100.00	0.00	**TOTAL**	100.00	100.00	100.00	0.00										
28 O					**28 O**					**28 O**					**28 O**					**28 O**				
Cu	0.48	0.91	0.76	0.07	**Cu**	0.47	1.01	0.71	0.11	**Cu**	0.57	0.92	0.77	0.09	**Cu**	0.38	0.83	0.64	0.11	**Cu**	0.70	0.89	0.78	0.05
Zn	0.00	0.05	0.03	0.01	**Zn**	0.00	0.04	0.03	0.02	**Zn**	0.00	0.00	0.00	0.00	**Zn**	0.00	0.05	0.03	0.01	**Zn**	0.00	0.05	0.04	0.01
Fe	0.00	0.94	0.27	0.16	**Fe**	0.01	0.40	0.17	0.07	**Fe**	0.46	1.74	1.09	0.26	**Fe**	0.04	0.37	0.13	0.08	**Fe**	0.04	0.22	0.12	0.05
Ti	0.00	0.04	0.03	0.01	**Ti**	0.00	0.01	0.01	0.00	**Ti**	0.04	0.15	0.08	0.03	**Ti**	0.00	0.04	0.02	0.01	**Ti**	0.00	0.07	0.03	0.01
Mg	0.00	0.03	0.01	0.01	**Mg**	0.00	0.03	0.02	0.01	**Mg**	0.00	0.00	0.00	0.00	**Mg**	0.00	0.06	0.03	0.01	**Mg**	0.00	0.01	0.01	0.00
Ca	0.02	0.09	0.05	0.01	**Ca**	0.00	0.11	0.03	0.03	**Ca**	0.00	0.01	0.01	0.00	**Ca**	0.03	0.13	0.07	0.03	**Ca**	0.01	0.05	0.02	0.01
Mn	0.00	0.02	0.02	0.01	**Mn**	0.00	0.02	0.02	0.00	**Mn**	0.00	0.01	0.01	0.00	**Si**	0.18	1.32	0.79	0.35	**Si**	0.00	0.10	0.04	0.02
K	0.00	0.07	0.02	0.02	**K**	0.00	0.05	0.02	0.01	**K**	0.00	0.05	0.02	0.01	**Al**	4.51	6.22	5.20	0.50	**Al**	5.31	6.19	5.74	0.24
Si	0.00	0.50	0.09	0.10	**Si**	0.00	2.10	0.22	0.41	**Si**	0.00	0.02	0.01	0.01	**P**	2.42	3.86	3.44	0.15	**P**	3.57	4.01	3.77	0.10
Al	4.83	6.13	5.50	0.25	**Al**	4.34	6.41	5.40	0.48	**Al**	4.04	5.64	4.84	0.38	**H***	12.74	25.01	17.59	2.69	**H***	15.17	19.72	17.76	1.08
P	3.58	4.16	3.89	0.12	**P**	2.40	4.08	3.35	0.30	**P**	3.25	4.25	3.62	0.22	**Total**	24.63	33.42	28.08	1.94	**Total**	26.36	29.62	28.24	0.77
										H*	14.33	27.31	20.55	2.93	**H***	0.38	0.83	0.64	0.11	**H***	0.23	0.83	0.58	0.17
										Total	25.84	35.09	30.33	2.11	**Total**	0.00	0.05	0.03	0.01	**Total**	0.00	0.05	0.03	0.01

*H2O determined by the difference of Total from 100

Cations calculated based on molecular formula of turquoise with 28 oxygen

Range, Average and Standard Deviation for Homogenous Material by Sample

BJ1					**BJ11**					**BJ12(1)**					**BJ12(2)**					**BJ12(3)**				
n=9	**MIN**	**MAX**	**AVG**	**STD**	n=14	**MIN**	**MAX**	**AVG**	**STD**	n=9	**MIN**	**MAX**	**AVG**	**STD**	n=12	**MIN**	**MAX**	**AVG**	**STD**	n=12	**MIN**	**MAX**	**AVG**	**STD**
CuO	6.65	8.09	7.44	0.43	**CuO**	7.47	9.04	8.19	0.47	**CuO**	6.17	7.61	7.00	0.45	**CuO**	4.75	7.82	7.11	0.80	**CuO**	6.56	7.57	7.21	0.32
ZnO	0.00	0.00	0.00	0.00	**ZnO**	0.00	0.39	0.35	0.04	**ZnO**	0.00	0.00	0.00	0.00	**ZnO**	0.00	0.55	0.39	0.10	**ZnO**	0.00	0.00	0.00	0.00
Fe2O3	1.86	3.01	2.28	0.34	**Fe2O3**	0.00	0.31	0.26	0.04	**Fe2O3**	1.99	4.78	2.97	1.03	**Fe2O3**	2.44	3.23	2.76	0.28	**Fe2O3**	2.15	9.16	3.75	2.05
TiO2	0.00	0.00	0.00	0.00	**TiO2**	0.00	0.00	0.00	0.00	**TiO2**	0.00	0.00	0.00	0.00	**TiO2**	0.00	0.00	0.00	0.00	**TiO2**	0.00	0.09	0.09	0.00
MgO	0.00	0.05	0.05	0.01	**MgO**	0.00	0.06	0.05	0.01	**MgO**	0.00	0.08	0.07	0.01	**MgO**	0.00	0.07	0.07	0.01	**MgO**	0.00	0.08	0.07	0.02
SiO2	0.00	0.53	0.22	0.16	**CaO**	0.27	0.44	0.38	0.05	**CaO**	0.21	0.27	0.23	0.02	**SiO2**	0.00	0.22	0.13	0.05	**CaO**	0.28	0.42	0.36	0.04
Al2O3	34.60	37.40	35.95	1.13	**MnO**	0.00	0.00	0.00	0.00	**SiO2**	0.19	0.50	0.32	0.13	**Al2O3**	34.88	38.87	36.34	1.14	**MnO**	0.00	0.00	0.00	0.00
P2O5	34.26	36.19	34.96	0.56	**K2O**	0.00	0.43	0.15	0.19	**Al2O3**	34.50	36.82	35.46	0.85	**P2O5**	34.05	36.74	35.40	0.72	**K2O**	0.06	0.27	0.14	0.06
Total	79.52	82.54	80.84	0.94	**SiO2**	0.00	0.07	0.07	0.00	**P2O5**	34.52	35.96	35.14	0.56	**Total**	80.11	83.20	81.83	0.97	**SiO2**	0.26	0.51	0.38	0.09
H2O*	17.46	20.48	19.16	0.94	**Al2O3**	35.53	36.80	36.07	0.39	**Total**	79.03	83.55	81.14	1.28	**H2O***	16.80	19.89	18.17	0.97	**Al2O3**	30.10	36.79	34.43	1.88
TOTAL	100.00	100.00	100.00	0.00	**P2O5**	32.68	35.25	34.20	0.73	**H2O***	16.45	20.97	18.86	1.28	**TOTAL**	100.00	100.00	100.00	0.00	**P2O5**	33.60	35.37	34.62	0.53
					Total	76.95	80.57	79.19	0.91	**TOTAL**	100.00	100.00	100.00	0.00						**Total**	79.83	82.10	80.98	0.67
					H2O*	19.43	23.05	20.81	0.91											**H2O***	17.90	20.17	19.10	0.70
					TOTAL	100.00	100.00	100.00	0.00											**TOTAL**	100.00	100.00	100.00	0.00
28 O					**28 O**					**28 O**					**28 O**					**28 O**				
Cu	0.67	0.83	0.75	0.05	**Cu**	0.74	0.91	0.82	0.05	**Cu**	0.62	0.77	0.71	0.05	**Cu**	0.48	0.79	0.72	0.08	**Cu**	0.66	0.77	0.73	0.03
Zn	0.00	0.00	0.00	0.00	**Zn**	0.00	0.04	0.03	0.01	**Zn**	0.00	0.00	0.00	0.00	**Zn**	0.00	0.05	0.04	0.01	**Zn**	0.00	0.01	0.01	0.00
Fe	0.19	0.30	0.23	0.03	**Fe**	0.00	0.03	0.02	0.01	**Fe**	0.20	0.49	0.30	0.11	**Fe**	0.24	0.33	0.28	0.03	**Fe**	0.22	0.94	0.38	0.21
Ti	0.00	0.00	0.00	0.00	**Ti**	0.00	0.00	0.00	0.00	**Ti**	0.00	0.00	0.00	0.00	**Ti**	0.00	0.00	0.00	0.00	**Ti**	0.00	0.00	0.00	0.00
Mg	0.00	0.01	0.01	0.00	**Mg**	0.00	0.01	0.01	0.00	**Mg**	0.00	0.02	0.02	0.01	**Mg**	0.00	0.01	0.01	0.00	**Mg**	0.00	0.00	0.00	0.00
Si	0.00	0.07	0.03	0.02	**Ca**	0.04	0.06	0.05	0.01	**Ca**	0.03	0.04	0.03	0.00	**Si**	0.00	0.03	0.02	0.01	**Ca**	0.04	0.06	0.05	0.01
Al	5.39	5.91	5.65	0.21	**Mn**	0.00	0.00	0.00	0.00	**Si**	0.03	0.07	0.04	0.02	**Al**	5.48	6.13	5.75	0.19	**Mn**	0.00	0.02	0.02	0.01
P	3.85	4.08	3.94	0.07	**K**	0.00	0.07	0.03	0.03	**Al**	5.35	5.77	5.58	0.16	**P**	3.85	4.16	4.02	0.09	**K**	0.01	0.05	0.02	0.01
H*	15.78	18.03	17.04	0.72	**Si**	0.00	0.01	0.01	0.00	**P**	3.84	4.08	3.98	0.09	**H***	15.01	17.65	16.28	0.79	**Si**	0.03	0.07	0.05	0.01
Total	26.79	28.31	27.64	0.51	**Al**	5.53	5.69	5.60	0.05	**H***	15.06	18.37	16.82	0.96	**Total**	26.07	28.09	27.08	0.60	**Al**	4.83	5.85	5.44	0.28
					P	3.58	3.98	3.82	0.11	**Total**	26.24	28.58	27.46	0.69						**P**	3.87	4.03	3.93	0.06
					H*	17.31	19.91	18.30	0.66											**H***	16.12	17.82	17.10	0.56
					Total	27.90	29.83	28.62	0.50											**Total**	27.05	28.2	27.708	0.39

*H2O determined by the difference of Total from 100

Cations calculated based on molecular formula of turquoise with 28 oxygen

BJ21					BJ43					BJ46					BJ47					BJ49				
n=9	**MIN**	**MAX**	**AVG**	**STD**	n=9	**MIN**	**MAX**	**AVG**	**STD**	n=9	**MIN**	**MAX**	**AVG**	**STD**	n=9	**MIN**	**MAX**	**AVG**	**STD**	n=9	**MIN**	**MAX**	**AVG**	**STD**
CuO	6.11	6.94	6.61	0.28	**CuO**	7.47	8.38	7.99	0.34	**CuO**	6.89	8.29	7.43	0.46	**CuO**	6.83	7.95	7.58	0.38	**CuO**	7.87	8.61	8.35	0.23
ZnO	0.00	0.38	0.36	0.02	**ZnO**	0.00	0.35	0.35	0.00	**ZnO**	0.00	0.37	0.37	0.00	**ZnO**	0.00	0.29	0.29	0.00	**ZnO**	0.00	0.07	0.05	0.01
Fe2O3	2.08	5.78	3.72	1.19	**Fe2O3**	1.10	1.63	1.32	0.16	**Fe2O3**	3.36	6.25	4.61	1.06	**Fe2O3**	1.06	1.97	1.45	0.31	**Fe2O3**	0.00	0.30	0.30	0.00
TiO2	0.00	0.00	0.00	0.00	**TiO2**	0.00	0.00	0.00	0.00	**TiO2**	0.00	0.14	0.12	0.01	**TiO2**	0.00	0.00	0.00	0.00	**TiO2**	0.15	0.31	0.24	0.04
MgO	0.00	0.12	0.09	0.03	**MgO**	0.00	0.05	0.05	0.00	**MgO**	0.00	0.05	0.05	0.00	**MgO**	0.00	0.08	0.07	0.02	**MgO**	3.45	4.31	3.81	0.28
SiO2	1.33	3.76	2.40	0.84	**CaO**	0.29	0.38	0.33	0.03	**CaO**	0.27	0.37	0.33	0.03	**CaO**	0.40	0.62	0.46	0.07	**CaO**	0.27	0.36	0.32	0.03
Al2O3	32.15	34.73	33.54	0.85	**MnO**	0.00	0.00	0.00	0.00	**MnO**	0.00	0.00	0.00	0.00	**MnO**	0.00	0.00	0.00	0.00	**SiO2**	0.34	0.58	0.46	0.08
P2O5	32.45	35.58	33.78	0.92	**K2O**	0.00	0.17	0.10	0.04	**K2O**	0.00	0.05	0.05	0.00	**K2O**	0.06	0.35	0.15	0.11	**Al2O3**	32.61	35.85	34.18	1.16
Total	77.63	82.63	80.28	1.45	**SiO2**	0.87	1.05	0.96	0.06	**SiO2**	0.00	0.00	0.00	0.00	**SiO2**	0.37	0.59	0.45	0.07	**P2O5**	33.12	35.43	34.38	0.64
H2O*	17.37	22.37	19.72	1.45	**Al2O3**	34.55	36.91	35.27	0.88	**Al2O3**	30.97	33.75	32.63	1.01	**Al2O3**	34.46	35.49	35.06	0.32	**Total**	80.44	83.47	81.81	1.14
TOTAL	100.00	100.00	100.00	0.00	**P2O5**	32.62	34.89	33.71	0.66	**P2O5**	32.85	34.89	33.78	0.63	**P2O5**	33.55	35.33	34.70	0.54	**H2O***	16.53	19.56	18.19	1.14
					Total	78.05	81.63	79.71	1.28	**Total**	77.23	79.94	78.89	0.90	**Total**	77.90	80.62	79.89	0.91	**TOTAL**	100.00	100.00	100.00	0.00
					H2O*	18.37	21.95	20.29	1.28	**H2O***	20.06	22.77	21.11	0.90	**H2O**	19.38	22.10	20.11	0.91					
					TOTAL	100.00	100.00	100.00	0.00	**TOTAL**	100.00	100.00	100.00	0.00	**TOTAL**	100.00	100.00	100.00	0.00					
28 O					**28 O**					**28 O**					**28 O**					**28 O**				
Cu	0.61	0.71	0.66	0.03	**Cu**	0.75	0.84	0.80	0.03	**Cu**	0.68	0.84	0.75	0.05	**Cu**	0.68	0.80	0.76	0.04	**Cu**	0.8	0.89	0.86	0.03
Zn	0.00	0.04	0.04	0.01	**Zn**	0.00	0.03	0.02	0.01	**Zn**	0.00	0.04	0.04	0.00	**Zn**	0.00	0.00	0.00	0.00	**Zn**	0.00	0.03	0.03	0.00
Fe	0.21	0.59	0.37	0.12	**Fe**	0.11	0.16	0.13	0.02	**Fe**	0.33	0.62	0.46	0.10	**Fe**	0.10	0.20	0.14	0.03	**Fe**	0.36	0.44	0.39	0.03
Ti	0.00	0.00	0.00	0.00	**Ti**	0.00	0.00	0.00	0.00	**Ti**	0.00	0.01	0.01	0.00	**Ti**	0.00	0.00	0.00	0.00	**Ti**	0.03	0.04	0.03	0.00
Mg	0.00	0.03	0.02	0.01	**Mg**	0.00	0.01	0.01	0.00	**Mg**	0.00	0.01	0.01	0.00	**Mg**	0.00	0.03	0.03	0.00	**Mg**	0.00	0.01	0.01	0.00
Si	0.18	0.50	0.32	0.11	**Ca**	0.04	0.05	0.04	0.01	**Ca**	0.04	0.05	0.05	0.01	**Ca**	0.06	0.09	0.07	0.01	**Ca**	0.02	0.04	0.03	0.01
Al	5.00	5.49	5.25	0.18	**Mn**	0.00	0.00	0.00	0.00	**Mn**	0.00	0.00	0.00	0.00	**Mn**	0.00	0.02	0.02	0.01	**Si**	0.05	0.08	0.06	0.01
P	3.67	4.00	3.80	0.11	**K**	0.00	0.03	0.02	0.01	**K**	0.00	0.01	0.01	0.00	**K**	0.01	0.06	0.03	0.02	**Al**	5.16	5.80	5.47	0.23
H*	15.82	19.40	17.48	1.07	**Si**	0.12	0.14	0.13	0.01	**Si**	0.00	0.00	0.00	0.00	**Si**	0.05	0.08	0.06	0.01	**P**	3.82	4.09	3.95	0.08
Total	26.80	29.29	27.91	0.76	**Al**	5.34	5.84	5.51	0.18	**Al**	4.85	5.32	5.10	0.17	**Al**	5.35	5.57	5.47	0.08	**H***	15.18	17.49	16.48	0.88
					P	3.62	3.94	3.78	0.10	**P**	3.65	3.94	3.80	0.09	**P**	3.70	3.97	3.89	0.09	**Total**	26.38	27.97	27.28	0.61
					H*	16.45	19.22	17.94	0.98	**H***	17.94	19.94	18.70	0.69	**H***	17.25	19.23	17.78	0.67					
					Total	27.29	29.32	28.354	0.72	**Total**	28.27	29.76	28.866	0.49	**Total**	27.84	29.26	28.199	0.49					

*H2O determined by the difference of Total from 100

Cations calculated based on molecular formula of turquoise with 28 oxygen

TM57					**TM66**					**TM68**					**TM70**				
n=12	**MIN**	**MAX**	**AVG**	**STD**	n=13	**MIN**	**MAX**	**AVG**	**STD**	n=11	**MIN**	**MAX**	**AVG**	**STD**	n=9	**MIN**	**MAX**	**AVG**	**STD**
CuO	5.27	6.26	5.70	0.32	**CuO**	6.82	9.64	7.77	0.81	**CuO**	6.51	7.95	7.20	0.43	**CuO**	6.65	9.18	7.80	0.84
ZnO	0.00	0.00	0.00	0.00	**ZnO**	0.00	0.00	0.00	0.00	**ZnO**	0.00	0.43	0.43	0.00	**ZnO**	0.00	0.00	0.00	0.00
Fe2O3	0.73	1.12	0.93	0.11	**Fe2O3**	0.84	1.90	1.42	0.28	**Fe2O3**	0.77	1.49	1.07	0.23	**Fe2O3**	1.83	2.57	2.18	0.23
TiO2	0.00	0.00	0.00	0.00	**TiO2**	0.00	0.00	0.00	0.00	**TiO2**	0.00	0.00	0.00	0.00	**TiO2**	0.00	0.00	0.00	0.00
MgO	0.00	0.00	0.00	0.00	**MgO**	0.00	0.09	0.09	0.00	**MgO**	0.00	0.00	0.00	0.00	**MgO**	0.00	0.11	0.10	0.01
CaO	0.00	0.09	0.09	0.00	**CaO**	0.00	0.21	0.15	0.03	**CaO**	0.00	0.09	0.09	0.00	**CaO**	0.11	0.23	0.17	0.04
MnO	0.00	0.00	0.00	0.00	**MnO**	0.00	0.00	0.00	0.00	**MnO**	0.00	0.00	0.00	0.00	**MnO**	0.00	0.00	0.00	0.00
K2O	0.00	0.10	0.08	0.01	**K2O**	0.00	0.09	0.07	0.02	**K2O**	0.00	0.08	0.06	0.01	**K2O**	0.00	0.12	0.08	0.03
SiO2	0.00	0.00	0.00	0.00	**SiO2**	0.00	0.14	0.11	0.02	**SiO2**	0.00	0.00	0.00	0.00	**SiO2**	0.00	0.14	0.12	0.02
Al2O3	30.88	37.38	33.54	2.07	**Al2O3**	35.86	38.55	37.14	1.06	**Al2O3**	34.99	40.33	37.56	1.92	**Al2O3**	30.34	34.06	32.64	1.42
P2O5	27.97	30.66	29.42	0.78	**P2O5**	30.41	34.88	31.91	1.21	**P2O5**	31.26	34.61	32.94	1.10	**P2O5**	27.30	30.10	28.54	0.94
Total	65.74	74.78	69.62	2.81	**Total**	74.87	84.47	78.48	2.45	**Total**	75.30	82.61	78.99	2.13	**Total**	68.73	74.84	71.46	1.83
H2O*	25.22	34.26	30.38	2.81	**H2O***	15.53	25.13	21.52	2.45	**H2O***	17.39	24.70	21.01	2.13	**H2O***	25.16	31.27	28.54	1.83
TOTAL	100.00	100.00	100.00	0.00	**TOTAL**	100.00	100.00	100.00	0.00	**TOTAL**	100.00	100.00	100.00	0.00	**TOTAL**	100.00	100.00	100.00	0.00
28 O					**28 O**					**28 O**					**28 O**				
Cu	0.47	0.60	0.53	0.04	**Cu**	0.66	1.01	0.77	0.10	**Cu**	0.51	0.79	0.70	0.08	**Cu**	0.62	0.90	0.74	0.09
Zn	0.00	0.00	0.00	0.00	**Zn**	0.00	0.00	0.00	0.00	**Zn**	0.00	0.04	0.04	0.00	**Zn**	0.00	0.00	0.00	0.00
Fe	0.06	0.09	0.08	0.01	**Fe**	0.09	0.19	0.14	0.03	**Fe**	0.07	0.14	0.11	0.02	**Fe**	0.01	0.25	0.18	0.07
Ti	0.00	0.00	0.00	0.00	**Ti**	0.00	0.00	0.00	0.00	**Ti**	0.00	0.00	0.00	0.00	**Ti**	0.00	0.00	0.00	0.00
Mg	0.00	0.00	0.00	0.00	**Mg**	0.00	0.02	0.02	0.00	**Mg**	0.00	0.00	0.00	0.00	**Mg**	0.00	0.02	0.02	0.00
Ca	0.00	0.01	0.01	0.00	**Ca**	0.00	0.03	0.02	0.01	**Ca**	0.00	0.01	0.01	0.00	**Ca**	0.01	0.03	0.02	0.01
Mn	0.00	0.00	0.00	0.00	**Mn**	0.00	0.00	0.00	0.00	**Mn**	0.00	0.00	0.00	0.00	**Mn**	0.00	0.00	0.00	0.00
K	0.00	0.02	0.01	0.00	**K**	0.00	0.02	0.01	0.00	**K**	0.00	0.01	0.01	0.00	**K**	0.00	0.02	0.01	0.01
Si	0.00	0.00	0.00	0.00	**Si**	0.00	0.02	0.01	0.00	**Si**	0.00	0.00	0.00	0.00	**Si**	0.00	0.02	0.01	0.00
Al	4.34	5.59	4.85	0.40	**Al**	5.43	6.25	5.76	0.25	**Al**	5.33	6.41	5.81	0.38	**Al**	4.50	5.20	4.85	0.27
P	2.86	3.29	3.05	1.30	**P**	3.30	4.08	3.56	0.20	**P**	3.39	3.86	3.66	0.15	**P**	2.89	3.20	3.05	0.11
H*	21.43	27.31	24.89	1.84	**H***	14.33	21.45	18.87	1.83	**H***	15.80	21.26	18.49	1.58	**H***	21.85	25.73	24.01	1.15
Total	30.95	35.09	33.409	1.3	**Total**	25.84	31	29.138	1.33	**Total**	26.94	30.81	28.778	1.12	**Total**	31.42	34.12	32.872	0.79

*H2O determined by the difference of Total from 100

Cations calculated based on molecular formula of turquoise with 28 oxygen

Hachita Mine

TM91					TM95					TM102					TM109				
n=9	**MIN**	**MAX**	**AVG**	**STD**	n=12	**MIN**	**MAX**	**AVG**	**STD**	n=9	**MIN**	**MAX**	**AVG**	**STD**	n=12	**MIN**	**MAX**	**AVG**	**STD**
CuO	7.54	9.20	8.32	0.61	**CuO**	6.58	8.09	7.14	0.51	**CuO**	5.47	8.51	7.27	0.97	**CuO**	6.21	8.09	7.67	0.52
ZnO	0.00	0.00	0.00	0.00	**ZnO**	0.00	0.00	0.00	0.00	**ZnO**	0.00	0.05	0.05	0.00	**ZnO**	0.00	0.14	0.09	0.07
Fe2O3	0.68	1.41	1.00	0.26	**Fe2O3**	1.79	2.95	2.34	0.33	**Fe2O3**	1.54	1.87	1.73	0.11	**Fe2O3**	0.32	1.74	1.33	0.37
TiO2	0.00	0.00	0.00	0.00	**TiO2**	0.00	0.00	0.00	0.00	**TiO2**	0.00	0.00	0.00	0.00	**TiO2**	0.00	0.00	0.00	0.00
MgO	0.00	0.00	0.00	0.00	**MgO**	0.00	0.16	0.14	0.04	**MgO**	0.00	0.00	0.00	0.00	**MgO**	0.00	0.00	0.00	0.00
CaO	0.00	0.09	0.08	0.01	**CaO**	0.00	0.20	0.14	0.04	**CaO**	0.56	0.74	0.66	0.07	**CaO**	0.00	0.14	0.11	0.02
MnO	0.00	0.17	0.17	0.00	**MnO**	0.00	0.00	0.00	0.00	**MnO**	0.00	0.00	0.00	0.00	**MnO**	0.00	0.00	0.00	0.00
K2O	0.00	0.09	0.07	0.01	**K2O**	0.00	0.11	0.08	0.02	**K2O**	0.17	0.27	0.22	0.03	**K2O**	0.00	0.11	0.09	0.04
SiO2	0.00	0.17	0.13	0.03	**SiO2**	0.31	0.88	0.52	0.16	**SiO2**	4.25	6.70	6.06	0.76	**SiO2**	0.00	0.18	0.13	0.03
Al2O3	34.26	38.62	37.12	1.25	**Al2O3**	33.61	37.59	35.44	1.59	**Al2O3**	32.00	35.69	33.72	1.37	**Al2O3**	33.15	38.70	36.26	2.13
P2O5	29.70	34.52	32.37	1.77	**P2O5**	29.84	32.14	31.29	0.71	**P2O5**	27.20	31.36	29.16	1.32	**P2O5**	29.15	33.00	30.98	1.54
Total	72.49	83.02	79.02	3.23	**Total**	74.78	79.75	76.94	1.66	**Total**	75.05	82.22	78.83	2.72	**Total**	71.77	80.90	76.52	3.75
H2O*	16.98	27.51	20.98	3.23	**H2O***	20.25	25.22	23.07	1.66	**H2O***	17.78	24.95	21.17	2.72	**H2O***	19.10	28.23	23.48	3.75
TOTAL	100.00	100.00	100.00	0.00	**TOTAL**	100.00	100.00	100.00	0.00	**TOTAL**	100.00	100.00	100.00	0.00	**TOTAL**	100.00	100.00	100.00	0.00
28 O					**28 O**					**28 O**					**28 O**				
Cu	0.72	0.95	0.83	0.08	**Cu**	0.64	0.80	0.70	0.05	**Cu**	0.53	0.87	0.73	0.10	**Cu**	0.59	0.82	0.75	0.06
Zn	0.00	0.00	0.00	0.00	**Zn**	0.00	0.00	0.00	0.00	**Zn**	0.00	0.00	0.00	0.00	**Zn**	0.00	0.01	0.01	0.00
Fe	0.07	0.14	0.10	0.03	**Fe**	0.17	0.29	0.23	0.03	**Fe**	0.16	0.19	0.17	0.01	**Fe**	0.10	0.18	0.14	0.02
Ti	0.00	0.00	0.00	0.00	**Ti**	0.00	0.00	0.00	0.00	**Ti**	0.00	0.00	0.00	0.00	**Ti**	0.00	0.00	0.00	0.00
Mg	0.00	0.00	0.00	0.00	**Mg**	0.00	0.03	0.03	0.01	**Mg**	0.00	0.00	0.00	0.00	**Mg**	0.00	0.00	0.00	0.00
Ca	0.00	0.01	0.01	0.00	**Ca**	0.00	0.03	0.02	0.01	**Ca**	0.08	0.11	0.09	0.01	**Ca**	0.00	0.02	0.02	0.01
Mn	0.00	0.02	0.02	0.00	**Mn**	0.00	0.00	0.00	0.00	**Mn**	0.00	0.00	0.00	0.00	**Mn**	0.00	0.00	0.00	0.00
K	0.00	0.01	0.01	0.00	**K**	0.00	0.02	0.01	0.00	**K**	0.03	0.05	0.04	0.01	**K**	0.00	0.02	0.02	0.01
Si	0.00	0.02	0.02	0.00	**Si**	0.04	0.11	0.07	0.02	**Si**	0.54	0.88	0.80	0.11	**Si**	0.00	0.02	0.02	0.00
Al	5.09	6.21	5.79	0.32	**Al**	5.06	5.85	5.44	0.30	**Al**	4.89	5.66	5.24	0.31	**Al**	4.91	6.12	5.56	0.46
P	3.17	3.96	3.62	0.27	**P**	3.27	3.60	3.45	0.09	**P**	2.98	3.51	3.26	0.18	**P**	3.11	3.71	3.41	0.25
H*	15.48	23.14	18.46	2.38	**H***	17.95	21.47	20.03	1.21	**H***	16.14	21.21	18.59	2.01	**H***	17.11	23.51	20.24	2.66
Total	26.69	32.22	28.83	1.74	**Total**	28.46	30.93	29.942	0.85	**Total**	27.23	30.75	28.92	1.45	**Total**	27.92	32.48	30.124	1.9

*H2O determined by the difference of Total from 100

Cations calculated based on molecular formula of turquoise with 28 oxygen

Hachita Mine

Hachita Mine

TM115					TM118					TM127				
n=9	**MIN**	**MAX**	**AVG**	**STD**	n=10	**MIN**	**MAX**	**AVG**	**STD**	n=5	**MIN**	**MAX**	**AVG**	**STD**
CuO	6.54	8.30	7.11	0.52	**CuO**	7.11	8.90	7.69	0.55	**CuO**	5.16	6.15	5.49	0.40
ZnO	0.00	0.00	0.00	0.00	**ZnO**	0.00	0.00	0.00	0.00	**ZnO**	0.00	0.05	0.05	0.00
Fe2O3	1.86	2.70	2.18	0.25	**Fe2O3**	1.89	2.44	2.25	0.16	**Fe2O3**	3.44	3.95	3.75	0.21
TiO2	0.00	0.13	0.13	0.00	**TiO2**	0.00	0.00	0.00	0.00	**TiO2**	0.00	0.13	0.13	0.00
MgO	0.00	0.00	0.00	0.00	**MgO**	0.00	0.17	0.17	0.00	**MgO**	0.00	0.00	0.00	0.00
CaO	0.00	0.00	0.00	0.00	**CaO**	0.00	0.10	0.10	0.00	**CaO**	0.18	0.25	0.21	0.03
MnO	0.00	0.00	0.00	0.00	**MnO**	0.00	0.00	0.00	0.00	**MnO**	0.00	0.00	0.00	0.00
K2O	0.00	0.10	0.10	0.00	**K2O**	0.00	0.08	0.07	0.01	**K2O**	0.00	0.13	0.10	0.03
SiO2	0.00	0.11	0.11	0.01	**SiO2**	0.00	0.24	0.16	0.05	**SiO2**	5.84	15.66	9.10	4.03
Al2O3	31.40	37.71	34.18	2.19	**Al2O3**	32.44	38.67	35.32	2.19	**Al2O3**	33.03	35.68	34.46	1.26
P2O5	28.80	30.92	29.79	0.62	**P2O5**	29.85	33.24	31.35	1.15	**P2O5**	21.07	28.38	25.42	3.01
Total	70.39	77.12	73.30	2.17	**Total**	71.99	83.07	76.80	3.53	**Total**	76.05	81.80	78.53	2.46
H2O*	22.88	29.61	26.70	2.17	**H2O***	16.93	28.01	23.20	3.53	**H2O***	18.20	23.95	21.47	2.46
TOTAL	100.00	100.00	100.00	0.00	**TOTAL**	100.00	100.00	100.00	0.00	**TOTAL**	100.00	100.00	100.00	0.00
28 O					**28 O**					**28 O**				
Cu	0.61	0.80	0.68	0.05	**Cu**	0.68	0.92	0.76	0.07	**Cu**	0.51	0.62	0.54	0.04
Zn	0.00	0.00	0.00	0.00	**Zn**	0.00	0.00	0.00	0.00	**Zn**	0.00	0.00	0.00	0.00
Fe	0.18	0.25	0.21	0.02	**Fe**	0.18	0.24	0.22	0.02	**Fe**	0.33	0.40	0.37	0.03
Ti	0.00	0.01	0.01	0.00	**Ti**	0.00	0.00	0.00	0.00	**Ti**	0.00	0.01	0.01	0.00
Mg	0.00	0.00	0.00	0.00	**Mg**	0.00	0.03	0.03	0.00	**Mg**	0.00	0.00	0.00	0.00
Ca	0.00	0.00	0.00	0.00	**Ca**	0.00	0.01	0.01	0.00	**Ca**	0.02	0.03	0.03	0.00
Mn	0.00	0.00	0.00	0.00	**Mn**	0.00	0.00	0.00	0.00	**Mn**	0.00	0.00	0.00	0.00
K	0.00	0.02	0.02	0.00	**K**	0.00	0.01	0.01	0.00	**K**	0.00	0.02	0.01	0.01
Si	0.00	0.01	0.01	0.00	**Si**	0.00	0.03	0.02	0.01	**Si**	0.75	2.10	1.20	0.55
Al	4.60	5.79	5.12	0.41	**Al**	4.81	6.24	5.43	0.48	**Al**	5.03	5.65	5.33	0.28
P	3.09	3.35	3.20	0.09	**P**	3.21	3.82	3.46	0.21	**P**	2.40	3.20	2.83	0.31
H*	19.89	24.57	22.61	1.50	**H***	15.48	25.53	20.32	2.93	**H***	16.33	20.59	18.79	1.82
Total	29.91	33.16	31.833	1.04	**Total**	26.72	34.44	30.224	2.2	**Total**	27.44	30.31	29.104	1.25

*H2O determined by the difference of Total from 100

Cations calculated based on molecular formula of turquoise with 28 oxygen

RH9					RH10					RH13				
n=18	**MIN**	**MAX**	**AVG**	**STD**	n=13	**MIN**	**MAX**	**AVG**	**STD**	n=12	**MIN**	**MAX**	**AVG**	**STD**
CuO	5.74	8.46	7.09	0.77	**CuO**	6.64	8.25	7.42	0.56	**CuO**	5.83	7.11	6.46	0.34
ZnO	0.00	0.00	0.00	0.00	**ZnO**	0.00	0.00	0.00	0.00	**ZnO**	0.00	0.00	0.00	0.00
Fe2O3	8.44	14.75	10.36	1.53	**Fe2O3**	7.76	10.83	9.14	0.86	**Fe2O3**	11.13	16.53	13.76	1.65
TiO2	0.39	0.59	0.49	0.06	**TiO2**	0.46	0.64	0.53	0.06	**TiO2**	0.97	1.30	1.16	0.09
MgO	0.00	0.00	0.00	0.00	**MgO**	0.00	0.00	0.00	0.00	**MgO**	0.00	0.00	0.00	0.00
CaO	0.00	0.00	0.00	0.00	**CaO**	0.00	0.07	0.07	0.00	**CaO**	0.00	0.00	0.00	0.00
MnO	0.00	0.05	0.05	0.00	**MnO**	0.00	0.00	0.00	0.00	**MnO**	0.00	0.00	0.00	0.00
K2O	0.07	0.17	0.12	0.03	**K2O**	0.13	0.23	0.18	0.03	**K2O**	0.09	0.26	0.18	0.05
SiO2	0.00	0.12	0.11	0.01	**SiO2**	0.00	0.12	0.11	0.02	**SiO2**	0.00	0.00	0.00	0.00
Al2O3	27.25	32.34	29.65	1.52	**Al2O3**	29.50	33.62	31.39	1.23	**Al2O3**	25.22	29.37	27.05	1.33
P2O5	28.82	33.39	30.84	1.12	**P2O5**	29.23	32.18	30.75	0.78	**P2O5**	28.89	30.98	29.75	0.63
Total	74.64	83.57	78.64	2.40	**Total**	77.30	81.25	79.43	1.35	**Total**	75.99	81.38	78.36	1.56
H2O*	16.43	25.36	21.36	2.40	**H2O***	18.75	22.70	20.57	1.35	**H2O***	18.62	24.01	21.64	1.56
TOTAL	100.00	100.00	100.00	0.00	**TOTAL**	100.00	100.00	100.00	0.00	**TOTAL**	100.00	100.00	100.00	0.00
28 O					**28 O**					**28 O**				
Cu	0.57	0.88	0.73	0.09	**Cu**	0.67	0.85	0.76	0.06	**Cu**	0.59	0.74	0.67	0.04
Zn	0.00	0.00	0.00	0.00	**Zn**	0.00	0.00	0.00	0.00	**Zn**	0.00	0.00	0.00	0.00
Fe	0.85	1.53	1.06	0.17	**Fe**	0.78	1.12	0.93	0.09	**Fe**	1.14	1.74	1.42	0.19
Ti	0.04	0.06	0.05	0.01	**Ti**	0.05	0.06	0.05	0.00	**Ti**	0.10	0.13	0.12	0.01
Mg	0.00	0.00	0.00	0.00	**Mg**	0.00	0.00	0.00	0.00	**Mg**	0.00	0.00	0.00	0.00
Ca	0.00	0.00	0.00	0.00	**Ca**	0.00	0.01	0.01	0.00	**Ca**	0.00	0.00	0.00	0.00
Mn	0.00	0.01	0.01	0.00	**Mn**	0.00	0.00	0.00	0.00	**Mn**	0.00	0.00	0.00	0.00
K	0.00	0.03	0.02	0.01	**K**	0.02	0.04	0.03	0.01	**K**	0.02	0.05	0.03	0.01
Si	0.00	0.02	0.02	0.01	**Si**	0.00	0.02	0.02	0.01	**Si**	0.00	0.00	0.00	0.00
Al	4.31	5.37	4.73	0.30	**Al**	4.68	5.39	5.03	0.23	**Al**	4.04	4.70	4.35	0.22
P	3.25	3.80	3.54	0.16	**P**	3.33	3.69	3.54	0.10	**P**	3.28	3.58	3.44	0.10
H*	15.48	22.03	19.28	1.73	**H***	17.33	20.38	18.65	1.03	**H***	17.44	21.34	19.69	1.12
Total	26.74	31.28	29.412	1.22	**Total**	28.02	30.28	28.995	0.74	**Total**	28.12	30.86	29.708	0.79

*H2O determined by the difference of Total from 100

Cations calculated based on molecular formula of turquoise with 28 oxygen

RH16					**RH17**					**RH19**				
n=7	**MIN**	**MAX**	**AVG**	**STD**	n=7	**MIN**	**MAX**	**AVG**	**STD**	n=12	**MIN**	**MAX**	**AVG**	**STD**
CuO	6.65	8.23	7.75	0.56	**CuO**	7.02	8.54	8.03	0.50	**CuO**	7.18	8.70	8.07	0.48
ZnO	0.00	0.00	0.00	0.00	**ZnO**	0	0.00	0.00	0.00	**ZnO**	0.00	0.00	0.00	0.00
Fe2O3	8.19	12.84	10.74	1.76	**Fe2O3**	4.58	9.04	6.50	1.58	**Fe2O3**	10.16	13.16	11.57	1.00
TiO2	1.00	1.46	1.21	0.17	**TiO2**	0.5	1.06	0.78	0.22	**TiO2**	0.43	0.94	0.69	0.15
MgO	0.00	0.00	0.00	0.00	**MgO**	0	0.00	0.00	0.00	**MgO**	0.00	0.00	0.00	0.00
CaO	0.00	0.00	0.00	0.00	**CaO**	0	0.00	0.00	0.00	**CaO**	0.00	0.07	0.07	0.01
MnO	0.00	0.00	0.00	0.00	**MnO**	0	0.00	0.00	0.00	**MnO**	0.00	0.00	0.00	0.00
K2O	0.07	0.21	0.12	0.05	**K2O**	0.08	0.13	0.10	0.02	**K2O**	0.11	0.25	0.15	0.04
SiO2	0.00	0.00	0.00	0.00	**SiO2**	0	0.00	0.00	0.00	**SiO2**	0.00	0.10	0.10	0.00
Al2O3	28.60	32.89	30.06	1.42	**Al2O3**	32.04	34.39	33.23	0.95	**Al2O3**	27.45	31.25	29.78	1.29
P2O5	29.18	32.45	30.95	1.08	**P2O5**	32.13	35.16	33.78	0.91	**P2O5**	30.51	34.48	32.30	1.14
Total	78.76	82.46	80.83	1.21	**Total**	80.07	85.31	82.44	1.73	**Total**	79.98	87.03	82.57	2.20
H2O*	17.54	21.24	19.17	1.21	**H2O***	14.69	19.93	17.56	1.73	**H2O***	12.97	20.02	17.43	2.20
TOTAL	100.00	100.00	100.00	0.00	**TOTAL**	100	100.00	100.00	0.00	**TOTAL**	100.00	100.00	100.00	0.00
28 O					**28 O**					**28 O**				
Cu	0.69	0.86	0.81	0.06	**Cu**	0.71	0.90	0.84	0.06	**Cu**	0.75	0.92	0.86	0.06
Zn	0.00	0.00	0.00	0.00	**Zn**	0	0.00	0.00	0.00	**Zn**	0.00	0.00	0.00	0.00
Fe	0.85	1.36	1.12	0.19	**Fe**	0.46	0.96	0.68	0.18	**Fe**	1.05	1.41	1.22	0.12
Ti	0.10	0.15	0.12	0.02	**Ti**	0.05	0.11	0.08	0.02	**Ti**	0.04	0.10	0.07	0.02
Mg	0.00	0.00	0.00	0.00	**Mg**	0	0.00	0.00	0.00	**Mg**	0.00	0.00	0.00	0.00
Ca	0.00	0.00	0.00	0.00	**Ca**	0	0.00	0.00	0.00	**Ca**	0.00	0.01	0.01	0.00
Mn	0.00	0.00	0.00	0.00	**Mn**	0	0.00	0.00	0.00	**Mn**	0.00	0.00	0.00	0.00
K	0.01	0.04	0.02	0.01	**K**	0.01	0.02	0.00	0.00	**K**	0.02	0.04	0.03	0.01
Si	0.00	0.00	0.00	0.00	**Si**	0	0.00	0.00	0.00	**Si**	0.00	0.01	0.01	0.00
Al	4.59	5.36	4.90	0.26	**Al**	5.14	5.64	5.39	0.20	**Al**	4.49	5.26	4.93	0.26
P	3.47	3.80	3.62	0.11	**P**	3.77	4.07	3.94	0.12	**P**	3.59	4.25	3.84	0.19
H*	16.20	19.30	17.69	0.97	**H***	13.91	17.78	16.11	1.29	**H***	12.61	18.49	16.30	1.79
Total	27.15	29.44	28.283	0.7	**Total**	25.51	28.22	27.043	0.89	**Total**	24.53	28.89	27.253	1.31

*H2O determined by the difference of Total from 100

Cations calculated based on molecular formula of turquoise with 28 oxygen

CH22					**CH23**					**CH27**			
n=12	**MIN**	**MAX**	**AVG**	**STD**	n=3	**MIN**	**MAX**	**AVG**	**STD**	n=9	**MIN**	**MAX**	**AVG**
CuO	6.52	7.93	7.04	0.45	**CuO**	6.65	6.83	6.74	0.09	**CuO**	5.57	7.18	6.49
ZnO	0.00	0.40	0.36	0.04	**ZnO**	0.45	0.51	0.48	0.03	**ZnO**	0.00	1.00	0.11
Fe2O3	0.62	1.00	0.77	0.13	**Fe2O3**	1.83	2.04	1.94	0.11	**Fe2O3**	0.47	0.26	0.71
TiO2	0.00	0.13	0.11	0.03	**TiO2**	0.00	0.00	0.00	0.00	**TiO2**	0.12	0.07	0.20
MgO	0.00	0.16	0.09	0.03	**MgO**	0.18	0.27	0.22	0.05	**MgO**	0.00	0.29	0.06
CaO	0.29	0.54	0.37	0.08	**CaO**	0.70	0.77	0.73	0.04	**CaO**	0.21	0.29	0.25
SiO2	6.67	7.60	7.19	0.28	**SiO2**	9.48	9.79	9.66	0.16	**SiO2**	1.44	1.70	1.58
Al2O3	32.80	38.44	35.83	1.90	**Al2O3**	33.21	36.47	34.31	1.87	**Al2O3**	31.29	36.58	34.11
P2O5	29.17	33.14	30.46	1.14	**P2O5**	29.86	30.68	30.23	0.41	**P2O5**	29.33	31.77	30.72
Total	77.11	86.01	81.92	2.64	**Total**	87.19	87.70	87.45	0.25	**Total**	69.35	77.63	74.09
H2O*	13.99	22.89	18.09	2.64	**H2O***	12.30	12.81	12.55	0.25	**H2O**	22.37	30.65	25.91
TOTAL	100.00	100.00	100.00	0.00	**TOTAL**	100.00	100.00	100.00	0.00	**TOTAL**	100.00	100.00	100.00
28 O					**28 O**					**28 O**			
Cu	0.64	0.83	0.71	0.06	**Cu**	0.68	0.72	0.70	0.02	**Cu**	0.51	0.69	0.62
Zn	0.00	0.04	0.03	0.01	**Zn**	0.05	0.05	0.05	0.00	**Zn**	0.00	0.01	0.01
Fe	0.06	0.10	0.08	0.01	**Fe**	0.19	0.21	0.20	0.01	**Fe**	0.04	0.09	0.07
Ti	0.00	0.01	0.01	0.00	**Ti**	0.00	0.00	0.00	0.00	**Ti**	0.01	0.02	0.02
Mg	0.00	0.03	0.02	0.01	**Mg**	0.04	0.05	0.04	0.01	**Mg**	0.00	0.01	0.01
Ca	0.04	0.08	0.05	0.01	**Ca**	0.10	0.11	0.11	0.01	**Ca**	0.03	0.04	0.03
Si	0.87	1.05	0.96	0.05	**Si**	1.31	1.32	1.32	0.01	**Si**	0.18	0.21	0.20
Al	4.99	6.22	5.65	0.39	**Al**	5.30	5.96	5.53	0.38	**Al**	4.51	5.59	5.09
P	3.20	3.86	3.45	0.17	**P**	3.42	3.54	3.50	0.07	**P**	3.05	3.49	3.29
H*	12.87	19.72	16.11	2.04	**H***	12.74	15.41	14.28	1.38	**H***	19.37	25.01	21.86
Total	24.63	29.61	27.05	1.46	**Total**	24.67	26.52	25.72	0.95	**Total**	29.42	33.42	31.19

*H2O determined by the difference of Total from 100

Cations calculated based on molecular formula of turquoise with 28 oxygen

Chalchihuitl
Mine

CH28					**CH34**				
n=12	**MIN**	**MAX**	**AVG**	**STD**	n=9	**MIN**	**MAX**	**AVG**	**STD**
CuO	6.63	7.33	6.96	0.24	**CuO**	3.88	5.12	4.46	0.39
ZnO	0.00	0.34	0.28	0.08	**ZnO**	0.00	0.00	0.00	0.00
Fe2O3	0.81	1.33	1.10	0.14	**Fe2O3**	2.09	3.72	2.71	0.51
TiO2	0.20	0.38	0.28	0.06	**TiO2**	0.14	0.28	0.19	0.05
MgO	0.08	0.16	0.13	0.03	**MgO**	0.18	0.30	0.23	0.04
CaO	0.41	0.59	0.51	0.06	**CaO**	0.76	0.92	0.83	0.06
SiO2	4.51	8.23	6.55	1.03	**SiO2**	3.65	9.73	6.46	2.34
Al2O3	32.69	35.62	34.25	0.75	**Al2O3**	32.82	35.32	33.87	0.69
P2O5	29.84	31.61	30.83	0.53	**P2O5**	30.09	33.41	31.81	1.17
Total	79.87	82.18	80.70	0.76	**Total**	78.57	82.08	80.57	1.21
H2O*	17.82	20.13	19.31	0.76	**H2O***	17.92	21.43	19.43	1.21
TOTAL	100.00	100.00	100.00	0.00	**TOTAL**	100.00	100.00	100.00	0.00
28 O					**28 O**				
Cu	0.67	0.74	0.70	0.02	**Cu**	0.38	0.50	0.44	0.04
Zn	0.00	0.03	0.03	0.00	**Zn**	0.00	0.00	0.00	0.00
Fe	0.08	0.13	0.11	0.02	**Fe**	0.20	0.37	0.27	0.05
Ti	0.02	0.04	0.03	0.01	**Ti**	0.01	0.03	0.02	0.01
Mg	0.02	0.03	0.03	0.01	**Mg**	0.03	0.06	0.05	0.01
Ca	0.06	0.09	0.07	0.01	**Ca**	0.11	0.13	0.12	0.01
Si	0.60	1.08	0.87	0.14	**Si**	0.48	1.29	0.85	0.31
Al	5.08	5.59	5.36	0.14	**Al**	5.10	5.49	5.25	0.11
P	3.33	3.56	3.46	0.07	**P**	3.36	3.71	3.54	0.12
H*	15.95	17.71	17.10	0.59	**H***	15.91	18.54	17.05	0.92
Total	26.89	28.15	27.72	0.42	**Total**	26.79	28.68	27.59	0.68

*H2O determined by the difference of Total from 100
Cations calculated based on molecular formula of turquoise with 28 oxygen

TF39					**TF44**					**TF46**				
n=12	**MIN**	**MAX**	**AVG**	**STD**	n=12	**MIN**	**MAX**	**AVG**	**STD**	n=12	**MIN**	**MAX**	**AVG**	**STD**
CuO	6.91	7.94	7.50	0.29	**CuO**	7.39	8.16	7.70	0.27	**CuO**	7.13	7.80	7.48	0.22
ZnO	0.00	0.00	0.00	0.00	**ZnO**	0.00	0.00	0.00	0.00	**ZnO**	0.00	0.51	0.43	0.07
TiO2	0.11	0.23	0.18	0.04	**Fe2O3**	0.74	1.18	0.91	0.13	**Fe2O3**	1.54	2.20	1.92	0.21
Fe2O3	0.87	1.46	1.16	0.17	**TiO2**	0.22	0.37	0.30	0.05	**TiO2**	0.00	0.00	0.00	0.00
MgO	0.00	0.05	0.05	0.00	**MgO**	0.00	0.00	0.00	0.00	**MgO**	0.00	0.04	0.04	0.00
CaO	0.12	0.19	0.16	0.02	**CaO**	0.10	0.18	0.15	0.02	**CaO**	0.12	0.18	0.15	0.02
SiO2	0.29	0.46	0.36	0.05	**SiO2**	0.00	0.14	0.11	0.02	**SiO2**	0.13	0.26	0.20	0.05
Al2O3	34.53	38.48	36.57	1.57	**Al2O3**	35.56	38.03	36.86	0.99	**Al2O3**	35.21	37.41	36.20	0.79
P2O5	32.78	35.17	33.90	0.73	**P2O5**	32.28	34.95	33.54	0.84	**P2O5**	33.02	35.03	33.69	0.66
Total	77.26	83.26	79.82	1.97	**Total**	77.96	82.47	79.56	1.19	**Total**	77.94	81.45	79.88	1.09
H2O*	16.74	22.74	20.18	1.97	**H2O***	17.53	22.04	20.44	1.19	**H2O***	18.55	22.06	20.12	1.09
TOTAL	100.00	100.00	100.00	0.00	**TOTAL**	100.00	100.00	100.00	0.00	**TOTAL**	100.00	100.00	100.00	0.00
28 O					**28 O**					**28 O**				
Cu	0.70	0.81	0.75	0.03	**Cu**	0.73	0.82	0.77	0.03	**Cu**	0.71	0.79	0.75	0.02
Zn	0.00	0.00	0.00	0.00	**Zn**	0.00	0.00	0.00	0.00	**Zn**	0.00	0.05	0.04	0.01
Fe	0.09	0.14	0.12	0.02	**Fe**	0.07	0.12	0.09	0.01	**Fe**	0.15	0.22	0.19	0.02
Ti	0.01	0.02	0.02	0.00	**Ti**	0.02	0.04	0.03	0.01	**Ti**	0.00	0.00	0.00	0.00
Mg	0.00	0.01	0.01	0.00	**Mg**	0.00	0.00	0.00	0.00	**Mg**	0.00	0.01	0.01	0.00
Ca	0.02	0.03	0.02	0.00	**Ca**	0.01	0.03	0.02	0.00	**Ca**	0.02	0.03	0.02	0.00
Si	0.04	0.06	0.05	0.01	**Si**	0.00	0.02	0.02	0.01	**Si**	0.02	0.03	0.03	0.01
Al	5.31	6.15	5.70	0.32	**Al**	5.49	6.03	5.74	0.19	**Al**	5.43	5.90	5.66	0.16
P	3.61	4.01	3.79	0.12	**P**	3.59	3.99	3.75	0.11	**P**	3.66	3.95	3.79	0.09
H*	15.17	19.72	17.78	1.50	**H***	15.79	19.21	18.01	0.91	**H***	16.58	19.26	17.82	0.82
Total	26.36	29.62	28.22	1.06	**Total**	26.80	29.28	28.42	0.66	**Total**	27.35	29.31	28.28	0.59

*H2O determined by the difference of Total from 100

Cations calculated based on molecular formula of turquoise with 28 oxygen

TF47					**TF49**				
n=12	**MIN**	**MAX**	**AVG**	**STD**	n=12	**MIN**	**MAX**	**AVG**	**STD**
CuO	7.65	8.42	8.00	0.27	**CuO**	8.01	8.74	8.36	0.25
ZnO	0.00	0.00	0.00	0.00	**ZnO**	0.00	0.00	0.00	0.00
Fe2O3	0.45	1.04	0.71	0.18	**Fe2O3**	0.93	1.75	1.26	0.31
TiO2	0.00	0.66	0.41	0.18	**SiO2**	0.00	0.11	0.09	0.02
MgO	0.00	0.07	0.07	0.00	**TiO2**	0.00	0.00	0.00	0.00
CaO	0.14	0.32	0.21	0.06	**MgO**	0.00	0.00	0.00	0.00
SiO2	0.24	0.77	0.45	0.17	**CaO**	0.10	0.15	0.12	0.02
Al2O3	35.66	38.70	37.03	1.31	**Al2O3**	35.74	38.40	36.92	1.01
P2O5	32.29	34.63	33.38	0.79	**P2O5**	32.94	34.25	33.57	0.46
Total	77.64	83.12	80.09	1.75	**Total**	78.40	81.69	80.25	1.02
H2O*	16.88	22.36	19.91	1.75	**H2O***	18.31	21.60	19.75	1.02
TOTAL	100.00	100.00	100.00	0.00	**TOTAL**	100.00	100.00	100.00	0.00
28 O					**28 O**				
Cu	0.76	0.86	0.80	0.03	**Cu**	0.80	0.89	0.84	0.03
Zn	0.00	0.00	0.00	0.00	**Zn**	0.00	0.00	0.00	0.00
Fe	0.04	0.10	0.07	0.02	**Fe**	0.09	0.18	0.13	0.03
Ti	0.00	0.07	0.04	0.02	**Ti**	0.00	0.00	0.00	0.00
Mg	0.00	0.01	0.01	0.00	**Mg**	0.00	0.00	0.00	0.00
Ca	0.02	0.05	0.03	0.01	**Ca**	0.01	0.02	0.02	0.00
Si	0.03	0.10	0.06	0.02	**Si**	0.00	0.01	0.01	0.00
Al	5.49	6.19	5.79	0.28	**Al**	5.57	6.08	5.80	0.20
P	3.57	3.94	3.75	0.12	**P**	3.69	3.91	3.79	0.06
H*	15.31	19.49	17.62	1.33	**H***	16.47	18.92	17.56	0.77
Total	26.50	29.52	28.16	0.96	**Total**	27.36	29.09	28.13	0.53

*H2O determined by the difference of Total from 100

Cations calculated based on molecular formula of turquoise with 28 oxygen

Separation of Microprobe Analyses of Homogeneous Turquoise Minerals

Numerical values = number of times that type of material was analyzed from the sample. (If the "Homogeneous" column is blank and a value appears in another for that sample area, those analyses were not included in averages of homogeneous material, i.e., they were not turquoise minerals.) X = identified within turquoise minerals of that sample.

Sample	Areas analyzed	Homogeneous	Variable density	Vein-like network	Inclusions	High-Fe	Notes
			Observed light/dark patches in images	Light/Dense veinlets w/in dark/light material	(other than high-Fe)	inclusions or data	Numbers in parentheses equal the # of analyses from that sample with measurable amounts of element unless otherwise indicated.
Hachita							
TM57	Area 1, 2, 3, 4	12	X				K (5), Ca (1)
TM66	Area 1, 2, 3, 4	13					Si (8), Ca (12), (Mg 1)
TM68	Area 1, 2, 3, 4	11					K (7), Ca (1), Zn (1)
TM70	Area 1, 2, 3	9					Ca (9), Si (5), K (4), Mg (2) Fe ~2%, low P
TM91	Area 1, 2, 3	9	X				K (7), Ca (3), Si (8) Subtle image variation (Area 2)
TM95	Area 1, 2, 3, 4	12					Si (12), K (10), Ca (9), Mg (2) Fe ~2%
TM102	Area 1, 2, 3	9	X	X			High Si (9), K (9), Ca (9), Zn (1) Low P, weathering (higher Fe?) between the homogeneous patches
TM109	Area 1, 2, 3	12					Si (9), Ca (7), K (2), Zn (2)
TM114	Area 1, 2, 3		X			9	High Fe ~14-17%, Si ~2-7%, K (9), Ca (9), Mg (6), Ti (7) Low P, low Al, weathering between the homogeneous patches
TM115	Area 1, 2, 3	9					Ti (1), Si (2), Fe ~2%, low end of P range for turquoises
TM118	Area 1,2	10					Si (8), K (5), Mg (1) Ca (1) Fe ~2%
TM127	Area 1	5					Spherules, Fe ~3%, Si ~5-15%, K (3), Ca (5), Ti (1), Zn (1), Low P
	Area 2					4	Inclusions in spherule center, High Fe ~15-25%, low P & Al, Si (4), Ca (4), Ti (2)
	Area 3		3				Clay area btwn spherules, High Al & Si, no Cu, no or low P, low Fe, Ca (3), Mg (1)
TOTAL		111	3			4	127

Sample	Areas analyzed	Homogeneous	Variable density	Vein-like network	Inclusions	High-Fe	Notes
			Observed light/dark patches in images	Light/Dense veinlets w/in dark/light material	(other than high-Fe)	inclusions or data	Numbers in parentheses equal the # of analyses from that sample with measurable amounts of element unless otherwise indicated.
Red Hill							
RH9	substandard	18	X	X			Ti (18), K (18), Si (4), Mn (2), Fe ~9-11% Weathering between the homogeneous areas
RH10	Area 1,2,3,4	13					Ti (13), Ca (2), K (13), Fe ~9-10% Area 4 had higher Cu
RH13	Area 1, 1-3, 2, 3, 4	12					Fe ~ 12-15%, Ti (3), K (3)
	Area 1, 4-6			3		X	Veinlets had Ca (3), Ti (3), K (3), Si (1), higher Fe 17-23%, lower Cu, Al, P
RH16	Area 1, 1-4			4		X	veinlets had Ti (4), K (4), High Fe 15-20%, low Al & P
	Area 1, 5-8	4					Ti (4), K (4), Fe ~10-12%
	Area 2, 1-3			3		X	Veinlets had Ti (3), K (3), High Fe 19-22%, low Al & P
	Area 2, 4-6	3					Ti (3), K (3), Fe ~8-12%
RH17	Area 1, 3	7					Ti (7), K (7), Fe 5-9%
	Area 2, 4			6		X	Veinlets had Ti (6), K (5), High Fe ~12-22%, lower Al
RH19	Area 1,2, 3, 4	12	X		X		Ti (12), Ca (2), K (12), Si (1), Fe ~10-13%
TOTAL		69		16			85

			Observed light/dark patches in images	Light/Dense veinlets w/in dark/light material	(other than high-Fe)	inclusions or data	Numbers in parentheses equal the # of analyses from that sample with measurable amounts of element unless otherwise indicated.
Blue J Artifacts							
BJ1	Area 1,2,3	9			X		Si (8), Mg (3), Fe ~1.9-3%
BJ11	Area 1,2,3,4	14			X		Zn (5), Mg (4), Ca (12), K (4), Si (1), low Fe (11) ~0-.31%
	Area 5				3		Inclusions (exsolution?) High Cu ~17-18%, Zn ~3-5%, low P, low Fe ~0-.28%, Ca (3), K (3), Si (3)
BJ12(1)	Area 1,2,3	9					Ca (9), Mg (2), Si (9)
	Area 4			4		X	Veinlets had High Fe ~11.7-27%, lower Al, Ca (4), Zn (1), Si (3)
BJ12(2)	Area 1,2,3	9					Zn (4), Mg (3), Si (3), Fe ~2-3%
	Area 4					3	Inclusions in spherules Higher Fe ~8-12%, lower Al, Zn (1), Si (1)
	Area 5	3	X				Less dense zone @ spherule rim, Zn (1), Si (2), Fe ~ 2-3%
BJ12(3)	Area 1, 3, 4	12		X			Si (12), Ca (12), K (12), Fe ~ 2-3 up to 9%
	Area 2			3		X	Veinlets had High Fe ~ 31-38%, less Al, Cu, P, Si, Ca & no K
BJ21	Area 1	3				X	Fe ~ 4-5%, Si ~1.3-1.6%, Mg (3)
	Area 2, 3	6					Fe ~ 2-4%, Si ~2-3.7%, Mg (3)
BJ43	Area 1,2,3	9					Si (9), Ca (9), Fe (9) ~1%
BJ46	Area 1,2,3	9					Fe ~ 3-6%, Ca (9), Ti (4), Zn (1), Mg (1), K (1)
	Area 4, 4-1				1		Inclusion had High Cu ~18%, high Zn ~4%, low P ~25%
	Area 4, 4-2					1	Inclusion had High Fe ~32%, high Ca ~13%, low Cu, Al, P, Si ~3.8%
BJ47	Area 1,2,3	9			X	X	Si (9), Ca (9), Mg (2), Zn (1), Fe (9) ~ 1%
BJ49	Area 1,2,3	9					Si (9), Fe (1), Ti (9), Zn (5), High Mg (9) ~3-4%
	Area 4				3		Inclusions (exsolution?) High Cu ~11-20%, high Mg ~2.9-3.9%, Fe ~3-8%, Ti (3), Zn (1), Ca (3), K (3), Si (3)
	Area 5		2				Less dense area High Mg ~3-4%, no Fe, Ti (2), Ca (2), Si (2), Zn (1)
TOTAL		101	2	7	7	4	121

Sample	Areas analyzed	Homogeneous	Variable density	Vein-like network	Inclusions	High-Fe	Notes
			Observed light/dark patches in images	Light/Dense veinlets w/in dark/light material	(other than high-Fe)	inclusions or data	Numbers in parentheses equal the # of analyses from that sample with measurable amounts of element unless otherwise indicated.
Chalchihuitl					14		
CH22	Area 1, 2, 3, 5	12			X	X	Si ~6-7%, (Ca (12), Zn (5), Mg (11), Ti (2), low Fe less than 1%
	Area 4		3				Less dense zone, lower P, Si, Cu, Fe (3), Mg (3), Zn (1), Ca (3)
CH23	Area 1, 2		6	X	X	X	P low ~22-25%, high Si ~16-19%, Fe ~5-7%, Cu 4-5%, Mg (6), Ca (6), low Al ~27-29%
	Area 3	3					P 29-30%, Al 33-36%, Fe 1-2% lower Si ~9%, Mg (3), Zn(3), Ca(3)
CH26	Area 1, 2, 3		9		X	X	P low ~21-26%, Si high ~15-19%, ~Fe 4-9%, Cu ~4-5%, Al ~26-29%, Mg (9), Ca (9)
	CH26B Area 1		1				Fe ~7%, lower Si ~14%
	CH26B Area 2				1		quartz, Si ~99%
CH27	Area 1				1		quartz, Si ~98%
	Area 2, 3, 4	9					Si ~1%, Cu ~5-7%, Fe less than 1%, Ti (9), Mg (3), Zn (1), Ca (9)
CH28	Area 1, 2, 3, 4	12			X	X	Si ~4-7%, Fe ~1%, Ti (12), Mg (12), Ca (12), Zn (4)
CH34	Area 1, 3, 4	9	X		X	X	Si ~3-8%, Fe ~2-3%, Cu 3.8-5%, Ti (9), Mg (9), Ca (9)
	Area 2		2		X	X	Si ~45-65%, Al ~19-32%
CH35	Area 1, 2, 3		9			X	low Cu ~2-3%, high Ti 1.3-2.8%, not turquoise mineral
	Area 4				1		Inclusion- higher Fe~3.9%, Cu 2.2%, Ca~1%, P~35%, Al~35%
TOTAL		45	30		3		78
Tiffany							
TF39	Area 1, 2, 3, 4	12	X				Si ~.3-.4%, Fe ~1%, Ti (12) Ca (12)
TF44	Area 1, 2, 3, 4	12	X		X	X	Fe ~1%, Si 0-.14%, Ti (12), Ca (12)
TF46	Area 1, 2, 3, 4	12	X		X	X	Si .13-.26%, Fe ~1-2%, Zn (7), Ca (12,)Mg (1)
TF47	Area 1, 2	12	X		X	X	Si .24-.77%, Fe less than 1%, Ca (12), Ti (9)
TF49	Area 1, 2, 3, 4	12	X				Si (3), Fe ~1%, Ca (12)
TOTAL		60					60

Appendix H: X-ray Diffraction

```
################################################################################
###                Match! Phase Analysis Report                  ###
################################################################################

Sample  : TM 95 Bulk Powder 40mA 45kV

****************************** Sample Data ********************************

File name     : tm95.rd
File path     : e:\
Data collected: 4/3/2008 2:46:24 PM
Data range    : 2.000∞ to 60.000∞
No. of points : 2901
Step size     : 0.020
Alpha2 subtr.?: No
Backgr.subtr.?: No
Data smoothed?: Yes
Radiation     : Cu-Ka1
Wavelength    : 1.540562 A

**************************** Matched Phases ******************************

Phase A:  (Turquoise)
-------
Formula sum      : Al6 Cu H16 O28 P4
Entry number     : 96-900-8100
FoM              : 0.863266
No. of peaks     : 500
Peaks in range   : 255
Peaks matched    : 229
Int. scale fct   : 0.53
Quant. (weight %): 63.34

Phase B:  (Vermiculite)
-------
Formula sum      : Al0.721 Fe0.24 H3 Mg1.338 O9 Si1.36
Entry number     : 96-900-0061
FoM              : 0.758061
No. of peaks     : 292
```

Peaks in range : 196
Peaks matched : 124
Int. scale fct : 0.27
Quant. (weight %): 1.43

Phase C: (Faustite)

Formula sum : Al6 H16 O28 P4 Zn0.927
Entry number : 96-900-9517
FoM : 0.707390
No. of peaks : 500
Peaks in range : 253
Peaks matched : 226
Int. scale fct : 0.17
Quant. (weight %): 20.38

Phase D: (Quartz)

Formula sum : O2 Si
Entry number : 96-900-5033
FoM : 0.664250
No. of peaks : 35
Peaks in range : 13
Peaks matched : 9
Int. scale fct : 0.00
Quant. (weight %): 0.00

Phase E: (Chalcosiderite)

Formula sum : Al0.54 Cu Fe5.46 H16 O28 P4
Entry number : 96-900-9360
FoM : 0.612730
No. of peaks : 500
Peaks in range : 275
Peaks matched : 231
Int. scale fct : 0.00
Quant. (weight %): 0.00

Phase F: (Illite)

Formula sum : Al2 H2 K O12 Si4
Entry number : 96-901-3719
FoM : 0.528504
No. of peaks : 261
Peaks in range : 74

Peaks matched : 60
Int. scale fct : 0.10
Quant. (weight %): 11.05

Phase G: (Chlorite)

Formula sum : H4 Mg3 O9 Si2
Entry number : 96-900-0159
FoM : 0.443159
No. of peaks : 94
Peaks in range : 94
Peaks matched : 69
Int. scale fct : 0.03
Quant. (weight %): 3.80

Phase H: (Muscovite-2M1)

Formula sum : Al2.16 F0.58 Fe0.42 H1.42 K0.97 Li0.38 Mg0.01 Na0.02 O11.42 Rb0.01 Si3.28
Entry number : 96-900-4645
FoM : 0.384216
No. of peaks : 301
Peaks in range : 131
Peaks matched : 100
Int. scale fct : 0.00
Quant. (weight %): 0.00

****************************** Candidates ********************************

Name	Formula	Entry No.	FoM
(Vermiculite)	H2 Mg3 O12 Si4	96-900-0017	0.709791
(Vermiculite)	H2 Mg3 O12 Si4	96-900-0010	0.709720
(Schoepite)	H18 O21 U4	96-900-4445	0.677247
(Vermiculite)	C12 H2 Al1.43 Fe0.48 Mg2.37 N2 O16 Si2.72	96-900-0209	0.615939
(Vermiculite)	C12 Mg3 N4 O12 Si4	96-900-0119	0.565318
(Turquoise)	Al3 Cu0.452 H8 O14 P2	96-900-9518	0.563717
(Vermiculite)	Al0.57 H1.4 Mg1.705 O7.86 Si1.43	96-900-0147	0.558719
(Quartz)	O2 Si	96-900-5026	0.539529
(Quartz)	O2 Si	96-900-5031	0.539492
(Quartz)	O2 Si	96-900-5028	0.539301
(Quartz)	O2 Si	96-900-5029	0.539266
(Quartz)	O2 Si	96-900-5034	0.539264
(Quartz)	O2 Si	96-900-5030	0.539243
(Quartz)	O2 Si	96-900-5027	0.539178

(Quartz) O2 Si 96-900-5032 0.538915
(Biotite) Al1.24 Fe1.4 H1.64 K0.98 Mg0.71 Na0.02 O12 Si1.36 Ti0.16 96-900-2308 0.537504
(Quartz) O2 Si 96-900-8093 0.535592
(Quartz) O2 Si 96-900-8094 0.534779
(Cristobalite) O2 Si 96-901-3428 0.534684
(Cristobalite) O2 Si 96-901-3427 0.532453
(Biotite) Al1.207 Fe0.4 K1.906 Mg0.512 Mn0.007 Na0.034 O12 Si2.808 Ti0.067 96-900-1583 0.516936
(Biotite) Al3.3 Fe3.512 K2 Mg7.164 O48 Si5.68 Ti1.344 96-900-0845 0.512598
(Cristobalite) O2 Si 96-900-1582 0.510516
(Biotite) Al1.216 Fe1.215 K0.946 Mg1.545 Mn0.018 Na0.032 O12 Si2.784 Ti0.225 96-900-1584 0.498169
(Biotite) Al1.208 Fe1.392 K Mg1.161 O12 Si2.792 Ti0.276 96-900-0744 0.487056
(Tridymite) O10 Si5 96-901-3394 0.484164
(Biotite) Al1.322 Fe0.864 K Mg1.638 O12 Si2.84 Ti0.336 96-900-0844 0.482422
(Biotite) Al1.999 K0.5 Mg2.001 O12 Si3 96-900-0469 0.463993
(Biotite) Al1.428 Ca0.001 Cr0.006 Fe1.296 K0.914 Mg1.245 Mn0.009 Na0.022 O12 Si2.764 Ti0.198 96-900-1354 0.461624
(Cristobalite) O2 Si 96-900-1581 0.460612
(Biotite) Al1.9 Fe1.44 H1.54 K0.95 Mg0.84 Na0.05 O12 Si2.64 Ti0.16 96-900-2307 0.460323
(Biotite) Al1.62 F0.04 Fe1.5 H1.8 K0.96 Mg0.76 Na0.04 O11.96 Si2.72 Ti0.22 96-900-2302 0.457704
(Biotite) Al1.84 Ba0.02 Ca0.02 Fe1.54 H1.6 K0.96 Mg0.7 Na0.03 O12 Si2.64 Ti0.2 96-900-2306 0.454643
(Biotite) Al1.78 Cl0.04 F0.16 Fe1.48 H1.56 K0.98 Mg0.7 Na0.02 O11.8 Si2.72 Ti0.16 96-900-2304 0.454406
(Biotite) Al1.96 Fe1.36 H1.56 K0.98 Mg0.72 Na0.02 O12 Si2.68 Ti0.16 96-900-2305 0.450010
(Biotite) Al1.9 Ba0.01 Ca0.03 F0.32 Fe1.38 H1.56 K0.96 Mg0.73 Na0.02 O11.68 Si2.68 Ti0.14 96-900-2303 0.447783
(Biotite) Al1.249 Ca0.009 Cr0.006 Fe1.239 K0.968 Mg1.401 Mn0.024 Na0.02 O12 Si2.832 Ti0.231 96-900-1353 0.445382
(Tridymite) O2 Si 96-900-0521 0.443633
(Tridymite) O2 Si 96-900-6969 0.443567
(Tridymite) O2 Si 96-901-3492 0.439755
(Tridymite) O2 Si 96-901-3494 0.438014
(Tridymite) O2 Si 96-901-3493 0.437581
(Biotite) Al1.27 Ca0.007 Cr0.006 Fe0.942 K0.915 Mg1.476 Mn0.024 Na0.015 O12 Si2.736 Ti0.39 96-900-1352 0.437515
(Biotite) Al Fe H2 K Mg2 O12 Si3 96-900-1269 0.436428
(Biotite) Al F H K Mg3 O11 Si3 96-900-0026 0.434513
(Biotite) Al Fe H2 K Mg2 O12 Si3 96-900-1268 0.429893
(Biotite) Al Fe H2 K Mg2 O12 Si3 96-900-1265 0.429447

(Quartz) O2 Si 96-900-9667 0.427943
(Biotite) Al Fe H2 K Mg2 O12 Si3 96-900-1266 0.420913
(Quartz) O2 Si 96-901-2601 0.420388
(Biotite) Al1.161 Ca0.004 Cr0.054 Fe0.588 K0.958 Mg1.602 Mn0.03 Na0.016 O12 Si2.932 Ti0.522 96-900-1349 0.419986
and 121 others...

****************************** Search-Match ********************************

Settings:

Profile data used? : No
Automatic zeropoint adaptation? : No
Minimum figure-of-merit (FoM) : 0.60
Parameter/influence 2theta : 0.50
Parameter/influence intensities : 0.00
Parameter multiple/single phase(s): 0.50

******************************* Restraints *********************************

Search string : inorganic_entries_only OR mineral_name=(Turquoise OR Chalcosid
erite OR Faustite OR Quartz OR Tridymite OR Cristobalite OR Ka
olinite OR Illite OR Muscovite OR Muscovite-2M1 OR Chlorite OR
Biotite OR Vermiculite) OR mineral_name=(Turquoise OR Chalcos
iderite OR Faustite OR Quartz OR Tridymite OR Cristobalite OR
Kaolinite OR Illite OR Muscovite OR Muscovite-2M1 OR Chlorite
OR Biotite OR Vermiculite) OR mineral_name=(Turquoise OR Chalc
osiderite OR Faustite OR Quartz OR Tridymite OR Cristobalite O
R Kaolinite OR Illite OR Muscovite OR Muscovite-2M1 OR Chlorit
e OR Biotite OR Vermiculite) OR mineral_name=(Turquoise OR Cha
lcosiderite OR Faustite OR Quartz OR Tridymite OR Cristobalite
OR Kaolinite OR Illite OR Muscovite OR Muscovite-2M1 OR Chlor
ite OR Biotite OR Vermiculite) OR mineral_name=(Turquoise OR C
halcosiderite OR Faustite OR Quartz OR Tridymite OR Cristobali
te OR Kaolinite OR Illite OR Muscovite OR Muscovite-2M1 OR Chl
orite OR Biotite OR Vermiculite) OR mineral_name=(Turquoise OR
Chalcosiderite OR Faustite OR Quartz OR Tridymite OR Cristoba
lite OR Kaolinite OR Illite OR Muscovite OR Muscovite-2M1 OR C
hlorite OR Biotite OR Vermiculite) OR mineral_name=(Turquoise
OR Chalcosiderite OR Faustite OR Quartz OR Tridymite OR Cristo
balite OR Kaolinite OR Illite OR Muscovite OR Muscovite-2M1 OR
Chlorite OR Biotite OR Vermiculite) OR mineral_name=(Turquois

e OR Chalcosiderite OR Faustite OR Quartz OR Tridymite OR Cristobalite OR Kaolinite OR Illite OR Muscovite OR Muscovite-2M1 OR Chlorite OR Biotite OR Vermiculite) OR mineral_name=(Turquoise OR Chalcosiderite OR Faustite OR Quartz OR Tridymite OR Cristobalite OR Kaolinite OR Illite OR Muscovite OR Muscovite-2M1 OR Chlorite OR Biotite OR Vermiculite) OR mineral_name=(Turquoise OR Chalcosiderite OR Faustite OR Quartz OR Tridymite OR Cristobalite OR Kaolinite OR Illite OR Muscovite OR Muscovite-2M1 OR Chlorite OR Biotite OR Vermiculite) OR mineral_name=(Turquoise OR Chalcosiderite OR Faustite OR Quartz OR Tridymite OR Cristobalite OR Kaolinite OR Illite OR Muscovite OR Muscovite-2M1 OR Chlorite OR Biotite OR Vermiculite) OR mineral_name=(Turquoise OR Chalcosiderite OR Faustite OR Quartz OR Tridymite OR Cristobalite OR Kaolinite OR Illite OR Muscovite OR Muscovite-2M1 OR Chlorite OR Biotite OR Vermiculite) OR mineral_name=(Turquoise OR Chalcosiderite OR Faustite OR Quartz OR Tridymite OR Cristobalite OR Kaolinite OR Illite OR Muscovite OR Muscovite-2M1 OR Chlorite OR Biotite OR Vermiculite) OR mineral_name=(Turquoise OR Chalcosiderite OR Faustite OR Quartz OR Tridymite OR Cristobalite OR Kaolinite OR Illite OR Muscovite OR Muscovite-2M1 OR Chlorite OR Biotite OR Vermiculite) OR mineral_name=(Turquoise OR Chalcosiderite OR Faustite OR Quartz OR Tridymite OR Cristobalite OR Kaolinite OR Illite OR Muscovite OR Muscovite-2M1 OR Chlorite OR Biotite OR Vermiculite) OR mineral_name=(Turquoise OR Chalcosiderite OR Faustite OR Quartz OR Tridymite OR Cristobalite OR Kaolinite OR Illite OR Muscovite OR Muscovite-2M1 OR Chlorite OR Biotite OR Vermiculite)

****************************** Peak List ********************************

Wavelength used for calculation of 2theta values: lambda = 1.540562 A

d[A]	2theta[∞]	Int.	FWHM	Matched
41.8672	2.1084	37.50	0.2800	
38.2715	2.3065	23.82	0.2800	
9.0262	9.7909	39.10	0.2800	A,C,E
8.8587	9.9765	49.32	0.2800	
8.7627	10.0862	57.28	0.2800	
7.2726	12.1599	23.00	0.2800	
7.1814	12.3148	22.35	0.2800	B,G

6.6057	13.3928	185.07	0.2800	A,C,E
6.4353	13.7491	44.96	0.2800	A,C
6.3557	13.9223	30.21	0.2800	E
6.1054	14.4959	354.72	0.2800	A,C,E
5.9270	14.9348	140.03	0.2800	A,C
5.7787	15.3202	26.62	0.2800	C,E,G
5.7143	15.4939	56.90	0.2800	A
5.5951	15.8263	29.06	0.2800	
5.5373	15.9924	24.08	0.2800	
5.4522	16.2438	27.35	0.2800	
5.3536	16.5450	24.13	0.2800	
4.9659	17.8470	28.01	0.2800	E,F,H
4.7487	18.6702	213.55	0.2800	A,B,C,E,G
4.2115	21.0776	23.98	0.2800	A,B,C,E,H
4.1722	21.2782	22.24	0.2800	A,C,E,G
4.1342	21.4762	30.20	0.2800	A,B,C,F,H
3.6500	24.3662	1000.00	0.2800	A,B,C,E,F
3.5350	25.1715	23.01	0.2800	B,E,G,H
3.4897	25.5040	30.85	0.2800	A,B,C,H
3.4725	25.6324	58.61	0.2800	
3.4107	26.1049	365.04	0.2800	A,B,C,D,E
3.3332	26.7233	156.13	0.2800	A,B,C,E,F,G,H
3.2580	27.3512	282.47	0.2800	A,B,C,E,H
3.0671	29.0906	98.68	0.2800	A,B,C,E,F,G,H
3.0168	29.5860	56.26	0.2800	A,C,E
2.9982	29.7744	36.94	0.2800	A,C,E
2.9760	30.0016	47.34	0.2800	A,B,H
2.9505	30.2667	30.09	0.2800	E,F
2.8860	30.9599	770.48	0.2800	A,B,C
2.8240	31.6570	33.30	0.2800	A,B,C,E,G,H
2.7191	32.9132	25.22	0.2800	A,B,C,E,F
2.5118	35.7169	128.67	0.2800	A,B,C,E,F
2.4987	35.9101	105.86	0.2800	A,B,E,F,G,H
2.4828	36.1482	26.81	0.2800	A,C,D,E,F,H
2.4708	36.3305	30.42	0.2800	A,C,E,F,H
2.4554	36.5662	44.54	0.2800	A,C,E,H
2.4475	36.6876	43.65	0.2800	B,C,E
2.4381	36.8340	27.07	0.2800	B,E,F,G
2.4290	36.9776	41.21	0.2800	A,B,C,E
2.4208	37.1072	56.35	0.2800	A,C,G
2.4050	37.3603	44.13	0.2800	A,C,E,H
2.3935	37.5459	70.00	0.2800	A,B,F,G,H
2.3855	37.6763	60.95	0.2800	A,B,C,E
2.3517	38.2388	35.99	0.2800	A,C,F,H
2.3360	38.5065	89.30	0.2800	A,B,C,E,G

2.2961	39.2024	120.34	0.2800	A,B,C,D,E,G,H
2.2192	40.6197	123.44	0.2800	A,B,C,E,F,G,H
2.1776	41.4316	32.55	0.2800	A,B,C,E,F,G,H
2.1705	41.5727	50.29	0.2800	A,B,C,F
2.1600	41.7837	30.49	0.2800	A,D,E,F,G,H
2.1056	42.9160	105.75	0.2800	A,B,C,E,F,G,H
2.0947	43.1501	26.40	0.2800	A,C,E,F,H
2.0789	43.4959	23.00	0.2800	A,B,E,G,H
2.0722	43.6427	25.86	0.2800	B,C,E,H
2.0557	44.0127	126.10	0.2800	A,B,C,E
2.0388	44.3965	22.11	0.2800	A,C,E,F,G,H
2.0068	45.1427	137.60	0.2800	A,B,C,D,E,F,G,H
1.9291	47.0695	22.94	0.2800	A,B,C,E,F,G,H
1.9249	47.1767	26.79	0.2800	C
1.9201	47.3018	22.50	0.2800	A,B,C,E,G,H
1.8949	47.9701	64.97	0.2800	A,B,C,E,F,G,H
1.8553	49.0609	31.09	0.2800	A,B,C,E,F,G,H
1.8490	49.2406	48.68	0.2800	A,C,H
1.8421	49.4368	76.19	0.2800	A,B,D,E,H
1.8370	49.5825	89.17	0.2800	A,B,C,E
1.8307	49.7643	79.04	0.2800	A,B,C,E,F
1.8143	50.2460	101.25	0.2800	A,B,C,E,H
1.8036	50.5643	40.50	0.2800	A,C,E,G
1.7966	50.7759	35.30	0.2800	B,E,G,H
1.7795	51.2980	50.58	0.2800	A,C,E,G
1.7758	51.4142	56.35	0.2800	A,B,C,E
1.7710	51.5627	26.75	0.2800	A,E,H
1.7613	51.8671	21.79	0.2800	A,B,C,E,F,H
1.7269	52.9820	33.44	0.2800	A,B,C,E,H
1.7201	53.2057	49.93	0.2800	A,B,C,E
1.7162	53.3359	44.61	0.2800	A,B,C,E,F,H
1.6726	54.8412	22.15	0.2800	A,B,C,D,E,F,H
1.6363	56.1641	30.56	0.2800	A,B,C,D,E,F,H
1.6325	56.3087	45.61	0.2800	A,C,E
1.6296	56.4171	45.68	0.2800	A,B,C,E,F,H
1.6018	57.4863	25.10	0.2800	A,B,C,E,H
1.5974	57.6596	35.61	0.2800	A,C,E,F,H
1.5918	57.8833	23.97	0.2800	A,B,C,E,F,H
1.5795	58.3772	30.77	0.2800	A,B,C,E,H
1.5757	58.5317	44.04	0.2800	A,B,C,E,F,H
1.5652	58.9625	27.79	0.2800	A,C,D,E,F,H
1.5612	59.1253	24.95	0.2800	A,E

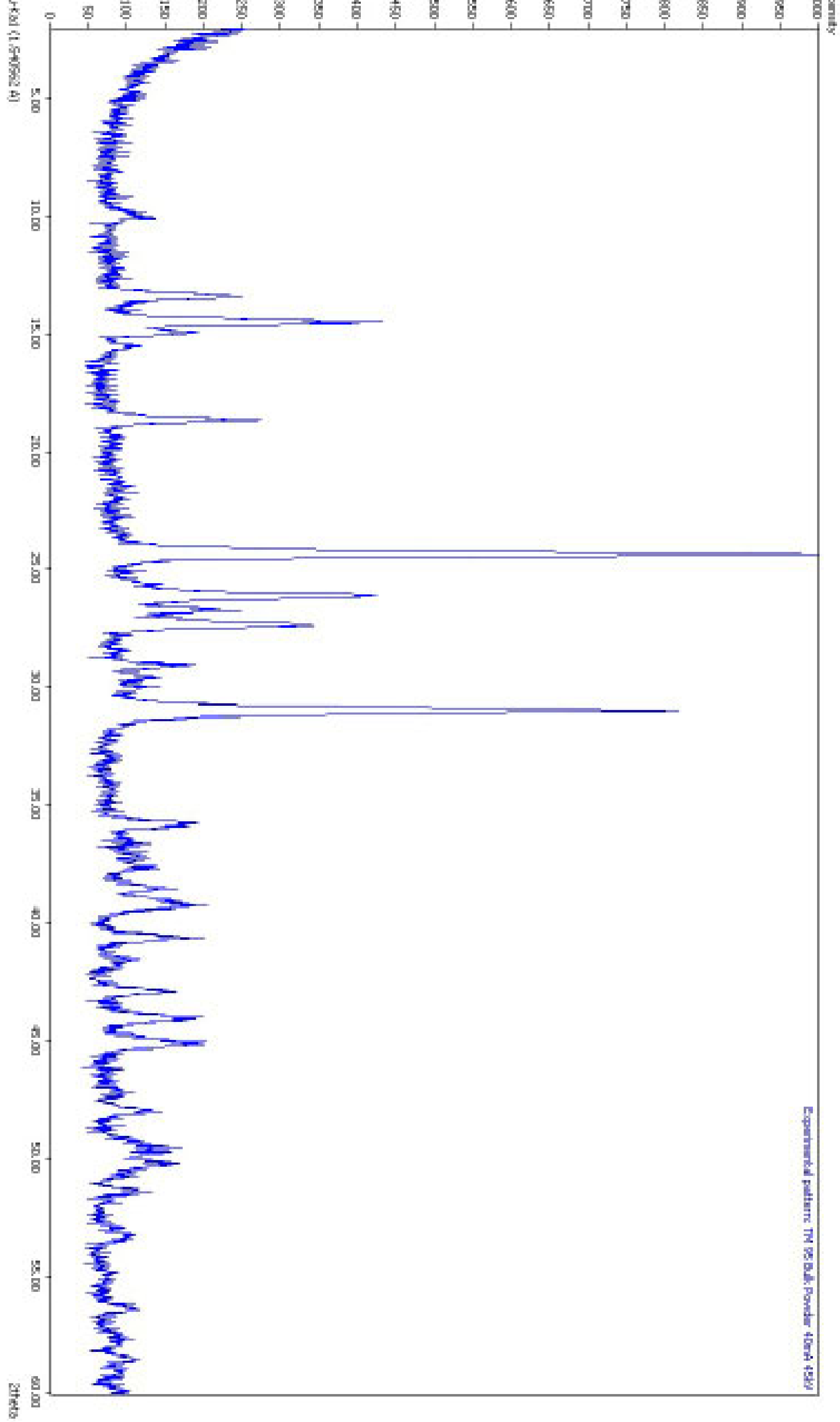

```
###############################################################################
###                 Match! Phase Analysis Report                    ###
###############################################################################

Licensee:

Sample  : TM109A random bulk powder 45k40m


****************************** Sample Data ********************************

File name     : tm109a.rd
File path     : e:\
Data collected: 4/2/2008 2:19:24 PM
Data range    : 2.000∞ to 60.000∞
No. of points : 2901
Step size     : 0.020
Alpha2 subtr.?: No
Backgr.subtr.?: No
Data smoothed?: Yes
Radiation     : Cu-Ka1
Wavelength    : 1.540562 A


**************************** Matched Phases *******************************

Phase A:  (Microcline)
-------
Formula sum      : Al K O8 Si3
Entry number     : 96-900-0702
FoM              : 0.869759
No. of peaks     : 255
Peaks in range   : 197
Peaks matched    : 162
Int. scale fct   : 0.58
Quant. (weight %): 36.00

Phase B:  (Bementite)
-------
Formula sum      : Mn6.683 O23 Si6
Entry number     : 96-900-1585
FoM              : 0.855617
No. of peaks     : 500
Peaks in range   : 500
Peaks matched    : 346
```

Int. scale fct : 0.00
Quant. (weight %): 0.00

Phase C: (Vermiculite)

Formula sum : H2 Mg3 O12 Si4
Entry number : 96-900-0010
FoM : 0.837680
No. of peaks : 291
Peaks in range : 190
Peaks matched : 101
Int. scale fct : 2.98
Quant. (weight %): 6.22

Phase D: (Kaolinite)

Formula sum : Al2 H4 O9 Si2
Entry number : 96-900-9235
FoM : 0.813647
No. of peaks : 254
Peaks in range : 91
Peaks matched : 85
Int. scale fct : 0.27
Quant. (weight %): 11.68

Phase E: (Albite)

Formula sum : Al Na O8 Si3
Entry number : 96-900-3703
FoM : 0.812245
No. of peaks : 252
Peaks in range : 159
Peaks matched : 120
Int. scale fct : 0.55
Quant. (weight %): 32.57

Phase F: (Quartz)

Formula sum : O2 Si
Entry number : 96-900-5018
FoM : 0.776947
No. of peaks : 35
Peaks in range : 12
Peaks matched : 12
Int. scale fct : 0.12

Quant. (weight %): 1.97

Phase G: (Metaswitzerite)

Formula sum : Fe0.875 H8 Mn2 O12 P2
Entry number : 96-901-1955
FoM : 0.759822
No. of peaks : 500
Peaks in range : 500
Peaks matched : 380
Int. scale fct : 0.11
Quant. (weight %): 0.92

Phase H: (Muscovite-2M1)

Formula sum : Al2.96 F0.02 Fe0.08 K0.92 Mg0.06 Na0.08 O11.98 Si2.92 Ti0.02
Entry number : 96-900-1955
FoM : 0.731021
No. of peaks : 300
Peaks in range : 130
Peaks matched : 110
Int. scale fct : 0.07
Quant. (weight %): 7.83

Phase I: (Tridymite)

Formula sum : O10 Si5
Entry number : 96-901-3394
FoM : 0.727713
No. of peaks : 53
Peaks in range : 52
Peaks matched : 27
Int. scale fct : 0.05
Quant. (weight %): 1.69

Phase J: (Biotite)

Formula sum : Al1.24 Fe1.4 H1.64 K0.98 Mg0.71 Na0.02 O12 Si1.36 Ti0.16
Entry number : 96-900-2308
FoM : 0.701346
No. of peaks : 301
Peaks in range : 137
Peaks matched : 88
Int. scale fct : 0.07
Quant. (weight %): 1.12

****************************** Candidates *********************************

Name Formula Entry No. FoM

(Vermiculite) Al0.721 Fe0.24 H3 Mg1.338 O9 Si1.36 96-900-0061 0.794346
(Vermiculite) H2 Mg3 O12 Si4 96-900-0017 0.791199
(Wagnerite) F5 Mg10 O20 P5 96-900-4737 0.783565
(Wolsendorfite) Ba0.72 H40.16 O126 Pb12.32 U28 96-900-2249 0.778653
(Co(C6H13N4)(C14H8O4S2)) C19 Cl Co N4 O4 S2 96-900-7858 0.776508
(K5[(UO2)10O8(OH)9](H2O)) H11 K5 O38 U10 96-900-4552 0.771116
(Wollastonite) Ca O3 Si 96-900-5779 0.766938
(Ramdohrite) Ag1.5 Pb3 S12 Sb5.5 96-901-1731 0.766803
(Wagnerite) F Mg2 O4 P 96-901-2770 0.758940
(Andorite VI) Ag Pb S6 Sb3 96-900-8386 0.756701
(Cannizzarite) Bi54 Pb46 S127 96-901-1203 0.754029
(Megacyclite) H46 K Na8 O46 Si9 96-901-3161 0.752606
(Vurroite) As4.71 Bi6.97 Cl3 Pb9.6 S27 Sn0.72 96-901-0439 0.751645
(Braithwaiteite) As6 Cu5 H18 Na O34 Sb0.96 Ti1.04 96-901-2855 0.751521
(Farneseite) Al21 Ca4.26 Cl0.24 F0.078 H10 K4.59 Na17.826 O111.512 S5.366 Si21
96-901-0734 0.750801
(Labyrinthite) Ca12 Ce0.102 Cl2.68 F0.68 Fe2.19 H11.56 K1.452 Mn0.81 Na34.53
O151.54 Si51.2 Sr0.735 Ti0.52 Zr6 96-901-2646 0.749965
(Becquerelite) Ca H22 O30 U6 96-900-2701 0.749616
(Hugelite) As2 H10 O21 Pb2 U3 96-901-1825 0.748066
(Paderaite) Ag0.2 Bi11.34 Cu7.09 Pb1.37 S22 96-900-4985 0.747951
(Vermiculite) Al0.57 H1.4 Mg1.705 O7.86 Si1.43 96-900-0147 0.746245
(Paderaite) Bi11.34 Cu7.32 Pb1.34 S22 96-900-4986 0.745579
(Tazieffite) As6.41 Bi4.59 Cd0.5 Cl4 H0.48 N0.12 Pb10.13 S26 Sn0.25 96-901-3678
0.745431
(CuCl(C2H4NO2)(CH4O)) C3 Cl Cu N O3 96-900-7725 0.744573
(Vermiculite) C12 Mg3 N4 O12 Si4 96-900-0119 0.743865
(Bergenite) Ba3.694 Ca2.306 H32 O64 P6 U9 96-900-4736 0.743730
(Yegorovite) H18 Na4 O19 Si4 96-901-3998 0.743226
(Microcline) Al0.93 K O8 Si3.07 96-900-0190 0.740801
(Cu(C21H24N4S3)I3CHCl3) C22 Cl3 Cu I3 N4 S3 96-900-7877 0.738778
(Biotite) Al1.208 Fe1.392 K Mg1.161 O12 Si2.792 Ti0.276 96-900-0744 0.737952
(Juabite) As4 Ca Cu10 H10 O34 Te4 96-900-4594 0.737926
(Inderite) B3 H15 Mg O13 96-900-7613 0.734935
(Schoepite) H18 O21 U4 96-900-4445 0.734447
(Fizelyite) Ag1.486 Pb3.436 S12 Sb5.215 96-901-3807 0.733921
(Na3H2As3O10) As3 H2 Na3 O10 96-900-7787 0.733764
(Metaschoepite) H34 O40 U8 96-901-1299 0.732139
(Hodrushite) Bi5.875 Cu4.25 S11 96-900-4833 0.731258

(Cebaite-(Ce)) C5 Ba3 Ce2 F2 O15 96-900-9389 0.730385
(Ezcurrite) B5 H5 Na2 O12 96-900-0296 0.730303
(Ca2Co.9Zn.1Si2O7) Ca2 Co0.9 O7 Si2 Zn0.1 96-901-1316 0.728583
(Biotite) Al1.216 Fe1.215 K0.946 Mg1.545 Mn0.018 Na0.032 O12 Si2.784 Ti0.225 96-900-1584 0.728490
(Ca2Co.9Zn.1Si2O7) Ca2 Co0.9 O7 Si2 Zn0.1 96-901-1317 0.726207
(Epididymite) Be2 H Na2 O16 Si6 96-901-0013 0.724868
(Epididymite) Be Na O8 Si3 96-900-0208 0.724868
(Carnallite) Cl3 H12 K Mg O6 96-900-0984 0.723638
(Feldspar) Al1.9 O8 Si2.1 Sr 96-900-2567 0.723614
(Antigorite) H62 Mg48 O147 Si34 96-900-4515 0.723518
(Mg2PO4OH) H Mg2 O5 P 96-901-1482 0.722968
(IMA2004-009) H Mg2 O5 P 96-901-1483 0.722968
(Na6[(UO2)(MoO4)4]) Mo4 Na6 O18 U 96-900-4622 0.721632
(Triploidite) Fe0.5 H Mn1.5 O5 P 96-900-8191 0.721579
([Co(C2H4N2)(C3H6N2)(C4H8N2)][Co(CN)6].H20) C30 Co4 N24 O2 96-900-7880 0.721532
and 318 others...

****************************** Search-Match ********************************

Settings:

Profile data used? : No
Automatic zeropoint adaptation? : No
Minimum figure-of-merit (FoM) : 0.60
Parameter/influence 2theta : 0.50
Parameter/influence intensities : 0.00
Parameter multiple/single phase(s): 0.50

****************************** Peak List **********************************

Wavelength used for calculation of 2theta values: lambda = 1.540562 A

d[A]	2theta[∞]	Int.	FWHM	Matched
39.7675	2.2197	95.47	0.1600	
36.6288	2.4100	88.14	0.1600	
32.9706	2.6774	35.73	0.1600	
20.8893	4.2264	41.44	0.1600	
15.7397	5.6102	38.04	0.1600	
10.1456	8.7085	49.34	0.1600	G,I
9.9605	8.8706	64.19	0.1600	H,J

7.6757	11.5190	36.90	0.1600	I
7.5292	11.7439	48.28	0.1600	B
7.1305	12.4031	311.24	0.1600	B,C,D,G,I
6.8744	12.8671	41.42	0.1600	B,G,I
6.6233	13.3571	35.33	0.1600	A,B,G,I
6.5201	13.5695	42.77	0.1600	
6.4646	13.6866	58.38	0.1600	A,B,G
5.8957	15.0144	259.48	0.1600	A,B,E
5.7140	15.4948	124.34	0.1600	B,E,G,I
5.0673	17.4868	473.14	0.1600	B,G,H,I,J
4.4566	19.9059	252.91	0.1600	B,C,D,E,H,I
4.4016	20.1575	139.66	0.1600	B,H,I,J
4.3666	20.3206	143.12	0.1600	B,C,D,I
4.3349	20.4710	166.08	0.1600	B,D
4.2985	20.6463	115.57	0.1600	B,C,G,H,I,J
4.2611	20.8294	181.23	0.1600	A,B,E,F,G,I
4.2226	21.0216	655.20	0.1600	B,C
4.1734	21.2721	136.34	0.1600	B,D,G,H,I,J
4.1326	21.4846	120.66	0.1600	B,C,D,I
4.0772	21.7802	87.00	0.1600	B,G,H,I,J
4.0401	21.9823	58.82	0.1600	B,C
4.0168	22.1117	75.46	0.1600	B,G,I
3.9436	22.5275	236.50	0.1600	A,C,G,H,I
3.8966	22.8026	58.59	0.1600	B,G,I,J
3.8811	22.8949	61.77	0.1600	A
3.8541	23.0576	119.23	0.1600	B,C,D,G,H
3.8137	23.3055	74.55	0.1600	B,G,J
3.7701	23.5783	349.52	0.1600	A,B,C
3.7290	23.8423	54.55	0.1600	B,D,E,G,H
3.6932	24.0765	63.82	0.1600	B,G
3.6602	24.2971	103.39	0.1600	B,C,G,J
3.6240	24.5434	236.85	0.1600	B,G
3.6075	24.6573	213.01	0.1600	A,B
3.5866	24.8039	210.85	0.1600	B,E,G
3.5667	24.9442	239.76	0.1600	A,B,D,E,H
3.5511	25.0557	249.38	0.1600	A,B,E,G,J
3.5135	25.3280	245.98	0.1600	C,G
3.4626	25.7068	501.19	0.1600	A,B,C,E,G,H
3.4295	25.9593	60.40	0.1600	B,D,G
3.3929	26.2445	50.26	0.1600	B,C,E,G,J
3.3380	26.6838	641.87	0.1600	A,B,D,E,F,H,J
3.3142	26.8791	749.37	0.1600	A,B,E,G,H
3.2832	27.1375	756.30	0.1600	A,B,C,E,G,J
3.2320	27.5757	724.09	0.1600	A,B,C,G
3.1214	28.5734	35.37	0.1600	B,C,E,G,H,J

3.0939	28.8327	418.53	0.1600	B,D,G
3.0648	29.1123	1000.00	0.1600	B,E,G
3.0247	29.5073	40.99	0.1600	B,C,G,J
2.9907	29.8508	311.10	0.1600	A,B,G,H
2.9653	30.1125	64.79	0.1600	B,E,G
2.9484	30.2894	103.81	0.1600	A,B,C,G
2.9306	30.4773	65.53	0.1600	A,B,G,J
2.8983	30.8258	254.69	0.1600	A,B,E,G
2.8599	31.2499	131.43	0.1600	B,C,D,E,G,H
2.7659	32.3408	123.11	0.1600	A,B,D,E,G,H
2.6045	34.4046	152.49	0.1600	A,B,G,J
2.5954	34.5296	119.10	0.1600	A,C,G,H
2.5757	34.8014	225.71	0.1600	A,B,C,E,G,H
2.5644	34.9603	268.89	0.1600	A,B,D,G,H
2.5522	35.1332	287.34	0.1600	A,B,D,G,H
2.5399	35.3084	228.20	0.1600	A,B,G,H,J
2.5311	35.4358	210.07	0.1600	A,B,C,D,G,J
2.4975	35.9287	119.83	0.1600	B,D,G,H,J
2.4878	36.0737	129.96	0.1600	A,B,D,E,G,H
2.4614	36.4740	37.39	0.1600	A,B,C,D,E,G,H
2.4568	36.5437	37.25	0.1600	A,B,E,F,G,H
2.4460	36.7115	43.73	0.1600	A,B,G,H,J
2.4190	37.1357	37.03	0.1600	B,C,G
2.4110	37.2635	42.33	0.1600	A,B,E
2.4038	37.3794	43.08	0.1600	A,B,C,G,H
2.3857	37.6736	104.21	0.1600	A,B,E,G,H
2.3783	37.7958	98.13	0.1600	A,B,C,D,E,G,H
2.3531	38.2159	115.29	0.1600	B,C,E,G,H,J
2.3413	38.4163	134.34	0.1600	B,D,E,G
2.3353	38.5187	137.98	0.1600	B,D,G
2.3254	38.6893	169.26	0.1600	A,B,E,G
2.3016	39.1053	98.61	0.1600	A,B,C,D,E,G,H,J
2.2865	39.3747	304.74	0.1600	A,B,C,D,G,J
2.2667	39.7319	43.30	0.1600	A,B,D,E,F,G,H,J
2.2363	40.2961	34.64	0.1600	A,B,C,D,E,F,G,H,J
2.2286	40.4415	41.17	0.1600	A,B,C,D,E,G,H
2.1981	41.0279	55.42	0.1600	A,B,C,G,H,J
2.1908	41.1705	38.51	0.1600	A,B,C,D,E,G,H,J
2.1638	41.7079	195.18	0.1600	A,B,C,D,E,G,J
2.1297	42.4065	83.91	0.1600	A,B,C,D,E,F,G,H,J
2.1227	42.5540	98.54	0.1600	B,G,H
2.1151	42.7140	85.24	0.1600	A,B,C,D,E,G
2.0690	43.7157	44.17	0.1600	A,B,D,E,G,H
2.0569	43.9857	40.15	0.1600	A,B,C,E,G,H
2.0163	44.9189	52.99	0.1600	A,B,C,E,G,H

2.0091	45.0891	101.64	0.1600	B,C,G,J
1.9988	45.3333	63.80	0.1600	B,C,D,E,G,J
1.9955	45.4124	60.05	0.1600	C,E,G,H,J
1.9874	45.6086	60.10	0.1600	D,F,G,H
1.9696	46.0432	299.44	0.1600	A,C,D,E,G,H
1.9556	46.3936	51.86	0.1600	A,G,H
1.9480	46.5834	57.29	0.1600	C,D,E,G,H,J
1.9409	46.7660	36.52	0.1600	A,E,G,H
1.9269	47.1249	153.21	0.1600	A,C,D,E,G,J
1.9220	47.2538	98.50	0.1600	A,C,D,E,G,H
1.9108	47.5473	48.44	0.1600	A,G,J
1.9041	47.7238	36.90	0.1600	C,D,E,G,J
1.8937	48.0027	34.52	0.1600	A,C,E,G,H,J
1.8510	49.1831	65.33	0.1600	A,C,G,H
1.8332	49.6914	38.76	0.1600	A,C,D,E,G,H,J
1.8164	50.1824	210.89	0.1600	A,C,D,E,F,G,H
1.7985	50.7173	326.05	0.1600	A,D,E,F,G,J
1.7731	51.4981	48.27	0.1600	A,C,D,E,G,H,J
1.6838	54.4466	47.02	0.1600	A,C,D,E,G,H,J
1.6818	54.5162	45.14	0.1600	C,D,E,G,H,J
1.6744	54.7789	60.34	0.1600	A,D,E,G,H,J
1.6696	54.9477	49.75	0.1600	A,D,F,G,H
1.6665	55.0611	90.14	0.1600	A,C,D,E,G,J
1.6617	55.2313	96.65	0.1600	D,G,H,J
1.6567	55.4132	60.93	0.1600	A,C,D,E,F,G,H,J
1.6494	55.6806	56.23	0.1600	A,D,E,G,H,J
1.6412	55.9843	46.43	0.1600	A,C,D,E,G,H
1.6333	56.2760	46.12	0.1600	A,D,E,G,H,J
1.6297	56.4146	49.46	0.1600	A,C,D,E,H
1.6257	56.5658	63.09	0.1600	A,C,E,G,H
1.6163	56.9220	51.94	0.1600	A,C,D,E,F,G,H,J
1.5955	57.7348	42.14	0.1600	A,C,D,E,G,H,J
1.5919	57.8777	44.17	0.1600	C,D,E,G,H,J
1.5705	58.7412	52.74	0.1600	A,C,D,E,H,J
1.5670	58.8877	50.99	0.1600	A,J

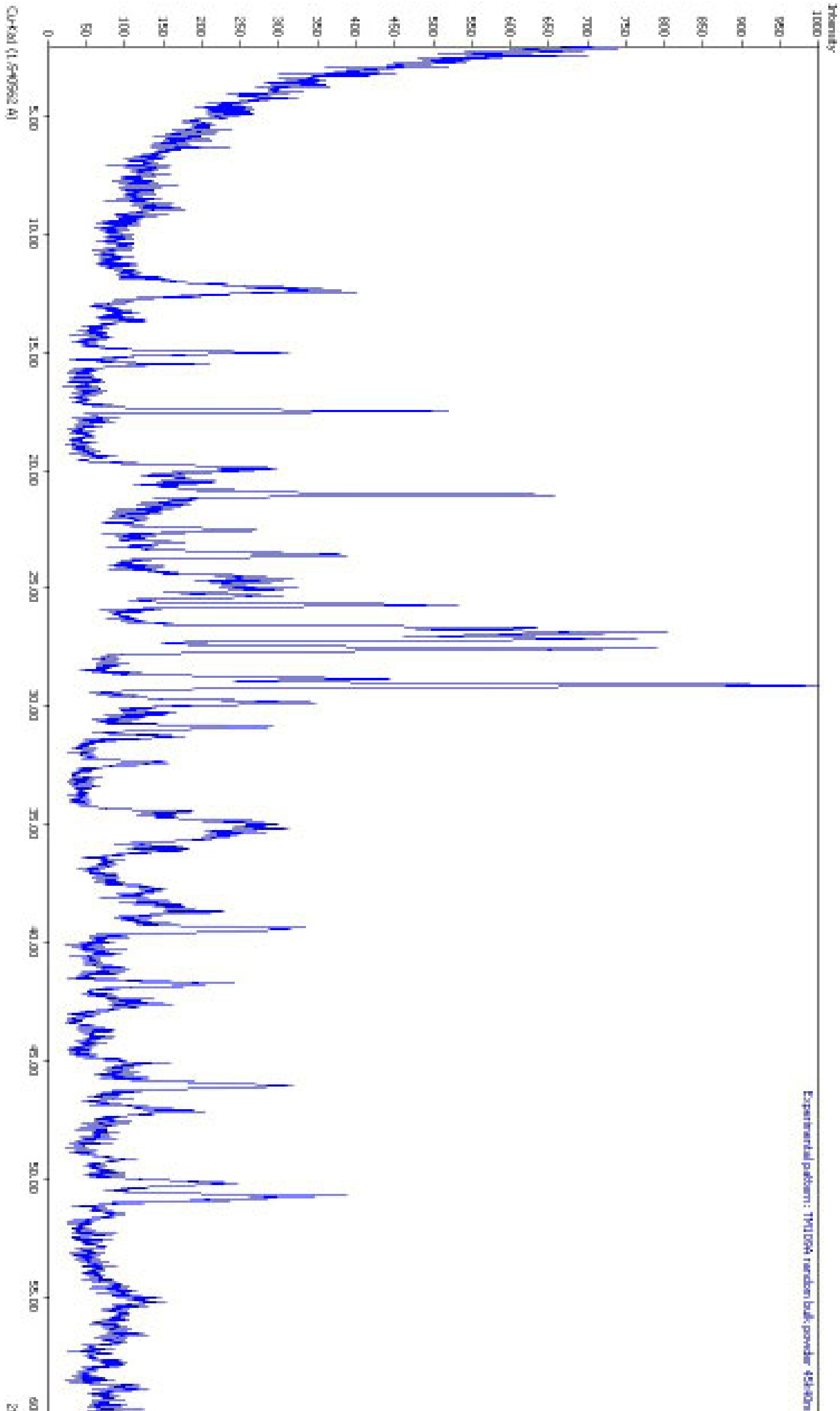

###
Match! Phase Analysis Report
###

Licensee:

Sample : TM109B bulk powder slide 45k40m

******************************* Sample Data ********************************

File name   : tm109b.rd
File path   : e:\
Data collected: 4/2/2008 2:20:24 PM
Data range   : 2.000∞ to 60.000∞
No. of points : 2901
Step size   : 0.020
Alpha2 subtr.?: No
Backgr.subtr.?: No
Data smoothed?: Yes
Radiation   : Cu-Ka1
Wavelength   : 1.540562 A

***************************** Matched Phases *******************************

Phase A: (Turquoise)

Formula sum   : Al3 Cu0.452 H8 O14 P2
Entry number   : 96-900-9518
FoM   : 0.880751
No. of peaks   : 500
Peaks in range   : 252
Peaks matched   : 207
Int. scale fct   : 0.52
Quant. (weight %): 39.39

Phase B: (Vermiculite)

Formula sum   : Al0.721 Fe0.24 H3 Mg1.338 O9 Si1.36
Entry number   : 96-900-0061
FoM   : 0.785371
No. of peaks   : 292
Peaks in range   : 196
Peaks matched   : 119

Int. scale fct : 0.00
Quant. (weight %): 0.00

Phase C: (Faustite)

Formula sum : Al6 H16 O28 P4 Zn0.927
Entry number : 96-900-9517
FoM : 0.679808
No. of peaks : 500
Peaks in range : 252
Peaks matched : 215
Int. scale fct : 0.25
Quant. (weight %): 19.72

Phase D: (Tridymite)

Formula sum : O2 Si
Entry number : 96-900-5270
FoM : 0.612350
No. of peaks : 144
Peaks in range : 144
Peaks matched : 115
Int. scale fct : 0.06
Quant. (weight %): 35.20

Phase E: (Chalcosiderite)

Formula sum : Al0.54 Cu Fe5.46 H16 O28 P4
Entry number : 96-900-9360
FoM : 0.593538
No. of peaks : 500
Peaks in range : 274
Peaks matched : 203
Int. scale fct : 0.03
Quant. (weight %): 1.71

Phase F: (Quartz)

Formula sum : O2 Si
Entry number : 96-901-2601
FoM : 0.565022
No. of peaks : 35
Peaks in range : 12
Peaks matched : 10
Int. scale fct : 0.00

Quant. (weight %): 0.06

Phase G: (Biotite)

Formula sum : Al1.208 Fe1.392 K Mg1.161 O12 Si2.792 Ti0.276
Entry number : 96-900-0744
FoM : 0.556223
No. of peaks : 300
Peaks in range : 138
Peaks matched : 89
Int. scale fct : 0.00
Quant. (weight %): 0.00

Phase H: (Chlorite)

Formula sum : Al0.865 Fe0.255 H4 Mg2.292 O9 Si1.588
Entry number : 96-901-0170
FoM : 0.532790
No. of peaks : 299
Peaks in range : 104
Peaks matched : 75
Int. scale fct : 0.02
Quant. (weight %): 1.86

Phase I: (Illite)

Formula sum : Al2 H2 K O12 Si4
Entry number : 96-901-3724
FoM : 0.512892
No. of peaks : 262
Peaks in range : 73
Peaks matched : 54
Int. scale fct : 0.03
Quant. (weight %): 2.07

Phase J: (Cristobalite)

Formula sum : O2 Si
Entry number : 96-900-1579
FoM : 0.474839
No. of peaks : 66
Peaks in range : 22
Peaks matched : 19
Int. scale fct : 0.00
Quant. (weight %): 0.00

******************************* Candidates *********************************

Name	Formula	Entry No.	FoM
(Vermiculite)	H2 Mg3 O12 Si4	96-900-0017	0.799065
(Vermiculite)	H2 Mg3 O12 Si4	96-900-0010	0.777892
(Vermiculite)	C12 Mg3 N4 O12 Si4	96-900-0119	0.631574
(Quartz)	O2 Si	96-900-8093	0.624433
(Tridymite)	O2 Si	96-900-0521	0.619143
(Tridymite)	O2 Si	96-901-3492	0.618079
(Quartz)	O2 Si	96-900-8094	0.616336
(Tridymite)	O2 Si	96-901-3493	0.612039
(Vermiculite)	Al0.57 H1.4 Mg1.705 O7.86 Si1.43	96-900-0147	0.592299
(Biotite)	Al1.24 Fe1.4 H1.64 K0.98 Mg0.71 Na0.02 O12 Si1.36 Ti0.16	96-900-2308	0.588796
(Tridymite)	O10 Si5	96-901-3394	0.584137
(Tridymite)	O2 Si	96-900-6969	0.581969
(Quartz)	O2 Si	96-900-5026	0.577466
(Quartz)	O2 Si	96-900-5027	0.577409
(Quartz)	O2 Si	96-900-5029	0.577150
(Quartz)	O2 Si	96-900-5031	0.576999
(Quartz)	O2 Si	96-900-5030	0.576977
(Quartz)	O2 Si	96-900-5028	0.576972
(Quartz)	O2 Si	96-900-5034	0.576706
(Quartz)	O2 Si	96-900-5033	0.576680
(Quartz)	O2 Si	96-900-5032	0.576343
(Turquoise)	Al6 Cu H16 O28 P4	96-900-8100	0.576047
(Tridymite)	O2 Si	96-901-3494	0.567780
(Vermiculite)	C12 H2 Al1.43 Fe0.48 Mg2.37 N2 O16 Si2.72	96-900-0209	0.567375
(Tridymite)	O2 Si	96-900-5271	0.562927
(Kaolinite)	Al2 H4 O9 Si2	96-900-9235	0.540389
(Biotite)	Al F H K Mg3 O11 Si3	96-900-0026	0.534422
(Quartz)	O2 Si	96-901-2605	0.532510
(Kaolinite)	Al2 H4 O9 Si2	96-900-9231	0.532226
(Biotite)	Al1.322 Fe0.864 K Mg1.638 O12 Si2.84 Ti0.336	96-900-0844	0.531206
(Biotite)	Al1.216 Fe1.215 K0.946 Mg1.545 Mn0.018 Na0.032 O12 Si2.784 Ti0.225	96-900-1584	0.528495
(Quartz)	O2 Si	96-901-2602	0.527849
(Biotite)	Al1.999 K0.5 Mg2.001 O12 Si3	96-900-0469	0.527725
(Cristobalite)	O2 Si	96-901-3428	0.524159
(Cristobalite)	O2 Si	96-900-8232	0.522838
(Chlorite)	Al0.865 Fe0.255 H4 Mg2.292 O9 Si1.588	96-901-0167	0.520552
(Cristobalite)	O2 Si	96-900-8231	0.519631

(Cristobalite) O2 Si 96-900-8234 0.519624
(Cristobalite) O2 Si 96-900-8233 0.519615
(Chlorite) Al0.865 Fe0.255 H4 Mg2.292 O9 Si1.588 96-901-0169 0.519603
(Cristobalite) O2 Si 96-900-8235 0.519601
(Cristobalite) O2 Si 96-901-3427 0.519581
(Biotite) Al3.3 Fe3.512 K2 Mg7.164 O48 Si5.68 Ti1.344 96-900-0845 0.518743
(Muscovite-2M1) Al2.16 F0.58 Fe0.42 H1.42 K0.97 Li0.38 Mg0.01 Na0.02 O11.42 Rb0.01 Si3.28 96-900-4645 0.514459
(Cristobalite) O2 Si 96-900-1581 0.514177
(Muscovite-2M1) Al2.24 F0.42 Fe0.47 H1.58 K0.96 Li0.27 Na0.01 O11.58 Rb0.03 Si3.24 96-900-4644 0.512258
(Chlorite) Al0.865 Fe0.255 H4 Mg2.292 O9 Si1.588 96-901-0166 0.511170
(Quartz) O2 Si 96-901-2606 0.503732
(Cristobalite) O2 Si 96-900-1582 0.503697
(Muscovite) Al2.748 Ba0.044 Cl0.005 Cr0.062 Fe0.039 H1.829 K0.857 Mg0.081 Na0.103 O11.995 Si3.11 Ti0.003 96-900-5472 0.503252
(Muscovite) Al2.88 Fe0.02 H4 K0.89 Mn0.02 Na0.1 O12 Rb0.01 Si3.08 96-900-4477 0.502977
and 120 others...

****************************** Search-Match ********************************

Settings:

Profile data used? : No
Automatic zeropoint adaptation? : No
Minimum figure-of-merit (FoM) : 0.60
Parameter/influence 2theta : 0.50
Parameter/influence intensities : 0.00
Parameter multiple/single phase(s): 0.50

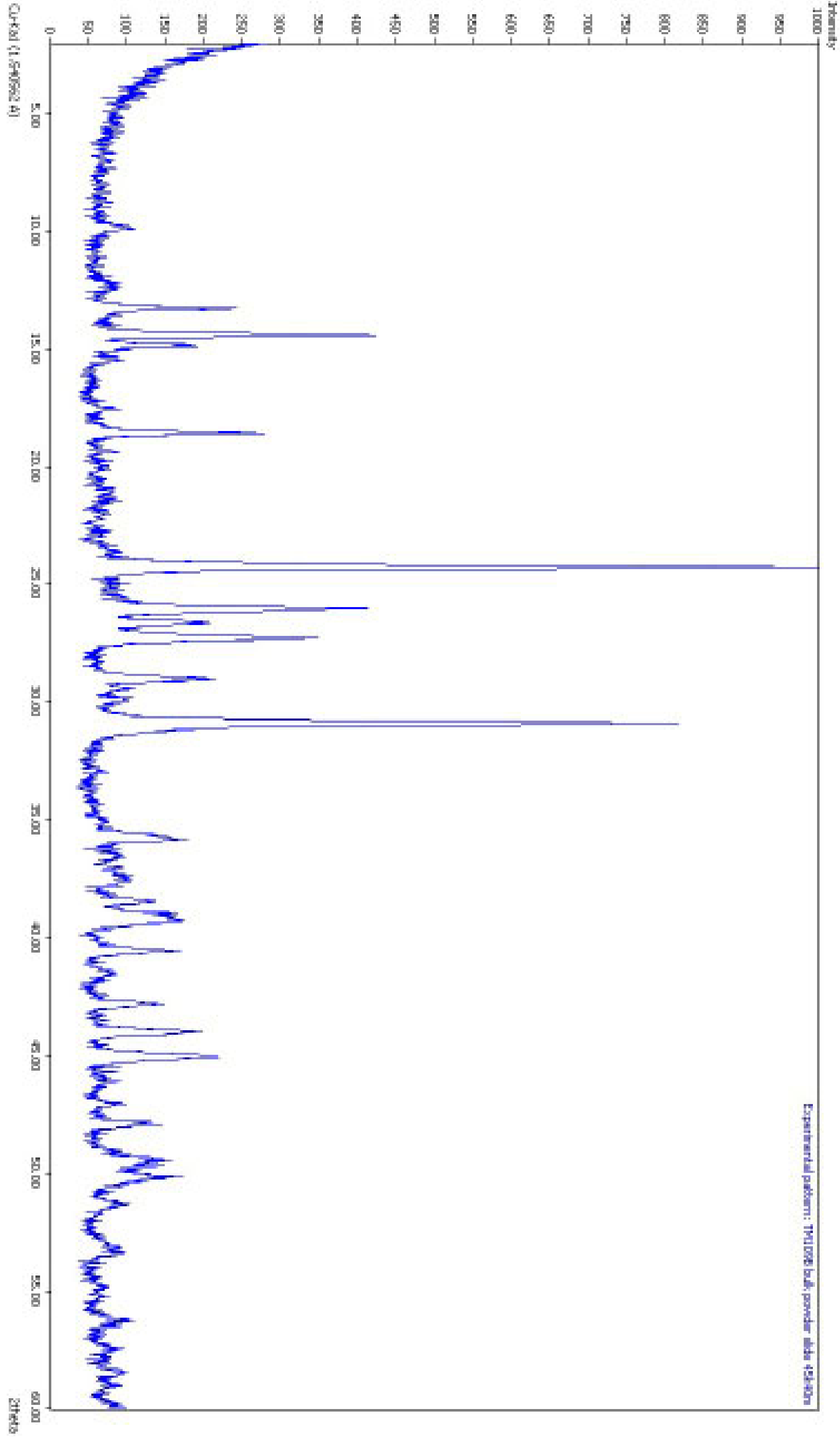

###
Match! Phase Analysis Report
###

Licensee:

Sample : TM114 powder slide mount 45k40m

******************************* Sample Data ********************************

File name : tm114.rd
File path : e:\
Data collected: 4/2/2008 4:24:12 PM
Data range : 2.000∞ to 60.000∞
No. of points : 2901
Step size : 0.020
Alpha2 subtr.?: No
Backgr.subtr.?: No
Data smoothed?: Yes
Radiation : Cu-Ka1
Wavelength : 1.540562 A

***************************** Matched Phases *******************************

Phase A: (Faustite)

Formula sum : Al6 H16 O28 P4 Zn0.927
Entry number : 96-900-9517
FoM : 0.876574
No. of peaks : 500
Peaks in range : 255
Peaks matched : 238
Int. scale fct : 0.63
Quant. (weight %): 50.63

Phase B: (Turquoise)

Formula sum : Al6 Cu H16 O28 P4
Entry number : 96-900-8100
FoM : 0.810633
No. of peaks : 500
Peaks in range : 255
Peaks matched : 244

Int. scale fct : 0.00
Quant. (weight %): 0.00

Phase C: (Chalcosiderite)

Formula sum : Al0.54 Cu Fe5.46 H16 O28 P4
Entry number : 96-900-9360
FoM : 0.767242
No. of peaks : 500
Peaks in range : 278
Peaks matched : 246
Int. scale fct : 0.22
Quant. (weight %): 11.92

Phase D: (Vermiculite)

Formula sum : Al0.721 Fe0.24 H3 Mg1.338 O9 Si1.36
Entry number : 96-900-0061
FoM : 0.747228
No. of peaks : 292
Peaks in range : 197
Peaks matched : 139
Int. scale fct : 0.00
Quant. (weight %): 0.00

Phase E: (Wollastonite-2M)

Formula sum : Ca O3 Si
Entry number : 96-901-1914
FoM : 0.726344
No. of peaks : 405
Peaks in range : 183
Peaks matched : 154
Int. scale fct : 0.35
Quant. (weight %): 14.02

Phase F: (Muscovite-2M1)

Formula sum : Al2.65 Fe0.12 K0.92 Mg0.06 Na0.08 O12 Si3.2 Ti0.04
Entry number : 96-900-1954
FoM : 0.653264
No. of peaks : 300
Peaks in range : 130
Peaks matched : 119
Int. scale fct : 0.08

Quant. (weight %): 12.68

Phase G: (Cristobalite)

Formula sum : O2 Si
Entry number : 96-900-8232
FoM : 0.629882
No. of peaks : 24
Peaks in range : 6
Peaks matched : 4
Int. scale fct : 0.05
Quant. (weight %): 0.46

Phase H: (Benyacarite)

Formula sum : Al0.14 F0.8 Fe1.78 H23.2 K0.32 Mg0.08 Mn1.5 O32.76 P4 Ti1.56
Entry number : 96-900-8435
FoM : 0.611689
No. of peaks : 500
Peaks in range : 377
Peaks matched : 287
Int. scale fct : 0.23
Quant. (weight %): 10.22

Phase I: (Tridymite)

Formula sum : O10 Si5
Entry number : 96-901-3394
FoM : 0.478478
No. of peaks : 53
Peaks in range : 52
Peaks matched : 34
Int. scale fct : 0.00
Quant. (weight %): 0.07

Phase J: (Quartz)

Formula sum : O2 Si
Entry number : 96-900-5031
FoM : 0.474670
No. of peaks : 35
Peaks in range : 13
Peaks matched : 10
Int. scale fct : 0.00
Quant. (weight %): 0.00

******************************* Candidates *********************************

Name Formula Entry No. FoM

(Vermiculite) H2 Mg3 O12 Si4 96-900-0010 0.713853
(Vermiculite) H2 Mg3 O12 Si4 96-900-0017 0.713328
(Lazurite) Al8.75 Ca2 Cl0.18 K0.17 Na9.77 O44.32 S2.88 Si9.25 96-901-1782 0.692961
(Brewsterite-Ba) Al2.15 Ba0.55 H10 K0.01 O21 Si5.85 Sr0.4 96-900-1789 0.678528
(Brewsterite-Sr) Al2.15 Ba0.24 H10 K0.01 O21 Si5.85 Sr0.67 96-900-1790 0.673968
(Brewsterite-Sr) Al2.05 Ba0.45 H10 K0.01 O21 Si5.95 Sr0.5 96-900-1788 0.670256
(Pb4Sb4Se10) Pb1.79 Sb2.21 Se5 96-900-7852 0.665182
(Brewsterite-Sr) Al1.98 Ba0.3 Ca0.14 H8 O20.9 Si6.02 Sr0.58 96-900-7480 0.656129
(Andorite VI) Ag Pb S6 Sb3 96-900-8386 0.653517
(Feldspar) Al1.9 O8 Si2.1 Sr 96-900-2567 0.643385
(Feldspar) Al1.9 O8 Si2.1 Sr 96-900-2568 0.641875
(HfCl4(C4H8O)2) C8 Cl4 Hf O2 96-900-7772 0.641482
(Leonite) H8 K2 Mg O12 S2 96-900-2639 0.640083
(Sarkinite) As H Mn2 O5 96-900-9578 0.631976
(Brewsterite-Sr) Al2 Ba0.24 H10 K0.01 O21 Si6 Sr0.71 96-900-7623 0.631426
(Brewsterite-Sr) Al2 Ba0.24 H9.667 K0.01 O21 Si6 Sr0.71 96-901-1177 0.631426
(Bavenite) Al2 Be2 Ca4 H2 O28 Si9 96-900-7488 0.631081
(Nordstromite) Bi7.92 Cu Pb2.08 S10.8 Se3.2 96-900-4158 0.628187
(Vyuntspakhkite-(Y)) Al2 H5 O18 Si3.882 Tm0.935 Y2.115 96-901-3991 0.627525
(Brewsterite-Ba) Al2.1 Ba0.9 H9.3 K0.02 Mg0.04 Na0.035 O20.88 Si5.9 96-900-5136 0.626249
(Fizelyite) Ag1.486 Pb3.436 S12 Sb5.215 96-901-3807 0.624470
(Freieslebenite) Ag Pb S3 Sb 96-901-1428 0.620992
(Freieslebenite) Ag Pb S3 Sb 96-900-8074 0.620788
(Ramdohrite) Ag1.5 Pb3 S12 Sb5.5 96-901-1731 0.619427
(Ronneburgite) K2 Mn O12 V4 96-900-2584 0.619186
(Hugelite) As2 H10 O21 Pb2 U3 96-901-1825 0.618882
(Tridymite) O2 Si 96-901-3494 0.618849
(2(H3AsO4).H2O) As2 H8 O9 96-900-7505 0.617408
(Fornacite) As0.925 Cr Cu H O9 P0.075 Pb2 96-900-8128 0.616251
(Feldspar) Al2 O8 Pb0.5 Si2 96-900-1785 0.614786
(Alloriite) C0.31 H18 Al12 Ca2.23 Cl0.17 K2.16 Na11.61 O61.79 S2.7 Si12 96-901-3997 0.612930
(Mereiterite) Fe H8 K2 O12 S2 96-900-2645 0.610124
(Grenmarite) Ca0.38 F2 Mn1.3 Na3.56 O16 Si4 Ti0.46 Zr2.3 96-900-5695 0.607545
(Feldspar) Al2 Ca0.2 O8 Si2 Sr0.8 96-900-3093 0.607070
(Cuspidine) Ca1.005 F Na0.995 O3.5 P 96-900-2506 0.605558
(Parwelite) As Mg0.92 Mn4.08 O12 Sb Si 96-901-2508 0.604902

(Leucite)	K0.9 O6 Si2	96-900-1799	0.604836
(Feldspar)	Al1.9 O8 Si2.1 Sr	96-900-2565	0.604111
(Carnallite)	Cl3 H12 K Mg O6	96-900-0984	0.603252
(Upalite)	Al H15 O23 P2 U3	96-900-9715	0.603190
(Zippeite)	H22 Mg2 O31 S2 U4	96-900-4762	0.600905
(Tridymite)	O2 Si	96-900-6969	0.594899
(Tridymite)	O2 Si	96-901-3492	0.594672
(Tridymite)	O2 Si	96-900-0521	0.594119
(Tridymite)	O2 Si	96-901-3493	0.593142
(Vermiculite)	C12 Mg3 N4 O12 Si4	96-900-0119	0.588798
(Turquoise)	Al3 Cu0.452 H8 O14 P2	96-900-9518	0.588690
(Vermiculite)	Al0.57 H1.4 Mg1.705 O7.86 Si1.43	96-900-0147	0.571523
(Cristobalite)	O2 Si	96-900-1580	0.569557
(Cristobalite)	O2 Si	96-900-9686	0.552408
(Cristobalite)	O2 Si	96-900-1581	0.550463

and 160 others...

****************************** Search-Match ********************************

Settings:

Profile data used? : No
Automatic zeropoint adaptation? : No
Minimum figure-of-merit (FoM) : 0.60
Parameter/influence 2theta : 0.50
Parameter/influence intensities : 0.00
Parameter multiple/single phase(s): 0.50

******************************* Peak List **********************************

Wavelength used for calculation of 2theta values: lambda = 1.540562 A

d[A]	2theta[∞]	Int.	FWHM	Matched
39.0887	2.2583	31.82	0.2400	
28.1660	3.1342	31.56	0.2400	
25.2346	3.4984	42.59	0.2400	
19.0785	4.6278	27.28	0.2400	
12.6576	6.9778	32.53	0.2400	
10.8562	8.1374	41.75	0.2400	
10.3850	8.5074	38.04	0.2400	H,I
9.9070	8.9186	52.96	0.2400	F
9.6674	9.1402	45.69	0.2400	
9.4307	9.3701	43.86	0.2400	

9.2558	9.5475	43.15	0.2400	C
9.0244	9.7929	89.33	0.2400	A,B
8.2901	10.6627	42.54	0.2400	I
8.0715	10.9523	30.80	0.2400	
7.8612	11.2463	27.53	0.2400	I
7.6035	11.6288	40.72	0.2400	E,H,I
6.8461	12.9205	38.72	0.2400	C,E,I
6.7164	13.1711	228.29	0.2400	C
6.6130	13.3779	66.99	0.2400	A,B,E,I
6.4799	13.6541	36.95	0.2400	A,C,H
6.2257	14.2143	450.25	0.2400	A,B,C,H,I
6.0454	14.6407	98.31	0.2400	A,B,C
5.7667	15.3523	40.77	0.2400	A,B,C,I
4.8583	18.2456	152.75	0.2400	C,E,F,I
4.8289	18.3574	207.69	0.2400	A,B,D,I
4.6614	19.0232	36.56	0.2400	C,E,H,I
4.6269	19.1661	27.27	0.2400	A,B,C,D,I
4.5168	19.6382	78.27	0.2400	A,B,D,F,I
4.2832	20.7204	36.35	0.2400	B,C,D,E,F,I,J
4.2509	20.8797	28.60	0.2400	A,D,H,I
4.2069	21.1008	47.41	0.2400	A,B,C,E,F,H,I
4.1412	21.4394	74.52	0.2400	A,B,C,D,E,F,G,I
3.7041	24.0049	1000.00	0.2400	A,B,C,D,E,F,H
3.6404	24.4317	31.42	0.2400	A,B,C,H
3.5503	25.0612	34.91	0.2400	C,D,E,F
3.5260	25.2367	36.64	0.2400	A,B,C,D,E
3.4649	25.6894	466.98	0.2400	A,B,F,H
3.4076	26.1291	46.12	0.2400	A,B,C,D,H
3.3688	26.4351	129.86	0.2400	A,B,C,E,H,J
3.3191	26.8386	450.27	0.2400	A,B,D,E,F,H
3.1355	28.4422	41.03	0.2400	A,B,D,E,H
3.1190	28.5958	89.67	0.2400	C,H
3.1060	28.7182	80.04	0.2400	E,F
3.0744	29.0194	66.81	0.2400	A,B,C,H
3.0406	29.3492	42.14	0.2400	A,B,C,D,E,H
3.0238	29.5160	71.31	0.2400	A,B,C,E
3.0045	29.7107	59.55	0.2400	A,C,H
2.9886	29.8723	59.11	0.2400	A,B,D,F,H
2.9371	30.4087	558.27	0.2400	C,E,H
2.9207	30.5832	491.39	0.2400	C
2.9089	30.7101	460.80	0.2400	A,B,D
2.8650	31.1932	46.29	0.2400	A,B,D,F,H
2.8412	31.4606	33.16	0.2400	A,B,C,D,E,H
2.7909	32.0429	27.15	0.2400	E,H
2.7783	32.1917	27.33	0.2400	F

2.7636	32.3683	30.18	0.2400	H
2.7526	32.5005	32.18	0.2400	D,H
2.7357	32.7080	33.89	0.2400	A,B,C,E
2.6784	33.4273	33.71	0.2400	C,D,E,H
2.6690	33.5488	34.71	0.2400	C,F,H
2.6568	33.7071	37.33	0.2400	D,H
2.6422	33.8996	32.63	0.2400	A,B,C,D,H
2.6273	34.0968	28.56	0.2400	A,B,C,D,E,H
2.5361	35.3637	147.62	0.2400	A,B,C,D,E,F,H
2.5118	35.7165	48.20	0.2400	A,B,C,G,H
2.5041	35.8305	36.71	0.2400	B,C,H
2.4940	35.9809	28.89	0.2400	B,C,D,F,J
2.4870	36.0857	44.35	0.2400	A,C,F
2.4799	36.1916	45.99	0.2400	E,F
2.4707	36.3307	51.50	0.2400	A,B,C,E,H
2.4552	36.5693	50.02	0.2400	A,B,C,F,H
2.4454	36.7210	56.15	0.2400	C,D,F
2.4291	36.9757	85.29	0.2400	A,B,C,D,H
2.4243	37.0513	81.34	0.2400	A,B,C,E,F,H
2.3720	37.9003	74.83	0.2400	A,B,C,D,F,H
2.3663	37.9944	70.48	0.2400	A,B,H
2.3423	38.3986	122.04	0.2400	A,B,C,E,F,H
2.3338	38.5445	128.67	0.2400	C,E
2.3173	38.8287	57.15	0.2400	A,B,C,D,E,H
2.3075	39.0018	106.95	0.2400	A,B,C,D,E,F,H,J
2.2632	39.7956	34.14	0.2400	A,B,C,D,E,F,H
2.2406	40.2147	88.93	0.2400	A,B,C,E,F,H
2.2334	40.3511	87.24	0.2400	A,C,D,F
2.2257	40.4954	30.61	0.2400	A,B,D,F,H
2.2159	40.6838	30.89	0.2400	C,D,E,H
2.2114	40.7702	32.06	0.2400	A,D,E,H
2.1993	41.0037	29.19	0.2400	A,B,C,D,E,F,H
2.1280	42.4423	55.50	0.2400	A,B,C,D,F,H
2.1212	42.5866	66.17	0.2400	A,D,E,F,H
2.1168	42.6785	70.95	0.2400	A,B,E,H
2.1045	42.9394	45.68	0.2400	B,C,F,H
2.0902	43.2490	89.82	0.2400	A,B,C,E,F,H
2.0830	43.4061	127.01	0.2400	B,C,H
2.0706	43.6793	97.43	0.2400	A,B,C,D,E,F,G,H
2.0440	44.2769	154.55	0.2400	A,B,C,D,F,H
2.0285	44.6332	44.97	0.2400	B,C,H
2.0232	44.7562	40.92	0.2400	A,B,C,D,E,F,H,J
1.9782	45.8326	30.85	0.2400	A,B,C,D,E,F,H
1.9640	46.1817	28.89	0.2400	A,B,C,D,E,F,H
1.9585	46.3213	28.36	0.2400	C,E,F,H

1.9476	46.5940	41.91	0.2400	A,B,C,F
1.9392	46.8087	71.04	0.2400	A,B,C,E,H
1.9311	47.0175	66.35	0.2400	A,B,C,D,F,H
1.9287	47.0777	67.58	0.2400	A
1.9210	47.2790	67.91	0.2400	A,B,C,E,H
1.9121	47.5115	39.35	0.2400	A,B,C,D,E,F
1.9060	47.6736	46.21	0.2400	A,B,C,E,H
1.8801	48.3724	30.71	0.2400	A,B,C,D,E,F,H
1.8660	48.7607	88.97	0.2400	A,B,C,E,F,H
1.8612	48.8952	112.28	0.2400	A,C,D,E,F,H
1.8565	49.0264	103.45	0.2400	A,B,C,H
1.8511	49.1810	74.14	0.2400	A,B,E,H
1.8462	49.3181	58.50	0.2400	A,B,C,D,E,F,H,J
1.8293	49.8067	158.18	0.2400	A,B,C,D,E,F,H
1.8164	50.1844	53.99	0.2400	A,B,C,D,E,F,H
1.8099	50.3761	49.28	0.2400	A,B,C,E,H
1.8034	50.5693	55.50	0.2400	A,C,E,H
1.7955	50.8102	48.23	0.2400	C,E,H
1.7909	50.9482	50.84	0.2400	A,B,C,D,E,F,H
1.7508	52.2024	35.50	0.2400	A,B,C,D,E,F,H
1.7441	52.4167	44.98	0.2400	A,B,C,D,H
1.7373	52.6377	60.00	0.2400	A,B,C,D,F,H
1.7317	52.8233	36.93	0.2400	A,B,C,D,E
1.7284	52.9312	40.22	0.2400	A,B,C,D,E,F,H
1.6906	54.2089	31.03	0.2400	A,B,C,D,E,F,H,J
1.6878	54.3081	31.07	0.2400	A,B,C,E,F,H
1.6840	54.4395	36.60	0.2400	A,B,C,D,E,F,H,J
1.6565	55.4213	32.11	0.2400	A,B,C,D,E,F,H
1.6490	55.6959	54.64	0.2400	B,C,D,E,F,H
1.6450	55.8424	53.17	0.2400	A,C,D,E,F,G,H
1.6413	55.9774	51.48	0.2400	A,B,D,E,F
1.6370	56.1391	35.54	0.2400	A,B,C,D,E,F,H,J
1.6290	56.4396	31.92	0.2400	A,B,C,F,H
1.6210	56.7448	38.79	0.2400	A,B,C,D,E,F,H
1.6172	56.8905	40.08	0.2400	B,C,D,E,F,H
1.6114	57.1123	48.82	0.2400	A,B,C,D,F,H
1.6060	57.3236	38.91	0.2400	A,B,C,D,E,H
1.6024	57.4610	41.31	0.2400	B,E,H
1.6000	57.5576	54.34	0.2400	A,B,C,F
1.5955	57.7329	46.70	0.2400	A,B,C,D,E,F,H
1.5910	57.9128	55.81	0.2400	D,E,F,H
1.5855	58.1349	40.00	0.2400	A,B,C,D,E,H
1.5803	58.3449	32.62	0.2400	A,B,D,E,F,H
1.5684	58.8289	41.22	0.2400	A,B,C,D,E,F,H,J
1.5641	59.0085	45.54	0.2400	A,B,C,E,H

1.5605	59.1561	33.26	0.2400	A,B,C,E,H
1.5565	59.3252	29.24	0.2400	A,C,E

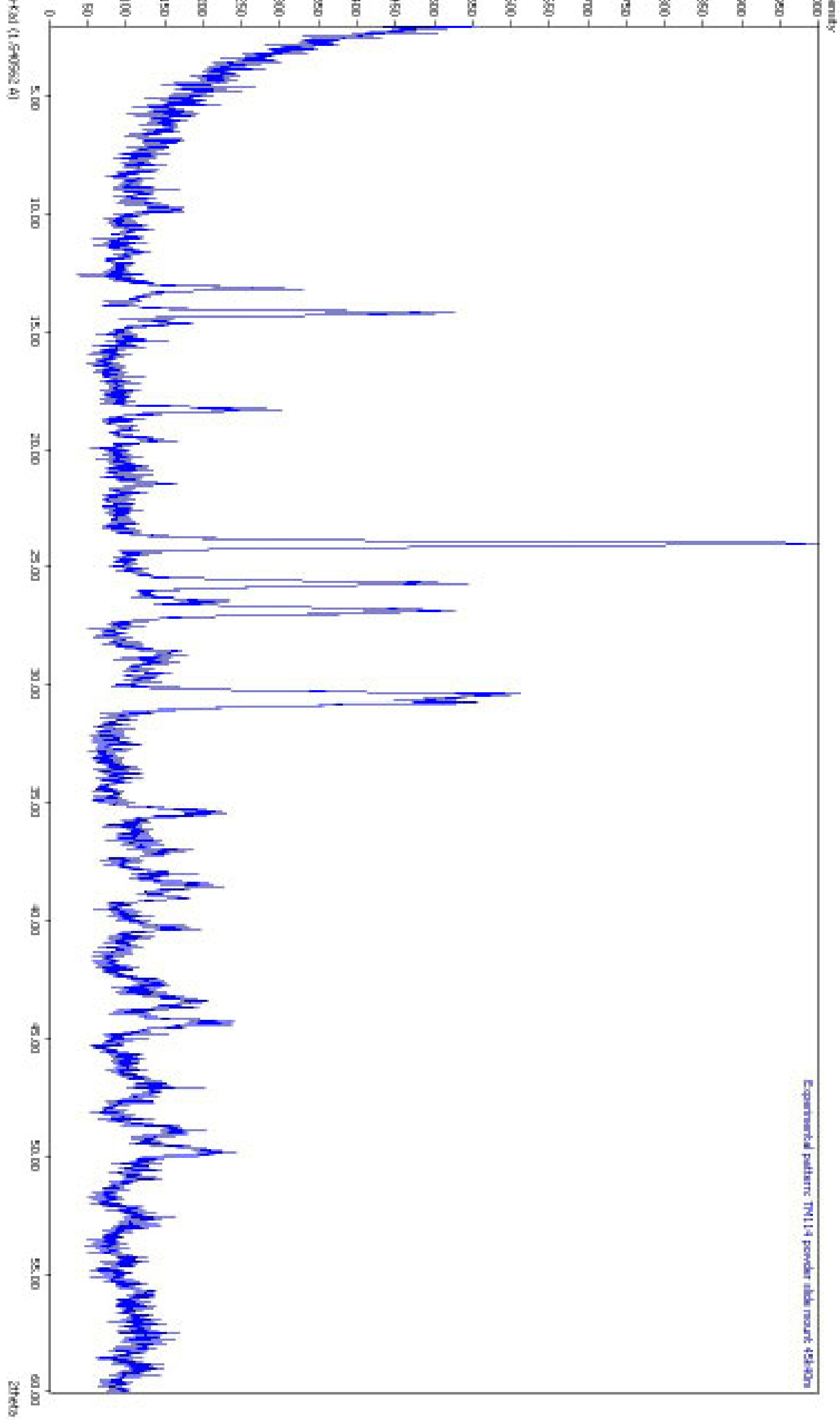

##
Match! Phase Analysis Report
##

Licensee:

Sample : TM 118 Bulk Powder 40mA 45kV

****************************** Sample Data ******************************

File name   : tm118.rd
File path   : e:\
Data collected: 4/3/2008 2:46:04 PM
Data range   : 2.000∞ to 60.000∞
No. of points : 2901
Step size   : 0.020
Alpha2 subtr.?: No
Backgr.subtr.?: No
Data smoothed?: Yes
Radiation   : Cu-Ka1
Wavelength   : 1.540562 A

**************************** Matched Phases ****************************

Phase A: (Chalcosiderite)

Formula sum   : Al0.54 Cu Fe5.46 H16 O28 P4
Entry number   : 96-900-9360
FoM   : 0.831460
No. of peaks   : 500
Peaks in range   : 273
Peaks matched   : 258
Int. scale fct   : 0.09
Quant. (weight %): 4.83

Phase B: (Microcline)

Formula sum   : Al0.93 K O8 Si3.07
Entry number   : 96-900-0190
FoM   : 0.797650
No. of peaks   : 254
Peaks in range   : 198
Peaks matched   : 191

Int. scale fct : 0.55
Quant. (weight %): 53.81

Phase C: (Turquoise)

Formula sum : Al3 Cu0.452 H8 O14 P2
Entry number : 96-900-9518
FoM : 0.793632
No. of peaks : 500
Peaks in range : 251
Peaks matched : 239
Int. scale fct : 0.06
Quant. (weight %): 4.62

Phase D: (Quartz)

Formula sum : O2 Si
Entry number : 96-900-5034
FoM : 0.767476
No. of peaks : 35
Peaks in range : 13
Peaks matched : 11
Int. scale fct : 0.05
Quant. (weight %): 0.70

Phase E: (Kaolinite)

Formula sum : Al2 H4 O9 Si2
Entry number : 96-900-9235
FoM : 0.763045
No. of peaks : 254
Peaks in range : 91
Peaks matched : 90
Int. scale fct : 0.21
Quant. (weight %): 13.92

Phase F: (Tridymite)

Formula sum : O2 Si
Entry number : 96-901-3494
FoM : 0.703839
No. of peaks : 500
Peaks in range : 198
Peaks matched : 151
Int. scale fct : 0.02

Quant. (weight %): 1.04

Phase G: (Illite)

Formula sum   : Al2 H2 K O12 Si4
Entry number   : 96-901-3722
FoM   : 0.698654
No. of peaks   : 263
Peaks in range   : 73
Peaks matched   : 71
Int. scale fct   : 0.23
Quant. (weight %): 19.70

Phase H: (Cristobalite)

Formula sum   : O2 Si
Entry number   : 96-900-8227
FoM   : 0.669571
No. of peaks   : 66
Peaks in range   : 22
Peaks matched   : 22
Int. scale fct   : 0.09
Quant. (weight %): 1.25

Phase I: (Vermiculite)

Formula sum   : Al0.721 Fe0.24 H3 Mg1.338 O9 Si1.36
Entry number   : 96-900-0061
FoM   : 0.612793
No. of peaks   : 292
Peaks in range   : 196
Peaks matched   : 152
Int. scale fct   : 0.03
Quant. (weight %): 0.13

****************************** Candidates ********************************

Name	Formula	Entry No.	FoM
(Friedelite)	Cl H9 Mn8 O24 Si6	96-901-2818	0.788433
(Kipushite)	Cu2.92 H7 O15 P2 Zn2.08	96-900-4178	0.782208
(Olympite)	Li Na5 O8 P2	96-901-2623	0.780999
(Triploidite)	Fe0.5 H Mn1.5 O5 P	96-900-8191	0.773394
(Triploidite)	Fe0.5 H Mn1.5 O5 P	96-900-8192	0.773196

(Sampleite) Ca Cl Cu5 H10 Na O20.56 P4 96-901-0784 0.772895
(Andorite VI) Ag Pb S6 Sb3 96-900-8386 0.772650
((NH4)2[(UO2)6(MoO4)7(H2O)2]) H4 Mo7 N3 O42 U6 96-900-4625 0.772271
(FeFe2(PO3OH)4(H2O)4) Fe3 H12 O20 P4 96-900-0989 0.770188
(Becquerelite) Ca H22 O30 U6 96-900-2701 0.770085
(Metaschoepite) H34 Na0.48 O37.91 U8 96-901-0195 0.769272
(Marinellite) Al18 Ca2.91 Cl0.99 H14 K5.37 Na15.5 O90.98 S4 Si18 96-900-5632 0.767492
(Metaschoepite) H34 Na0.47 O37.082 U8 96-901-0199 0.767026
(Sulfur) S 96-901-2364 0.766753
(Rosickyite) S 96-901-2366 0.766753
(Proudite) Bi18.8 Cu1.5 Pb14.5 S30 Se14 96-900-0516 0.765733
(Vyuntspakhkite-(Y)) Al2 H5 O18 Si3.882 Tm0.935 Y2.115 96-901-3991 0.765599
(Metaschoepite) H32 Na1.09 O38.328 U8 96-901-0196 0.764929
(Metaschoepite) H34 O40 U8 96-901-1299 0.764059
(Khademite) Al F H10 O9 S 96-900-9710 0.763716
(Metaschoepite) H34 Na1.16 O37.9 U8 96-901-0198 0.762577
(Cyanochroite) Cu H12 K2 O14 S2 96-901-2781 0.761110
(Cs2[(UO2)6(MoO4)7(H2O)2]) Cs3 H4 Mo7 O42 U6 96-900-4624 0.761093
(K5[(UO2)10O8(OH)9](H2O)) H11 K5 O38 U10 96-900-4552 0.759937
(Schoepite) H18 O21 U4 96-900-4445 0.759854
(Metaschoepite) H32 Na1.22 O39.09 U8 96-901-0197 0.759360
(Turquoise) Al6 Cu H16 O28 P4 96-900-8100 0.756986
(Poyarkovite) Cl Hg3 O 96-900-4522 0.755748
(Bavenite) Al2 Be2 Ca4 H2 O28 Si9 96-900-7488 0.755227
(Minguzzite) C6 H6 Fe K3 O15 96-901-2076 0.754370
(Proudite) Bi20 Cu2 Pb16 S28.12 Se18.38 96-901-3781 0.753203
(Cs2Cr3O10) Cr3 Cs2 O10 96-900-7958 0.752257
(Cu(C21H24N4S3)I3CHCl3) C22 Cl3 Cu I3 N4 S3 96-900-7877 0.751311
(Poldervaartite) Ca1.67 H2 Mn0.33 O5 Si 96-900-1565 0.751086
(Feldspar) Al1.9 O8 Si2.1 Sr 96-900-2568 0.751049
(Ca2SiO3OHOH) Ca2 O5 Si 96-901-1377 0.750974
(Uranopilite) H34 O38 S U6 96-900-4638 0.750859
(Mereiterite) Fe H8 K2 O12 S2 96-900-2645 0.750381
(Faustite) Al6 H16 O28 P4 Zn0.927 96-900-9517 0.749975
(Cosalite) Bi4 Cu0.12 Pb4 S10 96-900-8242 0.749869
(Threadgoldite) Al H17 O21 P2 U2 96-900-9609 0.749841
(Kentbrooksite) Ca2.1 Ce0.579 Cl0.3 F0.5 Fe0.15 H3.816 Hf0.051 K0.099 La0.342 Mn3.6 Na16.002 Nb0.4 Nd0.228 O77.11 Si25.6 Sr0.45 Ti0.099 Zr3.3 96-901-2639 0.749806
(Na18Mn3Ca3Zr3Si26O76*H2O) Ca2.1 Ce0.54 Cl0.17 F0.28 Fe0.15 H3.78 Hf0.051 K0.099 La0.312 Mn3.6 Na16.002 Nb0.4 Nd0.198 O77.11 Si25.6 Sr0.45 Ti0.099 Y0.099 Zr3.3 96-901-2640 0.748758
(Pb4Sb4Se10) Pb1.79 Sb2.21 Se5 96-900-7852 0.747291
(Tazieffite) As6.41 Bi4.59 Cd0.5 Cl4 H0.48 N0.12 Pb10.13 S26 Sn0.25 96-901-3678 0.746961

(Carminite)	As2 Fe2 H2 O10 Pb	96-900-0115	0.745991
(Na2[(UO2)(MoO4)2](H2O)4)	H6 Mo2 Na2 O14 U	96-900-4766	0.745200
(Parsonsite)	O10 P2 Pb2 U	96-900-3629	0.745196
(Parsonsite)	O10 P2 Pb2 U	96-900-2376	0.745040
(Bementite)	Mn6.683 O23 Si6	96-900-1585	0.744854
(Feldspar)	Al1.9 O8 Si2.1 Sr	96-900-2567	0.744597

and 300 others...

****************************** Search-Match ********************************

Settings:

Profile data used? : No
Automatic zeropoint adaptation? : No
Minimum figure-of-merit (FoM) : 0.60
Parameter/influence 2theta : 0.50
Parameter/influence intensities : 0.00
Parameter multiple/single phase(s): 0.50

******************************* Peak List *********************************

Wavelength used for calculation of 2theta values: lambda = 1.540562 A

d[A]	2theta[∞]	Int.	FWHM	Matched
38.9577	2.2659	38.51	0.3600	
36.8595	2.3949	36.11	0.3600	
34.6883	2.5448	29.82	0.3600	
26.6816	3.3086	30.24	0.3600	
18.0646	4.8877	28.78	0.3600	
17.7578	4.9722	41.36	0.3600	
16.8789	5.2313	27.97	0.3600	
15.9840	5.5244	26.47	0.3600	
14.7819	5.9741	34.80	0.3600	I
13.3276	6.6266	26.00	0.3600	
10.3828	8.5092	40.12	0.3600	
9.8296	8.9890	149.01	0.3600	A,G
8.3055	10.6429	25.83	0.3600	
7.8940	11.1994	32.57	0.3600	
7.7347	11.4309	32.92	0.3600	
7.6405	11.5723	38.36	0.3600	
7.4978	11.7932	75.04	0.3600	
7.1843	12.3099	205.77	0.3600	E,F,I

6.6396	13.3242	26.52	0.3600	A,B,C
6.5957	13.4132	32.03	0.3600	B
6.4957	13.6207	39.78	0.3600	B,C
6.4284	13.7639	49.49	0.3600	A,C
5.8165	15.2202	52.90	0.3600	A,B,C
4.9384	17.9471	67.00	0.3600	A,C,G,I
4.4348	20.0051	224.04	0.3600	A,B,C,E,G,I
4.3932	20.1962	174.91	0.3600	A,F
4.3615	20.3446	148.94	0.3600	E,F,G,I
4.3167	20.5578	150.78	0.3600	A,C,D,E,F,I
4.1961	21.1558	544.78	0.3600	B,F,I
4.1369	21.4621	105.73	0.3600	A,C,E,I
4.1020	21.6467	112.18	0.3600	C,F,G
4.0761	21.7859	90.03	0.3600	I
4.0444	21.9587	102.82	0.3600	C,F,H
4.0055	22.1748	59.30	0.3600	
3.9523	22.4772	73.71	0.3600	B,F,I
3.9146	22.6965	161.33	0.3600	A,B
3.8620	23.0097	65.05	0.3600	B,I
3.8309	23.1989	84.45	0.3600	A,E,F
3.8037	23.3671	57.88	0.3600	A,B,C,G,I
3.7564	23.6661	477.94	0.3600	A,B
3.6756	24.1936	88.54	0.3600	C,E,F,I
3.6000	24.7099	226.86	0.3600	A,B,G,I
3.5436	25.1091	211.86	0.3600	A,B,E,F
3.5380	25.1502	211.68	0.3600	A
3.5000	25.4274	156.80	0.3600	A,B,C,H,I
3.4786	25.5868	122.82	0.3600	C
3.4482	25.8163	399.17	0.3600	B,C
3.3910	26.2590	52.43	0.3600	A,C,D,E,F,I
3.3676	26.4448	65.32	0.3600	A,C,E
3.3210	26.8226	1000.00	0.3600	B,C,G
3.2767	27.1927	525.71	0.3600	B,C,F,G,I
3.2224	27.6600	599.65	0.3600	A,B,F,I
3.1830	28.0093	32.60	0.3600	A
3.1629	28.1903	34.39	0.3600	A,C,E,F,H,I
3.0635	29.1251	46.46	0.3600	A,C,E,F,G,I
3.0461	29.2955	110.98	0.3600	A,C,F
2.9834	29.9256	273.89	0.3600	A,B,C,F
2.9518	30.2530	34.59	0.3600	A,B,C,I
2.9146	30.6493	48.44	0.3600	A,B,G,I
2.8878	30.9404	179.81	0.3600	B,C,E,F,H,I
2.7558	32.4620	111.51	0.3600	B,C,E,F,I
2.6897	33.2831	60.30	0.3600	A,F,I
2.6683	33.5578	41.49	0.3600	A,C,G,I

2.5922	34.5731	159.03	0.3600	A,B,C,F,G,I
2.5614	35.0022	346.66	0.3600	A,B,C,E,F,G
2.5536	35.1133	315.65	0.3600	B,G,I
2.5437	35.2535	209.60	0.3600	A,B,E,I
2.5283	35.4752	91.01	0.3600	A,B,E,I
2.5160	35.6550	99.08	0.3600	A,B,C
2.5092	35.7545	111.01	0.3600	A,B,C,E,F
2.4820	36.1597	89.95	0.3600	A,B,C,D,E,F,G,H,I
2.4457	36.7153	92.21	0.3600	A,B,C,G,I
2.4062	37.3400	50.08	0.3600	A,B,C,F
2.4007	37.4302	47.82	0.3600	B,C,F,G,I
2.3788	37.7865	113.66	0.3600	A,B,C,E,F,I
2.3745	37.8589	114.26	0.3600	A,F
2.3558	38.1700	68.89	0.3600	B,C,F,G
2.3426	38.3930	61.78	0.3600	A,C,E,F,H
2.3339	38.5432	85.30	0.3600	A,C,E
2.3264	38.6725	86.98	0.3600	A,B,F,I
2.3179	38.8192	83.21	0.3600	A,B,C,F
2.3073	39.0044	59.95	0.3600	A,C,D,F,I
2.2966	39.1945	47.05	0.3600	A,B,C,E,F,I
2.2881	39.3459	31.16	0.3600	A,B,C,E,F,I
2.2753	39.5756	63.52	0.3600	A,B,F,I
2.2315	40.3858	29.38	0.3600	A,B,C,E,F,G,H,I
2.1995	41.0006	62.76	0.3600	A,B,C,F,G,I
2.1852	41.2798	25.75	0.3600	A,B,C,E,F,G,I
2.1577	41.8301	117.97	0.3600	A,B,C,D,E,F,G,I
2.1394	42.2068	34.79	0.3600	A,B,C,F
2.1328	42.3437	32.49	0.3600	A,E,F,I
2.1210	42.5901	115.70	0.3600	B,F,H,I
2.1080	42.8664	72.56	0.3600	A,B,C,E,F,G,H
2.0615	43.8817	53.08	0.3600	A,B,C,E,F,I
2.0511	44.1169	43.37	0.3600	A,B,C,F,G,H,I
2.0026	45.2422	127.15	0.3600	A,B,C,D,F,G,I
1.9980	45.3529	101.47	0.3600	A,B,E,F
1.9907	45.5273	93.52	0.3600	A,C,E,G,I
1.9768	45.8666	40.15	0.3600	A,B,C,F
1.9711	46.0075	86.11	0.3600	B,C,E,F
1.9655	46.1465	77.91	0.3600	A,B,C,I
1.9536	46.4443	50.57	0.3600	A,C,F,G
1.9428	46.7167	29.11	0.3600	A,B,C,E,F,G,H
1.9251	47.1731	55.94	0.3600	A,B,C,E,F,I
1.9180	47.3576	47.37	0.3600	A,B,C,F,I
1.9093	47.5872	28.32	0.3600	A,B,C,E,F,G,I
1.8855	48.2262	37.04	0.3600	A,B,C,F,G,H,I
1.8458	49.3308	34.70	0.3600	A,B,C,E,F,G,I

1.8386	49.5367	46.79	0.3600	A,B,C,D,E,F
1.8355	49.6256	49.39	0.3600	A,B,C,I
1.8274	49.8622	28.44	0.3600	A,B,C,E,F,G,I
1.8137	50.2632	99.54	0.3600	A,B,C,E,F,I
1.7944	50.8433	162.81	0.3600	A,B,F,I
1.7819	51.2240	38.83	0.3600	A,B,C,E,F
1.7757	51.4176	36.72	0.3600	A,B,C,I
1.7718	51.5378	29.64	0.3600	A,C,F
1.7693	51.6153	29.30	0.3600	A,B,C,F,H,I
1.7439	52.4233	34.34	0.3600	A,B,C,F,G,H,I
1.7003	53.8776	28.56	0.3600	A,B,C,E,F,G,H,I
1.6913	54.1879	64.67	0.3600	A,C,D,E,F,G,I
1.6862	54.3640	55.73	0.3600	A,B,C,E,F,G
1.6808	54.5510	48.31	0.3600	C,E,I
1.6756	54.7353	47.37	0.3600	C,D,E,F,I
1.6713	54.8879	55.03	0.3600	A,B,C,G,I
1.6672	55.0357	76.34	0.3600	B,E,G,I
1.6640	55.1509	74.37	0.3600	A,B,C,G
1.6588	55.3365	76.80	0.3600	A,B,E,G
1.6544	55.4965	78.49	0.3600	A,C,E,I
1.6500	55.6575	69.91	0.3600	A,B,E,F,G,I
1.6462	55.7998	76.05	0.3600	A,B,F,H
1.6426	55.9328	63.16	0.3600	A,B,F,G,I
1.6363	56.1648	70.31	0.3600	A,B,C,D,E,F,I
1.6283	56.4664	53.53	0.3600	A,B,C,E,F,G
1.6245	56.6104	70.87	0.3600	A,B,C,F,G,I
1.6175	56.8770	37.44	0.3600	A,B,C,E,F,H,I
1.5919	57.8768	40.63	0.3600	A,B,C,E,F,G,I
1.5877	58.0467	25.67	0.3600	A,B,C,E,F,G,H,I
1.5658	58.9371	37.29	0.3600	A,B,C,D,E,F,H,I

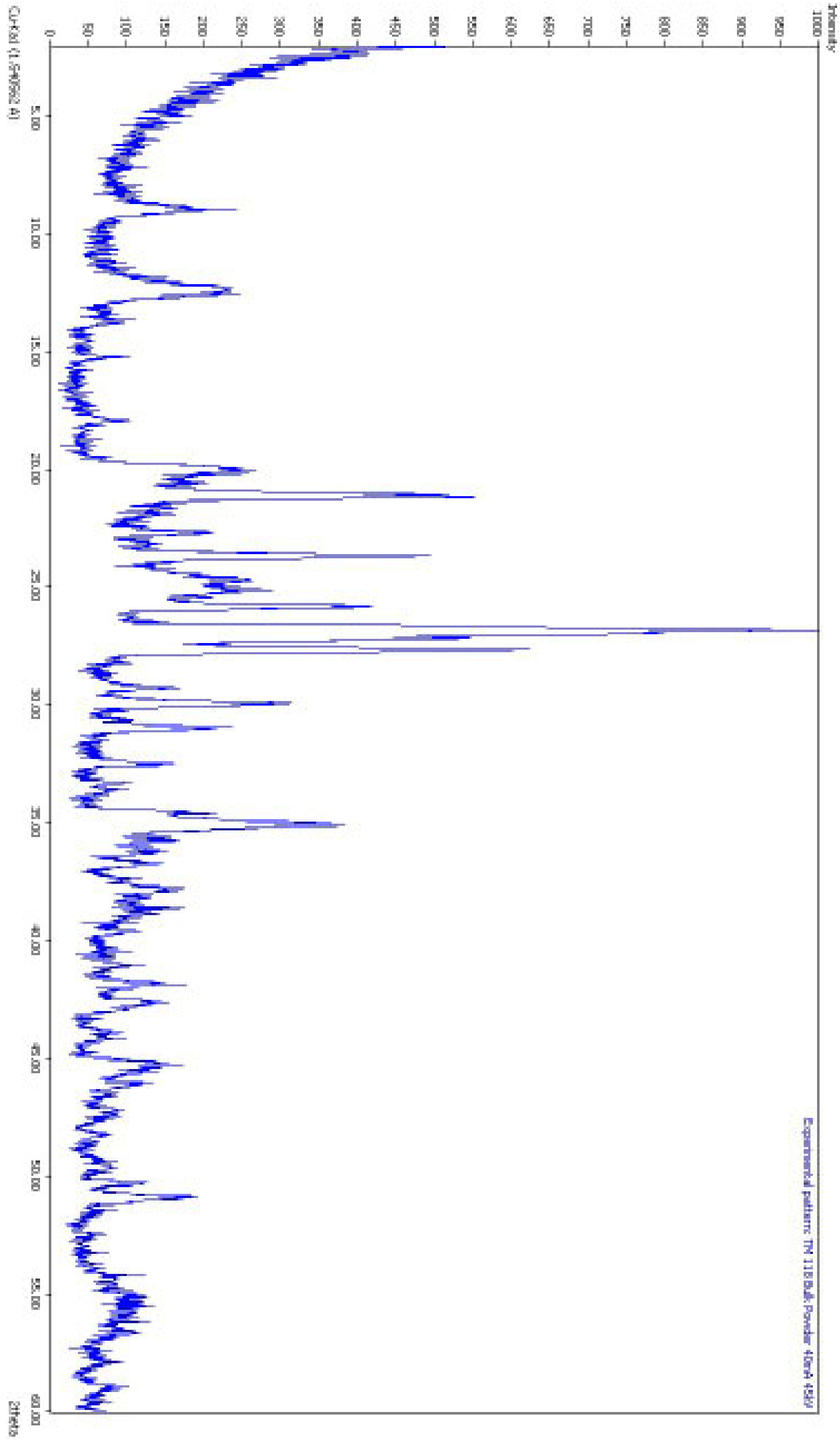

##
Match! Phase Analysis Report
##

Licensee:

Sample : TM127 random slide mount 45k40m

******************************** Sample Data ********************************

File name   : tm127.rd
File path   : e:\
Data collected: 4/2/2008 3:01:08 PM
Data range   : 2.000∞ to 60.000∞
No. of points : 2901
Step size   : 0.020
Alpha2 subtr.?: No
Backgr.subtr.?: No
Data smoothed?: Yes
Radiation   : Cu-Ka1
Wavelength   : 1.540562 A

****************************** Matched Phases ******************************

Phase A: (Turquoise)

Formula sum   : Al6 Cu H16 O28 P4
Entry number   : 96-900-8100
FoM   : 0.869336
No. of peaks   : 500
Peaks in range   : 225
Peaks matched   : 188
Int. scale fct   : 0.44
Quant. (weight %): 34.30

Phase B: (Ramdohrite)

Formula sum   : Ag1.5 Pb3 S12 Sb5.5
Entry number   : 96-901-1731
FoM   : 0.849825
No. of peaks   : 500
Peaks in range   : 500
Peaks matched   : 332

Int. scale fct : 0.24
Quant. (weight %): 2.94

Phase C: (Bementite)

Formula sum : Mn6.683 O23 Si6
Entry number : 96-900-1585
FoM : 0.811417
No. of peaks : 500
Peaks in range : 500
Peaks matched : 326
Int. scale fct : 0.29
Quant. (weight %): 11.52

Phase D: (Kaolinite)

Formula sum : Al2 H4 O9 Si2
Entry number : 96-900-9235
FoM : 0.765272
No. of peaks : 254
Peaks in range : 82
Peaks matched : 68
Int. scale fct : 0.30
Quant. (weight %): 18.47

Phase E: (Tridymite)

Formula sum : O10 Si5
Entry number : 96-901-3394
FoM : 0.738164
No. of peaks : 53
Peaks in range : 53
Peaks matched : 31
Int. scale fct : 0.09
Quant. (weight %): 4.15

Phase F: (Illite)

Formula sum : Al2 H2 K O12 Si4
Entry number : 96-901-3733
FoM : 0.694826
No. of peaks : 260
Peaks in range : 68
Peaks matched : 52
Int. scale fct : 0.31

Quant. (weight %): 28.48

Phase G: (Vermiculite)

Formula sum : Al0.721 Fe0.24 H3 Mg1.338 O9 Si1.36
Entry number : 96-900-0061
FoM : 0.657623
No. of peaks : 292
Peaks in range : 176
Peaks matched : 112
Int. scale fct : 0.04
Quant. (weight %): 0.14

****************************** Candidates ********************************

Name Formula Entry No. FoM

(Brewsterite-Ba) Al2.15 Ba0.55 H10 K0.01 O21 Si5.85 Sr0.4 96-900-1789 0.773750
(Vermiculite) C12 Mg3 N4 O12 Si4 96-900-0119 0.770486
(Brewsterite-Sr) Al2.05 Ba0.45 H10 K0.01 O21 Si5.95 Sr0.5 96-900-1788 0.759866
(Brewsterite-Sr) Al2.15 Ba0.24 H10 K0.01 O21 Si5.85 Sr0.67 96-900-1790 0.758559
(Upalite) Al H15 O23 P2 U3 96-900-9715 0.748393
(Brewsterite-Sr) Al1.98 Ba0.3 Ca0.14 H8 O20.9 Si6.02 Sr0.58 96-900-7480 0.748265
(KV(C9H12)2.C4H8O.0.5C4H8O2) C24 K O2 V 96-900-7861 0.746196
(Vermiculite) C12 H2 Al1.43 Fe0.48 Mg2.37 N2 O16 Si2.72 96-900-0209 0.746090
(Becquerelite) Ca O30 U6 96-900-1111 0.743822
((NH4)2[(UO2)6(MoO4)7(H2O)2]) H4 Mo7 N3 O42 U6 96-900-4625 0.742163
(Juabite) As4 Ca Cu10 H10 O34 Te4 96-900-4594 0.741083
(Antigorite) H62 Mg48 O147 Si34 96-900-4515 0.740244
(Phurcalite) Ca2 O23 P2 U3 96-900-4231 0.734933
(Khademite) Al F H10 O9 S 96-900-9710 0.732754
(K5[(UO2)10O8(OH)9](H2O)) H11 K5 O38 U10 96-900-4552 0.732535
(Epistilbite) Al0.726 Ca0.375 H4 O7.72 Si2.274 96-900-5581 0.731609
(Cs9Al9Si27O72*13H2O) Al4.34 Ca0.2 Cs4.16 H30 O42.35 Si13.66 96-901-2218
0.730682
(Antigorite) H58 Mg45 O138 Si32 96-900-4000 0.727592
(Megacyclite) H46 K Na8 O46 Si9 96-901-3161 0.725737
(Antigorite) H79 Mg48 O147 Si34 96-900-3104 0.722986
(Paderaite) Ag0.2 Bi11.34 Cu7.09 Pb1.37 S22 96-900-4985 0.721345
(Fettelite) Ag16 As3.596 Hg S15 Sb0.403 96-901-3617 0.720718
(Ca2Co.9Zn.1Si2O7) Ca2 Co0.9 O7 Si2 Zn0.1 96-901-1316 0.718717
(Paracoquimbite) Fe2 H9 O21 S3 96-900-0252 0.717866
(Ca2Co.9Zn.1Si2O7) Ca2 Co0.9 O7 Si2 Zn0.1 96-901-1317 0.717324
(Paderaite) Bi11.34 Cu7.32 Pb1.34 S22 96-900-4986 0.716546

(Turquoise) Al3 Cu0.452 H8 O14 P2 96-900-9518 0.716404
(Biotite) Al1.208 Fe1.392 K Mg1.161 O12 Si2.792 Ti0.276 96-900-0744 0.714518
(Bustamite) Ca Mn O6 Si2 96-900-8087 0.710466
(Ag10[(UO2)8O8(Mo5O20)]) Ag10 Mo5 O44 U8 96-900-4828 0.710084
(NaMg(H2PO3)3*H2O) H8 Mg Na O10 P3 96-900-7942 0.708491
(Zr(PO3)4) O12 P4 Zr 96-901-2851 0.707038
(Vonbezingite) Ca6 Cu3 O26 S3 96-900-1506 0.706910
(Tridymite) O2 Si 96-901-3493 0.706100
(Tridymite) O2 Si 96-900-0521 0.704182
(Tridymite) O2 Si 96-901-3492 0.703058
(Tridymite) O2 Si 96-900-6969 0.701899
(Carnallite) Cl3 H12 K Mg O6 96-900-0984 0.701478
(Makatite) H5 Na O7 Si2 96-900-8303 0.701178
(Na3Tl3[(UO2)(MoO4)4]) Mo4 Na3 O18 Tl3 U 96-900-4763 0.701160
(Leonite) H8 K2 Mn O12 S2 96-900-2642 0.701099
(Biotite) Al1.24 Fe1.4 H1.64 K0.98 Mg0.71 Na0.02 O12 Si1.36 Ti0.16 96-900-2308 0.697080
(Epistilbite) Al0.726 Ca0.36 H4 O7.945 Si2.274 96-900-5580 0.695240
(Proudite) Bi20 Cu2 Pb16 S28.12 Se18.38 96-901-3781 0.694317
(Nordstromite) Bi7.92 Cu Pb2.08 S10.8 Se3.2 96-900-4158 0.692989
((CH3)2NH2CuCl3) C2 Cl3 Cu N 96-900-9873 0.692931
(Proudite) Bi18.8 Cu1.5 Pb14.5 S30 Se14 96-900-0516 0.692449
(RUB-7) Mn3 O6 Rb2.08 96-900-5285 0.691944
(Kochite) Ca3.27 Ce0.08 F5.6 Fe0.24 Mn1.1 Na6.91 Nb0.1 O30.4 Si8 Ti0.87 Y0.04 Zr1.31 96-900-5610 0.690482
(Uranopilite) H34 O38 S U6 96-900-4638 0.690467
(Andorite VI) Ag Pb S6 Sb3 96-900-8386 0.689766
and 284 others...

****************************** Search-Match ********************************

Settings:

Profile data used? : No
Automatic zeropoint adaptation? : Yes
Minimum figure-of-merit (FoM) : 0.60
Parameter/influence 2theta : 0.50
Parameter/influence intensities : 0.00
Parameter multiple/single phase(s): 0.50

******************************* Peak List **********************************

Wavelength used for calculation of 2theta values: lambda = 1.540562 A

d[A]	2theta[∞]	Int.	FWHM	Matched
41.9547	2.1040	80.20	0.2000	
37.6353	2.3455	63.77	0.2000	
32.4522	2.7202	49.01	0.2000	
15.6208	5.6530	37.30	0.2000	C
13.9519	6.3298	41.64	0.2000	G
13.3280	6.6264	44.36	0.2000	
9.0229	9.7945	51.69	0.2000	A,C
8.1366	10.8645	39.25	0.2000	E
7.9711	11.0908	59.35	0.2000	B,E
7.8322	11.2881	80.05	0.2000	B
7.5467	11.7166	192.96	0.2000	C,E
7.3154	12.0885	273.77	0.2000	C,E
7.2372	12.2196	305.31	0.2000	B,D,G
6.9237	12.7750	45.34	0.2000	E
6.8594	12.8953	41.84	0.2000	B,C,E
6.6829	13.2374	115.48	0.2000	A,B,C,E
6.3343	13.9693	37.25	0.2000	C,E
6.1596	14.3678	286.70	0.2000	A,B
6.0020	14.7471	62.72	0.2000	A,C
4.7833	18.5340	128.12	0.2000	A,B,C,E,G
4.4379	19.9908	283.39	0.2000	A,B,C,D,E,F,G
4.3369	20.4613	149.79	0.2000	B,C,D,E,G
4.3027	20.6256	146.28	0.2000	C,E,F,G
4.2504	20.8821	334.16	0.2000	A,C,E
4.1737	21.2704	156.27	0.2000	A,C,D,E,G
4.1472	21.4079	121.38	0.2000	B,C,G
4.1217	21.5420	110.00	0.2000	A,D,E,F
4.0831	21.7482	108.40	0.2000	C,E
4.0456	21.9522	80.73	0.2000	A,B,C,G
4.0157	22.1178	81.79	0.2000	B,C,E
3.9819	22.3080	90.46	0.2000	B,C,E,G
3.9240	22.6413	57.16	0.2000	B,C,E
3.8675	22.9765	75.78	0.2000	B,F,G
3.8363	23.1658	60.98	0.2000	B,C,D
3.7966	23.4116	82.91	0.2000	A,B,C,G
3.7645	23.6140	86.94	0.2000	C,D
3.6702	24.2297	705.80	0.2000	A,C,G
3.6341	24.4741	175.15	0.2000	B,C
3.6108	24.6346	168.69	0.2000	B,C

3.5842	24.8204	193.76	0.2000	C,F,G
3.5662	24.9481	176.85	0.2000	B,C,D
3.5450	25.0996	132.17	0.2000	B
3.5053	25.3881	109.65	0.2000	A,B,G
3.4845	25.5426	124.78	0.2000	A,B,C
3.4263	25.9838	245.32	0.2000	A,B,C,D,G
3.3378	26.6855	1000.00	0.2000	A,B,C,D,F
3.2763	27.1962	198.63	0.2000	A,B,C,G
3.2331	27.5666	59.89	0.2000	B,C,G
3.0856	28.9121	93.78	0.2000	A,B,C,D,F
3.0513	29.2443	63.03	0.2000	B,C,G
3.0289	29.4654	46.85	0.2000	A,B,C
2.9825	29.9341	60.33	0.2000	A,C,G
2.9705	30.0580	43.75	0.2000	C
2.9554	30.2151	50.25	0.2000	B,C
2.9012	30.7937	512.43	0.2000	A,B,C,F,G
2.5859	34.6606	48.38	0.2000	A,B,C,F,G
2.5739	34.8266	57.88	0.2000	B,C,G
2.5631	34.9787	126.85	0.2000	A,B,C,D,F
2.5527	35.1255	143.53	0.2000	C,D,F,G
2.5426	35.2693	102.35	0.2000	B,C,D,G
2.5226	35.5586	160.57	0.2000	A,B,C
2.5097	35.7469	134.07	0.2000	A,B,C,D,F
2.4934	35.9896	130.20	0.2000	A,B,C,D,G
2.4837	36.1347	115.61	0.2000	B,C,D
2.4674	36.3818	68.66	0.2000	A,B,C,D
2.4547	36.5765	127.15	0.2000	A,B,C,F
2.4322	36.9277	64.56	0.2000	A,B,C,F,G
2.4222	37.0859	70.84	0.2000	A,B,C
2.4145	37.2076	52.46	0.2000	A,B,C
2.4037	37.3807	79.46	0.2000	A,B,C,F
2.3827	37.7235	92.97	0.2000	A,C,F,G
2.3732	37.8797	78.48	0.2000	A,C,D,G
2.3596	38.1061	93.93	0.2000	B,C
2.3456	38.3428	169.32	0.2000	A,B,C,D
2.3316	38.5824	130.19	0.2000	B,C,D
2.3182	38.8147	141.28	0.2000	A,B,C,F,G
2.3059	39.0297	145.58	0.2000	A,B,C,G
2.2951	39.2204	120.91	0.2000	A,B,C,D,G
2.2508	40.0256	36.65	0.2000	A,B,C,D,F,G
2.2281	40.4513	102.65	0.2000	A,B,C,D,F,G
2.2204	40.5964	69.88	0.2000	A,B,C,D,F,G
2.1238	42.5309	72.85	0.2000	A,B,C,D,F,G
2.1132	42.7557	72.53	0.2000	A,B,C,D,F
2.1074	42.8776	35.46	0.2000	A,B,C,D

2.0754	43.5731	40.18	0.2000	A,B,C,D,G
2.0621	43.8685	94.12	0.2000	A,B,C,D,F
2.0536	44.0595	52.23	0.2000	A,B,C,F,G
2.0278	44.6498	59.70	0.2000	A,B,C
2.0145	44.9608	80.03	0.2000	A,B,C,F,G
1.9777	45.8458	44.28	0.2000	A,B,D,F,G
1.9030	47.7541	55.22	0.2000	A,B,G
1.8988	47.8666	61.35	0.2000	A,B,D,F,G
1.8605	48.9139	36.18	0.2000	A,B,D,F,G
1.8559	49.0448	39.56	0.2000	A,B
1.8493	49.2305	58.53	0.2000	A,B
1.8433	49.4016	67.84	0.2000	A,B,D,G
1.8365	49.5964	74.94	0.2000	A,B,G
1.8294	49.8037	42.17	0.2000	A,B,D,F,G
1.8170	50.1672	153.82	0.2000	A,B,D,G
1.7839	51.1635	39.08	0.2000	A,B,D,F,G
1.7267	52.9873	38.82	0.2000	A,B,F,G
1.7193	53.2337	35.39	0.2000	A,B,G
1.7141	53.4062	35.96	0.2000	A,B,D,F,G
1.6826	54.4901	41.41	0.2000	A,B,D,F,G
1.6769	54.6886	60.98	0.2000	A,B,D,F,G
1.6708	54.9067	65.47	0.2000	A,B,F,G
1.6675	55.0235	70.32	0.2000	A,B,D,F,G
1.6588	55.3391	68.85	0.2000	D,F
1.6542	55.5051	39.26	0.2000	D,F,G
1.6525	55.5684	40.36	0.2000	A,D,F,G
1.6406	56.0047	40.26	0.2000	A,F,G
1.6365	56.1562	40.83	0.2000	A,D,G
1.6341	56.2488	41.09	0.2000	A,D,F
1.6234	56.6515	50.26	0.2000	A,G